PROBABILISTIC ANALYSIS OF HIGHWAY BRIDGE TRAFFIC LOADING

by

COLIN C. CAPRANI

OCTOBER 2005

Thesis submitted to the National University of Ireland, University College Dublin, School of Architecture, Landscape and Civil Engineering, in fulfilment of the requirements for the degree of Doctor of Philosophy

Dr. M.G. Richardson

Head of School

Prof. E.J. OBrien

Project Supervisor

DEDICATION

To my mother, Joan Caprani.

DECLARATION

The author hereby declares that this thesis, in whole or part, has not been used to obtain any degree in this, or any other, university. Except where reference has been given in the text, it is entirely the author's own work.

The author confirms that the library may lend or copy this thesis upon request, for academic purposes.

_____

Colin C. Caprani

October 2005

ABSTRACT

Many bridges of the world's highway networks have been in service for decades and are subject to escalating volumes of traffic. Consequently, there is a growing need for the rehabilitation or replacement of bridges due to deterioration and increased loading. The assessment of the strength of an existing bridge is relatively well understood, whereas the traffic loading it is subject to, is not as well understood. Accurate assessment of the loading to which bridges may be subject, can result in significant savings for highway maintenance budgets internationally. In recent years, a general approach has emerged in the research literature: the characteristics of the traffic at a site are measured and used to investigate the load effects to which the bridge may be subject in its remaining lifetime.

This research has the broad objective of developing better methods of statistical analysis of highway bridge traffic loading. The work focuses on short- to medium-length (approximately 15 to 50 m), single- or two-span bridges with two opposing lanes of traffic. Dynamic interaction of the trucks on the bridge is generally not included.

Intuitively, it can be accepted that the gap between successive trucks has important implications for the amount of load that may be applied to any given bridge length. This work describes, in quantitative terms, the implications for various bridge lengths and load effects. A new method of modelling headway for this critical time-frame is presented.

When daily maximum load effects (for example) are considered as the basis for an extreme value statistical analysis of the simulation results, it is shown that although this data is independent, it is not identically distributed. Physically,

this is manifest as the difference in load effect between 2- and 3-truck crossing events. A method termed composite distribution statistics is presented which accounts for the different distributions of load effect caused by different event types. Exact equations are derived, as well as asymptotic expressions which facilitate the application of the method.

Due to sampling variability, the estimate of lifetime load effect varies for each sample of load effect taken. In this work, the method of predictive likelihood is used to calculate the variability of the predicted extreme for a given sample. In this manner, sources of uncertainty can be taken into account and the resulting lifetime load effect is shown to be calculated with reasonable assurance.

To calculate the total lifetime load effect (static load effect plus that due to dynamic interaction), the results of dynamic simulations based on 10-years of static results are used in a multivariate extreme value analysis. This form of analysis allows for the inherent correlation between the total and static load effect that results from loading events. A distribution of dynamic amplification factor and estimates for a site dynamic allowance factor are made using parametric bootstrapping techniques. It is shown that the influence of dynamic interaction decreases with increasing static load effect.

ACKNOWLEDGEMENTS

In the course of any work such as this, it is inevitable that an author comes to rely on many people; the work that results is partly theirs: this is no exception. It is because of these people that these years have proved the best of my life.

To Prof. Eugene O'Brien, I have read many of your former students' comments, doubtful that one person could be so many wonderful things: I know now that they are right. I pushed your patience more than most, that we remain good friends is testament to your abilities. Thank you for everything, I hope you're happy with the results. Wife Number 2 herewith resigns!

To all of my family, here with us and gone before us, it simply wouldn't have happened without you. To Mam and Maurice; Anna, Connor, Jack and Carla; Stephen, Tracy and Joey; thank you. To the memories of Dad; Nanna and Grandad; and Honey; I know your support in the early years has me here.

To Ms. Aoife Banks, B.A., M.A. for going through this with me, suffering all the while, yet with little to show for it at the end – but my love, thank you.

To Dr. Mark Richardson, thank you for your advice in the early years, direct support in the latter, and the opportunity to repay the department in kind.

To the staff of the former Department of Civil Engineering, UCD for their expertise, friendships, humour, and fantastic Christmas parties, thank you. In particular, Dr's Arturo Gonzalez, Ciarán McNally, Paul Fanning, Ken Gavin, and John O'Sullivan all contributed in ways they cannot know. To Andrew and Naoimh in the office, many thanks for those special red-tape scissors. To the guys in the lab: Derek, Terry, Tom and, Paddy – thanks for the cheap therapy.

There have been many postgrads over the course of the last 1543 days and 68572 words, and I have learned so much from them. Thank you firstly to those with whom I have shared a room: Sinéad, Tom, Benny, Alissa, Abraham, Paraic, Colm and Niall. I appreciate them allowing me my Friday afternoon 'love-ins'. Thanks are due to many others: to Carden, Chisco, and Enda for the legend of Madrid; Drs. Archie, Brady and Tucker for proving it can be done; that Old Man Carl; Cillian, Gavin, and Noel for the coffees; and to the others, Lorraine O'G, Fionnuala, JJ, Diarmuid, Katherine, Shane and Continuity Shane, Davy G, Li, Lorraine F, Conor, Caroline, Aidan and Louis, thank you all. If there are some I've missed: my apologies.

To Joe Kindregan, thank you so much for years of humour, patience and support; I doubt you know of your import in this. To my former lecturers, now my colleagues, in DIT Bolton St., thank you for inspiring me to push harder. My apologies to my friends from home and 'first' college for missing out on so much of your lives: my thanks for understanding. To Dr Rod Goodfellow for his friendship, advice and direct aid early on, thank you.

I would also like to thank my many friends in, or of, UCD Canoe Club for four of the best years of my life, in particular Benoit Ferré-Cullen for inviting me in. The encouragement they offer – that saw me run Ubaye Gorge, for example – filtered through into this work: truly a remarkable collection of people.

To you the reader, whether you make it all the way through or fail in a valiant attempt, thank you.

Finally, I would like to thank all those people from whom, with or without their knowledge, I have learned.

TABLE OF CONTENTS

Chapter 1

INTRODUCTION

"One should aim not at being possible to understand, but at being impossible to misunderstand"   – Marcus Fabius Quintilian

Chapter 1 - INTRODUCTION

1.1 Background

The developed economies of the world have, as a prerequisite, a transport infrastructure that is efficient in the movement of goods and people. In such economies, the highway transport infrastructure was, in many cases, built in the decades following World War II. Hence, the bridges built for these highway networks have been in existence for a significant proportion of their design lifetime. Deterioration of these older bridges has been found in many countries; yet with economic growth, their importance has increased, as has the cost of their replacement or refurbishment.

Throughout the last century, as scientific knowledge broadened, more accurate standards for highway bridge design developed. Indeed the in-situ strength of bridges is now well understood relative to the in-situ loads to which bridges are subject. The highway bridge load models in bridge design codes are consequently quite conservative. Whilst acceptable for the majority of new bridges, where the cost of providing additional strength is minimal, the loading standards are conservative when applied to bridges in operation. In the past, when bridges were fewer in number, more lightly trafficked, and cheaper to repair or replace, the overall economic cost of conservative loading codes was small. Today, the rehabilitation of existing bridges to conservative code load requirements is therefore known to be an area in which savings can be made.

The factors just outlined have combined in recent years to significantly increase the value of accurate assessment of the loads to which a bridge may be subject. A general solution of the problem is emerging in which the characteristics of the

traffic at a given site are measured and used to investigate the load effects to which the bridge may be subject in its remaining lifetime.

Static weigh-station sites, typical of those used in law enforcement efforts, are known to produce biased measurements of traffic, due to the avoidance of grossly overloaded vehicles. Lately, unbiased measurement of real traffic is obtained by Weigh-In-Motion (WIM) systems. These systems have acknowledged measurement inaccuracies but produce unbiased data because the installations are not readily visible to traffic.

Even with modern WIM systems, the quantity of traffic data is usually limited: such data is generally expensive to obtain and measurement periods are consequently limited. To extend the amount of traffic data, synthetic traffic data can be generated, based upon the measured traffic characteristics, through the use of Monte-Carlo simulation. Such extended traffic records are then used for estimation of rare extreme load effects which may result from the traffic at the measurement site in the bridge lifetime. Even with this form of simulation, it is necessary to have some form of statistical extrapolation technique, based on the load effect history, to estimate a lifetime value of load effect.

1.2 Objectives and Scope

1.2.1 Objectives

The research described in this exposition has the broad objective of critically examining the statistical analysis of highway bridge traffic loading. It had been recognized that the contemporary literature on the subject included areas of subjectivity that can affect the results of an analysis. Thus the main thesis of this work is to further the level of knowledge regarding the calculation of the bridge loading that may be expected to occur with an acceptably low level of probability in the remaining lifetime of the bridge.

More specifically, with reference to previous work in the area, the objectives are:

1. to maximize the information gained from a limited amount of measured traffic data;

2. to develop appropriate software tools to produce robust information for further analysis;

3. to improve the statistical analyses performed on load effect histories such that robust and realistic estimates of lifetime maximum load effect are determined;

4. to introduce further statistical techniques through which introduced inaccuracies may be accounted for in the lifetime maximum load effect estimate.

1.2.2 Scope of work

This work focuses on short- to medium-length bridges (approximately 15 to 50 m) of two opposing lanes of traffic. While it is acknowledged that congested traffic may govern for bridges in the upper part of this length range, only free-flowing traffic is considered in this work. Vehicles of Gross Vehicle Weight

(GVW) greater than 3.5 tonnes are considered: lighter vehicles do not contribute significantly to the loading to which a bridge is subject, but their role in the spatial arrangement of traffic is acknowledged. Dynamic interaction of the trucks on the bridge is generally not considered. Only single and two-span bridges are examined and the load effects are limited to bending moment, shear force, stress and/or strain as appropriate to the problem under study.

1.3 Outline of the Research

1.3.1 Traffic modelling and simulation

The research presented herein is heavily reliant on the software tools developed as part of this work. The efficacy and power of the software has implications for the manner in which bridge load research is carried out: for example, larger sample sizes generally result in more accurate load effect prediction. Accordingly, in this work, the object-orientated approach to programming is used. An explanation of this method, and the programs based upon it, is given in Chapter 4. As a result of these developments, it is now possible to simulate 5 years of traffic for a typical heavily trafficked European trunk motorway on a typical high-specification desktop personal computer. This traffic may be used to assess load effects from any form of influence line or slices of an influence surface. The statistical analysis outlined later may then be applied to the complex of results gathered.

1.3.2 Headway modelling

Intuitively, the gap between successive trucks has important implications for the quantity of load that may be applied to a bridge: this work describes, in quantitative terms, the implications for various lengths and load effects. It is found that existing headway (gap plus the lead truck length) models do not focus on the small headways that are critical for bridge loading events. A new method of modelling headway for this critical range is presented: it exhibits less variability in load effect estimation; conforms to the physical requirements of traffic; and preserves measured headway distributions. This method is described in Chapter 5, along with comparisons to existing methods.

1.3.3 Composite distribution statistics

The load effect output from the process of measurement, modelling, and traffic simulation, requires a statistical analysis to permit estimations of future load effect values. Extreme value analysis assumes that the data to be analysed is independent (or, at most, has minor dependence) and identically distributed. When daily maxima (for example) are considered as the basis for further statistical analysis, it is shown here that although this data is independent, it is not identically distributed. Physically, this is manifest as the difference in load effect between 2- and 3-truck crossing events, for example. Intuitively, such events are not identically distributed, and as such, should not be mixed as a single distribution in an extreme value statistical analysis. A method termed composite distribution statistics is presented which accounts for the different distributions of load effect caused by different event types. Exact equations are derived, as well as asymptotic expressions which facilitate the application of the method. The method is checked against results derived from the exact distribution, and compares favourably. Also, the method is applied to the output from the simulation process and compared with the traditional approach. It is shown that the composite distribution statistics method can give significantly different results.

1.3.4 Prediction of extreme load effects

The **raison d'être** of the bridge loading model, and subsequent statistical analysis, is the prediction of extreme, or maximum lifetime, load effects. Basic prediction techniques are outlined in Chapter 3, but more advanced methods are required to reflect the complexity of the underlying process and its model, such as the method of composite distribution statistics developed as part of this work. Such extrapolation methods, are subject to substantial variability:

different samples give different estimates of lifetime load effect. To allow for this variability, the method of predictive likelihood is used in this work. This is a relatively new area of Frequentist statistics and is not yet adopted in many practical fields of research. Predictive likelihood yields many benefits for the bridge loading problem. Most importantly, the variability of the predicted extreme can be calculated. Further, sources of uncertainty, such as the random variation of the data and of the parameter fits to the data, can be taken into account. Therefore the result of a predictive likelihood analysis gives a measure of the uncertainty inherent in the bridge loading problem, and enables this uncertainty to be taken into account.

1.3.5 Multivariate extreme value analysis

The full spectrum of bridge traffic load modelling must account for the effect of dynamic interaction between the traffic and the bridge during crossing events. The modelling and simulation described in this work are strictly static analyses. To allow for the effects of dynamics at the return period of bridge loading, 10 years of traffic were simulated for a bridge which has been tested and modelled extensively by other authors. These results are used as a basis for dynamic models of crossing events. Both of these data sets form the basis of a multivariate extreme value analysis which allows for the correlation between the static and dynamic aspects of a crossing event. Using re-sampling techniques, estimates for a site dynamic allowance factor are made. It is shown that, while dynamic amplification may be large (around 30%) for some individual events, the allowance that should be made for dynamics to obtain an appropriate overall lifetime load effect value is much less (around 5%).

1.4 Layout of the Thesis

The process under study is described in this chapter and illustrated in Figure 1.1, where its integration into the chapters of this dissertation is shown.
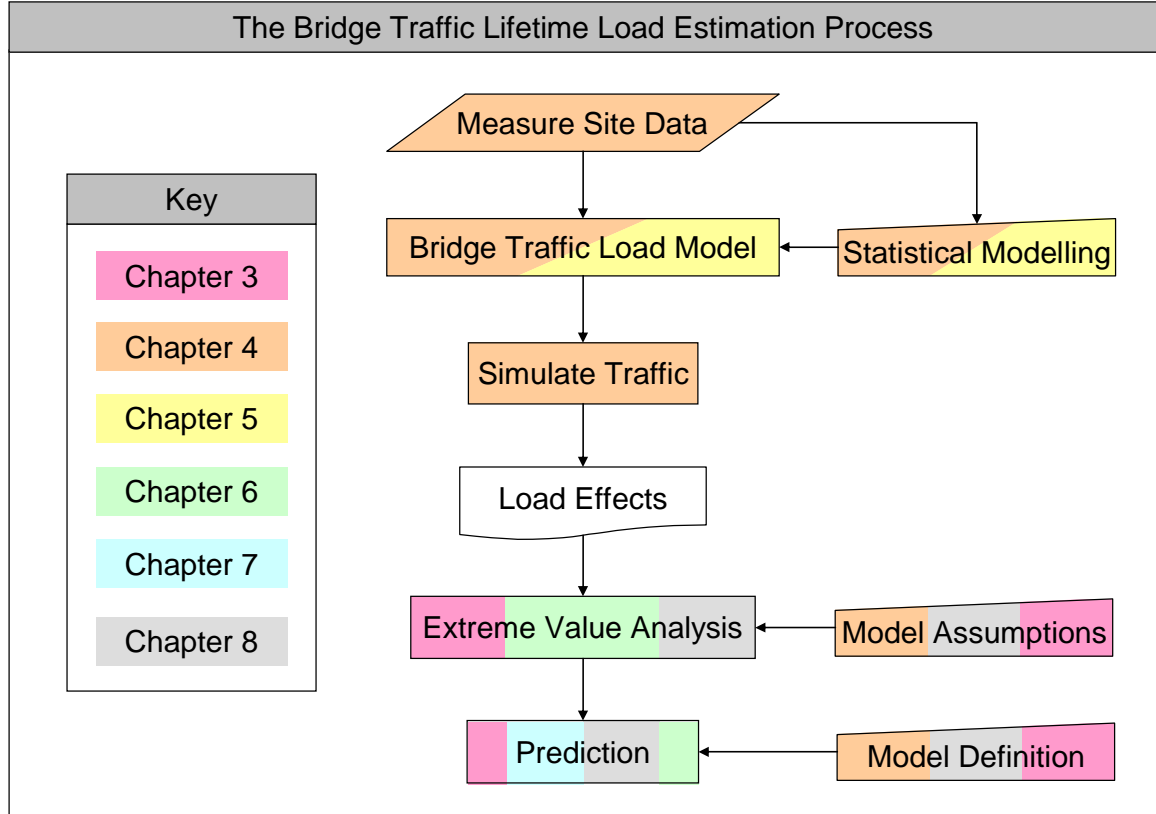
Figure 1.1: Load estimation process and chapter layout.

Chapter 2 gives more detailed information on the background to this work by surveying the scientific literature in the field. The areas of particular importance to this project are highlighted.

An introduction to the fundamental probability methods used in this work is given in Chapter 3. Particular attention is given to the areas of statistical analysis that are built upon in other parts of the work.

The bridge load models used are described in Chapter 4. Measurements of real traffic, taken from various sites, are described along with the development of a

sympathetic bridge traffic load model. The final part of this chapter describes the implementation of the traffic model, to generate data for further analysis.

It is shown in Chapter 5 that the headway model used is important to the types of event and values of load effect that result. A novel headway model is described, based on Headway Distributions Statistics of a particular site, termed HeDS. A comparison of HeDS with other headway models of the literature is made, and differences to existing models described

In Chapter 6 it is shown that the existing methods of fitting and extrapolating load effects do not reflect the underlying statistical phenomena. A method termed composite distributions statistics is proposed and shown to give good predictions when compared to known return levels. It is applied to the bridge loading problem and compared to the conventional means of extrapolation.

Chapter 7 presents the application of predictive likelihood theory to the bridge loading problem. It is shown that this method accounts for the variability of the data and parameter values in the composite distribution statistics model and a probabilistic assessment of future load effect is found.

A multivariate extreme value statistical analysis is presented in Chapter 8 in the context of relating lifetime static to total (the combination of the static and dynamic components of a bridge crossing event) load effect. A dynamic factor is derived which relates lifetime static load effect to lifetime total load effect and it is shown that required dynamic allowance decreases with increasing lifetime.

The conclusions reached by this work are presented in Chapter 9 along with areas in which further research may be directed.

Chapter 2

REVIEW OF THE LITERATURE

*"In literature as in love, we are astonished at what
is chosen by others"*   *– Andre Maurois*

Chapter 2 - **REVIEW OF THE LITERATURE**

2.1 Introduction

That the work herein attempts to improve and extend the work of other authors is testament to the importance to be placed upon those works. In particular, the work of Grave (2001) is to be noted as a basis for this research.

Initially, existing traffic models for the purposes of bridge load estimation, which are based on measurements, are discussed. Headway modelling in the literature is then reviewed as this has been a large focus of this research. Following this, the statistics used thus far in the analysis of bridge loading is examined. Also covered are the areas of the statistical literature which are relevant to this work.

It is the statistics currently used in the bridge load estimation research that is most relevant to this work. Indeed, the main area of progress in this research has been the adoption of extreme value theory for the estimation of bridge loads.

2.2 Bridge Traffic Load Estimation

2.2.1 Background

Of all the loads that a bridge may be subject to, traffic loading is probably the most difficult to predict. In the general reliability problem, traffic loading remains one of the most difficult variables to predict and incorporate. The assessment of load-carrying capacity is more readily understood and has been well researched (Melchers 1999, Bailey 1996).

Bridge Code Calibration

The development of recent bridge loading standards for the design and assessment of highway bridges has been predominantly based on the use of measured data and statistical extrapolations. Indeed, O'Connor (2001) outlines the development of codes such as the Ontario Highway Bridge Design Code (OHBDC), the Canadian Highway Bridge Design Code (CHBDC), the American Association of State Highway and Transportation Officials (AASHTO) **Standard Specification for American Highway Bridges**, the United Kingdom bridge design code, BD37/88 and the Eurocode for bridge traffic loading, Eurocode 1: Part 3, **Traffic Actions on Bridges**. All of these codes are calibrated for load effects that have been obtained from statistical analyses of the load effects that result from various forms of traffic model.

O'Connor and Shaw (2000) and Ryall et al (2000) provide other outlines of highway bridge loading codes and their development.

Weigh-In-Motion

The advent of Weigh-In-Motion (WIM) technology (Moses 1979) allowed the use of measured unbiased traffic streams for bridge load modelling. Before that,

traffic studies involved estimating the properties of traffic or sampling the population though the use of static weigh stations (Agarwal and Wolkowicz 1976), which are known to give biased results. It had been recognized (Agarwal and Wolkowicz 1976, Dorton and Csagoly 1977, OHBDC 1979) that measurement of the traffic characteristic at a site (or sites) is essential to any solution (O'Connor 2001).

Since the development of WIM, unbiased statistics of traffic characteristics have become available and this has resulted in more accurate traffic models as may be seen from the following section.

2.2.2 Simulation of traffic loading

Crespo-Minguillón and Casas (1997) and O'Connor (2001) note that there are three main types of traffic models for bridge load effect, split as follows:

- **Theoretical statistical models** – stochastic process theory and distributions representing traffic characteristics are used in statistical convolution to determine the distribution of traffic loads that result. O'Connor et al (2002); Fu and Hag-Elsafi (1995); Ghosn and Moses (1985); Ditlevsen (1994); and, Ditlevsen and Madsen (1994) are examples.

- **Static traffic configurations** – measured (or set) traffic data is used to calculate the load effects that result. Variation in the traffic stream is not allowed, therefore the quantity of traffic used is therefore of prime importance. This represents a significant drawback to this approach.

- **Simulation of real traffic flow** – measured traffic is used as the basis of statistical distributions of traffic characteristics. Monte-Carlo simulation is

used to generate synthetic, yet representative traffic which is then used to calculate load effects. In this way, unobserved traffic is allowed for.

Theoretical statistical models are not directly relevant to this work and as such are not considered further (refer to Grave 2001 for further reference). Use of measured or static traffic configurations is only relevant to two aspects of this work; the calculation of load effect from a given traffic stream and the subsequent statistical analysis for lifetime load effect. O'Connor (2001) provides a literature review of those authors dealing with static configurations and their associated extrapolations (Cooper 1995, 1997; Nowak 1991, 1993; for example).

It is the development of traffic models, based on measured traffic, which is directly relevant to this work – Grave (2001) and O'Connor (2001) provide thorough backgrounds on the research in this area. By basing traffic models – defined by statistical distributions for each of the traffic characteristics – on a set of measured traffic, the traffic model can be claimed to represent real traffic. The advantage offered by this approach is that unobserved traffic is allowed to occur randomly in computer simulations, whilst the overall characteristics remain those of the measured traffic. O'Connor (2001), Nowak (1993) and Crespo-Minguillón and Casas (1997) identify problems with the load effects that result when this process is not undertaken.

Bailey (1996)

Bailey (1996) develops a detailed statistical traffic load model for medium- to long-length bridges and allows for different types of traffic flow. The model is based on WIM measurements taken at various sites in Switzerland. The headway model used by Bailey is considered in Section 2.3.2 and Chapter 5.

In Bailey's model, the traffic composition is comprised of 14 different types of vehicle which make up 99% of Swiss truck traffic. The observed frequency of each vehicle type is used in the simulations.

Bailey considers axle groups as having a single weight, as the weight is generally evenly distributed between closely-spaced axles. A generalized bi-modal beta distribution is used to fit the observed axle group weights, shown in Figure 2.1. Correlation of this weight with the GVW is allowed for though generation of the other axle weights based on the axle group weight. Therefore random variation about perfect correlation (as assumed in Vrouwenvelder and Waarts, 1992) is allowed for. The procedure adopted for calculating axle weights is shown in Figure 2.2. The vehicles' geometries are modelled by a beta distribution for each of the axle spacings and overhangs of each type of truck in the classification. The flow rates used in this study are specified, rather than being based on the measured flow rates.
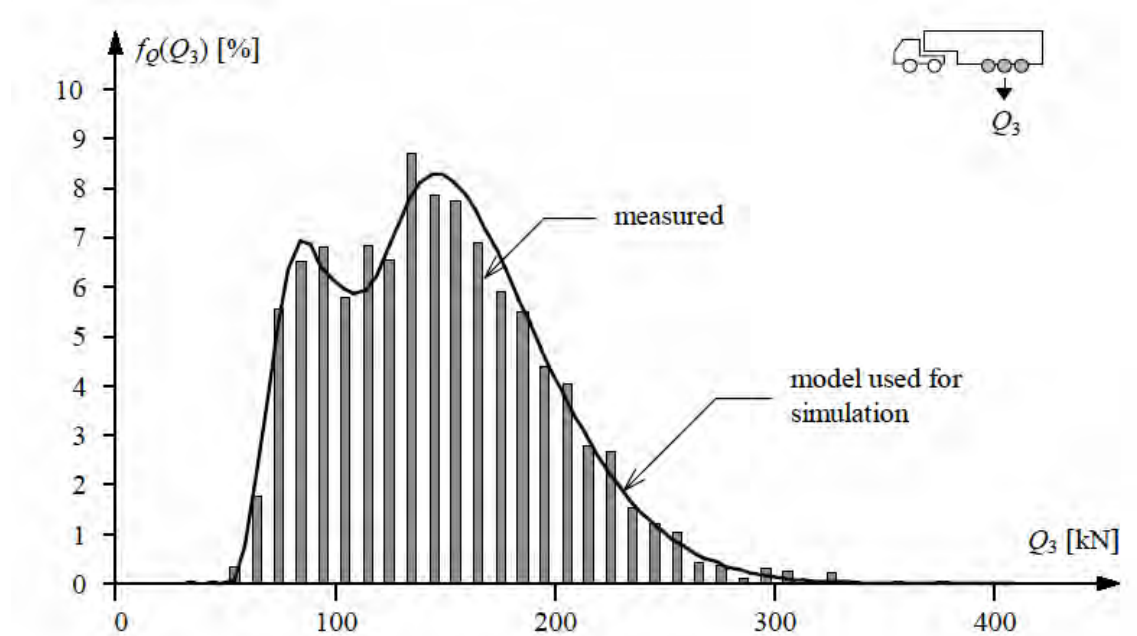
Figure 2.1: Axle-group weight distribution (after Bailey 1996).
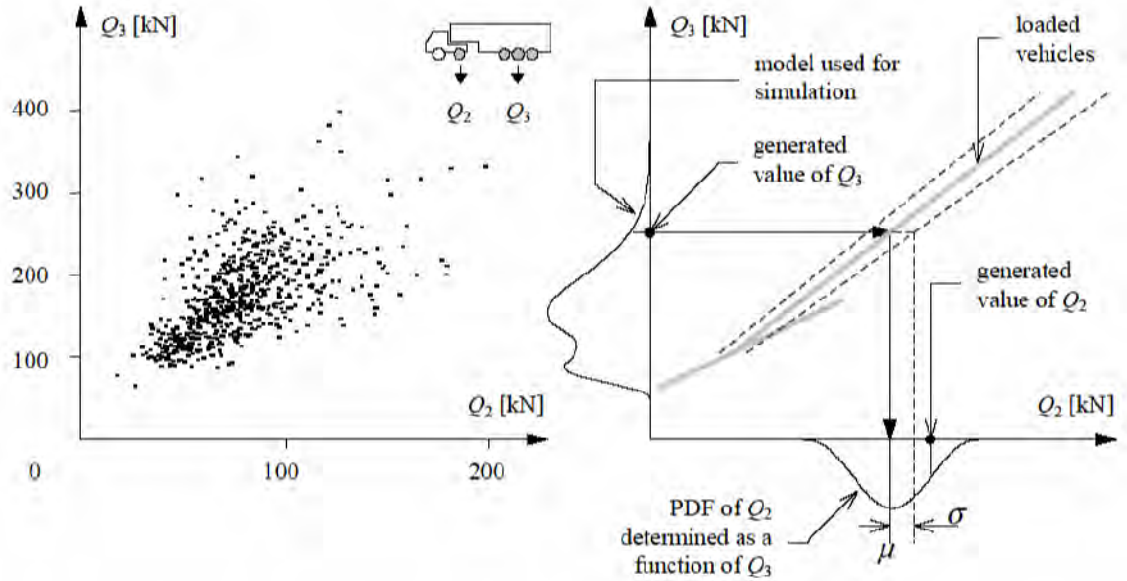
Figure 2.2: Modelling the axle weight relationships (after Bailey 1996).

Crespo-Minguillón and Casas (1997)

These authors present a substantial effort to develop a general and comprehensive traffic model for bridge loading. The generation of traffic and the modelling of each of the traffic characteristics, are explained in the following sequence:

1. The yearly mean daily flow is selected for the site under analysis.

2. Calibration curves for the flow (or traffic intensity) during the day of the week and the hourly variation are then used (shown in Figure 2.3).

3. A binomial decision making process is used to determine whether the traffic state will be jammed or free-flowing – the parameters of this process are not given by the authors, yet stated to be dependent on the hour. In this way then, the increased probability of traffic jams during rush hour is included.

4. Given the state of the traffic and its intensity, the traffic density can then be determined from measured intensity-density curves shown in Figure 2.4.
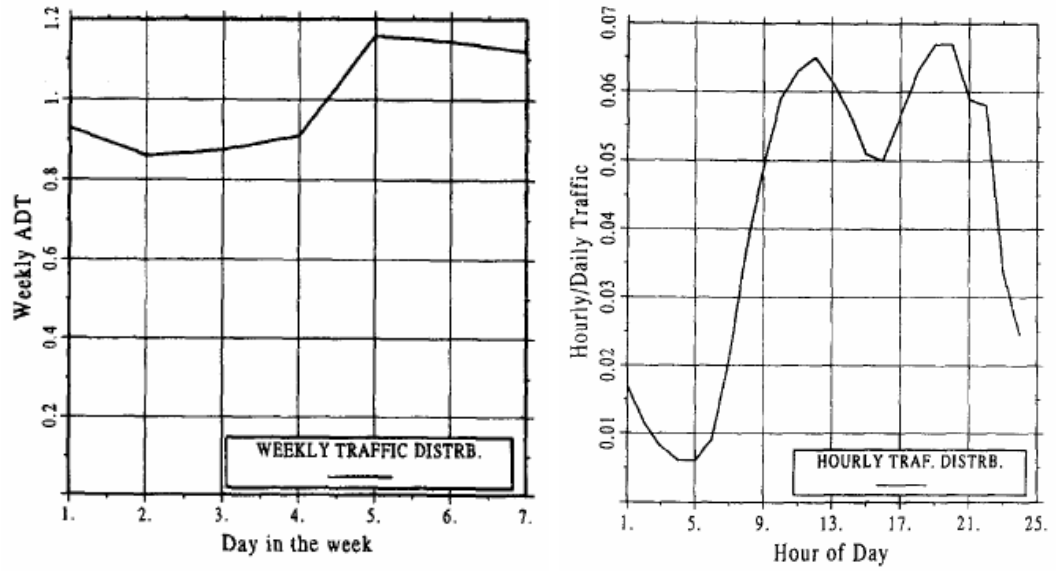
Figure 2.3: Calibration curves for traffic intensity

(after Crespo-Minguillón and Casas 1997).
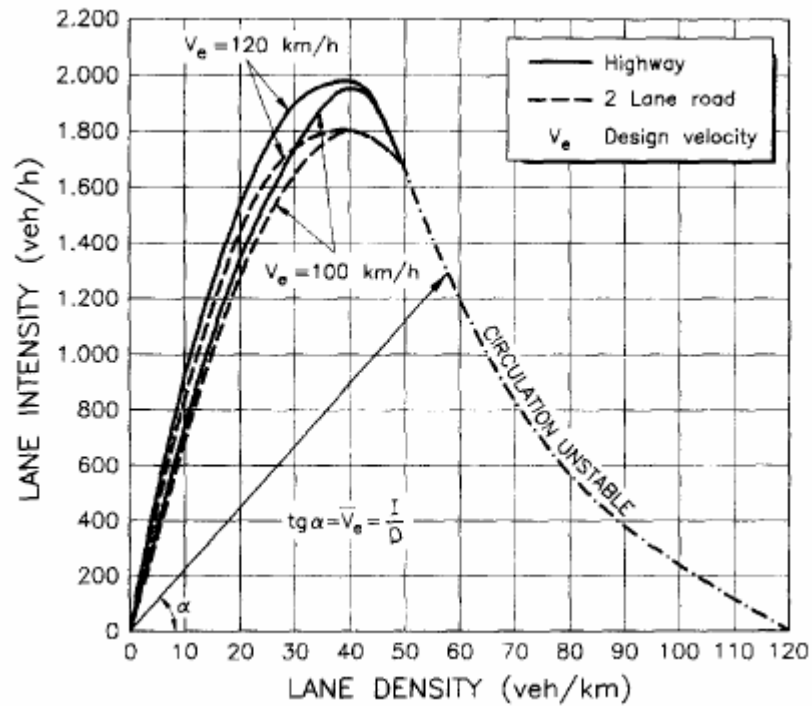
Figure 2.4: Intensity-density curves for traffic condition

(after Crespo-Minguillón and Casas 1997).

5. The traffic compositions are taken from measured WIM data at the site. The vehicle type, for the next vehicle arriving on the bridge, is calculated

using a Markov-chain method, with transition matrices based on those of the measured WIM data.

6. Velocities are then allocated to each vehicle based on a normalized velocity function (similar to that of headway, explained next) which can then be related to the intensity-density graph for the current flow condition.

7. Headway is assigned using the normalized headway model (Section 2.3 and Chapter 5). Different such models are specified for different forms of driver behaviour, heavy and light vehicles and lanes.

8. Weights and geometries are then allocated. Axle weights and GVW are allocated based on measured correlations (Table 2.1) between GVW and axle weights. Geometries are based on measured correlation coefficients for axle spacings. The GVW and axle weight distributions are defined numerically from measured cumulative distribution functions derived from the histograms of Figure 2.5.

In running this model across a bridge, the authors allow for interaction between the vehicles; that is, overtaking events, and changes in speed are modelled. Invariability this added complexity increases the number of design decisions that must be made.

Correlation matrix of weights for vehicles type 8. W_i = axle weight i; W_G = gross weight

	W_1	W_2	W_3	W_G
W_1	1.00	0.40	-0.74	-0.04
W_2	0.40	1.00	-0.89	0.11
W_3	-0.74	-0.89	1.00	-0.02
W_G	-0.04	0.11	-0.02	1.00

Table 2.1: Correlation values between axle weights and GVW

(after Crespo-Minguillón and Casas 1997).
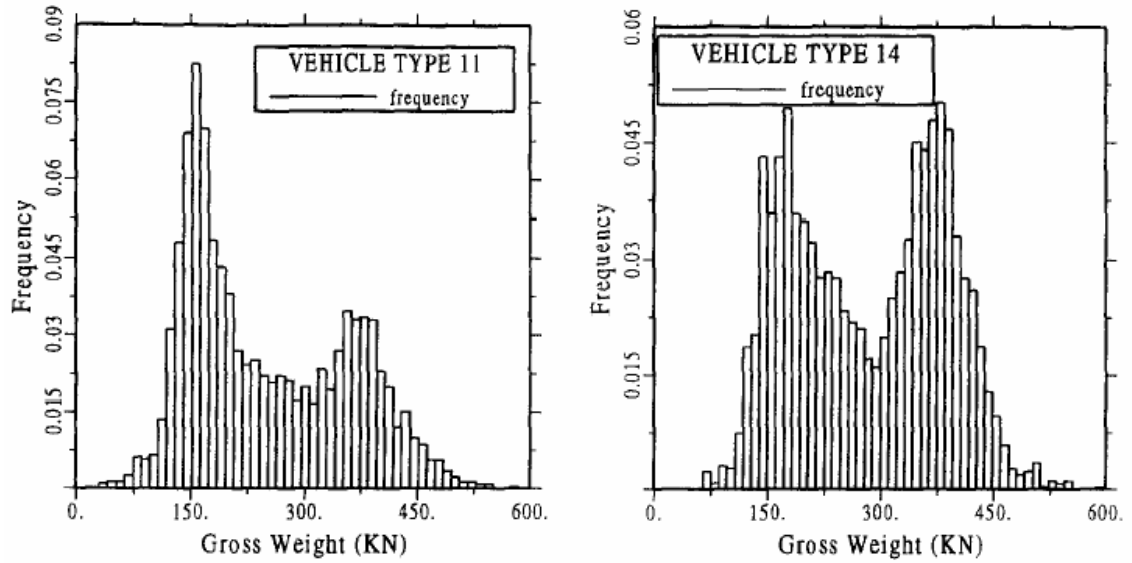
Figure 2.5: GVW histograms for two vehicle types

(after Crespo-Minguillón and Casas 1997).

Grave (2001)

Grave also develops a comprehensive traffic load model for use on short- to medium-length bridges. The traffic model in this research is largely based on the model developed by Grave. This model is therefore described in detail in Chapter 4. Some of the main aspects are discussed here, however.

Most of the traffic characteristics have been modelled statistically by Grave. Only traffic composition percentages and flow rates are deterministic. The headway model used by Grave is the same as that of Crespo-Minguillón and Casas (1997). The number of vehicle types is more limited than that of the other studies mentioned here, though Grave points out that the added complexity is not required for the WIM data under study (Chapter 4).

Other studies

The study by Harman and Davenport (1979), based on a survey of Canadian trucks by Agarwal and Wolkowicz (1976), is one of the first papers to use

Monte Carlo simulation of vehicles and headways to obtain load effects for further statistical analysis. However, the study is quite limited: it does not model real traffic flow; rather, a form of importance sampling of critical loading events on single lanes up to 90 m long is used. The authors use a mixed normal distribution with three modes to fit to the gross-weight ratio – defined as a truck's weight, divided by the legal weight limit – measured from several truck surveys. The geometries of the measured traffic and random GVWs (derived from the gross-weight ratio distribution) are used to generate a truck sample. Axle weights, as a proportion of GVW, are kept constant. Headways are randomly assigned based on a uniform distribution (see 2.3 for more information) and velocities are not required for this model.

Vrouwenvelder and Waarts (1992) describe a study in which a simplified traffic model for the estimation of lane loads (not bridge load effects) is developed. The main statistic of use is the distribution of gross vehicle weight (GVW). Axle weights, as a proportion of GVW, are kept constant. Different types of flow are considered, and deterministic headways are used. The observed frequencies of many different truck configurations are used in the model.

Other bridge loading traffic models are described but without the details being given, such as O'Connor (2001); Bruls et al (1996), and; Flint and Jacob (1996).

Discussion

Bailey (1996) uses the beta distribution for each of the traffic characteristics. This is a good distribution for such use: it is sufficiently flexible, and has upper and lower limits. It is difficult to compare this model to full site-specific models, as there appears to be no mechanism to incorporate hourly flow variation.

The model of Crespo-Minguillón and Casas (1997) is the most complex reviewed here. There may, however, be errors introduced through the use of numerical cumulative distribution functions to represent GVW histograms, for the reasons given in Section 2.4.4. Indeed, a substantial quantity of WIM data would be required to overcome these limitations. The complexity of the operations developed for passing the traffic across the bridge mean that subjective design decisions must be made, and this is a potential source of inaccuracy.

The model described by Grave (2001) is described and criticized in Chapter 4. Vrouwenvelder and Waarts's (1992) model does not claim to represent a full bridge load traffic model whilst that of Harman and Davenport (1979) is also simplistic, yet thorough for its use.

2.3 Headway Models

2.3.1 Introduction

Headway, or the distance from the front of one vehicle to the front of the next, is of great importance to bridge loading events. As is shown in Chapter 5, the types of loading events, and the values of the resulting load effects, are greatly influenced by the headway model adopted. Various methods of modelling the headway have been used by authors writing on Monte Carlo simulation for the analysis of the load effects induced on a bridge by the passage of trucks. Also, headway is of significance to the traffic engineering community. The headway models developed by both sets of researchers are reviewed next.

2.3.2 Headway modelling for bridge traffic loading

Poisson Process-Based Models

Traffic is often seen as a Poisson process and Grave (2001) gives a review of the literature on this subject. As a consequence of the Poisson process, the Exponential Distribution is used to model headway (Grave 2001, Bailey and Bez 1994, Bailey 1996). Often, this distribution is shifted to the right to allow for a minimum headway and is known as the Shifted Exponential Distribution:

$$F(t) = 1 - \exp\left[-\gamma(t - t_0)\right]$$
$$\text{where } \gamma = \frac{\lambda}{(\lambda t_0 - 1)} \tag{2.1}$$

and where t_0 is the minimum headway and λ is the flowrate (in trucks per hour). It may be seen from Figure 2.6 that this formulation gives inordinately high probabilities to values of headway close to the minimum allowed (Bailey 1996). Further, the minimum headway allowed is a subjective element in the

process and this has been the subject of study in this research (see Chapter 5). However, this formulation allows for the effect of flowrate upon the distribution of headways: a higher flowrate requires vehicles to travel closer together. This relationship is known to hold until the capacity of the highway is reached when flow breaks down and congestion results (see Figure 2.4 and Haight, 1963).
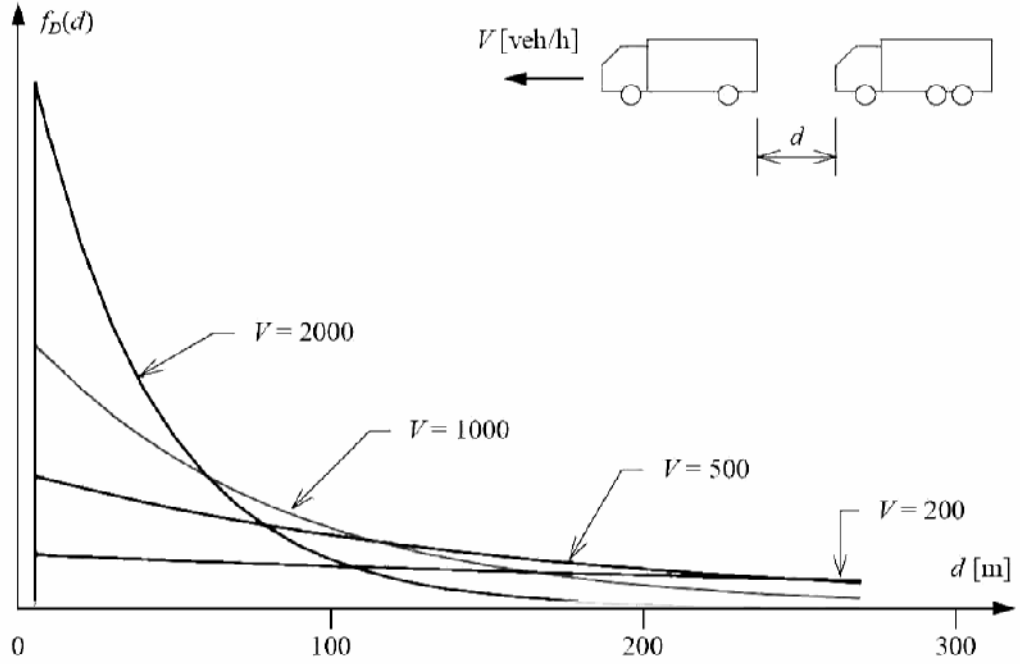
Figure 2.6: Headway (**d** plus lead truck length) PDF model (after Bailey 1996).

Harman and Davenport (1979) recognize that the usual Poisson process assumptions of traffic engineering are not wholly applicable to bridges as only short headways (0 to 97.5 m in their study) are of interest. Based on a study by Goble et al (1976), they assume that the probability density function (PDF) of short headway is a constant equal to the average number of trucks per unit time. Relative to the negative exponential distribution, this is expressed as:

$$F(t) = 1 - e^{-\lambda t} \approx \lambda t \tag{2.2}$$

where the symbols have their previous meaning. Also, Harman and Davenport limit the headway to be greater than 7.32 m, which allows for the front and rear overhangs of the truck bodies beyond the axles.

Gamma Distribution Model

The Gamma distribution function is an extension of the exponential distribution and passes through the origin – ensuring small probabilities for small headways:

$$F(t) = \frac{\Gamma(k, \gamma t)}{\Gamma(k)} \qquad (2.3)$$

where $\Gamma(k, \gamma t)$ is the incomplete Gamma function, and the parameters γ and $\mathbf{k}$ are analogous to the scale and location parameters but have physical interpretations of mean recurrence rate and the $\mathbf{k}$th arrival from a Poisson process. This distribution is used extensively in the background studies for the Eurocode for traffic loads on bridges (Bruls et al 1996, Flint and Jacob 1996, O'Connor et al 2002) and in other studies (O'Connor 2001, Getachew 2003). O'Connor (2001) finds that the parameters are dependent on the volume of flow, similar to the negative exponential distribution. His study also examines the effect of various periods for which the volume is obtained (be it 1, 3, 6 or 24 hours) on the characteristic extreme derived therefrom; concluding that flow periods based upon 1 hour give minimum variation of the extreme on average. The Gamma distribution does not, in its left tail, take account of the driver behaviour or other factors that must feature in very small headways. Further, this distribution passes through the origin; a check must therefore be performed such that the physical limitations of the process are not infringed. Bruls et al (1996), Flint and Jacob (1996) and O'Connor (2001) use the Gamma distribution but assume a minimum gap of 5 m, representing the distance from the back axle of the lead truck to the front axle of the following truck.

Driver Behaviour Models

Some authors have adopted headway models based on considerations of driver behaviour. Buckland et al (1980) proposed a simple method of calculating the headway based upon speed and a minimum distance:

$$h = 1.5 + \frac{v}{16} \cdot L \quad (m) \tag{2.4}$$

where **v** is the velocity (km/hr) and L is the truck length (m). It must be recognized that their study is confined to long-span bridges, but their model is worthy of consideration nonetheless. Such a model only accounts for flow indirectly though the velocity, does not account for driver behaviour, and has no facility for site-specific modelling.

The study by Vrouwenvelder and Waarts (1993) uses different headway models for different traffic conditions. They assume that, in free flowing conditions, the headway randomly lies in the range:

$$L \leq h \leq 30 - L \quad (m) \tag{2.5}$$

where the symbols have their previous meanings. Following a similar approach, for lengths up to 60 m, Nowak considers that gaps (headway minus the length of the lead vehicle) may be 4.5 or 9 m (Nowak at al 1991); may be 5 m conservatively, that is, bumper-to-bumper traffic (Nowak 1994); or, can vary between 5 and 30 m (Nowak 1993). These models may be reasonably realistic in terms of their acknowledgment of driver behaviour, but allow no facility for site-specific modelling and are subjective. Furthermore, there is no facility for modelling long headways which have an effect on the occurrence of trucks in another lane.

Normalized Headway Model

It is important to recognize that different headway distributions result from different truck flows – Figure 2.7(a) – and this has been noted in the literature (Bailey 1996, Crespo-Minguillón and Casas 1997, Grave 2001). Rather than fitting individual distributions for each flow, Crespo-Minguillón and Casas note that a single distribution resulted from consideration of a 'normalized headway', defined as the vehicles' headway divided by the average headway for a given flowrate – Figure 2.7(b). This distribution may be subsequently altered for the particular flow of the period of interest and where γ is the mean normalized headway and $\mathbf{Q}$ is the flow (trucks/hour), is:

$$F(t) = \frac{Q}{3600}\left[1 - e^{-\gamma t}\right] \tag{2.6}$$

(a)   (b)
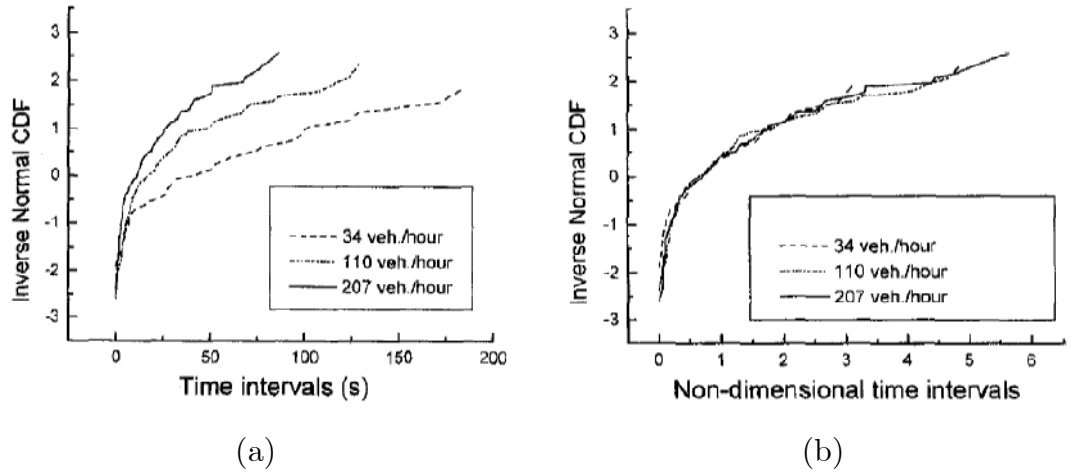
Figure 2.7: (a) Different headway distributions and, (b) Normalized headway variable, for different flows (after Crespo-Minguillón and Casas 1997).

For the sites mainly used in this study, Grave (2001) shows that, for the same flowrate, the distribution of headways is very similar. Further, Grave shows the effect of flowrate upon the headway distribution for the same sites and that in using the normalized headway distribution it is necessary to perform checks on the resulting trucks so that they do not overlap or come within 5 m.

2.3.3 Headways in traffic engineering

The traffic engineering community has been studying the headway of vehicles for many years (Haight 1963, Banks 2003). The general models are as described above, along with other more complex models which allow mixing of constrained and free flowing traffic (Grave 2001, Anon. 2003). Thamizh-Arasan and Koshy (2003), acknowledge that different flows and different traffic types follow different headway patterns. Also, at low flow rates, interaction between vehicles takes place at longer headways than at higher flow rates (Gazis 1974). Banks (2003) notes that drivers' different expectations of the traffic they are to face results in different headway distributions: in morning peak traffic there was no evident relationship between headway and speed, for speeds under 100 km/hr.

Many authors (Lieberman and Rathi 1992, Jensen 2003, Gazis 1974, HRB 1965) discuss the motivational aspect to the headway distribution: the ratio of drivers' actual- to desired-speed, and their aggression level, will affect how closely they are willing to drive to the vehicle in front. These factors affect the likelihood of overtaking, which in turn is controlled by the vehicle's positioning relative to vehicles in target lanes, further affecting the headway distribution. Drivers are also willing to operate at the mechanical limit of their vehicles, resulting in modified headways which allow for potential rapid deceleration of the driver's vehicle and the vehicle in front. Specifically of interest to this work, truck drivers exhibit different characteristics than other drivers: good route planning, commercial pressures, specialised training, high route familiarity and fatigue are factors affecting truck drivers. Also, the mechanical performances of trucks are known to be different – they are less able than other vehicles on the highway to respond quickly. All of these factors affect the headway distribution of trucks.

2.4 Determination of Extreme Load Effect

2.4.1 Introduction

The previous sections have examined the traffic models that are used in the literature to estimate bridge traffic load effect. The use of such models to determine lifetime load effect for a bridge, invariably involves some form of statistical analysis. It may be seen from Chapter 1 that the main objective of this work is the improvement of such statistical analyses. In this section, the statistical methods used in the literature are examined. Attention is given to areas of weakness in current practice that are addressed by this research.

The methods of statistical extrapolation used in the literature are quite varied. A general observation is that European authors, in recent years, are agreed on the adoption of some form of extreme value analysis. Conversely, American publications on the topic (Moses 2001, Ghosn et al 2003) are greatly influenced by the work of Nowak who generally uses a form of normal probability paper extrapolation. There are of course exceptions to these observations in both continents.

The following critique of the literature is broken into two sections: those dealing with extreme-value methods, and those using other methods. Such a layout reflects the importance of the extreme-value approach (Chapter 3) in this work.

2.4.2 General statistical methods

Harman and Davenport (1979)

Harman and Davenport consider single to five-truck events separately and then combine the results. The histograms for load effects caused by the five different types of loading event are shown in Figure 2.8 and may be seen to be

considerably different. Also shown for each type of loading event, are the histograms from the measured traffic configuration and from simulated traffic.
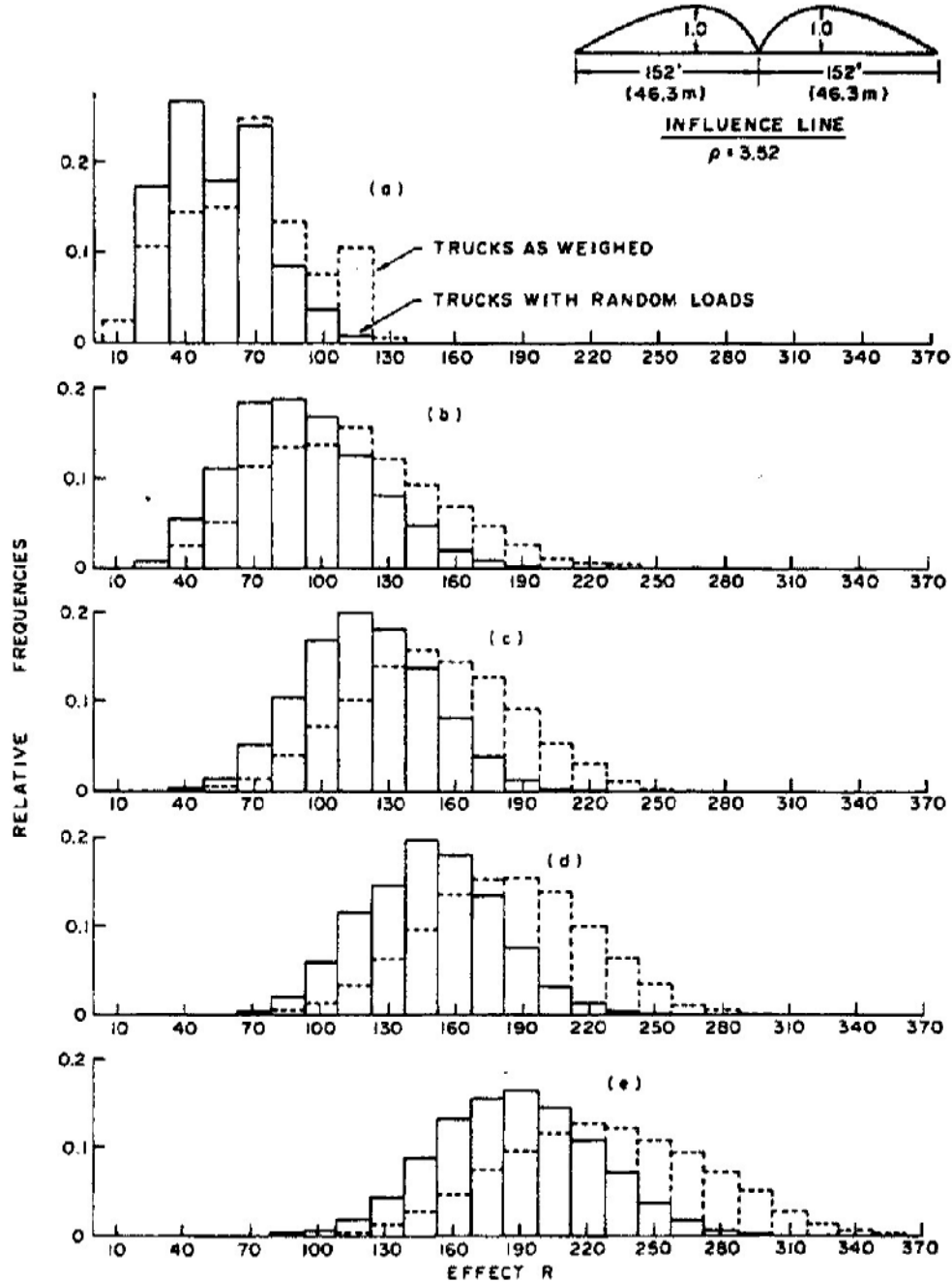
Figure 2.8: Histograms of load effect for different loading events, (a) – (e) represent 1- to 5-truck events (after Harman and Davenport 1979).

In Section 2.5.1, the method used by Harman and Davenport is explained in more detail, in the context of the statistical background to this work. Briefly

however, the statistical analysis used is as follows. Harman and Davenport note that each mechanism may be represented by a negative exponential function and fit straight lines on log-scale paper to data points from the upper tail of the parent histogram – the plotting position method is not described nor is the arbitrary cut off level for the upper tail (see Figure 2.9). These functions are compared with Gaussian (normal distribution) functions fitted to the whole distribution but especially weighted to best fit the mean.
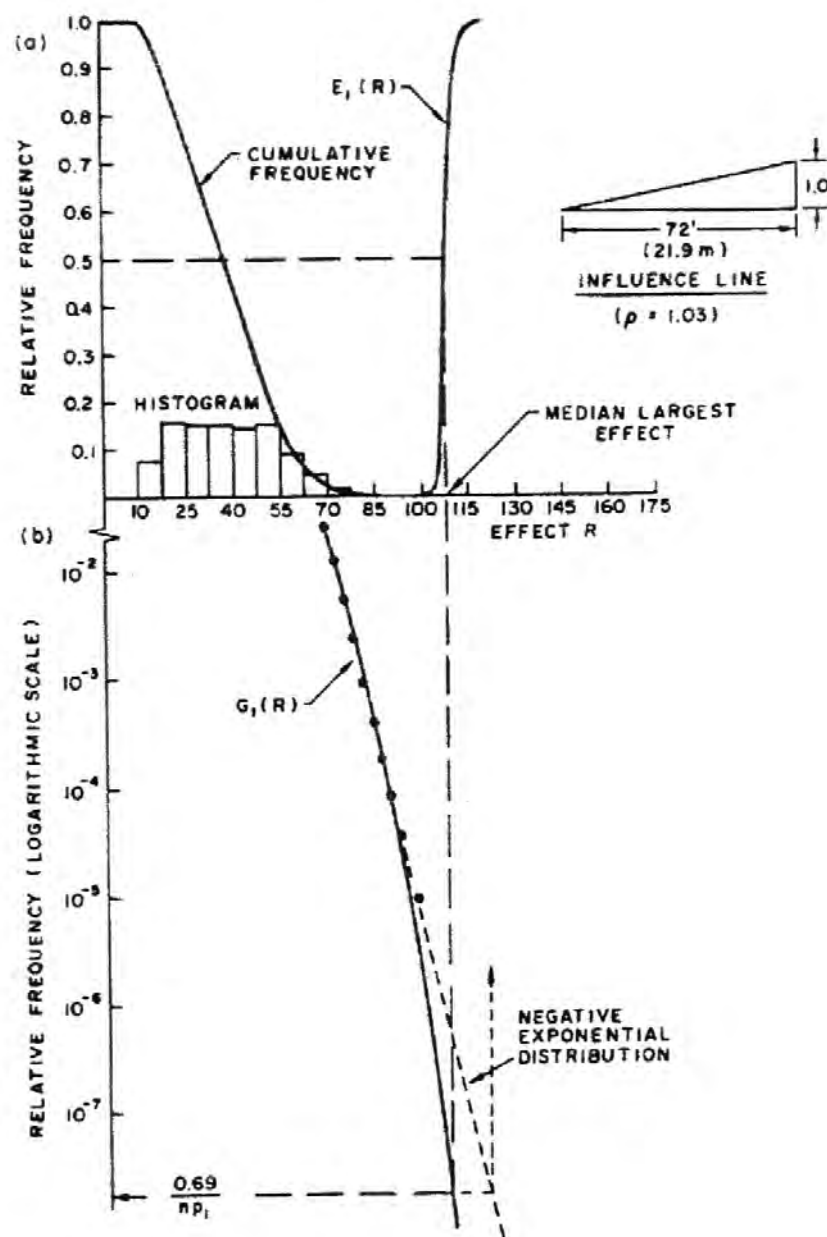
Figure 2.9: Extrapolation method (after Harman and Davenport 1979).

Nowak

Nowak has published widely on the subject of bridge load modelling. The truck survey carried out by Agarwal and Wolkowicz (1976) for the bridge load model of the Ontario Highway Bridge Design Code (OHBDC 1979) is used as the basis of most of the papers surveyed here: Nowak (1989), Heywood and Nowak (1989), Nowak et al (1991), Nowak and Hong (1991), and Nowak (1993). A contemporary truck survey is compared to the OHBDC survey in Nowak (1994). The OHBDC survey consists of 9250 trucks, especially selected as they appeared to be heavily loaded. This is assumed to correspond with a two-week period of traffic for a busy highway (see Nowak 1993 for example). Therefore, for a design lifetime of 75 years (used in most of the cited papers), the number of two-week periods is reported as 1500 (Nowak and Hong 1991) and 2000 (Nowak 1993). Based on these figures, the corresponding probabilities are reported as an inverse standard normal deviate as $z = 5.26$ (Nowak and Hong 1991) and $z = 5.33$ (Nowak 1993). The reason for the difference is due to the differing estimates of the number of weeks in the 75 year bridge lifetime.

Single- and two-lane shear force and bending moments are calculated for the trucks in the survey noted, taken individually. However, in the single-lane case, this is only done for spans up to 30 m as it is assumed that multiple trucks begin to feature thereafter (Heywood and Nowak 1989, Nowak and Hong 1991), though in later studies, the effect of headway is studied (Nowak 1993).

Based on the truck survey data, the results for the load effects are plotted on normal probability paper (see Chapter 3) for different spans. In the papers Nowak (1989), Heywood and Nowak (1989), Nowak (1991), and Nowak and Hong (1991) it appears that straight lines, superimposed on the tails of the distributions plotted, are used to extrapolate the load effects. This is specifically

stated as the case in Heywood and Nowak (1989). However, in the same paper it is recognized that towards the tail of the distributions, curvature is evident. The authors suggest that an exponential distribution may provide a reasonable fit in this case. In the remaining papers, Nowak (1993) and Nowak (1994), it appears that curved lines on normal probability paper are used to extrapolate for the load effects of various return periods. This can be seen in Figure 2.10, for example.
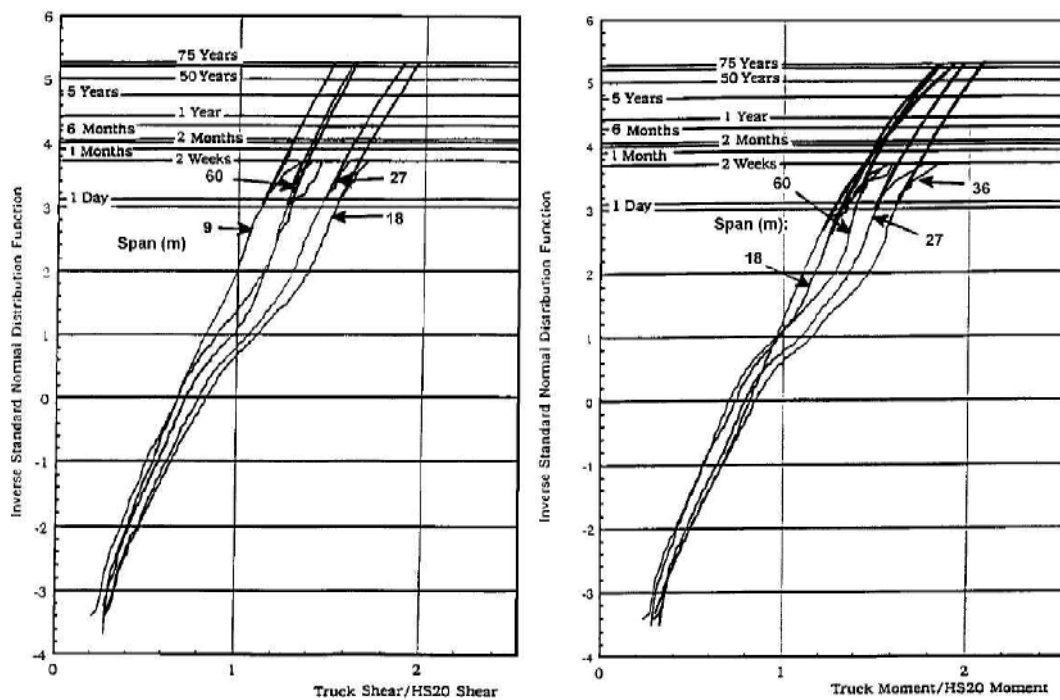
Figure 2.10: Load effect extrapolation for a range of spans (after Nowak 1993).

Nowak (1993) states that the cumulative distribution functions of load effect are raised to a power to obtain the mean and coefficient of variation of the maximum load effect – as shown in Figure 2.11. It is possible that it is this method that is used to extrapolate on the normal probability paper, though it is not explicitly stated. In a reply to a discussion about the extrapolation methods used in Nowak (1994), Nowak (1995) states that extrapolations based on the normal distribution are not used; rather, the power transform is used.
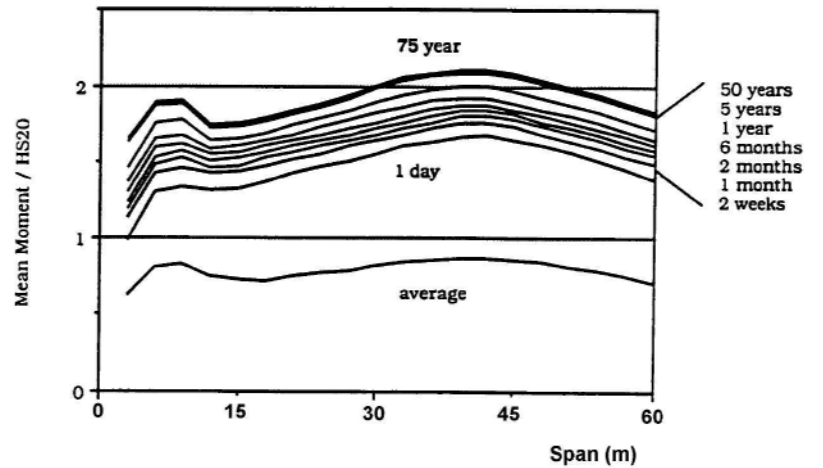
(a) Mean maximum moment;
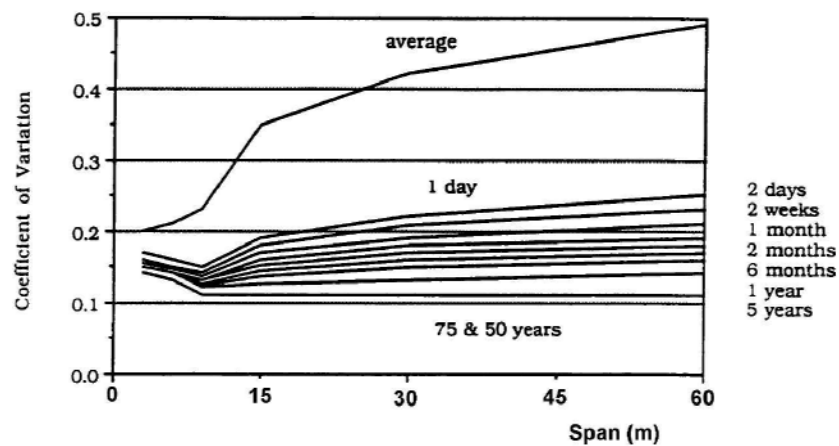
(b) Coefficient of variation;

Figure 2.11: Estimation of lifetime mid-span maximum moment

(after Nowak 1993).

Eurocode Background Studies

The background studies carried out for Eurocode 1: Part 3, **Traffic loads on bridges** (EC 1: Part 3: 1994) generated significant interest in bridge traffic load modelling in Europe. The important papers are described here.

Based on measured traffic samples, Bruls et al (1996) consider and compare several methods of extrapolation of the basic histogram of load effect:

- a half-normal curve fitted to the end of the histogram;

- a Gumbel distribution fit to the tail of the histogram;

- Monte-Carlo simulation of artificial traffic and Gumbel extrapolation.

Flint and Jacob (1996) consider various methods also, some of which are applied to the loading on the bridge, rather than the load effects resulting. The methods considered are:

- a half-normal curve fitted to the end of the histogram;

- Rice's formula for a stationary Gaussian process;

- Monte-Carlo simulation of artificial traffic and Gumbel extrapolation.

This last method, in the lists for both papers, amounts to an extreme value approach and will be considered further in Section 2.4.3. The half-normal and Gumbel distribution fits to the histograms suffer from some drawbacks as discussed in Section 2.4.4.

Rice's formula has been used extensively in the literature (Flint and Jacob 1996, O'Connor 2001, Cremona 2001, Getachew 2003). One of the problems involves the choice of a threshold (see Figure 2.12), above which data will be recorded. Given the histogram of the recorded data (see Figure 2.13), Cremona (2001) develops an optimal level (x_0) at which to set the threshold, based on minimization of the Kolmogorov-Smirnov statistic (see Figure 2.14). Getachew (2003) and Cremona (2001) describe the method in full. For the current purposes, it suffices to recognize that the fits depend on the threshold, the optimal level calculated, and the number and width of the histogram intervals.
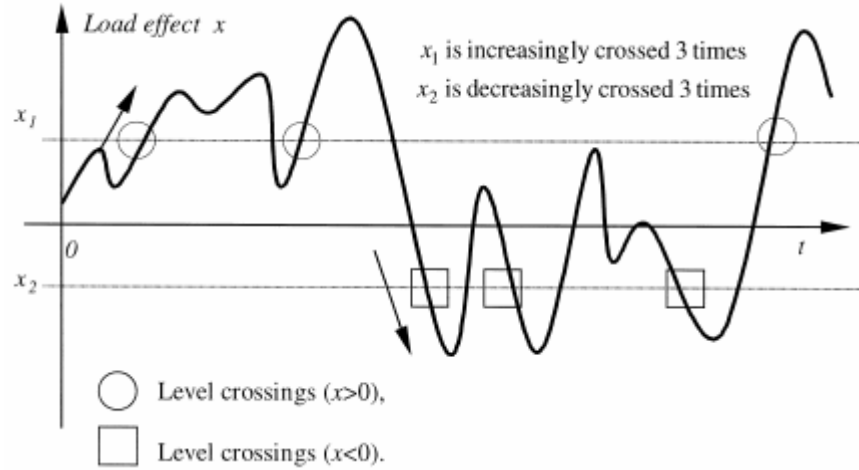
Figure 2.12: Basis for Rice's formula (after Cremona 2001).
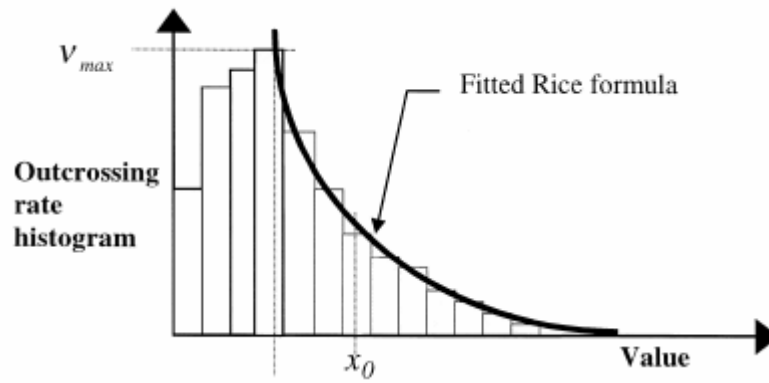
Figure 2.13: Histogram of out-crossings (after Cremona 2001).
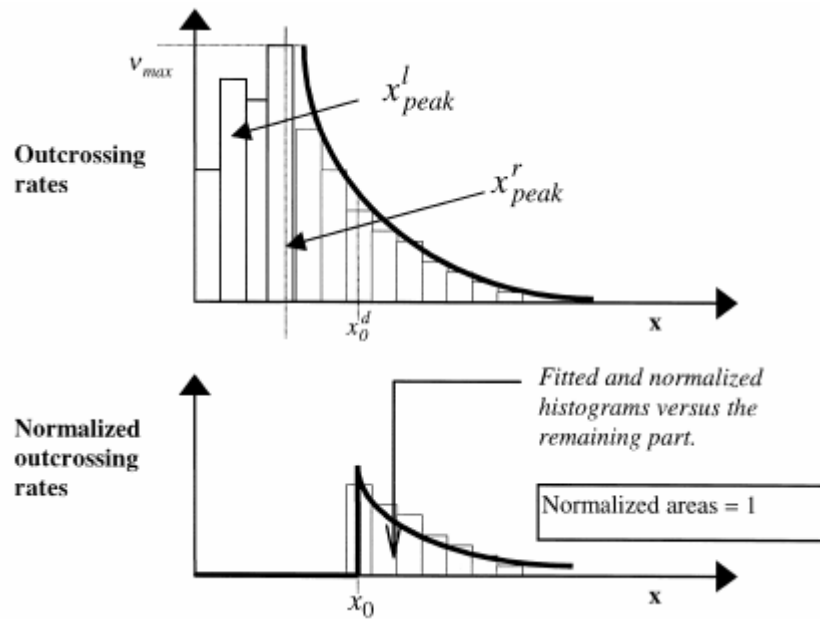
Figure 2.14: Basis of optimal fitting (after Cremona 2001).

Other Studies

Vrouwenvelder and Waarts (1993) do not attempt to estimate the load effects that result from their derived simplified lane load model. The extrapolations carried out are for truck weights and presences. Considering the truck weights alone, the authors use a truncated (at the lower tail) Weibull distribution on the upper mode of the gross vehicle weight (GVW) histogram. It is this fit that is used to extrapolate for the truck weight at the return period.

Even when sampling variability is removed, as in the case of the convolution methods noted earlier (Section 2.2.2), authors do not agree on the extrapolation method. Two such studies are described next.

Fu and Hag-Elsafi (1995) describe a probabilistic convolution method to obtain bending moments for single truck events. These authors obtain the distribution of moment for 2 years of traffic with an annual average daily truck-flow of 2000 vehicles. This is done by raising the original distribution to the power of $2 \times 365 \times 2000 = 1.46 \times 10^6$.

Ghosn and Moses (1985) describe a Markov-Renewel process to convolute for the bridge load effect distribution. The authors adopt a 0.1 (2.4 hour) daily maximum as their extreme data which is then fitted using a normal distribution on normal probability paper. The distribution thus estimated is raised to the power of $10 \times 365 \times 50$ to obtain the distribution of 50-year load effect.

Raising distributions to a power to obtain an 'exact' distribution of maxima is normally a cause for concern (Section 2.4.4), but as the authors use a convolution method, it may be presumed that the tail of the parent distribution has been calculated carefully. Therefore there should be little inaccuracy introduced in the distribution of maximum load effects.

2.4.3 Extreme value theory based methods

Introduction

After the simulation and modelling of loading events, a statistical analysis is required to estimate the lifetime load effect. Extreme value theory provides a theoretical and practical framework to carry out this analysis and prediction.

The extreme value theory utilized in extrapolating data to the return period required is well established. However it was not until recently that these theories were applied to the modelling of traffic loading on bridges. Many authors approach the problem by identifying the maximum load effect recorded during a loading event or in a reference period such as a day or a week, and then fit these maxima to an extreme value distribution. In all cases, the fitted distributions are used to extrapolate to obtain an estimate of the lifetime maximum load effect. This approach is based on the assumption that individual loading events are independent and identically distributed.

Irish-Based Literature

To determine the characteristic deflection of the Foyle Bridge, OBrien et al (1995) used 8 minute periods of measurements taken for each 4-hour rush hour period of a day. Each day of measurement is then represented by a 48 minute sample. The authors then consider the daily maximum deflection as an extreme value population. The Gumbel distribution is used to fit the data graphically on Gumbel probability paper. The extrapolation for the 1000-year return period is based on this distribution (shown in Figure 2.15). Interestingly, the authors establish the variance of the predicted load effect through the use of an empirical formula (Goda 1992).
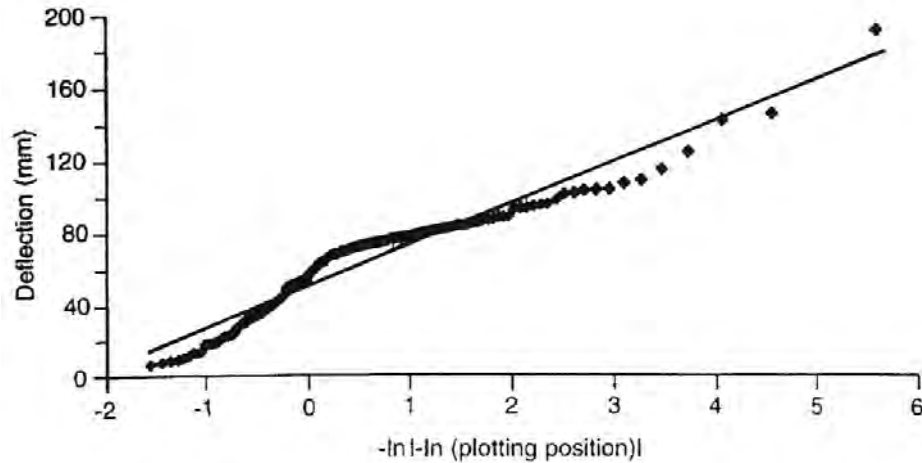
Figure 2.15: Gumbel extrapolation for the Foyle Bridge

(after OBrien et al 1995).

Grave et al (2000) describe the population of extreme values as the load effects caused by the 'critical' loading events, though critical is not qualified. A weighted least-squares approach is used to fit Weibull distributions to these critical load effects. This process is repeated to give an estimate of the distribution of characteristics values, though this distribution is not given. It is possible that the critical events are determined in a manner similar to that of Grave (2001). In this work, the 100 worst load effects noted during a 5-day simulation period are assumed to form an extreme value population. The data is plotted on Gumbel probability paper and straight lines are fitted. Such distributions form the basis for the extrapolation. The author uses the upper $2\sqrt{n}$ data points as recommended by Castillo (1988) for data that may not be convergent to an extreme value population.

In the simulations carried out as part of his work, O'Connor (2001) fits Gumbel and Weibull distributions to a population of 'extreme' load effects. The author does not specify the manner in which the 'extremes' are determined. Maximum likelihood fitting is carried out on a censored population. O'Connor (2001)

censors for the upper $\sqrt{n}$, $2\sqrt{n}$ and $3\sqrt{n}$ data points (Castillo 1988), and notes that different estimates of lifetime load effect result from different censoring.

In OBrien et al (2003), hourly maximum strain values are plotted on Gumbel probability paper. A least-squares, straight-line, fit is made to the upper $2\sqrt{n}$ data points similar to O'Connor (2001) and Grave (2001). Also, González et al (2003) use the Gumbel and Weibull distributions to extrapolate bridge load effect. The population upon which the distributions are fit is not described.

Getachew and OBrien (2005) fit the Generalized Extreme Value (GEV) distribution (Chapter 3) to the distribution of load effects from a number of simulated 2-truck meeting events representing two weeks of traffic. The fitting method is not identified, but is compared with histograms of load effect.

Bailey

Bailey has published widely on the estimation of traffic load on bridges. Most of the publications are based on his doctoral dissertation (Bailey 1996). The general approach is to use traffic models to derive load effects which are then statistically analysed. Bailey (1996) describes the use of plots of the mean and standard deviation of the load effects, as they change with the number of loading events, to estimate the appropriate extreme value distribution. Based on Bailey (1996), Bailey and Bez (1994 and 1999) describe a qualitative analysis of 500 simulated upper tails of mean maximum load effects plotted against the number of events contributing (see Figure 2.16). They determine that the Weibull distribution is most appropriate to model these tails and used maximum likelihood estimation. They report that the Fréchet distribution has been used by other authors and that, in comparison to the Weibull distribution, this approach leads to an overestimation of the load effects.
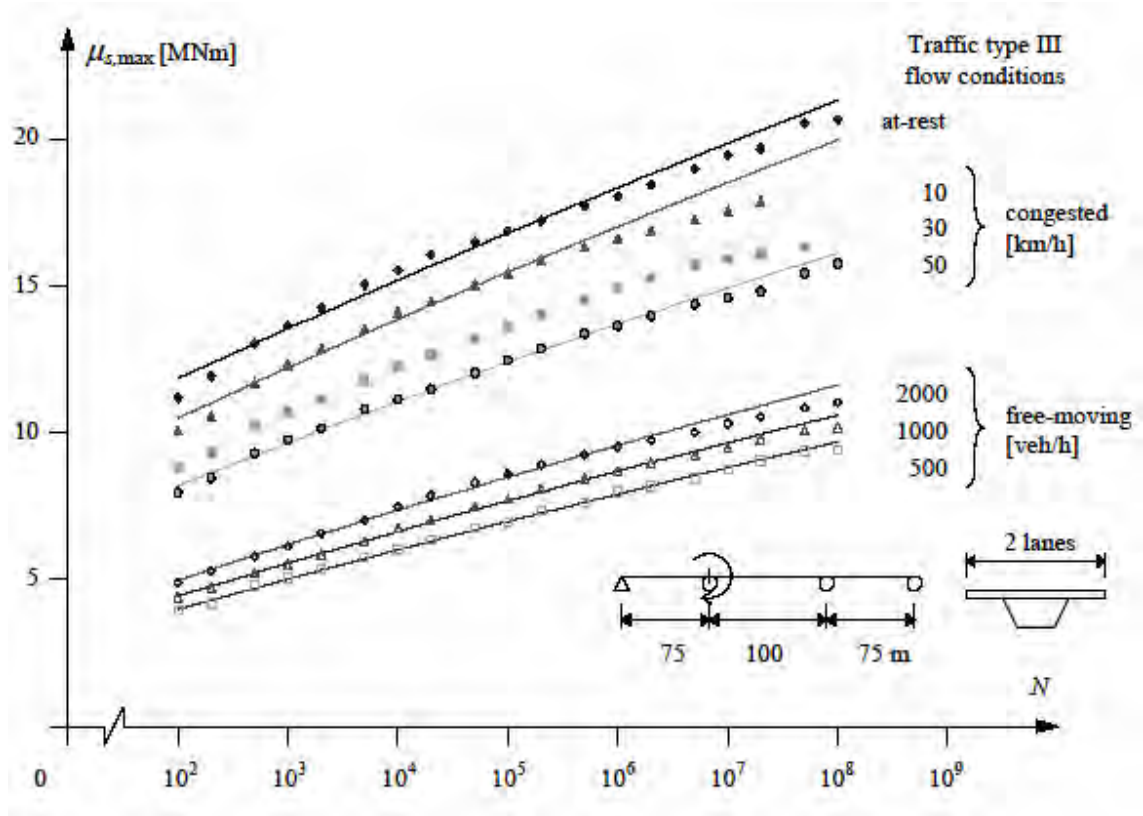
Figure 2.16: Mean maximum moment from N load events (after Bailey 1996).

Distributions are determined from the tail of the load effect histograms (though the tail region is not specified) by using fits based on a nonlinear least-squares technique – the Levenberg-Marqhuart method, described in Press et al (1993). Minimization of the chi-square statistic is used as the basis of the fit. The distributions thus determined are then raised to a power, as appropriate, to determine the distribution of maximum load effect (Bailey 1996, Bailey and Bez 1994, Bailey and Bez 1999) for a given number of loading events. Bailey and Bez (1994) also describe a weighted sum technique to allow for different traffic conditions.

Bailey and Bez (1999) and Bailey (1996) provide a parametric study of the parameters of the load effect distributions for many simulations. The results are used to express the parameters in terms of the traffic characteristics at the site.

Cooper

Cooper has published widely on the bridge loading problem as it relates to the United Kingdom. In Cooper (1995), a traffic model of about 81 000 measured truck events, which represents one year of traffic, is used to determine the distribution of load effects due to a 'single event'. The author raises this distribution to powers to determine the distribution of load effect for 1, 4, 16, 256 and 1024 such events – where 1024 events is stated to roughly correspond with 4.5 days of traffic. A Gumbel distribution is then fitted to this 1024-event distribution and used to extrapolate to a 2400 year return period.

Figure 2.17 shows this process, and the distribution of events obtained by raising the initial distribution to various powers is presented. It may be seen that two sharp peaks are progressively amplified as the power is increased (resulting in two sharp peaks in the distribution of 1024-event load effect). This is caused by sparse data in the tail of the initial distribution, amplified by the large power applied. This is an important limitation of the power method, and is returned to in Section 2.4.4.

In Cooper (1997), histograms of two-week traffic load effects are obtained from measured WIM data. The histograms are converted into cumulative distribution functions (CDFs), which are then raised to a power equal to the number of daily trucks, to give the distribution of daily maxima (Figure 2.18). The points of the CDF are then plotted on Gumbel paper and a straight line is fitted (Figure 2.19).
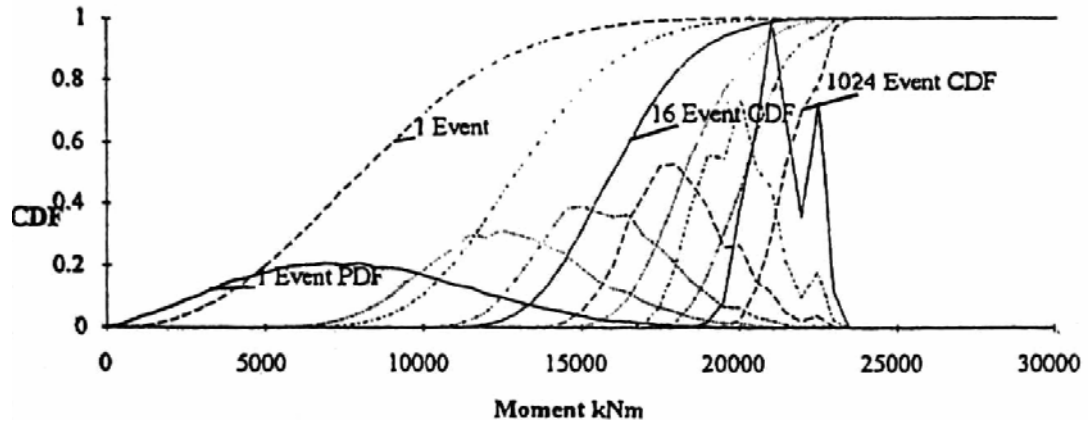
Figure 2.17: Densities and CDFs of extreme effects (after Cooper 1995).
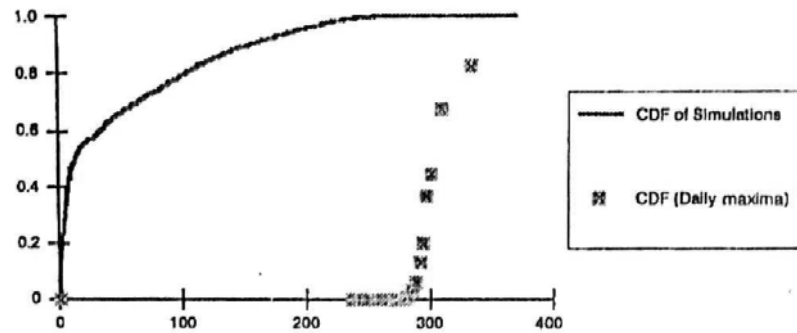
Figure 2.18: Individual event CDF and daily maxima CDF (after Cooper 1997).
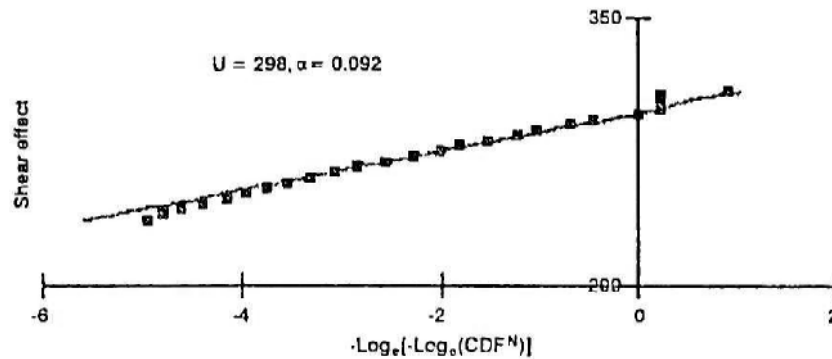
Figure 2.19: Daily maxima CDF fitted to Gumbel distribution

(after Cooper 1997).

Other Work

Crespo-Minguillón and Casas (1997) acknowledge the uncertainties involved in the extrapolation techniques of their contemporary literature. The authors plot the CDF of monthly maximum load effect on Gumbel probability paper and

note that it is not linear (Figure 2.20) – the plotting position method used is not stated and is not that of Chapter 3. The authors then adopt a peaks-over-threshold (POT) approach and use the Generalized Pareto Distribution (GPD) to model the exceedances of weekly maximum traffic effects over a certain threshold. The fitting method adopted is a least squares approach, minimized on the empirical distribution estimate. An optimal threshold is selected based on the overall minimum least-squares value and it is the distribution that corresponds to this threshold that is used as the basis for extrapolation.
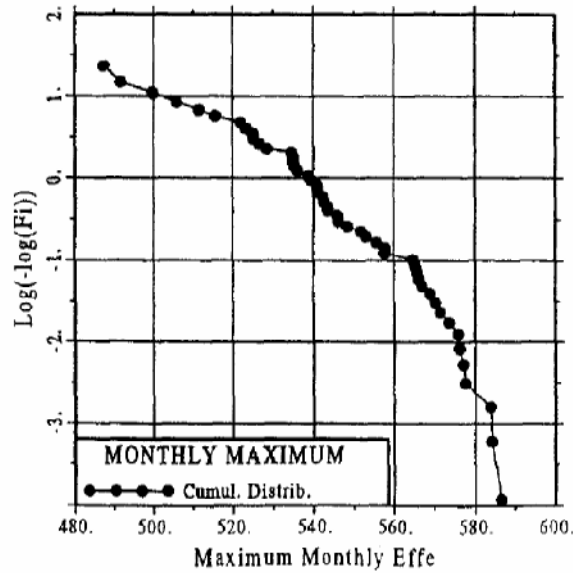
Figure 2.20: Monthly maxima plotted on Gumbel paper

(after Crespo-Minguillón and Casas 1997).

In Moyo et al (2002) the authors record strain measurements on a bridge. The daily maximum strain values are plotted on Gumbel probability paper and a least-squares fit is used to determine the parameters of the daily maxima Gumbel distribution. The authors also employ a method for deriving improved plotting positions taken from wind loading literature (Cook 1982).

Buckland et al (1980) use a Gumbel distribution to fit the 3-monthly maximum load effects and this is then used to extrapolate to any return period.

Getachew (2003) uses methods similar to those of O'Connor (2001). Gumbel and Weibull distributions are used to fit the "extreme" data (extreme is not qualified), and the results compared. The method given by Cremona (2001) is also used by Getachew (2003).

2.4.4 Discussion

It is clear that there are varying degrees of subjectivity in the literature. It does not induce confidence in the estimated lifetime load effect, when it is known that different decisions yield different results. It is one of the main objectives of this research to eliminate such subjective decisions in the statistical analysis of load effect data. It must also be recognized however, that subjectivity sometimes forms an essential part of any engineering solution to a problem, and Bardsley (1994) argues for this in the case of statistical extrapolation.

Choice of Population

It is important to choose a population that is in keeping with the limitations of the statistical model to be applied. In the works reviewed, Crespo-Minguillón and Casas (1997), Moyo et al (2002) and OBrien et al (1995) adhere to the recommendations of Gumbel (1958) for example. In these works, the form of the parent distribution is not established, and an extreme value distribution is fitted to the (presumed) population of maxima. Other authors surveyed describe an undefined 'extreme' population (O'Connor 2001, González et al 2003, Grave 2001, Grave et al 2000, and Getachew 2003) which may or may not meet the requirements of the theory. OBrien et al (2003) use the hourly maximum, whilst Ghosn and Moses (1985) use 2.4 hourly maxima, to form the extreme population. In the light of the hourly variation of traffic this does not meet the requirements of the extreme value theory; the initial population cannot be considered as identically distributed.

Other authors surveyed do not adopt the asymptotic extreme value theory and estimate the initial, or parent, distribution. They then estimate the theoretical exact distribution of maxima (Chapter 3) by raising the parent distribution to an appropriate power. Such authors include: Bailey (1996); Bailey and Bez (1994 and 1999); Cooper (1995 and 1997), and; Getachew and OBrien (2005).

The data upon which Nowak's and Harman and Davenport's result are based, represents a biased survey of trucks from 1976 and both sets of authors correctly identify this as a source of significant uncertainty (see, for example, Nowak 1993).

Distribution of Extreme Load Effects

Those authors that chose a sample of extreme values are faced with the problem of choosing a form of extreme value distribution. It is generally not acknowledged that, through use of the GEV distribution, such a decision is not required. Though Getachew and OBrien (2005) do use the GEV distribution, they use it to model the parent distribution of load effect, and not as an asymptotic approximation to the distribution extreme values. Therefore, the authors surveyed have introduced possible error by the adoption of different forms of extreme value distribution. It is recognized however (Bailey 1996, O'Connor 2001, for example), that traffic load effects normally exhibit Weibull-type behaviour and the authors that use this model are probably more accurate. This is not the general case however.

Other authors surveyed attempted to calculate the exact distribution of extreme load effect, based on a fit to the parent distribution (Bailey 1996; Bailey and Bez 1994 and 1999; Cooper 1995 and 1997; Getachew and OBrien 2005; Ghosn and Moses 1985; Nowak and Hong 1991; Nowak 1993). This is done by raising the initial distribution to an appropriate power. It is to be noted that Getachew

and OBrien (2005) do not do this but estimate the characteristic value directly from the parent distribution. The procedure followed by these authors is problematic in the light of the arguments of Coles (2001b) and Castillo (1988) which state that fitting parent distributions and raising them to a power to obtain an 'exact' distribution of maxima is inaccurate in most situations. This is so because the extreme tail may be of different form to the overall parent and consequent tail-fitting errors are raised to the same power. Therefore the resulting distribution may be significantly erroneous. Such problems can be seen in the work by Cooper (1995), reproduced in Figure 2.17. In this figure, it can be seen that a slight undulation in the 1-event distribution tail (more clearly observable in the tail of the 16-event PDF) becomes two sharp peaks in the distribution of the 1024-event load effect. Sparsity of data in the tail of the initial distribution (by definition) is the cause of this. Indeed, Cooper avoided compounding this error by raising the original distributions to a power, rather than using fitted distributions.

Nowak and Hong (1991) and Nowak (1993) also raise the distributions to the power of the number of repetitions of the survey: 1500 and 2000 respectively even though both studies are based on the same data and are estimating load effects for the same return period (75 years).

Estimation

The methods used in the examined literature to estimate, or fit, the parameters of the chosen distribution(s) to the data, are considerably varied. This is surprising as the statistical literature recognizes that the method of maximum likelihood gives minimum-variance estimates in general (Chapter 3). Only O'Connor (2001) appears to use maximum likelihood estimation.

Many of the authors use 'graphical' (but not necessarily graphed) methods to fit the data – that is, a vector of $(x, \hat{y})$ pairs representing the distribution is fitted to the $(x, \tilde{y})$ pairs representing the data. However, it is clear that data only provides the x-ordinates of its pairs – the y-ordinates are established through various plotting position formulae. Gumbel (1958) and Castillo (1988) discuss the choice of plotting position. Therefore, regardless of the actual fitting algorithm, subjectivity has been introduced. This is the case for OBrien et al (1995), Grave et al (2000), Grave (2001), OBrien et al (2003), Cooper (1995 and 1997), Moyo et al (2002), and Crespo-Minguillón and Casas (1997). The fitting algorithms used by these authors are all based on a form of least-squares fitting.

Some authors introduce subjectivity by basing their fits on 'binned' data; data grouped according to arbitrary (though regular once chosen) intervals of some value – the bin width. The application of Sturge's Rule (Benjamin and Cornell 1970) may reduce the effect, but it remains an area of subjectivity. Bruls et al (1996), Cooper (1995 and 1997), Cremona (2001), Flint and Jacob (1996), Getachew (2003), Getachew and OBrien (2005), O'Connor (2001), and Vrouwenvelder and Waarts (1993) fit distributions directly to histograms. Grave (2001) notes correctly that the form of distribution which results is greatly influenced by the number of intervals chosen, and O'Connor (2001) notes sensitivity of predicted extremes to the number of intervals. Further, as these distributions are fit to all, or a significant part, of a histogram of interest, the fit to the extreme values is not emphasized – by the very nature of extreme values. Therefore, such fits do not represent the extreme values well. Also, by raising such fits to a power amplifies the errors, as discussed earlier. The chi-squared fitting used by Bailey (1996) and Bailey and Bez (1994 and 1999) also requires the data to be 'binned' and the same problems therefore apply.

Choice of Thresholds

Many of the authors reviewed make decisions (and therefore introduce subjectivity) regarding various threshold choices. For instance, O'Connor (2001), Grave (2001), Grave et al (2000), OBrien et al (2003), Bailey (1996), and Bailey and Bez (1994 and 1999) fit the distributions to 'tail' data only. In some cases the decisions as to what constitutes tail data is not stated; in others the decision is based on Castillo's suggestion (Castillo 1988). Crespo-Minguillón and Casas (1997) are an exception to this as their model inherently requires the selection of a threshold, and their choice is rationally based on the overall least-squares value for all the thresholds considered.

Nowak also relies on extrapolating from the tails of load effect distributions. The level at which the tail (upon which the extrapolation is to be based) starts is not stated. The normal distribution-based extrapolations of the earlier papers (Heywood and Nowak 1989, for example) are therefore subjective to implement.

Summary

It can be seen that most authors exhibit sources of error under several of the categories and the errors in such works are therefore compounded. This has an effect on the characteristic load effect estimated from such methods. Also, it is clear that many authors describe subjective choices in their analyses.

2.5 Statistical Background

2.5.1 Composite Distribution Statistics

Introduction

Load effects can be the result of any number of loading events involving different numbers of trucks. In general, a load effect due to the passage of a single vehicle has a different distribution to that induced by the occurrence of multiple vehicles (see Figure 2.8 for example). Multiple truck presence events usually yield critical load effects. Normally, it is the maximum per day load effect that is used as the basis for the extreme value analysis which assumes independent and identically distributed (iid) data. Therefore, to mix load effects from different types of loading events violates the iid assumption used in extreme value analysis.

The problem of mixing different statistical generating mechanisms in an extreme value analysis has been examined by previous authors in different fields and their work is examined in this section.

Gumbel (1958)

In his summary, Gumbel (1958) states that "the initial distribution […] must be the same for each sample". Gumbel gives an example of the "the two sample problem" – a study of river discharges, where one series of floods is due to the melting of snow in the spring, and the other to autumnal rainfalls. Gumbel's approach to the problem is described as: take the largest value of each of two large samples, thus forming a couple. By repetition, obtain many such couples and then, for each couple, take the largest value. It is the distribution of this

final variable that is of interest. Gumbel notes that this distribution is the product of the two initial distributions of largest values.

Gumbel's reasoning is based on the following development. The basic results of probability (described in Chapter 3) state that for a value $\mathbf{x}$ and N random variables, $X_1, \ldots, X_N$:

$$P\left[x \geq X_1, \ldots, x \geq X_N\right] = \prod_{i=1}^{N} P\left[x \geq X_i\right] \qquad (2.7)$$

$$P\left[x \leq X_1, \ldots, x \leq X_N\right] = \prod_{i=1}^{N} P\left[x \leq X_i\right] \qquad (2.8)$$

This is so, regardless of the 'type' of random variable, X_i. That is, it is irrelevant whether X_i represents an extreme population or a parent population. Equation (2.8) is more useful, due to its relationship with the cumulative probability function (Chapter 3). Therefore,

$$F_C(x) = P\left[x \leq X_1, \ldots, x \leq X_N\right] = \prod_{i=1}^{N} F_{X_i}(x) \qquad (2.9)$$

where $F_{X_i}(x)$ represents the distribution of load effect resulting from different types of truck loading events, and so $F_C(\cdot)$ is the composite distribution of load effect. The load effect considered can be extreme or parent.

Wind Speed Analysis

The analysis of maximum wind speed is complex due to its nature. There are some similarities, though, with the bridge loading problem. Through study of the approaches taken in the wind speed literature, methods for analysing bridge loading can be adapted. Two of the more important papers are described next.

Gomes and Vickery (1978)

The work of Gomes and Vickery (1978) provides a direct analogy between the wind speed and bridge loading problems. They describe the problem of estimating the distribution of extreme wind speeds in mixed wind climates – climates in which wind may be caused by extensive pressure system storms, thunderstorms, hurricanes or tornados. They use the Gumbel distribution (Chapter 3) to model the extreme wind speeds from each of the mechanisms that occur at a particular site, and combine, without proof, as follows (in their notation):

$$P\big[V_M \leq v\big] = \prod_{q=1}^{Q} P\big[V_q \leq v\big] \tag{2.10}$$

where V_q is the annual maximum gust speed of the **q**th meteorological phenomenon and V_M is the annual maximum gust speed, regardless of the source. $P\big[V_X \leq v\big]$ is the cumulative distribution function of the variable **X**.

Also of importance in their paper, Gomes and Vickery consider the annual maximum gust speed from thunderstorms, with an unknown number of thunderstorms in any given year. Adapted slightly here, they derive the distribution of annual maximum gust speed from thunderstorms as:

$$G_T\big(v\big) = \int_0^{\infty} \big[F_T\big(v\big)\big]^n f_N\big(n\big)\, dn \tag{2.11}$$

where $F_T\big(\cdot\big)$ is the parent distribution of thunderstorm gust speed and $f_N\big(\cdot\big)$ is the probability density function of the number of thunderstorms per year, **N**. Clearly a functional form of (2.11) may be difficult to obtain and include in (2.10). Gomes and Vickery (1978) report a study which shows that

approximating the distribution of N by its mean value does not result in significant inaccuracy. Hence (2.11) may be written as:

$$G_T(v) \approx \left[F_T(v) \right]^{\bar{N}} \tag{2.12}$$

where $\bar{N}$ is the mean value of N. Gumbel (1958) describes a similar formulation to (2.11) for the exact distribution of maxima when the sample size itself is a random variable.

Cook et al (2003)

The paper by Gomes and Vickery (1978) was considered in detail by Cook et al (2003) in the light of more recent developments in statistics. Of note in this work, is their proof of (2.10), described next.

The authors consider two mechanisms; A and B which give values V_A and V_B and in general, for a given period, a pair of events $\{V_A, V_B\}$ can occur. Thus, there are four possible outcomes. Representing $\varnothing$ as the null set, the events are:

1. No events from either mechanism, $\{\varnothing, \varnothing\}$;
2. An event from both mechanism, $\{V_A, V_B\}$;
3. An event from A only, $\{V_A, \varnothing\}$;
4. An event from B only, $\{\varnothing, V_B\}$.

Given that the duration of the sampling period will be long enough such that an event from both mechanism occurs, the authors show that:

$$P\left[\hat{V} \leq v\right] = P\left[\hat{V}_A \leq v\right] \times P\left[\hat{V}_B \leq v\right] \tag{2.13}$$

They extend this to the general case by induction:

$$P\left[\hat{V} \leq v\right] = \prod_{i=1}^{n} P\left[\hat{V}_i \leq v\right] \tag{2.14}$$

This proof includes acknowledgement of the temporal aspect of the sample space considered. However, it is approximate as it considers the relative frequency of each of the possible outcomes, rather than the relative frequency of each of the mechanisms themselves. The authors solve this by modifying the contribution to (2.14) of a mechanism by considering its occurrence as a Poisson process.

Harman and Davenport (1979)

The study by Harman and Davenport noted earlier, also recognizes the composite nature of the bridge loading problem. In revised terminology, the load effect caused by the **i**-truck event has cumulative distribution function $F_i(\cdot)$ and the event has probability of occurrence, f_i. The distribution of load effect greater than a value, **r**, is then $\bar{F}_i(r) \equiv 1 - F_i(r)$. Therefore, the 'complete' distribution of load effect greater than **r** is given by Harman and Davenport as:

$$\bar{F}_C(r) = \sum_{i=1}^{5} f_i \cdot \bar{F}_i(r) \qquad (2.15)$$

which is an application of the theorem of total probability (Chapter 3). The cumulative distribution function of the largest load effect from a sample of size **n** is then given by:

$$G(r) = \left[1 - \bar{F}_C(r)\right]^n \cong \exp\left[-n\bar{F}_C(r)\right] \qquad (2.16)$$

which is reasonable for large **n**. Substitution of (2.15) into (2.16) yields:

$$G(r) = \prod_{i=1}^{5} \exp\left[-nf_i\bar{F}_i(r)\right] \qquad (2.17)$$

Section 2.4.2 describes the log-scale paper fitting procedure used by Harman and Davenport, based on (2.17).

2.5.2 Predictive Likelihood

Introduction

The relatively new theory of frequentist predictive likelihood can be used to estimate the variability of the predicted value, or predictand. Applications of predictive likelihood to real-world problems are sparse. Davison (1986) presents one in the context of his revised form of predictive likelihood. Lorén and Lundström (2005) present the only full paper (obtained for this work) on the application of predictive likelihood techniques; in their case, to the prediction of fatigue limit distributions for metals.

Fisher (1956) is the first clear reference to the use of likelihood as a basis for prediction in a frequentist setting. A value of the predictand ($\mathbf{z}$) is postulated and the maximized joint likelihood of the observed data ($\mathbf{y}$) and the predictand is determined, based on a model with parameter vector θ. The graph of the likelihoods thus obtained for a range of values of the predictand yields a predictive distribution. Such a predictive likelihood is known as the profile predictive likelihood. Denoting a normed likelihood by $\overline{L}\left(\theta;x\right)$ this is given by:

$$L_P\left(z \mid y\right) = \sup_{\theta} \overline{L}_y\left(\theta; y\right) \overline{L}_z\left(\theta; z\right) \tag{2.18}$$

It is to be noted that likelihood is not a probability and so the usual conditional probability rule does not apply. Mathiasen (1979) appears to be the first to study Fisher's predictive likelihood and notes some of its problems. Foremost for this work is the problem that it does not take into account the parameter variability for each of the maximizations of the joint likelihood function required (Lindsey 1996, Bjørnstad 1990). Lejeune and Faulkenberry (1982) propose a similar predictive likelihood, but include a normalizing function.

Predictive likelihood is a general concept (see Berger and Wolpert 1988) and in the literature many versions have been proposed. The paper by Bjørnstad (1990) is seminal in predictive likelihood for it collects all of the literature and examines each of the predictive likelihoods proposed. Bjørnstad notes that the Fisherian predictive likelihood of (2.18) "plays a central role in prediction". The other predictive likelihoods considered by Bjørnstad are those based on sufficiency principles put forth by Lauritzen (1974), Hinkley (1979) and Butler (1986). Based on the Lauritzen-Hinkley definition, Cooley and Parke put forward a number of papers dealing with the prediction issue (Coole and Parke 1987, Cooley et al 1989, Cooley and Parke 1990). However, their method relies on the assumption that the parameters are normally distributed, and they use Monte-Carlo simulation as a result. Leonard (1982) suggests a similar approach.

Davison (1986) provides a relevant example of the application of predictive likelihood methods to river discharges and wave heights. Though he uses a different form of predictive likelihood, the explanation of his approach with the GEV distribution (Chapter 3) is important to this work.

2.5.3 Multivariate Extreme Value Analysis

Allowing for the effect of the dynamic interaction between the bridge and the trucks which form a loading event is essential to determine the total load effect to which the bridge is be subject. As part of a study described in Chapter 8, dynamic interaction simulations are described for 10 years of monthly maximum events. To determine the lifetime total load effect for the bridge, the correlation between static and total load must be accounted for. As extreme values of two correlated variables are required, multivariate extreme value analysis is adopted.

The study of multivariate extreme value theory began in the 1950s (Galambos 1987). Coles (2001a) and Galambos (1987) agree that the work of Tiago de Oliveira was essential to its development – refer to Coles (2001a) and Galambos (1987) for references to his work.

An approach to the modelling of bivariate extreme value distributions, including consideration and estimation of several dependence structures, is presented by Tawn (1988). Several general models of extreme value distributions are examined by Tawn (1990) who also presents an application – the modelling of tri-variate extreme sea level data. Large dimensional problems in multivariate extreme value modelling are considered by Embrechts et al (2000). In this paper, the authors also present an application in the field of sea level analysis for flood protection. Coles and Tawn (1991) present a generalization of the peaks-over-threshold (POT) approach to the modelling of multivariate extreme values.

Capéraà et al (1997) present the modelling and estimation of extremal dependence functions. Klüppelberg and May (1998) also discuss the bivariate dependence functions and state that the only possible models are the mixed and logistic classes. Coles et al (1999) also discuss the dependence functions used in multivariate extreme value analysis. A thorough presentation of multivariate extreme value analysis and the modelling of dependence through the use of dependence structures and copulas is given by Demarta (2002). Segers (2004) also discusses the estimators of use for the bivariate extreme value dependence function of Pickands (1981) whilst Hefferenan (2005) gives a review of the dependence measures used in multivariate statistical modelling in recent years.

Literature on the statistical computational aspects of multivariate extreme value statistics is sparse. Stephenson (2004) presents a user guide to R (R

Development Core Team 2005) software for the analysis of multi- and uni-variate extreme analysis. The guide gives several applications of the theory and serves well as a collection of examples, and an introduction to the theory. Nadarajah (1997) and Stephenson (2003) both describe procedures to simulate multivariate extreme value distributions. This is important for the application of bootstrapping methods to the problem

There have been several applications of the theory, mostly in the statistical literature. Hawkes et al (2002) discuss the use of multivariate extreme value theory in estimating coastal flood risk due to combinations of high tides and wave surges. An application of bivariate extreme value analysis to the wave height and sea level problem of coastal flood defence is presented by Draisma and de Haan (2004). Zachary et al (1998) use the theory to estimate the loads caused on offshore structures by combinations of wave height, wave period and wind speed. An application of multivariate extreme value theory to structural design problems is considered by Coles and Tawn (1994); a detailed application to coastal engineering is presented. Also, Gupta and Manohar (2005) use multivariate extreme value theory in the analysis of random vibration problems. Specifically, a two span bridge subject to earthquake support motions is examined.

The multivariate extreme value analysis used in this work is based mainly on the work of Stephenson (2003 and 2004). The software developed as part of Stephenson's work has been used here – the evd library for the R (R Development Core Team 2005) language. Stephenson's work is, in turn, based on that of the many authors mentioned previously, most notably the work of Coles and Tawn.

2.6 Summary

This chapter presents the background literature to the various aspects of this research project. Initially, the contemporary work in the field of bridge traffic load models is presented, followed by some discussion. One area of significant development of such models is presented in detail as it forms a substantial part of the current research: that of headway modelling. The literature for the main theme of this work is then presented – methods of statistically analysing the results of bridge traffic load simulations. An extensive discussion is provided, in which various problems with the current methods are outlined. Following this, a section outlining the background statistical literature of this work is presented. General statistical literature is not presented, rather, the literature specific to the main areas of use in this work. General statistical literature is discussed in Chapter 3 instead.

Chapter 3

FUNDAMENTAL PROBABILISTIC METHODS

"Statistics in the hands of an engineer are like a lamppost to a drunk—they're used more for support than illumination"   *- AE Housman*

Chapter 3 - **FUNDAMENTAL PROBABILISTIC METHODS**

3.1 Introduction

Karl Pearson (1920) posed "the fundamental problem of statistics" as follows:

> *An 'event' has occurred p times out of p + q = n*
> *trials, where we have no a priori knowledge of the*
> *frequency of the event in the total population of*
> *occurrences. What is the probability of its occurring*
> *r times in a further r + s = m trials?*

That Pearson's 'problem' applies to the bridge loading problem is immediately apparent. Note also that prediction is an integral part to this "fundamental problem" – just as it is to the bridge loading problem. This chapter presents the background material necessary for the development and presentation of the statistical analyses used to solve Pearson's "fundamental problem".

Initially, the fundamental definitions of any random experiment are given, followed by the mathematical tools need to operate on random experiments. Inference from the outcomes of a statistical experiment is then considered: the method of maximum likelihood, which is of central importance to this work, is presented here. Following this, the statistics of extreme values is introduced and the basic definitions and limitations of the theories outlined. Finally, the problem of predicting future outcomes of a statistical experiment is addressed. The material introduced herein forms the background to the analyses carried out by many other authors in this field, as may be seen from Chapter 2.

3.2 Basic Results

The fundamentals presented in this section are required for further developments in this work as a whole. Standard texts that may be referred to for more information on these basic results are Mood et al (1974) and Ang and Tang (1975). Other highly relevant texts are Castillo (1988), Lindsey (1996), Coles (2001a), Cox and Hinkley (1974), Feller (1968), and Azzalini (1996).

3.2.1 Probability, events and sample spaces

The classical, or frequency **definition of probability** is:

> If a random experiment can result in **n** mutually exclusive and equally likely outcomes and if n_A of these outcomes have attribute **A**, then the probability of **A** is the fraction n_A/n.

The **sample space** is the collection of all possible outcomes of an experiment. Considering an experiment with a single die, the sample space would the integers 1 to 6, representing the six possible faces of the die. Sample spaces may be finite with discrete points, or infinite with continuous 'points'.

The terminology '**event A**' is used to represent an outcome of a statistical experiment that has attribute **A**. The **event space**, A , is defined as the collection of all permutations of events, or the collection of all subsets of the sample space. The sample space itself is a subset of the event space.

A **probability function**, $P[\cdot]$, is a set function with a domain of the event space and counterdomain the interval [0,1] on the real number line. $P[A]$ represents the probability of event **A**. Where Ω represents the sample space of an experiment, $P[\Omega]=1$, by definition. A **probability space**, denoted $(\Omega, A, P[\cdot])$,

describes the sample space, event space and probability function, respectively, for a given random experiment.

Given two events, A and B in A , the **conditional probability** of event A given that event B has occurred is defined as:

$$P[A \mid B] = \frac{P[AB]}{P[B]} \tag{3.1}$$

The division by $P[B]$ is equivalent to a re-scaling of the sample space for A. Conditional probabilities appear when an outcome is dependant on another outcome.
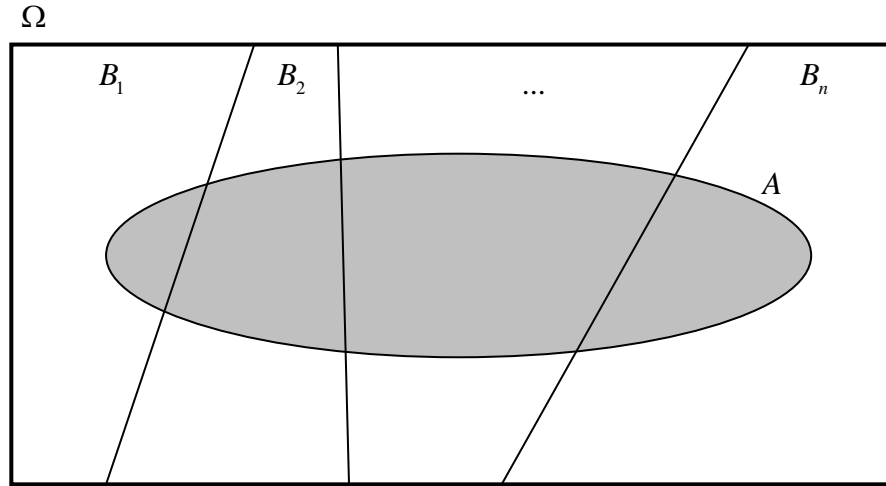
Figure 3.1: Illustration of the theorem of total probability

The **theorem of total probability**, illustrated in Figure 3.1, is defined as:

For a given probability space $(\Omega, A, P[\cdot])$, if $B_1, B_2, \dots, B_n$ is a collection of mutually exclusive events in A , satisfying $\Omega = \bigcup_{i=1}^{n} B_i$ and $P[B_i] > 0$ for $i = 1, 2, \dots, n$, then for every $A \in A$,

$$P[A] = \sum_{i=1}^{n} P[A \mid B_i] \cdot P[B_i] \tag{3.2}$$

In the cases where A does not depend on B, $P[A\,|\,B]=P[A]$, and the events A and B are therefore **independent**. For several events, and using (3.1), independence is defined as:

For a given probability space $(\Omega, A, P[\cdot])$, if $A_1, A_2, \ldots, A_n$ is a number of events in A , then these events are said to be independent if and only if:

$$
\begin{aligned}
P\big[A_i A_j\big] &= P\big[A_i\big] \cdot P\big[A_j\big] \\
P\big[A_i A_j A_k\big] &= P\big[A_i\big] \cdot P\big[A_j\big] \cdot P\big[A_k\big] \\
&\vdots \\
P\left[\bigcup_{i=1}^{n} A_i\right] &= \prod_{i=1}^{n} P\big[A_i\big]
\end{aligned}
\tag{3.3}
$$

Independence of events features largely in this research and the above definition is of central importance.

3.2.2 Random variables and distribution functions

Often it is not the occurrence of a particular event that is of interest, but rather, the value of an attribute realised by the event:

For a given probability space, $(\Omega, A, P[\cdot])$, a **random variable**, denoted X or $X(\cdot)$, is a function with domain Ω and counterdomain the real number line.

A random variable links the sample space with a unique real number; consequently all outcomes are described numerically. Another function is required to relate the realized value of the random variable to a probability:

The **cumulative distribution function** of a random variable **X**, denoted $F_X(\cdot)$, is that function with domain the real line and counterdomain the interval [0,1] which satisfies $F_X(x) = P[X \leq x] = P\big[\{\omega : X(\omega) \leq x\}\big]$.

$\{\omega : X(\omega) \leq x\}$ is read as the set of all points ω for which $X(\omega) \leq x$. The cumulative distribution function will normally be abbreviated to CDF. It is the cumulative aspect of this function (the '$\leq$') that urges another definition:

The **probability density function** of a random variable **X**, denoted $f_X(\cdot)$, is that function defined by:

$$
\begin{aligned}
f_X(x) &= \lim_{\Delta \to 0} \big(P[X \leq x + \Delta] - P[X \leq x]\big) \\
&= \frac{d F_X(x)}{dx}
\end{aligned}
\tag{3.4}
$$

The probability density function is abbreviated as PDF. It is to be noted that the above definitions relate to continuous random variables. The relationship between CDF and PDF is thus defined as:

$$
F_X(x) = \int_{-\infty}^{x} f_X(u) \, du
\tag{3.5}
$$

There are many forms of distributions and any of the textbooks given at the start of this section may be referred to for further information.

3.2.3 Probability paper

Graphical methods for the analysis of statistical data have a long history and an important place even in modern techniques; the histogram being the most prevalent – see Coles (2001a) for example. In this work, data and their corresponding statistical models are usually graphed on probability paper; a

graph in which the **x**-axis is in arithmetic scale, and the data is plotted at its value. The **y**-axis is modified to give the standard variate of the distribution under study, such that, when the data is plotted, a straight line reveals adherence to the distribution.

The plotting position of the data on probability paper is governed by the **empirical distribution function**: the CDF of a data set, $x_1, \ldots, x_n$. When the data is arranged in increasing order, for any one of the x_i exactly **i** of the **n** observations have a value less than or equal to x_i, therefore the cumulative probability is given by:

$$P[X \leq x_i] = \tilde{F}(x_i) = \frac{i}{n} \approx \frac{i}{n+1} \tag{3.6}$$

The adjustment is made such that $\tilde{F}(x_n) \neq 1$. The right hand side of (3.6) is the empirical probability. It is this probability that is used to identify the plotting position. Gumbel (1954) and Castillo (1988) discuss many other plotting positions. The choice of plotting position is not as important as it once was, as most inference is now done numerically rather than graphically.

Gumbel probability paper will be mostly used in this work and the Gumbel distribution is given by:

$$G_I(x) = \exp\left[\exp\left(\frac{x-\mu}{\sigma}\right)\right] \tag{3.7}$$

The standard Gumbel (or extremal) variate is:

$$s = \frac{x-\mu}{\sigma} \tag{3.8}$$

Therefore, the standard extremal variate, corresponding to the probability from the Gumbel distribution, s, and the empirical distribution, $\tilde{s}$, for a given data point, **x**, may be plotted on the **y**-axis once the following inversions are applied:

$$
\begin{aligned}
s &= -\ln\left[-\ln\left(G_I\left(x\right)\right)\right] \\
\tilde{s} &= -\ln\left[-\ln\left(\tilde{F}\left(x\right)\right)\right]
\end{aligned}
\tag{3.9}
$$

Should the extremal variates correspond for each of the data points, a straight line results. Thus, the comparison of the fitted data may be got by drawing a straight line through the data points. Figure 3.2 illustrates the concept: a straight line is fitted through the data points (in this case by maximum likelihood – see section 3.3.2). The left **y**-axis gives the standard extremal variate whilst the right **y**-axis gives the cumulative probability. The **x**-axis corresponds to the data values.
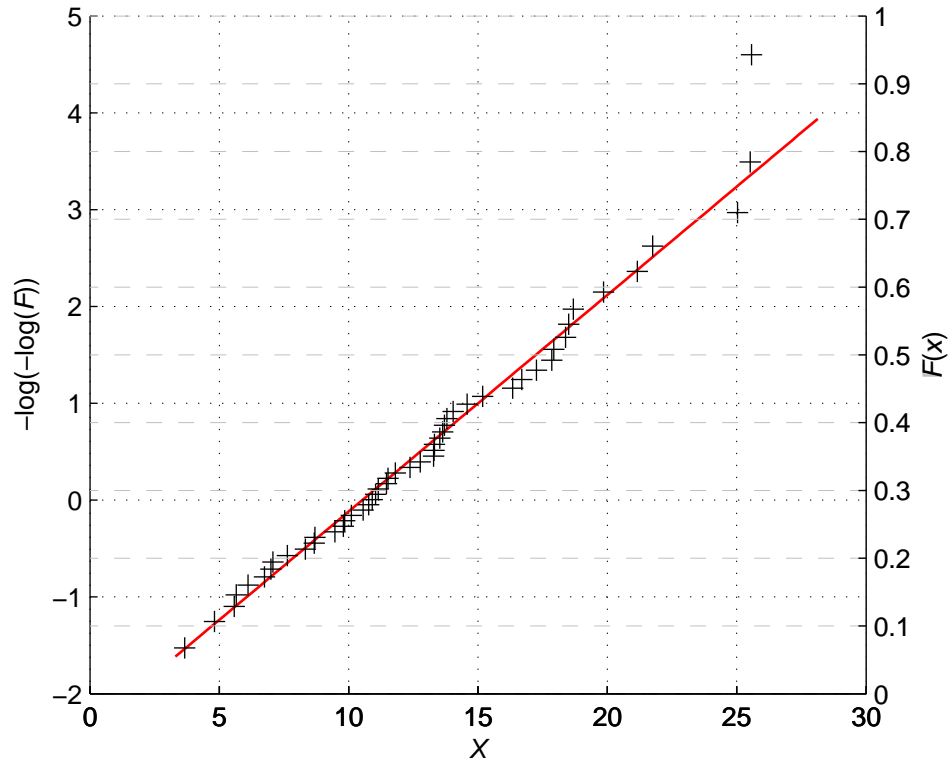
Figure 3.2: Gumbel paper probability plot.

It was previously stated that Gumbel paper is used, almost exclusively, in this research. However, it is not usually the Gumbel distribution being fit – rather the Generalized Extreme Value (GEV) distribution. This is a more flexible distribution that may exhibit curvature on Gumbel paper (or probability plot). Upward curvature reveals an asymptote to an **x**-axis value – corresponding to a physical limit on the statistical process. A curve asymptotic to a **y**-axis value (as well as a straight line) corresponds to a statistical mechanism with no physical limitation. Figure 3.3 gives two examples of GEV distributions plotted on Gumbel paper.
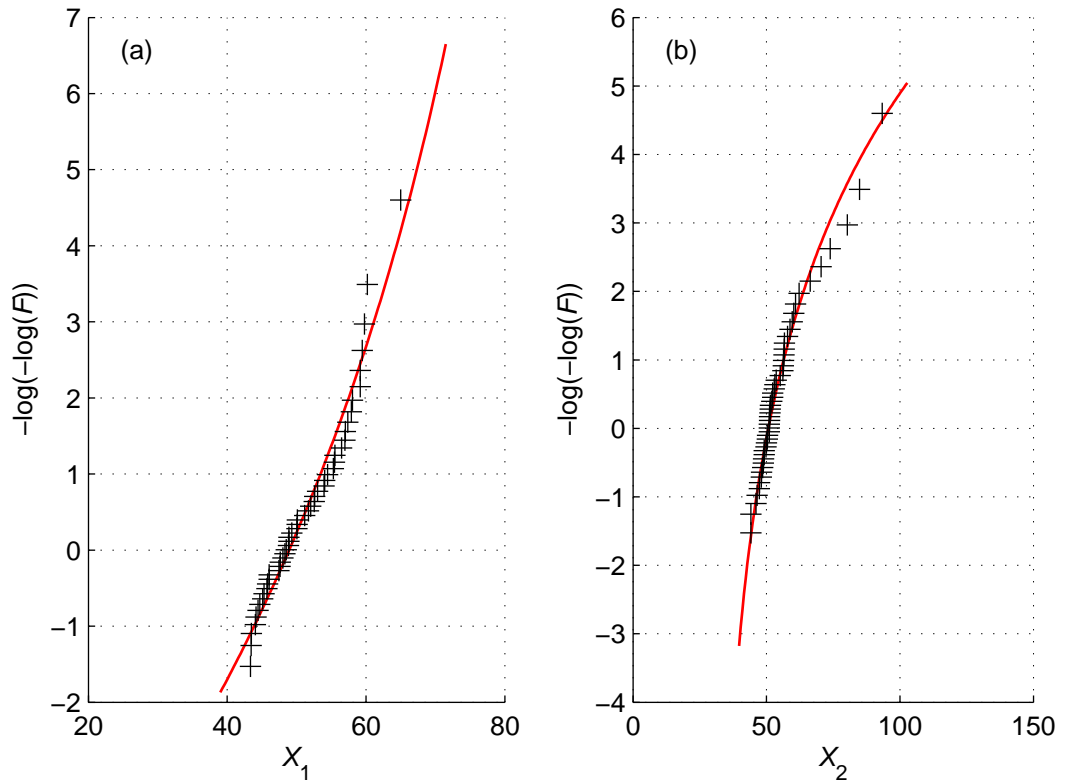
Figure 3.3: GEV distributions plotted on Gumbel probability paper: (a) bounded, and; (b) unbounded.

3.3 Statistical Inference

Azzalini (1996) defines statistical inference as the operation through which information provided by a sample of a population is used to draw conclusions about the characteristics of that population. The population is defined as the totality of elements about which information is desired, and the sample is defined as a collection of observed random variables taken from the population.

The following example will be developed through the following sections: consider a container holding 5000 small balls which are either black or white, of which the proportion of black balls is required. Rather than examining each of the 5000 balls, a sample could be taken at random from the container. Azzalini (1996) describes the reasons why this is often preferable. Suppose that 50 balls are drawn at random, of which 4 are found to be black. The proportion of black balls is $\hat{\theta} = 4/50$, in which the 'hat' notation shows that this is only an estimate of the true parameter value. It is reasonable to think that drawing another sample of 50 balls may not result in the same value for θ. However as of yet, it is the best estimate of the proportion of black balls in the population. Another issue is the sample size, and the amount of information it holds about the population: should 100 balls have been drawn and 8 found to be black, it is intuitive to expect extra 'information' about the estimate of θ from this larger sample.

Approximating the hypergeometric distribution with the binomial distribution (valid for the size of the sample), the probability that the random variable $\mathbf{Y}$ yields the observed number of black balls, $\mathbf{y}$, is:

$$P[Y = y] = \binom{50}{y} \theta^y (1 - \theta)^{50-y} \tag{3.10}$$

Approximating the set of possible values for θ as the interval $[0,1]$, it can be seen that (3.10) represents a family of probability distributions for each value of the parameter θ. Inference is identifying the true distribution of Y through estimation of the parameter θ (Silvey 1970, Lindsey 1996).

The Likelihood method of inference is mainly used in this work. As will be shown, it is a robust, accurate estimator with excellent asymptotic properties. It is also a minimal sufficient statistic (Zacks 1971) – it contains as much information about the distribution of the data as the data itself (Mood et al 1974). There are some known cases in which likelihood can give anomalous results (see for example, Zacks 1981), but these do not affect the work herein.

3.3.1 Likelihood

Edwards (1992) gives the first example of a likelihood argument and attributes it to Daniel Bernoulli, who states: "…one should choose the one which has the highest degree of probability for the complex of observations as a whole". Edwards (1992) himself also defines likelihood informally: "Our problem is to assess the relative merits of rival hypotheses in the light of observational or experimental data that bear upon them". Fisher first defined mathematical likelihood in 1912 in an undergraduate essay and continued to advance it, culminating in his paper "On the Mathematical Foundations of Theoretical Statistics" in 1922 (Fisher 1922, Alrich 1997). Fisher's idea is to examine the probability of having observed the data that was observed, given the proposed probability model. For a probability density $f_X(x;\theta)$ – where the notation indicates that the density is a function of the parameter (or vector of parameters) of the model – the **likelihood** of having observed a particular realization **x** is defined as:

$$L(\theta) = L(\theta; x) = c(\theta) \cdot f(x; \theta) \qquad (3.11)$$

where the notation emphasizes the dependence of the density upon the parameter, and similarly for the likelihood upon the data. The multiplicative constant is required to make the probability density a probability for each data point. For the set of **n** sample values the probability of having observed the observed values is:

$$L(\theta; x) = c(\theta) \cdot \left[f(x_1; \theta) \cdot f(x_2; \theta) \cdot \ldots \cdot f(x_n; \theta) \right]$$
$$L(\theta; x) = c(\theta) \cdot \prod_{i=1}^{n} f(x_i; \theta) \qquad (3.12)$$

In practice it is more convenient to work with the **log-likelihood** to avoid the multiplicative nature of the likelihood function:

$$l(\theta; x) = \log L(\theta; x) = c(\theta) + \sum_{i=1}^{n} \log f(x_i; \theta) \qquad (3.13)$$

Generally the constant $c(\theta)$ is not involved in any calculations using likelihood as one seeks knowledge of relative likelihoods and **c** is thus not relevant.

Returning to the example of the 5000 balls, it can be seen that for the single observed value $y = 4$, equation (3.10) corresponds to (3.11) and is thus the likelihood function for the parameter θ. This is graphed in Figure 3.4(a) which shows an increased likelihood for a parameter value around 0.05 to 0.10, relative to other possible values of the parameter. Also shown is the likelihood function for the case when the number of samples is 100 and the number of observed black balls in this sample is 8, as are the graphs of the likelihood ratio, which is the likelihood function, normalized on its maximum value, and the log-likelihood, for comparison.
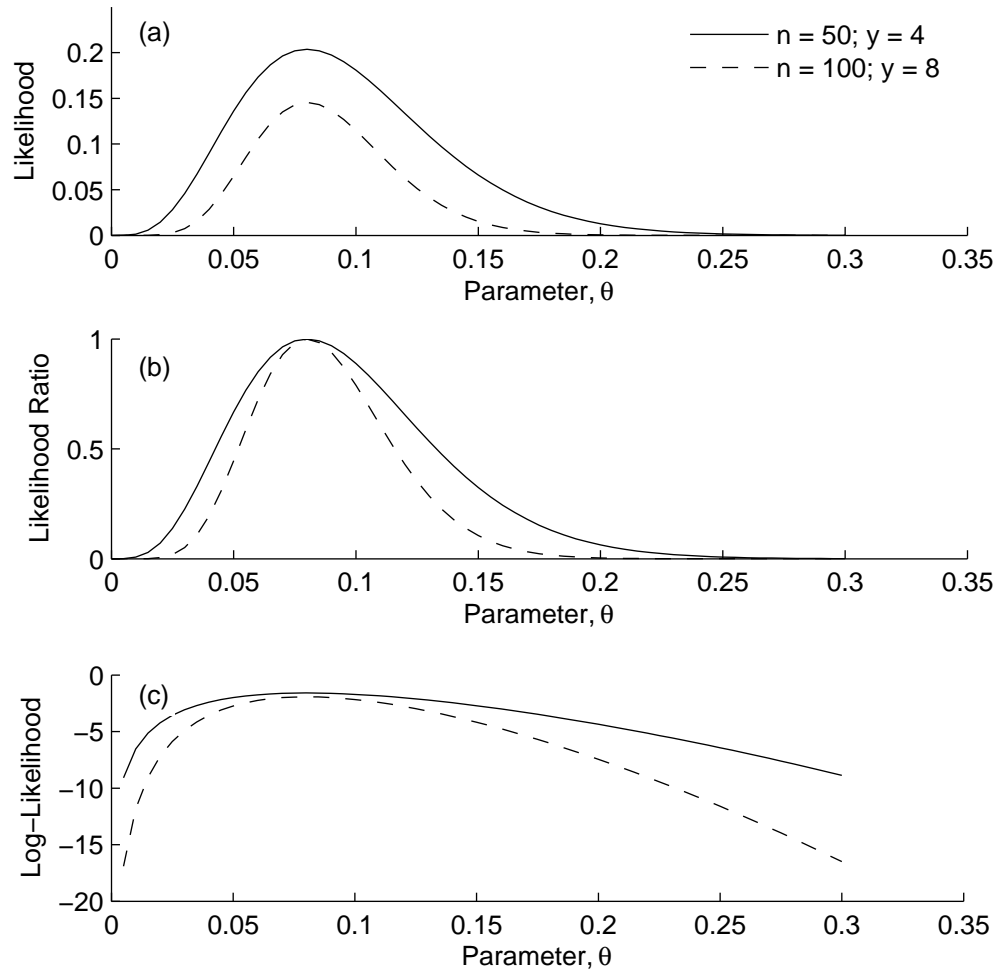
Figure 3.4: Likelihood functions for the 'ball' example: (a) absolute likelihood; (b) relative likelihoods, and; (c) log-likelihoods.

The question regarding the amount of 'information' held in the data was raised previously: more information regarding the 'true' value of θ should surely be available from a larger sample. Trivially, if the sample is the total population, then the amount of information about θ is at a maximum. This increase of information may be seen in the likelihood ratio and log-likelihood graphs – the width of the $n = 100$ curve is less than that of the $n = 50$ curve. This means a smaller range of likely parameter values, at any level of relative likelihood, results from the larger sample size, than for the smaller. Thus the $n = 100$ curve holds more information about the true parameter value, as expected.

3.3.2 Maximum likelihood and Fisher information

A mathematical definition of the information contained in the sample may be obtained by considering the log-likelihood function: the value of the parameter that maximizes the likelihood function is most likely to be the 'true' parameter value. This is the **Method of Maximum Likelihood**. A parameter value found in this way is denoted $\hat{\theta}$ to emphasize that it is an estimate; the notional 'true' value of the parameter is denoted θ_0. Using the log-likelihood function, the maximum likelihood estimate (MLE) of a parameter is the value that satisfies:

$$\frac{d\, l(\theta; x)}{d\theta} = 0 \tag{3.14}$$

Geometrically this is the slope of the tangent to the log-likelihood curve at its maximum (Figure 3.4). Using a Taylor series approximation about the MLE, the log-likelihood function is approximated as:

$$l(\theta) = l(\hat{\theta}) + (\theta - \hat{\theta}) \cdot \frac{d\, l(\hat{\theta})}{d\theta} + \frac{1}{2} \cdot (\theta - \hat{\theta})^2 \cdot \frac{d^2 l(\hat{\theta})}{d\theta^2} + \ldots \tag{3.15}$$

having dropped the dependency notation for brevity. Then approximately, incorporating (3.14) and dropping third-order and higher terms:

$$l(\theta) = l(\hat{\theta}) + \frac{1}{2} \cdot (\theta - \hat{\theta})^2 \cdot \frac{d^2 l(\hat{\theta})}{d\theta^2} \tag{3.16}$$

Empirically, equation (3.16) measures how informative the data is about the MLE. It states that the support offered by the data to $\hat{\theta}$, and some other value θ, differs by an amount proportional to the second derivative of the log-likelihood function about $\hat{\theta}$. Hence, the **observed (or Fisher) information** (Cox and Hinkley 1974) is defined as:

$$I\left(\theta\right) = -l''\left(\hat{\theta}\right) = -\frac{d^2l\left(\hat{\theta}\right)}{d\theta^2} \tag{3.17}$$

Referring to Figure 3.4(c), it is apparent that the curve for the larger sample size ($n = 100$) is narrower than that for the smaller sample size ($n = 50$) and is therefore more curved near the MLE than the log-likelihood function of the smaller sample. Hence, (3.17) may be perceived as the spherical curvature of the log-likelihood function at the estimate: its reciprocal is the radius of curvature at the estimate. The reciprocal is also the value of the Cramér-Rao lower bound for the variance of an unbiased estimator (Azzalini 1996, Mood et al 1974, Zacks 1971) – the smallest possible variability a parameter estimator can have.

Though the above has been presented relating to one-dimensional parameters, the theory is extendable to multi-dimensional parameters. In such cases the reciprocal of the information may be thought of as related to the volume under the likelihood surface. The square root of the determinant of the information matrix may be seen as a measure of the width of the likelihood surface (Edwards 1992). Also, the diagonal entries of $I\left(\theta\right)$ represent the variance of a parameter with respect to itself. Hence, the square root of the diagonal term corresponding to a parameter represents the standard error of that parameter.

Figure 3.5 shows two log-likelihood surfaces for the normal distribution. The flatter surface is derived from 50 random deviates of $N\left(100,5^2\right)$; the more curved surface is found from 200 random $N\left(100,5^2\right)$ deviates. This figure clearly shows that 'support' for differing values of μ and σ drops away much quicker for the larger data set. Put another way, the volume under the curve at its maximum is less; its reciprocal is the information, which is thus greater.
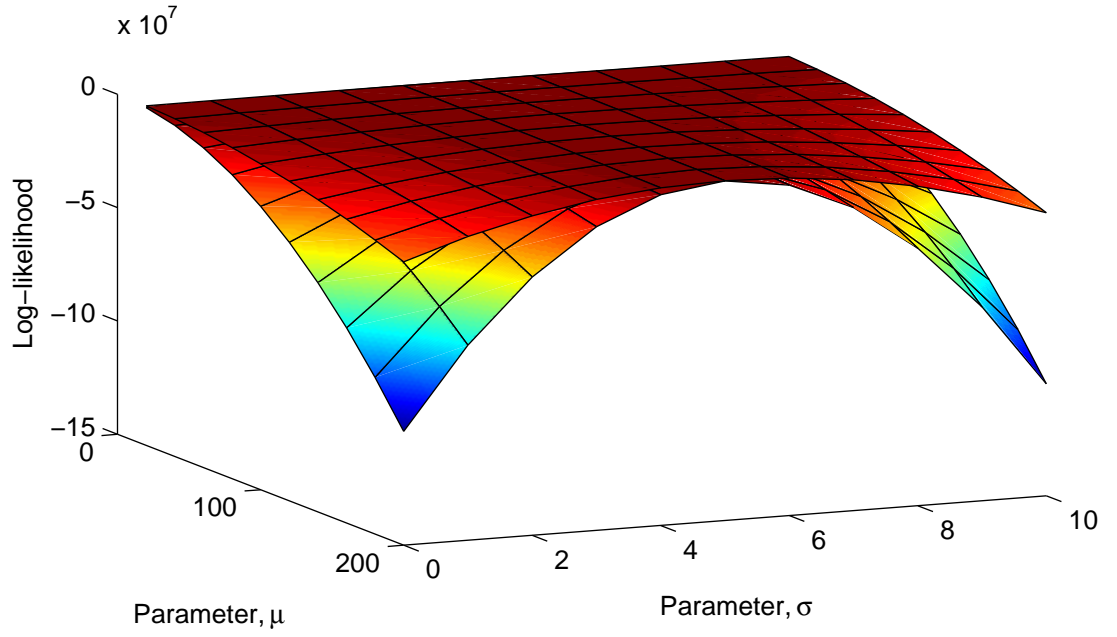
Figure 3.5: Log-likelihood surfaces of $N\left(100,5^2\right)$, for **n** = 50 and 200.

3.3.3 Asymptotic normality of an MLE

The maximum likelihood estimator has many properties desired of an estimator – refer to Azzalini (1996), Edwards (1992), and Mood et al (1974) for further information. Of direct relevance is that it is a Best Asymptotic Normal (BAN) estimator. An estimator (for example, maximum likelihood), $T(X)$, such that

$$\sqrt{n}T(X)\xrightarrow{\;d\;}N\left(\theta,\mathrm{var}(\theta)\right) \tag{3.18}$$

where **n** is the sample size, is said to be a BAN estimator if $\mathrm{var}(\theta)=I\left(\theta\right)^{-1}$ which indicates that the estimator is asymptotically normally distributed. In the multi-dimensional case, the reciprocal of the observed information is the usual variance-covariance matrix of the parameter estimates. Therefore, parameters of distributions estimated using maximum likelihood estimation may be taken to be asymtotically normally distributed; the accuracy of the approximation improves with increasing sample size due to the central limit theorem.

3.3.4 Profile likelihood and deviance

The previous section described the asymptotic distribution of maximum likelihood parameter estimates. Often, it is more useful to obtain an estimate of the actual distribution of a parameter (Barndorff-Nielsen 1983). In the uni-dimensional case this does not pose a problem: Figure 3.4 illustrates how the parameter estimate varies. As the likelihood function cannot provide an absolute statement of the suitability of a parameter estimate, the likelihood ratio graph of Figure 3.4(b) is particularly important in aiding estimates of parameter distributions. Having evaluated the log-likelihood, the likelihood ratio is given by the difference of two log-likelihoods. The **deviance function** is defined as:

$$D(\theta) = 2\left[l(\hat{\theta}) - l(\theta) \right] \tag{3.19}$$

As the log-likelihood is usually a negative quantity, the deviance is positive. The likelihood ratio is multiplied by 2 for reasons outlined by Lindsey (1996). The deviance, as defined in (3.19), is approximately chi-squared distributed with the number of degrees of freedom equal to the number of parameters in the model (Coles 2001a). With such knowledge, it is possible to work backwards from a pre-specified probability (such as 95%) to find the value of $l(\theta)$ that defines the confidence region. Figure 3.6 illustrates this for the ball example. It can be seen that the 95% confidence interval narrows for the larger sample size, reflecting the increase in information available. Also, it is of note that the confidence intervals are not symmetric about the MLE (corresponding to zero deviance). Thus the distribution of the likelihood estimate is skewed which is not compatible with the assumption of normality.
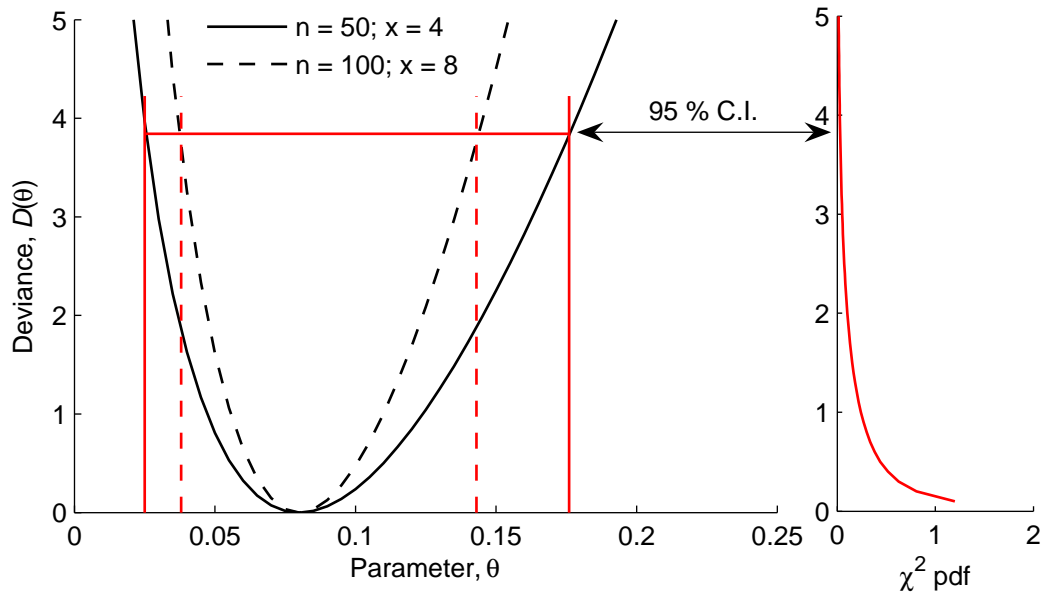
Figure 3.6: Deviance function and confidence intervals for the ball example samples (note that the χ^2 PDF graph is rotated 90°).

In multi-parameter cases, the application of the preceding method is more difficult. It may be seen from Figure 3.5 that the parameters are orthogonal in multi-dimensional space, though not independent. To estimate the distribution of a parameter, a notional 'slice' through the likelihood surface is made parallel to the axis of the parameter of interest – approximately, the resulting cross section is the **profile (log-)likelihood** of the parameter of interest. However, the 'slice' is in fact a point, as it must be taken at the MLEs of the other parameters, conditional on the current value of the parameter of interest. The profile log-likelihood of a parameter, θ_i, is defined as:

$$l_p\left(\theta_i\right) = \sup_{\bar{\theta}} l\left(\theta_i, \bar{\theta}\right) \tag{3.20}$$

where $\bar{\theta}$ denotes the restricted parameter vector which is θ without θ_i and sup may be read as 'the maximum of'. Thus, for each value of the parameter of interest, the profile log-likelihood is the maximized log-likelihood with respect to all of the other parameters. In the case of the example of Figure 3.5, the profile

likelihood for the μ parameter is shown in Figure 3.7. The 95% confidence intervals derived from the $\chi^2(0.95, 2)$ distribution – where the number of degrees of freedom is 2, corresponding to the number of parameters in the model – is also shown in Figure 3.7. Note also that each unit of the χ^2 distribution corresponds to two units of log-likelihood due to the deviance function. Further, it may be seen that the confidence intervals are close to symmetric about the MLE of the mean; the normal approximation in this case would be quite reasonable.
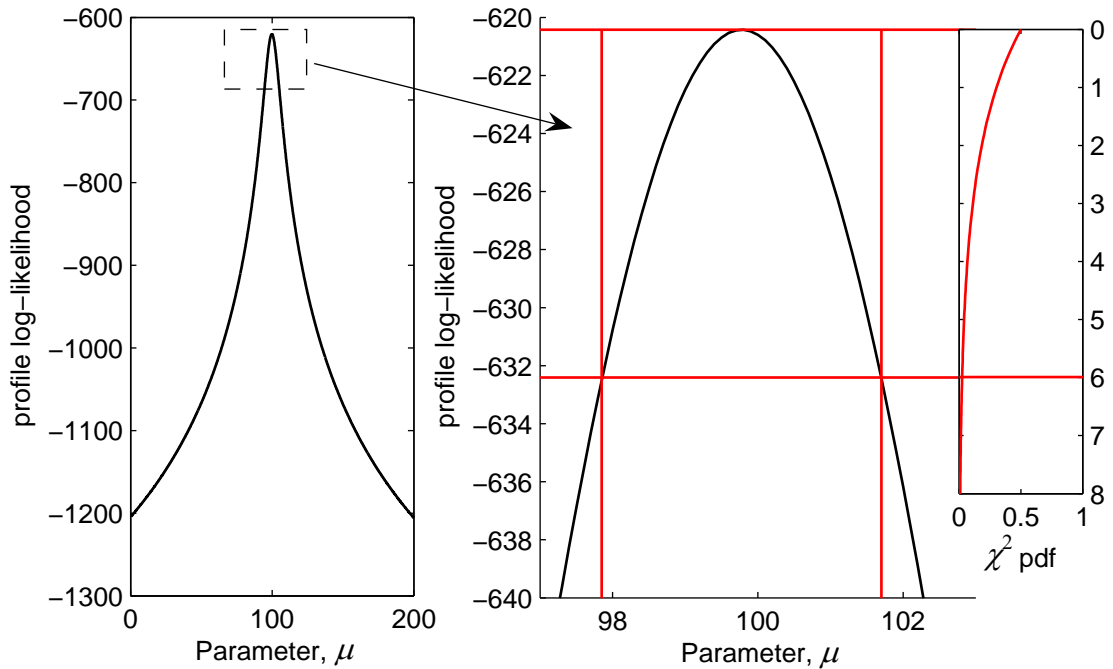
Figure 3.7: Profile likelihood for μ of N(100,5²), with confidence intervals got from $\chi^2(0.95,2)$.

Though only parameters have been examined here, the method of profile likelihood can be extended to cover any functional combination of the parameters. As will be shown in Chapter 7, this extension of profile likelihood has considerable benefit for the prediction of extreme values.

3.4 Statistics of Extremes

The statistics of extremes, or extreme value theory, is concerned with identifying trends in the extreme (maximum or minimum) values obtained from a set of samples. The theory has found extensive use in the practical sciences where decisions have to be made and not postponed until a better theory, or more data emerges (Castillo 1988, Coles 2001a). Bardsley (1994) argues that the theory has reached its zenith and that the results of an elaborate objective analysis are not significantly better than a subjective analysis by an experienced investigator. This view is certainly not as widespread as its counterpart. The statistical analyses used in this work employ extreme value theory throughout.

3.4.1 Basic formulation

Only the distribution of the maximum of a sample is considered here, though that of the minimum follows a similar formulation – refer to Castillo (1988), Ang and Tang (1984) and Galambos (1978) for more details on what follows.

Consider a set of **n** random variables, $X_1,\ldots,X_n$ and allow $Y = \max[X_1,\ldots,X_n]$. Given a set of observations, $x_1,\ldots,x_n$ for which $y = \max[x_1,\ldots,x_n]$. When the X_is are independent, the distribution function, $F_Y(\cdot)$, of y is:

$$F_Y(y) = P[Y \le y] = P[x_1 \le y;\ldots;x_n \le y] \tag{3.21}$$

which results because the largest of the x_is is less than or equal to **y** if, and only if, all of the x_is are less than or equal to **y**. If the X_is are **independent and identically distributed** (iid), then, similar to (3.3):

$$P[x_1 \le y;\ldots;x_n \le y] = \prod_{i=1}^{n} P[X_i \le y] \tag{3.22}$$

and therefore, where $F_X(\cdot)$ is the distribution function of $X_1, \ldots, X_n$:

$$F_Y(y) = \left[F_X(y) \right]^n \tag{3.23}$$

The distribution $F_X(\cdot)$ is known as the parent distribution. As the parent CDF is raised to the power of **n**, it is important that the parent distribution is both known and closely models the data – especially in the upper tail of the distribution (Coles 2001b, Castillo 1988). Any deviations of the model from the true distribution are raised to the power of **n** and can therefore distort the analysis. Also, explicit expressions for the distribution of the maxima are difficult to obtain from (3.23). These problems with this formulation have resulted in the development of the **asymptotic theory of extreme order statistics** – most notably associated with Fisher and Tippett (1928), though other authors were writing on this subject around the same time (Gumbel 1958).

3.4.2 Fisher-Tippett and Gnedenko

The asymptotic theory of extreme order statistics attempts to identify possible limiting forms of the distribution of the extreme as **n** tends to infinity, avoiding the degenerate results; 0 when $F_X(y) < 1$, and 1 when $F_X(y) = 1$. Fisher and Tippett (1928) recognized that the maximum of N sets of observations of **n** values of **X**, must also be the maximum of **n** values of **X**. Therefore any non-degenerate distribution must be of the same form, but linearly transformed by location and scale parameters (a_n and b_n respectively) that depend only on **n**:

$$G^n(y) = G(a_n + b_n y) \tag{3.24}$$

where $G(\cdot)$ indicates an extreme value distribution representing a limiting asymptotic form of the distribution of maxima. This equation is known as the **stability postulate** and any distribution that meets this equation is said to be

max-stable. With this as a basis, the limiting form of the distribution of the maximum from a parent distribution is:

$$\left[F_X(y)\right]^n = F_X(a_n + b_n y) \tag{3.25}$$

Fisher and Tippett gave three solutions to this equation, based on different values for a_n and b_n: the Type I, II and III limiting forms. Gnedenko (1943) established the strict mathematical conditions under which the Type I, II or III distributions form the limiting distribution for various forms of parent distributions – known as the **domain of attraction** of the parent distribution (Castillo and Sarabia 1992).

3.4.3 Jenkinson and von Mises

The three forms of limiting distributions, to which almost all distributions converge, are the Gumbel, Frechet and Weibull distributions (Gumbel 1958). Jenkinson (1955) and von Mises (1936) independently solved expression (3.25) for a single form: the Generalized Extreme Value distribution (GEV), given by:

$$G(y) = \exp\left\{-\left[1 - \xi\left(\frac{y-\mu}{\sigma}\right)\right]_+^{1/\xi}\right\} \tag{3.26}$$

where $[x]_+ = \max(x, 0)$ and where the parameters satisfy $-\infty < \mu < \infty$, $\sigma > 0$ and $-\infty < \xi < \infty$. The model has three parameters: location, μ; scale, σ; and shape, ξ. The Type II and III families correspond to the cases $\xi > 0$ and $\xi < 0$ respectively. The Type I family is the limit of $G(y)$ as $\xi \to 0$. The major benefit of using the GEV distribution is that, through inference on ξ, the data itself determines the correct tail model, avoiding the need to make a subjective **a priori** judgment on which of the Fisher-Tippett limiting forms to adopt.

The power of the concept of asymptotic limiting forms is that the actual form of the parent CDF $F_X(y)$ is not required for fitting the GEV (or indeed any of the extreme value distributions). It is worthy of note, however, that the speed of convergence with **n** repetitions of the parent distribution to the GEV varies: the normal distribution is notoriously slow, whist the exponential distribution converges rapidly (Cramér 1946). Figure 3.8 illustrates the exact and asymptotic (Gumbel) distributions from these two parent distributions – based on the constants a_n and b_n given by Galambos (1978) and Cramér (1946) and the methodology of Gumbel (1958).
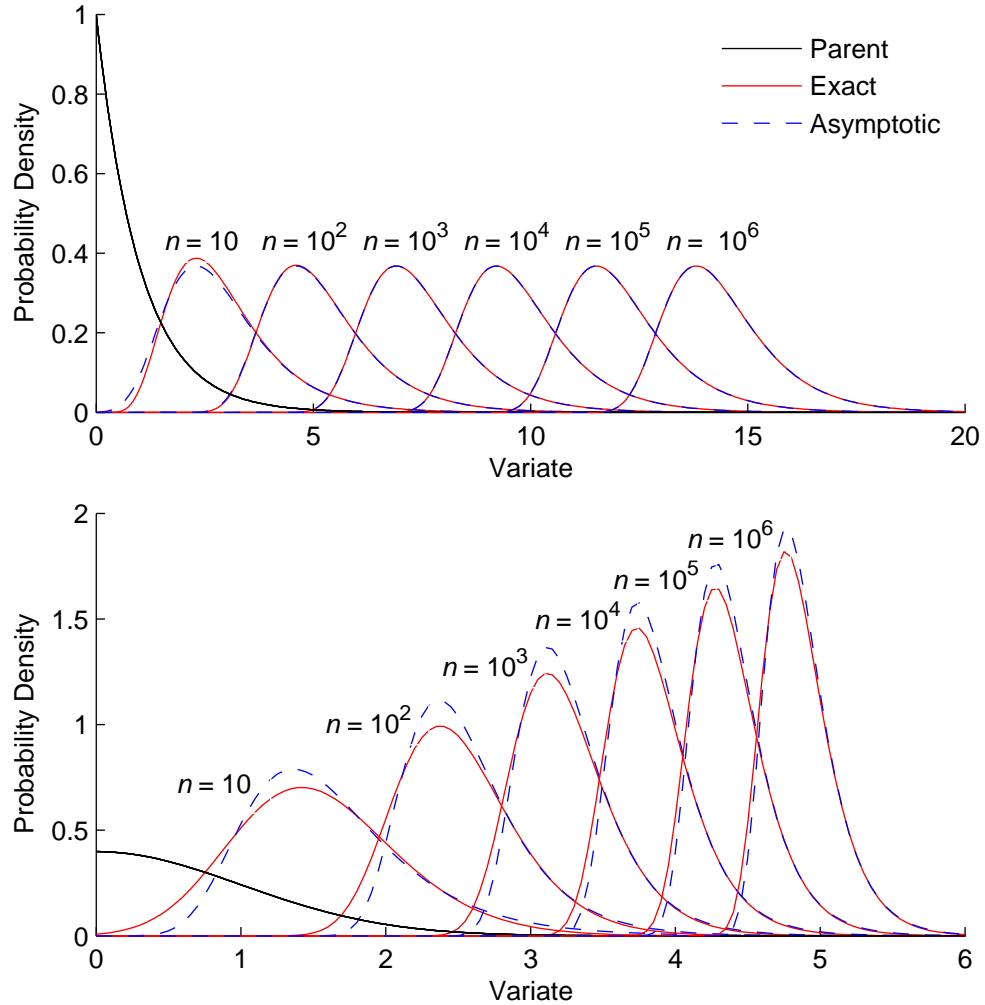
Figure 3.8: Asymptotic and exact distribution of maxima: (a) standard exponential distribution, and; (b) standard normal distribution.

From Figure 3.8, the difference in the speed of convergence for these two distributions is readily apparent. Castillo (1988) and Gomes (1984) discuss penultimate forms of asymptotic distributions; for suitable parameters the Weibull distribution (a particular case of the GEV distribution) can offer a better approximation of the distribution of maxima from a normal parent than its true asymptotic distribution (Gumbel). When it is necessary to check on the form of the parent, due to small sample sizes, speed of convergence tests may be used and are detailed in Galambos (1978).

3.4.4 Estimation

The method of maximum likelihood requires the maximization of the log-likelihood function. Optimization techniques often deal with minimizing functions. Hence minimization of the negative log-likelihood is usually performed. In this work, the GEV distribution is mostly used and Jenkinson (1969) gives the log-likelihood function for the GEV distribution:

$$l\left(\mu,\sigma,\xi;y\right)=-n\log\sigma-\left(1-\frac{1}{\xi}\right)\sum_{i=1}^{n}\log y_i-\sum_{i=1}^{n}y_i^{1/\xi} \qquad (3.27)$$

$$\text{where } y_i = 1 - \xi\left(\frac{x_i-\mu}{\sigma}\right) > 0 \quad \text{for } i = 1,\ldots,n \qquad (3.28)$$

For parameter combinations where $y_i < 0$ (which occurs when a data point x_i has fallen beyond the range of the distribution) the likelihood is zero and the log-likelihood will be numerically ill-defined. Solution of (3.27) is done by numerical means – there is no analytical solution. Jenkinson (1969) describes an approximate iteration technique for solving the equation which uses the **expected information matrix** (the matrix of second derivates of (3.27) with respect to each of the parameters). However Jenkinson only derived approximate values for this. Prescott and Walden (1980) detailed the elements

of the observed information matrix, $I(\theta)$, for the GEV distribution. They furthered this work (Prescott and Walden 1983) by proposing a Newton-Raphson technique which uses $I(\theta)$ and is found to converge quickly. Hosking (1985) presents an algorithm for the estimation of the parameters of the GEV distribution based on Prescott and Walden's proposal.

Good starting values for the minimization of the negative log-likelihood function of the GEV distribution are obtained from the method of probability weighted moments (PWMs) described by Hosking et al (1985). The exact solution requires iterative methods, but within the range usually encountered in practice, $\{-0.5 \leq \xi \leq 0.5\}$, Hosking et al (1985) have proposed an estimator, b_r, which uses the data, x_j, and is then used to solve for the other parameters in the sequence:

$$b_r = n^{-1} \sum_{j=1}^{n} \frac{(j-1)(j-2)\cdots(j-r)}{(n-1)(n-2)\cdots(n-r)} x_j \tag{3.29}$$

$$c = \frac{2b_1 - b_0}{3b_2 - b_0} - \frac{\log 2}{\log 3} \tag{3.30}$$

$$\hat{\xi} = 7.8590c + 2.9554c^2 \tag{3.31}$$

$$\hat{\sigma} = \frac{\hat{\xi}(2b_1 - b_0)}{\Gamma(1+\hat{\xi})(1 - 2^{-\hat{\xi}})} \tag{3.32}$$

$$\hat{\mu} = b_0 + \frac{\hat{\sigma}}{\hat{\xi}}\left[\Gamma(1+\hat{\xi}) - 1\right] \tag{3.33}$$

The PWM approach is written in C++ and used to initiate a C++ version of Hosking's (1985) algorithm. Data sets from Coles (2001a) are used to verify the output against published results. It is found, however, that there are cases in which Hosking's algorithm does not converge, or does not achieve the same minimum function value as the WAFO MATLAB toolbox (Brodtkorb et al 2000)

which was used occasionally to verify output. As a result, a more robust optimization method is implemented.

The Nelder-Mead (NM) optimization algorithm (Nelder and Mead 1965) is also known as the amoeba algorithm (**Numerical Recipes in C** – Press et al 1992) because of its slow robust movement across the **k**-dimensional surface of a function, where **k** is the dimension of the optimization problem. The NM algorithm is based on a simplex – a geometric shape with $k+1$ corners. Lagarias et al (1997) describe, in detail, the operations of the algorithm.

In the processing undertaken in the `AnalyseEvents` program (Chapter 4), the PWM method is used to initiate both the Hosking and NM algorithms – processing time is not substantial in any case. The program checks to see if the Hosking algorithm has a smaller negative log-likelihood than that of the NM algorithm. If not, the results of the NM algorithm are used. While good results can be obtained with manual re-injection of the Hosking algorithm, in general this is not possible for this research – the number of individual GEV fits is substantial for each run. Checks have been performed both against published results and other algorithms such as `WAFO` (Brodtkorb et al 2000) and `EVD` (Stephenson 2004) for the R-language (R Development Core Team 2005).

3.5 Prediction

Some of the solutions to Pearson's "fundamental problem of statistics" are described in this section. Initially the traditional extrapolation procedure – which uses a fitted distribution – is described. However, the variability of both the parameters and the data itself intuitively produce uncertainty in the estimate found in this manner. The delta method uses the asymptotic normality principle to estimate this variability, whilst the bootstrap method uses computational means to establish variability. Both methods are briefly described here.

3.5.1 The characteristic value and return period

The characteristic value is that value of a random variable that is expected to be exceeded once in a given return period. Given a random variable X, with distribution function $F_X(\cdot)$, the probability of exceeding a value, $\mathbf{u}$, is:

$$P\big[X > u\big] = 1 - F_X(u) \tag{3.34}$$

For a given return period, R, consider $\mathbf{n}$ repetitions of the sampling period, T_X, from which X was determined, such that:

$$n = \frac{R}{T_X} \tag{3.35}$$

In $\mathbf{n}$ such repetitions, the probability that the characteristic value, $\mathbf{u}$, will be exceeded is:

$$P\big[X > u \text{ in } n \text{ repetitions}\big] = n\big(1 - F_X(u)\big) \tag{3.36}$$

From the definition of a characteristic value, this probability must be equal to unity, that is, is expected to occur at least once in $\mathbf{n}$ repetitions, hence,

$$n\left[1-F_X(u)\right]=1$$
$$\Rightarrow F_X(u)=1-\frac{1}{n}$$

(3.37)

The characteristic value may therefore be determined by:

$$u=F_X^{-1}\left(1-\frac{1}{n}\right)$$

(3.38)

3.5.2 Extrapolation

In the work that follows, it will be usual to have a return period of 1000 years with each year comprising 50 working weeks of data with 5 working days per week, for reasons outlined in Chapter 4. The distribution obtained from the simulations is usually that of the maximum per day: the number of repetitions of the sampling period is then:

$$n_{1000}=1000\times50\times5=250\,000$$
$$\Rightarrow F_X(u_{1000})=1-\frac{1}{n_{1000}}=0.999996$$
$$\Rightarrow u_{1000}=F_X^{-1}(0.999996)$$

(3.39)

As described previously, this will correspond with a standard extremal variate derived from the Gumbel distribution as:

$$G_I^{-1}(0.999996)=-\log\left(-\log(0.999996)\right)$$
$$=12.429$$

(3.40)

An example of such extrapolation is shown in Figure 3.9 on Gumbel probability scale (Ang and Tang 1975, Section 3.2.3). Also, as the sampling period approaches the return period, the extrapolation distance decreases, intuitively resulting in an better estimate – though this needs to be proved using other methods.

There is inherent variability in the extrapolation process described: parameter estimates vary due to estimator uncertainty; the data varies; and different investigators may use different estimation techniques, which may or may not be biased. Prediction of a single number does not reflect the statistical nature of the underlying problem. Various methods for estimating the variability of the characteristic extreme are available; two are described next. Another method is preferred and described in Chapter 7 in relation to this research.
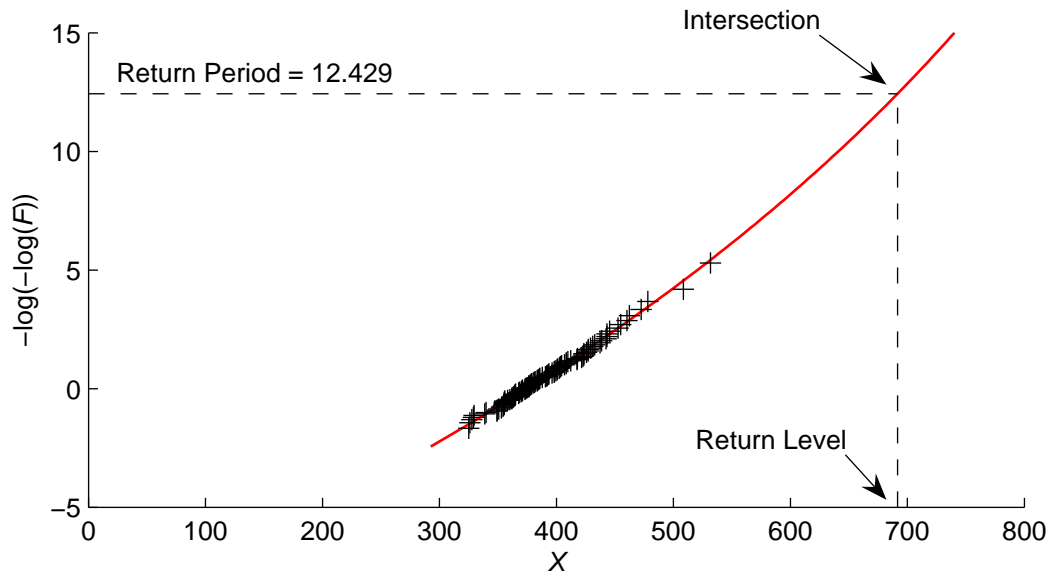
Figure 3.9: Sample extrapolation procedure.

3.5.3 The Delta Method and the normality assumption

The delta method for the approximation of moments of functions of random variables is usually based on a first-order Taylor series expansion of the function about the point of interest (Rice 1995, Oehlert 1992). Given a random variable X and a one-to-one function, $Y = g(X)$, the first-order Taylor approximation about the mean is:

$$Y = g(X) \approx g(\mu_X) + (X - \mu_X)\frac{d\,g(\mu_X)}{dx} \tag{3.41}$$

Noting that this is a linear function of $\mathbf{X}$, the linear transformation of variables rule (Mood et al 1974) gives:

$$\mathrm{Var}(Y) = \left(\frac{d\,g(\mu_X)}{dx}\right)^2 \cdot \mathrm{Var}(X) \tag{3.42}$$

Use of the matrix form of the Taylor series expansion (Beck and Arnold 1977) enables this to be extended to the case of several variables:

$$\mathrm{Var}(Y) = \nabla g(\mathbf{X}) \cdot \mathbf{V}_X \cdot \nabla g(\mathbf{X})^T \tag{3.43}$$

where $\mathbf{Y}$ is a scalar value of the function $g(\cdot)$ with parameter vector $\mathbf{X}$. $\mathbf{V}_X$ is the variance-covariance matrix of the parameter vector and $\nabla g(\mathbf{X})$ is the gradient vector of the function (Coles 2001a, Azzalini 1996, Efron and Tibshirani 1998, Lindsy 1996, Zacks 1971).

In (3.41) when $\mathbf{X}$ represents the (asymptotically) normally-distributed parameter(s) of a distribution, and as $\mathbf{Y}$ is a linear transformation of $\mathbf{X}$, then:

$$Y \xrightarrow{\ d\ } N\big(g(\mu_X), \mathrm{Var}(Y)\big) \tag{3.44}$$

where $\mathrm{Var}(Y)$ may be given by (3.42) for a single parameter function or (3.43) for a multi-parameter function.

For large sample sizes the delta method approximations give good results as a result of the central limit theorem (Mood et al 1974). However, for smaller sample sizes and where the linear approximation of the function in the region of interest is not good, the delta method can give inaccurate results (Rice 1995).

With respect to the GEV distribution used in this work, for $\mathbf{R}$ sampling periods, the maximum likelihood estimate of the characteristic value is got by rearranging the equality (3.37):

$$\hat{z}_R = g\left(R\right) = \mu + \frac{\sigma}{\xi} \cdot \left[1 - y_R^{\;\xi}\right] \tag{3.45}$$

where, $y_R = \log\left(1 - \dfrac{1}{R}\right)$. From (3.43), letting $\theta \equiv \mathbf{X} = \left(\mu, \sigma, \xi\right)^T$ and:

$$
\begin{aligned}
\nabla g\left(\theta\right) &= \nabla \hat{z}_R^{\,T} \\
&= \left[\frac{\partial z_R}{\partial \mu}; \quad \frac{\partial z_R}{\partial \sigma}; \quad \frac{\partial z_R}{\partial \xi}\right] \\
&= \left[1; \quad \xi^{-1}\left(1 - y_R^{\;\xi}\right); \quad \sigma\xi^{-2}\left(1 - y_R^{\;\xi}\right) - \sigma\xi^{-1}y_R^{\;\xi}\log y_R\right]
\end{aligned}
\tag{3.46}
$$

From (3.43) with the substitutions of (3.45) and (3.46) the distribution of $\hat{z}_R$ may be got from (3.44). The estimate notation on the parameters of the GEV was dropped for clarity: the expressions are evaluated at the estimates.

Implicit in methods like the delta method, is the central limit theorem and the assumption of asymptotic normality. Often it is not the case that the sample size is sufficient to converge to normality and the distribution may, in fact, be skewed. It is shown in Chapter 7 that the distribution of the bridge traffic load effect return level estimate is generally highly skewed and therefore highly non-normal. Therefore confidence limits, or variance estimates, based on the assumption of normality can give misleading results and should be avoided where possible.

3.5.4 Bootstrapping

The bootstrap has emerged as a fundamental tool in statistical analysis since its introduction (Efron 1979). This is, in part, due to the ready availability of

computing power and the intuitive nature of its application. Efron and Tibshirani (1993) and Davison and Hinkley (1997) both give thorough accounts of bootstrapping and its flexibility of use. Boos (2003) exemplifies the power of the bootstrap applied in a civil engineering, extreme value analysis, setting.

The bootstrap process (Figure 3.10) consists of re-sampling the original data (non-parametric bootstrap) or a model fitted to it (parametric bootstrap) and estimation of the statistic, $s(\cdot)$, of interest for the model. This process is repeated many times (bootstrap replications) and a distribution of the statistic of interest is found.
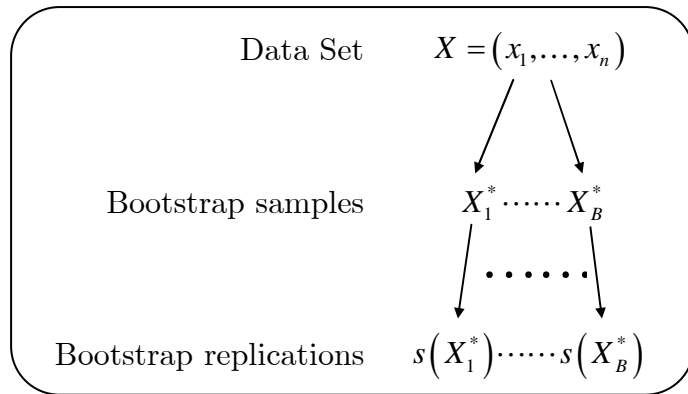
Figure 3.10: Illustration of the bootstrap process.

Extreme values are of particular importance to this work. Efron and Tibshirani (1993) describe a case where the bootstrap fails to give reasonable answers due to the sparsity of data in the tail, and the associated poor estimate of the true distribution by the empirical distribution (3.6).

As an illustration of this problem, and the non-parametric bootstrap process in general, consider a data set $x_1, \ldots, x_n$ randomly taken from a uniform distribution of bounds $[0, \theta]$. The maximum likelihood estimator for θ is:

$$\hat{\theta} = \max_{i=1,\ldots,n} x_i \qquad (3.47)$$
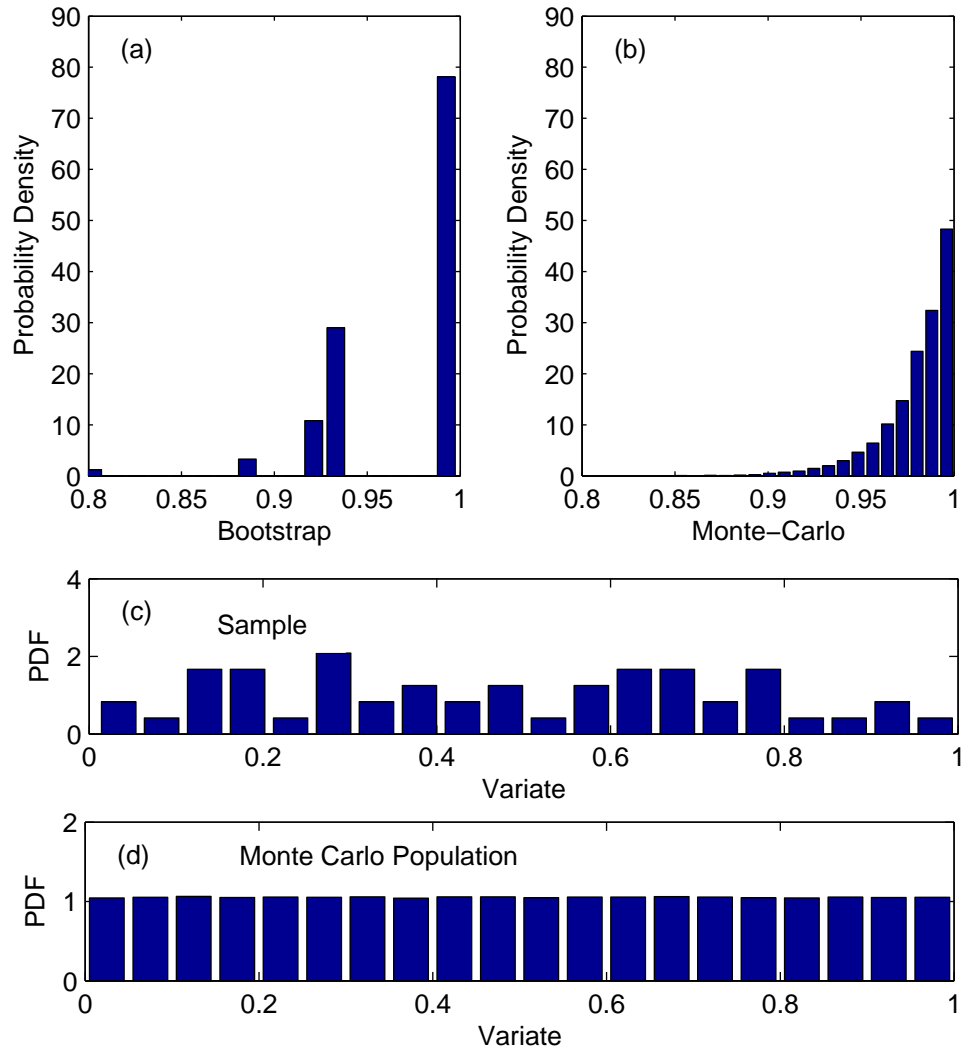
Figure 3.11: Problem noted by Efron and Tibshirani (1993): (a) non-parametric bootstrap estimate; (b) parametric bootstrap estimate; (c) sample histogram, and; (d) histogram of the parametric bootstrap populations.

For the interval $[0,1]$, $\theta_0 = 1$ and a sample of $\mathbf{n} = 50$ is generated on this interval from which $\hat{\theta} = 0.9858$; the histogram for the sample is shown in Figure 3.11(c). For each bootstrap replication, the data is sampled, with replacement, to provide a bootstrap sample from which an estimate of $\hat{\theta}_i^*$ is made. Such estimates are made for $\mathbf{B} = 1000$ bootstrap replications. The histogram of these estimates is shown in Figure 3.11(a). Further, to obtain an estimate of the actual distribution of $\hat{\theta}$, 1000 further samples of size $\mathbf{n} = 50$ were randomly

generated on the interval $[0,1]$. The resulting distribution of $\hat{\theta}$ is shown in Figure 3.11(b).

It can be seen from Figure 3.11 that the bootstrap distribution does not match that of the Monte-Carlo estimated distribution. Efron and Tibshirani (1993) refer the reader to Beran and Ducharme (1991) for further information on this problem. The example presented is a non-parametric bootstrap method; the parametric bootstrap method does not fail in this setting Figure 3.11(b). It is to be noted that the variability of the parameters of the parametric bootstrap cannot be taken into account (Efron and Tibshirani 1993); when compared to the method of Chapter 7, this becomes significant.

3.6 Summary

The basic statistical methods, essential to the work that follows, have been presented either in detail or by introduction and reference. Basic tools that will be used throughout this work, such as the method of maximum likelihood, probability paper, characteristic values, return periods and extrapolation have also been presented. More advanced tools that will be used further have also been presented, for example: profile log-likelihood, the bootstrap, Nelder-Mead solution of the GEV likelihood function, Fisher information, probability weighted moments, and the speed of convergence of the asymptotic extreme value distributions. Basic methods of prediction analysis such as the delta method and the bootstrap approach have also been presented.

Chapter 4

SIMULATION OF BRIDGE TRAFFIC LOADING

*"Anyone who attempts to generate random numbers
by deterministic means is, of course, living in a state
of sin"*   *– John Von Neumann*

Chapter 4 - SIMULATION OF BRIDGE TRAFFIC LOADING

4.1 Introduction

This chapter describes the measure, model and simulate phases of the bridge traffic load model used in this research. This approach has become more prevalent in recent years as more accurate unbiased measurements of real traffic have become available due to progress in Weigh-In-Motion (WIM) technology.

WIM measurement, and its accuracy, is investigation by many authors (Jacob and OBrien 2005, OBrien et al 2005). The implication of the accuracy of site measurements on resultant characteristic load effects has been studied by O'Connor (2001) and O'Connor et al (2002). The objectives of this research focus on the efficient use of expensive site data such that sufficiently accurate predictions of future load effect are made by further statistical analysis.

Basic statistical distributions of measured traffic characteristics form the input for the traffic model. Such an approach enables site-specific traffic characteristics to be generated which, even though not necessarily measured, represent those of the site. This chapter describes the modelling process undertaken for this research.

The software tools developed for this research are described in Section 4.5. The adoption of object-oriented programming techniques is shown to have significant benefit for traffic load simulation. Substantially increased periods of simulation are possible, increasing the amount of information available to the statistical analysis, which reduces uncertainty in the extreme.

4.2 Measurement of Highway Traffic

This work is based on traffic data from a number of European sites. The development of simulation methodologies is generally independent of the accuracy and amount of traffic data obtained from these sites. However, progress in the overall process does depend on having a sufficient quantity of data upon which reasonably general methods may be based.

WIM technology is the method through which the measured traffic data is obtained, and it is explained briefly in the following section. The work of Grave (2001) formed the early basis of this research programme and the sites analysed in his research are mainly used in this work. Those sites, and other sites also used, are described later in this section.

4.2.1 Weigh-In-Motion measurement

As outlined previously, highway traffic is essential to the bridge traffic load simulation process. Static weigh stations are generally not suitable for this purpose: it is known that traffic measured with such installations is often biased (Laman and Nowak 1997) as drivers of overweight trucks become aware of the installation and avoid the site. Therefore, for bridge traffic loading purposes, the measurement system must be unobtrusive so that unbiased data is gathered. Data should be recorded continuously for the duration of the recording period. Also, measurements of the traffic in free-flow are required to obtain headway, speed and overlapping data. WIM technology has been developed to meet these requirements. Pavement-based WIM systems use sensors located in the road to detect and weigh each of the axles. Alternatively, Bridge-WIM systems effectively use the bridge as a form of weighing scales. Either system can be used to collect traffic data that may be used in bridge loading studies. Recent

advances in the accuracy and durability of WIM technology have improved the accuracy of the measured truck and axle weight statistics (Jacob et al. 2002). O'Connor et al. (2002) have looked at the important issue of sensitivity of bridge loading to the accuracy of the original weight measurements.

Figure 4.1 illustrates the Bridge-WIM process; an example of a Bridge-WIM installation is shown in Figure 4.2 and a typical layout of the detectors is shown in Figure 4.3. For this layout, an example of the voltages realised by the passage of a truck is shown in Figure 4.4. A passing vehicle induces voltages in the axle detectors which give its speed, transverse position, number of axles, axle spacing and, importantly for flow and headway, the time stamp of arrival. The voltages induced in the strain transducers are processed with the axle detector information through a Bridge-WIM algorithm (OBrien et al 2005) to give the axle weights and GVW (Gross Vehicle Weight) for the vehicle.
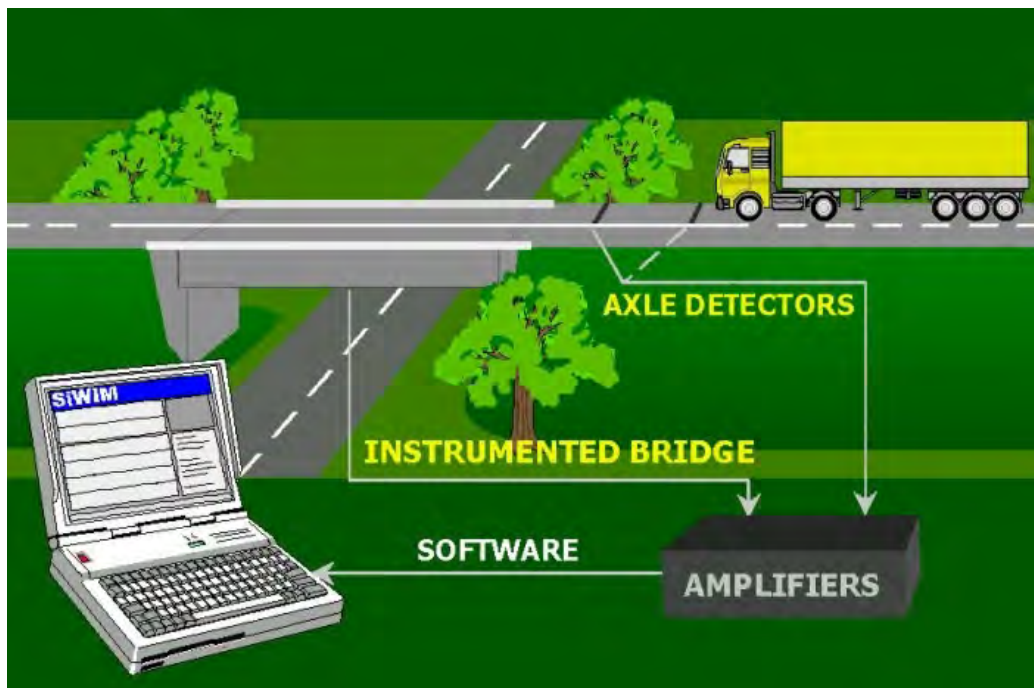
Figure 4.1: Bridge Weigh-In-Motion overview (courtesy of ZAG, Slovenia).

(a)   (b)

Figure 4.2: WIM installations: (a) road surface axles detectors; (b) bridge soffit strain transducers.
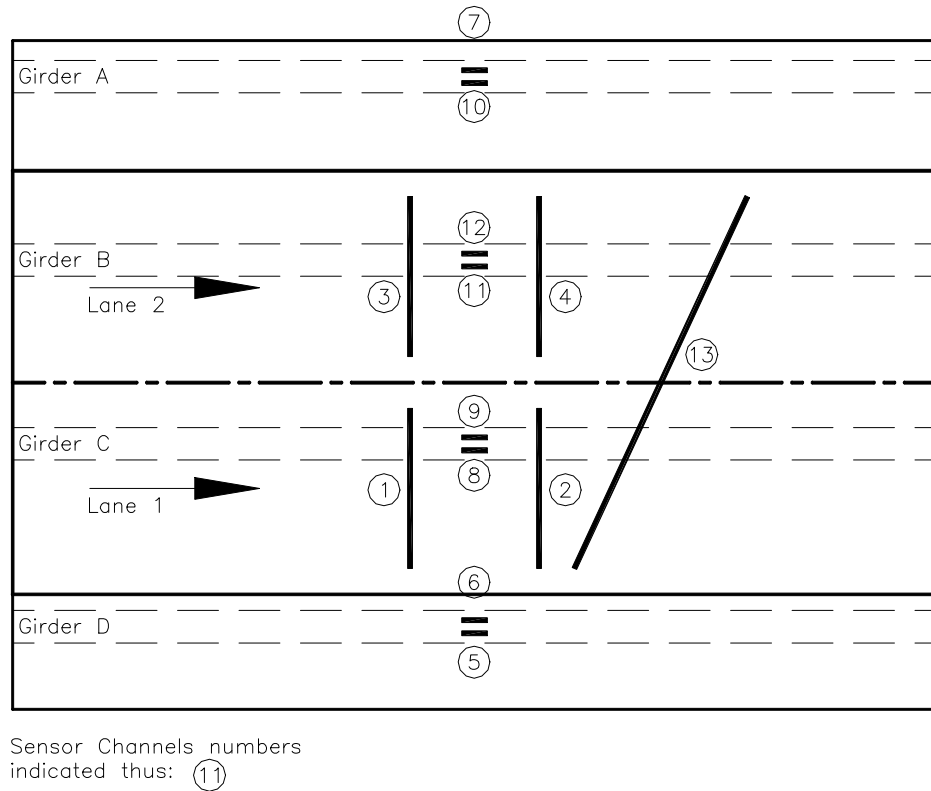
Figure 4.3: Typical Bridge-WIM installation showing the locations of axle detectors and strain transducers along with their channel numbers.
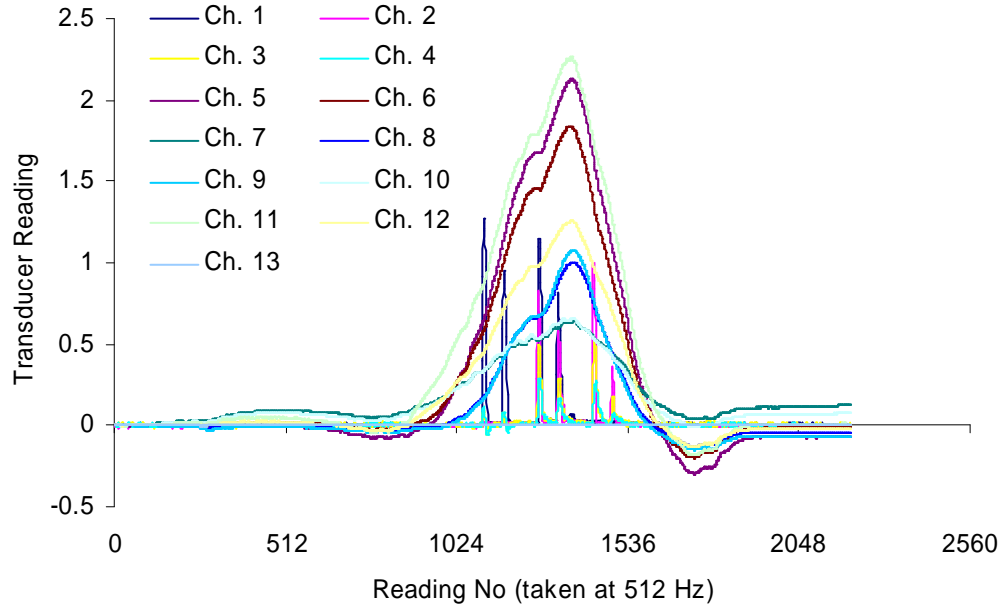
Figure 4.4: Sample Bridge-WIM data corresponding to the layout of Figure 4.3.

4.2.2 Description of sites and spans

French WIM Sites

Grave (2001) analyses the traffic characteristics of four French WIM sites in detail; the main characteristics of which are given in Table 4.1. These traffic data files were obtained from the **Laboratoire Central des Ponts et Chaussées** (LCPC) of Paris and some are deemed representative of general European traffic (Bruls et al 1996, O'Connor et al. 1998).

There are some limitations to the data from these sites that must be noted. Headway data for the A196 and A296 is not useable as truck arrivals were only noted to the nearest second – for accurate headway modelling (Chapter 5) it is required that times of arrival be noted to the nearest hundredth of a second. The recorded speeds for the Auxerre site are constant for each lane. Therefore, the speeds were given a variance in sympathy with that of the other sites.

Name of site	Auxerre (A6)	Angers (RN 23)	A196	A296
Road type	Motorway	National Route	Motorway	Motorway
Location	Near Auxerre	Near Angers	Near Ressons	Near Cambrai
Total no. of lanes	4	3	6	4
No. of lanes recorded	4	2	4	4
Time of recording	May 1986	April 1987	Sept. 1996	Sept. 1996
Duration of record	1 week	1 week	5 days	1 week
Average daily flow – Direction 1	3336	1536	8376	3024
Average daily flow – Direction 2	3408	1656	7536	3216

Table 4.1: The French WIM sites (Grave 2001).

Hrastnik Bridge, Slovenia

The Hrastnik Bridge (Figure 4.5) is analysed as part of a SAMARIS research project for European infrastructure needs. In total, 4 days of measurements were taken in April 2004. Average hourly flows of 25 and 24 for directions 1 and 2 respectively were recorded, though this is not a true representation due to the very low volume of truck traffic during the night. The peak truck flow occurs between 1100 and 1200 hours and is 59 and 55 trucks per hour for directions 1 and 2 respectively. The headway data got from this site is used to compare that of several European sites to aid the formation of the headway modelling method developed in Chapter 5.

Figure 4.5: Hrastnik Bridge, Slovenia.

Mura River Bridge, Slovenia

The Mura river bridge (Figure 4.6) is used to statistically analyse dynamic interaction of trucks and bridges. This is a two-lane, bi-directional, 32 m simply-supported bridge span which forms part of a multi-span structure. It consists of 5 longitudinal prestressed concrete beams, a reinforced concrete slab, and 5 transverse diaphragm beams. A 3-dimensional finite element model was developed by Brady (2004) for the bridge, and calibrated using field measurements. The use of this model is described in Chapter 8.

Figure 4.6: The Mura River Bridge.

4.2.3 Limitations of the WIM data

There are aspects to the WIM data recorded at the various sites that can limit the range of its applicability. An example of such an aspect is that only vehicles of greater than 35 kN were recorded at most of the sites but this is usual when the data is to be used for bridge loading purposes (Cooper 1995, Grave 2001, Galambos 1979). However, the incidence of lighter vehicles clearly has an affect on the spatial distribution of trucks, for example. Therefore, it is an implicit assumption that neglecting light vehicles does not have an affect on the bridge loading.

The age of some of the data sets used in this research could also be cause for concern. However, it is not the absolute value of characteristic load effect that is of interest in this work, rather the methodologies of use in its derivation. Therefore inaccuracies in the WIM data are not included in this work.

Of a more significant nature is the condensation of WIM data for 4-lane sites to input for the 2-lane bridge traffic loading model: the two outer lanes of such sites are used as the equivalent 2-lane traffic loading. This is a conservative assumption: it is well known that there is a tendency for cars to 'sort' themselves out from between trucks in a multi-lane environment (Hayrapatova 2006), resulting in a higher percentage of trucks than would usually be present on a two-lane road. The sorting phenomenon can be due to differences in desired speeds and differing speed restrictions, and may also be caused by small-vehicle drivers' preference for avoiding significantly larger neighbouring vehicles. An example of the sorting that occurs is shown in Figure 4.7.

Figure 4.7: Anecdotal evidence of sorting (A6 France, June 2005).

In conclusion, as this work is mainly concerned with developing procedures for the analysis of truck loading on bridges, and as general conclusions relating to truck traffic are not attempted, problems with specific data sets are not deemed significant. Further, should a detailed site-specific analysis be attempted, the measurement setup can be designed in advance to minimize factors that would contribute to error.

4.3 Statistical Considerations for Traffic Models

Traffic load models based on WIM data must faithfully represent the measured traffic. The statistics taken from a set of measured traffic data need to be carefully assessed to avoid introduced inaccuracy, or misrepresentation. In the following sections, the decisions and assumptions made in forming the traffic load model of this research are described. The underlying statistical relationships, temporal variations and considerations for subsequent extreme value analysis are discussed in relation to the measured WIM data.

4.3.1 Underlying statistical relationships

Traffic is a complex process and fundamentally is an outcome of many decisions made by many humans. For example, the peak in the GVW distribution near the legal limit reflects the economic-based decision-making of many hauliers. It is therefore possible to reason as to possible characteristics of traffic, and the relationships that may exist therein. Of course, not all such relationships are as the result of human intervention, other factors such as mechanical limitations can also play a part. In any case, many relationships do exist, and those important to bridge traffic load are assessed.

Speed and GVW

Due to the mechanical limitations of trucks, the acceleration and deceleration performance of heavily laden vehicles cannot be expected to match that of lighter vehicles. Drivers of such vehicles are expected to take this into account and drive at a safer, lower speed. Therefore it seems reasonable to expect a negative correlation between speed and GVW, and this is indeed the case (Figure 4.8), though it is not as significant as may be presumed.
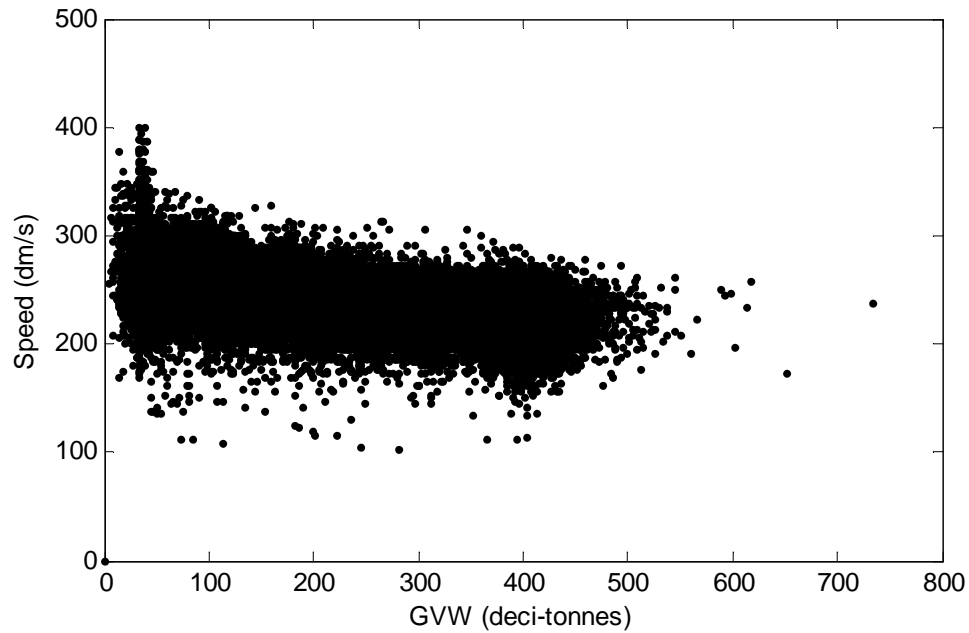
Figure 4.8: Speed and GVW relationship for the A196 site.

In the traffic model of this work, no allowance for this correlation is made. This is reasonable considering both the weakness of the correlation and the effect that speed has on the value of static loading events: it is headway that is more important.

Lead- and Following-Truck GVWs

Anecdotally, it would not be unusual for a fleet of similarly laden vehicles to leave a depot concurrently. Correlation between the GVW of these trucks may then be observed. On bi-directional two-lane bridges, such correlation could only occur with lead- and following-trucks. Further, correlated GVWs are only of interest if the trucks are sufficiently close to contribute to a same-lane 2-truck event. At a typical highway speed of 80 km/h, a vehicle travels nearly 90 m in 4 seconds. Therefore, for the Auxerre and A196 sites, lead- and following-truck GVWs are examined only when the headway is less than 4 seconds.

Histograms for the lead- and following-truck GVWs from the A196 and Auxerre sites are shown in Figure 4.9. It appears that there is little evidence for correlation – there does not appear to be significant differences between the lead- and following-truck GVW histograms for either site, allowing for some slight random variation. These histograms may be seen as the marginal distributions of a bi-variate frequency distribution which Figure 4.10 illustrates. It appears that the surface is reasonably symmetrical about the main diagonal. This further suggests that there is no significant correlation.
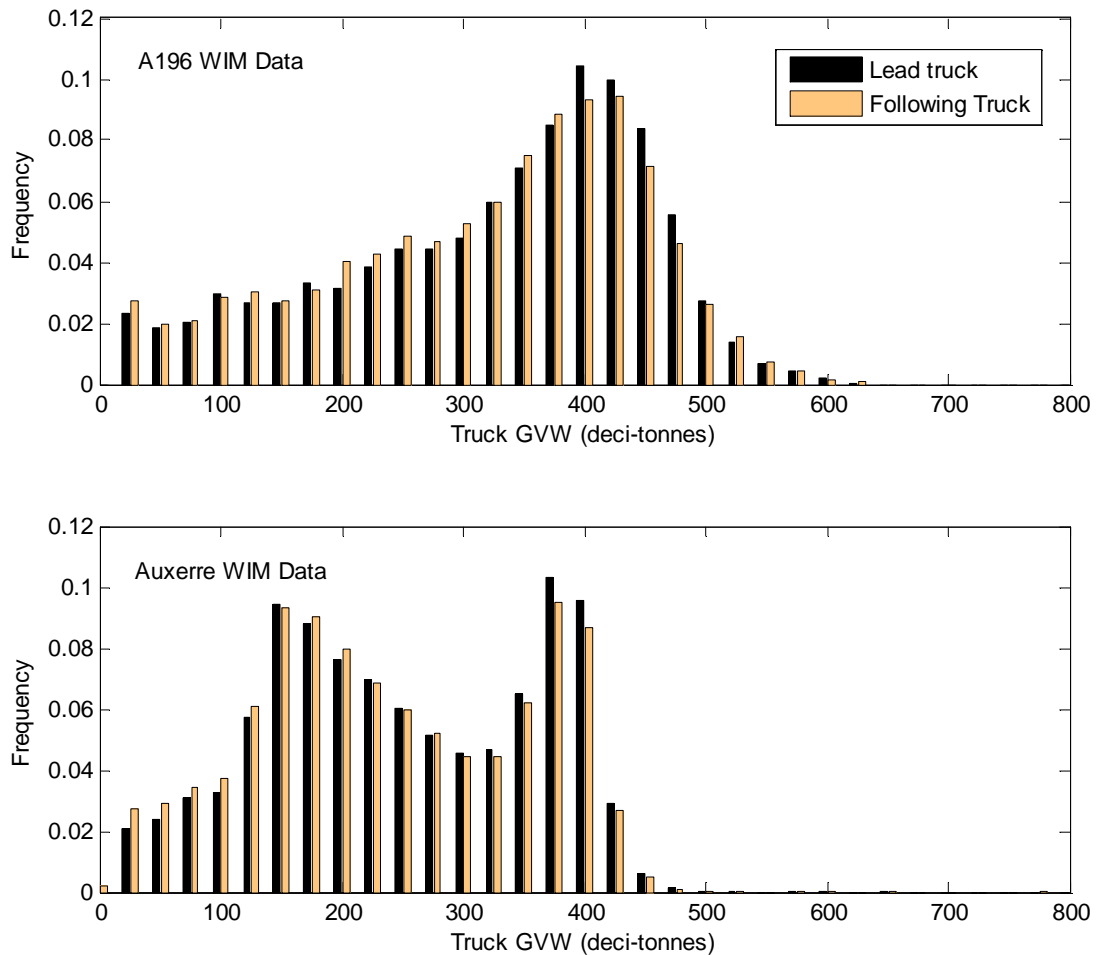
Figure 4.9: Histograms of lead- and following-truck GVWs for headways less than 4 seconds.
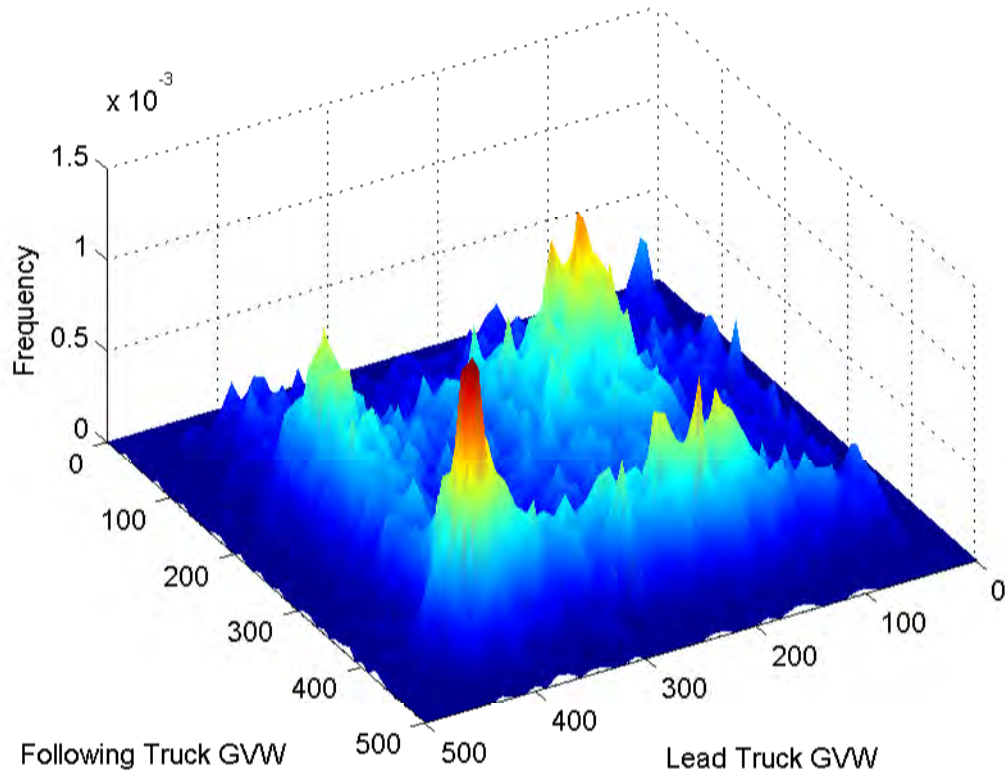
Figure 4.10: Frequency surface plot of the A196 lead and following truck GVW (in units of deci-tonnes).

The number of occurrences of trucks with correlated GVWs may not be of sufficient magnitude to noticeably affect the bi-variate distribution of all the trucks. It is therefore worthwhile to consider the deviations from true independence, which is represented as perfect symmetry about the main diagonal of the bi-variate distribution. Figure 4.11 shows the deviations from independence, represented as differences in the lower triangle from the upper triangle of the bi-variate distribution. There is no apparent pattern to the spread, though again it is possible that any real correlation may be swamped by random variation. Random error variation, by virtue of the central limit theorem is often thought to occur as normally distributed (Ang and Tang 1975, Mood et al 1974). The histogram of the deviations is also drawn in Figure 4.11. It can be seen that the variations appear to be normally distributed about zero.

It may thus be inferred that there is no apparent systematic deviation from true independence. It is to be acknowledged however, that correlated trucks, whilst so rare as to not distort the result presented from independence, may exist and may contribute to extreme events. As no information about such events is available, and based on the results presented here, in this work, no correlation between lead and following truck GVWs is allowed for.
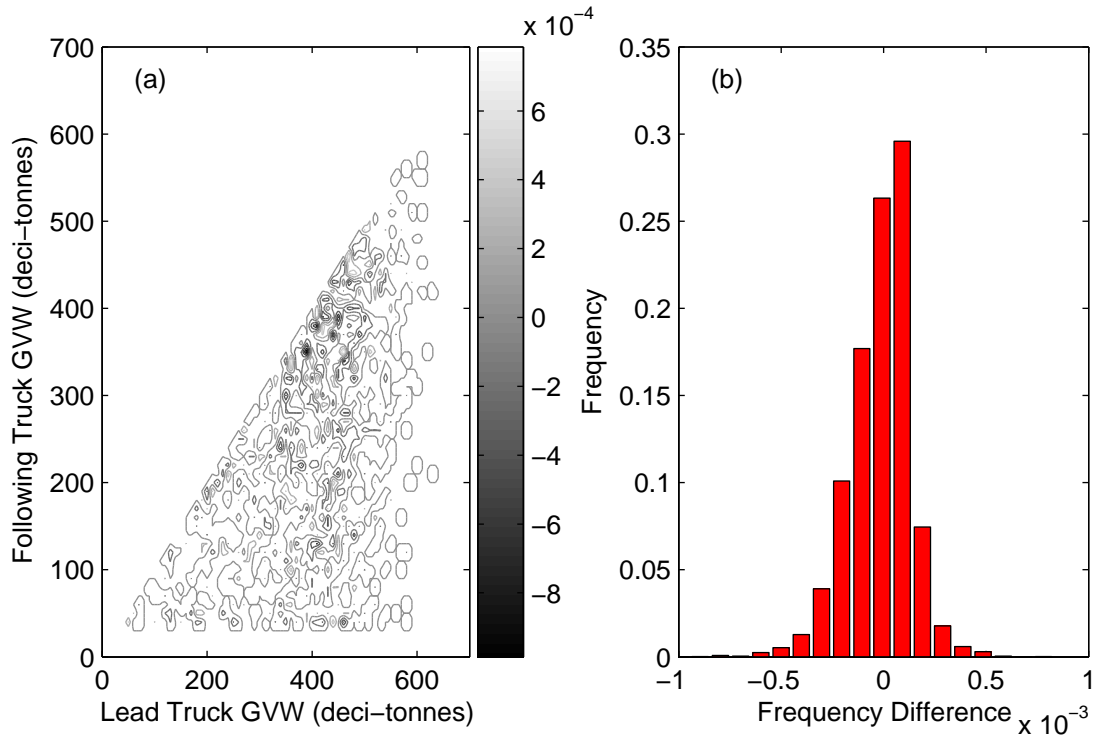
Figure 4.11: Deviations from true independence for A196 GVWs: (a) difference of lower triangle to upper triangle, and; (b) histogram of differences.

Correlation of Small Headways and Speed

Considering the characteristics of driver behaviour (Chapter 2), it is usual to presume that at higher speeds, distances between vehicles increase. The theory is that drivers aim to keep a sufficiently large time-gap to the vehicle in front, for their perceived reaction time, in case of incident. In this section it is investigated if there is correlation between speed and small headways. Truck drivers, however, are more highly trained and are often in communication with

other truck drivers. This may counter the previous argument. To test this, Angers WIM data is processed for the speeds of the lead and following trucks whose headway is less than 1.5 seconds. The results are plotted in Figure 4.12, along with linear trend lines for ease of interpretation. It can be seen there is not a positive correlation as may be thought, but rather a negative correlation. However, the correlation decreases when one considers the difference in speed. As the strength of correlation is small, it is reasonable to ignore any relationship between speed and headway, and this assumption is made in this research.
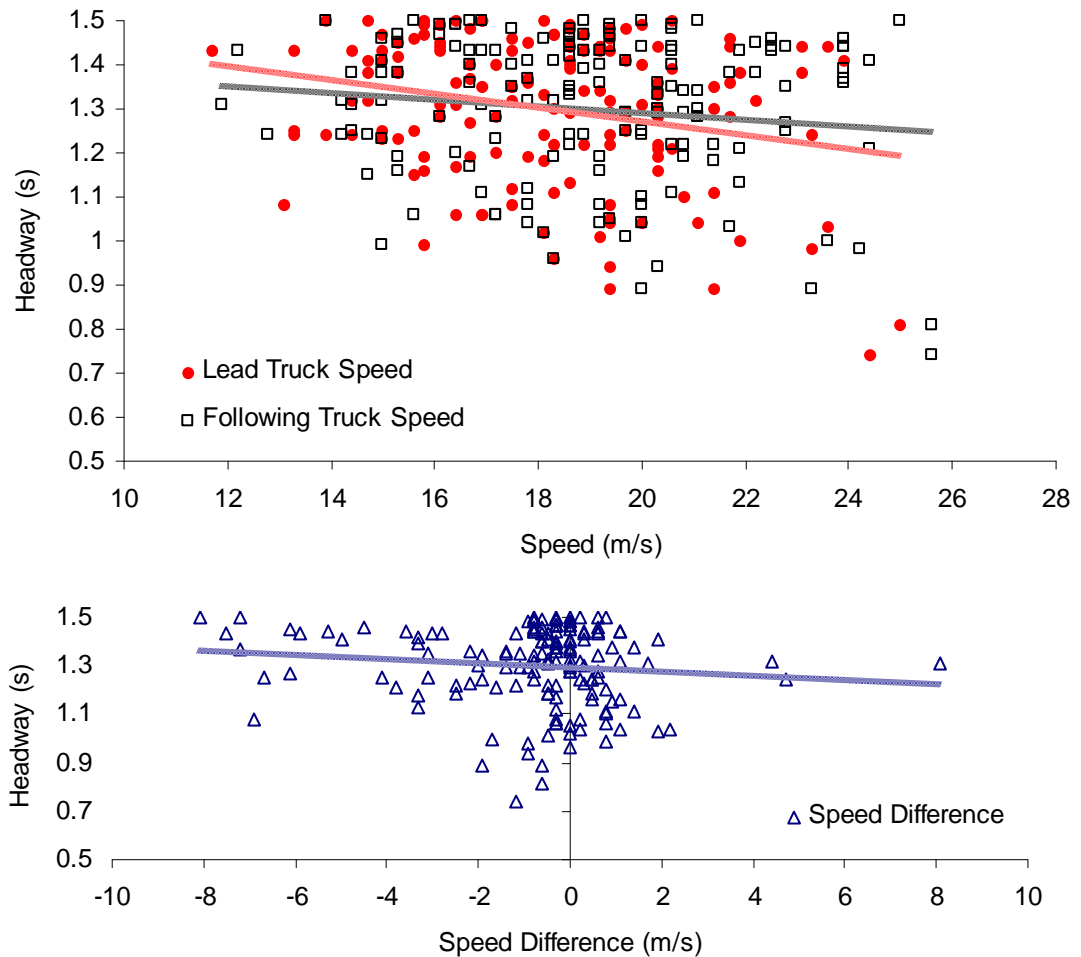
Figure 4.12: Speed and small headway correlation for Angers.

Included Correlations

Analysis of the WIM data for the French sites demonstrates that there are correlations that cannot be reasonably neglected. Grave (2001) has studied these sites in detail, and O'Connor (2001) has studied similar sites. In these studies it is found that, when axle weight is considered as a proportion of GVW, there is little correlation of axle-weights and GVW for 2- and 3-axle trucks. In contrast, Grave (2001), O'Connor (2001) and Bailey (1996) show and model the correlation between axle-weight and GVW for 4- and 5-axle trucks. This correlation is included in this work, as described in Section 4.4.1.

Whilst GVW and length are not explicitly related in the generated traffic, the individual axle spacings are generated and their sum defines the length. As the axle spacings' distributions are based on the measurements for the truck class (number of axles), the relationship between length and GVW is inherently catered for, though not explicitly. Further, as axle-spacings are modelled using tri-modal normal distributions, different forms of truck configurations within in each class are possible.

4.3.2 Representation of time

Temporal Variations

That traffic is dynamic is evident. Allowing for this temporal variation of traffic is therefore an important feature of any traffic model. In the following, two forms of variation are discussed: short-term, such as variations from hour to hour, and; long-term, such as an annual increase in traffic volume. The major consequence of such variations for bridge loading is in the headways between trucks: increasing the number of trucks in a given time interval reduces the headways, thereby increasing the likelihood of observing two or more same-lane trucks on the bridge concurrently.

It is well known that traffic is generally increasing year-on-year (European Commission 2004). Clearly, there are also seasonal variations, weekly variations, and, of course, daily variations. To allow for each of these variations, sufficient data must be obtained to estimate their distribution, thereby permitting modelling. As can be seen from the description of the sites given previously, there is often insufficient data to do this. In fact, there is only sufficient data to obtain reasonable estimates of the daily variation in traffic flow. As such, in this work, only daily variations in traffic flow are accounted for.

Hallenbeck (1995) studied temporal patterns of truck volumes in the United States. A significant finding is that weekend and weekday traffic exhibit different patterns. This is also the case for the sites studied in this work (Figure 4.13). Clearly this is due to the prevalence of economic activity on weekdays. Hallenbeck also notes that some sites may not exhibit this trend, depending on geographic location relative to industrial centres (for example). Another significant finding is that for sites with high truck volume, seasonal variations are stable, whereas the converse is true for sites with low truck volumes.
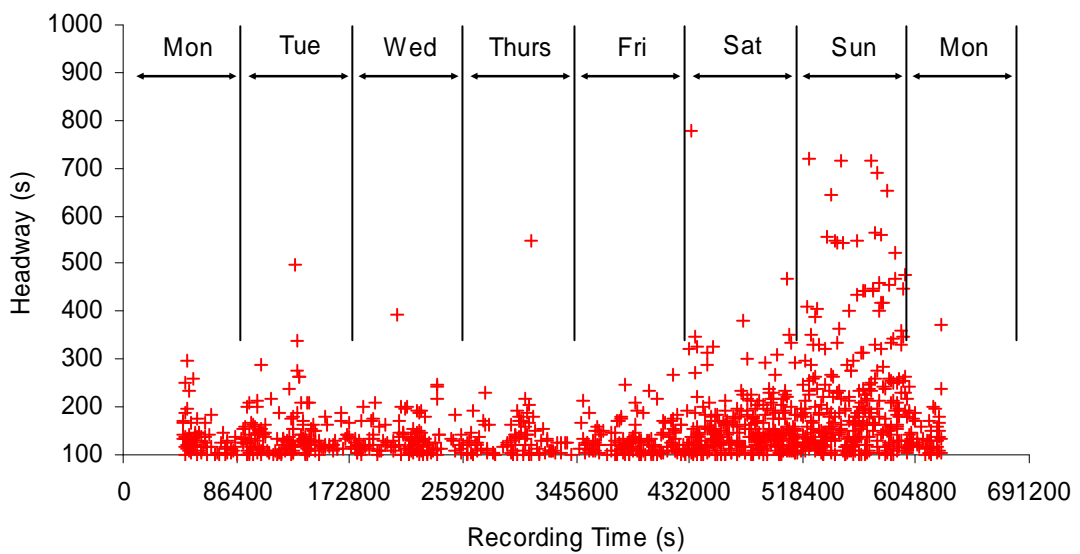
Figure 4.13: Large headways by day-of-week for Auxerre WIM data.

Homogenous Days

In the sites analysed for this work, traffic variations of periods longer than one day have insufficient data to form reliable estimates of their distribution. Therefore each day of simulation is based upon the same modelled variations: this is termed here as the 'homogenous day' model. That such a strategy is permissible, is based upon Hallenback's (1995) findings. Other authors have adopted strategies based on these finding also, in particular Cooper (1995 and 1997), Grave (2001) and Fu and Hag-Elsafi (1996). Notably, Crespo-Minguillón and Casas (1997) adopt a similar model but allow for variations with a period of one week. The homogenous day model accounts for the hourly fluctuations of traffic (with a period of one day) by using the average hourly flow measured for a given hour across all days of measurement. No account is made for daily, weekly, seasonal or annual variation in traffic. Such a model meets the requirements for ease of implementation and maximizes the use of available data. It is this model that is used in this research.

The Simulation Calendar

As will be shown in the following section, it is important for the data, upon which the extreme value analysis is performed, to be identically distributed. It would be unreasonable, in the light of the results presented above, to mix weekends and weekdays in the model due to their differing traffic properties. Some authors do, however, include weekend days in their studies (Ghosn & Moses 1985). In this work, only weekdays are modelled; therefore it is taken that 5 days of simulation represents one week of time.

Getachew (2003) notes that traffic during the holiday period in Sweden exhibits different properties than usual. Traditional holiday periods are well established across Europe. Such holidays, as well as public-holidays, are breaks in the

'economic calendar'. Therefore it is taken that the 'economic year' is equivalent to about 50 weeks of weekday traffic. In this study 5 days per week and 50 weeks per year is considered to represent a calendar year, that is, 250 'simulation days' per calendar year, representing the 250 working days per year.

For studies in which larger periods of traffic are simulated, monthly maxima are sometimes used instead of daily maxima (refer to Chapter 8 for an example). In this case, in this research, the term 'month' represents 25 working days and 10 such 'months' therefore represent a calendar year. This arrangement meets the requirements of ease of implementation whilst retaining a simple relationship to the calendar year.

4.3.3 Basis for extreme value analysis

Block Maxima Approach

The extreme value theory (Chapter 3) used to analyse the results of the simulations in this work has two major branches, the block maxima approach and the peaks over threshold (POT) approach.

The POT approach involves setting a threshold value and only recording those values which are greater than the threshold. An extreme value analysis may then be performed on the recorded values (Coles 2001a).

The block maxima method takes the single (usually) maximum from a set period of measurement. Many such periods give a population of maxima upon which an extreme value analysis may be performed. A pertinent example is the maximum wind speed per year (Cook et al 2003) – refer to Coles (2001a) for many others. It is possible to use a more general approach, termed Order

Statistics, and consider the top 5 or 10 values for a certain period – see Coles (2001a) and Smith (1986) for example.

The block maxima approach is wasteful of data; in environmental applications, for example, measurements are typically taken throughout the year and only lead to a single value (annual maximum). Another problem is that the second highest value in one block may be larger than the highest of another block; yet it is not accounted in the analysis. The POT approach avoids both of these problems. It, however, involves the choice of a threshold and the results of the method depend on the threshold choice.

The statistical analyses in this work are based on the block maxima approach. This method is readily applicable to the problems presented. Extension and adaptation of the method is relatively easy for further analysis. For this method, a block size is required, the length of which may not be arbitrary as maxima must be drawn from an iid (independent and identically distributed) sample. Coles (2001a) describes the temperature problem; daily temperatures will vary with the season, violating the iid assumption; seasonal blocks will also violate the iid assumption as summer and winter temperatures are not identically distributed.

Stationarity

Statistically, a random process which has characteristics that do not alter with time is said to be stationary and has the property of stationarity. Traffic, and thus its load effects, is therefore a non-stationary process, both over the short-term (hour to hour, for example) and the long-term. This may be seen from the discussion of Section 4.3.2. Clearly then, there may be problems with the modelling of the short- and long-term trends of traffic loading.

The extreme value theory applied in this work is based on the assumption of an underlying stationary process. For the theory to be strictly applicable then, this assumption must be met. A timeframe larger than the period of any variation incorporated into the traffic model meets this requirement - Figure 4.14. Therefore, as only hourly variations (with a period of one day) are included in this work, the stationarity requirement is met when a period of at least one day is chosen as the basis for further statistical analysis.
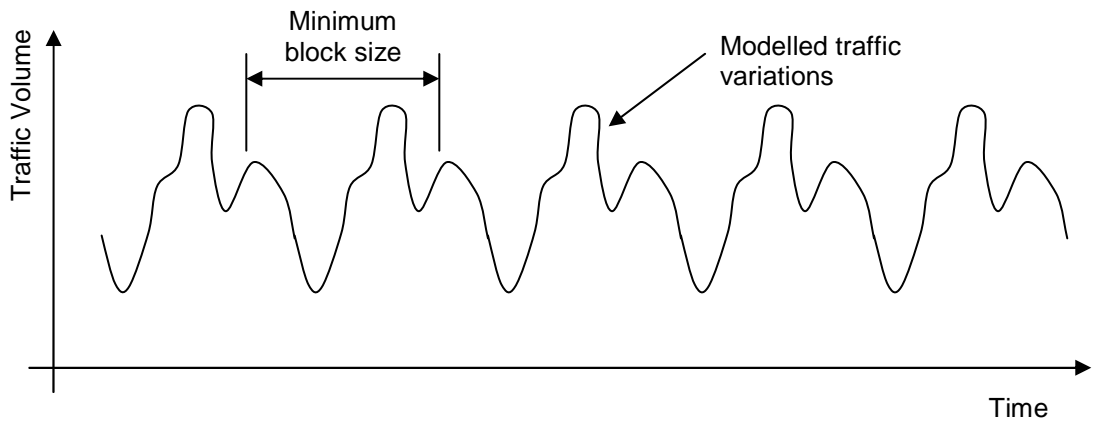
Figure 4.14: Extreme value analysis: required block size for the block maximum approach to traffic variations for iid samples.

In the long-term, the results of the statistical analysis are valid should the traffic characteristics not alter over the extrapolation period. Of course, this long-term stationarity is not met in practice. In this work, no allowance has been made to incorporate the effects of a change in the characteristics of the traffic over the long term.

Application

In this work, the problem of the choice of block size is analogous to that of Coles' temperature: the solution to which states that a timeframe larger than the period of any variation incorporated into a model must be used. Variations allowed for in the traffic model have a period of one day. As these variations

affect the resulting load effect, the iid assumption is violated. Therefore, any block size greater than, or equal to, one day does not violate the iid requirement.

Some authors (Grave 2001, Cooper 1995, Ghosn & Moses 1985) have chosen an arbitrary number of 'largest values' (such as the 'worst 100') or an inappropriate time period (such as 2.4 hours). Such a procedure is inherently subjective but it also mixes the extreme value approaches. A threshold is artificially introduced (the lowest of the data set) whilst the block maxima distribution (GEV) is then used instead of the Generalized Pareto Distribution, which is appropriate for a POT analysis. Such a scheme is therefore not recommended. Other authors recognize this and adopt the daily maxima approach; for example, OBrien et al (1995), Moyo et al (2002) and Cooper (1997).

4.4 Modelling Bridge Traffic Loading

4.4.1 Traffic characteristics

The traffic model required to simulate bridge load effects must be consistent with the measured traffic at the site it claims to represent. Yet, it is important that there is the potential for variation from the measured traffic in the model; otherwise the model would only represent multiple sets of the same traffic. By using parametric statistical distributions, the traffic model may remain sympathetic to the measurements, yet retain the capacity to differ.

Similarly to that of Grave (2001), the WIM data was analysed to determine the parameters of appropriate statistical distributions that characterize the measured traffic flow. The characteristics measured include the GVW, speed, headway, class of vehicle (based on the number of axles), flow rates, inter-axle spacing and the weight of each axle. The characteristics are modelled as described next.

Class Proportions

A truck's 'class' is defined here to be its number of axles. The traffic model uses the measured proportions of each class of vehicle. No allowance for variation from the measured proportions is made in the total amount of traffic simulated – variation exists within the days of this traffic, however.

Trucks with 6 axles or more are ignored. Grave (2001) shows that such trucks constitute a small proportion ($\leq 1\%$) of the measured traffic. Getachew and OBrien (2005) suggest that the effect of this assumption is not significant. However, it is possible that actual extreme events contain such vehicles, but due to a lack of data, they are not included in this work.

Gross Vehicle Weight

The distribution of GVW is known to be primarily bi-modal in nature (see Galambos 1979, for example). It is reasonably taken that this characteristic arises from peak frequencies of loaded and unloaded trucks. Figure 4.15 illustrates the GVW PDFs for a single site, showing that of each class and direction. It is clear that each class of vehicle exhibits strong bi-modal tendencies and it is usual to model such distributions with mixture of normal distributions. Bi- or tri-modal fits are used – it is useful to include a third mode (which does not have a clear physical interpretation) to increase the accuracy of the representation.
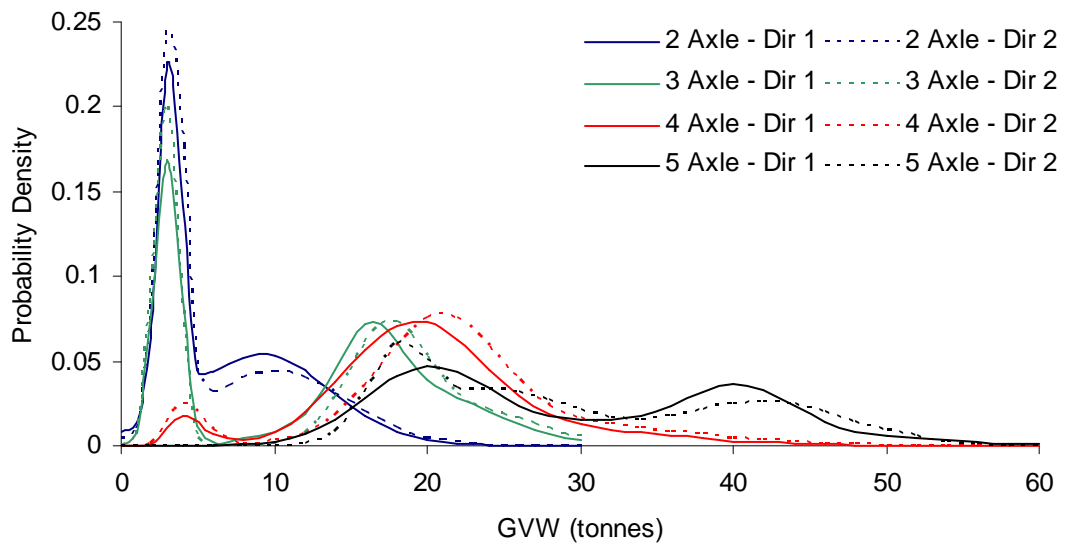
Figure 4.15: Example of GVW PDFs for each class and direction of a site.

Load effect is strongly affected by the shape of the GVW distribution and accurate fitting is therefore important. For this study, the method described by Grave (2001) was adopted: an iterative least-squares solution is found which gives special significance to the upper tails of the distributions by use of logarithmic plotting techniques. Such a method inherently entails a degree of subjectivity.

GVW is not considered as independent of direction (as may be seen from Figure 4.15). This allows for differing characteristics that may be observed on highways surrounding industrial areas, for example.

Axle Weights

Axle weights, when expressed as a proportion of GVW, are correlated with GVW for 4- and 5-axle trucks (Bailey 1996, O'Connor 2001, Grave 2001). For 2- and 3-axle trucks however, the correlation is not significant. Therefore, axle weights for these classes are modelled using bi- or tri-modal normal distributions. When generating the vehicle axle-weight characteristics, the axle weights are scaled appropriately to sum to the previously-generated GVW for that vehicle.

For 4- and 5-axle trucks, the correlation between GVW and axle-weights cannot be ignored. This is due to the uneven distribution of weight amongst the axles of a truck as its GVW increase. The rear tandem or tridem carries a portion of the load that increases with increasing GVW and it is assumed that the load carried by each axle in such axle groups is evenly distributed amongst the axles. The 4- and 5-axle truck model is based on fitting distributions to the measured proportions of GVW carried by each individual axle or axle-group: 12 five-tonne intervals of GVW are used. For each interval, the distribution of the proportion of GVW carried by first and second axles and the axle group is measured and then fitted using the normal distribution. This method requires the GVW to have been generated in advance.

As GVW is not independent of direction, and as axle weights are a function of GVW, axle-weight distributions are taken to be independent of direction.

Axle Spacings

Axle spacings are measured for each class of vehicle. Bi- or tri-model normal distributions are then used to model the measurements as appropriate. In this way, sub-classes of vehicle geometries are allowed for. Axle spacings are considered to be independent of direction.

Speed

Measured speeds are modelled using a normal distribution for each direction, independent of vehicle type or GVW (see Section 4.3.1).

Light Vehicles

The WIM data recorded often excludes vehicles of GVW less than 3.5 tonnes, as explained in Section 4.2.3. The model described and used in this research therefore excludes these vehicles. While insignificant in terms of the weight such vehicles contribute, their exclusion means that they do not affect the spatial disposition of trucks. The headway model of Chapter 5 is limited to the study of truck headways and its results are based on measured truck headways only.

By basing a headway model closely on the measured truck headways, the problems associated with the neglect of light vehicles are minimized. However, it may be that relationships existing in real traffic are lost in this way and there are no means to check this given the available data. More elaborate modelling based on comprehensive WIM data would be advantageous.

Discussion

In the modelling scheme described, the use of the normal distribution may not be ideal: its tails are unlimited in both directions, and there is no physical reason (and hence no theoretical justification) to expect normally distributed variables. Bailey (1996) uses the beta distribution for almost all of his traffic

characteristics, due to its flexibility and 'boundedness'. There is no doubt that more advanced modelling techniques could be applied to the modelling explained, though more data would be required to make the increase in accuracy gained from such an increase in sophistication meaningful.

4.4.2 Load Effect calculation

Influence line theory is used extensively in both the measurement and simulation stages of this work. Primarily, for this research, influence lines are used in the simulation stage of the analysis to determine the load effects caused by the passage of trucks. Both measured and theoretical influence lines are used, as well as influence lines determined from finite element analyses. Bridge-WIM systems use calibration runs (with vehicles of known geometry and axle-weights) to determine the actual influence lines of a bridge. Several calibration runs are required and the average influence line is used as input to the Bridge-WIM algorithm. The use of these measured influence lines extends the applicability of the load assessment procedure from mere theoretical considerations, to considerations of the actual behaviour of the bridge under investigation.

The software developed for this research requires an influence line to be specified by algebraic equations. For theoretical influence lines, the exact expressions are used whilst for measured influence lines, a number of quadratic or cubic polynomials are fit to segments of the influence line.

Theoretical Influence Lines

The theoretical influence lines used in this research are given in Table 4.2. Usually only influence lines 1 to 3 were post-processed statistically: they are deemed to represent a sufficiently wide variety of shapes such that sensitivity of load effect to the influence line shape alone may be detected
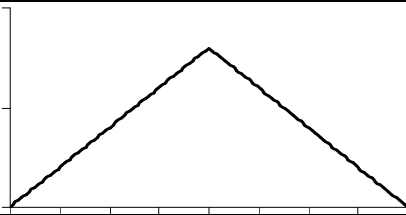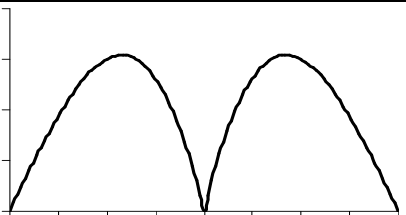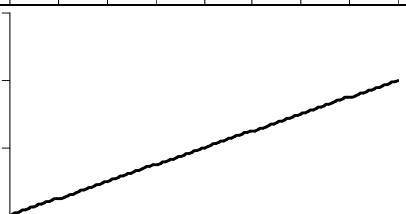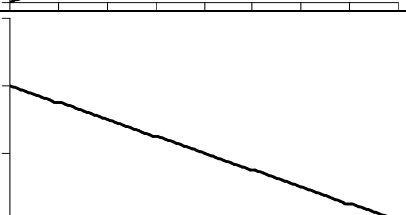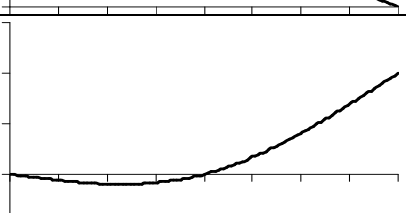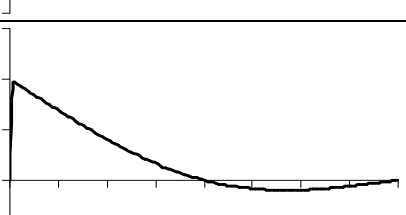
IL Index	Description	Graph
1	Bending moment at the centre of a simply-supported span.	
2	Bending moment over the central support of a two-span bridge.	
3	Right-hand support shear force for a simply-supported span.	
4	Left-hand support shear force for a simply-supported span.	
5	Right-hand support shear force for a two-span bridge.	
6	Left-hand support shear force for a two-span bridge.	

Table 4.2: Theoretical influence lines used.

Influence Lines for the Mura River Bridge

The influence lines for mid-span stress of the five longitudinal girders of the Mura River bridge study are based on a calibrated finite element model of the bridge rather than WIM measurements. Each girder has an influence line for each lane of travel and quadratic equations are fit for use in the simulations.

Figure 4.16 shows the general arrangement of the structure; Figure 4.17 gives the influence lines for the five girders for each lane of travel. As the driving lanes are not symmetrically located, the influence line for Beam 1, Lane 1 is not exactly the same as its symmetrical counterpart, Beam 5, Lane 2. Nonetheless, the difference is one of scale, and this fact was exploited in the algebraic representation of the influence surface to minimize the complexity of the model.
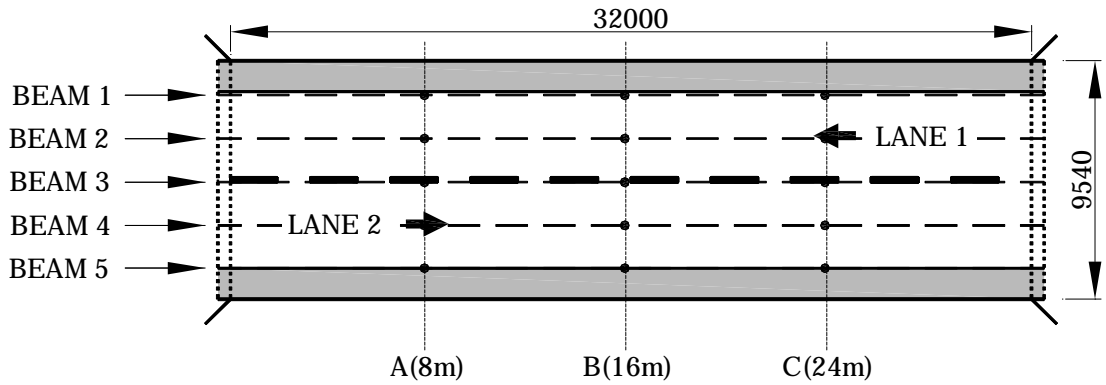
Figure 4.16: General arrangement of Mura River bridge.
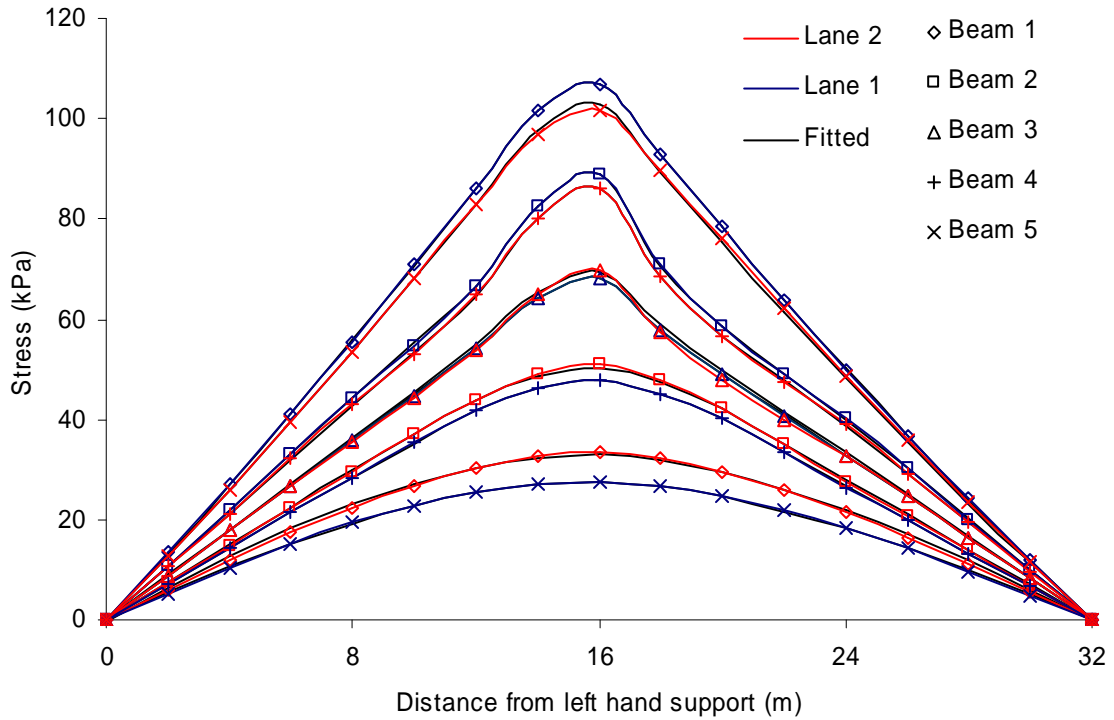
Figure 4.17: Influence lines for the Mura River bridge.

The quality of the fits to the finite element influence lines may be seen from Figure 4.17: these lines are drawn in black on the figure but are mostly obscured by the fits. Slight differences may be seen at the peak of Beam 5, Lane 2 and Beam 3, for both lanes, for example. These differences are deemed acceptable and have been shown to have a negligible impact on the results by static comparison of the finite element model results with the results of the load effect algorithm used in this research

4.5 Simulating Bridge Loading

4.5.1 Introduction

With the foundations laid in the previous sections of this chapter, the 'simulate' phase of the bridge traffic load calculation is discussed. Fundamentally, it is a Monte-Carlo simulation process that is used to generate artificial traffic which is used to calculate its associated load effects. Rubinstein (1981) gives a thorough introduction to the technicalities of the subject.

The software tools developed to generate random traffic and calculate the load effects therefrom are described in this section. Also described is software developed for other aspects of the research. Table 4.3 outlines the function and language used by the main tools developed. The first three programs are the most important to this work. Appendix A outlines the use of the programs.

Also given in Table 4.3 is the language used for the respective program. Different environments and languages were used as appropriate to the problem under study. In particular, the object-oriented programming approach was adopted for the large-scale numerical calculations. This is explained in more detail in Section 4.5.3 after the description of the random number generation process used for this work.

Name	Purpose	Language
GenerateTraffic	Generation of synthetic traffic file.	C++
SimulTraffic	Static analysis of loading events from a traffic file.	C++
AnalyseEvents	Statistical analysis of load effect data.	C++
ReadTrafficIn	Statistical analysis of the traffic characteristics of a traffic file.	C++
MCSim	Monte Carlo simulation from many distributions.	C++
TruckBrowser	Visualisation of the contents of a traffic file, truck by truck.	Visual Basic
AnimateEvents	Animation of the loading events.	Visual Basic
S.of.T.onBridges	Visual interface for GT, ST and AE.	Visual Basic
MultiMLE	Maximum likelihood fits of many distributions to a data set.	Matlab
PredLike	Predictive likelihood for a single data set.	Matlab
MMPredLike	Predictive likelihood for composite distribution statistics.	Matlab
MultiVarEVT	Analysis of total and static extreme load effect (Chapter 8).	R
UpDateGraphs	Interface for the amalgamation of results in many Excel files.	Excel VBA

Table 4.3: List of main software applications developed during this research

4.5.2 Random number generation

Generating the traffic requires Monte-Carlo simulation, the basic tool of which is a (pseudo-)random number generator (RNG). The prefix 'pseudo' indicates that the use of a computer is an inherently deterministic process and resulting deviates can only approximate true randomness (Knuth 1997). Rubinstein (1981) describes the importance of random number generation in Monte Carlo simulation and the fundamentals of computer-based RNGs.

The RNG initially used was `ran2()` of **Numerical Recipes in C** (Press et al 1993). This RNG takes the minimal sufficient RNG of Park and Miller (1988) and modifies it with the Bays-Durham shuffle. However, as the work herein progressed, it was discovered that there were some inconsistencies with the results got from this algorithm: numbers very close to unity were essentially deterministic (though the machine epsilon – a measure of the numerical precision of a computer – used is 2.2×10^{-16}). In generating sequences of maxima from a parent distribution, it is essential that numbers close to unity are random also. Further, as the number of trucks capable of being generated increased (to around 8.5×10^6), problems with period exhaustion and serial correlation became more likely (Press et al 1993).

To alleviate any possible problems with the RNG to be used, the virtual pseudo-random number generator described by L'Ecuyer et al (2002) was adopted, and all work presented herein is based on its use. This generator gives excellent results, even for values very close to unity. This is due to its double precision methodology. It can have multiple separate streams, each of which is based on the multiple recursive generator MRG32k3a (L'Ecuyer 1999) which has a period of 2^{57}; the seeds of each stream are separated by 2^{127} steps. This is useful when multiple random deviates are required: for example, the Box-Muller

transform for normal deviates requires two uniform deviates (Box and Muller 1955). In this case therefore, two separate streams of L'Ecuyer's RNG are ideal. This RNG is supported by published tests of its randomness (L'Ecuyer 1999, L'Ecuyer et al 2002).

4.5.3 Object-Oriented Programming

The three main programs developed for this work, `GenerateTraffic` (GT), `SimulTraffic` (ST) and `AnalyseEvents` (AE), are written using an object oriented (OO) programming. This method is different to traditional procedural programming as virtual 'objects' are coded to behave in ways similar to their real-life counterparts. More powerfully, abstract concepts may be used.

This work has mainly exploited the encapsulation principle of object oriented programming (Stroustrop 1997). Encapsulation allows different ideas, functions and data to be made distinct from the rest of the program – a 'black box' object or 'class'. The program uses the service that the class offers, without access to its inner details. This 'modularization' of the code has a number of advantages:

- Extension: problems usually associated with extending a piece of procedural code (trivially, difficulties in naming variables, for example) are avoided. Therefore it is easier to extend without affecting the logic of other parts of the program – for large programs this is a significant advantage.

- Reuse of code: it is only ever necessary to write the code for a certain feature, function, or class once – the class can be instantiated (declared) as often as required, and in many different guises in a single program or across several programs (such as is the case here). This is not the case with procedural programs in which more code must be added to each program.

As an example of the approach, the virtual object for the truck, a fundamental element in this work, is explained. The properties of the physical truck are

programmed into the CTruck class (for example, number of axles, GVW etc.). CTruck only allows the rest of the program access to these class members through an appropriate interface – this reduces logic errors in the program. In addition, CTruck has a number of actions it can perform; termed as class functions. For example, CTruck returns its time of arrival on the bridge, writes itself to file, or deletes itself when asked by an external function. Critical to this research, the CTruck class is treated as a single piece of data and (large) arrays (C++ STL <vector> class) of such objects are therefore used to contain the artificial trucks in the computer memory. As a fundamental object for all of the software required for this research, the CTruck class is used in all the programs.

As an example of an abstract class, the CEffect class encapsulates all the information pertaining to a crossing event for a particular influence line. It includes the comprising CTruck objects; the start time; truck arrangement at the instant of largest load effect; the maximum load effect and the (IL) index number of the load effect. Methods attached to the CEffect class allow it to write itself to a file, as well as answer any 'queries' regarding its contents. For a single crossing event, there are therefore 15 (the number of influence lines) instances of the CEffect class. These are, in turn, stored in another container class called CEvent. Therefore, in this application of CEvent the trucks are similar across all of the CEffect class members. As an example of the re-use of code possible, a different application of CEvent holds the CEffect variables for the daily maximum (for example) load effect for each of the influence lines. In this application of CEvent, the trucks for each CEffect object will be different, reflecting the different loading events critical for different influence line shapes.

One further significant benefit is that use of the OO approach allows proper integration of the C++ Standard Template Library (STL) – a library of

standard functions. Incorporating these efficient algorithms and structures allows the code to be more efficient in terms of memory and processing speed, easier to read and maintain, portable, and more robust.

4.5.4 GenerateTraffic

The generation of synthetic traffic is performed with the `GenerateTraffic` program. This program consists of the classes shown in Table 4.4, shown along with the purpose of each. It is to be noted that this program draws a lot of functionality from the C++ STL (Stroustrup 1997). The main alogorithms of this program are similar to those of Grave's (2001) program.

Class Name	Function
`Main.cpp`	Main function loop.
`CGlobals`	Communicates global variables to classes.
`CFilesIn`	Reads the traffic characteristics (model) input files.
`CRngStream`	Uniformly-distributed random number generator of L'Ecuyer et al (2002).
`CDistValues`	Changes uniform random deviates into deviates of other distributions using the inversion method (Rubinstein 1981).
`CGenTruckFlow`	Generates each of the traffic characteristics and assembles the `CTruck` variables.
`CTruck`	The basic truck object.
`CTruckGroup`	A collection of `CTruck` objects with some functionality.

Table 4.4: Outline of the `GenerateTraffic` program.

4.5.5 SimulTraffic

The `SimulTraffic` program passes the (generated or measured) traffic across a number of bridge lengths and calculates the load effects for each of the influence lines outlined previously. The function of this program is similar to that of Grave (2001). The program structure is given in Table 4.5.

Class Name	Function
`Main.cpp`	Main function loop.
`CGlobals`	Communicates the common variables to classes.
`CAnalyseEvents`	Post-processes the collection of `CEvent` objects and outputs results.
`CCalcEffect`	Returns load effects from influence lines based upon axle weight, axle position, lane number and bridge length.
`CCrossEvent`	Carries out the analysis of a significant crossing event given the comprising trucks and bridge length to be analysed.
`CEffect`	Stores information for a single load effect from a crossing event (refer to Section 4.5.3).
`CEvent`	The collection of `CEffect` for all load effects from a single crossing event, or, the collection of post-processed `CEvents` from `CAnalyseEvents`.
`CTestCrossingEvent`	Sequentially analyses the truck stream to determine the presence of a significant crossing event.
`CTruck`	The basic truck object
`CTruckGroup`	A collection of `CTruck` variables with some functionality

Table 4.5: Outline of the `SimulTraffic` program.

The traffic file output from `GenerateTraffic` (described in Appendix A) is read into `SimulTraffic`. When the traffic files are large (600-700 MB), this can create problems with memory on 32-bit machines. In this work, up to 5 years of traffic (1250 days) can be generated for Auxerre using `GenerateTraffic`. However, `SimulTraffic` can only cater for 4 years of Auxerre traffic because it must store the results from each crossing event as well as the original traffic file. Profiling of the code has shown that it is very efficient. The 32-bit architecture of the computers used means that the finite number of RAM addresses possible causes the limitations observed. Previous work (Grave 2001, O'Connor 2001) did not approach this limitation of 32-bit machines.

To minimize processing, only Significant Crossing Events (SCEs) are processed. These are defined as any Multiple Truck Presence Event (MTPE) or the occurrence of any truck with GVW over 40 tonnes. The program (`CTestCrossingEvent`) chronologically searches the truck traffic for such SCEs. When one is found, the trucks involved are passed to an algorithm (`CCrossEvent`) that uses all the influence lines programmed (`CCalcEffect`) to derive the induced load effect. The trucks are passed across the bridge in 0.02 seconds steps (less than 0.45 m for a speed of 80 km/h) as recommended by Grave (2001); at each step each load effect is calculated – this is in comparison with 0.2 seconds used by Bailey (1996), for example. The maximum value of each load effect is kept for further analysis, as well as the time it occurs at, and the front axle position of the first truck on the bridge.

Following the analysis of all the trucks (and the associated SCEs), a large collection of events (`CEvent`) is stored. The memory requirement for this is around 25% of the size of the traffic file input. Therefore, some initial post-processing of the results is done prior to outputting to file. Though strictly part

of the statistical analysis of the loading events, it is necessary to do this processing here due to the time and storage space otherwise required. Daily maximum and (as appropriate) monthly maximum load effects are output for each load effect and each day/month (see Section 4.3.3). This output then forms the input for the statistical analysis program `AnalyseEvents`.

4.5.6 AnalyseEvents

The statistical methodologies of Chapter 6 are incorporated into this program. Reference to this chapter is required for more information regarding the functions that the program performs – outlined next. The classes used in this program are given in Table 4.6.

The events read in from `SimulTraffic` output (`CReadEvents`) are separated for each load effect of interest. For reasons outlined in Chapter 6, it is necessary to analyse each of the types of MTPE, that is, whether it is a 2-, 3-truck event etc., separately. This means that, for each load effect, for each span, there are (normally) up to 4 to 5 different data vectors which are fitted (`CGEV`) using the GEV distribution (see Chapter 3). These fits are stored (`CGEVanal`) and then used in further statistical processing (`CMixMech`). For each load effect and each bridge length, the program outputs the predicted lifetime load effect for 28 different return periods (1 to 250 000 years, for completeness). Also output is information about the data and the fits that can be further processed to obtain illustrations of the fits and the extrapolation process. Further, the program outputs the input data for the analyses described in Chapter 7.

Class Name	Function
`Main.cpp`	Main function loop.
`CReadEvents`	Reads the events files output from `SimulTraffic`, performs various interface functions for the other objects and writes the effects of further interest to file.
`CEffect`	Stores information for a load effect from a crossing event (Section 4.5.3).
`CEvent`	The collection of `CEffect` for all load effects from a single crossing event, or, the collection of post-processed `CEvents` from `CAnalyseEvents`.
`CTruck`	The basic truck object.
`CPredExtrem`	Using `CMixMech`, calculates and writes the extrapolation results based on the input data.
`CMixMech`	Performs composite distribution statistics and outputs data for diagnostic plots.
`CGEVanal`	Stores the parameters, variance-covariance matrix and the data for a single GEV fit.
`CGEV`	Fits a GEV distribution to a given data vector.
`CSimplex`	Nelder-Mead minimization (Chapter 3) – used by CGEV.
`CKStest`	Performs a Kolmogorov-Smirnov test on fits to data.
`CMatrix`	A matrix class, used in the `CSimplex` class.
`CDistValues`	As per GT – used for bootstrapping in `CMixMech`.
`CRand`	Returns uniform random deviates using ran2() of **Numerical Recipes in C** (Press et al 1993) to `CDistValues`.

Table 4.6: Outline of the `AnalyseEvents` program.

4.6 Summary

This chapter has presented the means by which load effect data is obtained for a statistical analysis. Site measurements using WIM stations are described and the elements that may contribute to inaccuracies are mentioned. The use of the WIM measurements is also presented: traffic characteristics are analysed and statistically modelled to enable Monte Carlo generation of artificial traffic sets to extend the period of the original data. The duration of site measurements required is also noted as a possible source of inaccuracy in the process; however the methodology derived herein remains applicable. The use of the traffic files to calculate load effect data is also presented. It is shown that influence lines (either measured or theoretical) are used, in conjunction with the traffic files, to derive the load effect data for further use.

The programming approach adopted for this research is presented along with the main programs used in this work. It is shown that this enables large periods of traffic to be simulated which has benefits for the accuracy of the predictions derived therefrom. The functions and structures of the main programs are outlined by describing their constituent classes. The function of each of these classes is described and some detailed examples are discussed. Also, the main statistical analysis program is presented; the detailed operations of which are left to Chapters 6 and 7.

Chapter 5

HEADWAY MODELLING

"Statistics will prove anything, even the truth"
-Lord Moynihan

Chapter 5 - HEADWAY MODELLING

5.1 Introduction

5.1.1 Motivation

Load effects for the bridge lengths of interest in this research (20–50 m) are assumed to be governed by free-flowing traffic (Bruls et al 1996), once consideration has been given to dynamic effects of truck-bridge interaction. If it were not for the dynamic interaction, it is likely that such bridge lengths would instead be governed by traffic jam scenarios, as is the case for longer length bridges (Bailey 1996, Bruls et al 1996, O'Connor 2001, Hayrapetova 2006). For bridge loading purposes, the difference between these two forms of traffic (with respect to static load effect only) is the smaller gaps between the vehicles. It is for this reason that correctly modelling the gaps that occur in free-flowing situations is important in short- to medium-length bridges. It seems reasonable that more trucks at smaller gaps result in larger lifetime load effect values.

Accurate headway modelling is also essential in understanding the types of events that dictate the lifetime critical load effect. Some authors (e.g., Nowak and Hong 1991, Nowak 1993, Ghosn and Moses 1985) have only considered 2-truck meeting events for such cases. For short-length (20 to 30 m) bridges, the 2-truck meeting event is indeed important and is likely to strongly influence the bridge design. However, crossing events comprising more than two trucks are also possible and should not be ignored. Accurately modelling the headway could mean that same-lane trucks feature more frequently in the critical crossing events. As will be shown, the headway assumption has a significant effect on the number and type of loading events recorded.

5.1.2 Basis

In this work, the terminology used is:

- **Headway**: the time or distance between the front axle of a leading truck and the front axle of a following one (Thamizh-Arasan & Koshy 2003);

- **Gap**: the time or distance between the rear axle of the front truck and the front axle of the following truck;

- **AHF**: Average Hourly Flow – the average truck flow for a given hour, across all the days of measured traffic;

- **MGC**: Minimum Gap Criterion – a criterion governing the minimum gaps between lead and following trucks used in headway models;

- **HMT**: Headway Modified Truck – a truck that has had its headway modified due to the imposition of an MGC.

Headway and gap are related by the length of the lead truck. To assume too small a gap may be quite conservative whereas an excessively large gap effectively removes 3- and 4-truck meeting events from consideration. In this work, flows are broken into hourly intervals based on the work by O'Connor (2001), in which the effect of the period for the flow intervals (1, 3, 6 and 24 hours) on the characteristic extreme load effects is examined. He concludes that flow periods based upon hourly intervals give minimum deviations of characteristic load effect on average.

Accurate modelling of measured headways implicitly allows for the front and rear truck overhangs. Hence, no account has been made for these overhangs.

5.2 Analysis of Existing Headway Models

Existing headway models are presented in Section 2.3.2 in the context of the background literature to this research. The most recent of such models is tested to assess the sensitivity of the load effect results to the headway model later in this chapter: the normalized headway model of Crespo-Minguillón and Casas (1997).

5.2.1 Minimum Gap Criteria

The normalized headway model, when combined with a velocity distribution, results in a proportion of truck arrangements that violate the physics of traffic flow: simulated trucks occupy the same location, in the same lane, at a given instant. Crespo-Minguillón & Casas (1997) acknowledge that this has been an important source of error in previous work. It is therefore a central feature of headway models to adopt a Minimum Gap Criterion (MGC) to preclude such problems: Grave (2001), Bruls et al (1996), and Flint and Jacob (1996) all adopted a 5 m MGC; Bailey (1996) used a 5.5 m MGC which corresponds to a 0.25 second gap at a speed of 22 m/s (~80 km/h), and; Crespo-Minguillón and Casas (1997) do not specify what criterion they used, though they comment on allowing the simulated vehicles to react to vehicles in front. Such approaches are termed Minimum Gap Criterion as any vehicle combination that violates the criterion is modified in such a way that the criterion is met throughout the duration of the bridge loading event. In any crossing event, there are four critical cases in which the physics of traffic may be violated – as shown in Figure 5.1.
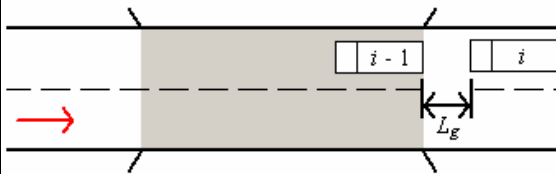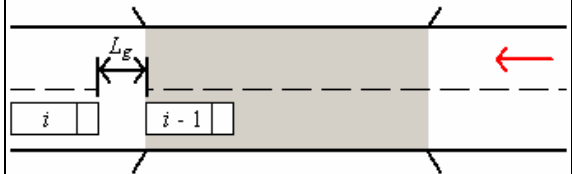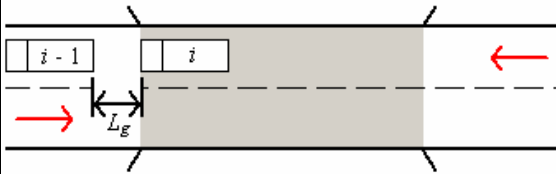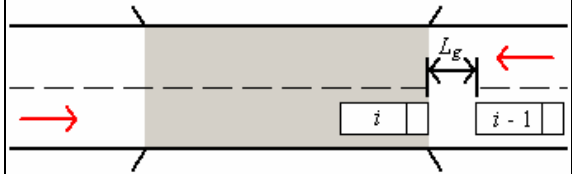
Lane 1	Lane 2
$V_i < V_{i-1}$	
Start of crossing event	Start of crossing event
$$t_i = \frac{L_g}{V_i} + \frac{L_{i-1}}{V_{i-1}} + t_{i-1}$$	$$t_i = \left(\frac{L_g + L_{Bridge}}{V_i} \right) - \left(\frac{L_{Bridge} - L_{i-1}}{V_{i-1}} \right) + t_{i-1}$$
$V_i > V_{i-1}$	
End of crossing event	End of crossing event
$$t_i = \left(\frac{L_g + L_{Bridge} + L_{i-1}}{V_{i-1}} \right) - \left(\frac{L_{Bridge}}{V_i} \right) + t_{i-1}$$	$$t_i = \left(\frac{L_g + L_{i-1}}{V_{i-1}} \right) + t_{i-1}$$

Figure 5.1: Critical truck overlapping scenarios: t is the arrival time; V is truck speed; L is truck length; subscripts i and $i-1$ denote the current and previous trucks respectively; L_g is the MGC; and L_{Bridge} is the bridge length.

The presented equations stipulate the time of arrival for the current truck, such that at its critical point (start or end of the crossing event) the MGC will be exactly met. It is in this manner that MGC-based headway models are made adhere to the physical limitations of the traffic process. The datum chosen for the arrival times is the right-hand side of the bridge. As the trucks are generated, their headway-velocity properties are checked against the requirements shown in Figure 5.1. Should a combination be found that violates the MGC, the time of arrival of the truck is modified using the appropriate

equation from Figure 5.1. The velocities of the trucks are not altered. In this work, such trucks are termed headway modified trucks (HMTs).

O'Connor (2001) and Bailey (1996) note that the shifted exponential distribution may also be used. In this case, no modification is needed, as there are no generated combinations that violate the MGC. However, this does not remove the subjectivity of the arbitrary choice of minimum gap and consequently this approach is not faithful to actual (measured) traffic.

5.2.2 Effect of Minimum Gap Criteria on headway distribution

In carrying out the process of checking the truck headway-velocity combinations, and modifying for the MGC when required, the measured headway distribution is not adhered to in the resulting generated traffic stream. In fact, all of the HMTs are effectively 'bunched' at the MGC-governed headway.

Figure 5.2 shows an example of the effect of imposing MGCs on generated headways in which 50 000 random headways, as defined by the normalized headway model, are generated for various flows. The PDF of these headways is shown as a black dashed line in each of the plots. For three MGCs, these random headways are checked and modified as described previously. The resulting histogram of headways, for the three MGCs is shown in each plot. As expected, 'bunching' of the modified headways at the MGC has severely distorted the headway PDF. It is to be noted that only headways under 4 seconds are illustrated.
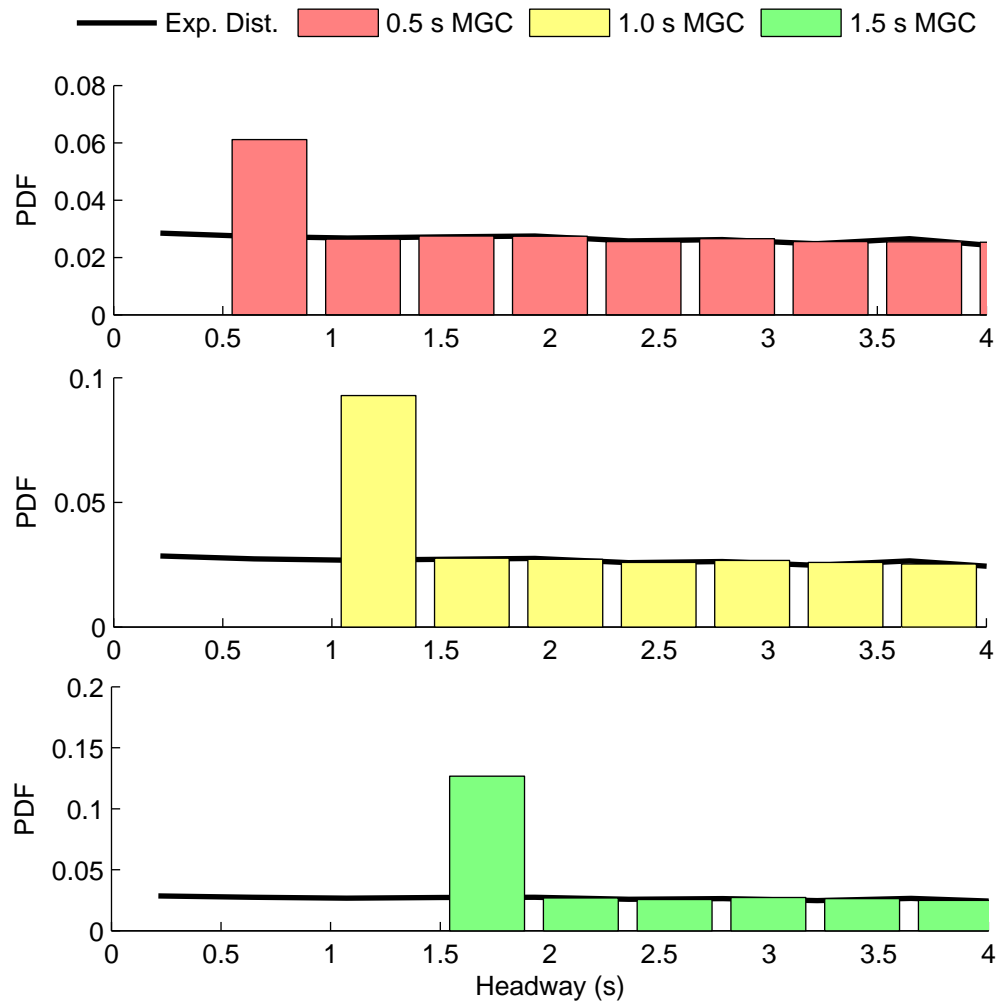
Figure 5.2: Effect of MGC modification to headway distribution for a flow of 100 trucks/hour.

5.2.3 The effect of Headway Modified Trucks

To assess the impact of the headway modifications previously outlined on load effect, four runs of 10 weeks simulation each are carried out based upon the Angers data. Only the events corresponding to a daily maximum (DM) load effect are processed for further use because these events form the basis for the statistical analysis. Space-time graphs (Gazis 1974) are used to understand the headways that are significant for bridge loading events (Figure 5.3 for example).

It is found that the duration of the daily maximum events varies for different load effects and spans but that the duration of most daily maximum events is around 4 seconds. However, when headways are required, due to the occurrence of same-lane trucks, they are smaller than 4 seconds – the total duration of the event. Such examinations of the critical events led to the general realization that it is headways under around 4 seconds that are most likely to contribute to the critical bridge loading events. The normalized headway model previously described is not focused on this important interval of headway.
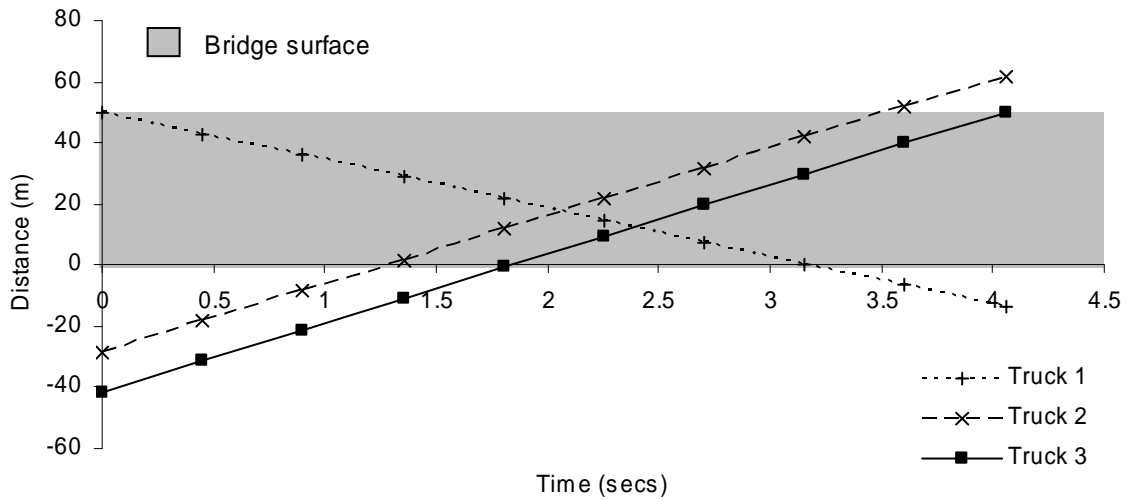
Figure 5.3: Typical space-time graph: 50 m bridge length, Load Effect 1.

The simulations are further analysed to determine the influence of the HMTs upon the loading events. It is found that, out of a total population of just over 654 725 trucks, 12 708 are HMTs – 1.9% of the population. However, HMTs constitute an average (for different load effects and bridge lengths) of 46.3% of the significant crossing events population. Of course, by definition, HMTs will have small headways and are thus liable to feature more than an 'average' headway truck. However, it is clear then that any inaccuracies in the headways generated may have significant impact on the loading events. It is with this motivation that the following headway model is proposed.

5.3 The Headway Distribution Statistics Model

5.3.1 Headways in a European context

Data sets from the A196, Angers, Auxerre and the Hrastnik Bridge sites are analysed for the occurrence of trucks with headways less than 4 seconds. The hourly mean flow (mean flow in an hour) for each hour of measurement is calculated, as is the incidence of trucks with headways less than 4 seconds for each hour.

The background literature (Section 2.3) has demonstrated that traffic is often approximated as a Poisson arrival process. According to this model, the number of trucks with headway less than 4 seconds (N_4), as a function of flow, is:

$$N_4 = Q \cdot \left[1 - \exp\left(-4 \cdot \frac{Q}{3600} \right) \right] \tag{5.1}$$

The curve defined by this model is shown in Figure 5.4 along with the processed data, as described previously. As the Poisson model is almost quadratic in this range, quadratic trend lines are fit to the data and shown for comparison.

There are several important points to be elicited from the relationships shown in Figure 5.4:

- Truck densities conform well to the Poisson assumption, though there is considerable variation about the model – especially for lower flows;
- Driver behaviour appears to be quite similar across Europe;
- The Lane 1 data from Angers does not appear to follow similar trends; this may be due to the road geometry at the site. For example, as it is a **Route Nationale**, access junctions can result in bunching of traffic as a vehicle slows to exit, or enters the traffic stream.
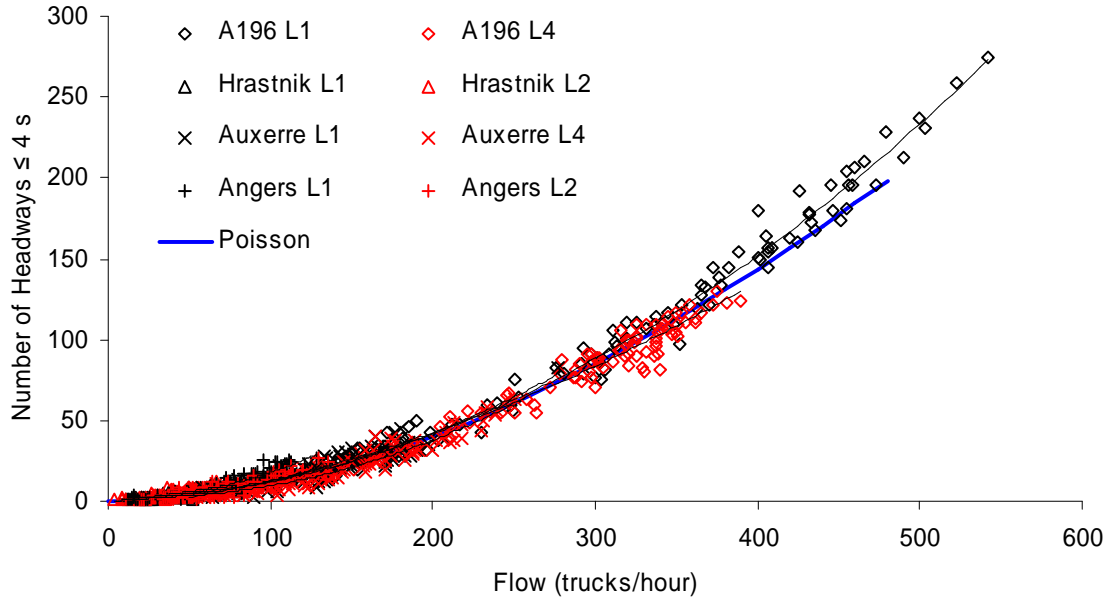
(a) Overall relationship;
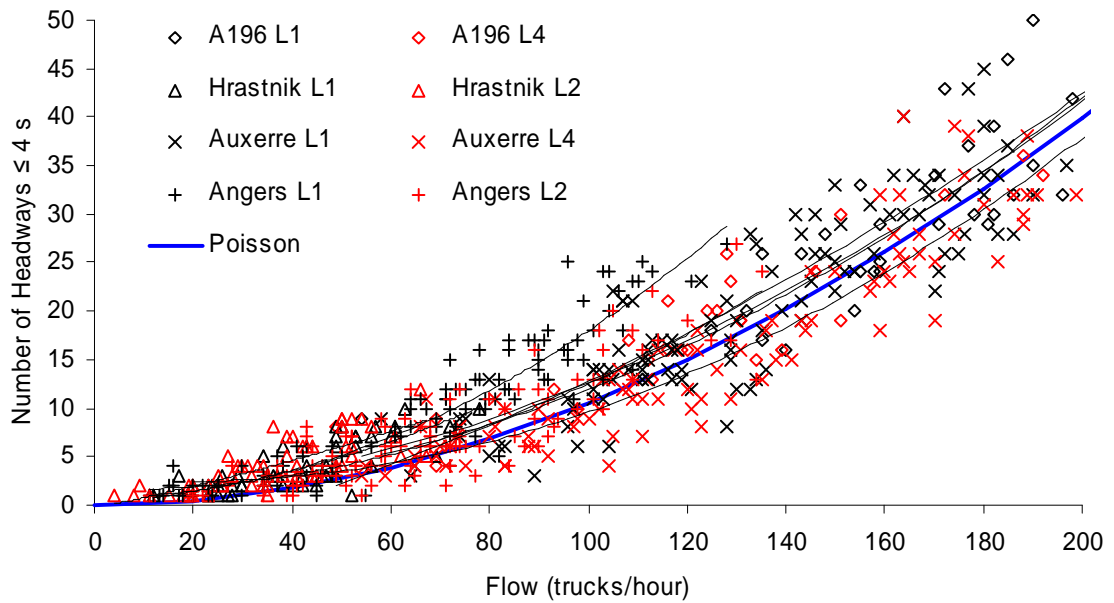
(b) Magnified view of lower flows;

Figure 5.4: Small headways at various European sites (L**i** refers to lane **i**).

It appears that at a macroscopic scale at least, headways in the range of interest are quite similar in different (European) countries. This is surely due to similar driver behaviour, regardless of country. Therefore any methodology may be reasonably specific and can expect to be applicable in a broad range of cases,

given sufficient data. Also, it may be possible to combine all the headway data into one model applicable throughout. However, exceptions such as the Angers Lane 1 data are always possible, and it is important not to draw too general an inference from a data set representing only one week of traffic from each site.

In the following development of a headway model, the weekday data from the A6 site, near Auxerre, is analysed to form the basis of the methodology. The characteristics of the site are described in Chapter 4. This headway model is based on the Headway Distribution Statistics measured at the site and is hereafter referred to as the HeDS model.

5.3.2 Investigation of very small headways

Very small headways are investigated to examine if driver perception of safe distance rather than traffic flow determines the headways (Koppa 1992, Lieberman & Rathi 1992). Up to a headway of 1.5 seconds, the correlation between hourly flow and headway is weak as can be seen from Figure 5.5. Hence, for such headways, it is reasonable develop a distribution of headway that is independent of flow.

To model the headways for less than 1.5 seconds, irrespective of flow and direction (because driver behaviour is surely independent of direction), the outside lanes of the Auxerre traffic file are processed for:

- The total number of trucks, 31 842;
- Each headway less than, or equal to, 1.5 seconds, i.e. measured data;
- The number of measured headways that occur less than, or equal to, increasing values of headway, as given in Table 5.1.
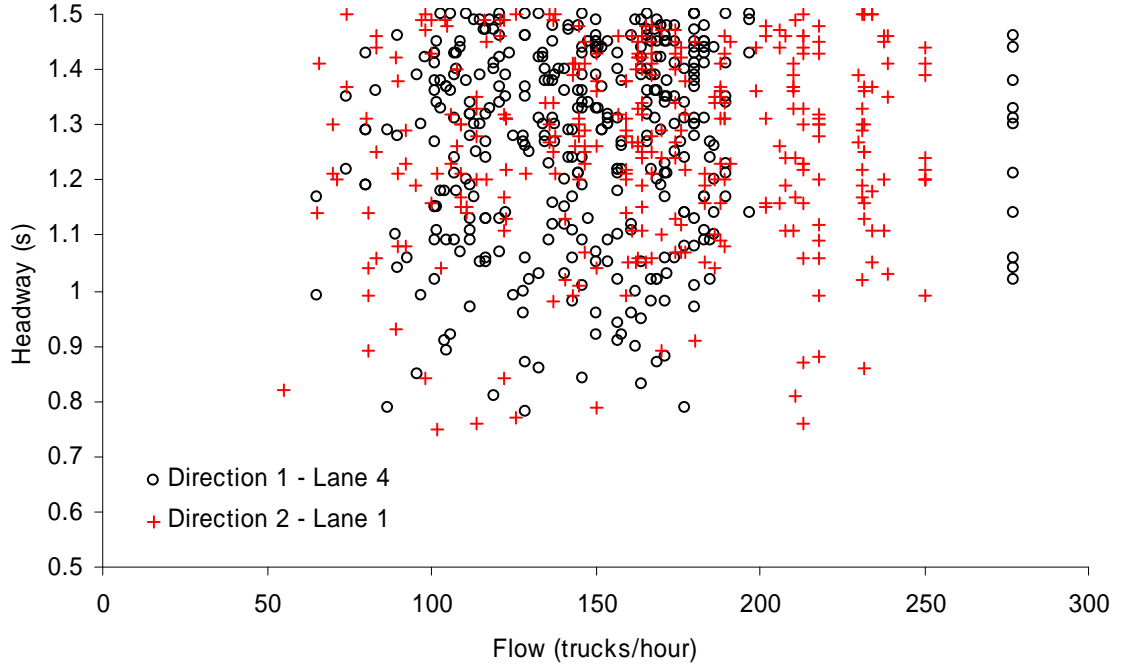
Figure 5.5: Occurrences of headways less than 1.5 seconds by flow.

h	N ≤ h	h	N ≤ h	h	N ≤ h
0.75	1	1.05	81	1.35	425
0.80	8	1.10	127	1.40	487
0.85	15	1.15	166	1.45	577
0.90	27	1.20	215	1.50	655
0.95	36	1.25	284		
1.00	55	1.30	339		

Table 5.1: The number, N, of headways occurring less than a specified headway,

h, in measured Auxerre traffic.

Two forms of headway distribution emerge:

- The distribution of headways less than, or equal to, 1.5 seconds, $F_{1.5}(\cdot)$;

- The distribution of all headways, $F_{Tot}(\cdot)$, though data is only gathered for headways in the interval of interest $[0,1.5]$.

The empirical distribution function (Section 3.2.3) for the measured data, $\tilde{F}_{1.5}(\cdot)$, is shown in Figure 5.6 (main plot). There is a change in the curvature of

the distribution at headway of about 1.0 seconds. It is therefore considered appropriate to use two fits: one for $h \leq 1.0$ seconds, and another for $1.0 \leq h \leq 1.5$. From Table 5.1 and the total number of trucks, $F_{Tot}^{-1}(1.5) = 0.02057$. This could be used to relate the probabilities of $\tilde{F}_{1.5}(\cdot)$ to those of $F_{Tot}(\cdot)$, but it is found that due to over-fitting of the large data set, the interface of the fits at 1.0 s is problematic. Therefore, using the data from Table 5.1, two quadratic fits are made, and are shown in the sub-plot of Figure 5.6:

$$F_{Tot}(h) = \begin{cases} a_1 h^2 + b_1 h + c_1 & \text{for } 0 \leq h \leq 1.0 \\ a_2 h^2 + b_2 h + c_2 & \text{for } 1.0 \leq h \leq 1.5 \end{cases} \tag{1.2}$$

Quadratic-equation, least-squares fits are used, as no probabilistic model could be justified as being more appropriate than any other. In the main plot of Figure 5.6, these quadratic fits are plotted (scaled appropriately) and may be compared with the empirical CDF: the comparison is quite good.
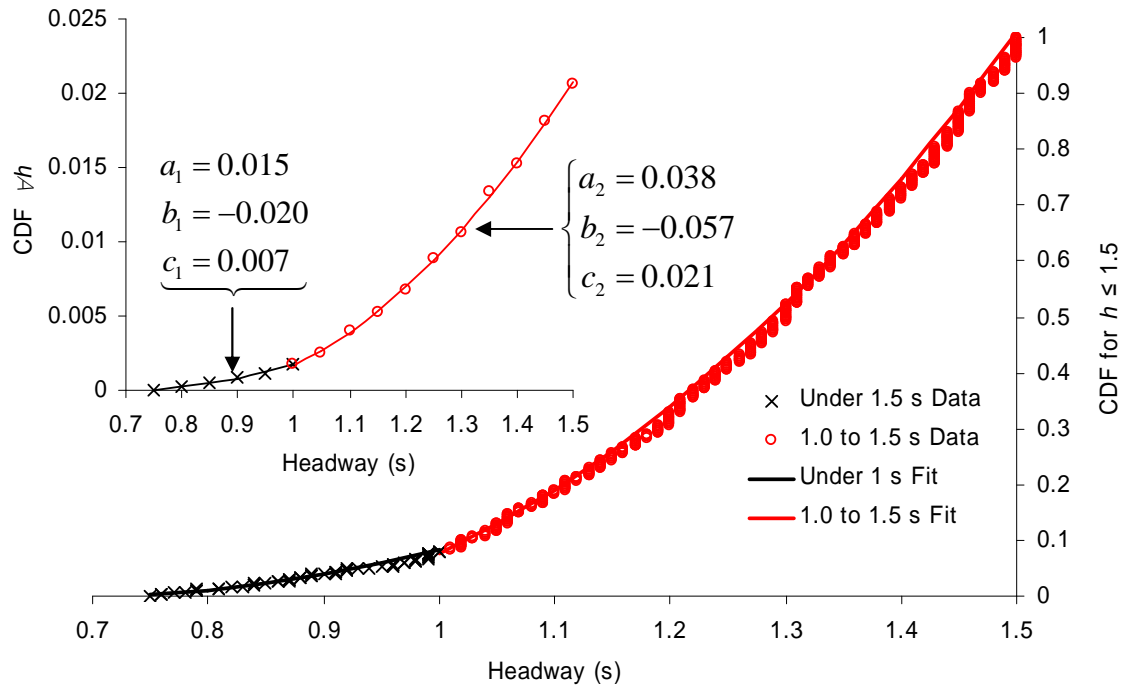
Figure 5.6: Cumulative distribution functions (for all flows combined) and quadratic fits for headways less than 1.5 seconds.

5.3.3   Headways between 1.5 and 4 seconds

It is not reasonable to assume that there is no correlation between headway and flow for headways between 1.5 and 4 seconds as is done for smaller headways. Instead the headway model must allow for differences due to varying flow. The hourly mean truck flows measured during the 5 working days of measurement at the Auxerre site are shown in Figure 5.7, by day, for both directions. Also shown is the AHF for each hour and each direction.
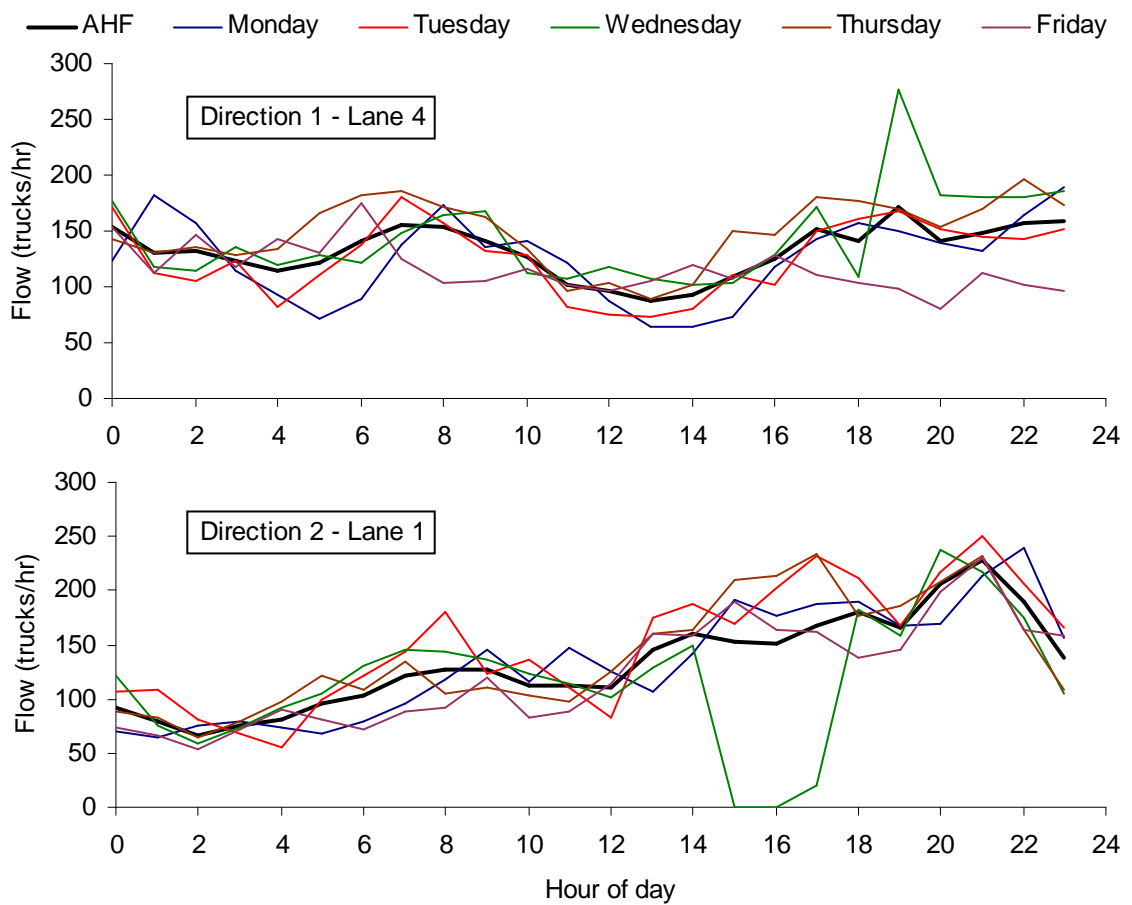
Figure 5.7: Daily variation and AHFs for both directions at Auxerre.

The AHF is determined from the flows that occur in a given hour across all of the days of data. It can be seen that the AHF closely follows the overall trend of the other days. This figure also illustrates one of the problems involved in site measurement: it can be seen that there are no measurements for Wednesday,

Direction 2, for 1500 and 1600 hours. That there is a small measurement for 1700 hours suggests that recording is temporarily stopped at 1500 but restarted close to 1800 hours. No adjustment is made to the AHF to account for this, though rational adjustment is clearly possible: interpolation based on the mean relationship exhibited in the other days, for example.

Figure 5.8 shows the flow histograms for both lanes separately, and the site as a whole; for both the measured flows and the calculated AHFs. The flow, and hence the headway distribution, varies considerably by hour. This has implications for the headway modelling: it would not be appropriate to assume a form of 'mean site flow' for the derivation of a headway model. This is in keeping with existing literature on the subject.
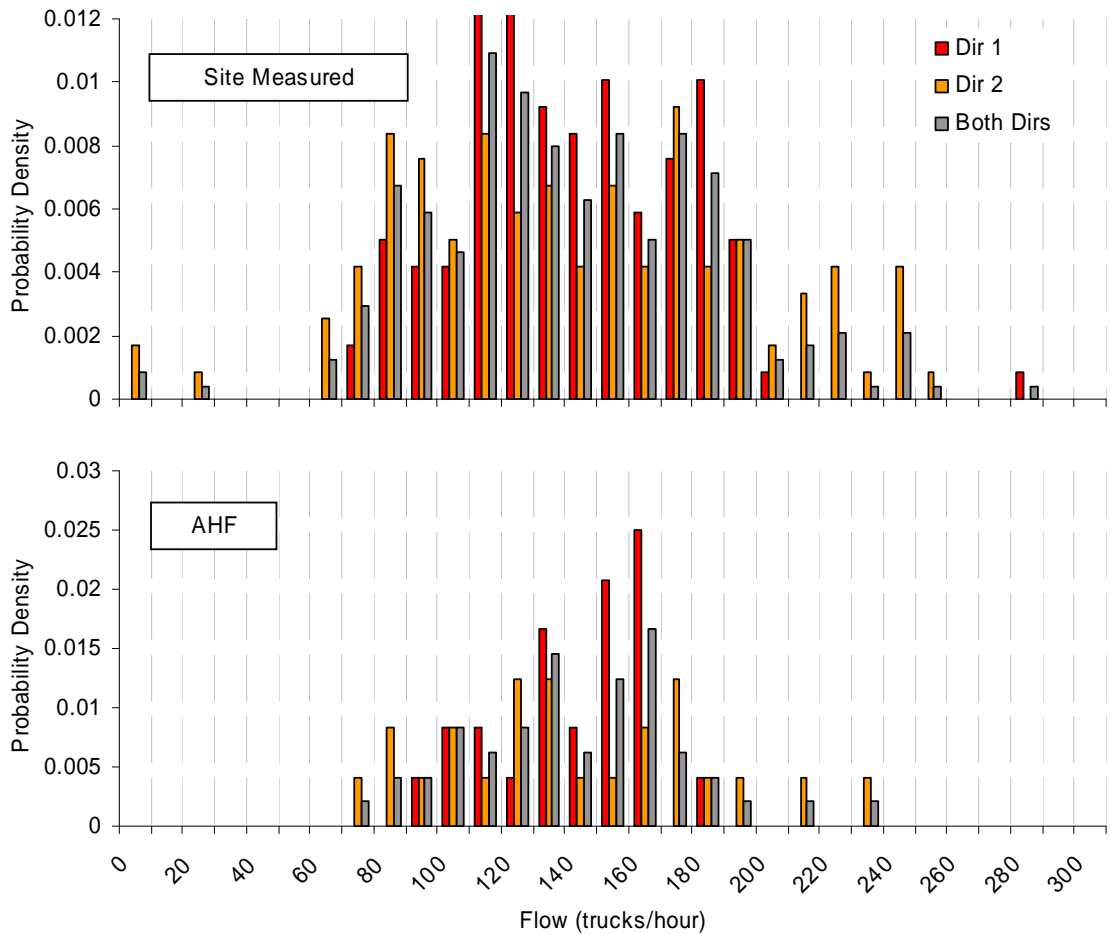
Figure 5.8: Histograms of measured Auxerre flows and resulting AHFs.

To accurately model the headway-flow relationship measured, for each hour of each day and direction, headway data and the corresponding mean hourly flow are noted. For each of the hours recorded, individual headway distributions are possible. However, there are two reasons not to use such distributions:

- It is unlikely that every AHF will have a corresponding flow with its associated headway distribution, regardless of the hour;
- It is unlikely that a single hour would have sufficient data for robust modelling.

Therefore, to maximize the use of the WIM data, yet to maintain faithful adherence to the WIM headway distributions, data from different hours is categorized by hourly flow in intervals of 10 trucks/hour. This is as shown in the histograms of Figure 5.8. Cumulative distribution functions (CDFs) of headway are then calculated for each interval. These CDFs for headway are illustrated in Figure 5.9. There is a general trend of increasing cumulative probability with increasing flow. There is some variation about this trend which is likely to be the result of the size of the data set. For the flow intervals for which there is a corresponding AHF (see Figure 5.8), the measured CDF is fit using quadratic equations (as previously). The fits are shown in Figure 5.10 and the parameters are given in Table 5.2.

Figure 5.11 shows the error in the fits described – expressed as a percentage of the measured probability – for the headway and flow under consideration. Immediately apparent is the flatness of large areas of the figure – corresponding with little error. However, it is also apparent that there are much larger percentage errors at low headways. For high flowrates, the error is about +38%; for low flows the error is about -17%. These high percentage errors are caused by the very small values of probability at low headways.
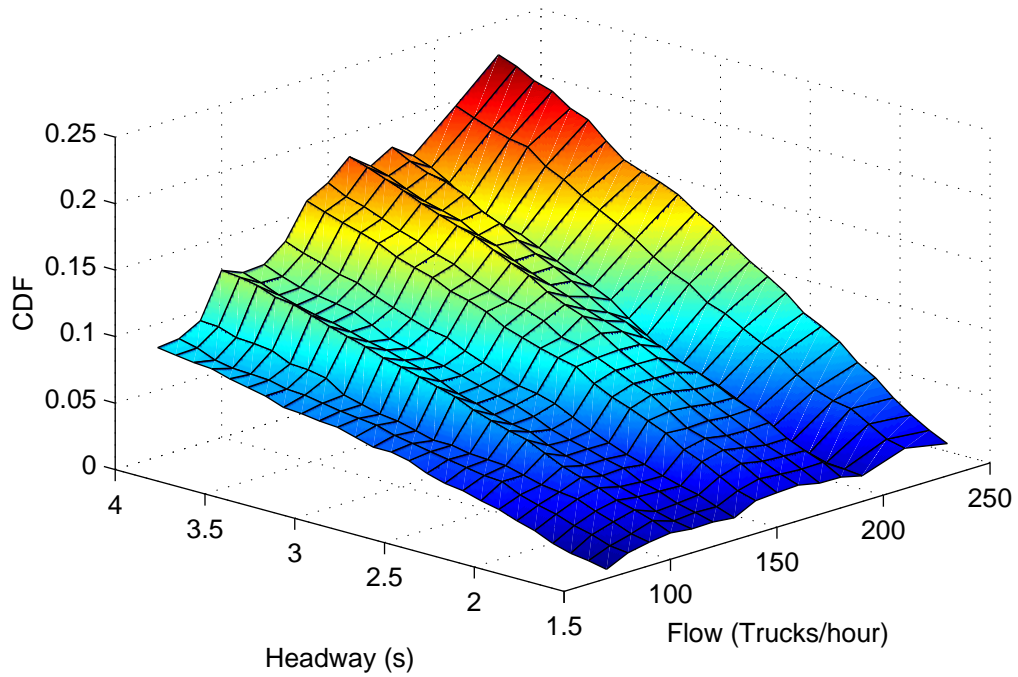
Figure 5.9: WIM headway CDFs corresponding to AHFs, categorized by flow increments of 10 trucks/hour.
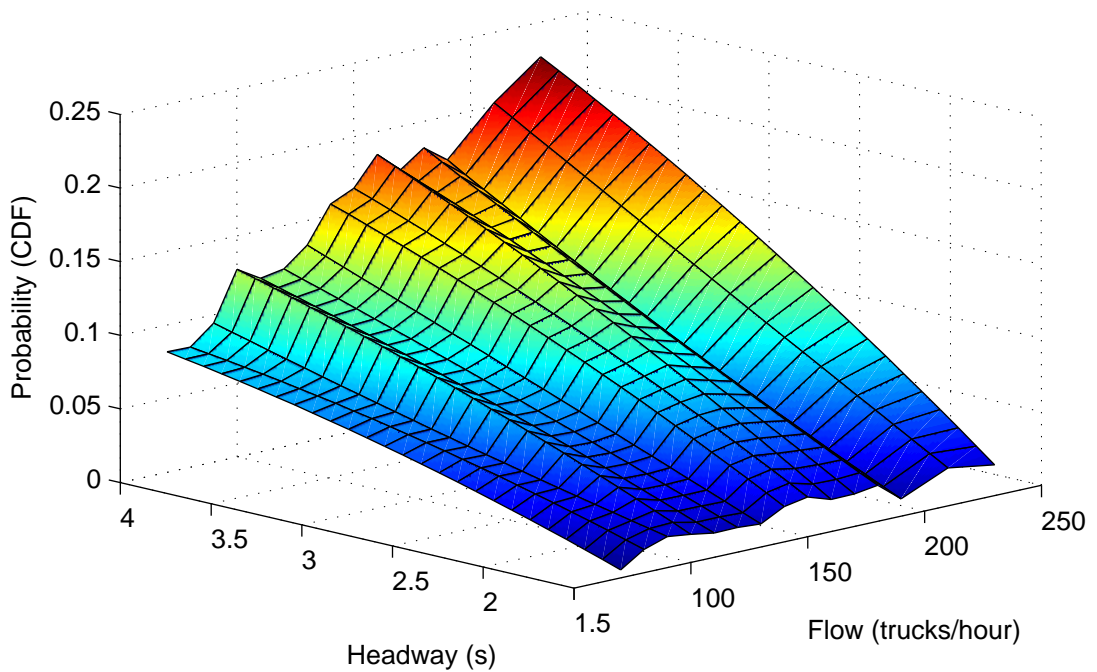
Figure 5.10: Modelled headway CDFs categorized by flow.

Flow	a	b	c	Flow	a	b	c
70	-0.004	0.055	-0.067	150	-0.005	0.080	-0.083
80	-0.004	0.050	-0.049	160	-0.005	0.092	-0.105
90	0.002	0.021	-0.014	170	-0.005	0.087	-0.097
100	-0.004	0.065	-0.069	180	0.002	0.052	-0.058
110	-0.003	0.055	-0.060	190	0.003	0.045	-0.063
120	-0.001	0.049	-0.053	210	0.000	0.068	-0.078
130	0.000	0.050	-0.058	230	-0.006	0.118	-0.141
140	-0.005	0.081	-0.086				

Table 5.2: Parameters of quadratic equations of CDFs by flow.
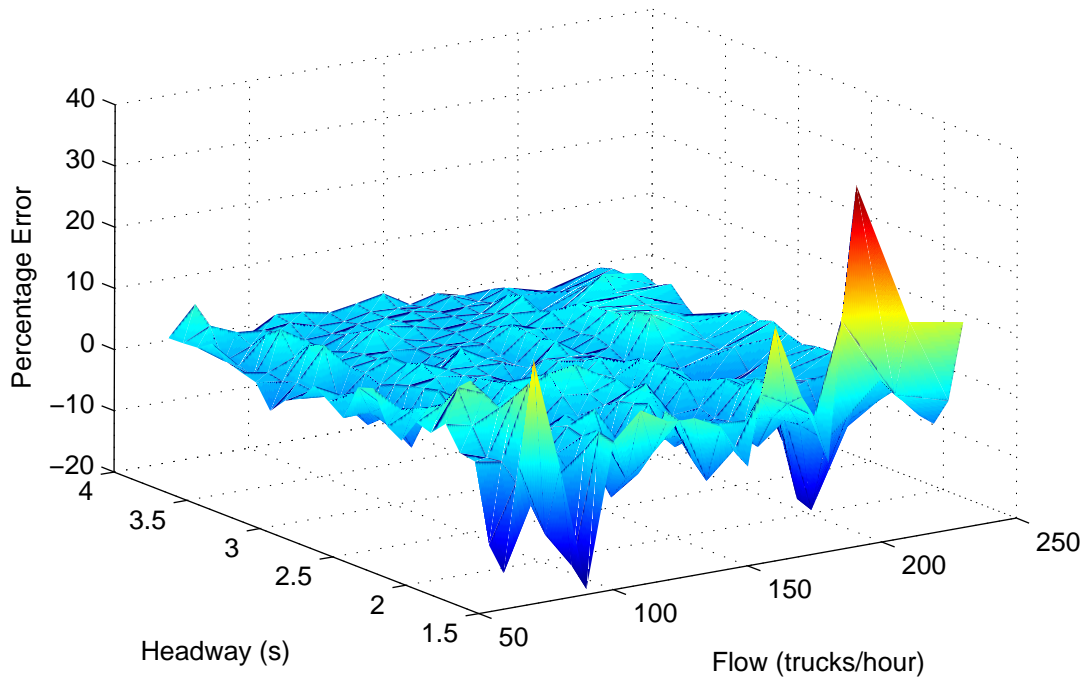
Figure 5.11: Percentage error of modelled to WIM headway CDFs.

Figure 5.9 shows that there is a relationship between cumulative distribution and flow for a given headway. Exploiting this through the use of a bi-variate quadratic surface fit would simplify the headway model. However, such a fit would yield larger errors than that of the individual flow rate fits explained above. As an example of such a procedure, a quadratic surface is fit to the measured CDF surface of Figure 5.9. The equation used is:

$$f\left(x,y\right)=Ax^2+By^2+Cx^2y+Dxy^2+Exy+Fx+Gy+H \qquad (1.3)$$

The parameters of the fit obtained by least squares evaluation are:

$$
\begin{array}{llll}
A = \text{-}0.00512 & B = 5.343E\text{-}07 & C = 1.819E\text{-}05 & D = \text{-}5.124E\text{-}07 \\
E = 0.00038 & F = 0.02229 & G = -0.00048 & H = \text{-}0.01641
\end{array}
\qquad (1.4)
$$

The fit obtained from this method is shown in Figure 5.12. The fit obtained by this method is not used in the work that follows, due to the higher errors observed when compared with the individual flow fits. However, given a larger data set, or more sites, the bi-variate fit method presented could be the superior model due to its ease of implementation and generality of application.
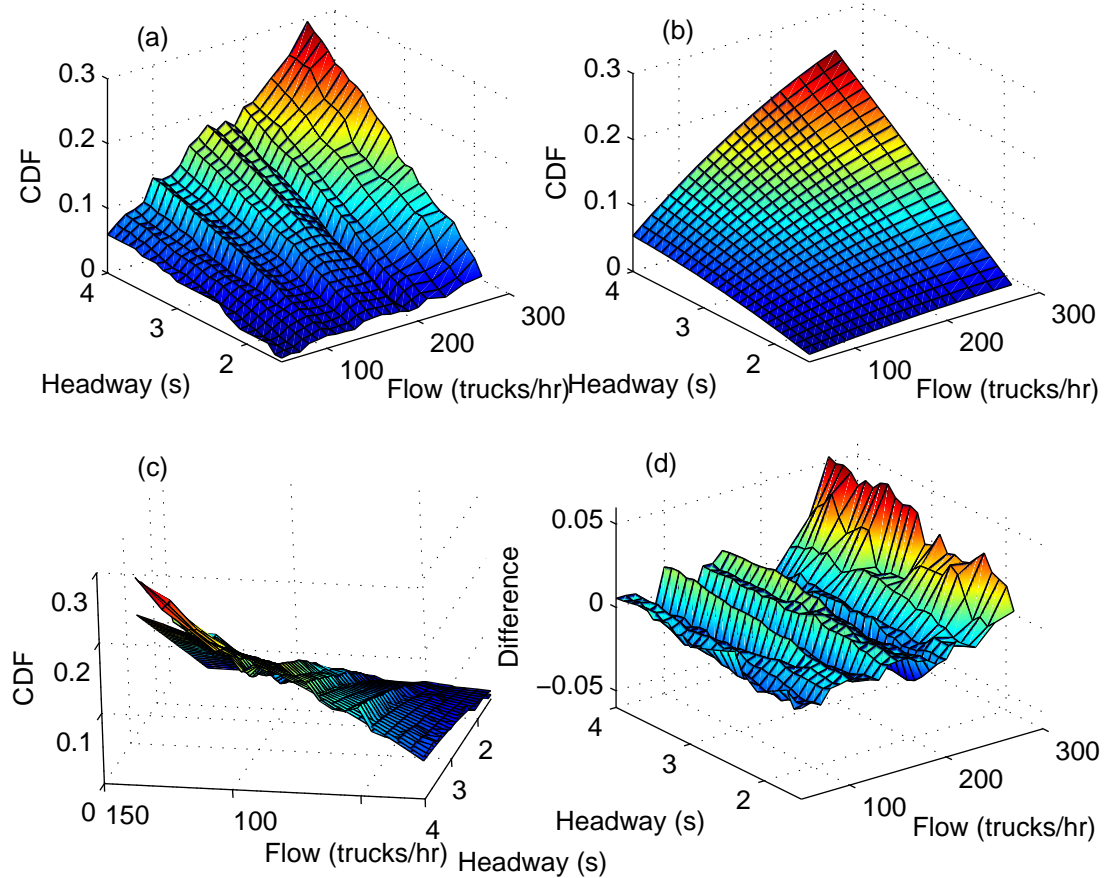
Figure 5.12: Bi-variate model of the headway-flow CDF relationship: (a) measured; (b) modelled; (c) both plotted together, and; (d) the differences.

5.3.4 Headways greater than 4 seconds

For bridges up to 50 m long, headways in excess of 4 seconds are not critical as at a typical highway speed of 80 km/h, a truck travels 89 m in this time. Therefore, such headways do not need to be modelled as accurately as smaller headways, and the normalized headway distribution of Crespo-Minguillón and Casas (1997), previously explained, is used for headways in this region.

5.3.5 Checks on generated headways

Checks are made to the generated headways so that it may be confirmed that physical limitations are not violated. The lack of correlation between speed and headway (Section 4.3.1) allows the following check:

Check 1:   For same-lane trucks concurrently present on the bridge, the speed of the following truck is made that of the lead truck, such that the headway is maintained all the way across the bridge.

Hence, the following truck cannot catch up with the lead truck and the measured headway statistics are maintained during the crossing. About 2.9% of trucks are modified in this manner for a typical Auxerre simulation. One further verification check is made on the generated headways:

Check 2:   If a truck has been adjusted in Check 1, the distance between the rear axle of the front truck and the front axle of the following truck is examined; if it is less than 1 m a warning is given.

No generated headway-velocity combination fails the second check: evidence that the proposed headway model is sympathetic to the measured traffic stream. That is, physical limitations are maintained, without arbitrary nose-to-tail distance stipulations.

5.4 Comparison of HeDS with other Methods

5.4.1 Simulation background

To investigate the proposed headway model, bridge lengths of 20, 30, 40 and 50 m are considered. In each case, three load effects are considered:

- Load Effect 1: Mid-span bending moment of a simply supported bridge;

- Load Effect 2: Left support shear in a simply-supported bridge;

- Load Effect 3: Central support bending moment of a two-span continuous bridge.

Fifty days of traffic are simulated and the daily maximum (DM) load effects identified in each case (for reasons given in Chapter 4). The results obtained using HeDS are taken as the reference for assessing other headway models. Other headway models considered are based on the normalized headway model, but with four different MGCs: 5 m, 10 m, 0.5 s and 1.0 s. In each of these cases, generated headways are checked and adjusted for gaps less than the MGC as described in Figure 5.1. Five sets of 50-day simulations for each of the headway models are generated to provide an indication of the repeatability of results.

For the time-based MGCs, the minimum distance is taken to be the minimum specified time gap multiplied by the speed of the following truck. That is, the truck for which the headway is to be modified.

5.4.2 The effect on event types and composition

For the five runs of 50 days carried out, the numbers of trucks involved in the daily maximum load effects are shown in Figure 5.13 for the HeDS model. For the other headway models, the composition of the daily maximum loading events, in terms of event type, is detailed in Figure 5.14.
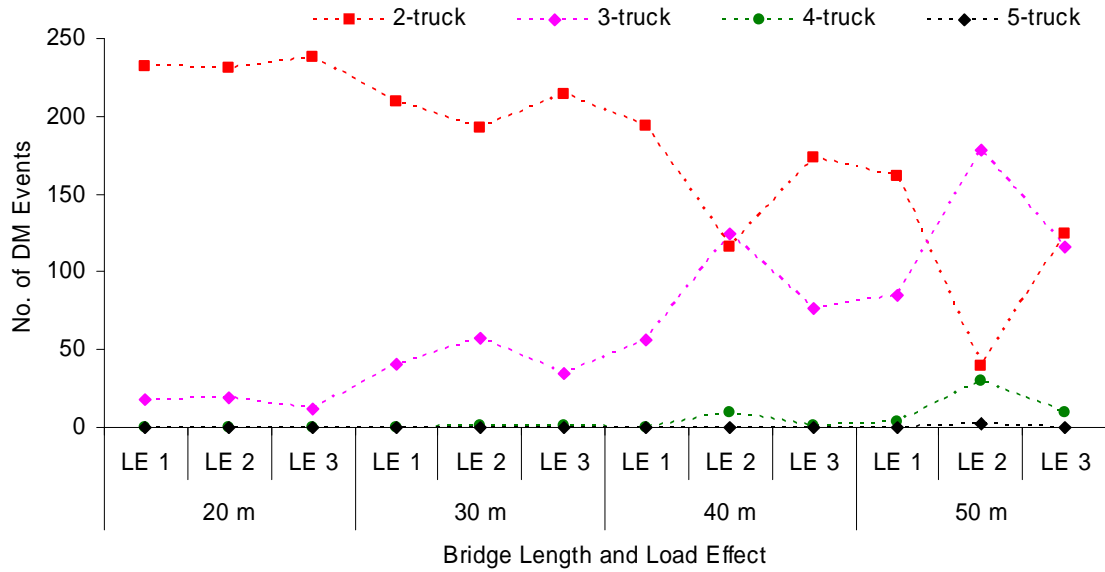
Figure 5.13: Mean composition of maximum-per-day load effects for HeDS.

From Figure 5.13 it can be seen, for example, that only two 5-truck events feature in the full 250 days of simulation (5 runs of 50 days each); both occurred at the 50 m bridge length and for Load Effect 2. There are no single truck loading events that feature in the HeDS daily maxima, but 2-truck events are important, particularly for shorter lengths. Also present are 3-truck events, particularly for greater lengths. This is most pronounced for Load Effect 2, where the influence line favours a lesser concentration of loading. Also, 4-truck events feature for 40 and 50 m bridge lengths.

For the MGC models, Figure 5.14 shows the difference in the number of i-truck DM events featuring, relative to the HeDS model and expressed as a percentage of the total number (250) of DM events. Again no 1-truck events feature as a maximum-per-day load effect. For the case of 2-truck events, all but one of the MGC models under-estimate the number of DM 2-truck events. With the exception of Load Effect 2 and bridge length 40 m, the 1.0 s MGC is similar to the HeDS results. The under-estimation of the 2-truck events by the other MGCs is mirrored by over-estimation of 3- and 4-truck events. Roughly, it

appears that about two-thirds of the under-estimate of 2-truck events corresponds to the over-estimate of 3-trucks, with the remaining third given to the 4-truck events. There is no significant variation for the 5-truck events, and very few are recorded.
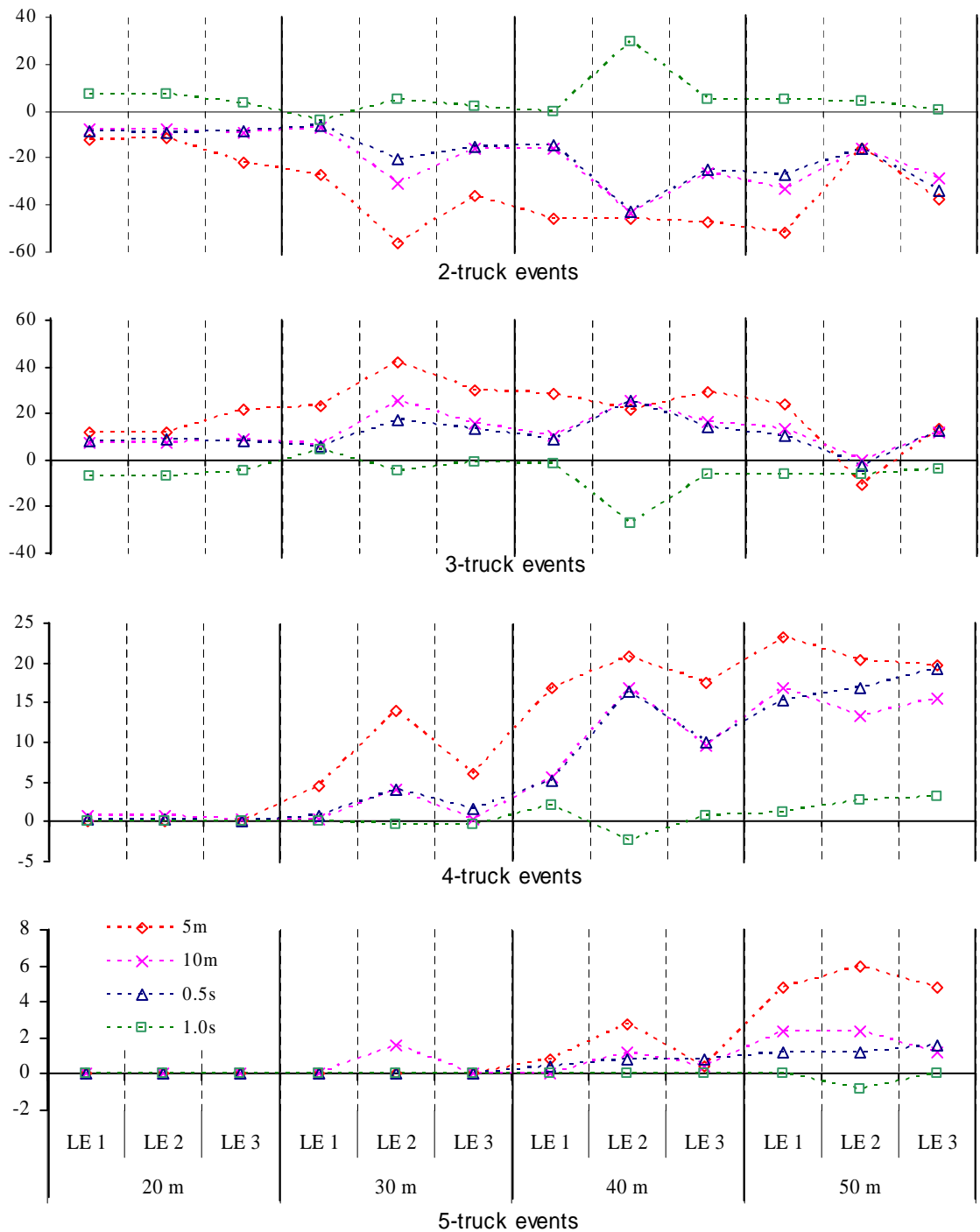
Figure 5.14: Percentage variation on mean DM event composition from HeDS.

5.4.3 The effect on load effect due to different events

Intuitively, it is evident that the headway mainly affects events in which following trucks feature. The majority of 2-truck events will be meeting events, and hence the load effects derived therefrom should not be unduly affected by differing headway models. Conversely, 3-truck events, by definition, will comprise two same-lane trucks and a single truck in the other lane. Hence, the load effect value may be quite sensitive to the headway model used.

Using HeDS as a reference, it is found that the three load effects studied exhibited very similar 'errors' when broken down into 2- and 3-truck events: Figure 5.15 details the average error in mean daily maximum load effect for 2-truck and 3-truck loading events only, relative to the HeDS model. Such a measure is considered to be generally representative of any changes to the underlying phenomena.

The 2-truck events plot of Figure 5.15 (see the scale of the y-axis), demonstrates that such events are not sensitive to the headway assumption used as expected, and random variation could easily account for the observed differences.

The 3-truck events plots, also shown in Figure 5.15, demonstrate that such loading events are particularly sensitive to the headway model used. In general the other headway models are conservative, presumably implying that more trucks have the same, or smaller, headways in comparison with HeDS. There is a notable error for the 1.0 s MGC on 20 m bridge lengths which is obviously caused by the imposition of a minimum headway of similar length to the bridge itself, thereby effectively removing the third truck.
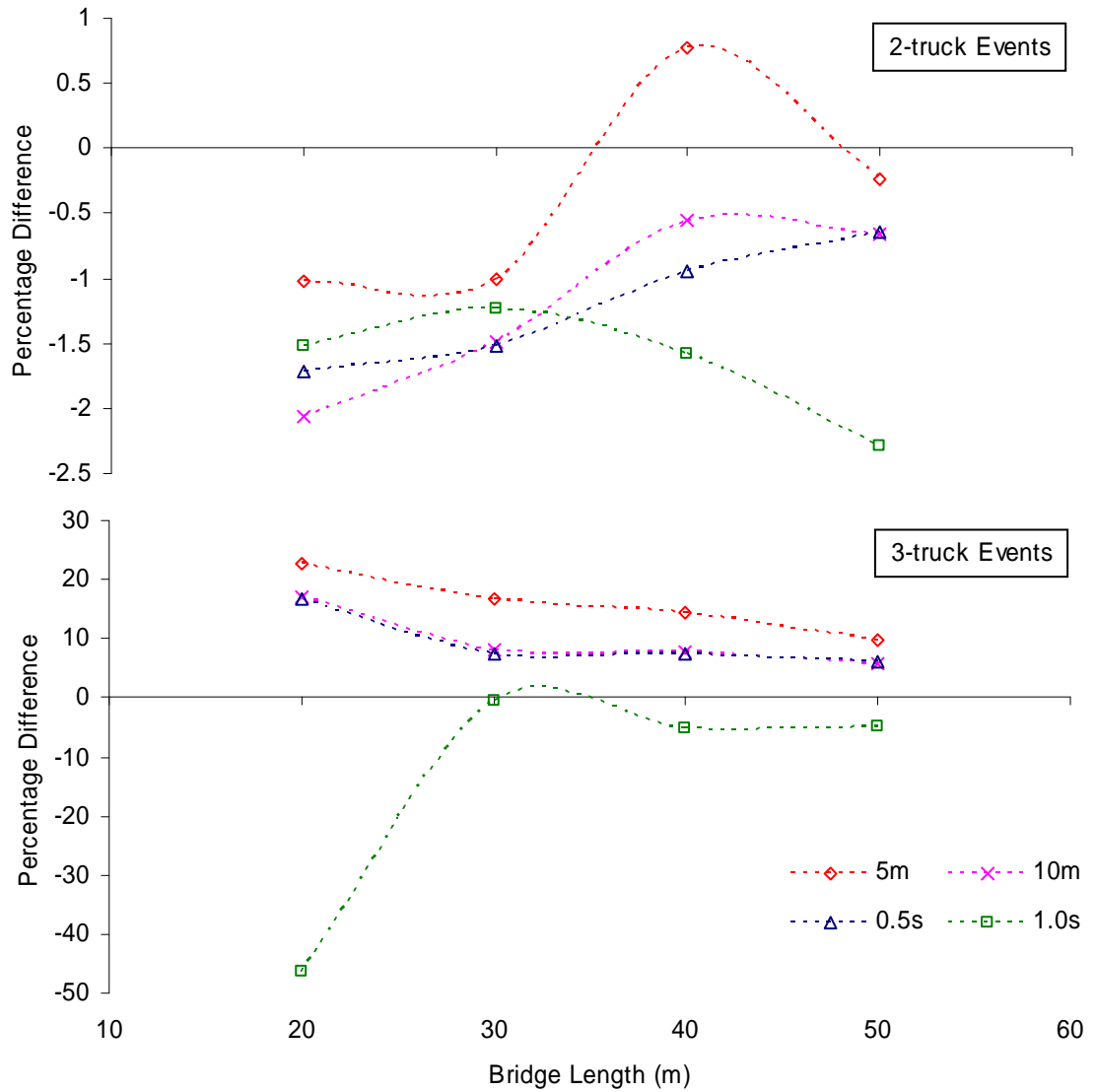
Figure 5.15: Mean change of load effect for different event types and headway models, relative to the HeDS model.

Given the enforcement of the minimum gap criteria shown, it is therefore evident that the conservatism in the other headway models arises from the 'bunching' of trucks' headways at the MGC – more trucks at small headways increases the chances of having a heavier truck closer than otherwise probable.

As stated at the outset of this chapter, Chapter 6 demonstrates that the statistical analysis to be carried out relies upon all of the event-types that occur on the bridge length. More importantly, Chapter 6 also demonstrates the

161

particular importance of the 3- and 4-truck events to the characteristic load effect values. Therefore, such inaccuracies in the MGC headway models have significant consequences.

5.4.4 The effect on daily maximum load effect values

Although extrapolation to the lifetime of the bridge is usual, that process may introduce uncertainty or mask the differences in the headway models. Hence the errors in the mean load effect, relative to the HeDS model average, of the 50 daily maxima are illustrated in Figure 5.16 for each of the three load effects considered. Five points are shown in each case, indicating the random variation between each run of fifty days.

It can be seen from Figure 5.16 that the daily maxima are quite sensitive to the gap assumption, particularly for the longer spans. That is, as more space becomes available to load, inaccuracies in the headway assumptions are amplified. For the load effects illustrated, most gap assumptions are conservative; up to about 15 - 20% in the case of the 5 m assumption. Errors for Load Effect 3 are similar to Load Effect 1 while those for Load Effect 2 are more variable and can be conservative or non-conservative. Thus it appears that the shape of the influence line features significantly.
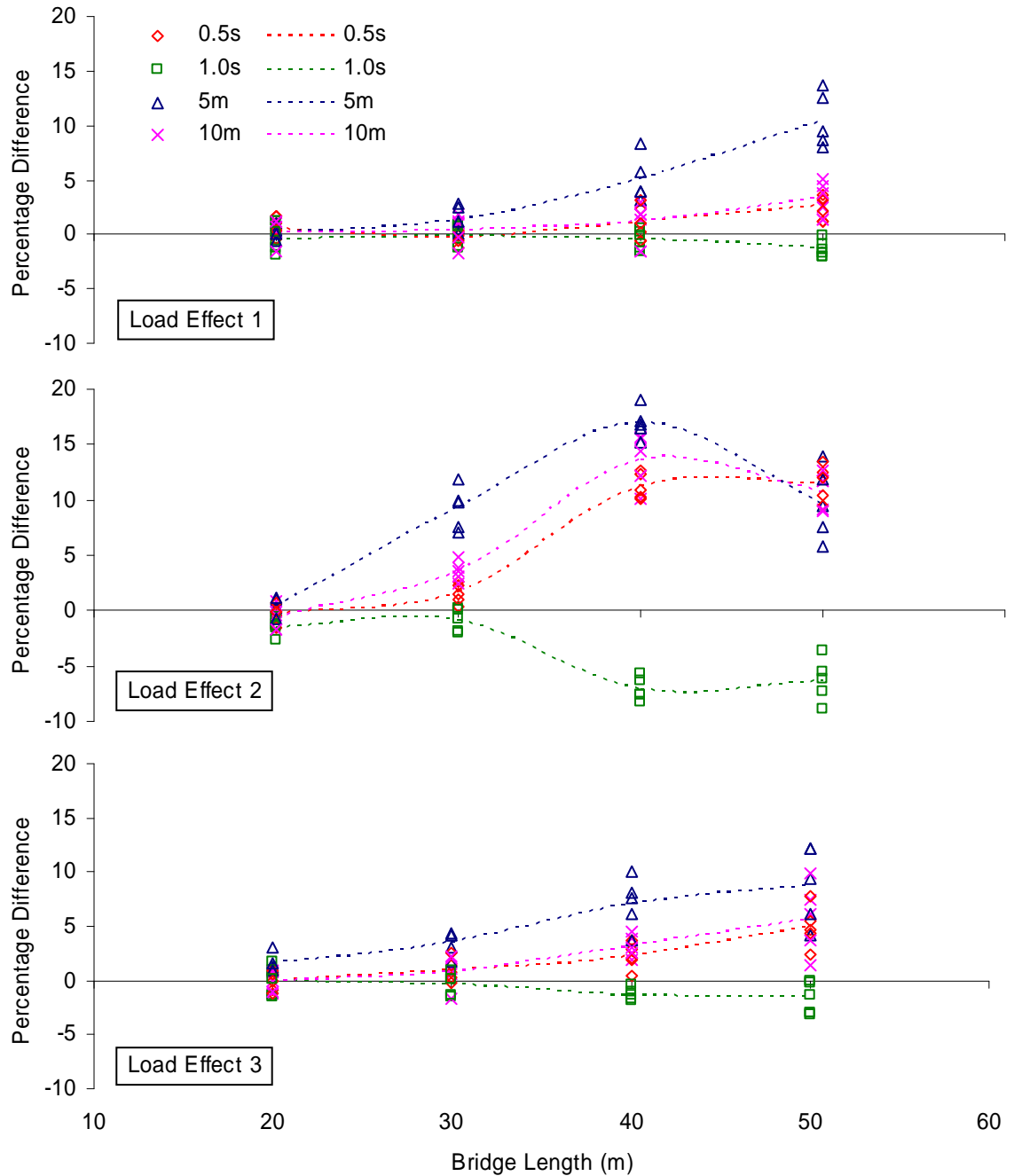
Figure 5.16: Percentage difference in mean DM load effect value relative to HeDS for various headway models.

5.4.5 The effect on characteristic load effect value

It is not the mean of the daily maximum load effects that is relevant for bridge assessment, rather the characteristic load effect. Further, for this application, it is only the relative values of characteristic load effect that are of interest.

However, given that there are five runs for each model; variability due to the generated traffic is part of each extrapolation. For each run, headway model, bridge length and load effect, daily maxima load effects are fit to a Gumbel distribution and extrapolated to a 1000-year return period – this procedure is explained in Chapter 3. In the light of the results of Chapter 6, these results are strictly comparative and not absolute.

The five HeDS results for each bridge length appear as points in Figure 5.17 whose means are the **x**-axes. The results for the other headway models, relative to the mean of the five HeDS calculations, are presented in Figure 5.18. For the different gap assumptions, there is significant variation in the results for each of the five runs, particularly for longer bridges. In general, there is considerably less variation in the five HeDS runs.
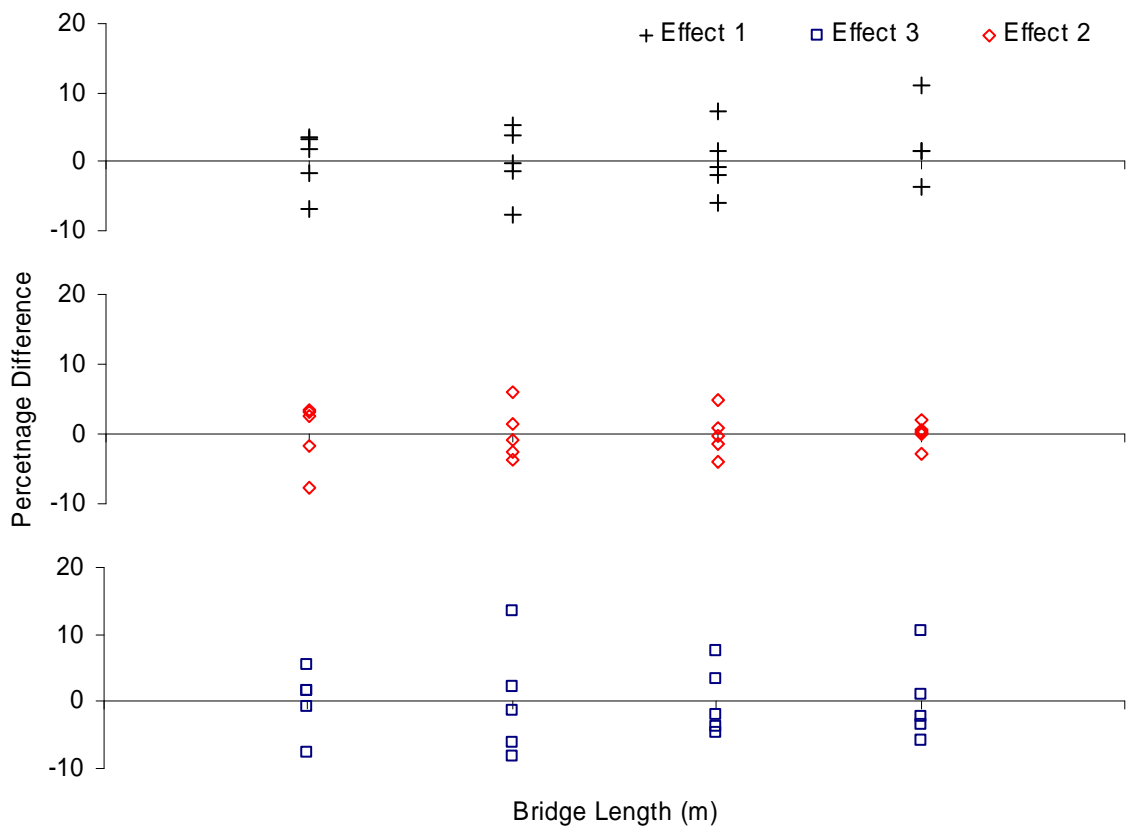
Figure 5.17: Variation in characteristic values calculated using HeDS.
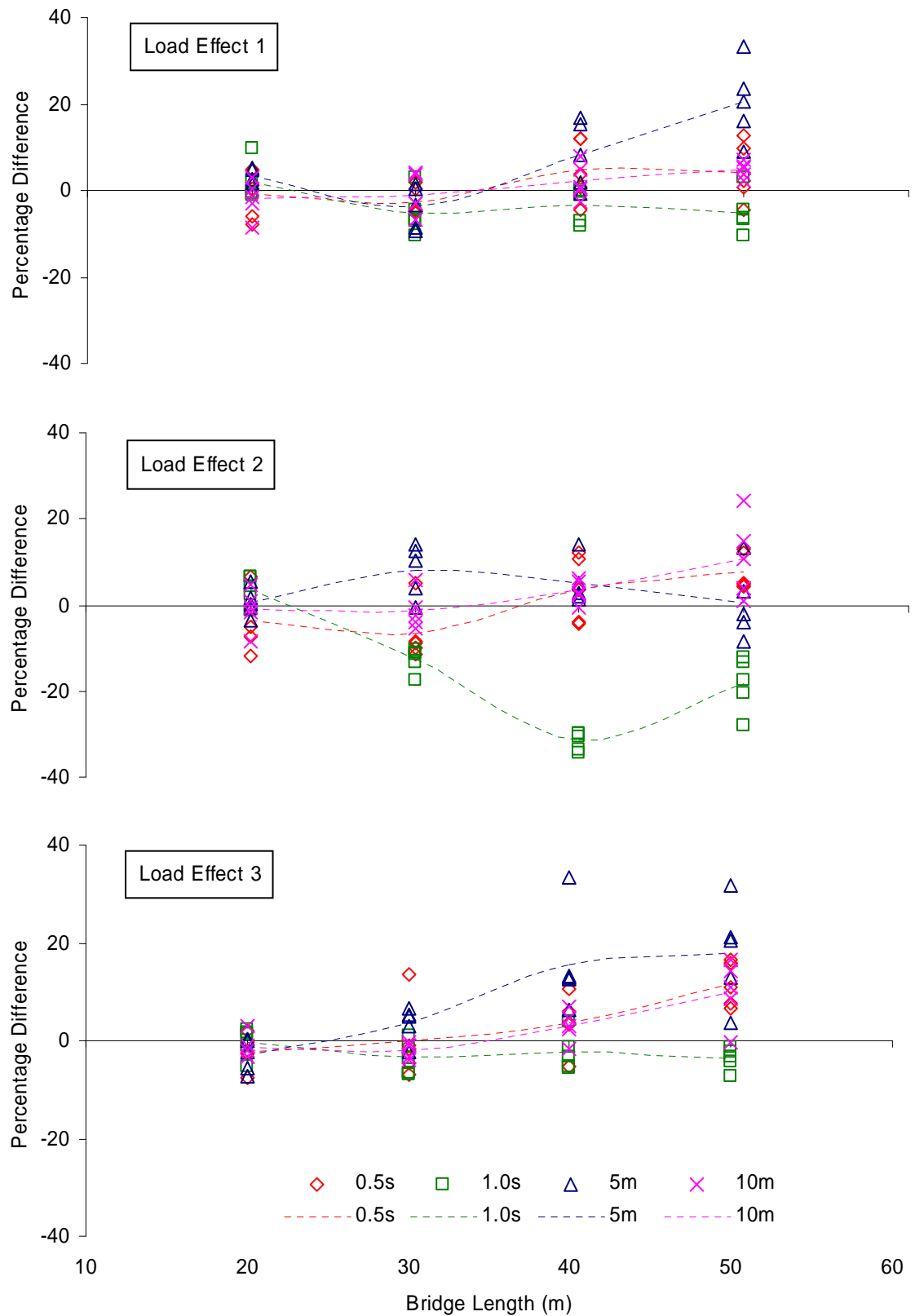
Figure 5.18: Variation in characteristic values, relative to mean HeDS value.

The gap assumptions result in substantial differences in characteristic value. While there is considerable variation between runs, it can be seen that the gap assumption strongly influences the mean result – by as much as 20% to 30%, depending on the assumption adopted. For Load Effects 1 and 3, the traditional approaches are generally conservative but for Load Effect 2 there is no clear trend.

There is a substantial non-conservative result from the 1.0 second gap assumption in 40 m bridges. The critical distance between point loads for central support moment in a bridge with two 20 m spans, is a little less than 20 m. The truck speeds are normally distributed but generally within 70 to 100 km/h, equivalent to ~20 to ~27 m in 1 second. Given a 10 m wheelbase for the following truck, the minimum distance between the two tridems implied by the 1.0 second minimum gap is 30–37 m. As a result, a 1.0 s MGC will cause Load Effect 2 to be underestimated for bridge lengths in the range 35–50 m. Figure 5.19 illustrates this point; it can be seen that the 1.0 s gap assumption has resulted in a considerably different truck arrangement to other methods.

Value: 2275.29   Distance: 5.352   Time: 27572.8

(a)

Value: 2215.85   Distance: 38.192   Time: 2813990

(b)

Value: 2162.8   Distance: 5.082   Time: 1617710

(c)

Value: 1708.47   Distance: -5.76   Time: 1456910

(d)

Value: 2170.95   Distance: 2.464   Time: 4038920
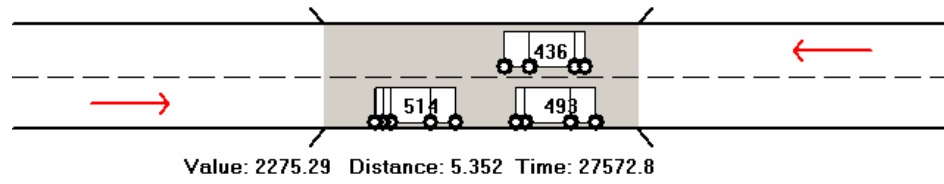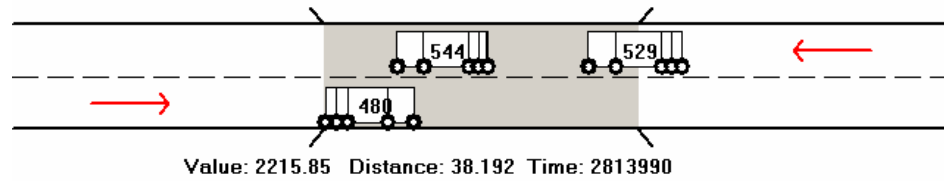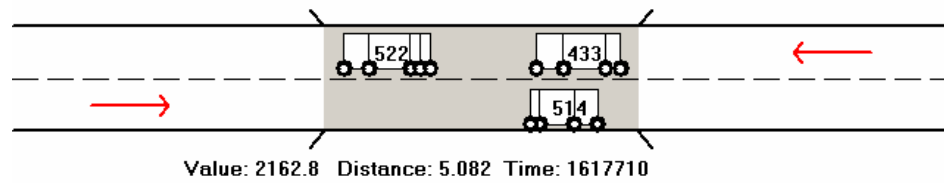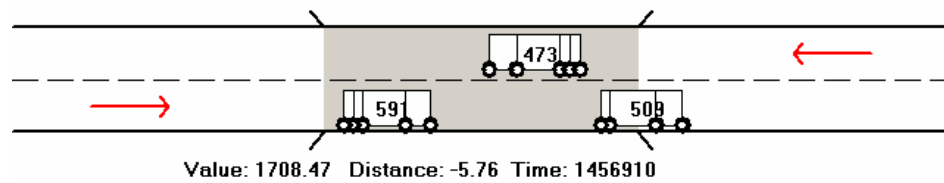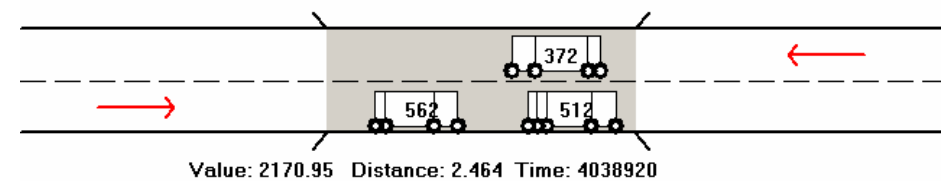
(e)

Figure 5.19: The critical 3-truck daily maximum events for Load Effect 2 and 40 m length for gap assumptions (a) 5 m; (b) 10 m; (c) 0.5 s; (d) 1.0 s, and for; (e) HeDS. GVW is shown on the trucks in units of deci-tonnes (i.e. kN/0.981).

5.5 Summary

The HeDS model presented appears to meet many of the requirements of a good headway model. It is relatively easy to implement, though quite involved to calculate initially. By using the features of the traffic - such as low correlation between headway and flow for small headways – the model is kept as simple as possible. The HeDS model is alternately conservative and non-conservative in comparison to the other models. Its results also typically lie between those of the 0.5 and 1.0 second MGC results. It appears that an MGC of around 0.7 - 0.8 seconds could give similar results to the HeDS model, were it to be required (however this is not recommended).

The influence line shape is found to be a determining factor in the accuracy of a given headway model when viewed in terms of its resulting load effects. It is found that 'peaked' influence lines (Load Effects 1 and 3), exhibit different responses to flatter influence lines (Load Effect 2). Generalizing further to influence lines not studied is suspect. Melchers (1999) notes a similar phenomenon in floor loading.

Through the implementation of the HeDS model, surprising results are found – such as the sensitivity of the Load Effect 2 influence line to the headway model used. More importantly, because the HeDS model does not artificially 'bunch' trucks at certain headways, these surprising results are able to be understood and explained by the nature of the physical process under study.

Chapter 6

STATISTICAL ANALYSIS OF MAXIMA

"Statistics: the only science that enables different experts using the same figures to draw different conclusions"   *– Evan Esar*

Chapter 6 - STATISTICAL ANALYSIS OF MAXIMA

6.1 Introduction

Gumbel (1958), in his summary, sets out the limitations of the asymptotic theory of extreme value statistics:

1. The observations from which the extreme values are drawn ought to be independent;

2. The observations must be reliable and be made under identical conditions. The initial distribution […] must be the same for each sample.

Collectively, this set of criteria forms the independent and identically distributed (iid) requirement on populations, upon which, an extreme value analysis is to be carried out.

A Bridge Loading Event (BLE) is defined as the presence for a continuous period of time of at least one truck on the influence area of the load effect of interest. BLEs are classified here on the basis of the number of trucks that contribute to the maximum load effect recorded during the event. Hence, for example, it is possible to have two trucks involved in a 1-truck BLE, provided only one contributes to the maximum load effect. Consequently, BLE-type is sensitive to the shape of the influence line for the load effect under consideration.

Single truck loading events are considerably more frequent than events involving more trucks, but the mean value of their load effect is relatively small as the GVW of individual trucks is limited. Multiple-truck loading events are rarer, but the combined weight of the multiple trucks can be much higher, so

the load effect tends to be larger. Load effect distributions that result from different types of BLE are therefore, in general, different.

This chapter addresses the impact of the iid limitation of extreme value analysis upon the bridge loading problem. Initially, load effect distributions caused by different types of loading event are studied and are shown to be non-iid. A method is then derived which accounts for the differences in load effect distribution and permits an extreme value analysis. This method is used in both theoretical and practical applications. The theoretical examples provide information on the behaviour of the method when its use is compared to known results. The practical application of the method is compared with a hybrid conventional approach derived from the current literature (Chapter 2).

6.2 Background

6.2.1 Distribution of load effects

The load effect resulting from a BLE, S_i, is the maximum load effect over the time period of the event. The distribution of S_i is termed the parent, or initial, distribution (Chapter 3) of load effect. The population that forms the basis of an extreme value analysis is the set of maximum load effect values, each the maximum of a sample of load effects which represent a period of time such as a day or month (Gumbel 1958). Depending on the form of the parent distribution, the extreme value distribution will asymptotically converge to one of Gumbel's (1958) extreme value distributions, or the Generalized Extreme Value (GEV) distribution (Chapter 3, Section 3.4). Should the parent distributions from different types of load effect be equivalent, then samples from those parents may be considered as identically-distributed. Conversely, should the parent distributions differ, then samples from those parents are not identically distributed. When such samples are 'mixed' together to form an extreme value population, the iid requirement of extreme value analysis is violated.

As a basis for the following work, 20 years (about 33×10^6 trucks) of truck traffic based on the Auxerre site, is simulated for Load Effects 1, 2 and 3 (see Chapter 4, Section 4.4.2) and for bridge lengths of 20, 30, 40 and 50 m. Single-truck events are only examined when the GVW of the truck is greater than 40 tonnes. A very large number of 1- and 2-truck loading events occur. As a result, only the first 50 000 load effect values are retained for further analysis. For 3- and 4-truck events, a smaller number of events occur and all load effect values are retained.

In total, for all bridge lengths and load effects, only seven 5-truck events were noted, all on a bridge length of 40 m. It is clear that 5-truck (and by the physical nature of the process, even 6-truck) events may contribute to the lifetime load effect. However, given the current simulation techniques such loading events are not readily observable. Indeed, the frequency of about seven events per 20 year period means that insufficient information is available to include these events in further analysis. It is only by extending the current computing techniques, or by some form of importance sampling, that the importance of 5- and 6-truck events may be assessed.

To determine the form of the parent distribution, S_i, for each type of loading event, a range of statistical distributions is considered, shown in Table 6.1. The WAFO Matlab toolbox (Brodtkorb et al 2000), and bespoke Matlab algorithms are used to obtain maximum likelihood fitting throughout. The relative quality of a fit is assessed from its log-likelihood value (Chapter 3).

For each load effect and for each span, there are up to 4 types of loading event of up to 50 000 values. Therefore, due to the large amount of processing involved, a preliminary study identifies those distributions that are to be considered for the full analysis – Table 6.1. Other distributions such as the Rayleigh, Beta, Gamma and Lognormal distributions do not fit the data nearly as well, and are not considered in the full analysis.

Fitted distributions	
Frechet	Gumbel
GEV	Normal
Generalized Gamma	Weibull

Table 6.1: Distributions considered for load effect parent distributions

An example of a set of fits is given in Figure 6.1; Appendix B gives the full results of the fits. The GEV distribution is noted especially in Figure 6.1 as it is the most frequent best fit. In fact, this is so for 42 out of 55 load effects and bridge length fits and the GEV distribution is close to the best in the remaining 13. However, there are some fits for which it is not sympathetic to the data – refer to Appendix B. This is the same problem noted in Chapter 2, Section 2.4.4 in relation to fits used by other authors. Clearly, in such cases, a more complex model would be appropriate. However, as the object here is to ascertain the overall behaviour of all of the load effect parent distributions, such cases are not investigated further. It is therefore assumed that the parent distributions of load effect are GEV-distributed. The parameters of the fits obtained for the GEV distribution are also given in Appendix B.
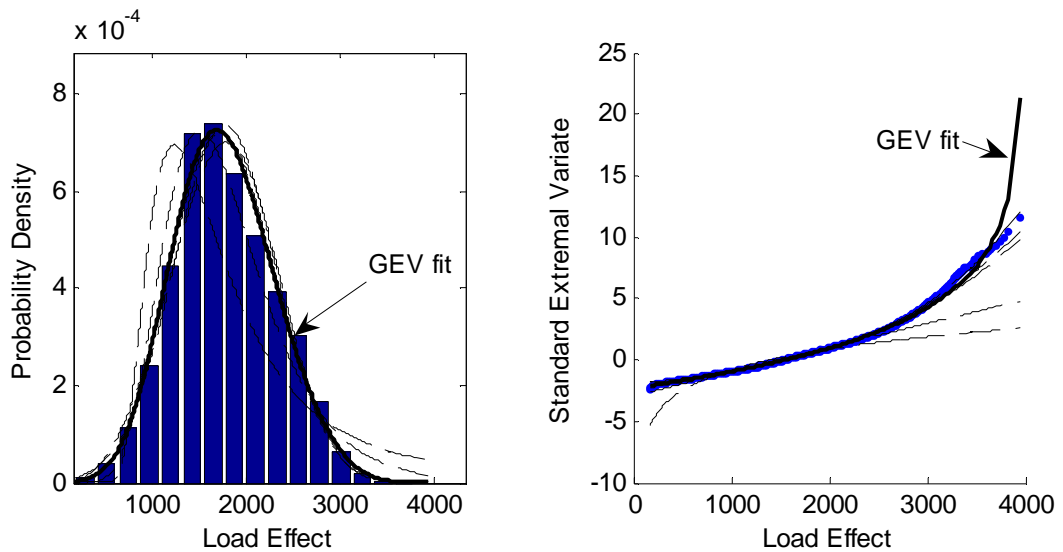
Figure 6.1: Parent distribution of load effect 1 due to 2-truck events on a 20 m bridge (fits to alternative distributions shown dashed).

The main aim of this analysis is to determine the form of the parent load effect distributions, and in doing so, to determine if they may be considered identical. Figure 6.2 shows the GEV distributions for Load Effect 1, all bridge lengths, and for all event-types. From this figure, and the main body of results given in

Appendix B, it can be seen that the distributions of load effect are different, depending on the composition of the loading event.
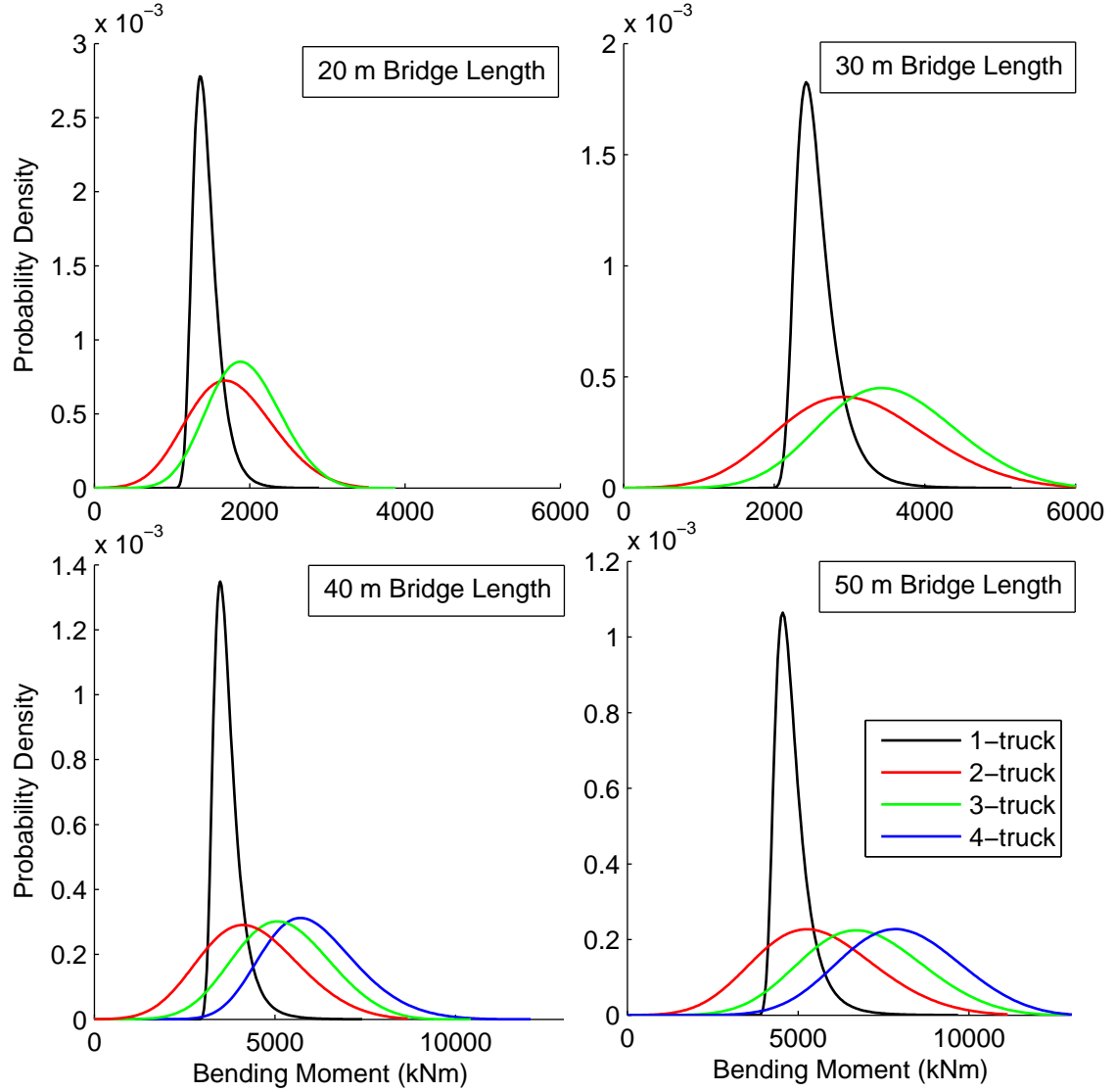
Figure 6.2: Parent distributions of Load Effect 1.

The GEV parameter values for Load Effect 1 are shown in Figure 6.3 for different event types and bridge lengths. Immediately apparent is the significant difference in the scale and shape parameters for the 1-truck events. Of particular physical significance is that the shape parameter indicates an unbounded distribution which is physically impossible. These values should be rejected for any real application. In such cases the fitting algorithm should be

limited to a shape factor of zero: the Gumbel distribution. To remain faithful to the simulated data, the negative shape parameters are kept here, and the implications are shown later to be problematic. The difference in the scale parameter is as a result of the limitation on 1-truck events: only those of trucks with GVW over 40 tonnes are included. Also, it is the 1-truck events that are least well fit by the GEV approximation to the parent distributions (Appendix B). For 2-, 3- and 4-truck loading events, it can be seen that for a given bridge length, the location changes slightly, the scale remains almost constant, and the shape parameter changes slightly.
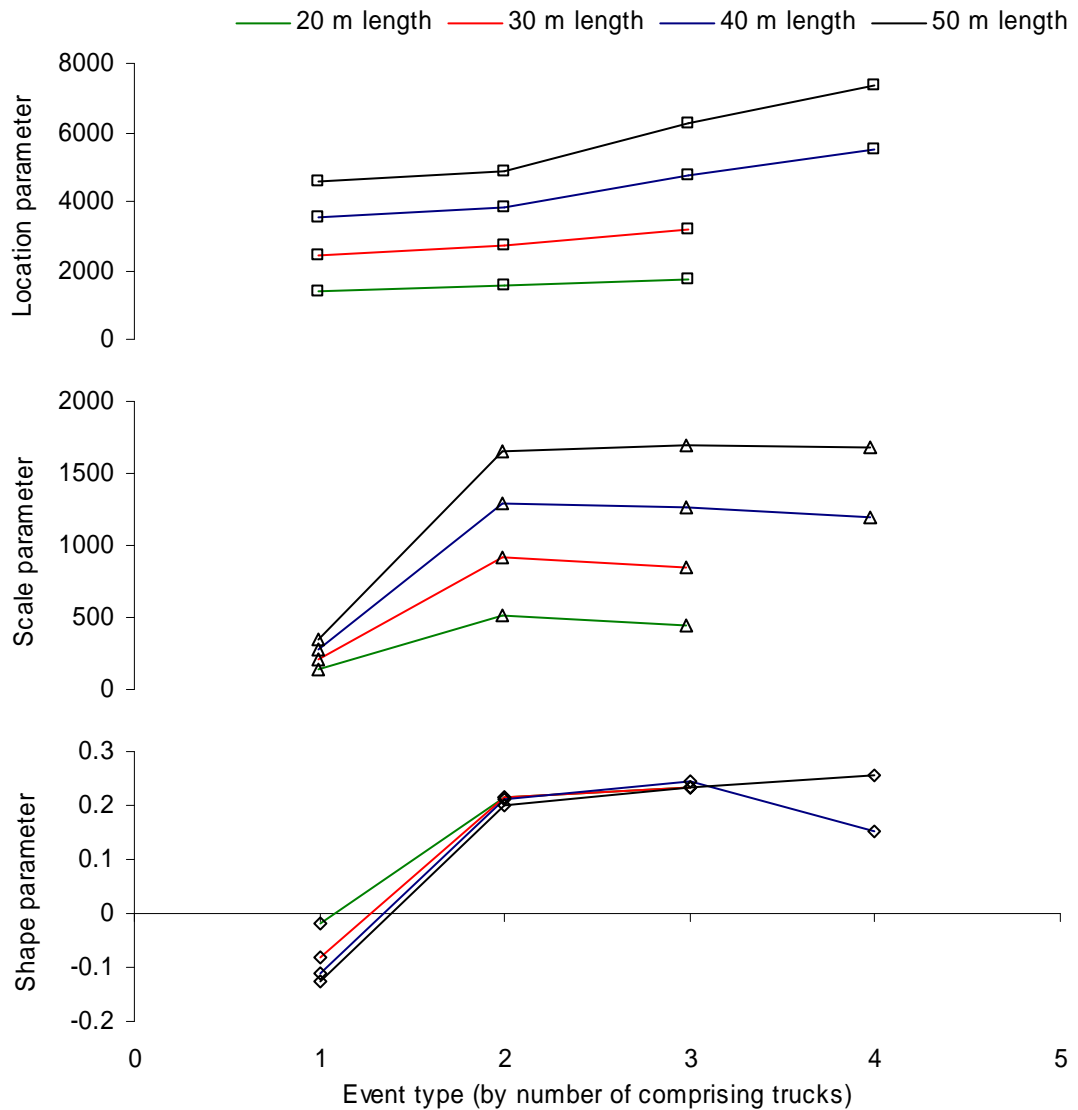
Figure 6.3: GEV parameter values for Load Effect 1.

The pattern of the GEV parameters illustrated in Figure 6.3 is repeated for the other load effects studied. Approximately, it appears that the location and scale parameters increase linearly with bridge length. To compare the relationship between the GEV parameters for different load effects (whose absolute values are significantly different), a normalization process is used, and is explained in more detail in Appendix B. For each load effect and bridge length, the 2-truck event location parameter value is scaled to a value of 100. This factor is then applied to the location and scale parameters of each of the fits for the other event types. Also, as a means of comparing the effect of bridge length, the location parameters for the 2-truck events of bridge lengths of 30, 40 and 50 m, are expressed relative to the normalized (100) 2-truck event location parameter of the 20 m bridge length. Thus, the effect of bridge length may be seen in Figure 6.4 – Load Effect 3 is not as sensitive to the bridge length as the other load effects – most probably due to its 'flatter' influence line shape.
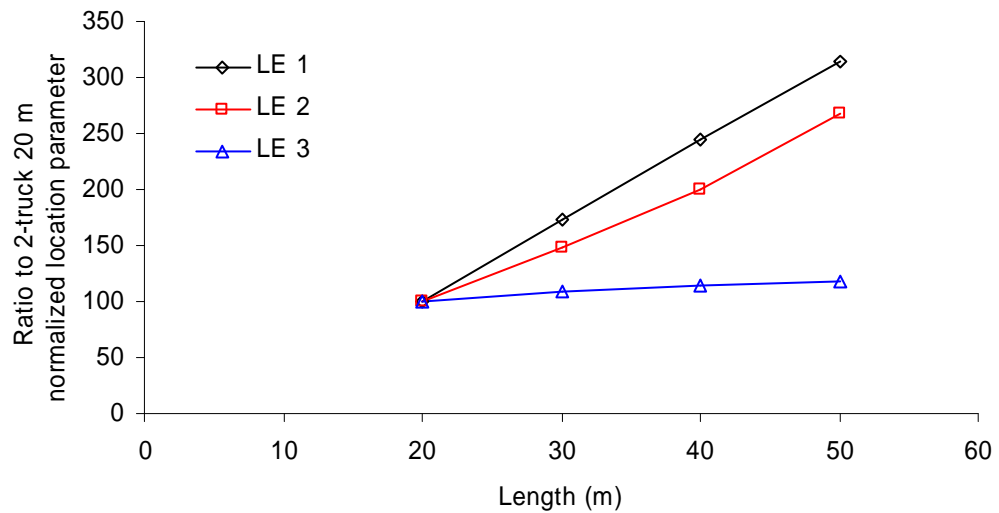
Figure 6.4: Effect of bridge length on 2-truck event location parameters.

The normalized parameter values for Load Effect 1 are shown in Figure 6.5. This form of representation makes it clear that, relatively, for the multiple truck events, the location parameter increases with increasing numbers of trucks in

the loading events; the scale parameter remains constant for events of over 1-truck; and, the shape parameter rises slowly. The 1-truck events exhibit a similar location value, but a lower scale value than the 2-truck event. This is expected as the 1-truck events are sampled only from trucks with GVW over 40 tonnes, whilst the 2-truck events represent all possible GVW values.
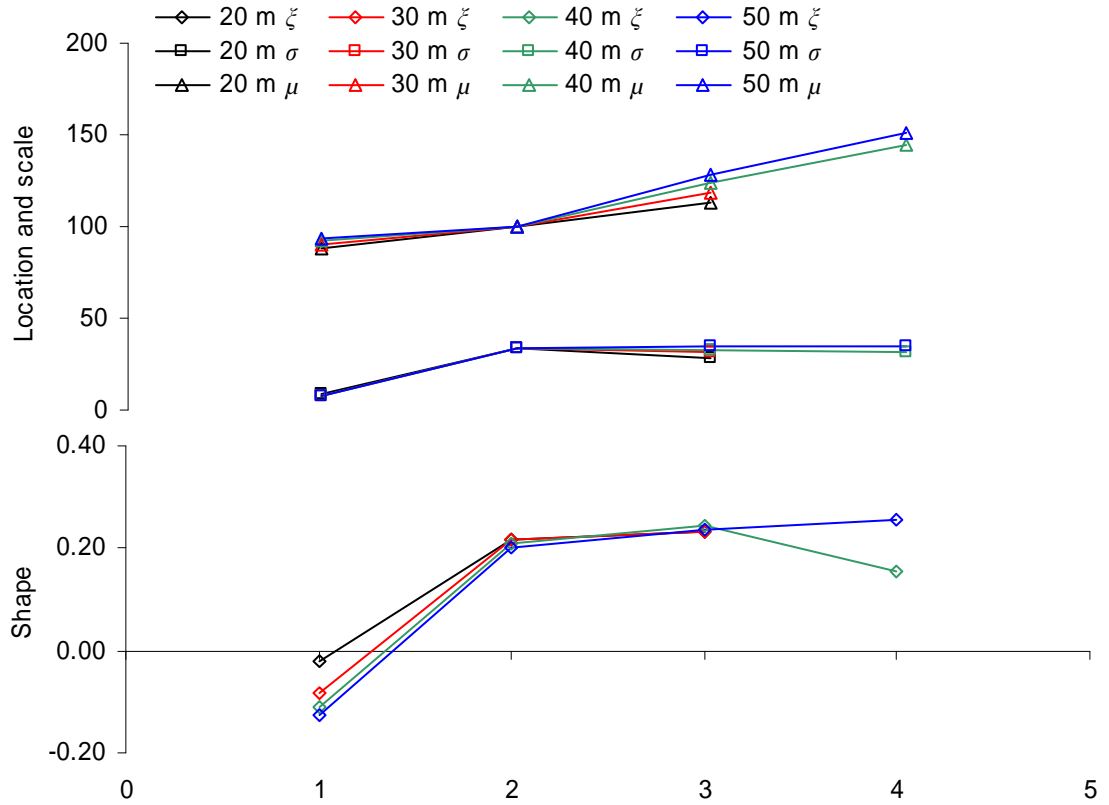
Figure 6.5: Normalized GEV parameter values for Load Effect 1.

The process of relating the parameters to the 2-truck event location value means that a global comparison of GEV parameters may be made, and this is shown in Figure 6.6. This figure is formed by superimposing the figures, similar to Figure 6.5 for each of the load effects. From this figure, for all spans and all load effects, a discernable relationship between the distributions of load effect for different event types is evident. The average parameter values from Figure 6.6 are determined, and used as the basis of further analysis in which a

representation of the relationship between the event types is required. These parameter values are given in Table 6.2.
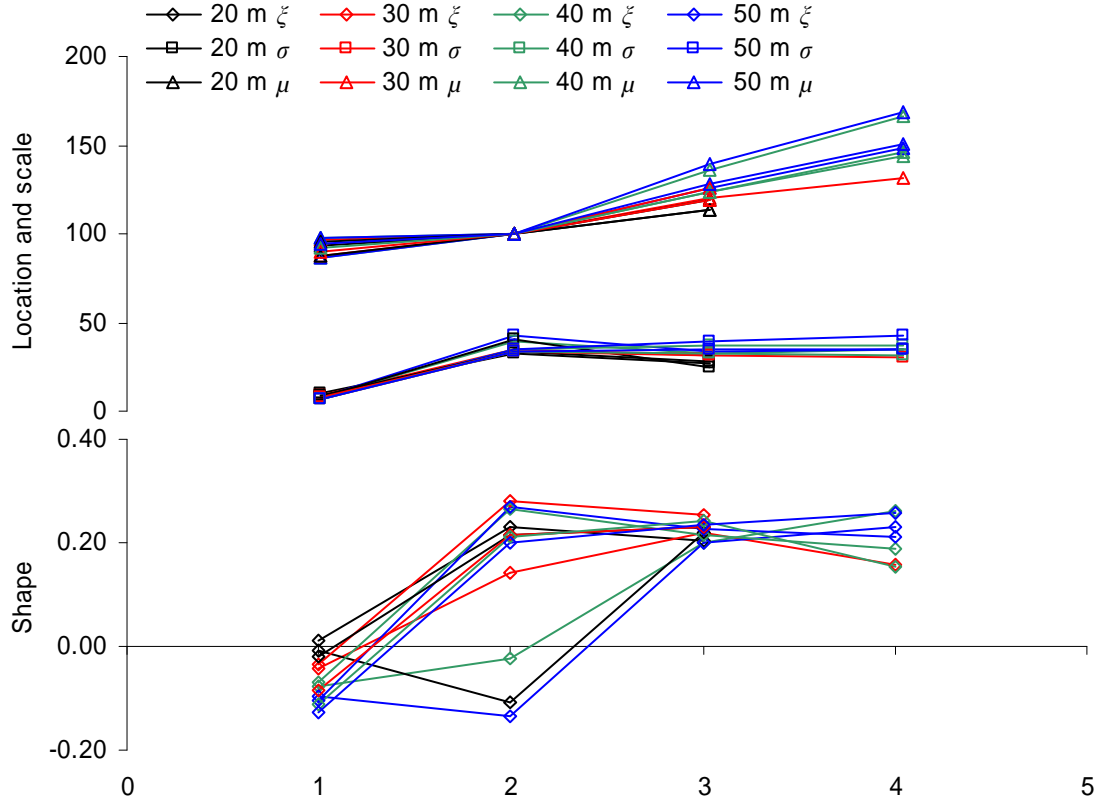
Figure 6.6: Normalized GEV parameter values for all load effects.

	1-truck	2-truck	3-truck	4-truck
Shape	-0.06	0.15	0.22	0.20
Scale	7.85	35.61	32.20	33.91
Location	92.21	100.00	123.85	146.73

Table 6.2: Mean normalized GEV parameters for event types.

6.2.2 Independence of events

Gumbel's first requirement for the use of extreme value theory states that observations from which extreme values are drawn ought to be independent. Independence requires that event-types are not reliant on the type of event preceding it. Intuitively it is reasonable that occurrences of bridge loading

events are independent: there is no rational mechanism though which a 2-truck event may be reasoned to 'cause' a subsequent 4-truck event, for example.

The assumption that occurrences of different event-types are independent is adopted in further analyses. Should mild dependence exist, however, the work of Castillo (1988) and Galambos (1978) demonstrates that standard extreme value theory may still apply.

6.2.3 Hybrid conventional approach

The previous sections have described how load effect values arising from different BLE-types are (surely) independent but not identically distributed. To take samples from such a mixture for use in an extreme value analysis violates the iid limitation of extreme value theory. However, the sensitivity of the results of an extreme value analysis to this violation cannot be readily assessed with usual extreme value approaches. Therefore some form of – what is termed here as – composite distribution statistics are required; this is developed in the following sections.

A hybrid 'conventional' approach to the bridge loading problem is used to compare with the composite distribution statistics developed as part of this research. This approach uses the absolute daily maximum load effect values, regardless of event-type, and maximum likelihood estimation is used to fit a GEV distribution to this population of 'mixed' maxima. In this way, many of the sources of error in the current literature are removed, such as: choice of population; the extreme value distribution used; the means of estimation; and the choice of threshold. Of course, the 'error' of interest, that of mixing non-iid data, is retained. The resulting comparisons therefore only have the 'mixing' as the basis for any differences.

6.3 Composite Distribution Statistics

6.3.1 Basis of development

A Bridge Loading Event (BLE) is defined in Section 6.1 as the presence for a continuous period of time of at least one truck on the influence area of the load effect of interest. Also, a BLE is classified on the basis of the number of trucks that contribute to the maximum load effect, S_i, recorded during the event. BLEs therefore have time duration: the time between instants when there are no trucks present on the bridge. The BLE so-defined is considered here as the fundamental event, in terms of probability theory (see Chapter 3).

The sample space of bridge loading events is constituted on the basis of the types of events that may occur. Of course, the sample space is not limited to any particular number of truck events but only 1- to 4-truck events are considered here. Therefore, in such a sample space, the events are deemed to be mutually exclusive and collectively exhaustive. Each BLE in this sample space also has a probability associated with it (relative frequency of occurrence).

The bridge lifetime is comprised of a large number of repetitions of the BLE sample space. In the bridge lifetime, many of each of the BLE-types may occur. Therefore, there are two frames of reference from which bridge loading events can be considered and, in general, different analyses result for each. The development described next is based on the fundamental event, described above, but permits inference on the bridge lifetime load effect.

6.3.2 Probability by event type

The BLE sample space is partitioned into n_t events, where n_t is the maximum possible number of trucks contributing to a maximum load effect. The

probability that the maximum load effect in the ith event, S_i, is less than or equal to some value s is then given by the Law of Total Probability:

$$P[S_i \leq s] = \sum_{j=1}^{n_t} F_j(s) \cdot f_j \qquad (6.1)$$

where $F_j(\cdot)$ is the cumulative distribution function for the maximum load effect in a j-truck event and f_j is the probability of occurrence of a j-truck event, where $j = 1, \ldots, n_t$.

For a given reference period (such as a day), n_d BLEs occur, and the distribution of the maximum value of the events, $\bar{S}$, is given by:

$$P[\bar{S} \leq s] = P\left[\max_{i=1}^{n_d} (S_i \leq s) \right]$$
$$= \prod_{i=1}^{n_d} P[S_i \leq s] \qquad (6.2)$$

This assumes that individual BLEs are independent. Substitution of (6.1) into (6.2) gives:

$$P[\bar{S} \leq s] = \left(\sum_{j=1}^{n_t} F_j(s) \cdot f_j \right)^{n_d} \qquad (6.3)$$

The number of BLEs in the reference period, n_d, is a random variable, and is in general different for each period. Gomes and Vickery (1978) note a similar issue with wind speeds, but report a study in which the approximation of the distribution of n_d by its mean value does not result in significant inaccuracy. Both Gomes and Vickery (1978) and Gumbel (1958) describe the inclusion of the variability of n_d in the analysis, but this is not attempted here. Therefore, in what follows, the expected value of n_d is used.

6.3.3 Asymptotic approximation

Considering only 1- and 2-truck events first, $n_t = 2$ and (6.3) reduces to a binomial expansion:

$$P\left[\overline{S} \leq s\right] = \left(f_1 F_1 + f_2 F_2\right)^{n_d} = \sum_{k=0}^{n_d} \binom{n_d}{k} f_1^k f_2^{n_d-k} F_1^k(s) F_2^{n_d-k}(s) \tag{6.4}$$

It is well known that a binomial distribution of the form,

$$\left(f_1 + f_2\right)^{n_d} = \sum_{k=0}^{n_d} \binom{n_d}{k} f_1^k f_2^{n_d-k} \tag{6.5}$$

converges to the normal distribution (for $n_d f_1 \geq 10$ approximately) with mean $n_d f_1$ and variance $n_d f_1 f_2$ (Feller 1968). Hence, the expansion of (6.5) is symmetrical with equal terms on either side of the mean – an illustrative example on this point follows this development. Rearranging (6.5), it can be expressed with terms in order of decreasing magnitude, as:

$$\left(f_1 + f_2\right)^{n_d} = \binom{n_d}{n_d f_1} f_1^{n_d f_1} f_2^{n_d f_2} + 2\sum_{k=1}^{n_d f_2} \binom{n_d}{n_d f_1 + k} f_1^{n_d f_1 + k} f_2^{n_d f_2 - k} \tag{6.6}$$

Equation (6.4) can be expressed in a similar form but, in this case, only the combined coefficient and $f_1^{n_d f_1 + k} f_2^{n_d f_2 - k}$ terms are symmetrical:

$$
\begin{aligned}
\left(f_1 F_1 + f_2 F_2\right)^{n_d} =\ & \binom{n_d}{n_d f_1} f_1^{n_d f_1} f_2^{n_d f_2} F_1^{n_d f_1} F_2^{n_d f_2} \\
& + \sum_{k=1}^{n_d f_2} \binom{n_d}{n_d f_1 + k} f_1^{n_d f_1 + k} f_2^{n_d f_2 - k} \left[F_1^{n_d f_1 - k} F_2^{n_d f_2 + k} + F_1^{n_d f_1 + k} F_2^{n_d f_2 - k} \right]
\end{aligned}
\tag{6.7}
$$

where the distributions $F_i(s)$ are written as F_i for clarity. As $F_1(s)$ and $F_2(s)$ are very close to unity for extrapolations to long return periods, they can be expressed as:

$$F_i(s) = 1 - \delta_i \text{ where } i = 1, 2 \tag{6.8}$$

for small δ_i. A Taylor series expansion gives:

$$F_i^m = (1 - \delta_i)^m = 1 - m\delta_i + \frac{1}{2}m(m-1)\delta_i^2 - \ldots \tag{6.9}$$

which is well approximated by the first two terms. Introducing the functions,

$$g_i^{+k} \equiv 1 - (n_d f_i + k)\delta_i \text{ and } g_i^{-k} \equiv 1 - (n_d f_i - k)\delta_i$$

equation (6.7) then becomes:

$$\begin{aligned}
(f_1 F_1 + f_2 F_2)^{n_d} &= \binom{n_d}{n_d f_1} f_1^{n_d f_1} f_2^{n_d f_2} (1 - n_d f_1 \delta_1)(1 - n_d f_2 \delta_2) \\
&+ \sum_{k=1}^{n_d f_2} \binom{n_d}{n_d f_1 + k} f_1^{n_d f_1 + k} f_2^{n_d f_2 - k} \left(g_1^{-k} \cdot g_2^{+k} + g_1^{+k} \cdot g_2^{-k} \right)
\end{aligned} \tag{6.10}$$

Ignoring second-order terms, $\left(g_1^{-k} g_2^{+k} + g_1^{+k} g_2^{-k} \right)$ reduces to $(1 - n_d f_1 \delta_1)(1 - n_d f_2 \delta_2)$. Using equation (6.6), equation (6.10) then becomes:

$$(f_1 F_1 + f_2 F_2)^{n_d} = (f_1 + f_2)^{n_d} (1 - n_d f_1 \delta_1)(1 - n_d f_2 \delta_2) \tag{6.11}$$

Given that $f_1 + f_2 = 1$ (representing the area under the probability density curve), and again using (6.9), this can be simplified to:

$$P\left[\bar{S} \leq s \right] = F_1^{n_d f_1} F_2^{n_d f_2} \tag{6.12}$$

If the parent distributions are extreme value distributed, then, by the stability postulate described in Section 3.4.2, $\left[F_1(s) \right]^{n_d f_1}$ and $\left[F_2(s) \right]^{n_d f_2}$ are also extreme value. Otherwise $\left[F_1(s) \right]^{n_d f_1}$ and $\left[F_2(s) \right]^{n_d f_2}$ converge asymptotically to an extreme value distribution if $\mathbf{n_d f_1}$ and $\mathbf{n_d f_2}$ are sufficiently large with respect to

the particular parent distributions. In such cases therefore, equation (6.12) becomes:

$$P\left[\bar{S} \le s\right] = G_1(s)G_2(s) \tag{6.13}$$

where $G_1(\cdot)$ and $G_2(\cdot)$ are extreme value distributions appropriate to each parent distribution.

For n_t event types, the multivariate normal distribution approximation to the multinomial distribution (Bishop et al 1975) may be used obtain a corresponding result:

$$P\left[\bar{S} \le s\right] = \prod_{j=1}^{n_t} G_j(s) \tag{6.14}$$

This result is similar to those described in Chapter 2, Section 2.5.2.

To avoid **a priori** decisions on the tail behaviour of the parent distribution, $G_i(\cdot)$ is considered to be of GEV form. By fitting to maxima of each event-type separately, the parameters of each distribution, $G_i(\cdot)$, namely μ_i, σ_i, and ξ_i, are determined. Hence equation (6.14) becomes:

$$P\left[\bar{S} \le s\right] = \exp\left[-h(s)\right] \tag{6.15}$$

where

$$h(s) = \sum_{j=1}^{n_t}\left[1-\xi_j\left(\frac{s-\mu_j}{\sigma_j}\right)\right]^{1/\xi_j} \tag{6.16}$$

6.3.4 Illustrative example

To illustrate the binomial nature of the $n_t = 2$ case, an example is considered in which there are 5 events in a day. The probability of a 1-truck event is 3/5 and the probability of a 2-truck event is 2/5; that is, the expected values are 3 and 2 for 1-truck and 2-truck events. Therefore, from (6.1), the parent distribution of load effect is given by:

$$P[S_i \leq s] = \frac{3}{5}F_1(s) + \frac{2}{5}F_2(s)$$
(6.17)

The distribution function for the maximum-per-day load effect, $\bar{S}$, is then given from (6.3) as:

$$P[\bar{S} \leq s] = \left[\frac{3}{5}F_1(s) + \frac{2}{5}F_2(s)\right]^5$$
(6.18)

The binomial expansion can be used to evaluate (6.18):

$$\left(f_1 F_1 + f_2 F_2\right)^n = \left(f_1^5\right)F_1^5 + \left(5f_1^4 f_2\right)F_1^4 F_2 + \left(10f_1^3 f_2^2\right)F_1^3 F_2^2$$
$$+ \left(10f_1^2 f_2^3\right)F_1^2 F_2^3 + \left(5f_1 f_2^4\right)F_1 F_2^4 + \left(f_2^5\right)F_2^5$$
(6.19)

in which the distributions $F_i(s)$ are written as F_i for clarity. The bracketed terms reflect the different probabilities related to all possible occurrences of the events, that is, there may be

- 5 1-truck events (probability equals f_1^5);
- 4 1-truck and 1 2-truck events (probability equals $5f_1^4 f_2$);
- 3 1-truck and 2 2-truck events (probability equals $10f_1^3 f_2^2$);
- 2 1-truck and 3 2-truck events (probability equals $10f_1^2 f_2^3$);
- 1 1-truck and 4 2-truck events (probability equals $5f_1 f_2^4$);
- 5 2-truck events (probability equals f_2^5).

Clearly, of the above possibilities, some are more likely than others. Further, the expected values should have the highest probability of occurrence, that is, 3 1-

truck and 2 2-truck events should have the highest probability. This may be seen best in the histogram which shows the weights of each term in the above expansion. Although possible, the occurrence of 5 2-truck events is seen to be very unlikely whereas the occurrence of 5 1-truck events is relatively more likely, as is expected.
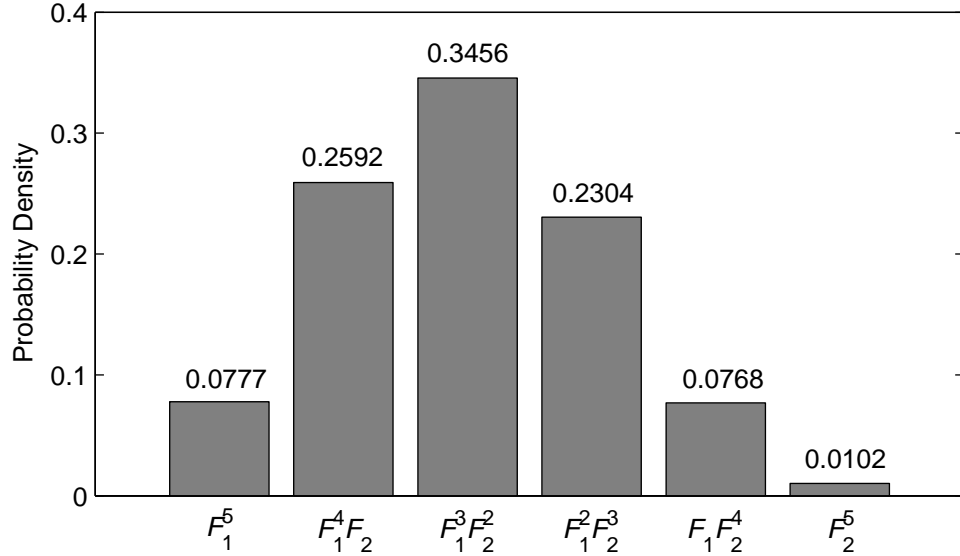
Figure 6.7: Histogram of term-weights for the illustrative binomial example.

The preceding arguments demonstrate that as n_d increases, the weights of the terms at the extremities decreases. That is, a mixture of the expected number of occurrences from each event-type becomes more and more probable.

6.3.5 Theoretical comparisons

A theoretical comparison of equation (6.14) with the conventional approach is difficult. Most of the statistical literature deals with likelihood ratio tests for nested models (Lehman 1986) but there are tests for non-nested models such as that proposed by Voung (1987). Unfortunately these tests do not strictly apply in this case, as the distributions for comparison are derived from different data sets, and a different number of data points. Also, comparison of the fits to the

overall daily maxima (for example) is misleading – the conventional approach will generally be better, as the composite distribution statistics approach is not fitted to the same set of maxima.

Based on the lack of theoretical means to evaluate the performance of the proposed method, some theoretical examples are used and are described in the following section.

6.4 Application to Theoretical Examples

6.4.1 Introduction

Aims

A theoretical comparison of the method of composite distribution statistics (CDS) against the hybrid conventional approach – described in Section 6.2.3 – is theoretically difficult, as has been noted previously. Therefore, the comparison is made through numerical examples for which the exact answer is known. Thus, the performance of CDS against the conventional method is assessed.

Procedure

The studies presented stipulate the parent distributions of load effect. Therefore, via equation (6.3), the exact distribution of load effect is known. Further, random values of daily maximum values from each component mechanism are simulated. Such data samples form the basis of the application of CDS and the conventional method; the results from both methods can be compared to the exact answer for a given return period, or the exact distribution. In this way, the studies mirror the real-life application of the proposed method and its behaviour in such problems can be assessed.

6.4.2 Sample problems and results

Many individual studies have been performed based on the approach outlined above; three such studies are presented here: the first and second are designed to reflect the true relationships between mechanisms that comprise the loading events; the third study, based on arbitrary parameters, provides insight into the nature of the asymptotic theory of extreme order statistics, and cases in which careful consideration of its applicability is required.

In each of the first two studies, six examples are carried out, based on all possible permutations of event-types, in an attempt to understand the influence of each event-type on the lifetime load effect. The six examples are derived from the different event-types as given in Table 6.3. Each event-type has an associated distribution and number of occurrences per day, for each of Studies 1 and 2, and these are described for each study in the following sections.

Example	1-truck	2-truck	3-truck	4-truck
1	✓	✓		
2	✓	✓	✓	
3	✓	✓	✓	✓
4		✓	✓	✓
5			✓	✓
6		✓	✓	

Table 6.3: Composition of the examples in Studies 1 and 2.

Study 1 – GEV Normalized Parent Distributions

In this study, the parent distributions obtained in the 20-year simulations of Section 6.2.1 are normalized (as described in Appendix B), and are used to approximate the inherent relationships between real parent load effect distributions. The parameters of each event-type are given in Table 6.4. To avoid unnecessary computation, these parent distributions are used to obtain daily maximum distributions (for each event-type) by linear transformation of the parent distribution, based on the stability postulate, as described in Appendix B.1.

The derived daily maximum distributions are used to randomly generate 1000 samples for each event-type, and this data forms the basis of the CDS approach. Further, the samples are processed to obtain the overall maximum load effect for each day, and this data forms the basis of the Conventional approach. Both

the CDS and Conventional models are then used to estimate the 100-year return level. This whole process is repeated 100 times to arrive at a distribution of predicted return level. The exact distribution for 100-year return level is derived from the stipulated distributions by application of equation (6.3).

	1-truck	2-truck	3-truck	4-truck
ξ	-0.06	0.15	0.22	0.20
σ	7.85	35.61	32.20	33.91
μ	92.21	100.00	123.85	146.73
$n_d f_j$	3102	2566	517	19

Table 6.4: Parameters of mechanisms for Study 1.

Figure 6.8 shows a typical set of random samples for each of the event-types, as well as the overall daily maximum values. The CDS and Conventional fits are also shown in the figure. It can be seen that the CDS converges towards the Conventional. It does so, as it is allowing for the possible occurrence of large effects from any of the 2-, 3-, or 4-truck events. The Conventional does not allow for this and follows the governing 4-truck simulation data.

In fact, for each of the examples of this study in which the 1-truck event is included, it governs the extreme due to the negative shape parameter. As noted earlier, it is physically impossible that 1-truck events are unbounded and hence in any real application the shape parameter should be limited to zero. Therefore as the GEV fits to the parent distribution of load effect for 1-truck events do not correctly reflect the underlying phenomenon, this distribution is not appropriate: a more complex (composite) distribution is required for proper inclusion of 1-truck loading events.
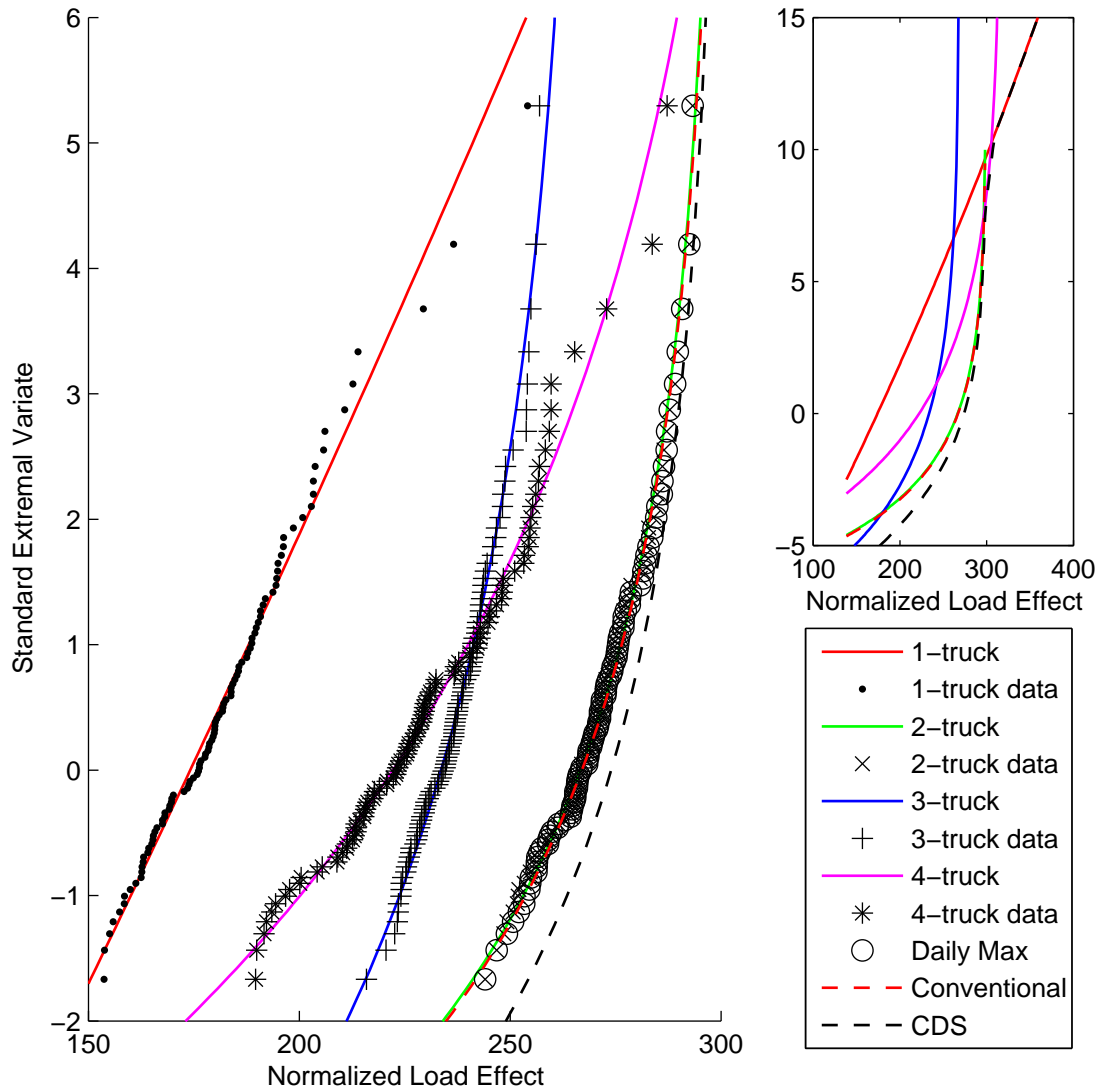
Figure 6.8: Study 1, Example 3: Typical extrapolation of 1- to 4-truck mechanisms from normalized, measured parent distributions.

Also of interest from Figure 6.8 is the 'crossover' point of several mechanisms at a normalized load effect value of about 300. As this crossover point occurs outside the range of the random samples, the Conventional method does not account for the governing mechanism beyond the crossover. However, in such cases the CDS method reflects the mixing that occurs, and properly reflects both the mixing of distributions and any clear governing distribution.

All of the event-types are included in Example 3 and the GEV-fitted distributions of results for this example are shown in Figure 6.9. It can be seen that the CDS method accounts for the divergent tail of the 1-truck governing mechanism, whereas the Conventional method does not: the 1-truck mechanism is not sufficiently dominant in the simulation range for the Conventional method to reflect this. Figure 6.9(a) shows that the exact distribution of the 100-year return level exhibits two distinct modes; the lower of which reflects the situations in which the 1-truck event does not govern, rather the 2- and 4-truck events govern. The implications of including physically impossible shape parameter values (<0) upon the lifetime load effect are apparent. It is therefore important that any real application takes the physical phenomenon into account and limits the possible range of distributions, as appropriate.

The parameters of the GEV distributions fitted to the distribution of return level estimates (for each of the 100 runs), are used to calculate the mean and (pseudo-)coefficient of variation (μ/σ^2) for each example for the CDS and Conventional methods. For each example, the mean is expressed as a ratio of the mode of the exact 100-year return level distribution, calculated from equation (6.3). The results are shown in Figure 6.10.

From Figure 6.10 it is apparent that the CDS method estimates the return level with good accuracy, and has a low coefficient of variation for the examples in which the 1-truck mechanism is not included. The Conventional method does not estimate the return level as accurately but has a lower coefficient of variation for the examples including the 1-truck mechanism.
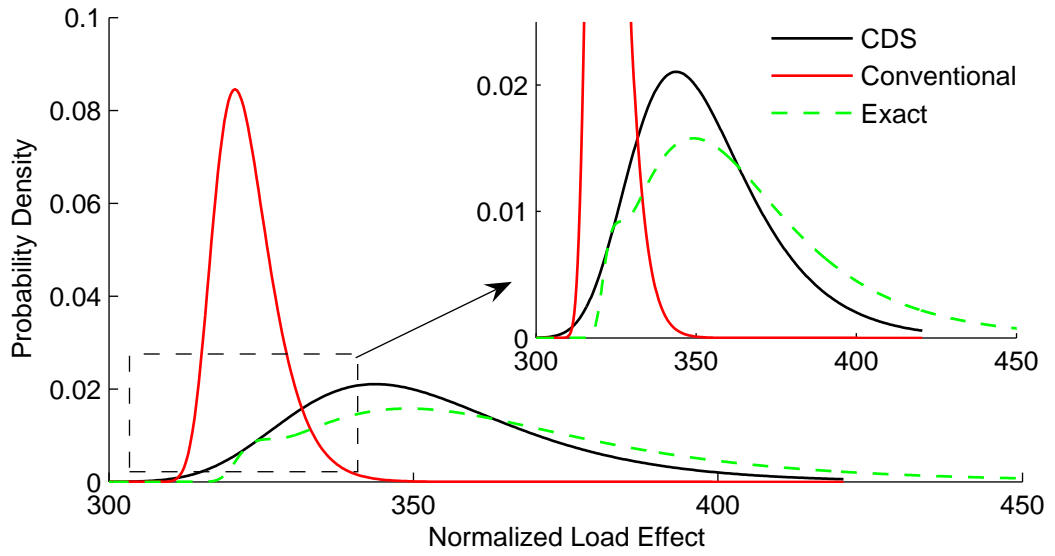
(a) Distributions of 100 return level values;
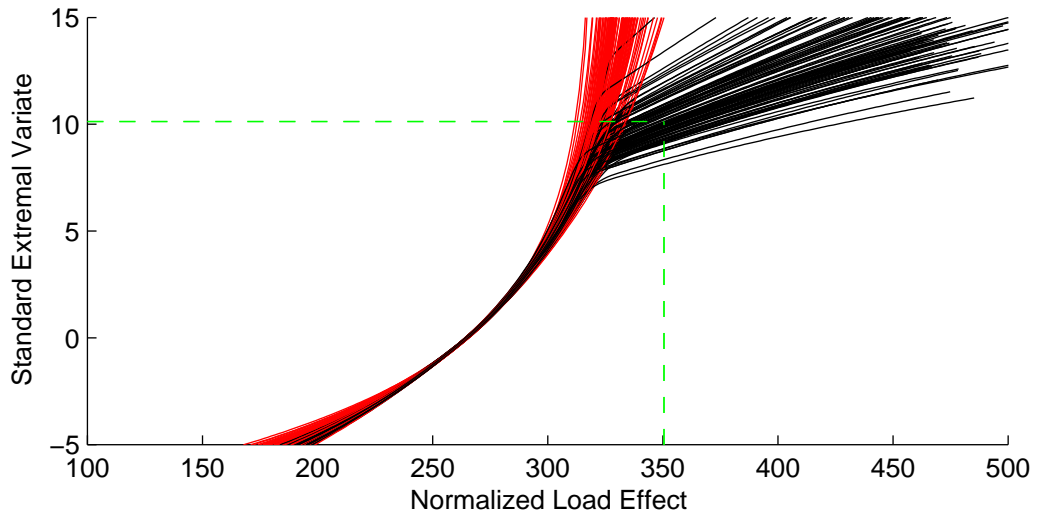
(b) 100 CDS and Conventional extrapolations and the exact mode;

Figure 6.9: Study 1, Example 3: 100-year return level estimates from CDS and conventional methods.

In this study, it is clear that the apparent 'misfitting' of the 1-truck parent distribution has severely distorted the results. In the following study however, this effect does not arise as the parent distribution is reverted from measured distributions of daily maxima.
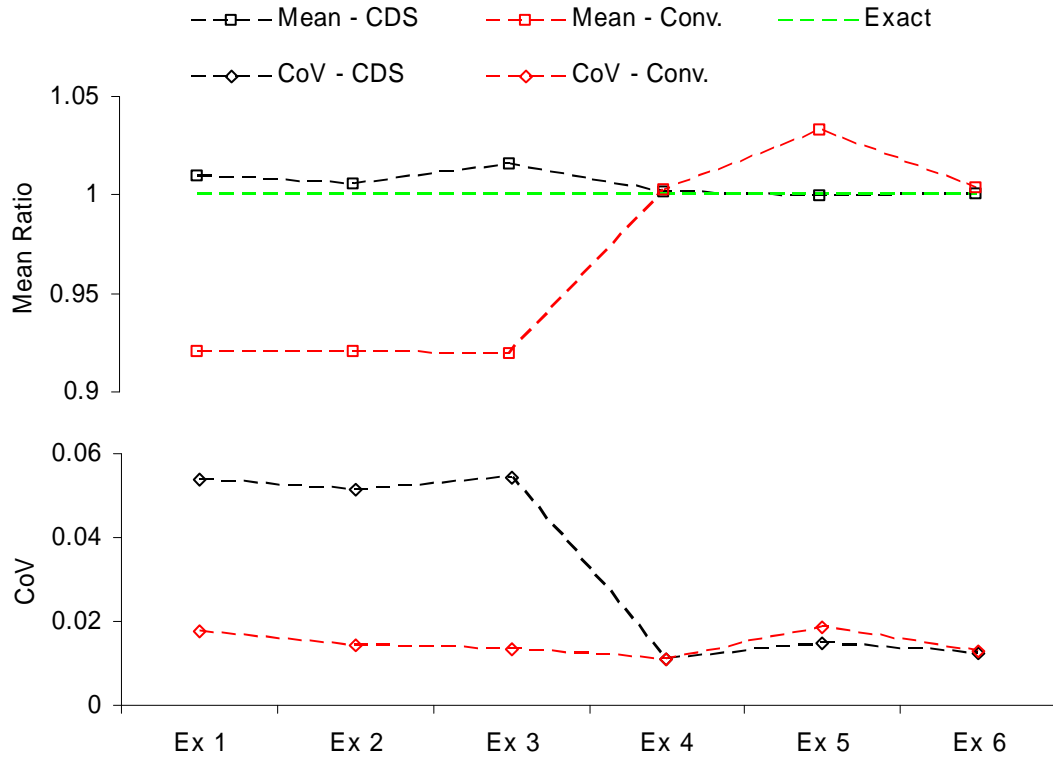
Figure 6.10: Results for Study 1 examples.

Study 2 – GEV Normalized Reverted Parent Distributions

Similarly to the previous study, this study uses GEV parent distributions to approximate parent distributions that may be found in reality. In this case, however, the problems of measuring and fitting parent distributions do not arise because 'reverted' parent distributions are used. These distributions are obtained from daily maximum distributions for each mechanism derived from the full simulation of 1000 days of Auxerre traffic. A backwards application of the stability postulate (as explained in Appendix B) is used to obtain the parent distributions that would result in the observed daily maximum distributions. Again however, and as explained in Appendix B, the parameters of the distributions are normalized to reflect the underlying relationship between the mechanisms regardless of load effect and bridge length.

The parameters of the mechanisms used in this study are given in Table 6.5; the individual examples are made up of different combinations of event-types, as given in Table 6.3. The procedure employed is as per Study 1. Figure 6.11 shows a typical random data set, along with the CDS and Conventional fits to the data.

	1-truck	2-truck	3-truck	4-truck
ξ	0.06	0.09	0.28	0.21
σ	1.41	2.37	9.99	22.76
μ	71.93	100	67.42	21.92
$n_d f_j$	3102	2566	517	19

Table 6.5: Parameters of mechanisms for Study 2.
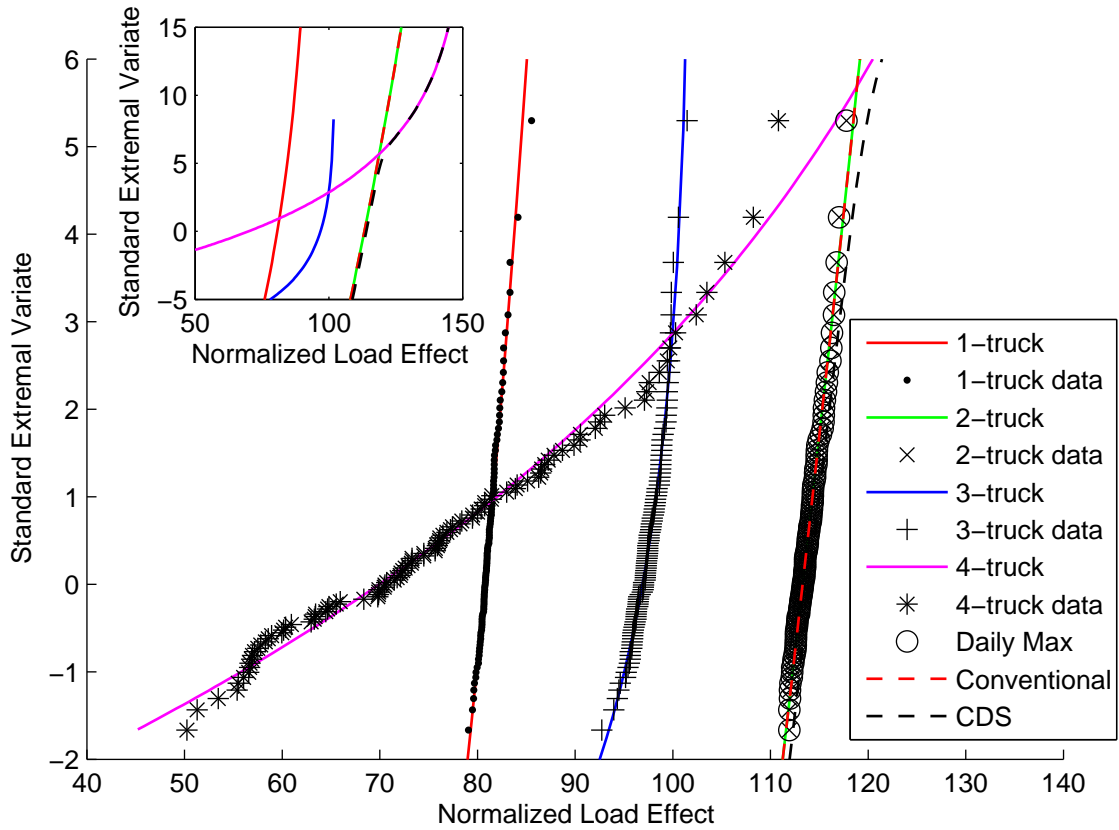
Figure 6.11: Study 2, Example 3: Typical extrapolation of 1- to 4-truck mechanisms from normalized, reverted parent distributions.

It is clear from Figure 6.11 that the 2-truck event governs in the range of the data, and the Conventional fit reflects this at the extreme level. The CDS distribution reflects the 4-truck distribution at the extreme range however, and it is this event-type that governs.

The GEV distributions fitted to the collection of 100 CDS and Conventional estimates of return level are shown in Figure 6.12. It can be seen that, due to the reasons outlined, the Conventional method underestimates the return level. The difference between the Conventional and CDS distribution modes is not large. It is the skewed nature of the CDS distribution that is significant: its 90-percentile is similar to that of the exact distribution.

Similarly to Study 1, the parameters of the GEV distributions fitted to the distribution of return level estimates are used to calculate the mean and coefficient of variation for each example. The results are shown in Figure 6.13. It is clear that the CDS means accurately reflect the mode of the exact 100-year return level distribution. The accuracy of the Conventional method appears to be dependent on the types of mechanisms included in the example.

Of note from this study, and Study 1, is the absolute value of the normalized load effects for Example 3 from each study. The exact modes are approximately 350 and 123 for Studies 1 and 2 respectively. This large difference is, in part, due to the inaccurate representation of the 1-truck event in Study 1. However, this is not the sole reason, and differences between the parent distributions of the other event-types from Study 1 to Study 2 also feature. It is clear that inference on the lifetime load effect level from parent distributions is very sensitive to the parameters of those parent distributions.
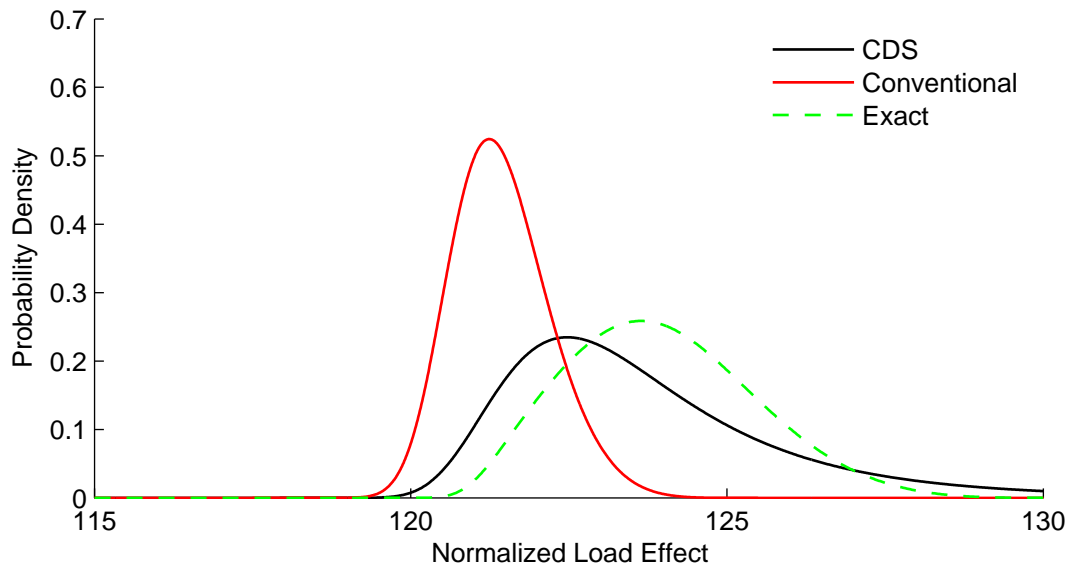
(a) Distributions of 100 return level values;
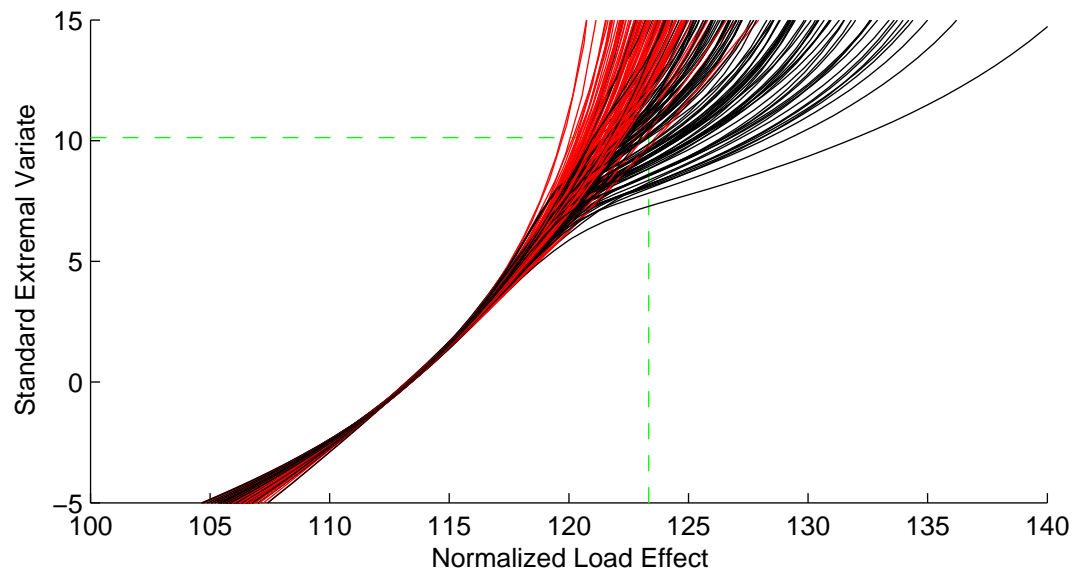
(b) 100 CDS and Conventional extrapolations and the exact mode;

Figure 6.12: Study 2, Example 3: 100-year return level estimates from CDS and conventional methods.
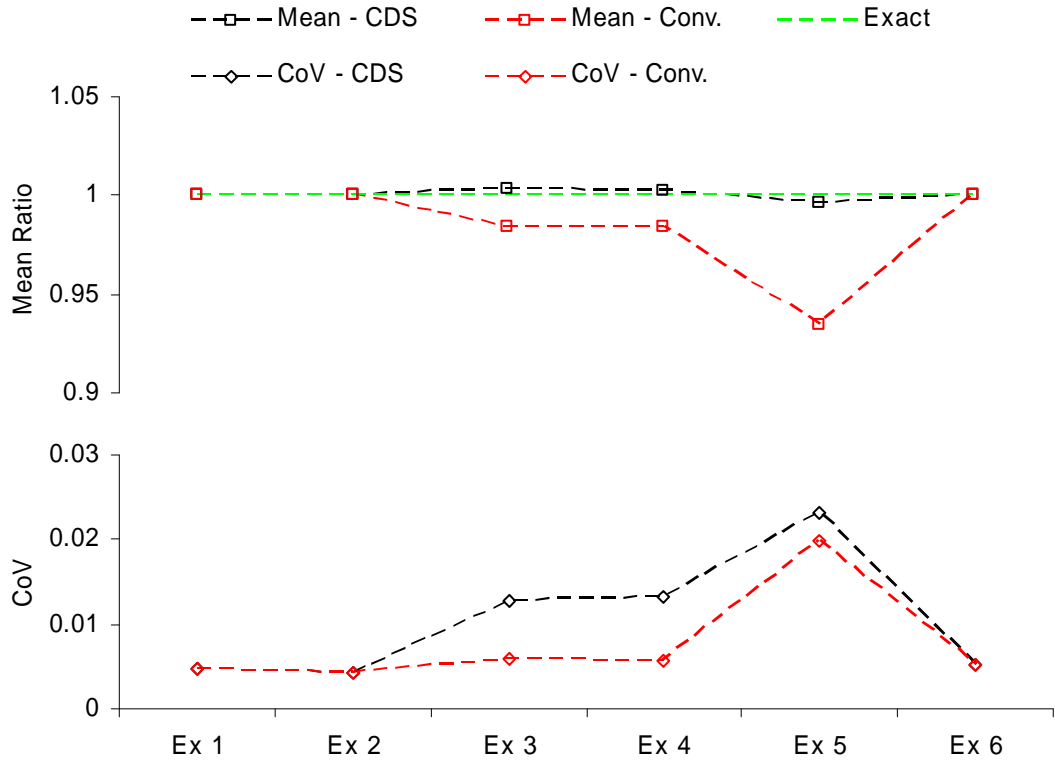
Figure 6.13: Results for Study 2 examples.

Study 3 – Normal Distribution Examples

Through various other studies, it is found that the CDS method described can appear to 'fail' at times. However, this is typically caused by inappropriate application of extreme value theory. In such cases, the use of 'exact' distributions of extreme may be more appropriate than the use of asymptotic extreme value theory.

This point is considered through use of the normal distribution as the basis of two statistical generating mechanisms. The normal distribution is very slow to converge to asymptotic extreme value form (Cramér 1946, Fisher and Tippett 1928). Theoretically, distributions of maxima from a normal parent converge asymptotically to the Gumbel extreme value distribution (Castillo 1988). Therefore, the Gumbel distribution is used as the appropriate extreme value distribution. Also considered is fitting of the 'exact' distribution of maxima,

$F^n(\cdot)$. In this case however, **n** is also considered as a parameter of the distribution as it is typically not known – only the data set of maxima is known.

The Gumbel distributions are fitted using maximum likelihood, as are the 'exact' distributions of maxima. The log-likelihood function for fitting the distribution of maxima, $F^n(\cdot)$, with unknown **n**, is given by:

$$l(x;\mu,\sigma,n) = \sum_{i=1}^{m} \log\left[n \cdot f(x;\mu,\sigma) \cdot F^{n-1}(x;\mu,\sigma) \right] \qquad (6.20)$$

Equation (6.20) is true for any distribution, but in this case, $F(\cdot)$ and $f(\cdot)$ represent the normal cumulative distribution and probability density functions respectively. This expression arises from equations (3.13) and (3.23). Numerical minimization of the negative log-likelihood is used to find those parameters that maximize the likelihood function.

The two normal distributions are taken as $N_1(420,30^2)$ and $N_2(380,45^2)$; the relative frequencies of occurrence are $f_1 = 0.9$ and $f_2 = 0.1$. It is to be noted that $\mu_1 > \mu_2$ yet $\sigma_1 < \sigma_2$ whilst $f_1 \gg f_2$. It is considered that 1000 events per time-period (block) occur and 1000 samples of block maximum are taken for each distribution, as is the absolute maximum for each block. These two data sets are used as the basis for two distinct applications of CDS and Conventional fitting. The two applications of CDS are based on individual Gumbel fits, which represents equation (6.13), and individual $F^n(\cdot)$ fits, representing equation (6.12). The Conventional fitting is done using a Gumbel distribution, to represent rigorous application of asymptotic extreme value theory. The sample data is randomly generated directly from the $F^n(\cdot)$ distributions to save unnecessary computation. The exact distribution is calculated from equation (6.3). The results are presented Figure 6.14.
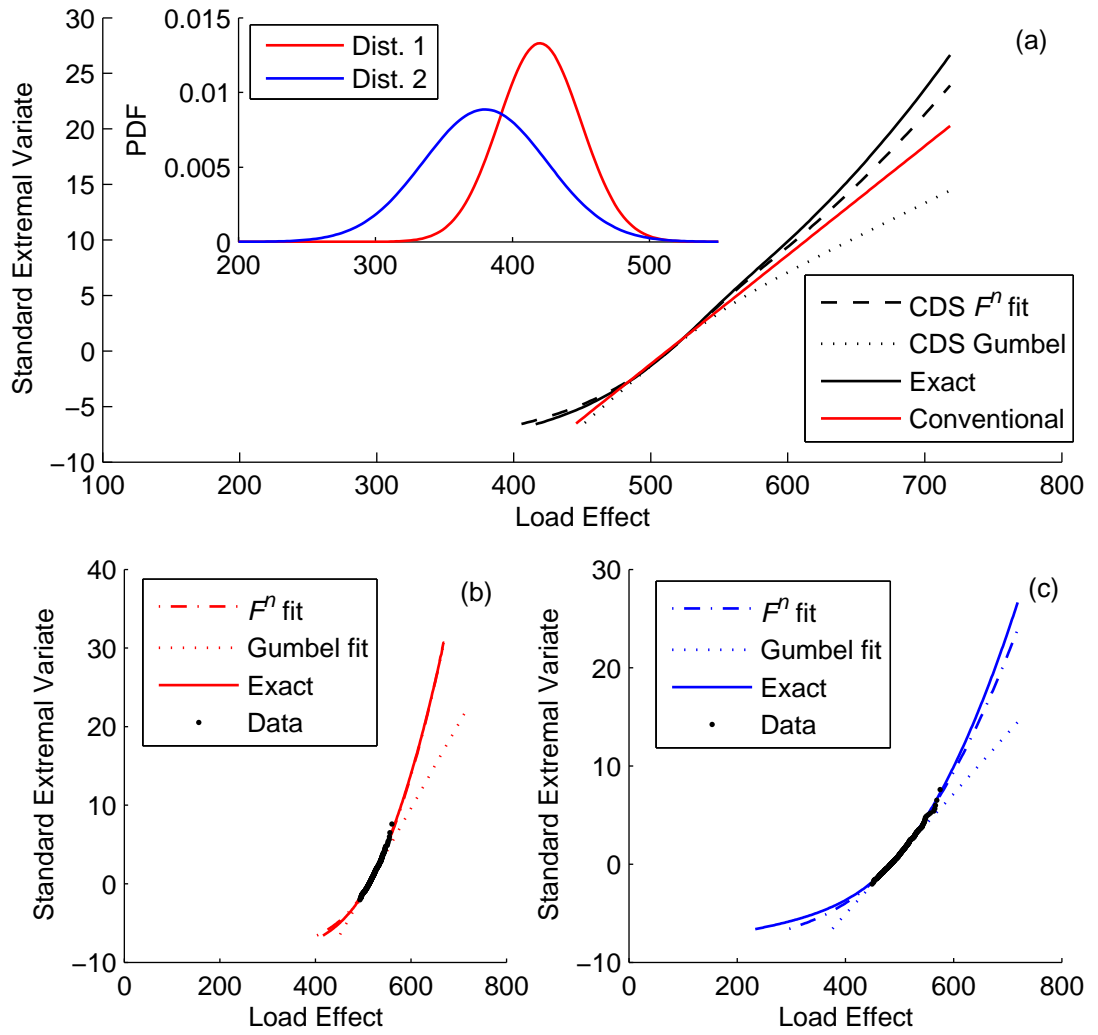
Figure 6.14: Example of improper use of asymptotic extreme value theory: (a) composite results; (b) $N_1\left(420, 30^2\right)$ distribution; (c) $N_2\left(380, 45^2\right)$ distribution.

The results show that the Conventional approach can appear more accurate than the CDS method, if asymptotic extreme value behaviour is assumed – Figure 6.14(a), CDS Gumbel distribution. However, when lack of convergence is allowed for by fitting an 'exact' distribution of maxima, or by using the upper $2\sqrt{n}$ data (Castillo 1988), the disparity is removed – Figure 6.14(a), CDS $F^n(\cdot)$ distribution. The disparity is caused by inaccurate fits to the individual distributions – Figure 6.14(b) and (c). The Conventional distribution appears reasonable as it is fitted to the governing distribution in the simulation data.

Effect of Sample Size

The framework of Example 3, Study 2 is used (as this includes all mechanisms, and is not biased by the 1-truck parent distribution estimate) to study the effect of different sizes of samples of daily maxima upon which the individual (and overall) daily maximum fits are made. Sample sizes of 100, 250, 500, 750 and 1000 (as previously) are used as the basis of the procedure outlined previously. For each of these sample sizes, there are, therefore, fitted GEV distributions for the CDS and Conventional methods of the 100-year return level estimates.

The results of the distributions based upon different sample sizes are shown in Figure 6.15 – for clarity only three of the distributions based upon the different samples sizes are shown. For both the Conventional and CDS approaches, it can be seen that with increasing sample size the variance decreases and the modes of the distributions shift slowly to the right. This is most probably caused by the increased number of load effect values from the 'governing' mechanism as the sample size increases. However, it can be seen that the CDS distribution is converging towards the exact distribution, whereas that of the Conventional method is converging to a different solution.

For the full set of samples analysed, Figure 6.16 shows the ratios of the mean CDS and Conventional results to the mode of the exact distribution (as previously described) and the coefficient of variation for the CDS and Conventional methods. It is clear to see that the mean is consistently accurate, regardless of sample size for the CDS method, whereas that of the Conventional method converges to an inaccurate value. This is caused by reasons outlined above. Further, the coefficient of variation of the CDS method decreases with increasing sample size and appears to be converging to an asymptotic value approximately that for a sample size of 1000.
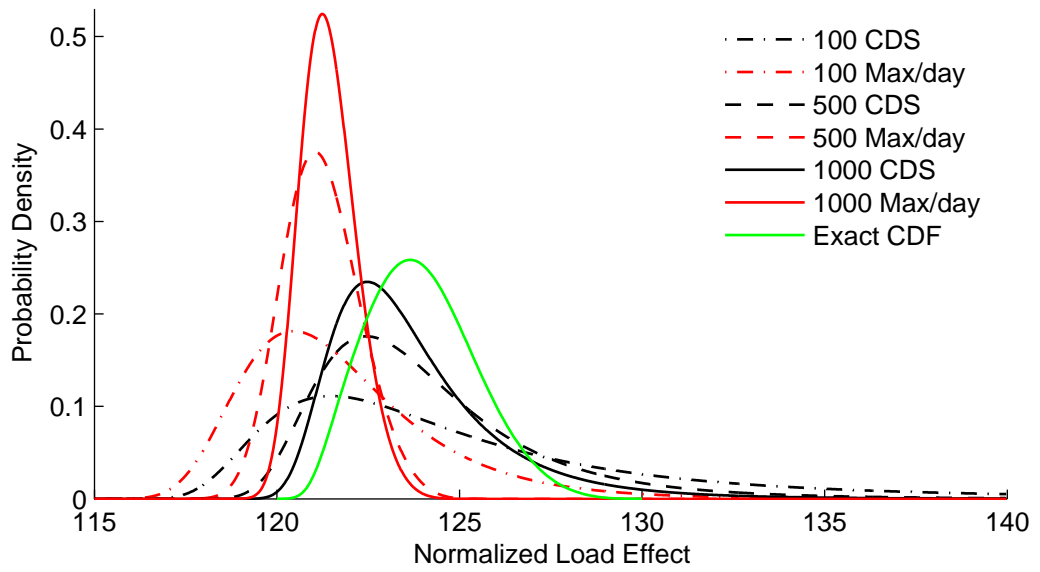
Figure 6.15: Effect of sample size, Example 3, Study 2.
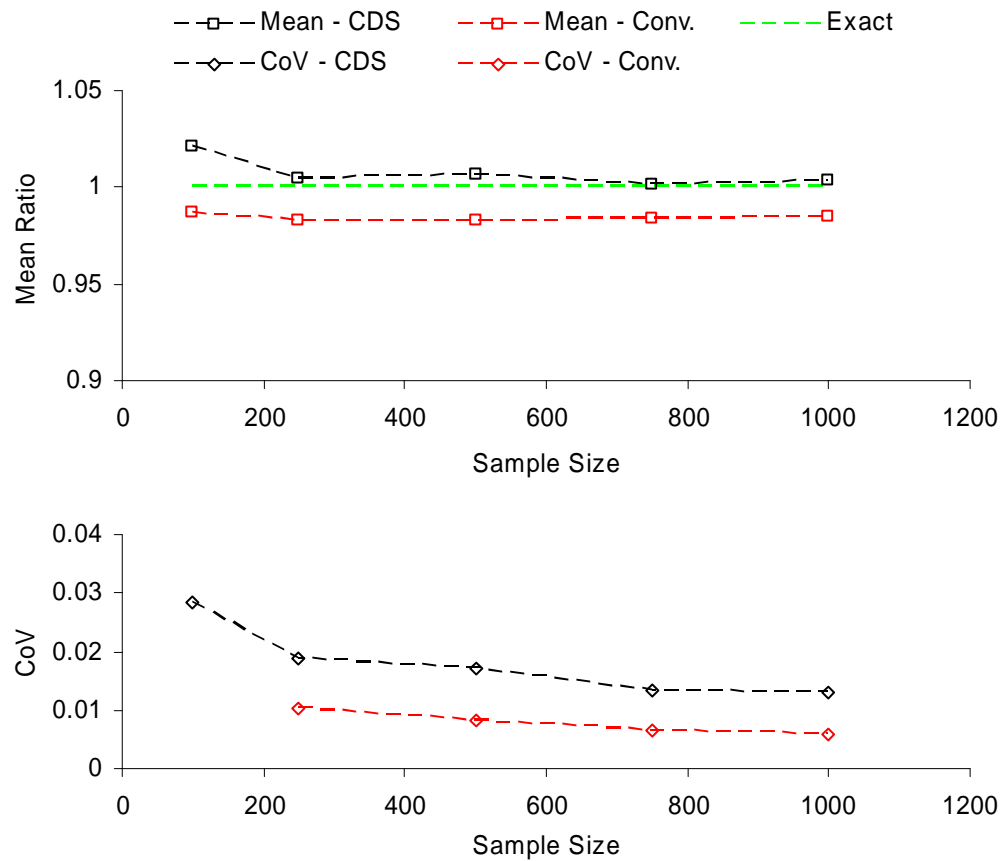
Figure 6.16: Results of sample size effect study for Example 3, Study 2.

6.4.3 Discussion of results

The results presented in Section 6.4.2 exhibit strong evidence that the CDS method outperforms the Conventional approach in the estimate of known return levels. It is also demonstrated that caution in its application is required, in order to adhere carefully to the requirements of asymptotic extreme value theory. However, an approach that uses the CDS method and avoids such problems is also presented.

Whilst it is clear that the conventional method can be reasonably accurate (Study 1 – Examples 4 and 5 and Study 2 – Examples 1 and 5), it is also apparent that this is due to favourable mixing of the comprising mechanisms in the simulation range. Therefore, the quality of the Conventional approach estimate is subject to the vagaries of the data – this should not be so for robust estimation and inference. Conversely, it appears that the CDS method does not require favourable data to return a reasonable estimate.

Through comparison of Example 3 of Studies 1 and 2, it appears the Conventional method performs well when the return level is not sensitive to the shape parameter of the 1-truck event. However, when the behaviour of this mechanism is outside the simulation data period, the Conventional approach does not reflect the distribution of return level accurately. Thus, it is possible to conclude that the CDS method is more robust and reflects the exact distribution of return level better.

Briefly, the results presented also demonstrate the inaccuracies that can result from incorrect evaluation of parent distribution data – it is better to work with extreme values (Castillo 1988, Coles 2001b), though this leads to data wastage.

6.5 Application to Bridge Traffic Loading

6.5.1 Introduction

The implications of the use of the Composite Distribution Statistics (CDS) method for the bridge traffic load problem are assessed in this section. Accordingly, a 1000-day simulation of Auxerre traffic on bridge lengths of 20, 30, 40 and 50 m is carried out for:

- Load Effect 1: Bending moment in the centre of a simply-supported beam;

- Load Effect 2: Bending moment over the central support of a two-span beam;

- Load Effect 3: Right-hand support shear force in a simply-supported beam,

as described in Chapter 4, Section 4.4.2. Other simulation periods are also used to assess the impact of the simulation period, and are compared to the results of Section 6.4.2.

As described in Chapter 4, only significant crossing events (SCEs) are processed. Also, when an SCE is identified, the truck(s) are moved in 0.02 second intervals across the bridge and the maximum load effects for the event identified. The pertinent data for the application of the CDS method, as well as that for the Conventional approach, is retained for the following analysis. The load effect values for a 1000-year return period are also calculated for both methods and compared. Maximum likelihood fitting and GEV distributions are used throughout.

6.5.2 Results of full simulation

For the load effects and bridge lengths described, 1000-year return period characteristic values, calculated from the CDS and Conventional approaches, are presented in Table 6.6. Immediately apparent is the general similarity of results, but it is also clear that some of the differences are significant – up to about 13%. This phenomenon is similar to that of the results presented in Section 6.4.2 (as may be expected), and is due to the particular nature of the mixing of the individual mechanisms that occurs.

Load Effect	Length (m)	CDS	Conventional	Percentage Difference
1	20	4067	4060	-0.2
	30	7852	7861	0.1
	40	10701	10732	0.3
	50	13893	14141	1.8
2	20	1067	1064	-0.3
	30	1643	1770	7.7
	40	2921	3297	12.9
	50	3785	3941	4.1
3	20	922	920	-0.2
	30	963	960	-0.3
	40	1079	1086	0.7
	50	1185	1195	0.8

Table 6.6: Comparison of 1000-year characteristic values.

Appendix B presents all of the results of this simulation. The fits to each of the mechanisms for all load effects and lengths is given, as well as the Conventional fit. Figures showing the data, fits, and the CDS and Conventional extrapolations for each of the bridge lengths and load effects are also given.

6.5.3 Governing mechanisms and mixing

The cases for which there is little difference between the CDS and Conventional approaches, reflect those for which little mixing of the mechanisms occur. That is, there is a clear 'governing' distribution, or event-type.

For a 20 m bridge length, and for the load effects examined, 2-truck loading events govern the extreme values. Physically, this is most probable as other forms of loading events require same-lane trucks. A spatial arrangement of loading events that includes same-lane trucks – when headway requirements are met – most often results in trucks that are only partially located on the bridge length – two examples are shown in Figure 6.17. Accordingly, loading events that allow the full length of a truck on the bridge length (or influence line) are expected to govern the extreme, and this is borne out in the results.

Value: 1607.46   Distance: -1.736   Time: 483019

(a) Load Effect 1;

Value: 643.124   Distance: -5.63   Time: 8620820
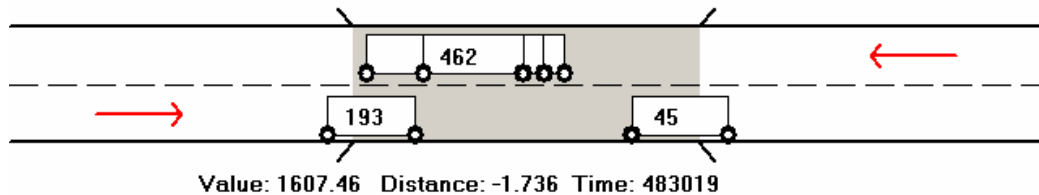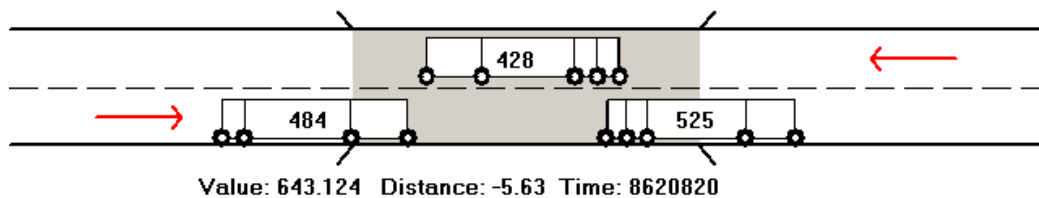
(b) Load Effect 2;

Figure 6.17: 3-truck events on 20 m bridge length (GVW is shown in deci-tonnes on the trucks).

For a bridge length of 30 m, 2-truck events mainly govern but some 3- and 4-truck events occur at the upper end of the simulation period. These events are not sufficient to affect the governance of the extreme, but this result may be reliant on the simulation period.

For bridge lengths of 40 and 50 m, it can be seen from Table 6.6 that the conventional approach is less accurate. It may be inferred from the theoretical examples of Section 6.4.2 that this is caused by mixing of the events. Indeed this is generally the case.

Of particular note, is the large difference for the 40 m bridge length, Load Effect 2 result, shown in Figure 6.18. This figure shows the individual fits along with the Conventional and CDS methods and the 100- and 1000-year return periods. For clarity, the data is not shown (but can be seen in Appendix B).
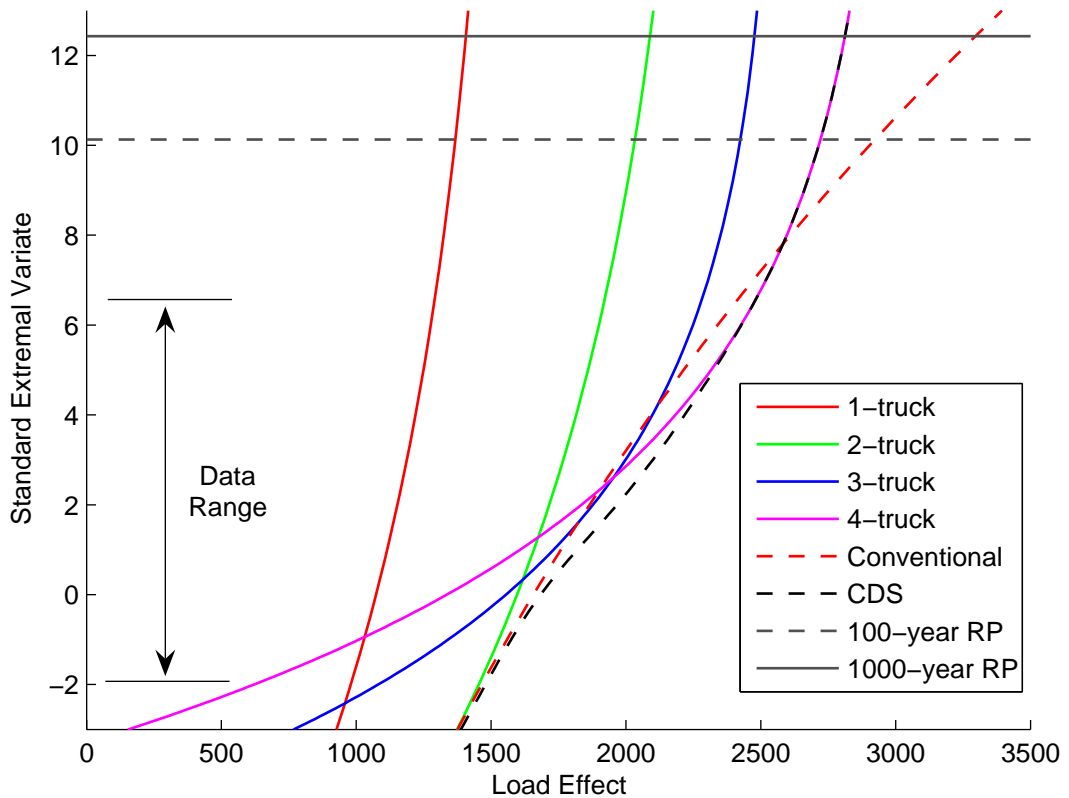
Figure 6.18: Distributions for 40 m bridge length and Load Effect 2.

Initial examination of Figure 6.18 shows that 1-truck events, and above a certain level, 2-truck events, do not govern. It is therefore mainly 3- and 4-truck events that govern this load effect, which is to be expected given the shape of the influence line (Chapter 4, Section 4.4.2). Therefore, the Conventional fit is mainly comprised of these event-types; the net effect of this uneven mixture is to produce the distribution shown in Figure 6.18.

In contrast to the behaviour of the Conventional method noted, the CDS method faithfully follows the envelope defined by, firstly the 3-truck event, but then the 4-truck event. The behaviour of the CDS distribution at the crossover point of the 3- and 4-truck mechanism is also of note: it is slightly removed from either curve, reflecting that a load effect could be from either event, and is thus more likely (and consequently has a lower y-value) than as if from one event-type. This behaviour can also be seen at the crossover of the 2- and 3-truck curves. Such crossover-point behaviour of the CDS is general and is always observed at crossover points.

It is important to note that physically, given the shape of the influence line, it is to be expected that 4-truck events should govern the extreme. This appears to be recognized by the results, but possibly not as strongly as may be expected: there is only a slight difference in the 3- and 4-truck curves at the extreme values in Figure 6.18. A longer simulation period may result in an increased importance of 4-truck events. Further, the observed behaviour is subject to random variation (similarly to the examples of Section 6.4.2) and it is possible that there may be a smaller difference between the two methods for other samples.

6.5.4 Effect of simulation period

The implications of the length of the simulation period chosen are assessed, relative to the 1000-day period. Though this is studied in the context of the examples of Section 6.4.2, it is studied here to assess the effect upon the actual application of the CDS and Conventional methods.

Simulation periods of 50-, 250- and 500-days are used to compare with the results of the 1000-day simulation described in the previous section. The percentage difference of the CDS and Conventional results, relative to the 1000-day CDS result, are shown in Figure 6.19.

In general, it is apparent from Figure 6.19 that the difference tends to reduce for increasing sample size, or simulation period. With some exceptions, the CDS method gives smaller differences than the Conventional method, though not significantly. There is a change in behaviour for the 500-day results: larger negative differences are observed for the Conventional approach than for the other simulation periods. The difference is significant for Load Effect 2, and this is in keeping with the results outlined for the 1000-day simulation. It is clear, however, that the other CDS percentages do not exhibit this behaviour and are reducing for this larger period.

Generally, the differences observed due to the simulation period are quite variable. It is difficult to infer upon the systematic effect of a longer simulation period therefore. Indeed it seems plausible that more than 1000-days of data is needed before differences stabilize. It must be noted however, that all such results are subject to random variation and the only true comparison is one that accounts for this.
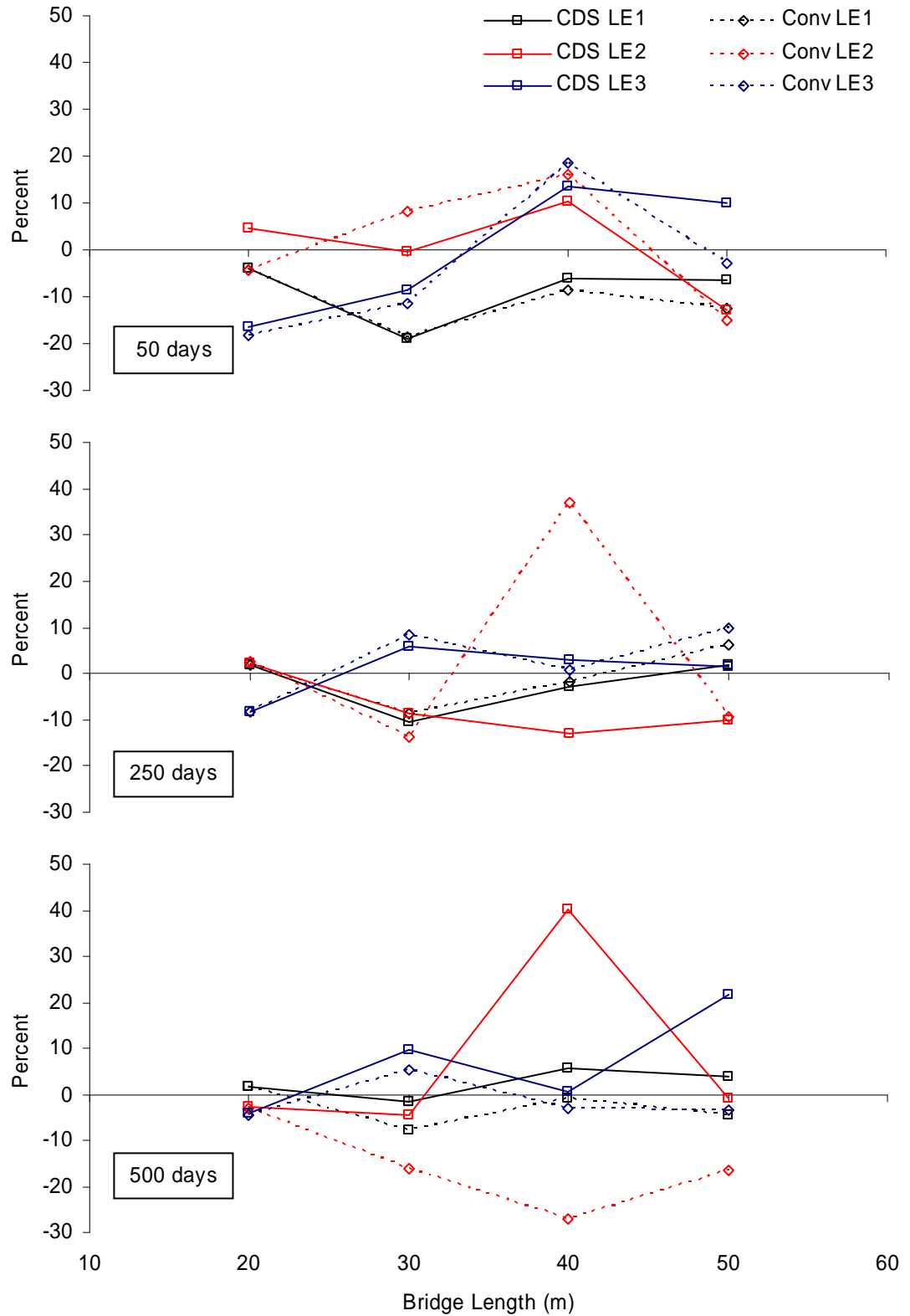
Figure 6.19: Deviations of extrapolated load effects for different simulation periods to those from a 1000-day period.

6.6 Summary

A detailed analysis of load effect is presented at the outset of this chapter. This analysis assesses the two primary assumptions of extreme value theory with respect to bridge loading events. It is shown that whilst the events may be considered as independent, they are not identically distributed. The implications of this for standard extreme value analysis of bridge loading events are outlined through the derivation of a method that recognizes these facts – the method of Composite Distribution Statistics (CDS).

The CDS method is shown to give different results to a hybrid Conventional approach, defined by the best features of models in the literature. From the analysis of load effect distributions presented, theoretical examples are developed though which the performance of the proposed method is assessed and compared with that of the Conventional approach. It is shown that the violation of the assumption of identically distributed data by the Conventional method, results in different predictions (in some cases significantly so) to the CDS method, which acknowledges the differences in distributions of the data.

The CDS method is applied to full traffic simulations on a range of bridge lengths and load effects. It is shown that some forms of loading event tend to govern certain lengths and load effects, and that this behaviour is dependent on the physical nature of the bridge loading problem. Also, it is clear that it is not reliable to assume that a particular event-type governs, as mixing of the distributions occurs. Further, it is also noted that the random variation of the results of simulations can mask systematic behaviour. As a result, it seems prudent to account for this random behaviour in the predictions made.

Chapter 7

PREDICTION ANALYSIS

"Prediction is very difficult, especially about the future"   *- Neils Bohr*

Chapter 7 - PREDICTION ANALYSIS

7.1 Introduction

The examples presented in Chapter 6 demonstrate the variability in the predicted extreme that exists even for well-defined initial distributions. As the parent distribution is known in these examples, this variability is due to the random sampling of the distribution and the random nature of the fitted parameter vectors. It is to be expected that this also occurs with the results of a bridge load simulation. Therefore a method, reliant on a specific set of sample data, is required to estimate the variability attributable to these sources.

In this work, the theory of predictive likelihood is used to estimate the variability in the bridge lifetime load effect prediction. The Eurocode (EC1: Part 3: 1994) requires bridges to be designed for the load effect with 10% probability of exceedance in a 100-year bridge lifetime – the characteristic value. Therefore, predictive likelihood is used to estimate the distribution of 100-year load effect (including many sources of variability) and thereby estimate the characteristic load effect.

Predictive likelihood is based on the likelihood function, explained in Chapter 3. Through its use, the credibility of different possible lifetime load effect values, given the data, is assessed. In this way, postulated lifetime load effect values are formed into a distribution of lifetime values based on their relative likelihood. Through this approach, sources of variability can be accounted for and the resulting distribution reflects this.

The statistical literature on predictive likelihood is limited to analysis based on simple distribution forms. Application of predictive likelihood to the bridge

loading problem is complicated by the composite distribution statistics approach. However, it may be seen from the results of Chapter 6 that this method is required to model the distribution of block-maximum load effect. Therefore, the theory of predictive likelihood is outlined in general terms first. Following this, application of the theory to both single- and multi-distribution problems is considered. Application to a published example is then considered to evaluate the performance of predictive likelihood, and aspects relating to its implementation are examined. The theoretical examples of Chapter 6 are also reviewed with predictive likelihood and application to the bridge loading problem follows.

7.2 Theoretical Development

7.2.1 Empirical description

Before the mathematical details of the theory of predictive likelihood are expounded, the method is qualitatively explained. Consider first the GEV parent distribution, and the distribution of maxima of samples of size 100, shown in Figure 7.1. The level corresponding to a probability of 1-1/100 is the mode of the distribution of maxima and this return level is ordinarily obtained through extrapolation (Chapter 3). When the PDF is obtained from data using maximum likelihood, a value of the likelihood function results. Similarly, a likelihood value can be obtained from the distribution of maxima of Figure 7.1 for a predicted value corresponding to a probability of 1-1/100. The idea of predictive likelihood is to propose a value of prediction – the predictand – and to maximize both the likelihood of the data and the likelihood of the predictand simultaneously. By repeating this process for a range of values of predictand, the values of joint likelihood may be plotted and used to form a distribution of likelihood for the predictand.
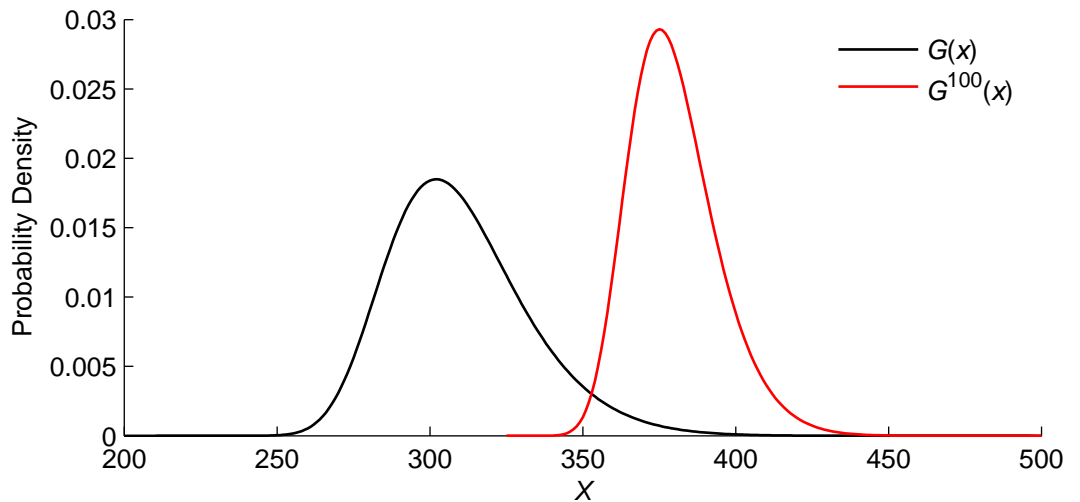
Figure 7.1: Parent distribution and distribution of maxima for $G(x; 300, 20, 0.1)$.

7.2.2 Predictive likelihood in the literature

Fisherian Predictive Likelihood

Likelihood inference on prediction is based on the initial suggestion of Fisher (1956). Fisherian predictive likelihood (also termed profile predictive likelihood) is defined as:

$$L_P(z \mid y) = \sup_\theta L_y(\theta; y) L_z(\theta; z) \qquad (7.1)$$

This formulation states that the likelihood of the predictand, **z**, given the data, **y**, is proportional to the likelihood of both the data (L_y) and the predictand (L_z) for a maximized parameter vector, θ. It can be seen that the parameter vector of the distribution is considered as the nuisance parameter and is eliminated by maximization. To form a distribution of the predictand, a range of predictand values is considered and the Fisherian predictive likelihood calculated for each. The results are then usually normalized to represent a distribution (see Lejeune and Faulkenberry 1982, for an early example).

Following the description in Chapter 3, and denoting the PDF of the distribution by $g(\cdot)$, the likelihood function for the data vector, **y** is:

$$L_y(\theta; y) = \prod_{i=1}^{n} g(y_i; \theta) \qquad (7.2)$$

For a postulated value of **z**, and denoting the PDF of the predictand by $g_z(\cdot)$, the likelihood function is:

$$L_z(\theta; z) = g_z(z; \theta) \qquad (7.3)$$

as there is only a single value: **z**. Similarly to ordinary likelihood, it is easier to use the log-likelihoods – maximization of this function is equivalent to

maximization of the likelihood function itself. Therefore, (7.1), in conjunction with (7.2) and (7.3), is written as:

$$\log\left[L_P\left(z\mid y\right)\right]=\sup_{\theta}\left\{\log\left[L_y\left(\theta;y\right)\right]+\log\left[L_z\left(\theta;z\right)\right]\right\}$$
$$=\sup_{\theta}\left\{\sum_{i=1}^{n}\log\left[g(y_i;\theta)\right]+\log\left[g_z(z;\theta)\right]\right\}$$

(7.4)

This function is evaluated for a range of values of **z**. The area under the curve of $\left\{L_p,z\right\}$ is normalized to unity and a distribution of the predictand results.

Mathiasen (1979) notes some problems with the Fisherian predictive likelihood. Of particular relevance to this work is that each function maximization does not account for the variability of the derived parameter vector, θ.

Modified Predictive Likelihood

Many forms of predictive likelihood have been proposed in the literature to overcome the problems associated with the Fisherian formulation – Chapter 2. In this work, the predictive likelihood method proposed by Butler (1989), based on that of Fisher (1956) and Mathiasen (1979) and also considered by Bjørnstad (1990), is used. Lindsey (1996) describes the reasoning behind its development. This predictive likelihood is the Fisherian, modified so that the variability of the parameter vector of each maximization is taken into account.

Edwards (1992) describes the meaning of the likelihood (multi-dimensional) surface at the point of maximum likelihood – Chapter 3. In particular, the determinant of the Fisher information matrix, $\left|I\left(\theta\right)\right|$, may be seen as the volume under the surface of the likelihood function at the maximum likelihood estimate (MLE). Therefore larger volumes (determinants) represent less information and vice versa as smaller volume indicates a narrower likelihood function which corresponds to more confidence (information) about the

parameter values. Mathematically, it is the absolute value of the determinant that is taken as volumes cannot be negative. Further, it is the square root of the determinant that is used as a measure of the variability of the parameter vector in the region of the estimate. Edwards (1992), for example, explains this as relating the width of the likelihood surface at some point below the maximum to the information matrix linearly: it is the square root of the determinant that indicates the 'multi-dimensional width' of the likelihood surface at the estimate. This metric thus forms a measure of credibility for a given parameter vector

To allow for the effect of parameter variability on Fisherian predictive likelihood, the width of the likelihood surface is used to weight the values of Fisherian predictive likelihood obtained for each parameter vector corresponding to each of the values of predictand. In this way, the variability of the parameters is included in a relative sense. Of course as the resulting function is normalized to a distribution, this relativity is adequate.

One further modification is required to the Fisherian predictive likelihood. The parameter vector determined for each value of the predictand, based on the maximization of (7.4), is dependent on both the data, y, and z and is therefore denoted θ_z, whereas that for the data solely is denoted θ. Therefore the parameter transform modification, $|\partial\theta_z/\partial\theta|$, is required so that the problem is in the domain of the 'free' parameter vector, θ (refer to Thomasian (1969) for further information on parameter transformations).

The modified profile predictive likelihood that results from these modifications to the Fisherian predictive likelihood is given as:

$$L_{MP}\left(z\,|\,y\right) = \frac{L_P\left(z\,|\,y;\theta_z\right)}{\left|\dfrac{\partial\theta_z}{\partial\theta}\right|\sqrt{\left|I\left(\theta_z\right)\right|}} \qquad (7.5)$$

Butler (1989) points out that the parameter transform $\left|\partial\theta_z/\partial\theta\right|$ is constant. Therefore normalization of the area under $L_P\left(z\mid y;\theta_z\right)\big/\sqrt{\left|I\left(\theta_z\right)\right|}$ amounts to evaluation of $\left|\partial\theta_z/\partial\theta\right|$ and hence $L_{MP}\left(z\mid y\right)$ is the density of the predictand.

7.2.3 Specific formulations

Introduction

Having outlined the general theory of predictive likelihood, the formulation used in applications of the theory in the statistical literature is considered. The extension of the method to problems of composite distribution statistics is then outlined.

The GEV distribution is used throughout the work that follows and, though also given in Chapter 3, several aspects are repeated here for reference. The distribution function of the GEV is given by:

$$G\left(y;\theta\right)=\exp\left\{-\left[1-\xi\left(\frac{y-\mu}{\sigma}\right)\right]^{1/\xi}\right\} \tag{7.6}$$

where $\theta=\left(\mu,\sigma,\xi\right)$. The PDF and likelihood function are, respectively:

$$g\left(y;\theta\right)=G\left(y;\theta\right)\cdot\sigma^{-1}\left\{1+\xi\left(\frac{y-\mu}{\sigma}\right)\right\}^{-1/\xi-1} \tag{7.7}$$

$$\log\left[L_y\left(\theta;y\right)\right]=l_y\left(\theta;y\right)$$
$$=-n\log\sigma-\left(1-\frac{1}{\xi}\right)\sum_{i=1}^{n}\log x_i-\sum_{i=1}^{n}x_i^{1/\xi} \tag{7.8}$$

where $x_i=1-\xi\left(\dfrac{y_i-\mu}{\sigma}\right)$ and is the reduced variate of the GEV distribution.

Single Mechanism Predictive Likelihood

The terms of equation (7.4) are determined in the context of a single GEV distribution problem. The likelihood of the data, $L_y(\theta; y)$, is as defined in Chapter 3 and is given in (7.8) for the GEV distribution. Following the definition of likelihood in Chapter 3, that of the predictand, $L_z(\theta; z)$, requires use of the distribution of z: an example is shown in Figure 7.1. Following Section 3.4.1, the distribution of the predictand, from m repetitions of the sample block size, is given by:

$$g_z(z;\theta) = m \cdot g(z;\theta) \cdot \left[G(z;\theta) \right]^{m-1} \tag{7.9}$$

and it is this PDF that is graphed in Figure 7.1. In this equation, the parameter vector θ is based upon the data y alone. Therefore, the likelihood of observing a given predictand, z, is simply $\log\left[g_z(z;\theta) \right]$ and this is the approach used by Davison (1986). It is also possible, using the GEV transforms of Appendix B, to derive the parameters of the $g_z(z;\theta)$ distribution explicitly.

It may be thought that the maximization of this function may be governed by the data vector, y, as it consists of n elements, whereas the predictand is a single value. However, the contribution made to this joint log-likelihood function is of order m, and if m and n are comparable, then the contributions from the predictand and the data are also comparable.

Composite Distribution Predictive Likelihood

Application of predictive likelihood to the method of composite distribution statistics (CDS) is complicated by the nature of the composite distribution, where for N mechanisms, its distribution is:

$$G_C(y) = \prod_{j=1}^{N} G_j(y)$$

$$= \exp\left\{-\sum_{j=1}^{N}\left[1-\xi_j\left(\frac{y-\mu_j}{\sigma_j}\right)\right]^{1/\xi_j}\right\}$$

(7.10)

The probability density function $g_C(y)$ can be evaluated numerically and central differences are used in this work. The likelihood of the data for the CDS distribution is defined in this work to be the joint likelihood of each of the mechanisms of the CDS distribution:

$$\log\left[L_y(\theta;y)\right] = l_y(\theta;y)$$

$$= \sum_{j=1}^{N}\left\{\sum_{i=1}^{n_j}\log\left[g_j\left(\theta_j;y_{j,i}\right)\right]\right\}$$

(7.11)

where $g_j(\theta_j;y_j)$ is the PDF of the jth loading event. Also, the distribution of a maximum of **m** sample repetitions is defined by:

$$G_{Z,C}(z) = \left[G_C(z)\right]^{m}$$

$$g_{Z,C}(z) = m \cdot g_C(z) \cdot \left[G_C(z)\right]^{m-1}$$

(7.12)

The likelihood of the predictand, given the initial distribution is:

$$\log\left[L_z(\theta;z)\right] = \log\left[g_{Z,C}(z)\right]$$

$$= \log\left\{m \cdot g_C(z) \cdot \left[G_C(z)\right]^{m-1}\right\}$$

(7.13)

This formulation is difficult to implement and other formulations have also been considered. However, these have not exhibited the same level of performance. Therefore, numerical tools have been employed to ensure robustness in the formulation presented, and these are outlined in Section 7.3.3.

7.3 Performance and Implementation

7.3.1 Introduction

Though the theory and formulation of the predictive likelihood approach have been stated, its performance must be compared to other methods with the same goal. A data set, with associated published results, is used as the basis for several methods of estimating the distribution of return levels for a 100-year lifetime. In this way, the behaviour of predictive likelihood is examined. However, only the single distribution formulation can be assessed in this way.

Predictive likelihood analysis is dependent on substantial numerical computation. Its sensitivity to inputs such as sample size, the order of the sample data, as well as final distribution fitting, is assessed. The algorithms used in this work are also explained. Though the formulation is clearly defined, specific approaches are used to enable robust estimation.

7.3.2 Performance evaluation

Coles (2001a) describes a study of the annual maximum sea levels at Port Pirie, Australia. An extreme value analysis, based on the GEV distribution, is presented; the results of which may be used as a basis for what follows. The data set is available as part of the `ismev` library for the $\mathbf{R}$ language ($\mathbf{R}$ Development Core Team 2005) and is shown in Figure 7.2.

The maximum likelihood estimates of the GEV parameters for the Port Pirie data are found to correspond to those of Coles (2001a) and are:

$$\hat{\theta} = \left(\hat{\xi}, \hat{\sigma}, \hat{\mu} \right) = \left(0.050, 0.198, 3.875 \right) \qquad (7.14)$$
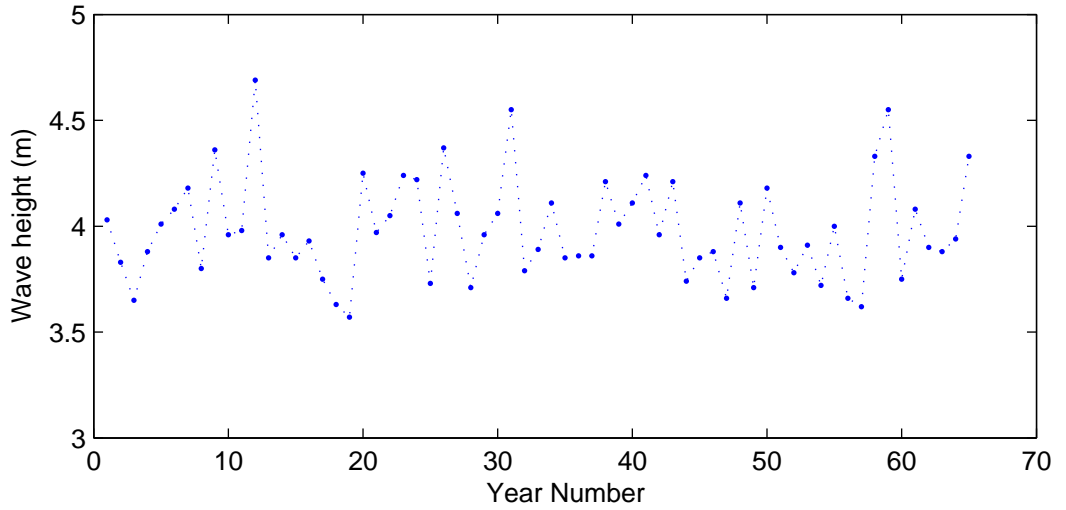
Figure 7.2: Annual maximum sea levels at Port Pirie, Australia.

In general, for the **n**-block return period, the return level, z_n, is that value that satisfies the equation:

$$1 - \frac{1}{n} = \exp\left\{-\left[1 - \xi\left(\frac{z_n - \mu}{\sigma}\right)\right]^{1/\xi}\right\} \qquad (7.15)$$

Solving this for z_n, gives:

$$z_n = \mu + \frac{\sigma}{\xi}\left\{1 - \left[-\log\left(1 - \frac{1}{n}\right)\right]^{\xi}\right\} \qquad (7.16)$$

The maximum likelihood estimate of z_n is got by substitution of the maximum likelihood parameter estimates, $\hat{\theta} = \left(\hat{\xi},\ \hat{\sigma},\ \hat{\mu}\right)$ into (7.16). In the case of the Port Pirie data, and for a 100-year return period, this yields $\hat{z}_{100} = 4.688$ and again corresponds to that of Coles (2001a).

Parametric Bootstrap and the Delta Method

A parametric bootstrap is used to assess the variability of the 100-year return level for the Port Pirie data. The distribution fitted to the data, defined by the

parameters of (7.14), is used to generate synthetic blocks of data of the same size as the original set. A shortfall of this approach is that the parametric bootstrap method does not account for parameter variability. A GEV distribution is fit to each synthetic data set and used to estimate the 100-year return level. 100 such return levels are got, and the results are shown in Figure 7.3. Also shown in this figure is the result of the application of the delta method, described in Chapter 3, which assumes asymptotic normality of the predictand. It can be seen that this is not reasonable as the distributions are quite different.
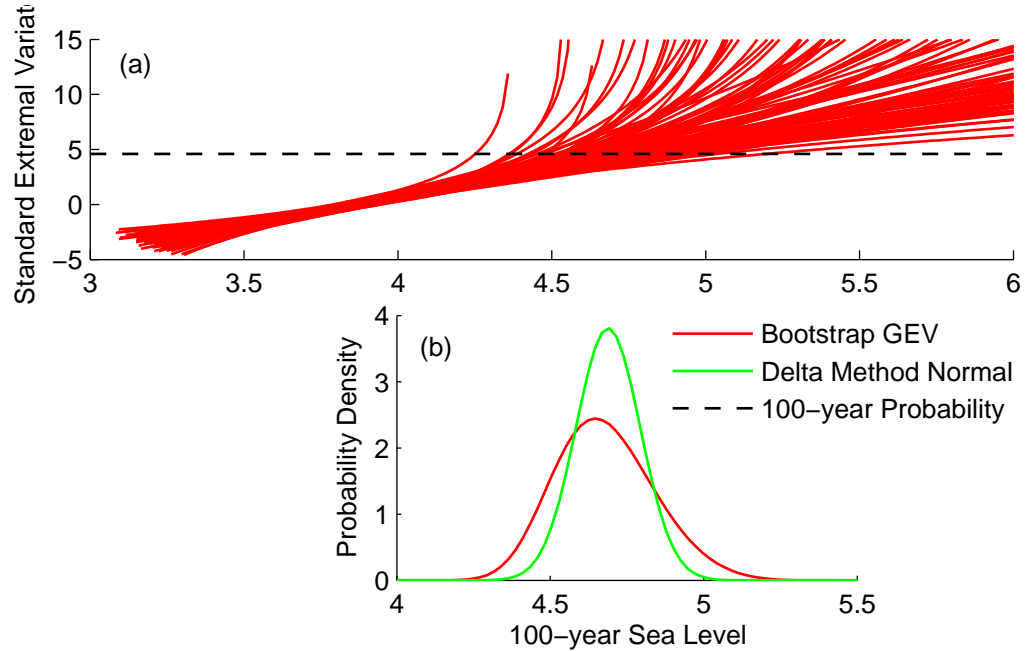
Figure 7.3: Parametric bootstrap and delta method approaches; (a) bootstrap replications on Gumbel paper, and (b) the return level distributions.

Profile Likelihood for Return Level

Many authors (Coles 2001a, Smith 2001, Gilli and Këllezi 2005) use the profile likelihood technique to estimate the distribution of the predictand. The method involves re-parameterizing the GEV distribution in terms of a given value of z_n, as follows from (7.16):

$$\mu = z_n - \frac{\sigma}{\xi}\left\{1-\left[-\log\left(1-\frac{1}{n}\right)\right]^{\xi}\right\} \qquad (7.17)$$

Use of the location parameter given by (7.17) in the likelihood equation of the GEV distribution – equation (7.8) – renders the problem in terms of the parameters $\theta = (\xi, \sigma, z_n)$. Then, for a range of values of z_n, the remaining parameters are maximized for each z_n. The likelihood values that result from each z_n maximization give the profile likelihood for z_n – as noted in Chapter 3.

Figure 7.4 shows the profile likelihood curve that results from the application of this method (shown as the 're-parameterized' curve) to the Port Pire data. Also given in this figure is the location of the maximum profile likelihood estimate (which is the same, by definition, as the likelihood function estimate), and the upper and lower 95% confidence intervals derived from the method outlined in Chapter 3, Section 3.3.4. Explanation of the predictive likelihood curve follows.
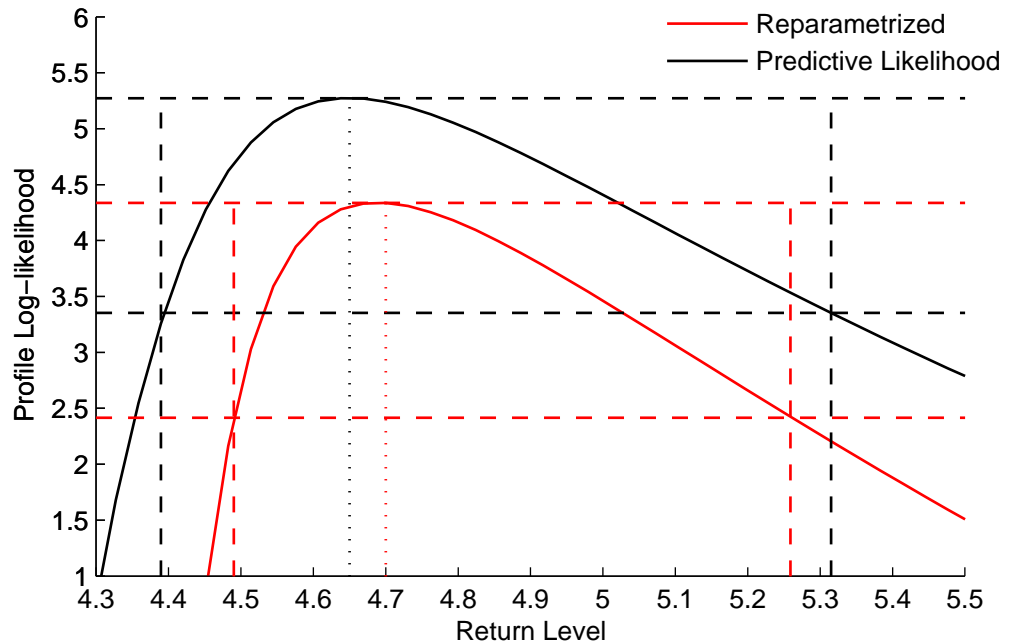
Figure 7.4: The profile likelihood for return level and predictive likelihood methods applied to the Port Pirie data.

Predictive Likelihood

The single distribution method of predictive likelihood (Section 7.2.3) is applied to the Port Pirie data. The results of the Fisherian and modified predictive likelihood approaches are kept separate in order that the effect of the modifications for parameter variability may be seen.

Firstly, the Fisherian predictive likelihood is evaluated for a range of return levels, shown in Figure 7.4 along with the profile likelihood approach. It is not the absolute value of this curve that is of interest, rather its relative values. The results are more easily assessed though consideration of the maximum predictive likelihood estimate of z_{100} and the 95% confidence intervals. It can be seen that this approach gives wider confidence bands for the return level than those of the profile likelihood method. Also, and of significance, is that the maximized estimate of return level is different – in this case, $\hat{z}_{100} = 4.638$.

The explanation for the differences in these two approaches provides useful insight into the predictive likelihood approach. Only one value of return level is considered: the maximum (and re-parameterized profile) likelihood estimate, $\hat{z}_{100} = 4.688$. For this return level, Figure 7.5 illustrates the two approaches. The component likelihood values for both methods and both the data and predictand are given in Figure 7.5. It can be seen that the profile-likelihood approach gives a higher value at which the data likelihood is maximized compared with that of the predictive likelihood $(4.34 > 4.30)$. This is to be expected, as this method is based solely on the data. However, as the predictive likelihood approach is balancing both the data and the predictand, its joint likelihood (data and predictand) is greater than that of the profile likelihood approach $(5.25 > 5.19)$. This is due to the difference in the likelihood of the predictand under the two approaches $(0.96 > 0.85)$.
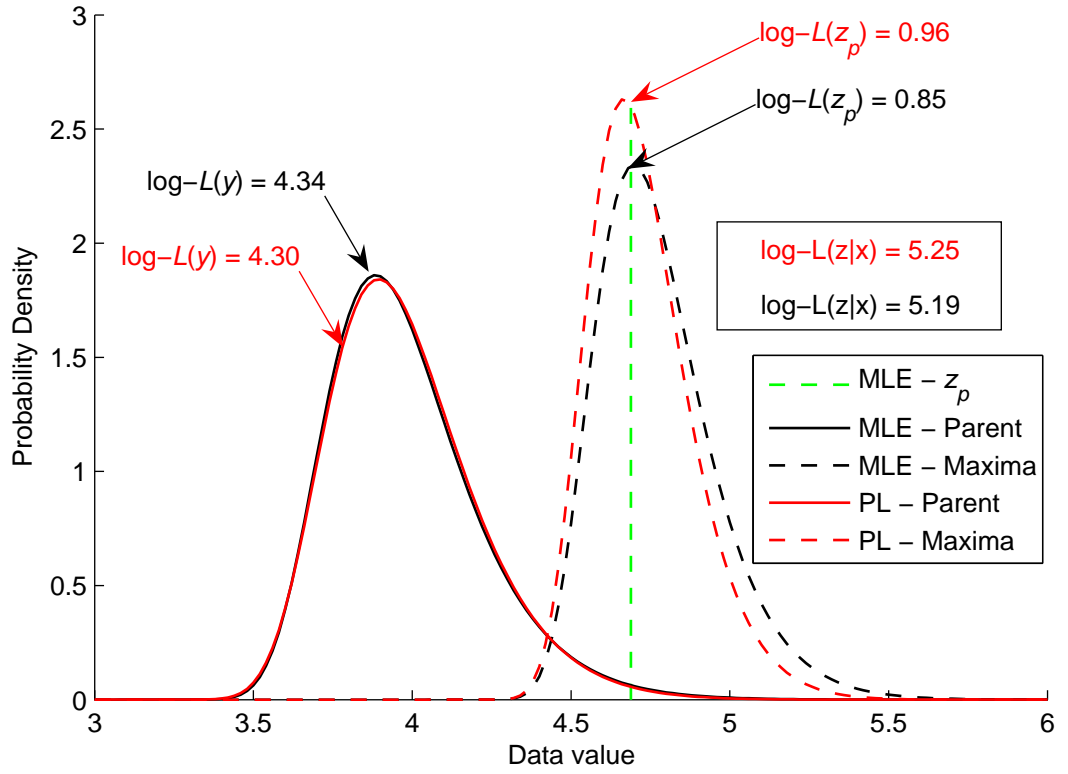
Figure 7.5: Comparison of profile likelihood (red elements) and predictive likelihood (black elements) approaches for a single return level.

In the above description, under both models the distribution of maxima is that of equation (7.9). Also, (as commented upon earlier) the contribution to the predictive likelihood of the predictand can be significant, and in this case is only one order removed from that of the data.

For this example, Figure 7.6 shows the basis of the modifications required to allow for the variability of the parameter vector. Figure 7.7 illustrates the Fisherian and Modified Predictive Likelihood distributions, along with the weighting term applied to L_P to determine L_{MP}. It can be seen that the weighting results in a slightly longer upper tail for L_{MP}, reflecting the uncertainty in the parameters. However, the difference overall is slight.
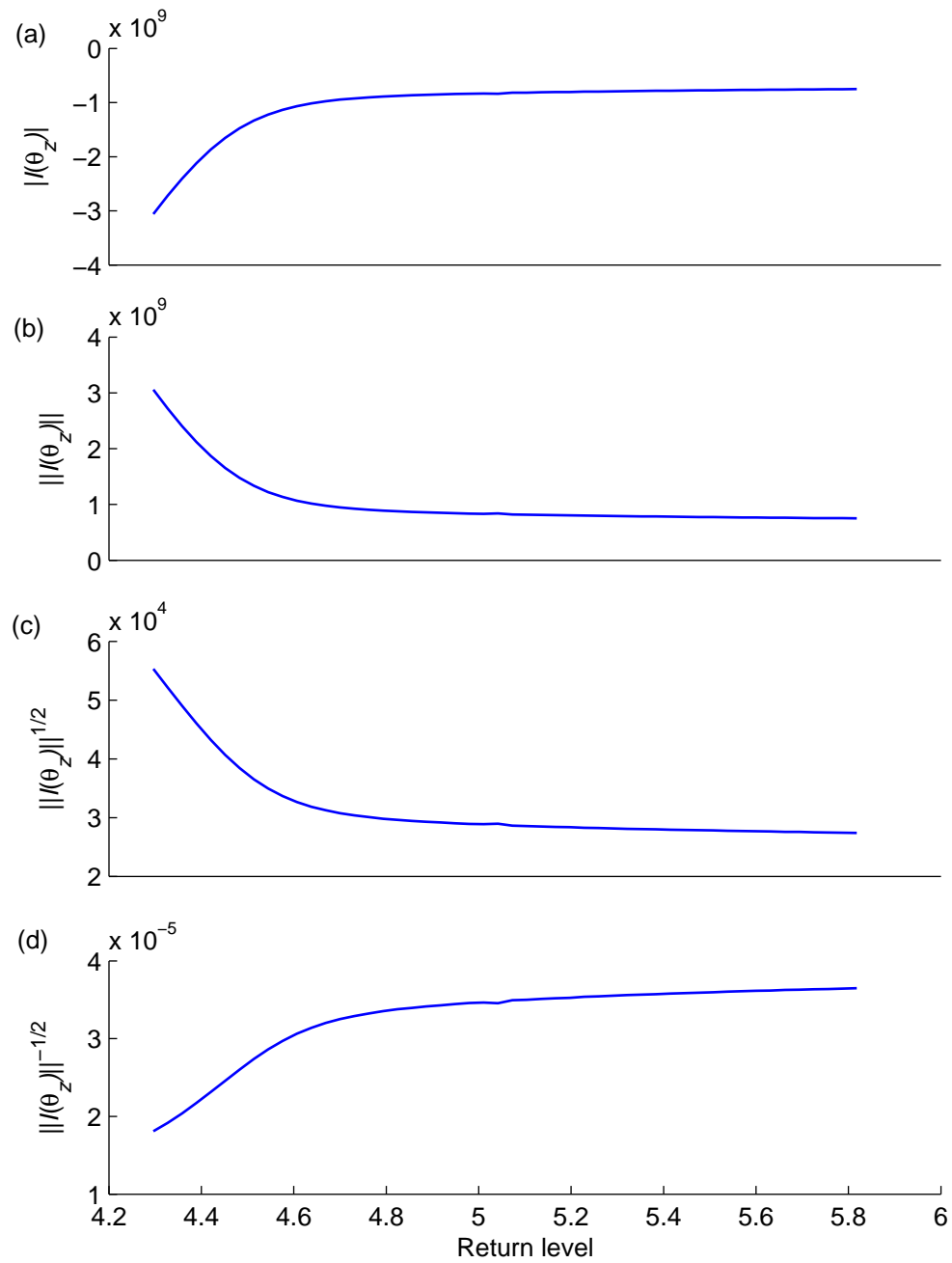
Figure 7.6: Modification for parameter variability for the Port Pirie example: (a) determinant; (b) volume under the likelihood surface; (c) multi-dimensional likelihood surface width, and; (d) resultant relative weighting factor.
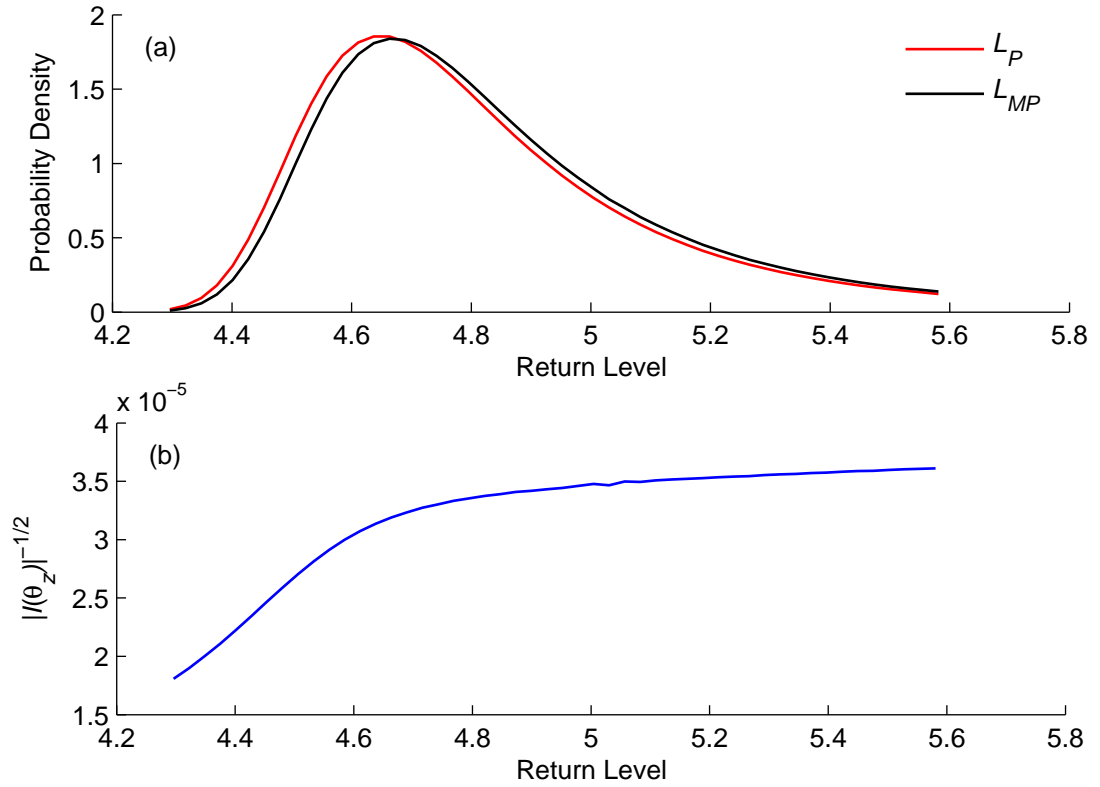
Figure 7.7: Fisherian, L_P, and Modified Predictive Likelihood, L_{MP}, results: (a) distributions, and; (b) modification weights for parameter variability.

Comparison of Approaches

A comparison of the distributions obtained from each of the methods outlined is given in Figure 7.8. It is clear that each distribution has a mode of approximately the same value. This is to be expected and usually lies at the maximum likelihood return level estimate. What is also clear, and of more importance, is the skewness of the distributions: the bootstrap distribution does not exhibit much skewness (and, by definition, neither does the delta method distribution). In the light of the results of the profile and modified predictive likelihood results, this underestimation of the skewness of the distributions is problematic. It is possible that a non-parametric bootstrap study may exhibit better behaviour, though it is not studied here.

The profile and modified predictive likelihood approaches compare quite well. Of significance though, is the larger variance of the modified predictive likelihood. This difference (as considered above) is due to a combination of the allowances for parameter variability and the joint likelihood of the data and predictand.
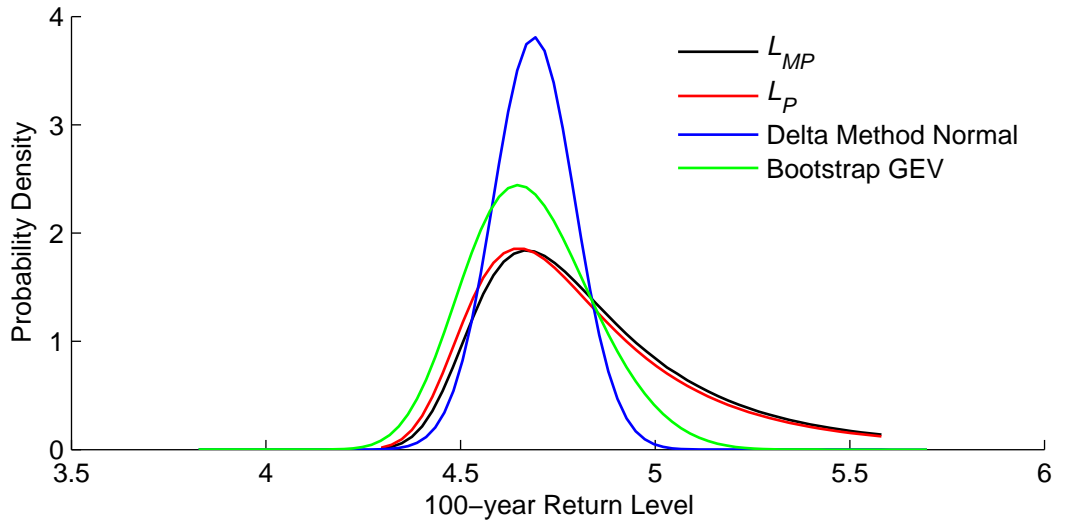
Figure 7.8: 100-year return level distributions for the Port Pirie data.

7.3.3 Implementation aspects

Save for Davison (1986), the statistical literature on predictive likelihood does not generally consider its implementation. The algorithm used is presented, along with some of the incident calculations. Following this, aspects related to the numerical computations are examined.

CDS Predictive Likelihood Algorithm

For each value of the predictand, equation (7.1) is maximized with the terms given by equations (7.11) and (7.13) (and correspondingly for the single mechanism predictive likelihood). As up to four event types are in a typical CDS problem, the maximization has a set of up to 12 parameters. Sequential quadratic programming optimization is used in this work to minimize the

negative of the predictive likelihood function. A MATLAB toolbox is developed for this purpose as part of this work.

In the optimization, each GEV parameter vector must be limited to operate on the data corresponding to its event-type. Therefore the optimization must be performed with parameter bounds appropriate for each event-type. The bounds used in this work are based on deviations from the ordinary maximum likelihood estimates. The location and scale parameters are allowed to vary as:

$$\frac{\lambda}{\psi} \leq \lambda \leq \psi\lambda; \quad \text{where } \lambda = \{\mu, \sigma, \xi\} \tag{7.18}$$

between bounds of $\psi = 1.1$ for μ, σ and $\psi = 1.4$ for ξ. Whilst seemingly restrictive, such tight bounds have been found necessary to prevent interaction of parameters on data from other event-types. However, once such interaction is prevented in this manner, the optimized parameter values remain within their bounds.

For numerical stability, it is found beneficial for each iteration of the optimization to start on the initial maximum likelihood estimate, rather than the final estimates of the previous iteration. Though more computationally expensive, each iteration is therefore independent, and the risk of divergence of the solution is reduced. However, there remain situations in which an iteration can diverge from solution. Therefore an intermediate optimization is carried out to provide initial parameter estimates for each iteration – the function is constrained to return the predictand it is optimizing for by the following:

$$z - G_C^{-1}(p_z; \theta) = 0 \tag{7.19}$$

where p_z is the probability level for the predictand, $\mathbf{z}$. Having obtained the parameter vector that solves this constraint function, the second optimization is commenced with this parameter vector as the start point.

This process may be explained by reference to Figure 7.5. The first optimization obtains the parameter vector that has the predictand as the mode of the distribution of $\mathbf{n}$-block maxima, $g_z(z;\theta)$. The second optimization releases this requirement, and the predictand is allowed to occur anywhere within $g_z(z;\theta)$, once the overall function is maximized.

The solution that results at each iteration is then processed using numerical derivatives to determine the (up to 12×12-dimension) Hessian matrix of the solution – the observed information matrix. Also, the maximized value of predictive likelihood is brought forward to the analysis for the distribution of predictive likelihood.

Establishing the Predictive Distribution

Curves of log predictive likelihood, such as those of Figure 7.4, are used to determine the predictive Fisherian distribution $f_{L_P}(z;y)$. Firstly, the log predictive likelihoods are defined as:

$$l_P(z\mid y) = \log\left[L_P(z\mid y)\right] \tag{7.20}$$

and its maximum value – as per Figure 7.4, for example:

$$\hat{l}_P(z\mid y) = \sup_z\left[l_P(z\mid y)\right] \tag{7.21}$$

Then, the curve of likelihood ratios is determined as:

$$f_{L_P}^*(z;y) = \exp\left\{l_P(z\mid y) - \hat{l}_P(z\mid y)\right\} \tag{7.22}$$

This curve is then normalized to the predictive distribution:

$$f_{L_P}\left(z;y\right) = \frac{f_{L_P}^*\left(z;y\right)}{\int f_{L_P}^*\left(z;y\right)} \tag{7.23}$$

The points so-defined, can be seen in Figure 7.9(a) for example.

Fitting the Predictive Distribution

It is to be noted that only discrete values of L_P are calculated at discrete intervals of return level. Therefore, for this work, a GEV distribution is fitted through the discrete points that result after normalization of the area under the points to unity. A least-squares fit through these points is not appropriate as it unduly weights the larger relative likelihoods by assigning a weight of unity to all points (Weight Function 1). To counteract this effect, a weight equal to the reciprocal of the y-value could be used so that the least-squares fit is biased to smaller magnitudes (Weight Function 2). However, as it is the upper tail that is of primary interest, the approach adopted in this work is to use a weigh of unity for all points below the mode of the distribution, and to use a weight equal to the reciprocal of the y-value for points above the mode (Weight Function 3). The application of these fitting methods is shown in Figure 7.9. It can be seen that the weighting results in a slightly longer upper tail for L_{MP}, reflecting the uncertainty in the parameters. However, the difference overall is slight.

From Figure 7.9, it can be seen that the upper tail is well approximated by each fit resulting from Weight Functions 2 and 3 and is not fitted quite as well by Weight Function 1 (standard least-squares). However, it can also be seen that Weight Function 3 provides a better fit near the mode of the data than Weight Function 2. Therefore, this weight function is used in this work as it describes both the upper tail and the mode reasonably well.
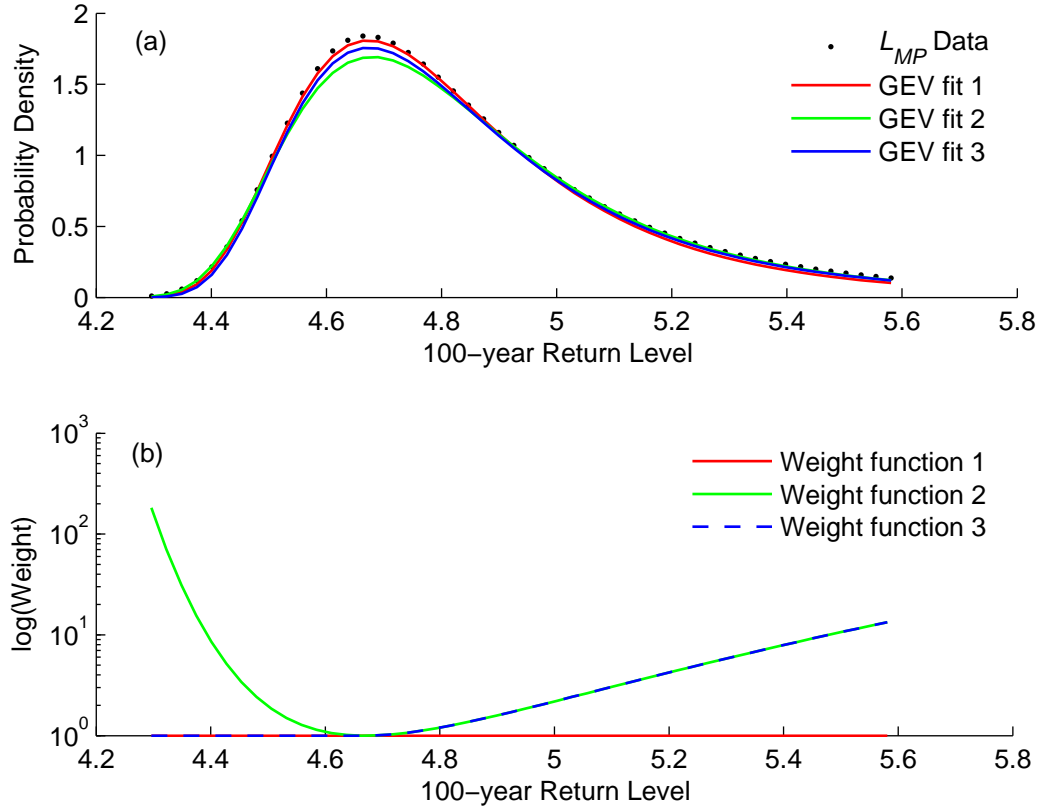
Figure 7.9: GEV distribution fits to the discrete predictive likelihood results; (a) the three distributions resulting from (b) the three weight functions.

Effect of Data Scale

Due to the small order of numbers involved in predictive likelihood, numerical problems can arise from the state of the information matrix. An example is the numerical differentiation involved in calculating the information matrix. A useful measure of its stability with respect to numerical computations is the matrix condition number (Golub and Van Loan 1996). Low order condition numbers are said to be well-conditioned whereas condition numbers of large order are considered ill-conditioned. The condition numbers of the information matrices evaluated at each predictand as part of the Port Pirie data are shown in Figure 7.10. The system is reasonably well-conditioned.
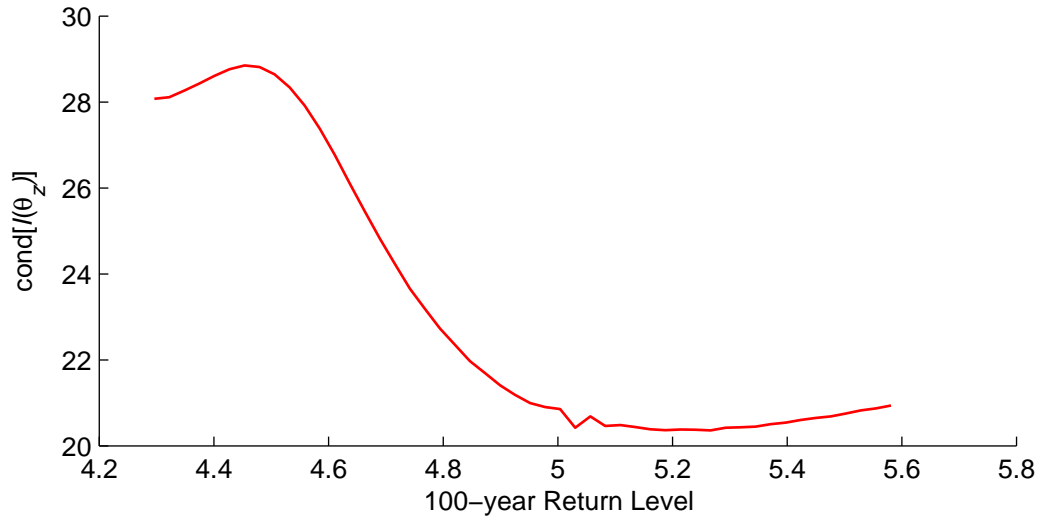
Figure 7.10: Information matrix condition numbers for the Port Pirie predictive likelihood example.

In this work, it has been found necessary to scale the input data to the predictive likelihood algorithm so that its order is less than 10. Higher order numbers exhibit severe ill-conditioning of the matrices with resultant effects on the modified predictive likelihood distribution. Figure 7.11 shows an example of these problems in which the Port Pirie data is scaled by a factor of 100. The plot corresponds to Figure 7.6 and Figure 7.10 and may be compared. It can be seen that the effect of the scale of the data is significant.

Also examined, is the influence of sample size and the inherent random variation of the data. Random numbers are generated from a GEV distribution $\theta = (0.15; 0.45; 1.0)$ for various sample sizes and used as the basis for a predictive likelihood analysis. This is repeated three times and the results plotted in Figure 7.12(a) and (b). It can be seen that as the sample size increases there is considerable variability in the determinant of the information matrix, but that the condition number is stable for sample sizes of about 150.
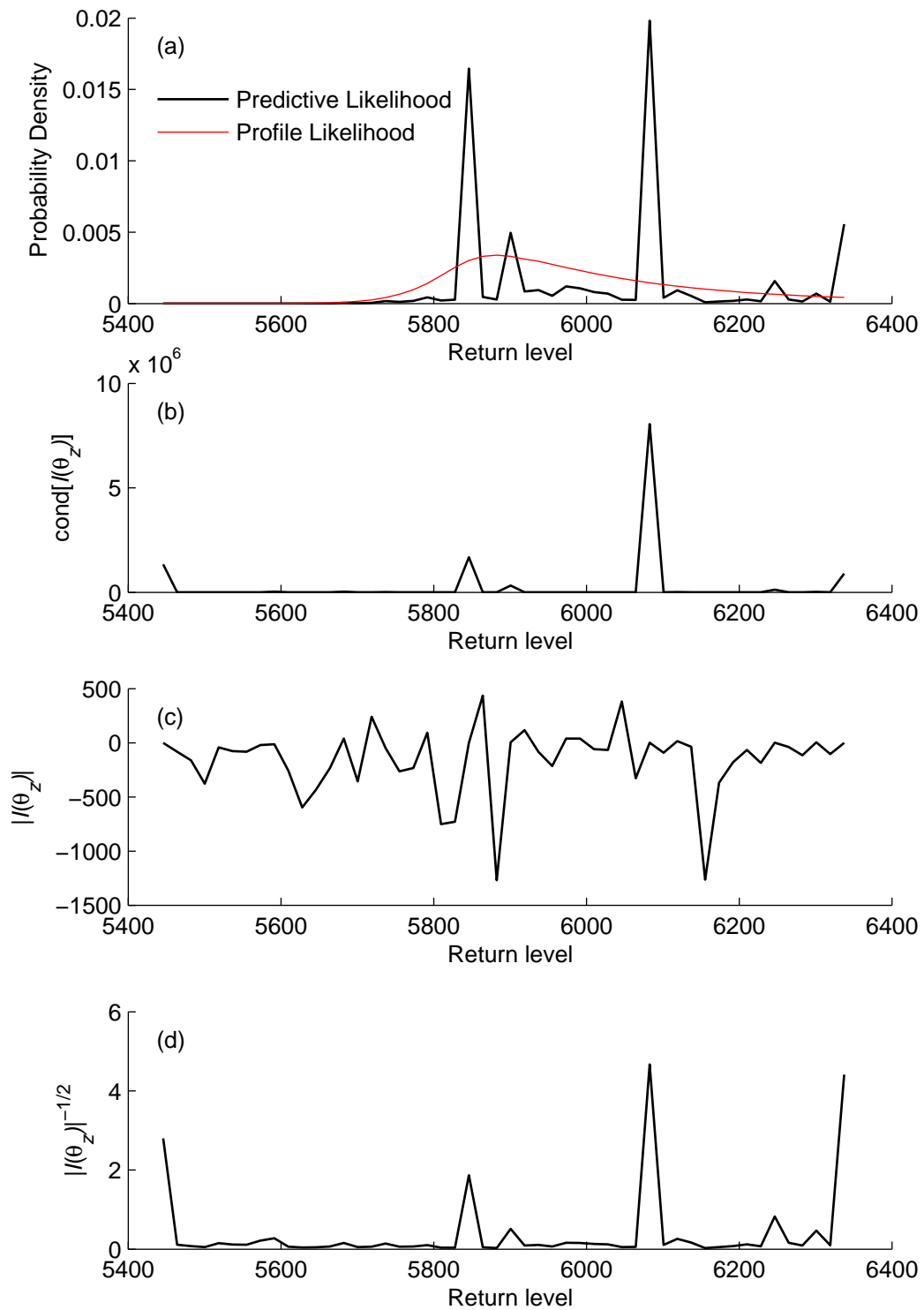
Figure 7.11: Information matrix diagnostics for the scaled Port Pirie data: (a) resultant distributions; (b) condition numbers; (c) determinant, and; (d) weight.
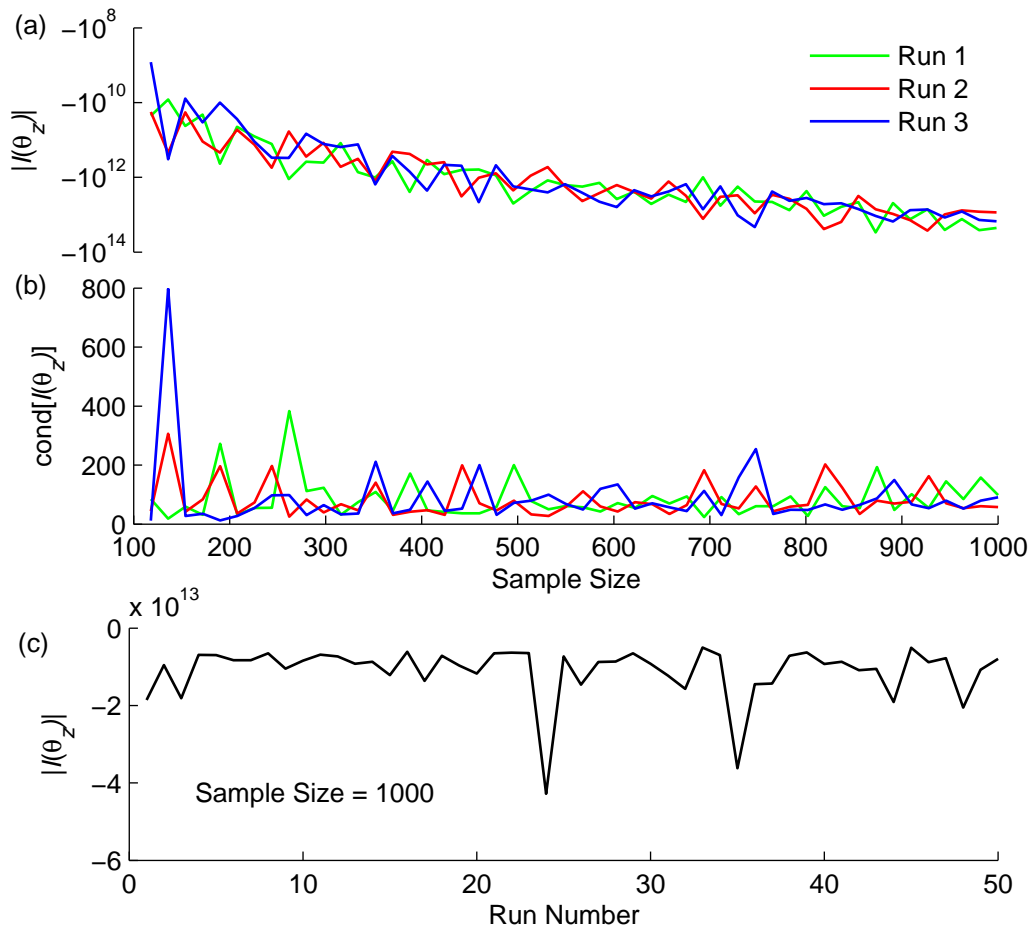
Figure 7.12: Numerical stability: (a) variation of the determinant of 3 runs with increasing sample size; (b) the condition number of the information matrix for those 3 runs, and; (c) the determinant for many runs of a single sample size.

The variability of the determinant for a given sample size is also examined, and the results are shown in Figure 7.12(c). It can be seen that there is variability but the determinant remains within a certain order.

7.4 Results of Application

7.4.1 Application to theoretical examples

The examples presented in Chapter 6 stipulate distributions that reflect the usual relationship between loading events. Samples from these distributions are used to simulate the statistical analysis of bridge traffic loading. These examples are used here to assess the accuracy of the composite distribution predictive likelihood presented in Section 7.2.3. A random data sample is generated and a predictive likelihood analysis is performed. The results are assessed against the simulated distribution of return level which are given in Chapter 6, but repeated here also.

For Example 3 of Study 1, the results are shown in Figure 7.13. The CDS determined return level is shown in the figure (Sample Return Level), along with the exact 100-year return level distribution (Exact) determined from the stipulated parent distributions. Also shown is the GEV-fitted distribution of simulated return levels (CDS Sims) as reported in Chapter 6. These results are compared with the predictive likelihood distributions: the first are the individual points of predictive likelihood (CDS-PL) and the second is the GEV distribution fitted to these points (PL-GEV), as explained previously. It is to be noted that the modification due to parameter variability is not made here as the information matrices exhibit numerical instability.

The results displayed in Figure 7.13 are generally excellent: the mode and the upper tail of the exact distribution are well represented by the predictive likelihood distribution. The left tail is not approximated as well. Considering that the 100-year return level of the sample is to the right of the actual mode, the predictive likelihood distribution displays robustness in its estimation of the

mode of the exact distribution. Further, the estimation of the load effect with 10% probability of exceedance in 100 years through the use of predictive likelihood coincides well with that of the exact distribution.
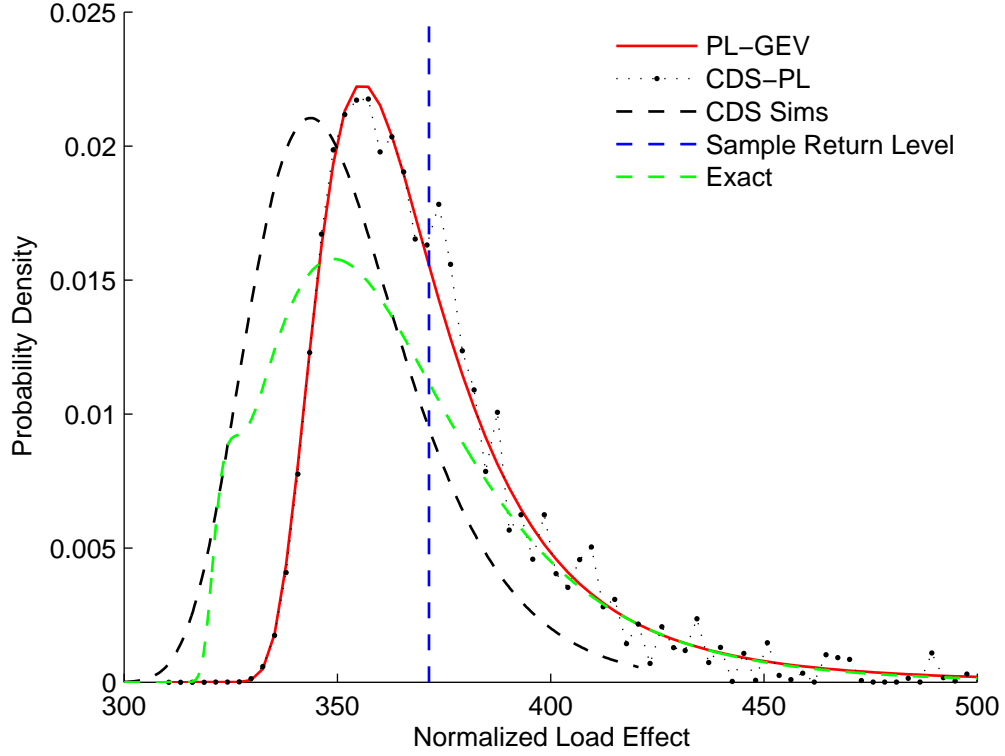
Figure 7.13: Predictive likelihood result for Study 1, Example 3 of Chapter 6.

The same procedure is used with the distributions of Study 2, Example 3 in Chapter 6 and the results are plotted in Figure 7.14. In this case the results are not as good as the previous example. The predictive likelihood distribution (CDS-PL) is shown without a GEV distribution fit, as it would clearly not be appropriate. The distributions of simulated 100-year return level from Chapter 6 (CDS Sims) and exact 100-year return level are given. The 100- and 1000-year return levels, estimated from the sample using usual extrapolation, are plotted, as well as those estimated directly from the predictive likelihood distribution using numerical integration (PL 50 and 90-percentiles respectively).
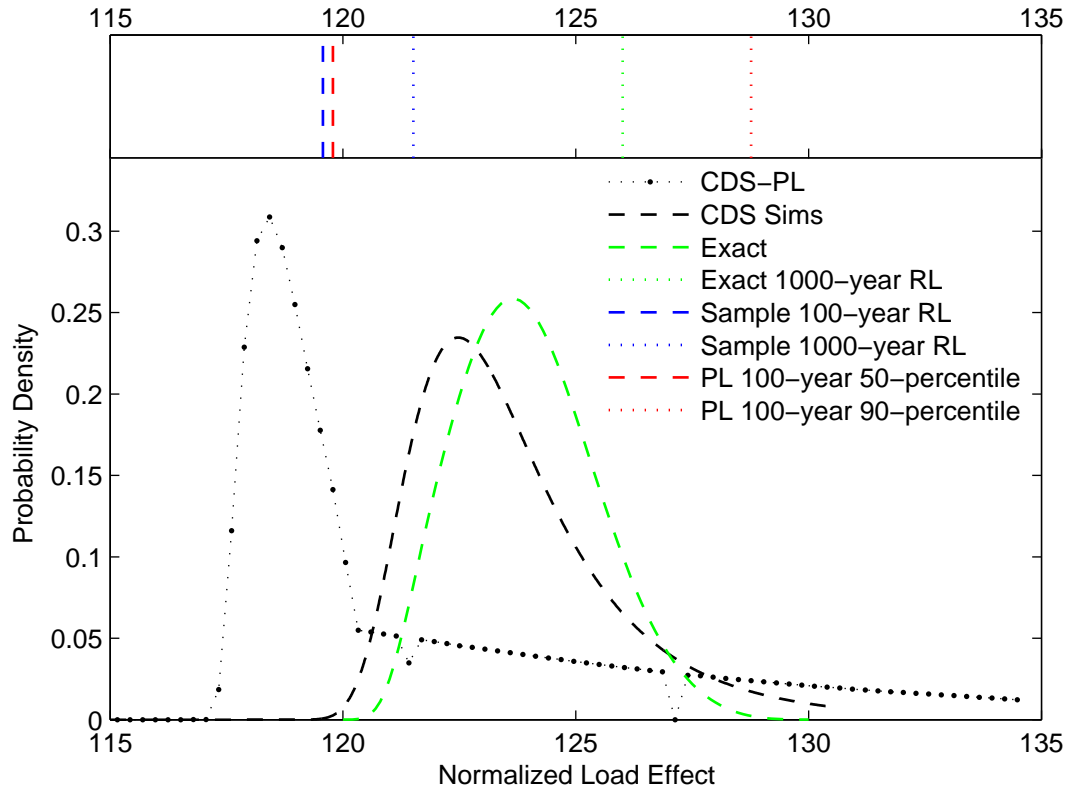
Figure 7.14: Predictive likelihood result for Study 2, Example 3 of Chapter 6.

It is clear from Figure 7.14 that the predictive likelihood distribution (CDS-PL) does not reflect the exact 100-year return level distribution well. In fact the predictive likelihood distribution exhibits composite behaviour – it is a distribution formed from differing underlying phenomena. It does not require knowledge of the component distributions to observe that this is indeed the case. Figure 7.15 shows the distribution history of the predictive likelihood maximizations, from which it may be seen, that initially, the 1-truck mechanism governs until z moves past its region of influence, at which point the 4-truck mechanism begins to govern. This results in the discontinuity in the derived distribution, as well as the long upper tail. There is a discernable gap in the sequence of 4-truck distributions at the discontinuity level from which it is clear that the 4-truck mechanism begins to govern.
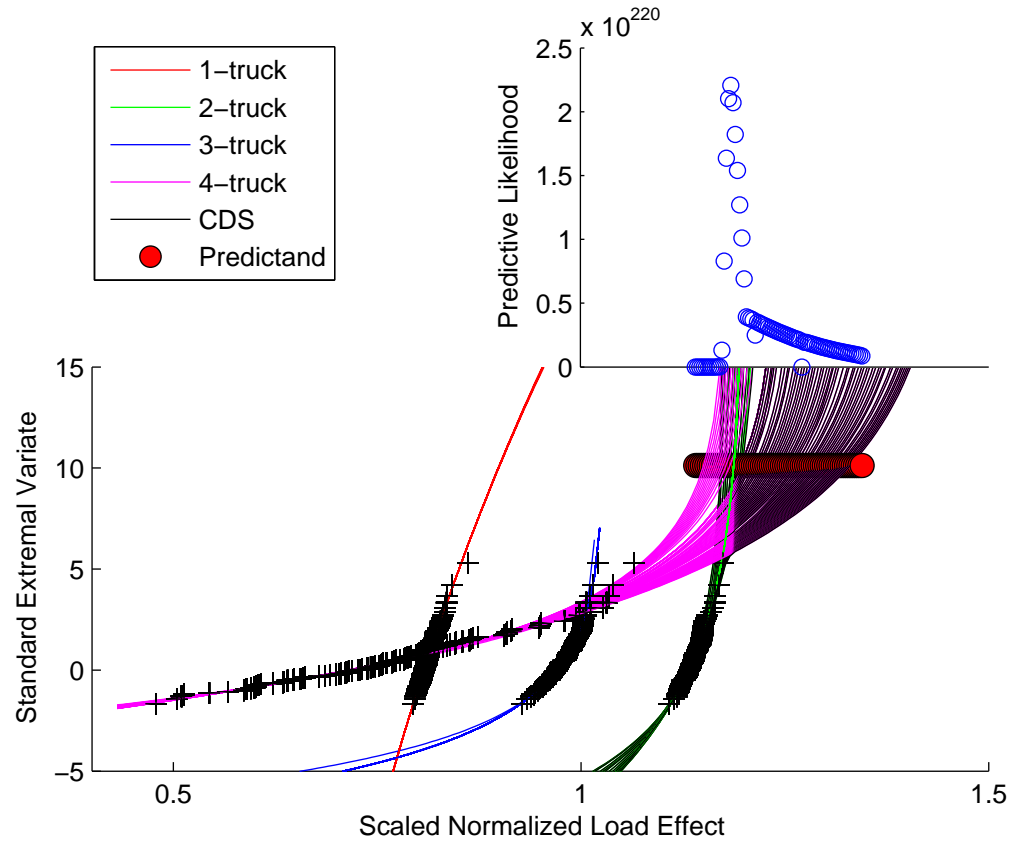
Figure 7.15: History of predictive likelihood maximizations (overlaid plot), showing each predictand, data (crosses), and the component distributions.

Before further consideration of the result, it is important to recognize that the load effect with 10% probability of exceedance in 100 years is conservatively estimated by the predictive likelihood distribution (PL 90-percentile). Therefore, in a practical application, use of the predictive likelihood approach remains better than estimation of the 1000-year return level, which may be seen from Figure 7.14 to be non-conservative.

To investigate further, the stipulated (Given) and sample-fitted (Sample) parent distributions are given in Figure 7.16. Also given, for direct comparison, are the exact and predictive likelihood distributions from Figure 7.14. It can be seen from Figure 7.16(b) that at the 100-year extrapolation level, the 2- and 4-truck

distributions based on the sample are very close, and are quite different from the exact distributions. It may be inferred that this has led to the large mode of the predictive likelihood distribution: both 2- and 4-truck events are contributing. In the case of the exact distribution, with which the derived predictive likelihood distribution is being compared, it can also be seen from Figure 7.16(b) that, at the level of interest, the 4-truck distribution clearly governs. Such governance results in the clear uni-modal exact distribution observed.

To conclude, it appears that two factors have combined to result in a predictive likelihood distribution that does not closely resemble the exact distribution:

- Due to sampling variability the GEV fits are quite different to the exact fits at the return level of interest, and this results in the crossover point being close to the return level of interest (100-year level);

- The crossover point of the given distributions is slightly below the return level of interest, and so there is little mixing in the exact distribution.

Though these factors have combined to give an inaccurate distribution of 100-year return level, the 1000-year return period derived from the predictive likelihood distribution (128.8) still shows smaller error than the usual extrapolation technique (121.5) when compared with the exact return level (126.0). Further, factors that combine to give inaccurate predictive likelihood distributions may be identified from the data and other techniques may be employed in these cases, such as the application of CDS to individual predictive likelihood distributions for each mechanism.
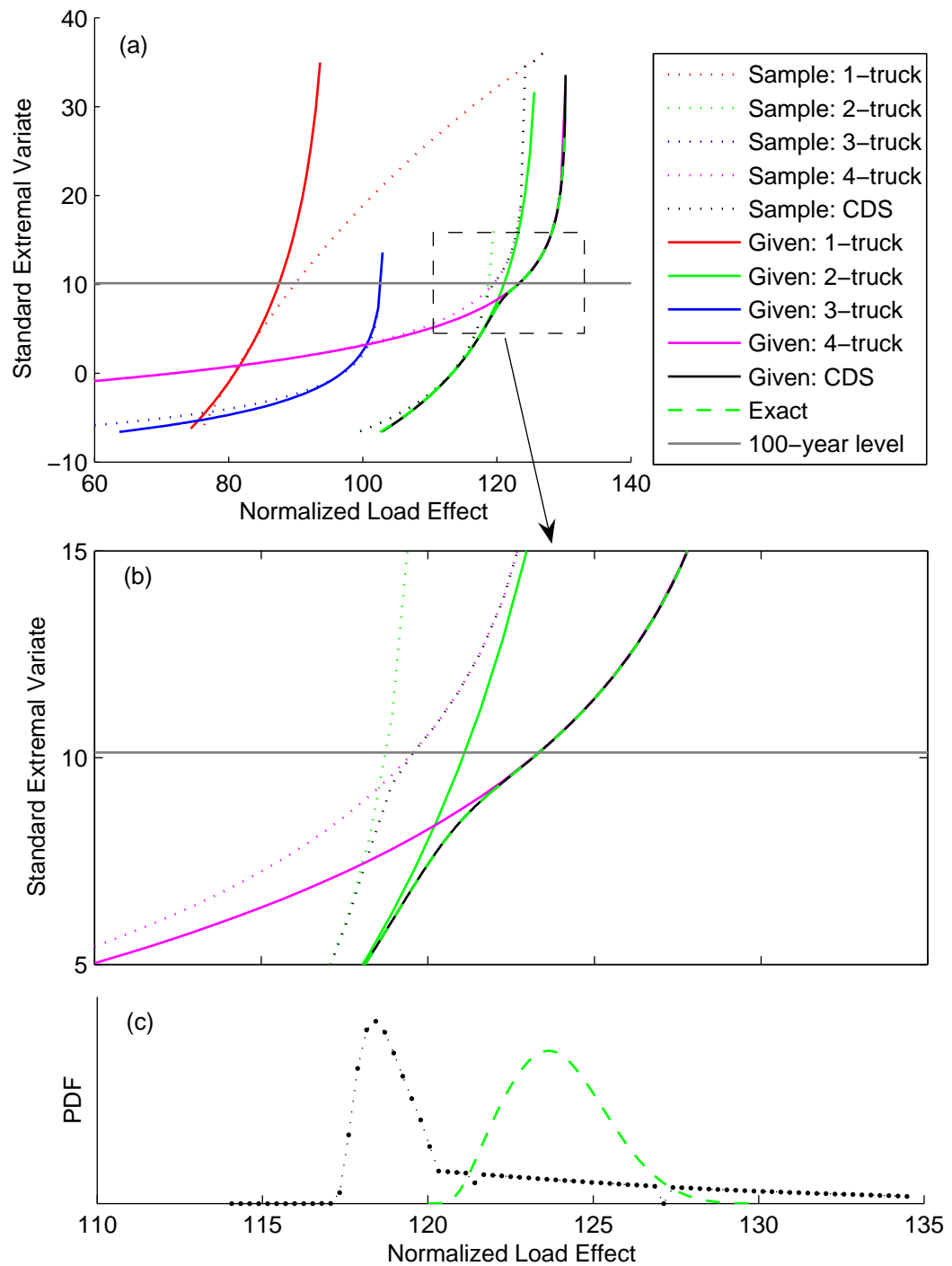
Figure 7.16: Examination of Study 2 exact (Given) and sample-fitted (Sample) distributions: (a) key and legend; (b) region of interest; (c) Exact and PL distributions.

7.4.2 Application to Bridge Loading

The results of the 1000-day simulation of Auxerre traffic presented in Chapter 6, are analysed using predictive likelihood. In general the information matrices exhibited considerable numerical instability and so the modification for parameter variability is not made to the results presented. In any case, this modification is generally slight – as may be seen from Figure 7.7(a). The predictive distributions of 100-year load effect are presented in Figure 7.17 to Figure 7.19. Also shown in these figures is a GEV fit to the predictive distribution. The GEV distribution is considered reasonable as it is sufficiently flexible to fit a wide range of uni-modal predictive likelihood curves, and also is the exact form of the distribution of return level through application of the stability postulate. Further, the load effect with 10% probability of exceedance in 100 years is indicated both for the predictive likelihood points (PL RL) and the GEV fit to these points (GEV PL fit). Also given in each figure is the usual 1000-year CDS-derived return level (CDS RL). Appendix C provides tables of results as well as plots showing the predictive likelihood optimizations.

It is clear that some of the GEV fits to the raw predictive likelihood points are not obtained through fully objective means. In such cases, the approach is to fit the upper tail more closely than either the lower tail or the mode. Due to the numerical nature of the predictive distributions themselves, such GEV fits may be considered as a smoothing process. In any case, the results have been derived from both the fits and the raw distributions and may be seen to be comparable. The percentage differences, relative to the GEV fit, for the load effect with 10% probability of exceedance in 100 years are shown in Figure 7.20.
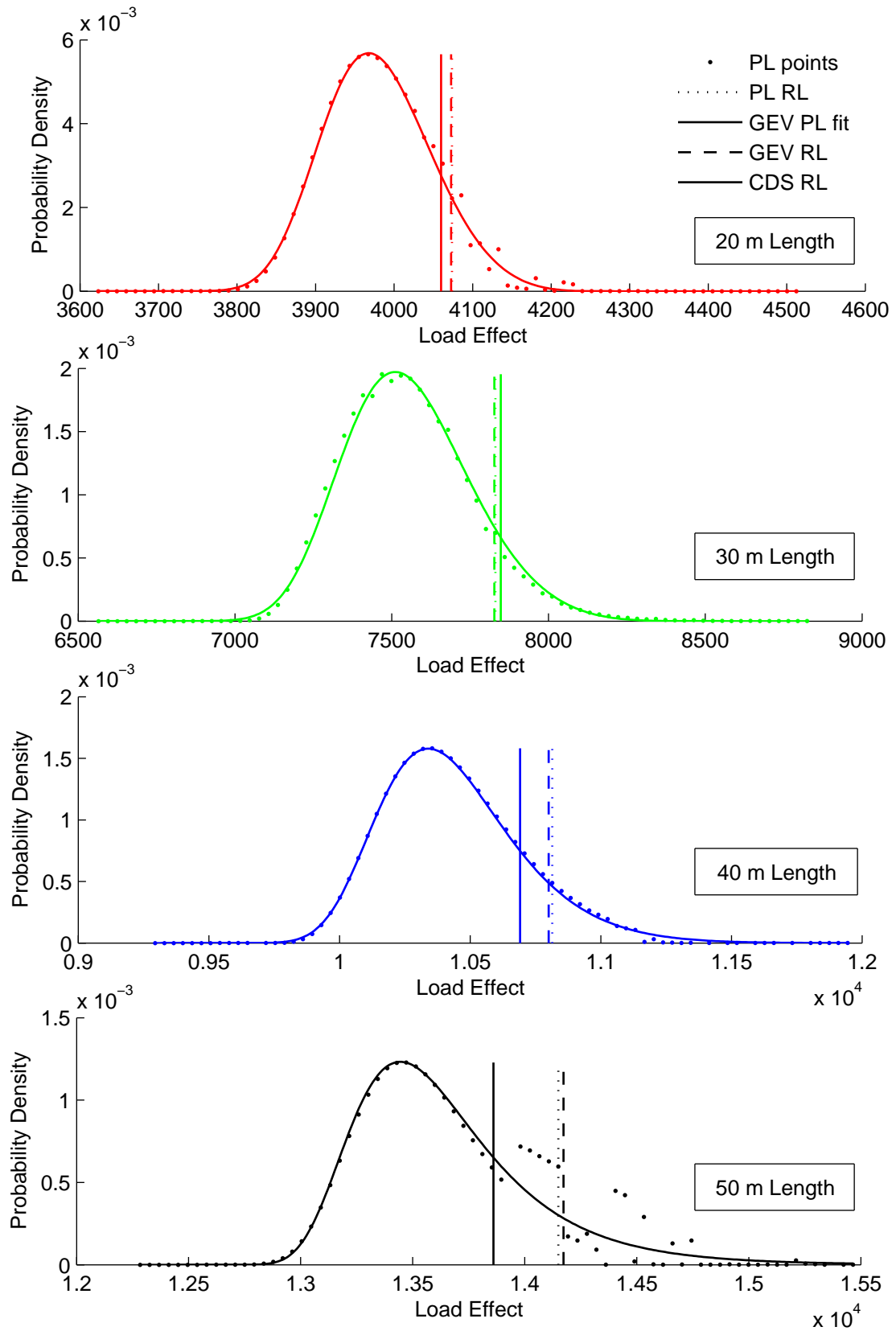
Figure 7.17: Characteristic load effect prediction for Load Effect 1.
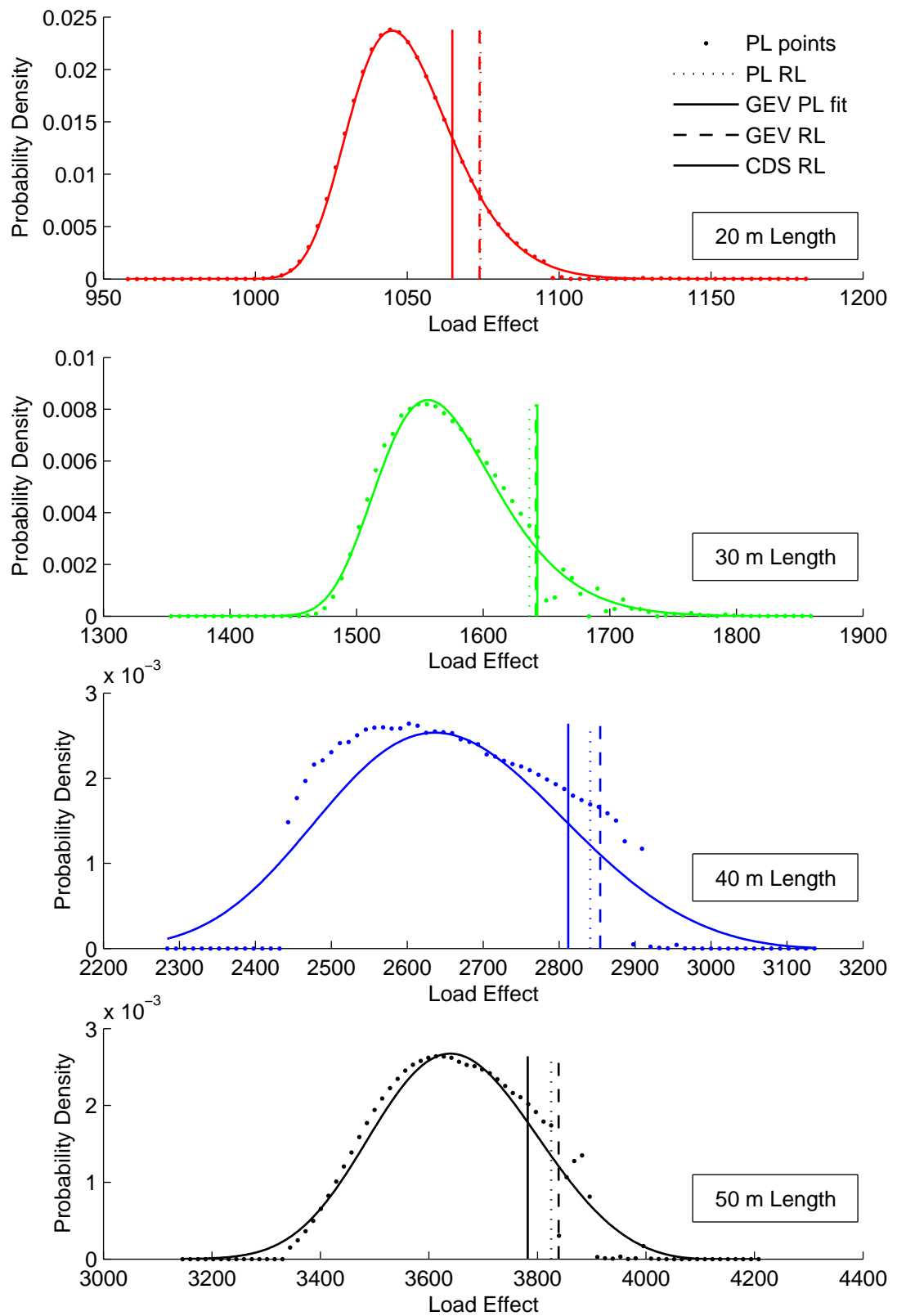
Figure 7.18: Characteristic load effect prediction for Load Effect 2.
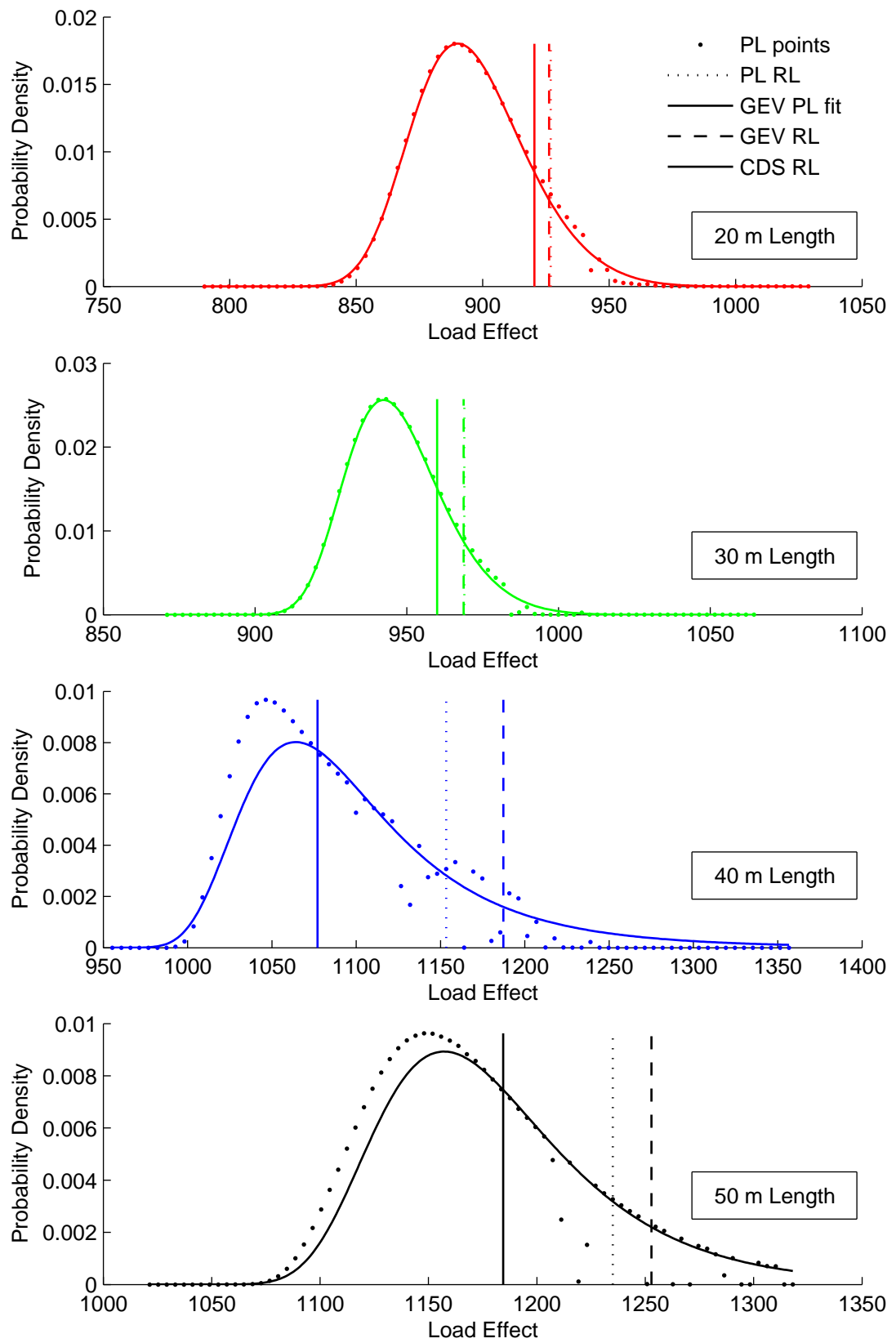
Figure 7.19: Characteristic load effect prediction for Load Effect 3.
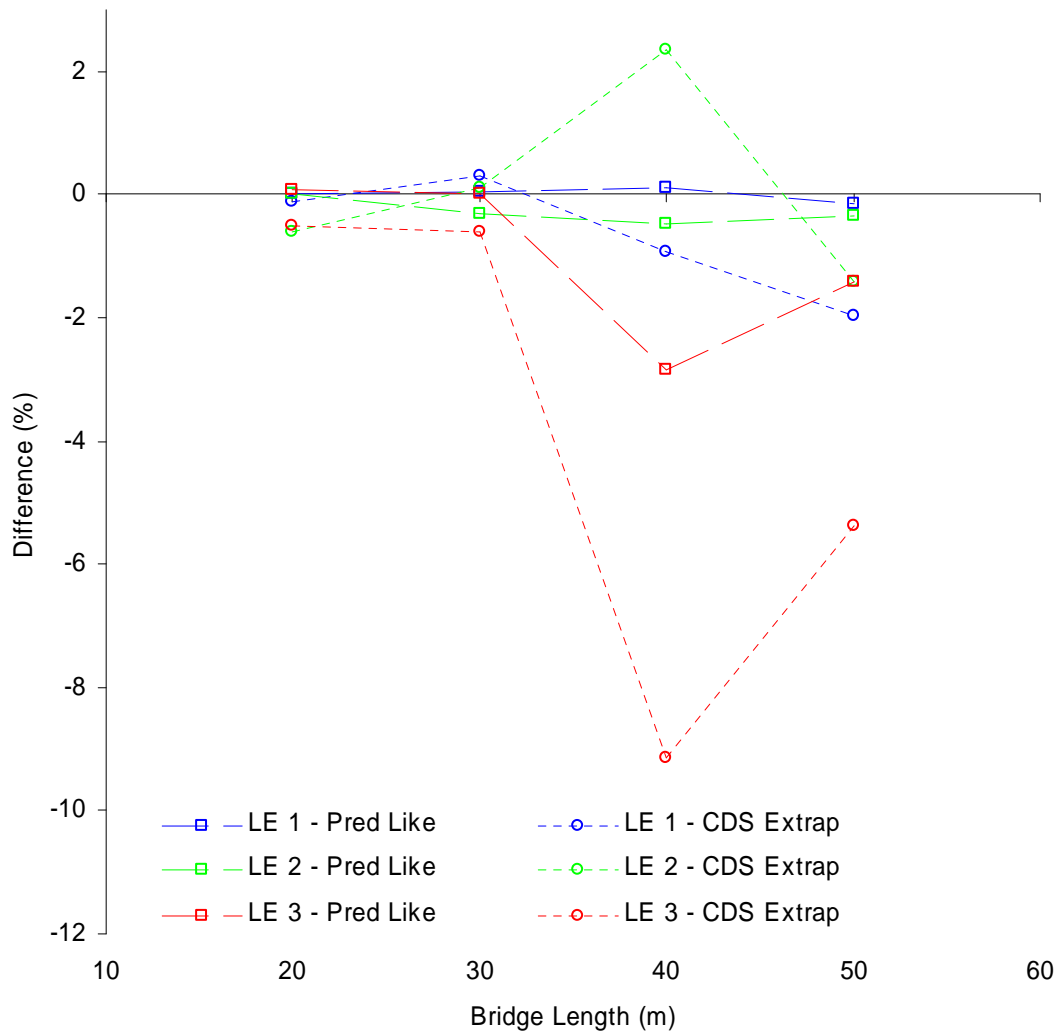
Figure 7.20: Differences in characteristic load effect prediction for different methods relative to the GEV fit to the predictive likelihood results.

It is evident from Figure 7.20 that the process of estimating the lifetime load effect directly from the predictive likelihood distribution, or the GEV fit to it, does not significantly affect the result – the maximum difference is about 3% for Load Effect 2, 40 m bridge length. Of more significance however, is the fact that the usual method of extrapolation to a 1000-year return period results in general non-conservative results (with the exception of Load Effect 2, 40 m bridge length), compared with either of the predictive likelihood-based results. The differences are not substantial, and this provides evidence that the results are

robust. Further, in the light of the results of Section 7.4.1, it may be surmised that the predictive likelihood results are closer to the actual lifetime load effect than those of the usual CDS extrapolation technique.

The net effect of the CDS and predictive likelihood approaches is compared to the hybrid Conventional approach of Chapter 6, Section 6.2.3 in Figure 7.21. It can be seen that, when compared with the GEV fitted predictive likelihood lifetime load effects, the Conventional approach is non-conservative for Load Effects 1 and 3, whilst for Load Effect 2 it is conservative. The magnitudes of the differences are also significant for bridge load estimation.
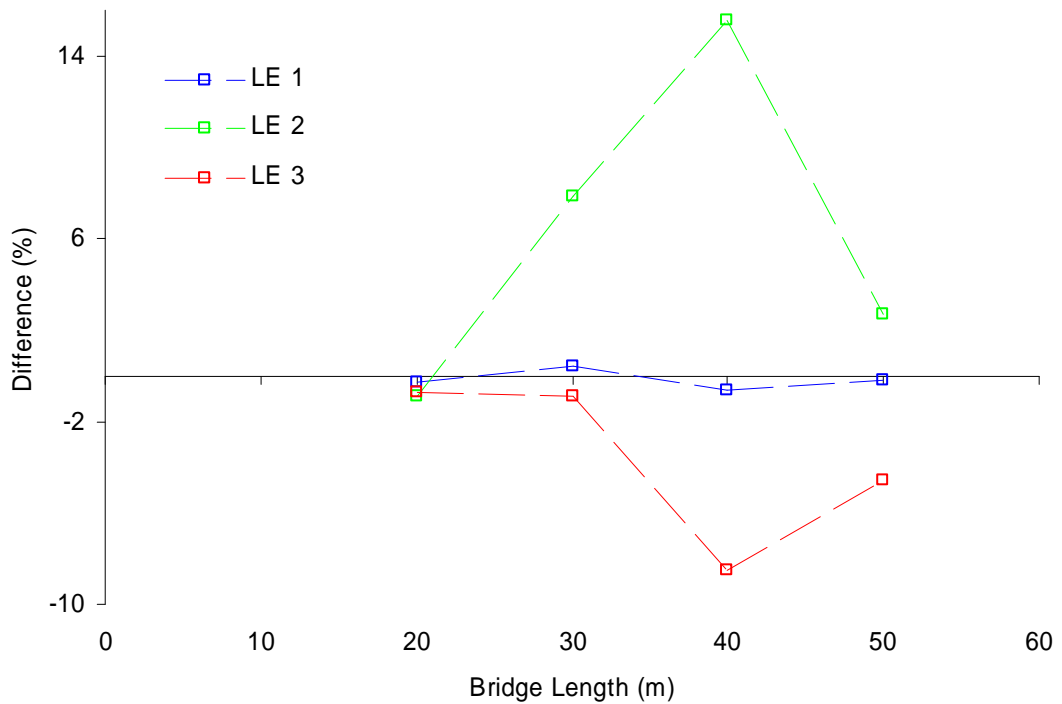
Figure 7.21: Conventional approach result relative to the GEV PL results.

7.5 Summary

In this chapter, the method of predictive likelihood is presented and applied to the bridge loading problem. Firstly, the approach used in the statistical literature is demonstrated and compared with published results for relevant examples and other methods of obtaining predictive distributions. Issues affecting the accuracy of the technique, mostly relating to the numerical processing, are examined and identified.

An extension of predictive likelihood is presented which caters for composite distribution statistics problems. This method is then applied to problems for which the results are known. Situations favourable and unfavourable to the accuracy of the method are identified therefrom and shown to be identifiable in a practical application. The method is then applied to the results of bridge load simulations. Predictive likelihood generally gives larger lifetime load effect values than the usual return period approach. This is as a result of inclusion of sources of variability within the predictive likelihood distribution. Finally the sum-total effect of the composite distribution statistics and predictive likelihood methods is established in comparison to the hybrid Conventional approach. The differences in lifetime load effects are considerable, yet within reason, and are also dependent on the influence line and bridge length. This is to be expected from the physical nature of the problem.

Chapter 8

TOTAL LIFETIME LOAD EFFECT

*"Statistics, as you all know, is the most exact of the
false sciences"*   *- John Thurloe*

Chapter 8 - TOTAL LIFETIME LOAD EFFECT

8.1 Introduction

Often in engineering it is not the outcome of a single stochastic process that is of interest, but the combination of several processes. For example, critical combinations of sea level and wave height are of interest to designers of coastal defences. The work presented thus far has focused on a single outcome from truck crossing events: static load effect.

It is well known that truck crossing events cause the truck and bridge to interact dynamically. With such interaction there is an associated dynamic component to the loading that results. When this is allowed for, the load effect is known as the total load effect – as distinct from that due to static considerations only. The total load effect is usually greater than the static load effect, but can be less in some cases.

From studies that separate the dynamic and static loads induced by loading events, the dynamic amplification factor (DAF) is defined as:

$$\varphi = \frac{S_{Total}}{S_{Static}} \tag{8.1}$$

where S represents the load effect under consideration. Many studies have been carried out to determine, either by measurement or simulation, the DAFs that occur under certain circumstances (Brady 2004). Based on such studies, bridge loading models include allowances for dynamics.

The Eurocode (EC 1: Part 3, 1994) load model for normal traffic loading (LM1) is given in Figure 8.1(a) for a two-lane bridge. These loads, so-defined, include

an allowance for dynamic interaction, given by Figure 8.1(b). The origins of this work are presented by Bruls et al (1996). O'Connor (2001) also provides a thorough background.

The Eurocode load model is developed from simulation of static traffic actions, as described in Chapter 2. The dynamic amplification factors of Figure 8.1(b) are applied to the 1000-year characteristic static load effects. As the worst static and dynamic cases are combined, such loading is conservative because it does not recognize the reduced probability of two extremes (static and dynamic aspects) occurring simultaneously.
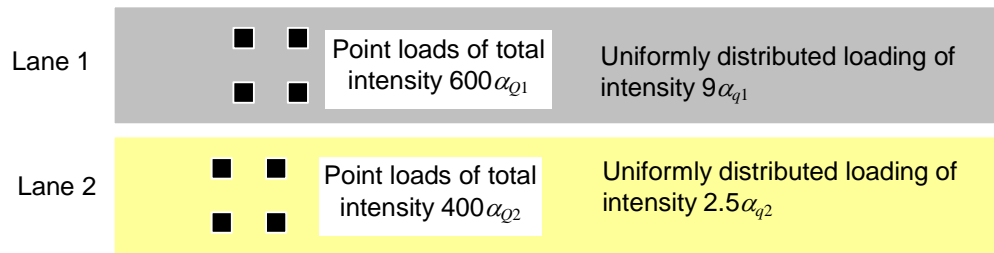
(a) Static Loading;
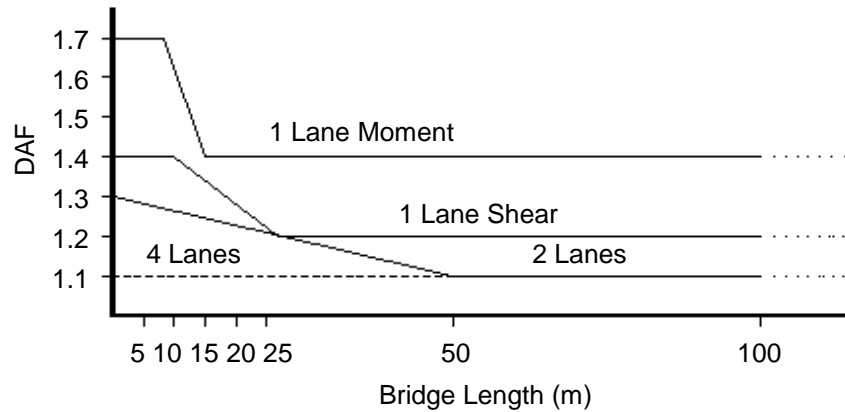
(b) Allowance for Dynamic Interaction;

Figure 8.1: Eurocode Load Model.

The bridge-truck(s) interaction is sufficiently complex that the dynamic aspect of the load effect may be considered as a random variable. Therefore, with any given crossing event, there are two resulting processes: static and total load

effect. For the assessment of bridges, it is critical combinations of these two processes that are of interest.

Multivariate extreme value theory is the statistical tool that is used to analyse critical combinations of several processes. Such an approach is more reasonable as it includes the respective probabilities of occurrence. This theory is used here to incorporate the dynamic interaction of the bridge and trucks into an extreme value analysis for total load effect. The results of this analysis are used to determine a dynamic allowance factor that may be applied to the results of static simulations to determine an appropriate lifetime total load effect. The analysis is performed for a notional site, derived from two well-studied sites.

8.2 Multivariate Extreme Value Theory

8.2.1 Background

In the univariate setting used thus far, the selection of block maxima is straightforward through the ordering of data from individual realizations. For multivariate processes though, the ordering of the data is complicated by the nature of the data. For example, in the case of bridge loading, a high-dynamics loading event does not necessarily have an associated high static load effect. It is usual in multivariate extreme value analyses to adopt the componentwise maxima approach (Coles 2001a, Demarta 2002). Considering the bivariate case, each realization, **i**, has an associated vector of outcomes, (X_i, Y_i), one for each of its statistical processes. For a block of **n** realizations, the vector of componentwise maxima is:

$$\mathbf{M}_n = (M_X, M_Y) \tag{8.2}$$

where

$$M_X = \max_{i=1,\ldots,n} X_i, \quad M_Y = \max_{i=1,\ldots,n} Y_i \tag{8.3}$$

Similarly to the univariate extreme value approach of Chapter 3, the distribution of $\mathbf{M}_n$, as $n \to \infty$, is a bivariate extreme value distribution if:

$$
\begin{aligned}
P[M_X \leq x, M_Y \leq y] &= G(x, y) \\
&= \lim_{n \to \infty} F^n(x, y)
\end{aligned}
\tag{8.4}
$$

for some extreme value distribution $G(x, y)$. This simplistic exposition avoids the normalizing constants required to account for degenerate cases – refer to Demarta (2002) and Tawn (1988) for further details.

In general, the marginal distributions,

$$G_X(x) = G(x, \infty)$$
$$G_Y(y) = G(\infty, y)$$

(8.5)

will be of GEV form (see Chapter 3, Section 3.4.3). One distribution that satisfies (8.4) is therefore:

$$G(x, y) = G_X(x) \cdot G_Y(y)$$

(8.6)

but this distribution represents the case when the maxima are independent and is not the general case. Therefore a form of dependence measure is required for a general multivariate extreme value distribution.

8.2.2 Correlation, copulae and dependence

Correlation Coefficients

The most widely used measure of dependence between random variables is Pearson's correlation coefficient (Mood et al 1974):

$$\rho(X, Y) = \frac{\mathrm{Cov}(X, Y)}{\sigma_X \sigma_Y}$$

(8.7)

where $\mathrm{Cov}(X, Y) = \mathrm{E}(XY) - \mathrm{E}(X)\mathrm{E}(Y)$. This function reduces the complexity of any relationship between the random variables to a scalar value. Moreover, this form of correlation coefficient only measures the linear relationship between parameters – of course many other relationships are possible. Other forms of correlation coefficient are also used such as Kendall's tau (ρ_τ) and Spearman's rho (ρ_S) correlation coefficient, both of which are types of rank-correlation. In the bivariate case, they are related to Pearson's correlation by:

$$\rho_\tau = \frac{2}{\pi}\sin^{-1}\rho$$

$$\rho_S = \frac{6}{\pi}\sin^{-1}\frac{\rho}{2}$$

(8.8)

Deterministic examples that fool these correlation measures are easy to find (such as exponents, logarithms, etc.). Figure 8.2 presents a random example in which two sets of a 1000 random deviates are generated according to two different models. However, both of the marginal distributions are distributed as standard normal deviates, and $\rho(X,Y) = 0.7$ in both cases. It is clear from Figure 8.2(b) that there is significant tail-dependence between the two marginal distributions – this would have clear implications for extreme value statistics, for example. It is therefore clear that more complex dependency measures are required to preserve any observed relationship between the data vectors in a multivariate extreme value analysis.
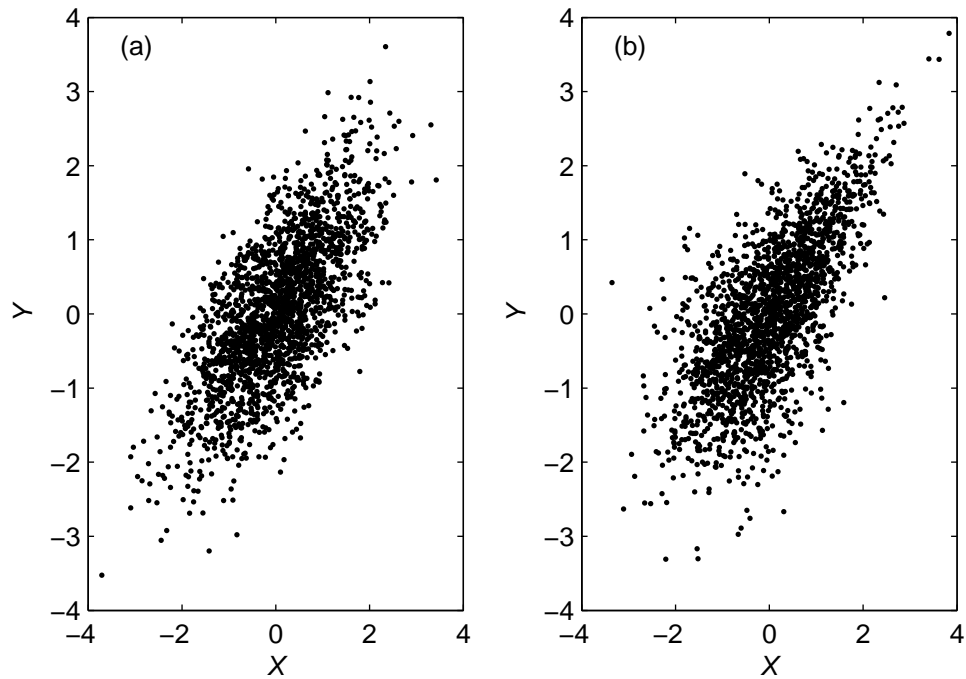
Figure 8.2: Bivariate dependences of standard normal distributions,

$\rho(X,Y) = 0.7$: (a) Gaussian copula, and (b) Gumbel copula.

Copulae

A function that links marginal distributions is known as a copula. Denoted as $C(\cdot)$, a copula is defined as:

$$F(x_1,\ldots,x_d) = C\left(F_1(x_1),\ldots,F_d(x_d)\right) \tag{8.9}$$

where $F_i(x_i)$ is the marginal distribution of the ith component. Every multivariate distribution has a copula (this is Sklar's theorem – see Demarta 2002, for example). From this representation, it can be seen that multivariate distribution modelling can be divided into two separate parts: modelling the marginal distributions; and, modelling the dependences through a copula. It is in this way that appropriate marginal and dependence structures can be developed separately and then combined.

There are several restrictions on copulae, most easily summed up by noting that a copula may be considered as a multivariate distribution function with uniform marginals – as may be clear from (8.9). A trivial example is the independence copula, for which $C_{Ind}(u,v) = u \cdot v$, and this is the copula of use in (8.6).

Figure 8.3 plots the bivariate Gumbel (or logistic) copula, given by:

$$C_{Gu}(u,v) = \exp\left\{-\left[(-\log u)^{1/\beta} + (-\log v)^{1/\beta}\right]^{\beta}\right\} \tag{8.10}$$

where β is the dependency measure. It is this copula that is used to link the standard normal marginal distributions of Figure 8.2(b). Embrechts et al (2003) provide the link between a copula and Kendall's tau. When applied to the Gumbel copula, this reduces to:

$$\rho_\tau = 1 - \frac{1}{\beta} \tag{8.11}$$

It is by inverting (8.11) and (8.8) that Figure 8.2(b) is drawn.

Embrechts et al (2003) and Demarta (2002) also provide another statistic based on the copula – that of tail dependence. Tail dependence is a measure of the amount of dependence in the upper (or lower) quadrants of a multivariate distribution – see Figure 8.2 for example – and is given by:

$$\lambda_U = \lim_{q \to 1} P\left[X > G_X^{-1}(q) \,|\, Y > G_Y^{-1}(q) \right] \tag{8.12}$$

provided that the limit $\lambda_U \in [0,1]$ exists. If $\lambda_U \in (0,1]$, $\mathbf{X}$ and $\mathbf{Y}$ are said to be asymptotically dependent in the upper tail; if $\lambda_U = 0$, $\mathbf{X}$ and $\mathbf{Y}$ are said to be asymptotically independent in the upper tail. Tail dependence is a copula property, and for the Gumbel copula, given by (8.10), it is given by:

$$\lambda_U = 2 - 2^\beta \tag{8.13}$$
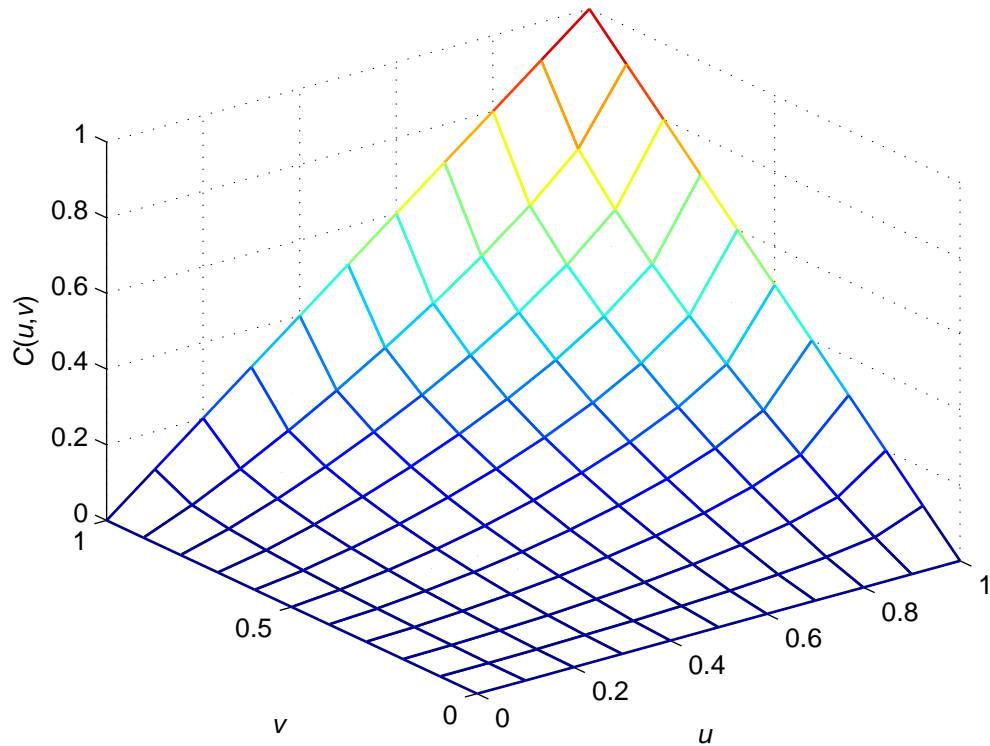
Figure 8.3: Gumbel copula function.

When multivariate data is analysed to find extremes, the copula representing the dependence structure also becomes extreme (Segers 2004). Pickands (1981) provides an extreme-value copula:

$$C_{EV}(u,v) = \exp\left\{ \log(uv) A\left(\frac{\log(v)}{\log(uv)} \right) \right\} \tag{8.14}$$

where the function $A(\cdot)$ is known as the Pickands dependence function. Every copula has an associated dependence function, and it is this function which solely determines the interrelationship between the marginal distributions (Demarta 2002). In order that $C_{EV}(u,v)$ be a copula, there are restrictions on $A(\cdot)$: $A(0) = A(1) = 1$ and $\max(\omega, 1-\omega) \leq A(\omega) \leq 1$ for $0 \leq \omega \leq 1$. Also, for independence $A(0.5) = 1$ whilst for perfect dependence, $A(0.5) = 0.5$.

8.2.3 Bivariate extreme value distributions

Tawn (1988) describes the use of the extreme value copula. For the bivariate extreme value case, the GEV distribution is used to fit each marginal of the data. Transformed random variables are defined as the exponent of these marginal GEV distributions:

$$z_1 = \left[1 - \xi_1 \left(\frac{x - \mu_1}{\sigma_1} \right) \right]^{1/\xi_1}_{+} ; \quad z_2 = \left[1 - \xi_2 \left(\frac{y - \mu_2}{\sigma_2} \right) \right]^{1/\xi_2}_{+} \tag{8.15}$$

where $h_{+} = \max(h, 0)$ and the GEV parameters are obtained using maximum likelihood fits to the data vectors $\mathbf{X}$ and $\mathbf{Y}$ separately. As a result of this transformation, the marginal distributions are now of the form:

$$G_X(z_1) = e^{z_1}; \quad G_Y(z_2) = e^{z_2} \tag{8.16}$$

Similarly to the univariate case, any multivariate extreme value distribution must be max-stable (as defined in Chapter 3). For the bivariate case with marginals given by (8.16) this requirement is met, as:

$$G^n(x, y) = G(nx, ny) \tag{8.17}$$

Pickands (1981) shows that, through the use of the extreme value copula and the exponential marginals of (8.16), a general form of bivariate extreme value distribution is:

$$G(x, y) = \exp\left\{-(x+y) A\left(\frac{y}{x+y}\right)\right\} \tag{8.18}$$

where $A(\cdot)$ is the Pickands dependence function previously mentioned:

$$A(\omega) = \int_0^1 \max\left\{(1-\omega)q, \omega(1-q)\right\} dH(q) \tag{8.19}$$

where $H(\cdot)$ is a distribution function on $[0,1]$. It is this last representation that gives rise to the restrictions on $A(\cdot)$ noted previously. It can be seen from the above developments, that inference on the bivariate extreme value distribution depends only upon inference on $A(\cdot)$. Further, different choices of $H(\cdot)$, subject to the restrictions on $A(\cdot)$, give rise to different forms of bivariate extreme value distribution. Indeed, Stephenson (2005) discusses eight different forms of bivariate extreme value distributions that have emerged in the literature. Of particular interest in this work, for reasons to be given, is the Gumbel bivariate extreme value distribution:

$$G_{Gu}(x, y) = \exp\left\{-\left(z_1^{1/\alpha} + z_2^{1/\alpha}\right)^{\alpha}\right\} \tag{8.20}$$

where $0 < \alpha < 1$ and is similar to the dependence measure β of $C_{EV}(u,v)$. Independence is represented by $\alpha = 1$ and complete dependence occurs when $\alpha \to 0$. Coles (2001a) gives the choice of distribution function $H(\cdot)$ that leads to this bivariate extreme value distribution. Capéraà et al (1997) describe the fitting of the dependence function $A(\cdot)$, upon which this work is based.

8.2.4 Structure variable analysis

As it is usually some combination of the individual variables comprising the multivariate analysis, Coles (2001a) describes the structure variable approach to inference on componentwise combination. This is expressed as a function of the individual components of the vector of componentwise maxima:

$$Z = \phi(\mathbf{M}_n) = \phi(M_X, M_Y) \tag{8.21}$$

Hence $\mathbf{Z}$ is the structure variable of this bivariate problem. The function may be $\phi = \max$, $\phi = \min$, $\phi = \Sigma$ for example. In the present context, total and static load effects are being considered and the dynamic allowance is the ratio. Hence:

$$Z = \phi(M_X, M_Y) = \frac{M_X}{M_Y} \tag{8.22}$$

Denoting the bivariate density of (M_X, M_Y) by $g(\cdot)$, the distribution of $\mathbf{Z}$ is:

$$P[Z \leq z] = G_Z(z) = \int_{V(z)} g(x, y)\, dx\, dy \tag{8.23}$$

where

$$V(z) = \{(x, y) : \phi(x, y) \leq z\} \tag{8.24}$$

in which the notation refers to the set of all (x, y) such that $\phi(x, y) \leq z$. This relationship is presented figuratively for simple $\phi(x, y)$ in Figure 8.4.

Clearly integration of (8.23) is not trivial for general ϕ. Coles (2001a) shows that for some functions its evaluation is not necessary ($\phi = \max$, for example). However, in the current context a more elaborate analysis is required. Coles also describes the univariate structure variable method, in which – for the current context – the distribution of $\mathbf{Z}$ is estimated by calculation of:

$$Z_i = \frac{M_{X,i}}{M_{Y,i}}; \quad i = 1, \ldots, n \tag{8.25}$$

and subsequent GEV fitting to the Z_i. Coles describes several drawbacks of this approach, not least that the GEV distribution cannot be justified on any theoretical grounds.
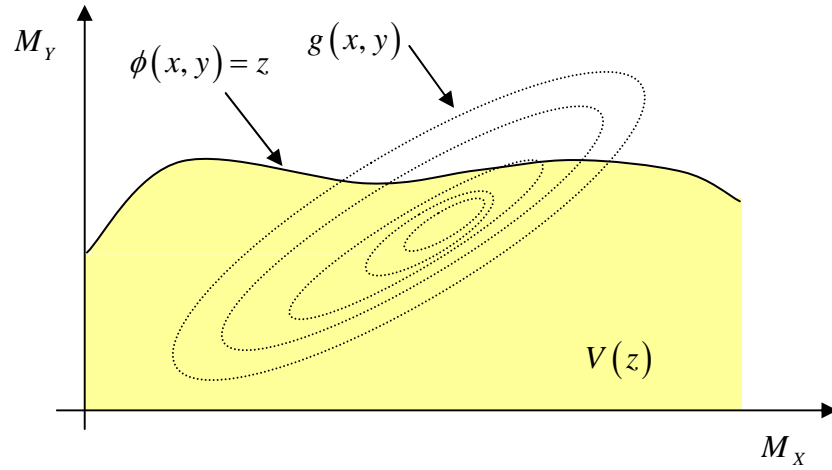
Figure 8.4: Figurative representation of the structure variable approach.

8.3 Statistical Analysis for Lifetime Load Effect

8.3.1 Site-specific traffic load effect

The Mura River Bridge, described in Chapter 4, is used in conjunction with WIM data from the A6 motorway near Auxerre, France, as the basis of this analysis. A finite element model of the bridge has been developed by Brady (2004), in which dynamic behaviour of the model has been calibrated against measured responses for single and two-truck meeting events. The notional site defined by the bridge and traffic is the basis for the application of multivariate extreme value analysis to determine lifetime dynamic allowance factors.

For this site, 10 years of bi-directional, free-flowing traffic data is generated and this traffic is passed over the influence line for Beam 1 to determine the load effects that result. Each year of simulation is broken into 'months' of 25 days each and there are thus 10 such months in each year of simulation – as described in Chapter 4, Section 4.3.2. As a basis for further analysis, the events corresponding to monthly-maximum static load effect are retained. This is done to minimize the number of events that are to be dynamically analysed, as well as providing a shorter extrapolation 'distance'.

It is to be noted that events are not separated for the application of composite distribution statistics. From the results of Chapter 6, it is not expected that this will cause much inaccuracy due to the behaviour of load effects from similarly shaped influence lines to that here. In any case, the work that follows illustrates the general methodology, and this can be extended for CDS statistics readily.

The 100 monthly-maximum loading events obtained from the simulations are analysed using the finite element bridge-truck interaction models developed by

Brady (2004) and Gonzalez (2001). Rattigan (2006) carried out the dynamic simulations as part of his doctoral research. Figure 8.5 illustrates a sample truck model and shows the model used for the bridge. Thus, the results of the simulations described is a population of 100 monthly-maximum loading events for which both total and static load effects are known; therefore the DAF for each is also known.

(a)   (b)
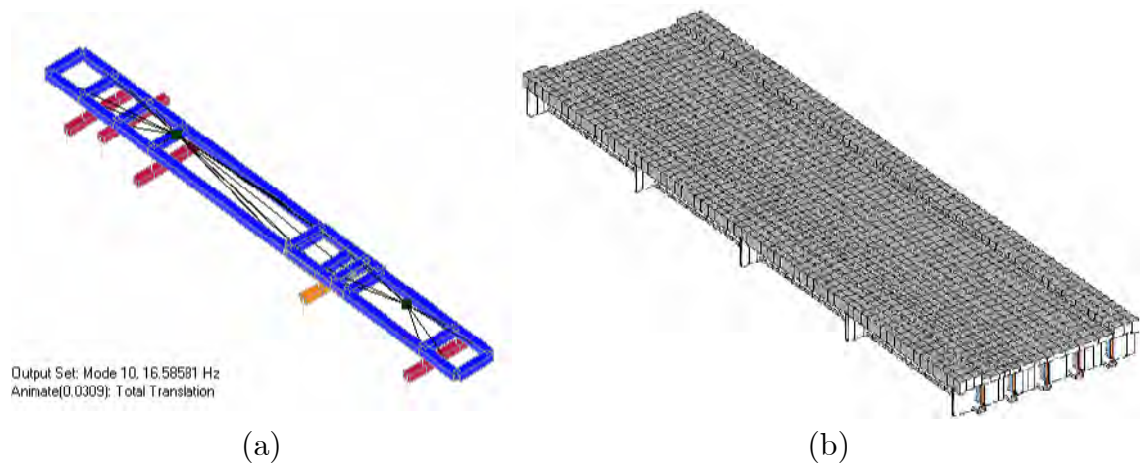
Figure 8.5: Finite element models of (a) 5-axle truck and (b) bridge.

Of the 100 monthly-maximum events, 20 are found to be 1-truck events, 77 to be 2-truck events and 3 are 3-truck events. This reflects the balance of frequency of occurrence with higher load effects observed in Chapter 6 and is also a function of the influence shape.

The influence surface for Beam 1 is asymmetrical; therefore trucks in Lane 1 dominate, reducing the effect of trucks in Lane 2. Therefore the monthly-maximum events are derived from the occurrence of heavy trucks in Lane 1, and trucks with less extreme GVW in Lane 2. Figure 8.6 illustrates some examples of the monthly-maximum events; the prevalence of heavy trucks in Lane 1 (top lane) is evident.
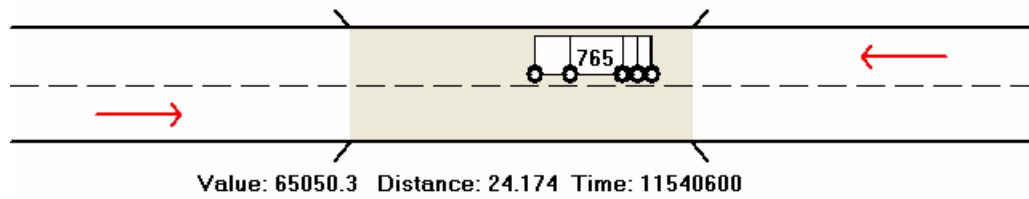
(a) 1-truck;
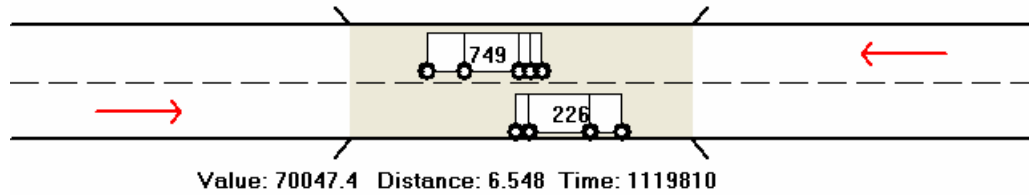
(b) 2-truck;
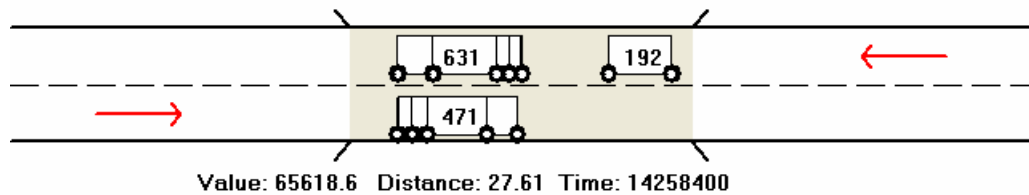
(c) 3-truck;

Figure 8.6: Examples of monthly-maximum events – GVW is noted on each truck in deci-tonnes and Lane 1 is uppermost.

8.3.2 Preliminary statistical investigation

Scatter plots of various variables are drawn, to investigate the results. Figure 8.7 shows the total and static load effect values of individual maximum-per-month loading events as a scatter plot. The results are in units of tenths of N/mm^2, for numerical stability purposes. There is a relationship between static and total load effect – as may be expected.

Scatter plots of DAF against total and static load effect are given in Figure 8.8. There is a positive correlation between DAF and total load effect. A less

significant relationship between DAF and static load effect can be seen from Figure 8.8.
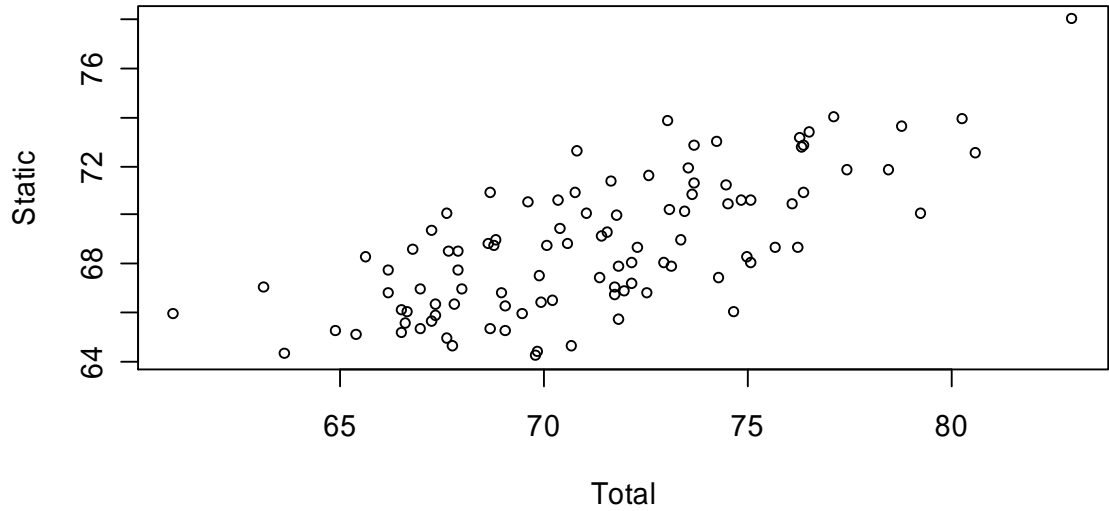
Figure 8.7: Maximum-per-month static and total load effect (dN/mm^2).
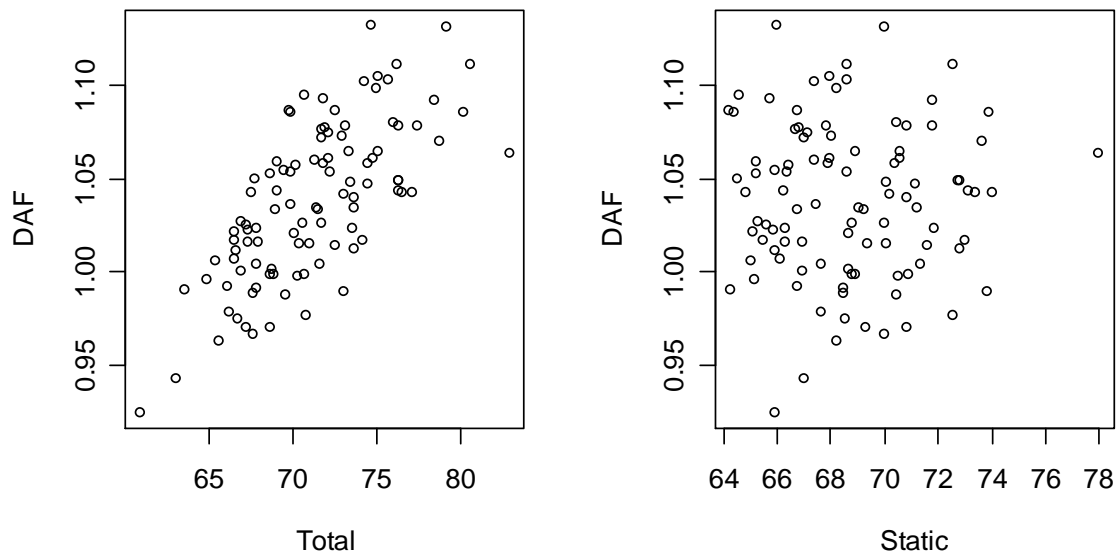
Figure 8.8: Scatter plots of DAF against total and static load effect (dN/mm^2).

It is possible, and conservative, to analyse this data in the following manner. The marginal distributions of total and static load effect can be estimated – the GEV distribution would be ideal for this. A distribution of dynamic ratio could then be numerically calculated as the quotient of these two distributions, and

possibly fitted with its own GEV distribution. This procedure, however, fails to recognize the correlation between the variables, and is therefore conservative. For later comparison, the 90-percentile of the dynamic ratio distribution that results from this procedure is about 1.23 and this will be seen to be considerably different to the results of a more appropriate analysis.

8.3.3 Multivariate extreme value analysis

In the analysis that follows, software developed by Stephenson (2005) is used in conjunction with bespoke algorithms, written in the $\mathbf{R}$ language for statistical computing ($\mathbf{R}$ Development Core Team 2005). Stephenson's (2003) method for simulating multivariate extreme value random variables is also used.

To include the apparent relationship between the total and static load effect values, bivariate extreme value distributions (BEVD) are adopted. In the first instance BEVD is used to model the parent distribution of monthly maxima, and later it is used to model the lifetime distribution.

The data is fitted using the Gumbel logistic bivariate extreme value distribution, given in equation (8.20). The marginal distributions are estimated using GEV distributions. The transformed variable approach of equation (8.15) is used. The results of the fit can be seen in Figure 8.9: subplots (a) and (b) show the quality of fit to the marginal distributions whilst Figure 8.9(c) shows a contour plot of the bivariate probability density function.
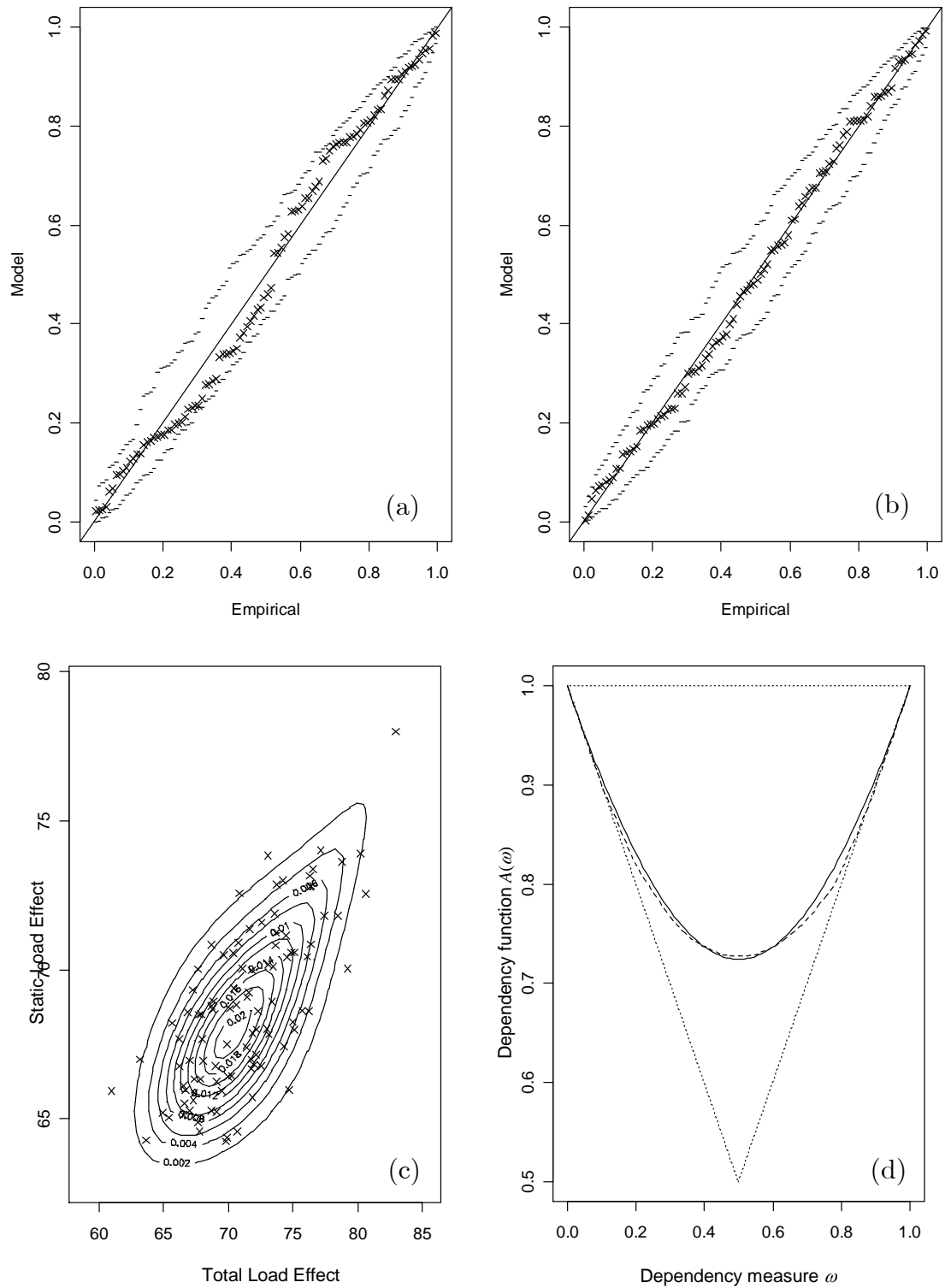
Figure 8.9: Results and diagnostic plots of the BEVD fit (dN/mm^2): (a) Marginal distribution of total load effect; (b) marginal distribution of static load effect; (c) bivariate distribution, and; (d) dependency structure.

Figure 8.9(d) is of particular importance: this plot describes the empirical and fitted dependence structure of the data; the function $A(\cdot)$. From the properties of $A(\cdot)$ discussed earlier, the line $A(\omega)=1$ in Figure 8.9(d) represents perfect independence, whilst the triangular envelope describes perfect dependence. The solid line represents the fitted dependence structure, whilst the dashed line is the empirical estimate of the dependence in the data. It can be seen, therefore, that the dependence function is modelled quite well - this is the determining factor in the use of the Gumbel bivariate extreme value distribution in this work. The parameters of the BEVD model are given in Table 8.1.

Marginal Distributions					
Total Load Effect			Static Load Effect		
μ	σ	ξ	μ	σ	ξ
69.72	3.851	0.2071	67.56	2.423	0.1233
Dependence Measures					
BEV dependence parameter			Tail dependence		
$\alpha = 0.5347$			$\lambda_U = 0.5514$		

Table 8.1: Parameters of fitted parent bivariate extreme value distribution.

8.3.4 Bootstrapping for lifetime load effects

To estimate the distribution of lifetime load effect, and as it is not considered feasible to raise the fitted parent distribution to an appropriate power, a parametric bootstrapping approach is used. The 100-year lifetime of the bridge is simulated in each bootstrap replication. To do this, 1000 (100 years with 10 'months' per year) synthetic monthly-maximum events are simulated from the BEVD model. The component-wise maxima (that is the, the maximum static effect, and the maximum total effect) are recorded. These values are therefore not related through an individual loading event. In this way, the maximum

total and static load effects from 1000 bootstrap replications of the bridge lifetime are noted; these points are given in Figure 8.10.

(a)   (b)   (c)
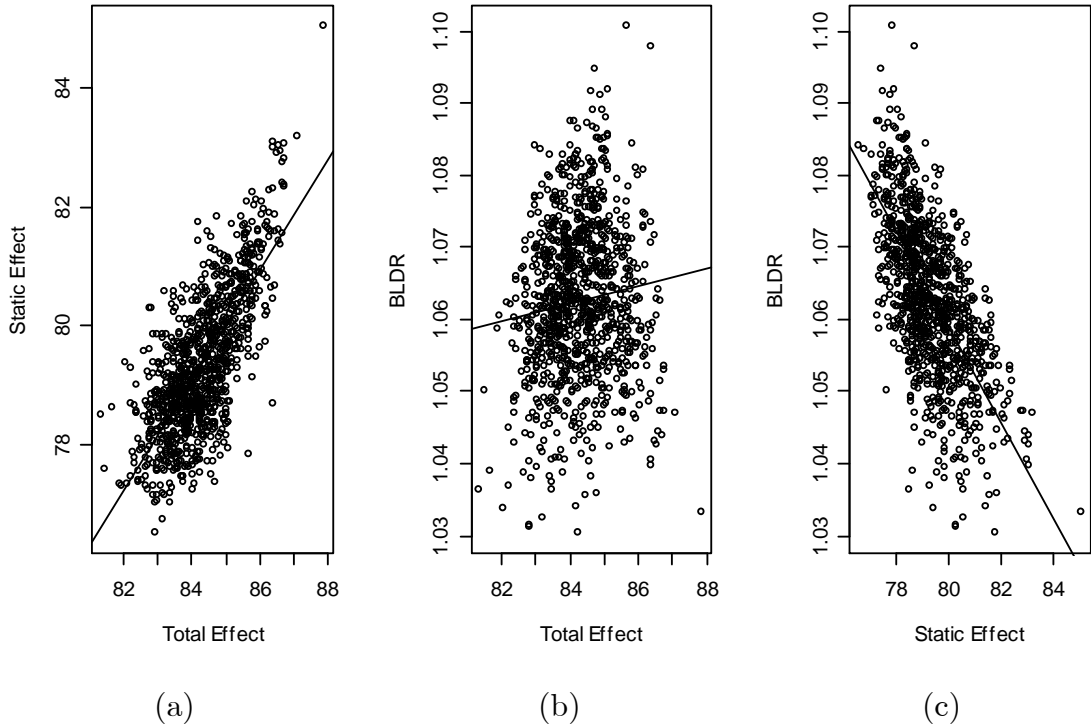
Figure 8.10: Scatter plots (showing linear regression lines) of (a) Total against Static load effect; and, Bridge Lifetime Dynamic Ratio against (b) Total, and; (c) Static load effect (dN/mm^2).

The ratio of static lifetime load effect to total lifetime load effect is termed here as the Bridge Lifetime Dynamic Ratio (BLDR). This recognizes that the same event is not necessarily responsible for the maximum lifetime total and maximum lifetime static load effects. Various plots are given in Figure 8.10 relating to the output from the bootstrap replications. It can be seen that there is strong positive correlation between the total and static load effect; little linear correlation between the BLDR and total effect, and; a strong negative linear correlation between BLDR and static effect. This is significant; it means that the dynamic ratio is falling as more extreme load effects are considered.

Applying the univariate structure variable analysis method of Section 8.2.4 and equation (8.25), the distribution of BLDR is shown in Figure 8.11, fitted with a GEV distribution, $\theta = \left(\mu = 1.058; \sigma = 0.0109; \xi = 0.22442 \right)$. It is to be noted that allowance for the relationship between the load effect components has reduced the 90-precentile dynamic allowance from 1.23 for perfect independence (as previously noted), to around 1.08 for modelled dependence.

For design purposes, the structure variable analysis described is not fully appropriate: it is not a probabilistic return level of BLDR that is required, rather a value of BLDR that 'links' the characteristic static load effect value to the characteristic total load effect value through some form of dynamic ratio.
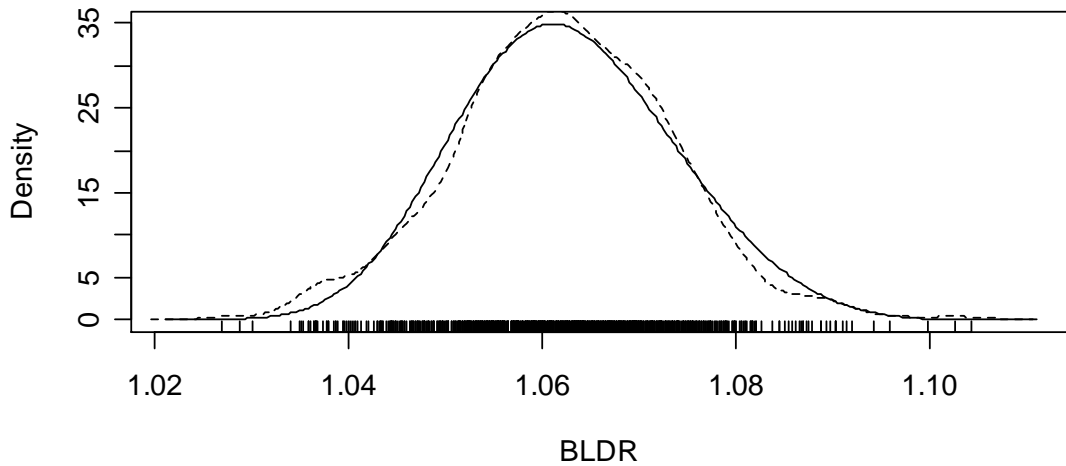
Figure 8.11: Empirical and fitted distribution of Bridge Lifetime Dynamic Ratio.

8.3.5 Assessment Dynamic Ratio

Due to the relationships apparent from Figure 8.10, a Gumbel bivariate extreme value distribution is fitted to the simulated lifetime maxima; the results are shown in Figure 8.12 and the parameters given in Table 8.2.
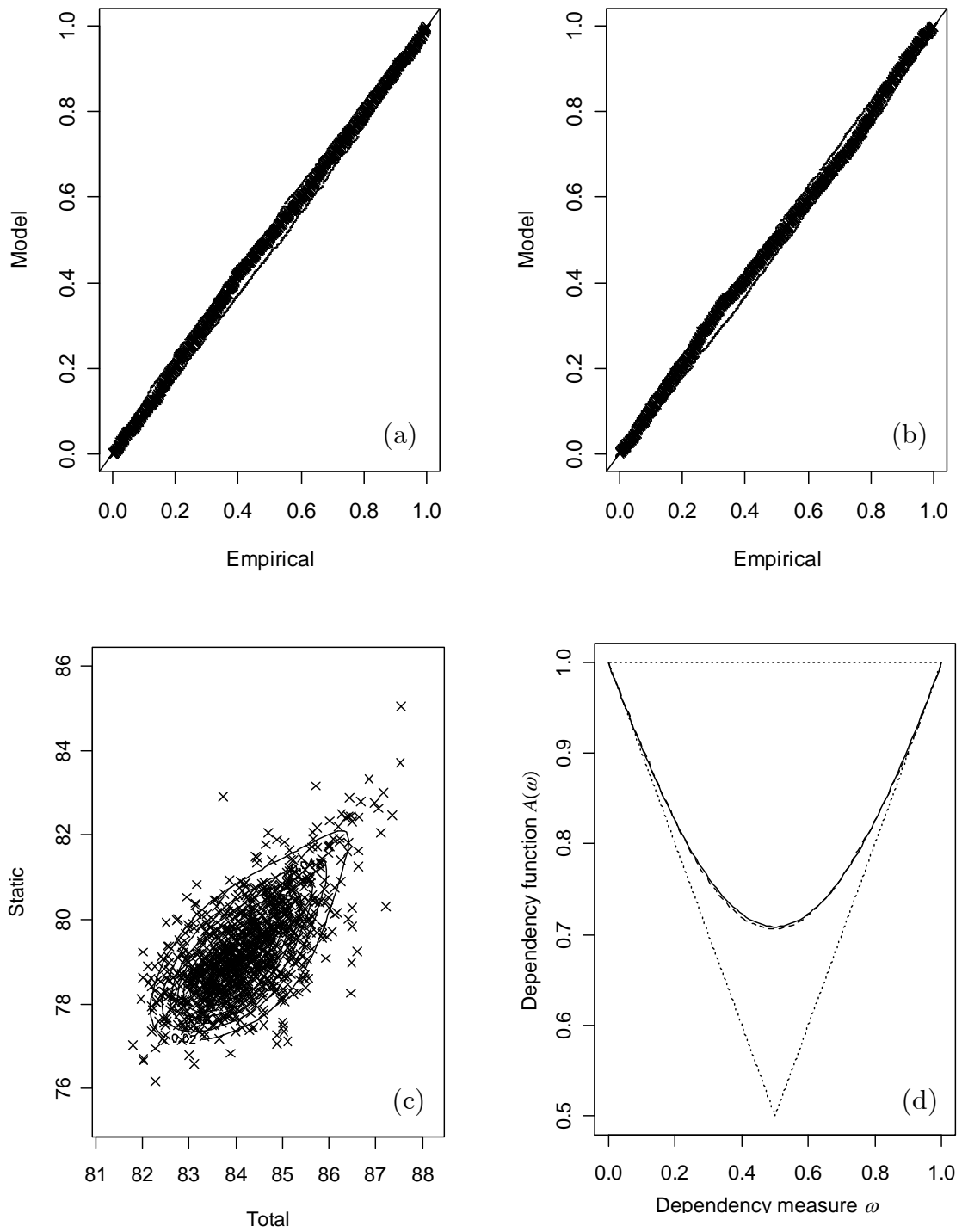
Figure 8.12: Bivariate extreme value lifetime load effect distribution (dN/mm^2): (a) Marginal distribution of total load effect; (b) marginal distribution of static load effect; (c) bivariate distribution, and; (d) dependency structure.

Marginal Distributions					
Total Load Effect			Static Load Effect		
μ	σ	ξ	μ	σ	ξ
83.86	0.950	0.2425	78.81	1.079	0.1566
Dependence Measures					
BEV dependence parameter			Tail dependence		
$\alpha = 0.5513$			$\lambda_U = 0.5346$		

Table 8.2: Parameters of 100-year lifetime fitted BEVD distribution.

Figure 8.12(d) shows that there is dependence between the static and total load effect values for bridge lifetime – even though they are not related through individual loading events, and this must be a result of the dependence in the parent distributions. To relate the density plot of the bridge lifetime load effects and parent distribution, they are equally scaled and plotted in Figure 8.13.

It is not the distribution of BLDRs that is of interest, rather, a BLDR that corresponds to a certain quantile for each of the marginal distributions. Such a BLDR is termed an Assessment Dynamic Ratio (ADR) and is defined as:

$$\varphi_q = \frac{G_X^{-1}(q)}{G_Y^{-1}(q)} \tag{8.26}$$

where **q** is the quantile of interest and the marginal distributions are defined in (8.5). For Eurocode design, $q = 0.9$ for a 100-year design life: this is the appropriate value to relate lifetime static to total load effect values, and is shown in Figure 8.14. In general, φ_q is not monotonically increasing in **q** as it is subject to the form of the marginals. Where it is so, it is possible to define a distribution of ADR as:

$$G_\varphi(z) = \int_{Q(z)} \varphi_q \, dq \tag{8.27}$$
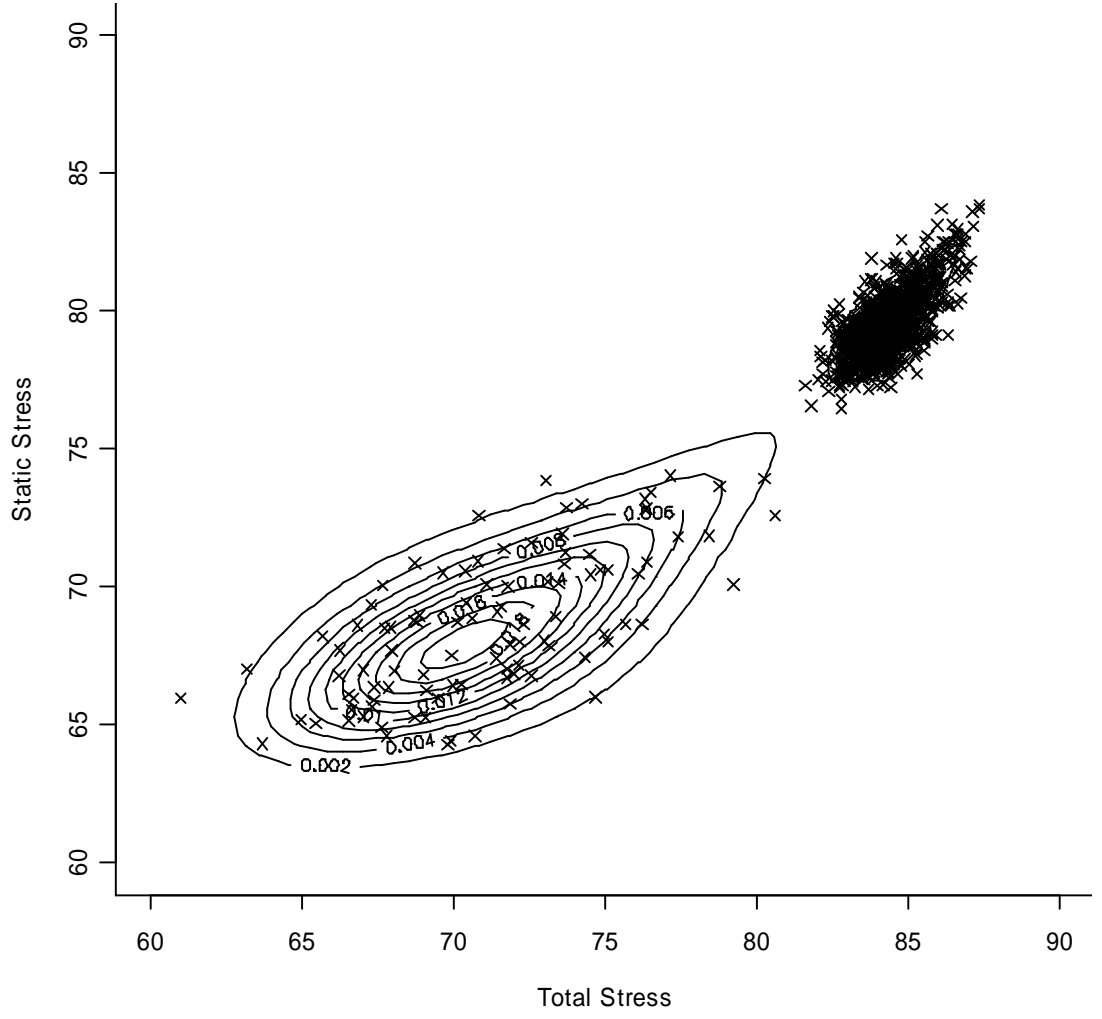
Figure 8.13: Parent and lifetime bivariate distributions (dN/mm²).

where, using the notation of (8.24),

$$Q(z) = \{q : \varphi_q \leq z\} \tag{8.28}$$

In appropriate cases, as outlined above, this is derived as:

$$G_\varphi^{-1}(q) = \varphi_q \tag{8.29}$$

hence, the probability density function may be derived as:

$$g_\varphi(z) = \left(\frac{d\varphi_q}{dz}\right)^{-1} \tag{8.30}$$

Numerical differentiation is required for the evaluation of the PDF, so defined.
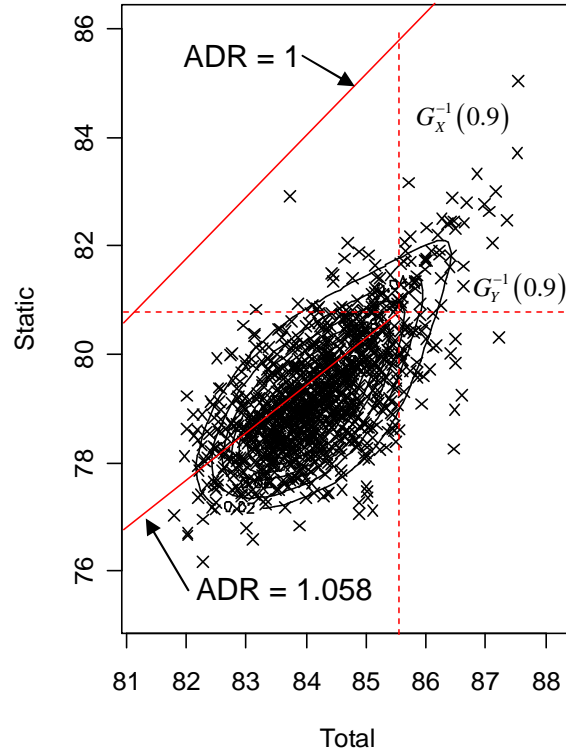
Figure 8.14: Representation of the ADR for the Eurocode quantile.

For many discrete quantiles – illustrated in Figure 8.15 – the total and static load effects are determined from the marginal distributions of the bivariate lifetime load effect distribution and the results are presented in Figure 8.16.

The main theme that emerges from Figure 8.16 is that as load effect (be it static or total) increases, the ADR tends towards unity. This is manifest in Figure 8.16(b) and (c): in (b) it is clear that as the quanntile increases, the ADR reduces; whilst in Figure 8.16(c) it is apparent that the line of ADR is curving towards the line representing an ADR of unity as both load effects increase. For design however, in the 100-year lifetime of this bridge and traffic as measured, the ADR has not yet reached unity and it is the 90-percentile of ADR is appropriate. This value corresponds with an ADR of 1.0576.
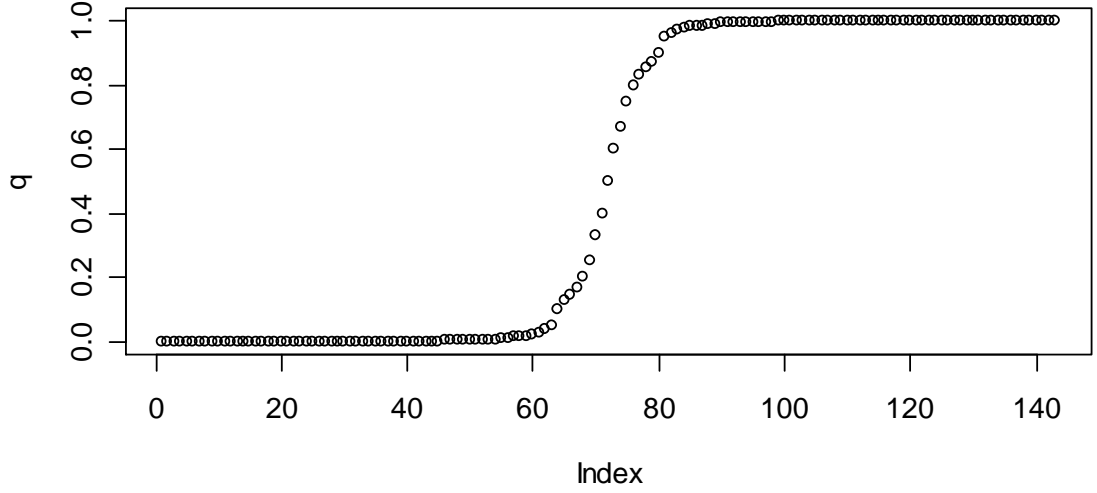
Figure 8.15: Quantiles used for evaluating the ADR.

The parameters of the marginal distributions result in a monotonically decreasing function φ_q in $\mathbf{q}$ – Figure 8.16(b). To apply the analysis of equations (8.27) to (8.30), the ADR is re-parameterized as:

$$\tilde{\varphi}_q = 1 - \varphi_q \tag{8.31}$$

and $\tilde{\varphi}_q$ is monotonically increasing in $\mathbf{q}$ as may be seen from Figure 8.17(b). Numerical differentiation is used to derive the points of Figure 8.17(a) from:

$$g_{\tilde{\varphi}}(z) = \left(\frac{d\tilde{\varphi}_q}{dz}\right)^{-1} \tag{8.32}$$

Using the curve-fitting methods outlined in Chapter 7, Section 7.3.3, a GEV distribution is fitted to the points of $g_{\tilde{\varphi}}(z)$ and is shown in Figure 8.17(a). The parameters of this distribution are: $\theta = \left(\xi = -0.1624; \sigma = 0.002463; \mu = -0.0642\right)$. This distribution may be used to find the return period at which $\tilde{\varphi}_q = 0$ and no allowance for dynamic interaction is required. The probability this occurs at is 0.99996 and so the return period for zero dynamic interaction is 26659 repetitions of the sampling period; and so in total, 2 665 970 years. Based on

this large figure, it is reasonable to note that some dynamics must feature as an element of loading for this specific notional site.
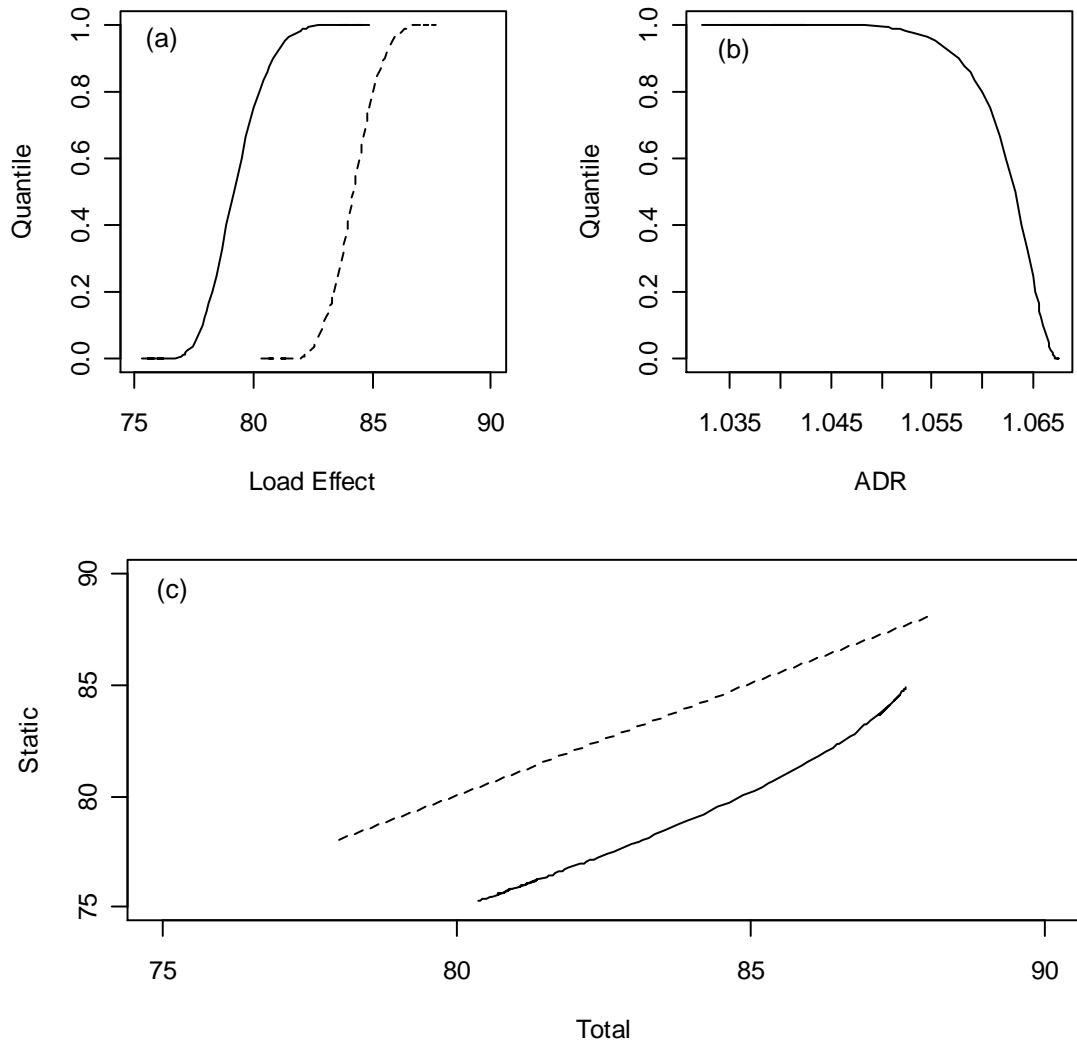
Figure 8.16: 100-year ADR diagnostics: (a) marginal CDFs (dN/mm²), (b) ADR by quantile, and (c) ADR against marginals and an ADR of unity (dashed).
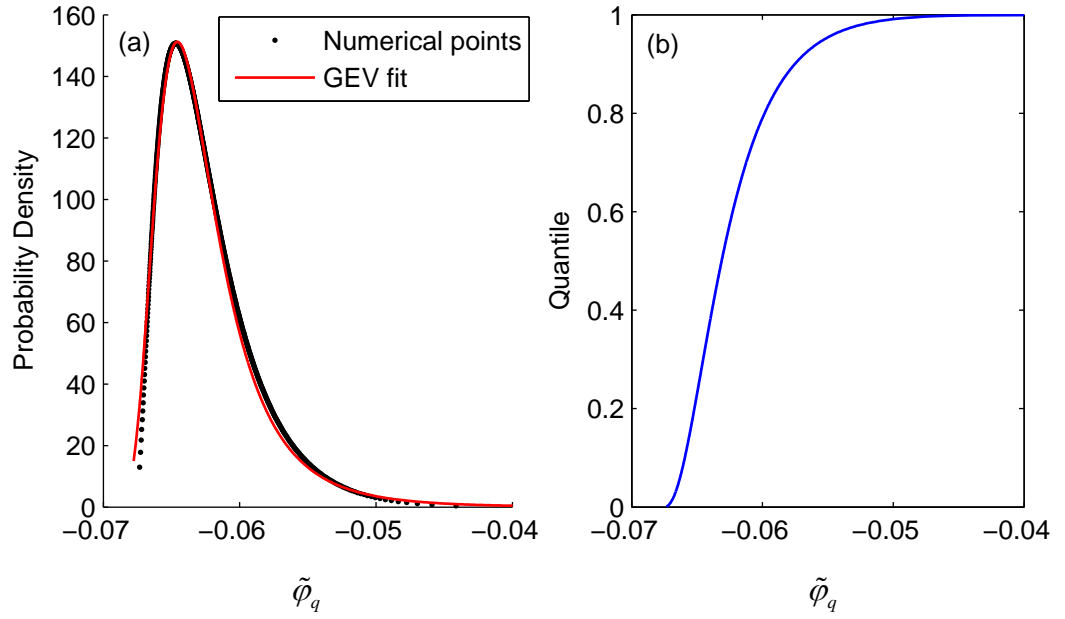
Figure 8.17: Re-parameterized 100-year ADR: (a) numerical and fitted PDF; and, (b) CDF.

To further investigate the effect of the lifetime upon these analyses, the process is repeated for a 1000-year lifetime. The results are presented in Figure 8.18 and Table 8.3. Though not an appropriate engineering measure, it is useful to compare the 90-percentiles of the 100- and 1000-year lifetime ADRs. That of the new analysis is 1.0350, as compared with 1.0576. It seems that the convergence to unity is quite slow, which suggests that the dynamic component of load is robust as found from the preceding analysis. This provides further evidence that dynamic loading cannot be discounted in a bridge load assessment for this notional site. However, it is also clear from the comparison that the influence of dynamics upon bridge loading is smaller than currently thought and decreases with return period.

In the development outlined, many repetitions of the results are calculated and it is to be noted that the results are not sensitive to random variation and are robust as a result.
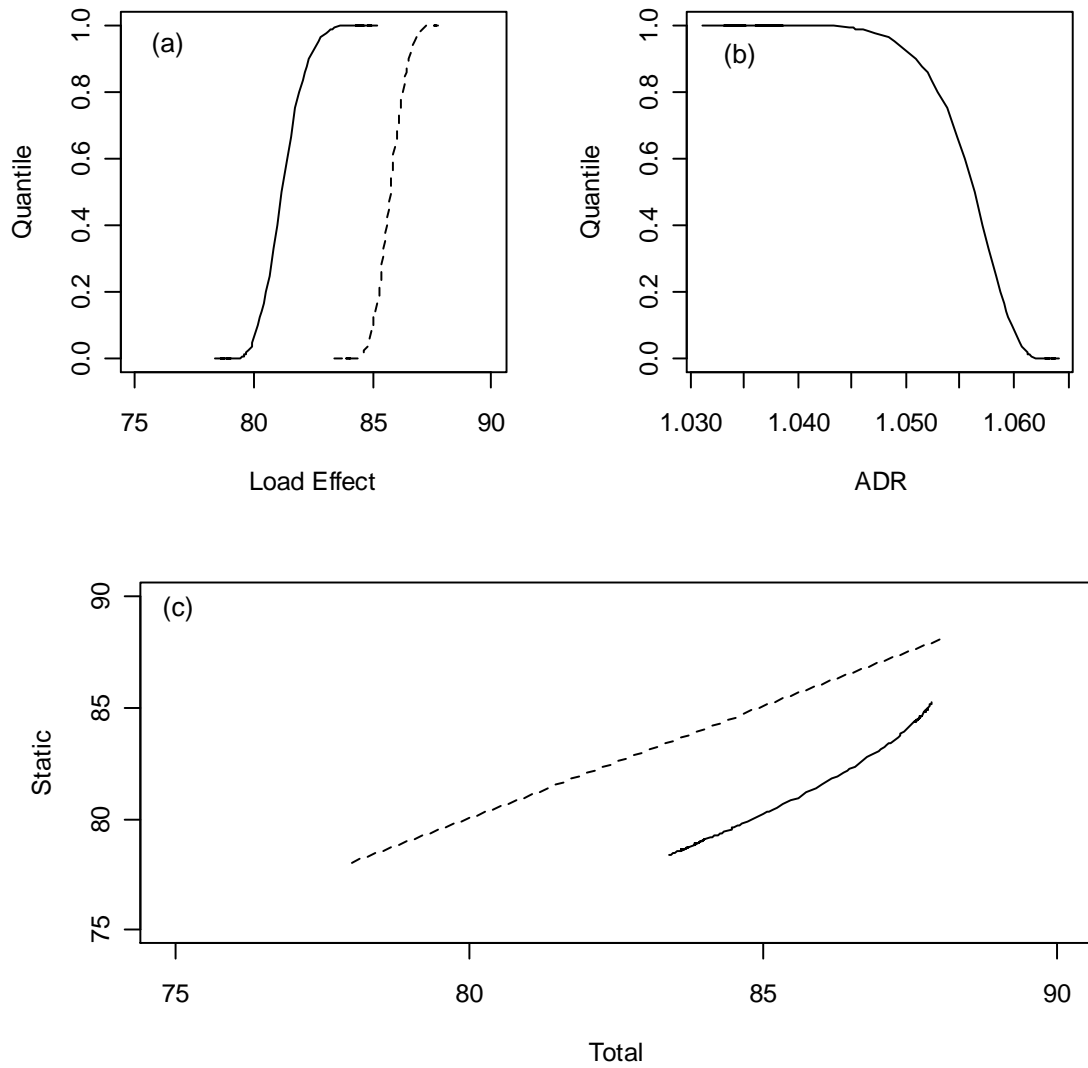
Figure 8.18: 1000-year ADR diagnostics: (a) marginal CDFs (dN/mm²), (b) ADR by quantile, and (c) ADR against marginals and an ADR of unity (dashed).

Marginal Distributions					
Total Load Effect			Static Load Effect		
μ	σ	ξ	μ	σ	ξ
87.36	0.102	0.2435	84.08	0.268	0.1668
Dependence Measures					
BEV dependence parameter			Tail dependence		
$\alpha = 0.5522$			$\lambda_U = 0.5346$		

Table 8.3: Parameters of 1000-year lifetime fitted BEVD distribution.

8.4 Summary

In this chapter, the current means of allowing for dynamic interaction of bridge and truck(s) is reviewed and shown to be conservative. Simulations of static load effect are used to obtain monthly maximum loading events, which are then modelled dynamically to obtain the total load effect: that which results from the dynamic interaction of the bridge and trucks. It is shown that there is significant statistical correlation between the two variables, and dependence models are described that allow for this.

Bivariate extreme value analysis is used to model the monthly maximum total and static load effects, and allow for their inter-dependence. Parametric bootstrapping is used to generate a history of lifetimes from the fitted bivariate distribution. In this manner, a distribution of bridge lifetime dynamic load ratio is derived. It is again shown to be bivariate, with a similar dependence structure to the monthly maximum events, even though the variables are no longer related through a single event. An alternative method to the univariate structure variable approach is also given and used to derive the assessment dynamic ratio for a given quantile.

It is shown that the dynamic allowance reduces with increasing load effect and that, for the bridge and traffic studied, the design dynamic allowance required is 5.8% of the static load effect. It is also shown that this allowance decreases slowly with increasing lifetime and that the lifetime at which 0% dynamics is attributable is around 2.7×10^6 years. Whilst the dynamic allowance results presented here are specific to this bridge and traffic, the method presented is general.

Chapter 9

CONCLUSIONS

"There are three kinds of lies: lies, damn lies and statistics"   *– Benjamin Disraeli*

Chapter 9 - CONCLUSIONS

9.1 Introduction

The research undertaken and summarized in this dissertation is intended to further knowledge in aspects of the probabilistic analysis of highway bridge traffic loading. The need for more accurate forms of such analyses is outlined in the **Introduction** to this work. Indeed, significant savings may result in bridge management budgets as a result of reduction in bridge rehabilitation and replacement needs. When considered on a national (Irish), or international (European Union) level, the accumulation of such reductions in expenditure can have significant socio-political impact. It is hoped that this work contributes to this goal.-

The objectives of this research are summarized here as:

1. to maximize the use of measured traffic;

2. to improve the statistical analyses for lifetime load effect;

3. to remove inaccuracies in the lifetime load effect estimate.

The developments in headway modelling (Chapter 5) and progress in traffic simulation (Chapter 4) contribute to the first objective. The method of composite distribution statistics (Chapter 6) and the bivariate extreme value analysis (Chapter 8) contribute to the second objective. The predictive likelihood analysis (Chapter 7) and aspects of the bivariate extreme value analysis (Chapter 8) both contribute to the final objective.

9.2 Executive Summary

Purpose of the research

- There is an increasing need for the rehabilitation/replacement of bridges due to deterioration and increased loading;

- The strength assessment of bridges is relatively well understood compared to that of loading;

- Better assessment of loading can result in significant maintenance budget savings internationally.

Main aims

To further knowledge in the following aspects of the probabilistic analysis of highway bridge traffic loading:

1. maximize the use of measured traffic, which is difficult and expensive to obtain;

2. improve the statistical analyses for lifetime load effect to better reflect the underlying phenomenon;

3. remove inaccuracies in the lifetime load effect estimate, taking into account sources of variability.

Methodology

1. Measured traffic characteristics at a site were used to develop a traffic model for that site;

2. The bridge traffic load model was used to determine the load effects resulting;

3. Statistical analyses were carried out on the load effects to determine the lifetime characteristic load effect.

Main findings

1. Existing headway models are overly simplistic and a new headway model (HeDS) was developed which is suitable for bridge traffic load modelling.

2. Current statistical analyses are overly subjective and may not adhere to the iid requirements of the extreme value approach. A revised methodology was developed which accounts for the requirements of extreme value theory and uses Composite Distribution Statistics (CDS).

3. Existing prediction methods do not account for variability of the prediction. Predictive likelihood was used and extended to include CDS analysis. It results in good estimation of the prediction variability by removing many sources of variability.

4. Current dynamic allowances are derived from the worst dynamic loading, and applied to the worst static loading; this does not account for the joint probability of occurrence. Multivariate extreme value statistics was used to find the relationship between static and total load effect and was used to derive an appropriate level of Assessment Dynamic Ratio. It was found that the influence of dynamic interaction decreases with increasing static load effect, and on one site, ~6% dynamic allowance is required.

Implications

1. The means of modelling traffic characteristics has a significant effect upon the resultant characteristic load effect.

2. Predictive likelihood and CDS should be used to evaluate a distribution of 100-year load effect from which design values may be obtained.

3. If the required dynamic allowance is ~6%, free-flowing traffic is not the governing case for short-to-medium length bridges. Traffic jam models must then be used instead for these bridge lengths.

9.3 Review of Main Findings

9.3.1 Simulation

In the early years of this work, the majority of effort was expended on the generation and simulation of bridge traffic loading. The software developed by Grave (2001) was re-written with many small improvements. Of significance though, was the improvement in memory management which made possible a vastly increased period of simulation. It was a consistent theme though this work that an increase in the quantity of data reduces the variability of any statistical analysis. Consequently, the software tools developed enabled the advances made in this work.

9.3.2 Headway modelling

Various forms of headway model exist in the literature and it was shown that an assumption relating to a minimum gap is a common feature. The effect of this assumption was tested and load effects were shown to be sensitive to it. Whilst actual traffic is a complex process, a minimum gap does not exist; rather, a representation based directly on measured traffic is appropriate and avoids the need for assumption.

Headway distribution statistics (HeDS) were derived that meet the requirements just outlined. The method involves the identification of headway distributions from measured flows that correspond to the hourly flows in the traffic load model. The headway behaviour of vehicles in these measured flows was used as a basis for the model. In recognition of the lack of justification for any particular distribution function, quadratic fits were made to individual measured headway distributions. A lack of correlation of headway with flow, for headways under 1.5 s, enables a more general model for small headways to be

used; one that is independent of flow. Headways above this figure were modelled with reducing fidelity as headway increases, dependent on flow.

The application of the HeDS method was compared with several forms of minimum gap assumptions that may be made. Of note in the findings was the effect of influence line shape upon the results: load effects in which critical distances between loads are similar to the minimum gap were found to be underestimated relative to the HeDS model. This phenomenon was explained through the physical process of traffic loading events.

Whilst the HeDS model is detailed and models measured traffic well, it is involved to derive the parameters for a particular site. This makes it impractical for general application, for without substantial site measurements – to an accuracy of 0.01 seconds – and appropriate software tools, it is too highly fitted to a particular site for use on another. However, these are quantitative concerns: the methodology developed was shown to accurately represent the measured traffic and results in loading events that do not violate the physical limitations of the traffic process. Therefore, for the purpose for which it is intended, that of site-specific traffic load modelling, the HeDS model is considered as the most representative headway model to date.

9.3.3 Composite distribution statistics

It was demonstrated that the distribution of daily maximum traffic load effects, upon which extreme value statistics are performed, is a composite, or mixed, distribution. Standard extreme value theory requires samples that are independent and identically distributed. It was shown that load effects resulting from different compositions of loading event (be they 1-, 2-, 3- or 4-truck events, for example) are distributed differently. Whilst it was shown that such loading

events are independent, it was also shown that it is not reasonable to treat them as identical. A method termed Composite Distribution Statistics (CDS) was developed which accounts for the different parent distributions of load effect, and combines them to determine the characteristic load effect.

Theoretical examples, for which the distributions of lifetime 'load effect' are known were used to verify the CDS approach against a hybrid conventional approach, adapted from the literature. It was shown for several examples that the CDS method corresponds to the exact distribution far more closely than the hybrid conventional approach. That it is not exact, is a function of sampling variability, as parametric bootstrapping is used.

In application to the bridge loading problem, the CDS results, in comparison with those of the conventional approach, were found to depend on the bridge length and influence line. The greatest observed difference was for bending moment at the central support of a two span bridge of overall length 40 m.

The CDS method is relatively easy to apply, although it requires more data to be used. It was shown to identify mechanisms which do not contribute to block-maximum load effects in the measurement period, but which govern the lifetime load effect. It is for this reason that use of the CDS method has shown that the conventional approach can miss the event-type that actually governs the extreme load effect for the lifetime of interest.

9.3.4 Predictive likelihood

The theory of predictive likelihood has emerged recently as a means to assess the relative likelihood of different outcomes given the data. There are few references to its application outside the statistical literature. The theory was presented in this work and extended to allow for the CDS method. Initially, the

standard form of predictive likelihood was applied and compared to published data and results. In this manner the behaviour of the method was examined.

A composite distribution statistics form of predictive likelihood was applied to theoretical examples for which the exact distribution of lifetime load effect is known. In one case, the predictive distribution corresponded very well to the exact distribution; in general this was not the case. The results of a predictive likelihood analysis were shown to be dependent on the quality of the data's resultant representation of the underlying (stipulated) distributions. Of significance however, was that in each case, predictive likelihood estimated the design load effect either conservatively or similar to the exact value.

The form of predictive likelihood outlined in the preceding paragraph was applied to the results of 4-years of simulated traffic loading on several bridge lengths for several load effects. These results were generally found to exceed those of the traditional return period extrapolation approach. This is as expected as predictive likelihood accounts for parameter variability. This finding has implications for lifetime load effect assessment: it is preferable to estimate the 100-year distribution of lifetime load effect and use its 90-percentile value, rather than the traditional form of extrapolation to a 1000-year return period. As the results differ, and as predictive likelihood accounts for more variability, it is to be preferred.

9.3.5 Bivariate extreme value analysis

The dynamic allowance applied to extreme load effect is known to be conservative: it is improbable that a loading event with extreme dynamic interaction corresponds to an extreme static loading event. A procedure was developed which accounts for these relative probabilities, and was applied to a

notional site to determine the optimum value and form of dynamic allowance for lifetime load effect. Bivariate extreme value theory, in combination with parametric bootstrapping, was used for this purpose.

Based on 10 years of simulated monthly-maximum (static) load events, total (static and dynamic components) load effect data, derived using finite element modelling of bridge-truck(s) interaction, was obtained. It was shown that significant correlation exists between total and static load effect and subsequent extrapolation had to account for this. Copula-based bivariate extreme value distributions were shown to represent the data well. Based on this distribution, a parametric bootstrapping approach was used to estimate sets of lifetime maximum static and total load effect.

At a level of lifetime maximum total and static load effect, it was shown that dependence still existed between the two types of load effect – in spite of the data points not originating from the same loading events. The standard univariate structure variable method was shown to be unsuitable because of the nature of the problem, and an alternative approach was developed to establish an appropriate lifetime dynamic allowance. This approach integrates total and static load effects into a multivariate extreme value theory model that allows joint extrapolation. There is no comparable approach in the literature reviewed.

The 90-percentile allowance derived from a 100-year bivariate lifetime load effect distribution was shown for a specific site to be 5.8%. Further, it was shown that the influence of dynamic interaction upon extreme loading events diminishes with increasing lifetime. These findings, if found to be general, have significant implications for the modelling and assessment of existing bridges.

9.4 Overview and Further Research

9.4.1 Overview

It is fair to say that, given the literature examined for this work, statistical analysis of the bridge loading problem is far behind that of other areas such as wind speed and flood prediction analysis. This is in spite of the potential significance of its application, alluded to in Section 9.1.

The implications of the results in this work are elaborated. Firstly, more accurate means of modelling traffic characteristics clearly affects the resultant load effect. It is therefore a requirement to derive optimum modelling strategies. Secondly, predictive likelihood and the CDS method should be used to evaluate a distribution of 100-year load effect and appropriate percentiles extracted for design rules. Such a form of analysis means that event-types that do not feature in the simulation period may yet contribute to the lifetime load effect, and parametric variability is allowed for in the resultant distribution. Thirdly, and possibly most importantly, if it is verified that dynamic allowances can be as low as 6% at the lifetime load effect level, free-flowing traffic can no longer be considered as the governing case for short-to-medium length bridges. Traffic jam scenarios would then need to be studied extensively in the context of these bridge lengths, and research into the dynamics of bridge-truck interaction for such bridges would be affected.

9.4.2 Further research

Throughout this work, many appealing avenues for further research opened, yet remained unexplored. It is fervently hoped that these opportunities will not be lost, and that they may bear rewards for the interested.

Traffic Simulation

In this topic, several areas for further research are:

- **Traffic characteristics modelling**: the distributions of traffic characteristics used in the models, most notably that of GVW, have a significant effect on the resulting loads. The use of the normal distribution is widespread, yet has no justification: not least that it assigns probabilities to negative numbers. More accurate modelling of tail distributions is also important: weighted likelihood may prove useful.

- **Headway modelling**: a generalized form of the HeDS method developed would be beneficial for application to numerous sites simultaneously. This is reasonable as driver behaviour is mostly location-independent.

- **Correlation of trucks**: it is essential that a means to model measured correlation between trucks is established both for bi- and uni-directional bridges. As the number of lanes modelled increases this becomes more important. A form of Markov-Chain modelling using measured transition matrices could be appropriate.

- **Traffic jam analysis**: To allow for the occurrence of traffic jams, and include the resultant load effects, is essential – especially so, given the result of Chapter 8. The CDS method is easily extended to allow for this.

- **Multiple-lane bridges**: to generalize the developments made in this work, it is necessary to extend the two-lane bridge models described here to multi-lane bridge models.

- **Simulation strategy**: the simulations of traffic loading have maximized the possibilities of 32-bit computer architecture. Approaches such as 64-

bit programming, parallel-processing or continuous simulation are needed to investigate the extreme loading events further. Importance sampling, and the approach of Castillo et al (1997) are other possibilities, but full-scale simulation of bridge loading is nonetheless required.

Statistical Analysis

In this topic, several areas for further research are:

- **Peaks-Over-Threshold (POT) analysis**: there is an enormous wastage of data from the block maxima approach. This can be minimized through the use of POT analysis. A CDS implementation of this form of theory is yet to be done, though straightforward. It is envisaged that this form of analysis will have less variability in the extreme.

- **Bootstrapping**: predictive likelihood is but one approach to the estimation of the variability of the extreme. Bootstrapping is very versatile; both the parametric and non-parametric forms could be used for this purpose.

- **Penalized likelihood for parameter evaluation**: the extrapolation results are sensitive to the shape parameter estimate, which generally has wider confidence intervals than the other GEV parameters. A form of penalized likelihood inference could be used to reduce the accuracy of the scale and location parameters, increasing that of the shape parameter accordingly.

General

There are also some general areas for further investigation:

- **Dynamics of extreme events**: though statistically derived, it is necessary to verify that extreme lifetime loading events exhibit little dynamics.

Further, it would be beneficial to have a loading history that allows for dynamic interaction, possibly through calibrated simplified two-dimensional models.

- **Assessment procedures:** from the research presented here, it is clear that its application to actual bridge assessment will not take place without effort. Thus it is necessary to derive assessment procedures based on this, and other work for implementation in practice.

The areas for potential research outlined are not exhaustive by any measure and others are sure to open as this work is built upon.

REFERENCES

"The ideal engineer is a composite ... He is not a scientist, he is not a mathematician, he is not a sociologist or a writer; but he may use the knowledge and techniques of any or all of these disciplines in solving engineering problems"

– N. W. Dougherty

REFERENCES

Miscellaneous

The quotations used at the beginning of each chapter are taken from various sources. The work of Van As (2004) is used and is to be noted as the inspiration for the inclusion of others' insights. Websites such as www.quotationspage.com are also used.

This dissertation uses the language and style defined by the **Oxford English Dictionary** and **The Oxford Guide to Style: Hart's Rules for the 21st Century**, both published by the Oxford University Press.

Listing

Agarwal, A.C. and Wolkowicz, M. (1976), **Interim Report on Ontario Commercial Vehicle Survey**, Research and Development Branch, Ontario Ministry of Transportation and Communications, Downsview Ontario.

Aldrich, J. (1997), 'R.A. Fisher and the making of maximum likelihood 1912-1922', **Statistical Science**, **12**(3), pp. 162-176.

Ang, A.H.S. and Tang, W.H. (1975), **Probability Concepts in Engineering Planning and Design**, Vols I and II, Wiley and Sons.

Anon. (2003), 'Literature review – models of headway distribution' [online], available from: http://www.cse.polyu.edu.hk/~activi/BAQ2002/Vehicle/29.doc, [Accessed: 26 April 2004].

Azzalini, A. (1996), **Statistical Inference based on the Likelihood**, Chapman and Hall.

Bailey, S.F. (1996), **Basic Principles and load models for the structural safety evaluation of existing bridges**, Ph.D. Dissertation, Thesis No. 1467, École Polythechnique Fédéral de Lausanne.

Bailey, S.F. and Bez, R. (1994), 'A parametric study of traffic load effects in medium span bridges', **Proceedings of the Fourth International Conference on Short and Medium Span Bridges**, Halifax, Canada, pp. 503-514.

Bailey, S.F. and Bez, R. (1999), 'Site specific probability distribution of extreme traffic action effects', **Probabilistic Engineering Mechanics**, **14**(1), pp. 19-26.

Banks, J.H. (2003), 'Average time gaps in congested freeway flow', **Transportation Research Part A**, **37**, pp. 539-554.

Bardsley, W.E. (1994), 'Against objective statistical analysis of hydrological extremes', **Journal of Hydrology**, **162**, pp. 429-431.

Barndorff-Nielsen, O. (1983), 'On a formula for the distribution of the maximum likelihood estimator', **Biometrika**, **70**, pp. 343-365.

BD 21 (1993), **Design Manual for Roads and Bridges**, Vol. 3, Section 4, Part 3, Department of Transport, United Kingdom.

Beck, J.V. and Arnold, K.J. (1977), **Parameter Estimation in Engineering and Science**, Wiley, New York.

Benjamin, J. R. and Cornell, C. A. (1970), **Probability, Statistics and Decision for Civil Engineers**, McGraw-Hill.

Beran, R. and Ducharme, G.R. (1991), **Asymptotic Theory for Bootstrap Methods in Statistics**, Les Publications CRM, Centre de Recherches Mathematiques, Universite de Montreal, Montreal, Canada.

Berger, J.O. and Wolpert, R.L. (1988), **The Likelihood Principle**, 2nd edn., Institute of Mathematical Statistics, Lecture Notes – Monograph Series Vol. 6, Hayward, California.

Bishop, Y.M.M., Fienberg, S.E. and Holland, P.W. (1975), **Discrete Multivariate Analysis: Theory and Practice**, MIT Press, Cambridge, Massachusetts.

Bjørnstad, J.F. (1990), 'Predictive likelihood: a review', **Statistical Science**, 5(2), pp. 242-254.

Boos, D.D. (2003), 'Introduction to the bootstrap world', **Statistical Science**, **18**(2), pp. 168-174.

Box, G. E. and Muller, M. E. (1958), 'A note on the generator of normal deviates', **Annals of Mathematical Statistics**, **29**, pp. 610-611.

Brady, S.P. (2003), **The Influence of Vehicle Velocity on Dynamic Amplification in Highway Bridges**, PhD Thesis, University College Dublin, Ireland.

Brodtkorb, P.A., Johannesson, P., Lindgren, G., Rychlik, I., Rydén, J., and Sjö, E. (2000), 'WAFO - a Matlab toolbox for analysis of random waves and loads', **Proceedings of the 10th International Offshore and Polar Engineering conference**, Seattle, Vol. III, pp. 343-350.

Bruls, A., Calgaro, J.A., Mathieu, H. and Prat, M. (1996), 'ENV1991 – Part 3: The main models of traffic loads on bridges; background studies', **Proceedings of IABSE Colloquim**, Delft, The Netherlands, IABSE-AIPC-IVBH, pp. 215-228.

Bruls, A., Croce, P., Sanpaolesi, L. and Sedlacek, G. (1996), 'ENV1991 – Part 3: Traffic Loads on Bridges; calibration of load models for road bridges', **Proceedings of IABSE Colloquium**, Delft, The Netherlands, IABSE-AIPC-IVBH, pp. 439-453.

Buckland, P.G., Navin, P.D., Zidek, J.M. and McBride, J.P. (1980), 'Proposed vehicle loading for long span bridges', **Journal of Structural Engineering**, ASCE, **106**, No. ST4, pp. 915 - 931.

Butler, R.W. (1986), 'Predictive likelihood inference with applications' (with discussion), **Journal of the Royal Statistical Society**, **Series B**, **48**, pp. 1-38.

Butler, R.W. (1989), 'Approximate predictive pivots and densities', **Biometrika**, **76**, pp. 489-501.

Capéraà, P., Fougres, A.L., and Genest, C. (1997), 'A nonparametric estimation procedure for bivariate extreme value copulas', **Biometrika**, **84**, pp. 567-577.

Castillo, E. (1988), **Extreme Value Theory in Engineering**, Academic Press, New York.

Castillo, E. and Sarabia, J.M. (1992), 'Engineering analysis of extreme value data: selection of models', **Journal of Waterway, Port, Coastal, and Ocean Engineering**, ASCE, **118**(2), pp. 129-146.

Castillo, E., Solares, C. and Gómez, P. (1997), 'Estimating extreme probabilities using tail simulated data', **International Journal of Approximate Reasoning**, **17**, pp. 163-189.

Choi, E.C.C. and Tanurdjaja, A. (2002), 'Extreme wind studies in Singapore. An area with mixed weather system', **Journal of Wind Engineering and Industrial Aerodynamics**, **90**, pp. 1611-1630.

Coles, S.G. (2001a), **An Introduction to Statistical Modeling of Extreme Values**, Springer-Verlag, London.

Coles, S.G. (2001b), 'The use and misuse of extreme value models in practice', in **Extreme Values in Finance, Telecommunications, and the Environment**, ed. Bärbel Finkenstädt and Holger Rootzén, Chapman and Hall/CRC.

Coles, S.G., Heffernan, J. and Tawn, J.A. (1999), 'Dependence measures for multivariate extremes', **Extremes**, **2**, pp. 339-365.

Coles, S.G. and Tawn, J.A. (1991), 'Modelling extreme multivariate events', **Journal of the Royal Statistical Society**, **Series B**, **53**, pp. 377-392.

Coles, S.G. and Tawn, J.A. (1994), 'Statistical methods for multivariate extremes: an application to structural design (with discussion)', **Applied Statistics**, **43**, pp. 1-48.

Cook, N.J. (1982), 'Towards better estimation of extreme winds', **Journal of Wind Engineering and Industrial Aerodynamics**, **9**, pp. 295-323.

Cook, N.J., Harris, R.I. and Whiting, R. (2003), 'Extreme wind speeds in mixed climates revisited', **Journal of Wind Engineering and Industrial Aerodynamics**, **91**, pp. 403-422.

Cooley, T.F., Parke, W.R. and Chib, S. (1989), 'Predictive efficiency for simple non-linear models', **Journal of Econometrics**, **40**, pp. 33-44.

Cooley, T.F. and Parke, W.R. (1987), 'Likelihood and other approaches to prediction in dynamic models', **Journal of Econometrics**, **35**, pp. 119-142.

Cooley, T.F. and Parke, W.R. (1990), 'Asymptotic likelihood-based prediction functions', **Econometrica**, **58**(5), pp. 1215-34.

Cooper, D.I. (1995), 'The determination of highway bridge design loading in the United Kingdom from traffic measurements', **Pre-Proceedings of the First European Conference on Weigh-in-Motion of Road Vehicles**, ed. B. Jacob et al., E.T.H., Zürich, pp. 413-421.

Cooper, D. I. (1997), 'Development of short span bridge-specific assessment live loading' in **Safety of Bridges**, ed. P.C. Das, Thomas Telford, pp. 64-89.

Cox, D.R. and Hinkley, D.V. (1974), **Theoretical Statistics**, Chapman and Hall, London.

Cramér, H. (1946), **Mathematical Methods of Statistics**, Princeton University Press, Princeton, New Jersey.

Cremona, C. (2001), 'Optimal extrapolation of traffic load effects', **Structural Safety**, **23**, pp. 31-46.

Crespo-Minguillón, C. and Casas, J.R. (1997), 'A comprehensive traffic load model for bridge safety checking', **Structural Safety**, **19**, pp. 339-359.

Davison, A.C. (1986), 'Approximate predictive likelihood' **Biometrika**, **73**, pp. 323-332.

Davison, A.C. and Hinkley, D.V. (1997), **Bootstrap Methods and Their Application**, Cambridge University Press, Cambridge.

Demarta, S. (2002), **Multivariate Extreme Value Theory and Copulas**, Diploma Thesis, ETH Zentrum, Switzerland, available from: http://www.math. ethz.ch/~demarta/diplom.pdf.

Ditlevsen, O. (1994), 'Traffic loads on large bridges modelled as white-noise fields', **Journal of Engineering Mechanics**, ASCE, **120**(4), pp. 681-694.

Ditlevsen, O. and Madsen, H.O. (1994), 'Stochastic vehicle-queue-load model for large bridges', **Journal of Engineering Mechanics**, ASCE, **120**(9), pp. 1829-1847.

Dorton, R.A. and Csagoly, P.F. (1977), **The Development of the Ontario Bridge Code**, Research and Development Branch, Ontario Ministry of Transportation and Communications, Downsview Ontario, Canada.

Draisma, G. and de Haan, L. (1995), **Estimating bivariate extremes**, Technical Report EUR--04, Erasmus University, Rotterdam, Neptune project T400, available from: http://www.few.eur.nl/few/people/ldehaan/neptune/.

EC 1 (1994): **Basis of design and actions on structures, Part 3: Traffic loads on bridges**, European Prestandard ENV 1991-3: European Committee for Standardisation, TC 250, Brussels.

Edwards, A.W.F. (1992), **Likelihood: An Account of the Statistical Concept of Likelihood and its Application to Scientific Inference**, 2nd edn., Johns Hopkins University Press, Baltimore.

Efron, B. (1979), 'Bootstrap methods: another look at the jackknife' **Annals of Statistics, 7**, pp. 1-26.

Efron, B. and Tibshirani, R. J. (1993), **An Introduction to the Bootstrap**, Chapman and Hall, London.

Eichinger, E. (2002), 'A case study in bridge assessment – weigh-in-motion meaurements on a reinforced concrete bridge', **Assessment of Bridges and Highway Infrastructure**, ed. E.J. OBrien, Institution of Engineers of Ireland, Dublin, pp. 81-96.

Embrechts, P., de Haan, L. and Huang, X. (2000), 'Modelling multivariate extremes', **Extremes and Integrated Risk Management**, ed. P. Embrechts, **RISK Books**, pp. 59-67.

Embrechts, P., Lindskog, F. and McNeil, A. (2003), **Modelling Dependence with Copulas and Applications to Risk Management**, chapter in **Handbook of Heavy Tailed Distributions in Finance**, ed. S. Rachev, Elsevier, pp. 329-384.

Eurpoean Commission (2004), **European Union Energy and Transport in Figures 2004**, available from: http://europa.eu.int/comm/ energy_transport/figures/ pocketbook/.

Eymard, R. and Jacob, B. (1989), 'Un nouveau logiciel: le programme CASTOR pour le calcul des actions et des sollicitations de traffic dans les ouvrages routiers', **Bull. Liaison des LPC**, No. 199, pp. 71-80.

Feller, W. (1968), **An Introduction to Probability Theory and its Applications, Volume I**, 3rd edn., Wiley, New York.

Fisher, R.A. (1956), **Statistical Methods and Scientific Inference**, Oliver and Boyd, Edinburgh.

Fisher, R.A. and Tippett, L.H.C. (1928), 'Limiting forms of the frequency distribution of the largest or smallest number of a sample', **Proc. Cambridge Philosophical Society**, XXIV, Part II, pp. 180-190.

Flint, A.R. and Jacob, B.A. (1996), 'Extreme traffic loads on road bridges and target values for their effects for code calibration', **Proceedings of IABSE Colloquium**, Delft, The Netherlands, IABSE-AIPC-IVBH, pp. 469-478.

Fu, G. and Hag-Elsafi, O. (1995), 'Bridge Evaluation for Overloads Including Frequency of Appearance', **Applications of Statistics and Probability**, ed. Favre and Mébarki, Rotterdam, pp. 687-692.

Galambos, J. (1978), **The Asymptotic Theory of Extreme Order Statistics**, John Wiley and Sons, New York.

Gazis, D.C. (1974), **Traffic Science**, Wiley, New York.

Getachew, A. (2003), **Traffic Load Effects on Bridges**, Ph.D. Thesis, Structural Engineering, Royal Institute of Technology Stockholm, Sweden.

Getachew, A. and OBrien, E.J. (2005), 'Simplified site specific models for determination of characteristic traffic load effects for bridges', **4th International Conference on Weigh-In-Motion – ICWIM4**, ed. E.J. OBrien et al, National Taiwan University, pp. 341-350.

Ghosn, M. and Moses, F. (1985), 'Markov renewal model for maximum bridge loading', **Journal of Engineering Mechanics**, ASCE, **111**(9), pp. 1093-1104.

Ghosn, M., Moses, F. and Wang, J. (2003), **Design of Highway Bridges for Extreme Events**, National Cooperative Highway Research Program (NCHRP) Report 489, Washington D.C.

Gilli, M. and Këllezi, E. (2005), 'An application of extreme value theory for measuring financial risk', in print, available from: http://www.unige.ch/ses/metri/gilli/evtrm/GilliKelleziEVT.pdf.

Goble, G.G., Moses, F. and Pavia, A. (1976), 'Applications of a bridge measurement system', Transportation Research Board, National Research Council, Washington D.C., Transportation Research Record 579, pp. 36-47.

Goda, Y. (1992), 'Uncertainty of design parameters from viewpoint of extreme statistics', **Journal of Offshore Mechanics and Arctic Engineering**, Transactions of the ASME, **114**, pp. 76-82.

Golub, G. and Van Loan, C. (1996), **Matrix Computations**, 3rd edn., John Hopkins University Press, Baltimore, Massachusetts.

Gomes, M.I. (1984), 'Penultimate limiting forms in extreme value theory', Annals of the Institute of Statistical Mathematics, 36, pp. 71–85.

Gomes, L. and Vickery, B.J. (1978), 'Extreme wind speeds in mixed climates', Journal of Wind Engineering and Industrial Aerodynamics, 2, pp. 331–344, 1977/1978.

Gonzalez, A. (2001), Development of Accurate Methods of Weighing Trucks in Motion, PhD Thesis, Department of Civil Engineering, Trinity College Dublin.

Gonzalez, A., O'Connor, A.J. and OBrien, E.J. (2003), 'An assessment of the influence of dynamic interaction modelling on predicted characteristics load effects in bridges', in Proceedings of the 3rd International Conference on Current and Future Trends in Bridge Design, Construction and Maintenance, ed. B.I.G. Barr et al., Shanghai, China, Sep./Oct., Thomas Telford, pp. 241-249.

Gnedenko, B. (1943), 'Sur la distribution limited u terme maximum d'une série aléatoire', Annals of Mathematics, 44, pp. 423-453.

Grave, S.A.J. (2001), Modelling of Site-Specific Traffic Loading on Short to Medium Span Bridges, Ph.D. Thesis, Department of Civil Engineering, Trinity College Dublin.

Grave, S.A.J., OBrien, E.J. and O'Connor, A.J. (2000), 'The determination of site-specific imposed traffic loadings on existing bridges', Bridge Management 4, ed. M.J. Ryall et al, Thomas Telford, pp. 442-449.

Gumbel, E. J. (1958), Statistics of Extremes, Columbia University Press.

Gupta, S. and Manohar, C.S. (2005), 'Multivariate extreme value distributions for random vibration applications', **Journal of Engineering Mechanics**, ASCE, **131**(7), pp. 712-720.

Haight, F.A. (1963), **Mathematical Theories of Traffic Flow**, Academic Press, New York.

Hallenbeck, M. (1995), 'Seasonal patterns of truck loads and volumes in the United States', **Proceedings of the First European Conference on Weigh-In-Motion of Road Vehicles**, ETH Zürich, Switzerland, pp. 121-129.

Han, Z. (2003), **Actuarial Modeling of Extremal Events Using Transformed Generalized Extreme Value Distribution and Transformed Generalized Pareto Distribution**, Ph.D. Thesis, The Ohio State University.

Harman, D.J. and Davenport, A.G. (1979), 'A statistical approach to traffic loading on highway bridges, **Canadian Journal of Civil Engineering**, **6**, pp. 494-513.

Hawkes, P.J., Gouldby, B.P., Tawn, J.A. and Owen, M.W. (2002), 'The joint probability of waves and water levels in coastal engineering design', **Journal of Hydraulic Research**, **40**(3), pp. 241-251.

Hayrapetova, A. (2006), **Micro-Simulation Modelling of Traffic Loading on long Span Bridges**, in print, Ph.D. Thesis, University College Dublin, Ireland.

Heffernan, J.E. (2005), 'Nonparametric estimation of the Bivariate Extreme Value distribution using a limiting conditional representation', **Extremes**, in print, available from http://www.maths.lancs.ac.uk/~currie/Papers/bev.cond.pdf.

Heywood, R.J. and Nowak, A.S. (1989), 'Bridge live load models', **International Conference on Structural Safety and Reliability**, San Francisco, pp. 2147-2154.

Hinkley, D.V. (1979), 'Predictive likelihood', **Annals of Statistics**, **7**, pp. 718-728; corrigendum, **8**, p. 694.

Hosking, J.R.M. (1985), 'Algorithm AS215: maximum-likelihood estimation of the parameters of the Generalized Extreme-Value distribution', **Applied Statistics**, **34**(3), pp. 301-310.

Hosking, J. R. M., Wallis, J. R. and Wood, E. F. (1985), 'Estimation of the Generalized Extreme Value distribution by the method of Probability-Weighted Moments', **Technometrics**, **27**, pp. 251-261.

HRB (1965), **Highway Capacity Manual**, Highway Research Board, 87, National Academy of Sciences, National Research Council, 1328.

James, G. (2005), 'Analysis of Traffic Load Effects on Railway Bridges using Weigh-in-motion Data', **4th International Conference on Weigh-In-Motion – ICWIM4**, ed. E.J. OBrien et al, National Taiwan University, pp. 351-362.

Jacob, B. and OBrien, E.J. (1998), 'European specification on weigh-in-motion of road vehicles (COST 323)', **Pre-proceedings of 2nd European Conference on Weigh-in-Motion of Road Vehicles**, ed. E.J. OBrien and B. Jacob, Lisbon, Sept., European Commission, Luxembourg, pp. 171-183.

Jacob, B. and OBrien, E.J., (2005), 'Weigh-in-motion: recent developments in Europe', **4th International Conference on Weigh-In-Motion – ICWIM4**, ed. E.J. OBrien et al, National Taiwan University, pp. 3-13.

Jenkinson, A. F. (1955), 'The frequency distribution of the annual maximum (or minimum) of meteorological elements', **Quarterly Journal of the Royal Meteorological Society**, **81**, pp. 158–171.

Jenkinson, A.F. (1969), **Statistics of extremes**, in **Estimation of maximum floods**, World Meteorological Office, Technical Note No. 98, WMO-No. 233, TP126, pp. 183-227.
(Courtesy of Ms. Jane Burns, Library, Met Éireann, www.met.ie)

Jensen, R. (2003), **Traffic Simulation** [online], available from: http://www.daimi.au.dk/~rud/sc/bin/report.pdf, [Accessed: 5 April 2004].

Klüppelberg, C. and May, A. (1998), **The dependence function for bivariate extreme value distributions – a systematic approach**, Technical report, Center of Mathematical Sciences, Munich, October, available from: http://citeseer.ist.psu.edu/114798.html.

Knuth, D.E. (1997), **The Art of Computer Programming, Volume 1: Fundamental Algorithms**, 3rd edn., Addison-Wesley.

Koppa, R.J. (1992), **Human Factors**, chapter in **The Theory of Traffic Flow**, Turner-Fairbank Highway Research Center, Federal Highway Administration, ed. A.K. Rathi et al, [online], available from: http://www.tfhrc.gov/its/tft/tft.htmfs, [Accessed: 5 April 2004].

Kotz, S. and Nadarajah, S. (2000), **Extreme Value Distributions: Theory and Applications**, Imperial College Press, London.

Lagarias, J.C., Reeds, J.A., Wright, M.H. and Wright, P.E. (1998), 'Convergence properties of the Nelder-Mead simplex method in low dimensions', **SIAM Journal on Optimization**, **9**(1), pp. 112-147.

Lagarias, J.C., Reeds, J.A., Wright, M.H. and Wright, P.E. (1996) 'Convergence properties of the Nelder-Mead simplex algorithm in low dimensions', Technical Report 96-4-07, ATandT Bell Laboratories, April, available from: http://www.math.lsa.umich.edu/~lagarias/doc/neldermead.ps.

Laman, J.A. and Nowak, A.S. (1997), 'Site-specific truck loads on bridges and roads', **Proceedings of the Institution of Civil Engineers – Transportation**, **123**, May, pp. 119-133.

Lauritzen, S.L. (1974), 'Sufficiency, prediction and extreme models', **Scandinavian Journal of Statistics**, **1**, 128-134.

L'Ecuyer, P. (1999), 'Good parameter sets for combined multiple recursive random number generators', **Operations Research**, **47**(1), pp. 159-164, available from: http://www.iro.umontreal.ca/~lecuyer/papers.html.

L'Ecuyer, P., Simard, R., Chen, E.J. and Kelton, W.D. (2002), 'An objected-oriented random-number package with many long streams and substreams', **Operations Research**, **50**(6), pp. 1073--1075.

Lehman, E.L. (1986), **Testing Statistical Hypotheses**, 2nd edn., Wiley Series in Probability and Mathematical Statistics, New York.

Lejeune, M. and Faulkenberry, G.D. (1982), 'A simple predictive density function', **Journal of the American Statistical Association**, **77**, pp. 654-657.

Leonard, T. (1982), 'Comment on "A simple predictive density function" by M. Lejeune and G.D. Faulkenberry', **Journal of the American Statistical Association**, **77**, pp. 657-658.

Lieberman, E. and Rathi, A.K. (1992), **Traffic Simulation**, chapter in **The Theory of Traffic Flow**, Turner-Fairbank Highway Research Center, Federal Highway Administration, ed. A.K. Rathi et al, [online], available from: http://www.tfhrc.gov/its/tft/tft.htmfs, [Accessed: 5 April 2004].

Lindsey, J.K. (1996), **Parametric Statistical Inference**, Oxford University Press, Oxford.

Lorén, S. and Lundström, M. (2005), 'Modelling curved S-N curves', **Fatigue and Fracture of Engineering Materials and Structures**, **28**, pp. 437-443.

Mathiasen, P.E. (1979), 'Prediction functions', **Scandinavian Journal of Statistics**, **6**, pp. 1-21.

Melchers, R.E. (1999), **Structural Reliability Analysis and Prediction**, 2nd edn., John Wiley and Sons, Chichester.

Mises von, R. (1936), 'La distribution de la plus grande de n valeurs', **Revue Mathématique De l'Union Interbalcanique**, **1**, pp. 141-160. Reproduced in **Selected Papers of Richard von Mises**, Vol. 2, pp. 271-294, American Mathematical Society, Rhode Island, 1964.

Mood, A.M., Graybill, F.A., and Boes, D.C. (1974), **Introduction to the Theory of Statistics**, 3rd edn., McGraw-Hill, Statistics Series.

Moses, F. (1979), 'Weigh-in-motion system using instrumented bridges' **Journal of the Transportation Division**, ASCE, **95**(TE3), pp. 233–249.

Moses, F. (2001), **Calibration of Load Factors for LRFR Bridge Evaluation**, National Cooperative Highway Research Program (NCHRP) Report 454, Washington D.C.

Moyo, P., Brownjohn, J.M. and Omenzetter, P. (2002), 'Highway bridge live loading assessment and load carrying estimation using a health monitoring system', **Proceedings of the First European Workshop on Structural Health Monitoring**, ed. D. L. Balageas, Cachan (Paris), France.

Nadarajah, S. (1999), 'Simulation of multivariate extreme values', **Journal of Statistical Computation and Simulation**, **62**, pp. 395-410.

Nelder, J. A. and Mead, R. (1965), 'A simplex method for function minimization', **The Computer Journal**, **7**, pp. 308-313.

Nowak, A.S. (1989), 'Probabilistic basis for bridge design codes', **International Conference on Structural Safety and Reliability**, San Francisco, pp. 2019-2026.

Nowak, A.S. (1993), 'Live load model for highway bridges', **Structural Safety**, **13**, pp. 53-66.

Nowak, A.S. (1994), 'Load model for bridge design code', **Canadian Journal of Civil Engineering**, **21**, pp. 36-49.

Nowak, A.S. and Hong, Y.K. (1991), 'Bridge live load models', **Journal of Structural Engineering**, ASCE, **117**(9), pp. 2757-2767.

Nowak, A.S., Hong, Y.K., Hwang, E.S. (1991), 'Bridge load models', **ICASP 6**, pp. 880 – 887.

Nowak, A.S. (1995), 'Load model for bridge design code: reply', **Canadian Journal of Civil Engineering**, **22**, p. 293, in reply to Sexsmith (1995).

OBrien, E.J., Caprani, C.C., Žnidarič, A. and Quilligan, M. (2003), 'Site-specific probabilistic bridge load assessment', **Proceedings of the 3rd International Conference on Current and Future Trends in Bridge Design, Construction and Maintenance**, ed. B.I.G. Barr et al., Shanghai, China, Thomas Telford, Sep./Oct., pp. 341-348.

OBrien, E.J., Gonzalez, A., Žnidarič, A. and McNulty, P. (2002), 'Testing of a bridge weigh-in-motion system in cold environmental conditions', **Third International Conference on Weigh-in-Motion (ICWIM3)**, ed. B. Jacob et al, Iowa State University, May, pp. 69-78.

OBrien, E.J. and Jacob, B. (1996), 'Applications of weigh-in-motion', in **3rd Slovenian Congress on Roads and Transport**, Road and Transportation Research Association of Slovenia, Bled, Slovenia, pp. 417-425.

OBrien, E.J., O'Connor, A.J. and Gonzalez, A. (1997), **Eurocode for traffic loads on Road Bridges – Calibration for Irish Conditions**, Report No. 97-006, Department of Civil Engineering, Trinity College Dublin.

OBrien, E.J., Quilligan, M.J. and Karoumi, R. (2005), 'Calculating an influence line from direct measurements', **Proceedings of the Institution of Civil Engineers**, **Bridge Engineering**, in print.

OBrien, E.J., Sloan, T.D., Butler, K.M. and Kirkpatrick, J. (1995), 'Traffic load fingerprinting of bridges for assessment purposes', **The Structural Engineer**, **73**(19), pp. 320-324.

OBrien, E.J., Žnidarič, A., Brady, K., González, A. and O'Connor, A.J. (2005), 'Procedures for the assessment of highway structures', **Transport, Proceedings of the Institution of Civil Engineers**, **158**, Issue TR1, pp. 17-25.

O'Connor, A.J. (2001), **Probabilistic Traffic Load Modelling for Highway Bridges**, Ph.D. Thesis, Department of Civil Engineering, Trinity College Dublin.

O'Connor, A.J., Jacob, B., OBrien, E.J. (1998), 'Effects of traffic loads on road bridges – preliminary studies for the re-assessment of the traffic load model for Eurocode 1, Part 3', **Pre-Proceedings of the second European Conference on Transport Research**, ed. E.J. OBrien and B. Jacob, pp. 231-242.

O'Connor, A.J., Jacob, B., OBrien, E.J. and Prat, M. (2001), 'Report of current studies performed on normal load model of EC1-Traffic Loads on Bridges', **Revue Francaise du Genie Civil**, Hermes Science Publications, **5**(4), pp. 411-434.

O'Connor, A.J., OBrien, E.J. and Jacob, B. (2002), 'Use of WIM data in development of a stochastic flow model for highway bridge design and

assessment', **Pre-Proceedings of the Third International Conference on Weigh-In-Motion**, ed. B. Jacob et al, Orlando, pp. 315-324.

O'Connor, C. and Shaw, P. (2000), **Bridge Loads: An International Perspective**, Spon Press.

Oehlert, G.W. (1992), 'A note on the delta method', **American Statistician**, **46**, pp. 27–29.

OHBDC (1979, 1983, 1991), **Ontario Highway Bridge Design Code**, Ontario Ministry of Transportation, Downsview, Ontario.

Park, S.K. and Miller, K.W. (1988), 'Random number generators: good ones are hard to find', **Communications of the ACM**, **31**(10), pp. 1192 – 1201.

Pearson, K. (1920), 'The fundamental problem of practical statistics', **Biometrika**, **13**, pp. 1-16.

Pickands, J. (1981), 'Multivariate extreme value distributions', **Proceedings of the 43rd Session of the International Statistical Institute**, **49**, pp. 859–878.

Prescott, P. and Walden, A.T. (1980), 'Maximum likelihood estimation of the parameters of the Generalized Extreme-Value distribution', **Biometrika**, **67**, pp. 723-724.

Prescott, P. and Walden, A.T. (1983), 'Maximum likelihood estimation of the parameters of the three-parameter Generalized Extreme-Value distribution from censored samples', **Journal of Statistical Computation and Simulation**, **16**, pp. 241-250.

Press, W. H., Teukolsky, S.A., Vetterling, W.T. and Flannery, B.P. (1992), **Numerical Recipes in C**, 2nd edn., Cambridge University Press.

R Development Core Team (2005), **R: A language and environment for statistical computing**, R Foundation for Statistical Computing, Vienna, Austria, available from: http://www.r-project.org.

Rattigan, P. (2007), Ph.D. Thesis not yet in print, School of Architecture, Landscape and Civil Engineering, UCD, Ireland.

Rice, J.A. (1995), **Mathematical Statistics and Data Analysis**, 2nd edn., Duxbury Press, Belmont, California.

Rubenstein, R. Y. (1981), **Simulation and the Monte Carlo Method**, John Wiley and Sons.

Ryall, M.J., Parke, G.A.R. and Harding, J.E. (2000), **The Manual of Bridge Engineering**, Thomas Telford, London.

Segers, J.J.J. (2004), **Non-parametric inference for bivariate extreme-value copulas**, CentER Discussion Paper 2004-91. available from: http://center.uvt.nl/ staff/segers/publications.html.

Sexsmith, R.G. (1995), 'Load model for bridge design code: discussion', **Canadian Journal of Civil Engineering**, **22**, pp. 292-293, discussion of Nowak (1994).

Silvey, S.D. (1970), **Statistical Inference**, Penguin.

Silvey, S.D. (1975), **Statistical Inference**, 1st edn. (reprinted with corrections), Chapman and Hall, London.

Smith, R.L. (1986), 'Extreme value theory based on the r-largest annual events', **Journal of Hydrology**, **86**, pp. 27-43.

Smith, R.L. (2003) – **Statistics of Extremes with Applications in Environment, Insurance and Finance**, lectures from: SEMSTAT conference on Extreme Value Theory, Gothenburg, CRC/Chapman and Hall, 2001; available from: http://www.stat.unc.edu/postscript/rs/semstatrls.ps.

Stephenson, A. G. (2003), 'Simulating multivariate extreme value distributions of logistic type', **Extremes**, **6**(1), pp. 49-59.

Stephenson, A.G. (2005), **A Users Guide to the** `evd` **Package (Version 2.1)**, May, available from http://cran.r-project.org/.

Stroustrup, B.J. (1997), **The C++ Programming Language**, 3rd edn., Addison Wesley.

Tawn, J.A. (1988), 'Bivariate extreme value theory: models and estimation', **Biometrika**, **75**, pp. 397-415.

Tawn, J.A. (1990), 'Modelling multivariate extreme value distributions', **Biometrika**, **77**, pp. 245-253.

Thamizh-Arasan, V. and Koshy, R. Z. (2003), 'Headway distribution of heterogeneous traffic on urban arterials', **Journal of the Institution of Engineers (India)**, **84**, pp. 210-215.

Thomasian, A.J. (1969), **The Structure of Probability Theory with Applications**, McGraw-Hill, New York.

Van As, S.C. (2004), **Applied Statistics for Civil Engineers**, available from www.up.ac.za/academic/civil/divisions/transportation/scvanas/statbook.pdf.

Voung Q.H. (1987), 'Likelihood ratio tests for model selection and non-nested hypotheses', **Econometrica**, **57**(2), pp. 307-333.

Vrouwenvelder, A.C.W.M. and Waarts, P.H. (1993), 'Traffic loads on bridges', **Structural Engineering International**, **3/93**, pp. 169-177.

Zachary, S., Feld, G., Ward, G. and Wolfram, J. (1998), 'Multivariate extrapolation in the offshore environment', **Applied Ocean Research**, **20**, pp. 273-295.

Zacks, S. (1971), **The Theory of Statistical Inference**, Wiley Series in Probability and Mathematical Statistics, New York.

Zacks, S. (1971), **Parametric Statistical Inference: Basic Theory and Modern Approaches**, International Series in Nonlinear Mathematics, Pergamon Press, Oxford.

Žnidarič, A., Lavric, I. and Kalin, J. (2002), 'The next generation of bridge weigh-in-motion systems', **Pre-Proceedings of the Third International Conference on Weigh-In-Motion**, ed. B. Jacob et al, Orlando, pp. 219-230.

Žnidarič A., OBrien E.J., Dempsey, A. and Baumgartner, W. (1999), 'Weighing in motion with instrumented bridges', **Pre-Proceedings of Second European Road Research Conference**, Brussels, pp. 212-213.

Appendix A

PROGRAM DESCRIPTIONS

"Ignorance gives one a large range of probabilities"   *- George Eliot*

Appendix A - **PROGRAM DESCRIPTIONS**

A.1 Introduction

This appendix describes the function and use of the three main programs developed as part of this research. Two of the programs, `GenerateTraffic` and `SimulTraffic` are based on programs of the same name by Grave (2001) written in `FORTRAN`. The programs are all object-orientated and were written in the `C++` language, as described in Chapter 4.

In summary, the function of the three main programs is:

1. `GenerateTraffic`: Uses Monte-Carlo simulation to generate a traffic-file whose statistical distributions match the input distributions;
2. `SimulTraffic`: Simulates the effect of the traffic-file crossing the bridge and produces, for each effect, a block maximum value;
3. `AnalyseEvents`: Filters the output from `SimulTraffic` and returns the extrapolated value for a range of return periods.

In using these three programs, with the exception of the Traffic Data Input Files, all files must be located in the same folder as the three `*.exe` files. All output files will also be written into this folder.

The algorithms used by these programs are explained in general terms throughout the text, but especially Chapters 4 and 5. Grave (2001) should be referred to for further information.

A.2 GenerateTraffic

A.2.1 Input

The input for this program is in two parts; first, the user specified information, that is, the customisation of the output to the users needs. Second, the statistical parameters of the truck traffic for the site under consideration. This input is considerably more complex to prepare than that of the user information. Both are described next.

User Information Input File

The user information input file is called `GTin.txt`; its format is as follows:

Line	Entry
1	10
2	50
3	2
4	2
5	1
6	0

Line 1: This is the number of days for which traffic is required; on a Pentium 4 ℝ processor with 1 GB of RAM, up to about 1250 days (5 years) of traffic can be generated.

Line 2: This specifies the maximum span for which the traffic file is to be used. This value is used in checking headways for headway models other than HeDS – refer to Chapter 5 for more information.

Line 3: The index of the site giving the weight parameters – Table A.1.

Line 4: The index of the site giving the flow rate data – Table A.1.

Line 5:   Boolean variable for the traffic to be generated: 1 for bidirectional, 0 for uni-directional. In this work, proper correlation has not been included for uni-directional traffic; refer to Chapter 4.

Line 6:   Headway model to be used, see Table A.1.

Site Indices		Headway Models	
Index	Site	Index	Model Type
1	Angers	0	HeDS
2	Auxerre	1	5 m
3	A196	2	10 m
4	B224	3	0.5 s
5	A296	4	1.0 s
6	SAMARIS D1		
7	SAMARIS D2		
8	SAMARIS D3		
9	SAMARIS S1		
10	SAMARIS S2		
11	SAMARIS S3		
12	SAMARIS D		
13	SAMARIS S		

Note:

1. SAMARIS sites: D – Dutch, S – Slovenian, sites 12 and 13 are notional sites, composite of the three same-country sites.

2. Headway models 1 to 4 are MGC models – refer to Chapter 5.

Table A.1: Input indices for site and headway models.

Traffic Data Input Files

This input consists of several files which need to be located in a folder, named after the site which is located in the `C:\Traffic\` folder. The site is then given an index number which is hard coded in the program for future use. The files then placed in this folder are of type comma separated values (`*.csv`). These file types are easily created in a spreadsheet program.

Axle Spacing

File name: `Asall.csv`

This file stores the axle spacing data for all classes of trucks measured at the site. The values must be separated by commas, and importantly, the last value must have a comma after it. An example is:

```
1,50.7,3.7,0,0,0,0,0,0,0,0,0,
0,0,0,0,0,0,0,0,0,0,0,0,
0,0,0,0,0,0,0,0,0,0,0,0,

0.65,34.1,6.9,1,11.5,1.7,0,0,0,0,0,0,
0.268,34,1.5,0,0,0,0,0,0,0,0,0,
0.082,61.5,6,0,0,0,0,0,0,0,0,0,

0.672,30.6,1.5,0.153,34.7,3,0.317,11.8,0.6,0,0,0,
0.328,30.2,3.9,0.386,54.8,8.6,0.598,12.1,1.7,0,0,0,
0,0,0,0.461,59.5,3.4,0.085,18.3,0.9,0,0,0,

0.041,23.2,1.4,0.133,42,5.6,1,10.9,1.7,1,11,1.7,
0.959,30.4,1.8,0.867,51.2,3.4,0,0,0,0,0,0,
0,0,0,0,0,0,0,0,0,0,0,0,
```

This data is more easily understood viewed in tabular form, Table A.2.

Class	Line	Spacing 1-2			Spacing 2-3			Spacing 3-4			Spacing 4-5		
		ρ	μ	σ	ρ	μ	σ	ρ	μ	σ	ρ	μ	σ
2-Axle	1	1	50.7	3.7	0	0	0	0	0	0	0	0	0
	2	0	0	0	0	0	0	0	0	0	0	0	0
	3	0	0	0	0	0	0	0	0	0	0	0	0
	4												
3-Axle	5	0.65	34.1	6.9	1	11.5	1.7	0	0	0	0	0	0
	6	0.268	34	1.5	0	0	0	0	0	0	0	0	0
	7	0.082	61.5	6	0	0	0	0	0	0	0	0	0
	8												
4-Axle	9	0.672	30.6	1.5	0.153	34.7	3	0.317	11.8	0.6	0	0	0
	10	0.328	30.2	3.9	0.386	54.8	8.6	0.598	12.1	1.7	0	0	0
	11	0	0	0	0.461	59.5	3.4	0.085	18.3	0.9	0	0	0
	12												
5-Axle	13	0.041	23.2	1.4	0.133	42	5.6	1	10.9	1.7	1	11	1.7
	14	0.959	30.4	1.8	0.867	51.2	3.4	0	0	0	0	0	0
	15	0	0	0	0	0	0	0	0	0	0	0	0

Table A.2: Axle spacing input file description.

Traffic data may be fitted by a mix of a number of Normal distributions; that is, the data may be multi-modally normally distributed. There are three parameters required for each of the modes: the weight, ρ; the mean, μ, and; the standard deviation, σ. The maximum number of modes allowed for is three; hence the 3×3 tabular format of the data. The units of the data are as per traffic file convention explained in the Output section.

Axle Weights

File name: `Aw2&3.csv`

This file contains the axle weight information for the 2- and 3- axle trucks of the site. The values must be separated by commas, and importantly, the last value must have a comma after it. An example is given, and explained in Table A.3:

```
0.560,33.4,3.7,0.440,59.4,7.4,0.000,0.0,0.0,
0.440,40.6,7.4,0.560,66.6,3.7,0.000,0.0,0.0,
0.000,0.0,0.0,0.000,0.0,0.0,0.000,0.0,0.0,

0.066,20.4,1.5,0.769,34.6,6.8,0.558,30.5,5.9,
0.522,26.0,4.9,0.227,39.2,2.2,0.442,37.7,3.5,
0.412,38.7,8.6,0.004,54.4,3.7,0.000,0.0,0.0,
```

Class	Row	Weight Axle 1			Weight Axle 2			Weight Axle 3		
		ρ	μ	σ	ρ	μ	σ	ρ	μ	σ
2-Axle	1	0.56	33.4	3.7	0.44	59.4	7.4	0	0	0
	2	0.44	40.6	7.4	0.56	66.6	3.7	0	0	0
	3	0	0	0	0	0	0	0	0	0
	4									
3-Axle	5	0.066	20.4	1.5	0.769	34.6	6.8	0.558	30.5	5.9
	6	0.522	26	4.9	0.227	39.2	2.2	0.442	37.7	3.5
	7	0.412	38.7	8.6	0.004	54.4	3.7	0	0	0

Table A.3: Axle weight for 2- and 3-axle trucks input file description.

File name: `Aw4&5.csv`

This file contains the axle weight information for the 4- and 5-axle trucks. It has been found that the axle weights of the 4- and 5-axle trucks depend on the Gross Vehicle Weight (GVW). Thus the data governing these axle weights have been assembled for 12 classes of truck GVW, beginning at 25 kN and increasing in steps of 50 kN. An example of the data file is given:

```
0.0,0.0,0.0,0.0,0.0,0.0,
20.9,39.8,39.3,5.2,6.9,7.3,
25.6,36.5,38.0,5.4,4.8,5.7,
23.9,35.5,40.7,4.3,4.6,5.2,
20.3,36.1,43.6,3.6,4.6,5.4,
17.4,34.9,47.7,3.0,4.1,5.5,
14.8,33.4,51.8,2.1,3.1,4.1,
14.5,33.6,51.9,1.5,2.6,3.2,
13.9,32.4,53.7,1.3,2.3,3.1,
11.9,31.4,56.7,0.9,1.4,0.9,
0.0,0.0,0.0,0.0,0.0,0.0,
0.0,0.0,0.0,0.0,0.0,0.0,

0.0,0.0,0.0,0.0,0.0,0.0,
0.0,0.0,0.0,0.0,0.0,0.0,
19.1,36.5,44.5,6.0,7.4,7.2,
23.6,32.8,43.7,4.6,4.2,5.0,
21.4,33.4,45.3,3.2,4.8,5.4,
18.1,33.8,48.1,2.4,4.5,5.5,
15.7,32.3,52.0,1.8,3.8,4.7,
14.3,31.0,54.6,1.5,3.3,3.9,
13.4,29.6,57.1,1.2,2.9,3.4,
12.7,27.7,59.6,1.0,2.7,3.1,
0.0,0.0,0.0,0.0,0.0,0.0,
0.0,0.0,0.0,0.0,0.0,0.0,
```

The values must be separated by commas, and the last value must have a comma after it. A single line separates the 4- and 5-axle data. The six entries for each line, or GVW range of truck, represent the parameters of the single-mode Normal distributions for the first (W1) and second (W2) axles and the total weight of the tandem or tridem (WT) in the order shown in Table A.4.

Mean W1	Mean W2	Mean WT	SD W1	SD W2	SD WT

Table A.4: Axle weight for 4- and 5-axle trucks input file description.

This has resulted from previous research which has found that the weights of the axles in the tandem or tridem of 4- and 5-axle trucks (respectively) are equal and thus the tandem/tridem may be considered as one weight. The calculated tandem/tridem weight will be divided by the number of axles to give each axle a weight in the processing of this data.

Traffic composition and flow

File name: `Class%.csv`

This file holds the data for the percentage of trucks in each class and for each direction. The values must be separated by commas, and the last value must have a comma after it. An example is given and explained in Table A.5:

```
27.2,30.1,
4.5,6.0,
37.2,37.4,
31.1,26.5,
```

Class	Direction 1	Direction 2
2-Axle	27.2	30.1
3-Axle	4.5	6
4-Axle	37.2	37.4
5-Axle	31.1	26.5

Table A.5: Traffic composition input file explanation.

File name: `FlowR.csv`

This file holds the average number of trucks, for the hour under consideration, for both directions, for each hour of a typical working day. The values must be separated by commas, and importantly, the last value must have a comma after

it. Column 1 holds the 24 hourly flow rates for direction 1 and similarly for direction 2. An example is

```
25.4,41.0,
16.4,35.8,
14.4,40.2,
17.2,33.0,
24.8,44.6,
42.0,56.4,
58.0,86.4,
68.8,103.2,
78.8,106.2,
90.6,111.8,
97.2,109.4,
96.0,99.8,
65.2,59.8,
56.4,74.6,
85.4,83.2,
84.6,74.6,
92.8,93.8,
89.4,91.8,
100.8,69.6,
91.6,57.8,
73.0,45.0,
76.4,44.2,
63.0,53.8,
37.6,47.8,
```

Gross Vehicle Weight

File name: `GVWpdf.csv`

This file holds the parameters of the distributions that characterize the GVW and speed of each class of truck for both directions. An example of this file is:

```
1,194.5,27.4,0.152,44.2,6.5,0.069,51.2,9.7,0.583,231.1,61.9,0.274,199.9,36.7,
0,0,0,0.395,76.4,20.7,0.887,166.3,53.2,0.24,176.6,29.6,0.553,308.7,49.9,
0,0,0,0.453,117.4,30.5,0.044,268.4,34.7,0.177,331,30.1,0.173,383.2,35.4,

1,181.1,22.4,0.143,46.5,8,0.093,56.4,12.4,0.493,243.6,64.6,0.16,205.3,40.1,
0,0,0,0.524,82.9,23.8,0.653,141.5,31.1,0.301,162.1,28.8,0.441,300.6,53.6,
0,0,0,0.333,132.3,31.8,0.254,218.5,33.4,0.206,361.9,31.6,0.399,400.4,35.9,
```

Again this is best explained by reference to Table A.6. In this table the entry 3×3 refers to the allowance for multi-modal distributions (up to a maximum of three modes) and includes, for each mode, the weight, mean and standard deviation, as explained for the `Asall.csv` file. The values must be separated by commas, and importantly, the last value must have a comma after it.

	Speed	2-Axle GVW	3-Axle GVW	4-Axle GVW	5-Axle GVW
Direction 1	3×3	3×3	3×3	3×3	3×3
Blank Line					
Direction 2	3×3	3×3	3×3	3×3	3×3

Table A.6: GVW input file explanation.

Headway

File name: `HeDS.csv`

Only the HeDS headway model requires an input file. An example is:

```
15,0,0,0,
0,0.011855673,-0.014268241,0.004048786,
0,0.039251526,-0.05978246,0.02212043,
70,-0.004412997,0.054824101,-0.066907905,
80,-0.004685721,0.052127816,-0.053475193,
90,0.001537014,0.020896587,-0.013787689,
100,-0.003853623,0.064555837,-0.069172155,
110,-0.002530238,0.054511802,-0.059714977,
120,-0.001307981,0.048010242,-0.051645258,
130,-0.000487752,0.049738587,-0.057875119,
140,-0.004995115,0.081041256,-0.086465967,
150,-0.004547469,0.080310658,-0.083351351,
160,-0.004938412,0.092219287,-0.105416601,
170,-0.005000644,0.086893379,-0.097048852,
180,0.001987438,0.052114614,-0.058245039,
190,0.003366332,0.044909211,-0.063187142,
210,0.000379907,0.068461437,-0.077769612,
230,-0.006466786,0.117770005,-0.141174818,
```

Line 1 indicates the number of flow-dependent headway models (always less than, or equal to, 24). Lines 2 and 3 give the parameters of the quadratic-fit headway CDF for under 1.0 s and between 1.0 s and 1.5 s respectively. The following lines (15 in this example, from Line 1), return the parameters of the quadratic fit to the headway CDF for that flow (trucks per hour) of the first column. Refer to Chapter 5 for further information. The values must be separated by commas, and importantly, the last value must have a comma after it.

A.2.2 Output

The trucks are output in the traffic file specified in `GTin.txt` input file. The format of the output follows the convention adopted by CASTOR-LCPC and other users – Table A.7.

Characteristic	Unit	Format
Head		I4
Day		I2
Month		I2
Year		I2
Hour		I2
Minute		I2
Second		I2
Second/100		I2
Speed	dm/s	I3
Gross Vehicle Weight - GVW	kg/100	I4
Length	dm	I3
No. Axles		I1
Direction		I1
Lane		I1
Transverse Location In Lane	dm	I3
Weight Axle 1	kg/100	I3
Spacing Axle 1 - Axle 2	dm	I2
Weight Axle 2	kg/100	I3
Spacing Axle 2 - Axle 3	dm	I2
"	"	"
Spacing Axle 8 - Axle 9	dm	I2
Weight Axle 9	kg/100	I3

Note: the format entries refer to I**X**, as an integer of length **X**.

Table A.7: Traffic-file structure.

An example of the program output for several trucks is:

```
1001 1 1 2 0 12618155  54 43211 18 2743 27 0  0 0   0 0   0 0   0 0   0 0   0 0   0
1001 1 1 2 0 2 412133 137 67311 18 5441 6626 17 0   0 0   0 0   0 0   0 0   0 0   0
1001 1 1 2 0 2 598157  64 43211 18 3243 32 0   0 0   0 0   0 0   0 0   0 0   0 0   0
1001 1 1 2 0 44354134 336133511 18 7839 7040 6327 6327 63 0   0 0   0 0   0 0   0
1001 1 1 2 0 93062152 117 67311 18 3941 3926 39 0   0 0   0 0   0 0   0 0   0 0   0
```

A.3 SimulTraffic

A.3.1 User input file

The input file is called STin.txt; its format is as follows:

Line	Entry
1	WbQb.txt
2	4
3	20,30,40,50,
4	2
5	400

Line 1:   This specifies the name of the traffic file to be read in.

Line 2:   This specifies the number of bridge lengths over which the traffic file will be passed. The number supplied here must match the number of values supplied in Line 3.

Line 3:   The different bridge lengths to be examined are specified here. As can be seen in the example decimal points can be used as can integer lengths. The values must be separated by commas, and importantly, the last value must have a comma after it.

Line 4:   This specifies the number of directions in the traffic file (1 or 2).

Line 5:   The GVW limit for single truck events in deci-tonnes. Single truck events with GVW lower than this value will not be processed.

Other options are currently hard-coded into the program. Input file definition of these options will be included in further implementations. These options are:

- Output monthly maxima or daily maxima;

- Output the effect value from all events, used for estimating parent distributions of load effect;

- Maximum number of event-types possible – currently set at 7-truck events, none of which have been found to occur in free-flowing traffic on short- to medium-length bridges. However, in future implementations traffic jam scenarios will be modelled and this option will become important, but it is easily increased.

- Simulation calendar options: currently the number of days per 'month' is set at 25, and the number of 'months' per year set at 10.

- Presently every effect is calculated, of which there are 15. As this is wasteful when some effects are not of interest, future implementations could allow the user to specify the effects of interest.

A.3.2 Output

File name: `Span_X_Y_i.txt`

The output from `SimulTraffic` consists of a set of files for each span examined.

In the filename, **X** represents the bridge length, **Y** the file-type, be it daily maximum (Y = "DM"), monthly maximum (Y = "MM"), or all events (Y = "All"). The index **i** represents the event-type results in the file, for example, **i** = 2 for the 2-truck event results.

For block maxima results (Y = "DM" or "MM") the output file contains the events of type **i** identified, the trucks involved and the load effect values. An example of a single 3-truck daily maximum event for a 30 m bridge length follows:

Line	Data
1	1
2	1 0 0 0 0
3	2 1021.29 9917.74 -0.814 3
4	1001 1 1 5 2451672273 396105511 0 623214250 6412 6412 64 0 0 0 0 0 0 0 00
5	1001 1 1 5 2451750256 362109511 0 463012152 6514 6514 65 0 0 0 0 0 0 0 00
6	1001 1 1 5 2451771217 479111522 0 563115056 9112 9112 91 0 0 0 0 0 0 0 00
7	3 530.84 74249.7 35.916 3
8	1001 1 1 520372825246 280112511 0 583410252 4013 4013 40 0 0 0 0 0 0 0 00
9	1001 1 1 520372967245 368118411 0 503212667 9619 96 0 0 0 0 0 0 0 0 0 00
10	1001 1 1 520373065208 504104422 0 60301666113913139 0 0 0 0 0 0 0 0 0 00
11	4 637.684 9917.62 1.79 3
12	1001 1 1 5 2451672273 396105511 0 623214250 6412 6412 64 0 0 0 0 0 0 0 00
13	1001 1 1 5 2451750256 362109511 0 463012152 6514 6514 65 0 0 0 0 0 0 0 00
14	1001 1 1 5 2451771217 479111522 0 563115056 9112 9112 91 0 0 0 0 0 0 0 00
15	5 414.73 74249.7 35.916 3
16	1001 1 1 520372825246 280112511 0 583410252 4013 4013 40 0 0 0 0 0 0 0 00
17	1001 1 1 520372967245 368118411 0 503212667 9619 96 0 0 0 0 0 0 0 00
18	1001 1 1 520373065208 504104422 0 60301666113913139 0 0 0 0 0 0 0 0 0 00
19	6 379.172 9917.84 -2.984 3
20	1001 1 1 5 2451672273 396105511 0 623214250 6412 6412 64 0 0 0 0 0 0 0 00
21	1001 1 1 5 2451750256 362109511 0 463012152 6514 6514 65 0 0 0 0 0 0 0 00
22	1001 1 1 5 2451771217 479111522 0 563115056 9112 9112 91 0 0 0 0 0 0 0 00
23	7 0 0 0 0
24	8 0 0 0 0
25	9 0 0 0 0
26	10 0 0 0 0
27	11 0 0 0 0
28	12 0 0 0 0
29	13 0 0 0 0
30	14 0 0 0 0
31	15 0 0 0 0

Line 1: The index of the block maximum: if it is a DM file it is the day number, and if it is an MM file it is the month number. These indices are cumulative through the simulation results, thus a four-year simulation will have monthly maximum indices up to 40.

Lines 2-3: This is the effect information line. The format is:

Load Effect ID	Value	Time	Distance	No. of trucks

The effect time, in seconds, is from the start of the first year of simulation. The distance is the position of the first axle of the first truck on the bridge relative to the bridge datum, at the time of the crossing event maximum effect being reached. In this file, no 3-truck event is noted for Load Effect 1. Line 3 is similar.

Line 4-6: These lines provide the full truck information from the traffic file for all the trucks involved in the event for later processing.

Line 7+: The format of lines 2-6 continues for each of the effects calculated.

For the case in which Y = "All" and all of the effect values are required, the file format is simpler:

1-truck values	2-truck values	3-truck values	etc

An example output is:

```
1313.7      2210.45     2763.5
1365.06     1247.76     0
…           …           …
```

The number of rows is equal to the maximum number of events noted for all of the event-types. In this example (from a 20 m bridge length) it can be seen that in the simulation period, only 1 3-truck event was recorded.

A.4 AnalyseEvents

A.4.1 Input

The input file is called `AEin.txt`; its format is as follows:

Line	Entry
1 2 3	4 Span_20_DM, Span_30_DM, Span_40_DM,Span_50_DM, 1,1,1,0,0,0,0,0,0,0,0,0,0,0,0,

Line 1:   This specifies the number of block maxima events files to be input.

Line 2:   This line specifies the 'root names' of the block maxima events files to be processed – the program automatically finds each of the event-type files associated with the root. The number of files must match the number of Line 1; the values must be separated by commas and the last value must have a comma after it.

Line 3:   This line identifies the Load Effect output required: 1 if it is required and 0 if it is not. The index of the digit corresponds to the Load Effect ID. Thus, the above example will provide output for Effects 1, 2, and 3. Once again, the values must be separated by commas and the last value must have a comma after it.

A.4.2 Output

There are three types of file output. The first is used for graphical examination of the statistical analysis. The second is used as input for the predictive likelihood program used in Chapter 7. Finally, the results of the extrapolations are output.

Analysis and Graphing File

File name: `Span_X_Y_G_i.txt`

This file holds the results of the composite distribution analysis of Chapter 6 as well as Gumbel paper plotting information for each value. In the filename, **X** and **Y** are as previously, "G" represents the graph file, and **i** is the load effect for which the analysis is run. The file format is complex, and an `Excel` ® spreadsheet is available to read and plot the results in files of this type. The structure is:

1-truck event	2-truck event	Etc.	Conventional	
GEV 1×3 cell	GEV 1×3 cell	GEV 1×3 cell	GEV 1×3 cell	
$N_1 \times 3$	$N_2 \times 3$	$N_j \times 3$	$N \times 4$	

The GEV 1×3 cells give the GEV parameter vector for that event-type (or the daily maximum load effect values if the Conventional fit). The corresponding $N_j \times 3$ results give the N_j effect values with the corresponding fit and empirical plotting positions (standard extremal variates). The $N \times 4$ matrix at the end returns the daily maximum load effect values along with the empirical, CDS, and Conventional plotting positions.

Predictive Likelihood Input

File name: `Span_X_Y_PL_i.txt`

This file is the input file for the predictive likelihood analysis. Its format is simple; for each day (row) it lists the daily maximum load effect value for each event-type (column) recorded. This is similar to the "All" `SimulTraffic` files.

Extrapolation Results

File name: `Span_X_Y_D_EV.txt`

The extrapolated results for a range of return periods are included in this file. All effects are output into this file; its format is read by an `Excel` ® file and used to plot graphs. An example follows in which the first column is the load effect index; the second, the return period in years; the third, the CDS prediction; and the fourth, the Conventional prediction. It can be seen that the extrapolation breaks down after 2500 years due to a bounded result.

```
1      1.0101       3750.68      3750.41
1      1.02041      3751.71      3751.24
1      1.04167      3753.43      3752.94
1      1.06383      3755.17      3754.67
1      1.08696      3756.95      3756.43
1      1.11111      3758.76      3758.22
1      1.25         3768.3       3767.75
1      1.42857      3779.08      3778.39
1      1.66667      3791.07      3790.46
1      2            3805.29      3804.44
1      2.5          3822.04      3821.13
1      3.33333      3842.84      3841.99
1      5            3871.31      3870.19
1      10           3916.98      3915.28
1      100          4048.43      4040.6
1      200          4075.82      4071.98
1      250          4084.9       4081.53
1      333.333      4097.53      4093.47
1      500          4114.44      4109.62
1      1000         4142.45      4135.44
1      1250         4149.19      4143.31
1      2500         4176.32      4166.42
1      25000        0      4230.68
1      50000        7.11642e+024     4246.77
1      62500        1.21256e+046     4251.67
1      83333.3      -1.#INF     4257.79
1      125000       -1.#INF     4266.07
1      250000       -1.#INF     4279.32
```

Appendix B

MAXIMA

"A thousand probabilities do not make one fact"
- John Thurloe

Appendix B - MAXIMA

B.1 GEV Transforms

Introduction

Based on the stability postulate, a distribution of maximum values from a parent distribution that is of GEV form, is itself a GEV distribution (Chapter 3, Section 3.4.2). The distribution of maximum values, $F_Y(\cdot)$, from a parent distribution $F_X(\cdot)$ is given by:

$$F_Y(x) = \left[F_X(x) \right]^n \tag{B.1}$$

The stability postulate requires of any extreme value distribution that a linear transform of the variable **x** gives:

$$G^n\left(x;\theta\right) = G\left(a_n + b_n x; \theta^*\right) \tag{B.2}$$

where the transformation parameters a_n and b_n are reliant on **n** and the parameter vectors of the distributions are θ and θ^* respectively. In this work, it is of interest to find the new parameter vector θ^* that result from the transform of (B.2).

Determination of a_n and b_n

The GEV distribution has three parameters: location, μ; scale, σ, and; shape, ξ, and the equation of the GEV CDF is:

$$G(x) = \exp\left\{ -\left[1 - \xi\left(\frac{x-\mu}{\sigma} \right) \right]_+^{1/\xi} \right\} \tag{B.3}$$

where $x_+ = \max(x,0)$ and the parameters satisfy $-\infty < \mu < \infty$, $\sigma > 0$ and $-\infty < \xi < \infty$. Based on (B.3), and proceeding as follows:

$$G(a_n + b_n x) = G^n(x) \tag{B.4}$$

$$\left(\log \left[G(a_n + b_n x) \right] \right)^\xi = \left(\log \left[G^n(x) \right] \right)^\xi \tag{B.5}$$

Introducing (B.3) gives:

$$1 - \xi \left[\frac{(a_n + b_n x) - \mu}{\sigma} \right] = n^\xi - n^\xi \xi \left(\frac{x - \mu}{\sigma} \right) \tag{B.6}$$

Multiplying out and collecting terms gives:

$$\left[1 - \frac{\xi a_n}{\sigma} + \frac{\xi \mu}{\sigma} \right] + \left[\frac{-b_n}{\sigma} \right] x = \left[n^\xi - \frac{n^\xi \xi \mu}{\sigma} \right] + \left[-\frac{n^\xi \xi}{\sigma} \right] x \tag{B.7}$$

Thus:

$$
\begin{aligned}
1 - \frac{\xi a_n}{\sigma} + \frac{\xi \mu}{\sigma} &= n^\xi - \frac{n^\xi \xi \mu}{\sigma} \\
\frac{-b_n}{\sigma} &= -\frac{n^\xi \xi}{\sigma}
\end{aligned}
\tag{B.8}
$$

and solving gives:

$$
\begin{aligned}
a_n &= \frac{\sigma}{\xi} \left(1 - n^\xi \right) + \mu \left(n^\xi + 1 \right) \\
b_n &= \xi n^\xi
\end{aligned}
\tag{B.9}
$$

The parameters a_n and b_n are useful when it suffices to modify the input variable, **x**. However, often it is preferable to know the parameters, θ^*, of the new distribution, $G^n(x;\theta) \equiv G^*(x;\theta^*)$ and this result follows.

Determination of θ^*

Based on (B.3) and (B.4), and using subscripts **n** for the individual parameters to show that they are considered as functions of **n**:

$$-\left\{1-\xi\left[\frac{(a_n+b_n x)-\mu}{\sigma}\right]\right\}^{1/\xi} \equiv -\left\{1-\xi_n\left[\frac{x-\mu_n}{\sigma_n}\right]\right\}^{1/\xi_n} \tag{B.10}$$

As (B.4) is a linear transform of the distribution, its shape will not alter. This feature has been noted in other work (Han 2003) also. Therefore, $\xi = \xi_n$ and:

$$1-\xi\left[\frac{(a_n+b_n x)-\mu}{\sigma}\right] = 1-\xi_n\left[\frac{x-\mu_n}{\sigma_n}\right] \tag{B.11}$$

However, from the previous derivation of a_n and b_n, it is also known that:

$$1-\xi\left[\frac{(a_n+b_n x)-\mu}{\sigma}\right] = n^{\xi}\left[1-\xi\left(\frac{x-\mu}{\sigma}\right)\right] \tag{B.12}$$

and so,

$$n^{\xi}\left[1-\xi\left(\frac{x-\mu}{\sigma}\right)\right] = 1-\xi_n\left[\frac{x-\mu_n}{\sigma_n}\right] \tag{B.13}$$

By expanding and collecting terms:

$$\left[n^{\xi}+\frac{n^{\xi}\xi\mu}{\sigma}\right]+\left[-\frac{n^{\xi}\xi}{\sigma}\right]x = \left[1+\xi_n\frac{\mu_n}{\sigma_n}\right]+\left[\frac{\xi_n}{\sigma_n}\right]x \tag{B.14}$$

and solving with $\xi = \xi_n$ gives:

$$\sigma_n = \frac{\sigma}{n^{\xi}}$$

$$\mu_n = \frac{\sigma}{\xi}\left(1-\frac{1}{n^{\xi}}\right)+\mu \tag{B.15}$$

B.2 Parent Distributions of Load Effect

The results of the parent distribution study of Chapter 6, Section 6.2 are reported here. Six distributions are fitted to the load effect data resulting from the 20-year simulation study of the Auxerre traffic. The distributions fitted are: Frechet, GEV, Generalized Gamma, Gumbel, Normal, and Weibull – refer to Brodtkorb et al (2000) for further details on the distributions and the fitting algorithm.

In the figures that follow – Figure B.2 to Figure B.52 – two subplots are given. The right hand plot gives a histogram of the data, binned according to Sturge's Rule (Benjamin and Cornell 1970), along with the probability density functions of the fitted distributions. It is to be noted that maximum likelihood fitting is used, and the fits are not reliant on the number of bins in the histogram. The left hand plot shows the data and fitted distributions on Gumbel probability paper (Chapter 3, Section 3.2.3).

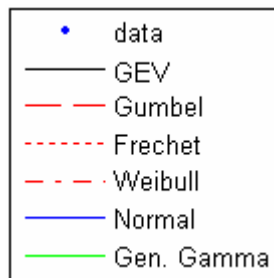The legend used in the plots is given by Figure B.1.

Figure B.1: Legend of parent distribution figures.

In Table B.1 to Table B.12, the maximum likelihood parameter estimates and likelihood function values are given for the corresponding figures.
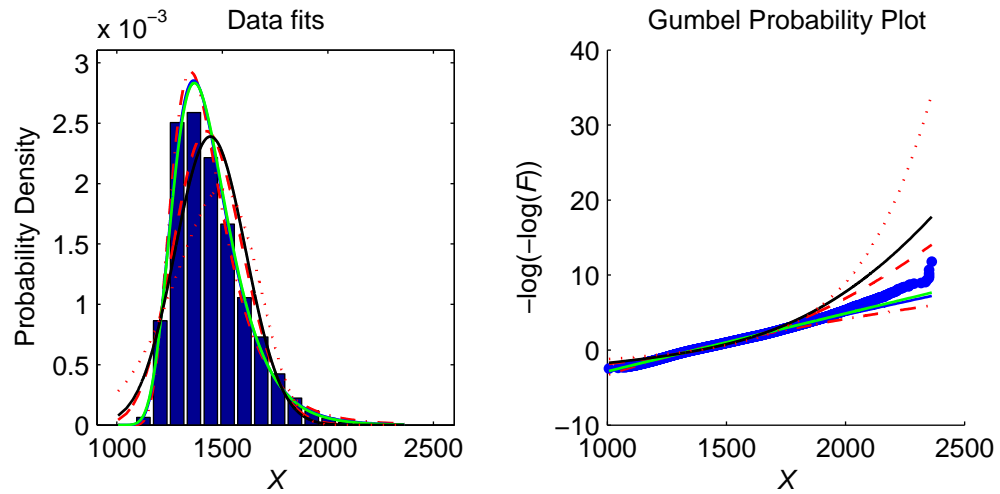
Load Effect 1

Figure B.2: Parent distribution for Load Effect 1; Length 20 m; 1-truck event.
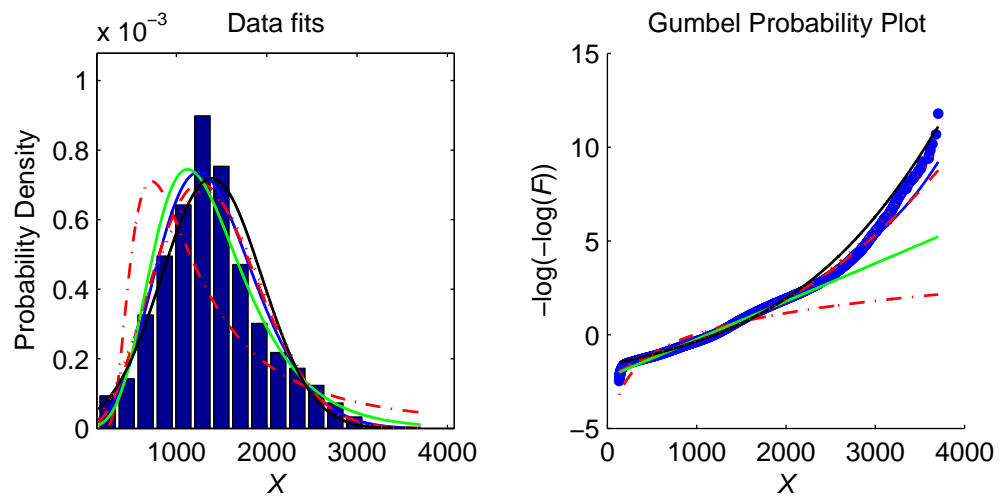

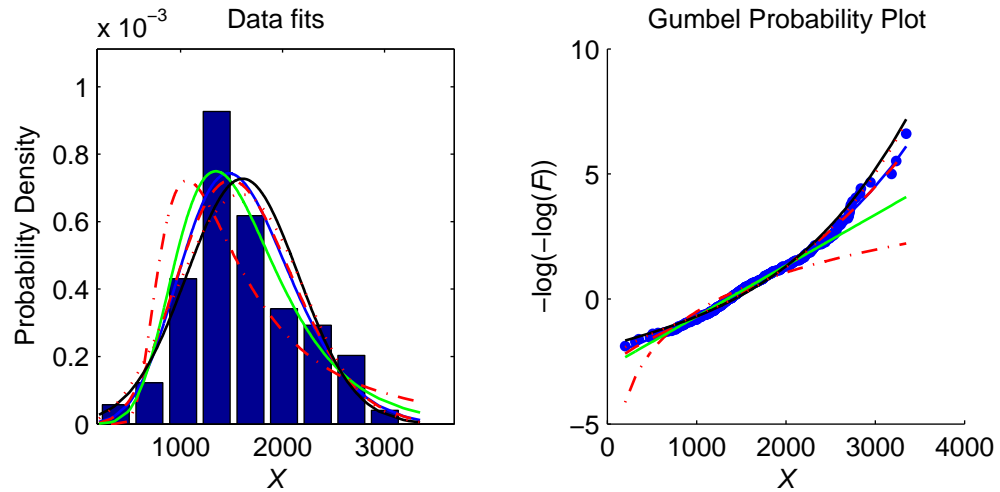Figure B.3: Parent distribution for Load Effect 1; Length 20 m; 2-truck event.

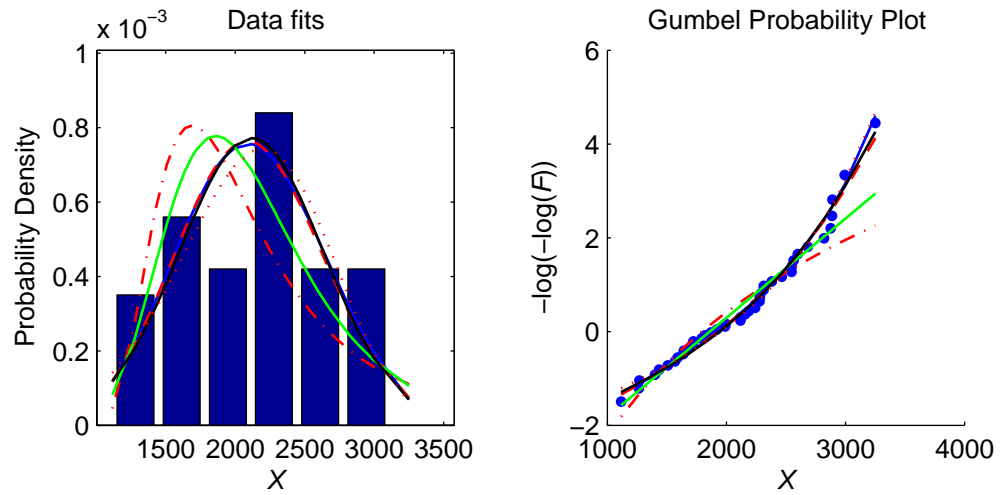Figure B.4: Parent distribution for Load Effect 1; Length 20 m; 3-truck event.

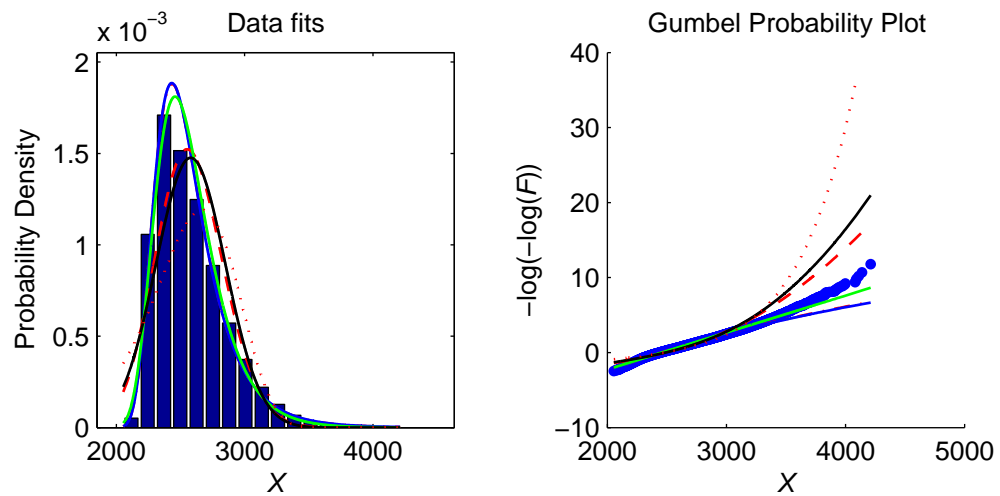Figure B.5: Parent distribution for Load Effect 1; Length 20 m; 4-truck event.

Figure B.6: Parent distribution for Load Effect 1; Length 30 m; 1-truck event.
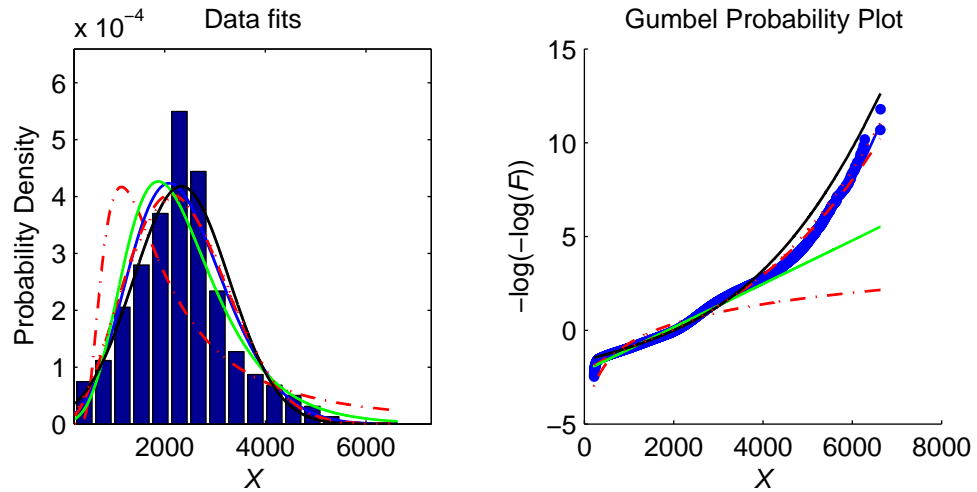
Figure B.7: Parent distribution for Load Effect 1; Length 30 m; 2-truck event.

Figure B.8: Parent distribution for Load Effect 1; Length 30 m; 3-truck event.

Figure B.9: Parent distribution for Load Effect 1; Length 30 m; 4-truck event.
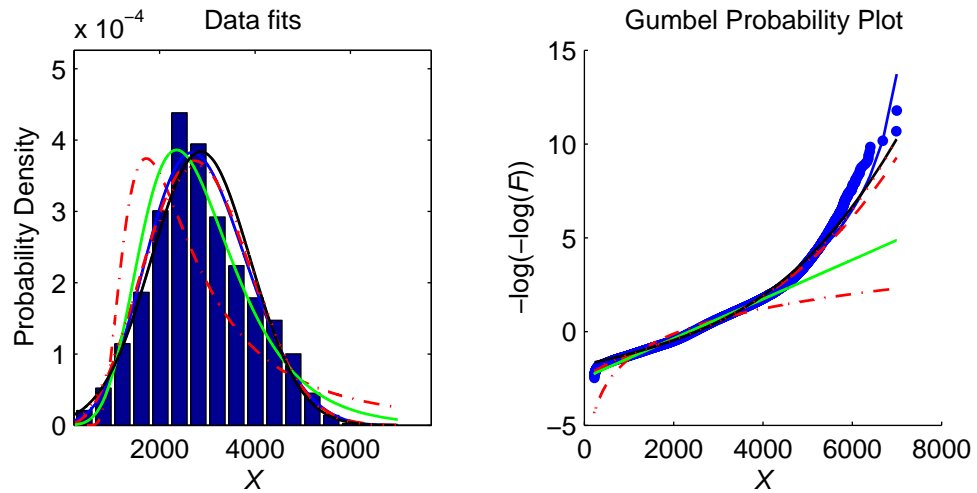
Figure B.10: Parent distribution for Load Effect 1; Length 40 m; 1-truck event.

Figure B.11: Parent distribution for Load Effect 1; Length 40 m; 2-truck event.

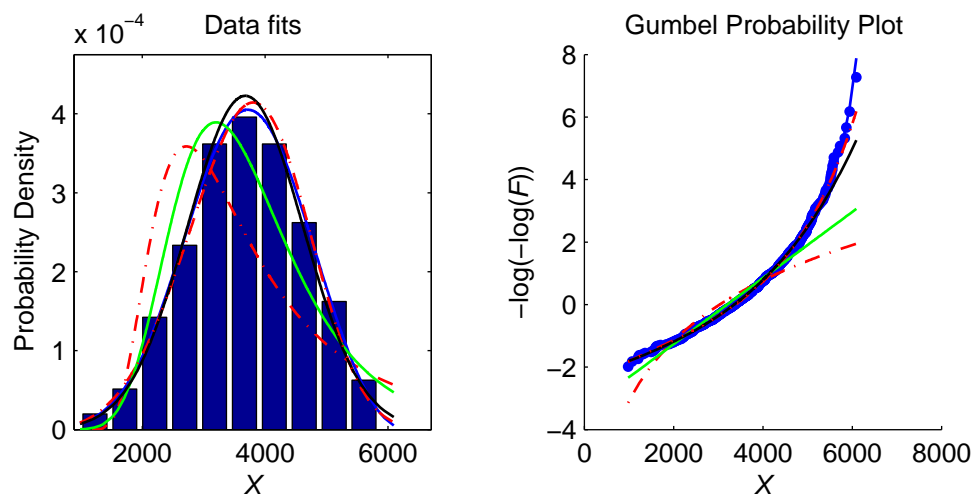Figure B.12: Parent distribution for Load Effect 1; Length 40 m; 3-truck event.

Figure B.13: Parent distribution for Load Effect 1; Length 40 m; 4-truck event.

Figure B.14: Parent distribution for Load Effect 1; Length 50 m; 1-truck event.

Figure B.15: Parent distribution for Load Effect 1; Length 50 m; 2-truck event.

Figure B.16: Parent distribution for Load Effect 1; Length 50 m; 3-truck event.

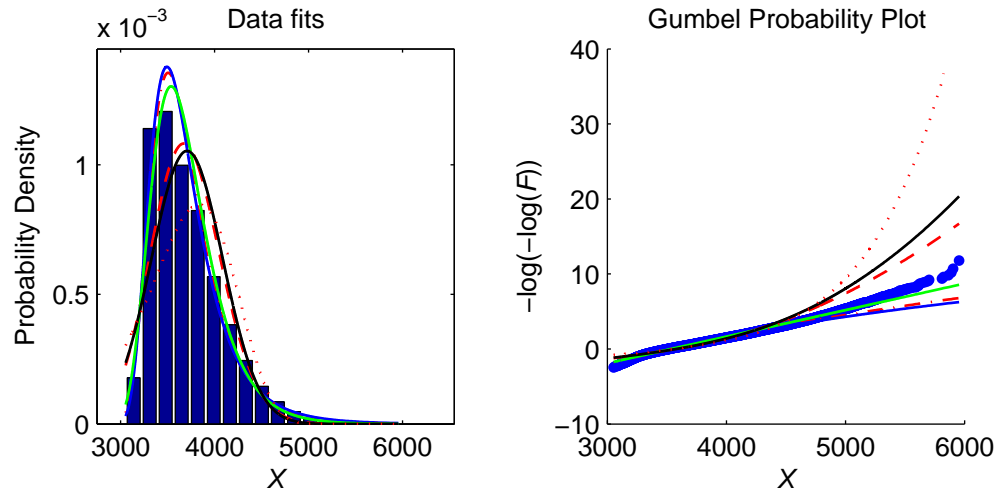Figure B.17: Parent distribution for Load Effect 1; Length 50 m; 4-truck event.

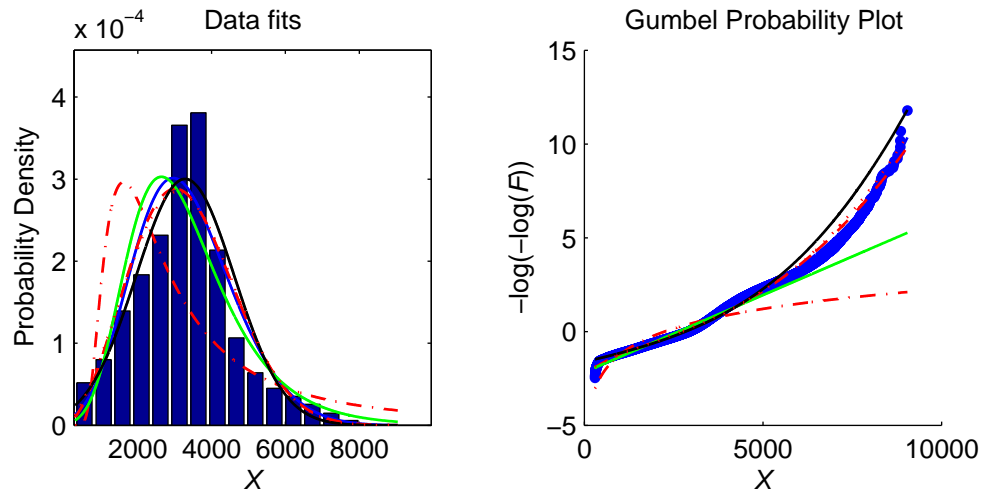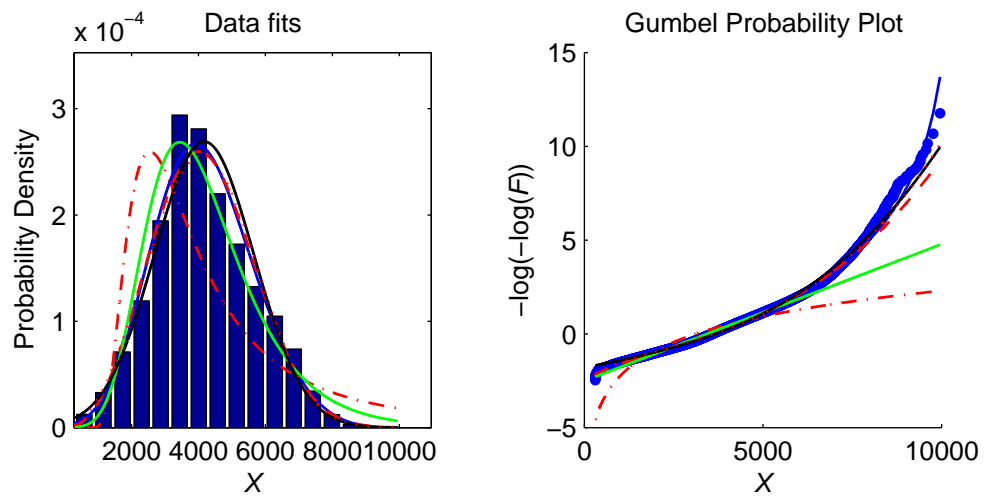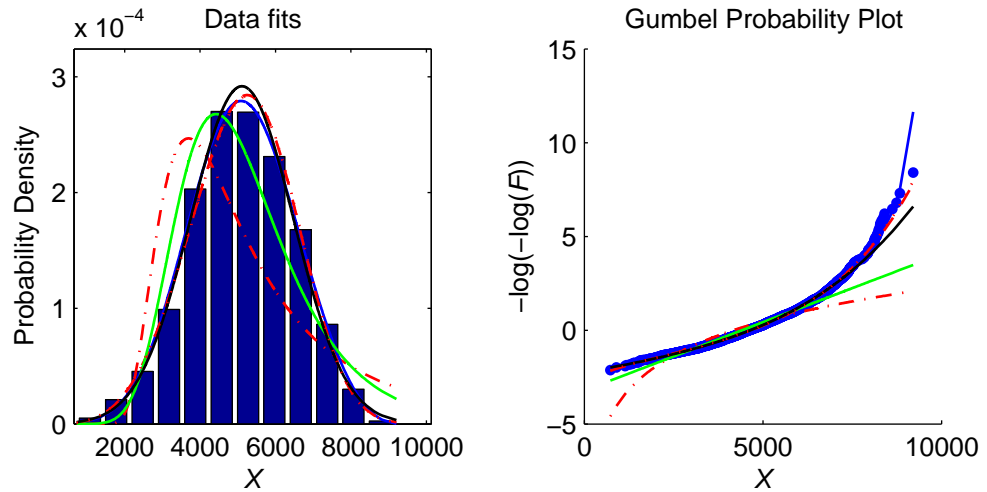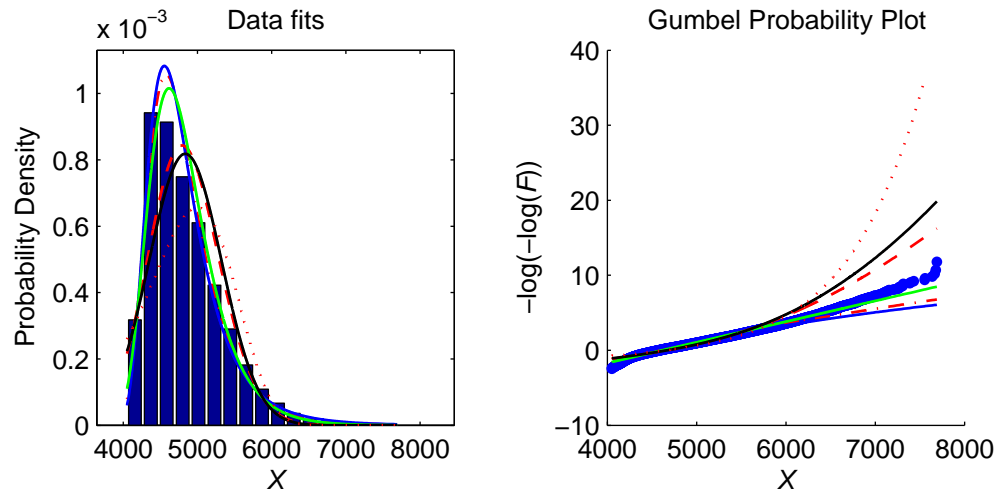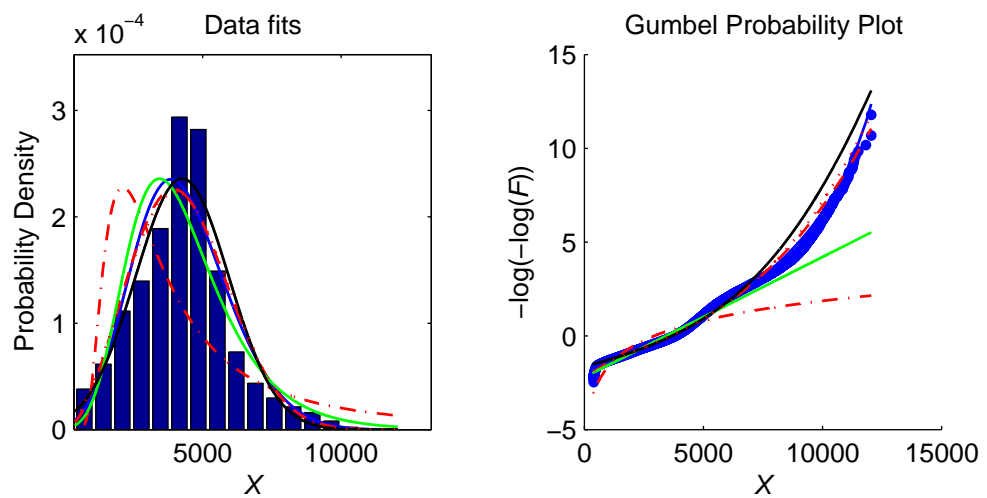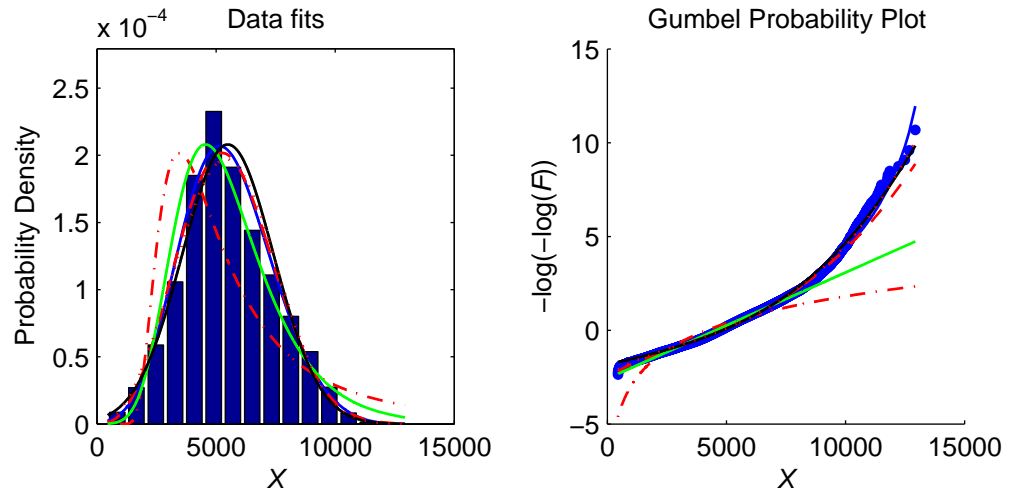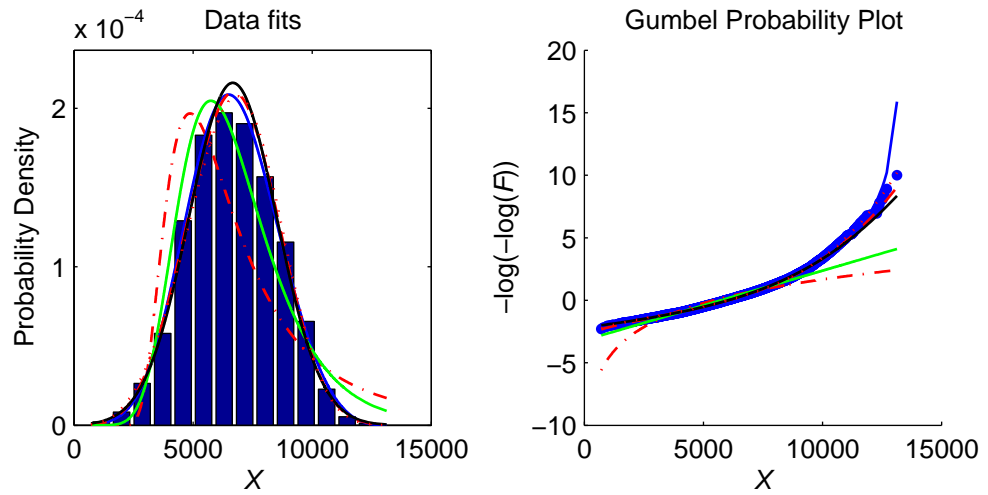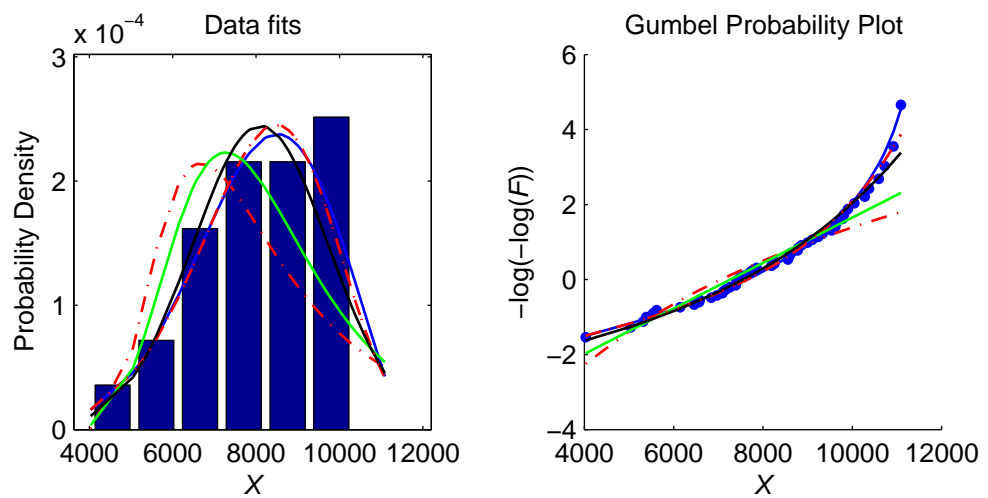Figure B.18: Parent distribution for Load Effect 1; Length 50 m; 5-truck event.

Load Effect 1			Bridge Length: 20 m		
1-truck event					
Rank	Distribution	Log-likelihood	Parameter vector		
1	GEV	-323847.141	-0.019	132.263	1367.717
2	Gumbel	-323860.871	133.177	1369.073	0
3	Frechet	-324047.776	1362.45	10.526	0
4	G.Gamma	-326654.495	52.069	52.716	1.193
5	Normal	-328081.551	1447.053	29301.24	0
6	Weibull	-333932.985	1526.075	7.893	0
2-truck event					
Rank	Distribution	Log-likelihood	Parameter vector		
1	GEV	-385335.694	0.216	520.381	1559.618
2	G.Gamma	-385445.184	1.665	1566.336	2.658
3	Weibull	-385631.057	1961.525	3.572	0
4	Normal	-385653.126	1767.051	293093.8	0
5	Gumbel	-387697.957	508.306	1501.27	0
6	Frechet	-400048.057	1408.774	2.476	0
3-truck event					
Rank	Distribution	Log-likelihood	Parameter vector		
1	G.Gamma	-3096.768	2.849	1351.638	2.607
2	Normal	-3097.202	1936.845	205595.9	0
3	GEV	-3097.411	0.232	444.544	1766.556
4	Weibull	-3102.732	2114.646	4.634	0
5	Gumbel	-3121.817	438.704	1712.3	0
6	Frechet	-3187.918	1648.311	3.447	0

Table B.1: Maximum likelihood estimates for Load Effect 1; Length 20 m.

Load Effect 1			Bridge Length: 30 m		
1-truck event					
Rank	Distribution	Log-likelihood	Parameter vector		
1	GEV	-346881.545	-0.083	202.058	2442.359
2	Frechet	-346881.549	2442.396	12.086	0
3	Gumbel	-347099.567	209.337	2451.598	0
4	G.Gamma	-350825.662	66.34	72.411	1.174
5	Normal	-352290.826	2576.791	77169.2	0
6	Weibull	-358836.6	2707.09	8.507	0
2-truck event					
Rank	Distribution	Log-likelihood	Parameter vector		
1	GEV	-413859.151	0.215	919.7	2708.019
2	G.Gamma	-414029.825	1.672	2708.792	2.598
3	Normal	-414208.382	3074.6	918464.1	0
4	Weibull	-414232.152	3415.927	3.496	0
5	Gumbel	-416226.575	901.181	2605.242	0
6	Frechet	-429924.1	2437.324	2.381	0
3-truck event					
Rank	Distribution	Log-likelihood	Parameter vector		
1	GEV	-35776.032	0.232	841.859	3210.828
2	G.Gamma	-35783.746	2.583	2582.014	2.632
3	Normal	-35792.337	3536.071	747383.9	0
4	Weibull	-35829.671	3872.117	4.482	0
5	Gumbel	-36026.91	828.93	3109.515	0
6	Frechet	-36819.263	2991.096	3.288	0

Table B.2: Maximum likelihood estimates for Load Effect 1; Length 30 m.

Load Effect 1			Bridge Length: 40 m		
1-truck event					
Rank	Distribution	Log-likelihood	Parameter vector		
1	GEV	-363001.375	-0.112	274.398	3515.703
2	Frechet	-363030.241	3520.639	12.662	0
3	Gumbel	-363362.076	288.577	3532.809	0
4	G.Gamma	-367475.032	59.34	145.803	1.262
5	Normal	-368866.396	3706.613	149758.4	0
6	Weibull	-375640.745	3889.085	8.73	0
2-truck event					
Rank	Distribution	Log-likelihood	Parameter vector		
1	GEV	-431223.95	0.21	1296.957	3816.512
2	G.Gamma	-431424.95	1.829	3622.188	2.454
3	Normal	-431614.018	4336.929	1842592	0
4	Weibull	-431714.037	4819.181	3.461	0
5	Gumbel	-433471.274	1273.204	3674.693	0
6	Frechet	-447398.819	3440.284	2.388	0
3-truck event					
Rank	Distribution	Log-likelihood	Parameter vector		
1	GEV	-159468.648	0.243	1259.681	4733.953
2	G.Gamma	-159491.738	2.138	4233.303	2.907
3	Normal	-159505.807	5210.643	1643540	0
4	Weibull	-159631.17	5706.861	4.474	0
5	Gumbel	-160663.122	1245.428	4575.346	0
6	Frechet	-164329.456	4411.416	3.298	0
4-truck event					
Rank	Distribution	Log-likelihood	Parameter vector		
1	GEV	-317.454	0.153	1192.759	5510.345
2	G.Gamma	-317.508	20.942	295.78	1.008
3	Gumbel	-317.928	1131.472	5414.258	0
4	Normal	-318.136	6049.425	1721393	0
5	Weibull	-318.968	6581.442	4.931	0
6	Frechet	-319.378	5294.196	4.906	0

Table B.3: Maximum likelihood estimates for Load Effect 1; Length 40 m.

Load Effect 1			Bridge Length: 50 m		
1-truck event					
Rank	Distribution	Log-likelihood	Parameter vector		
1	GEV	-375319.191	-0.126	348.303	4588.909
2	Frechet	-375378.98	4598.21	12.938	0
3	Gumbel	-375754.312	369.098	4613.477	0
4	G.Gamma	-380080.66	52.663	271.864	1.377
5	Normal	-381385.459	4836.421	247098	0
6	Weibull	-388263.633	5071.358	8.844	0
2-truck event					
Rank	Distribution	Log-likelihood	Parameter vector		
1	GEV	-443622.176	0.201	1655.568	4890.481
2	G.Gamma	-443833.479	1.946	4471.025	2.369
3	Normal	-444018.782	5563.557	3026370	0
4	Weibull	-444198.834	6181.224	3.448	0
5	Gumbel	-445814.898	1631.988	4716.974	0
6	Frechet	-459889.633	4410.749	2.363	0
3-truck event					
Rank	Distribution	Log-likelihood	Parameter vector		
1	G.Gamma	-439936.63	2.049	5718.775	2.936
2	GEV	-439957.173	0.235	1689.558	6258.307
3	Normal	-439964.06	6906.131	2965658	0
4	Weibull	-440282.917	7569.56	4.413	0
5	Gumbel	-443095.194	1675.072	6052.249	0
6	Frechet	-452945.748	5814.015	3.164	0
4-truck event					
Rank	Distribution	Log-likelihood	Parameter vector		
1	Normal	-3227.292	7982.878	2802193	0
2	G.Gamma	-3227.595	2.167	6681.794	3.41
3	GEV	-3228.617	0.257	1676.817	7369.156
4	Weibull	-3230.704	8654.902	5.268	0
5	Gumbel	-3259.666	1698.502	7145.363	0
6	Frechet	-3320.757	6985.525	4.045	0

Table B.4: Maximum likelihood estimates for Load Effect 1; Length 50 m.
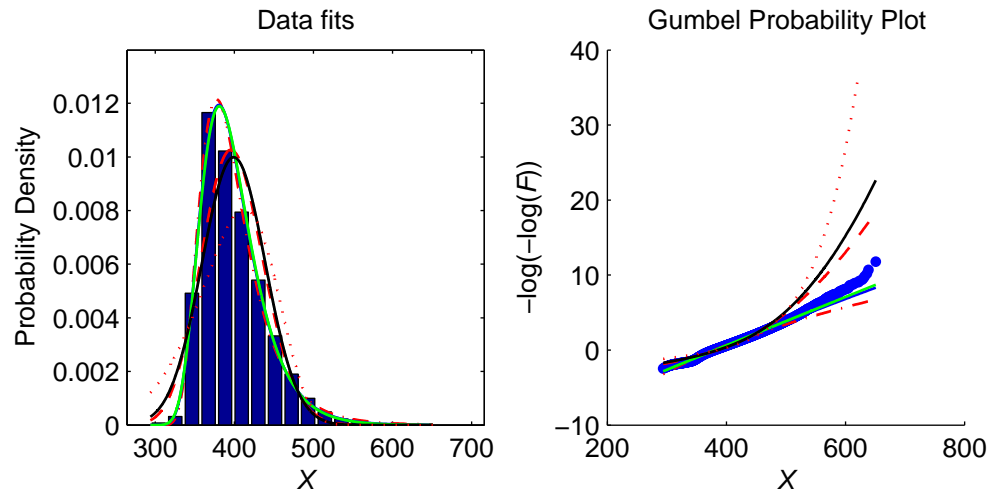
Load Effect 2

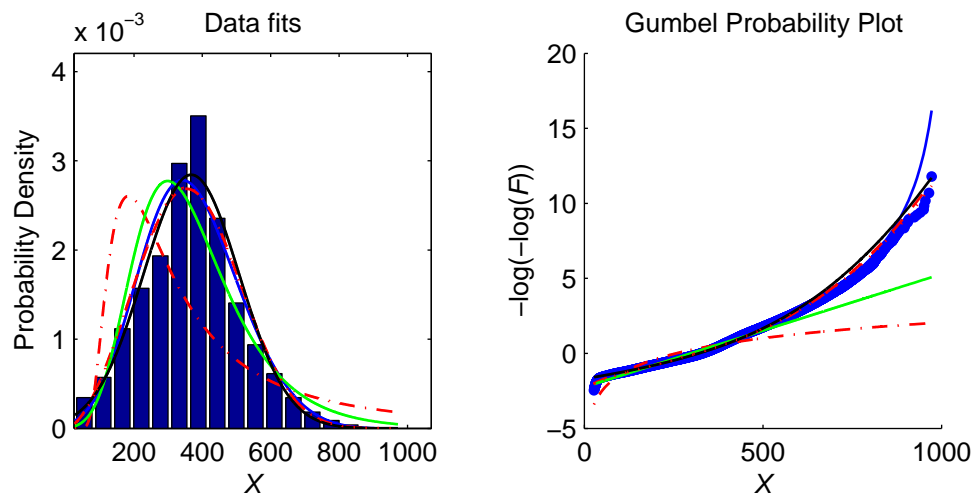Figure B.19: Parent distribution for Load Effect 2; Length 20 m; 1-truck event.

Figure B.20: Parent distribution for Load Effect 2; Length 20 m; 2-truck event.

Figure B.21: Parent distribution for Load Effect 2; Length 20 m; 3-truck event.

Figure B.22: Parent distribution for Load Effect 2; Length 20 m; 4-truck event.

Figure B.23: Parent distribution for Load Effect 2; Length 30 m; 1-truck event.

Figure B.24: Parent distribution for Load Effect 2; Length 30 m; 2-truck event.
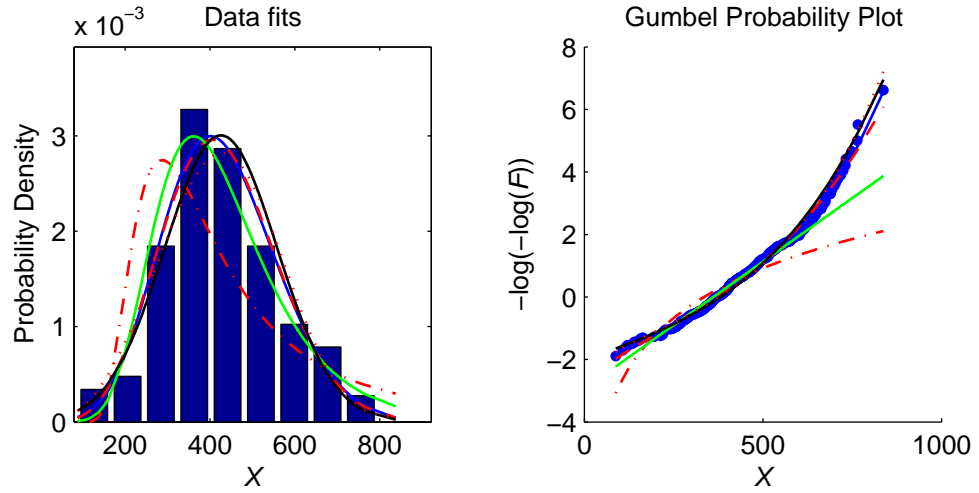

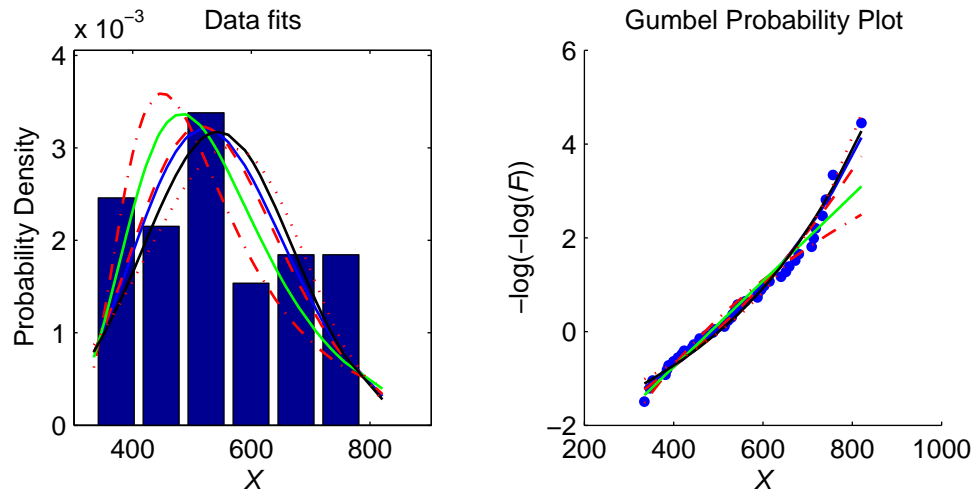Figure B.25: Parent distribution for Load Effect 2; Length 30 m; 3-truck event.
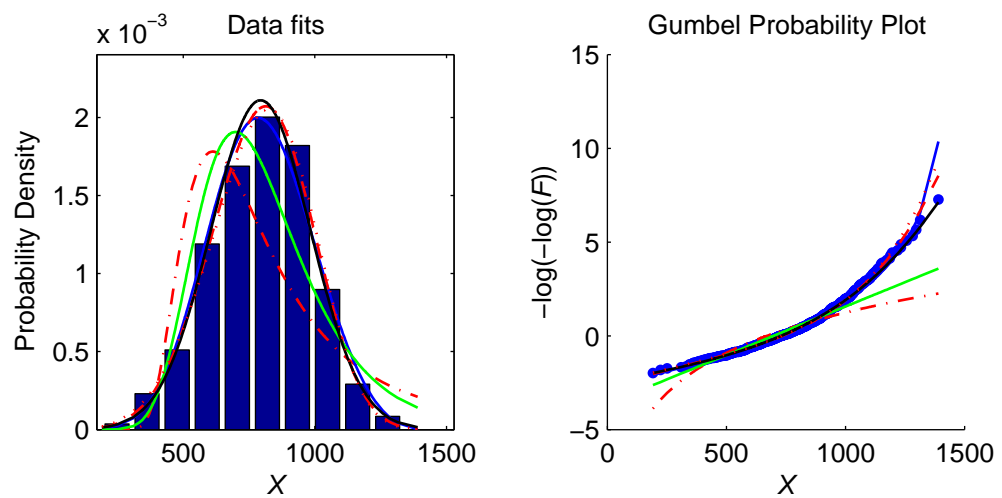
Figure B.26: Parent distribution for Load Effect 2; Length 30 m; 4-truck event.
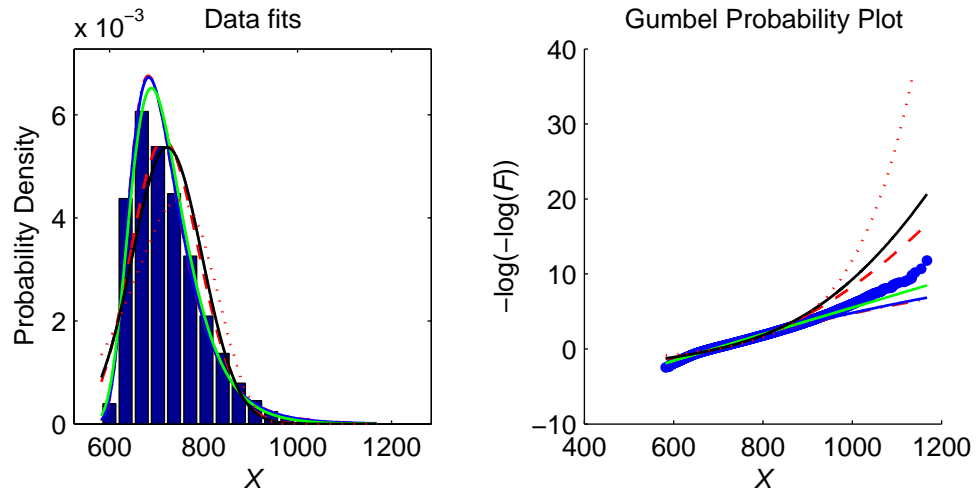
Figure B.27: Parent distribution for Load Effect 2; Length 40 m; 1-truck event.
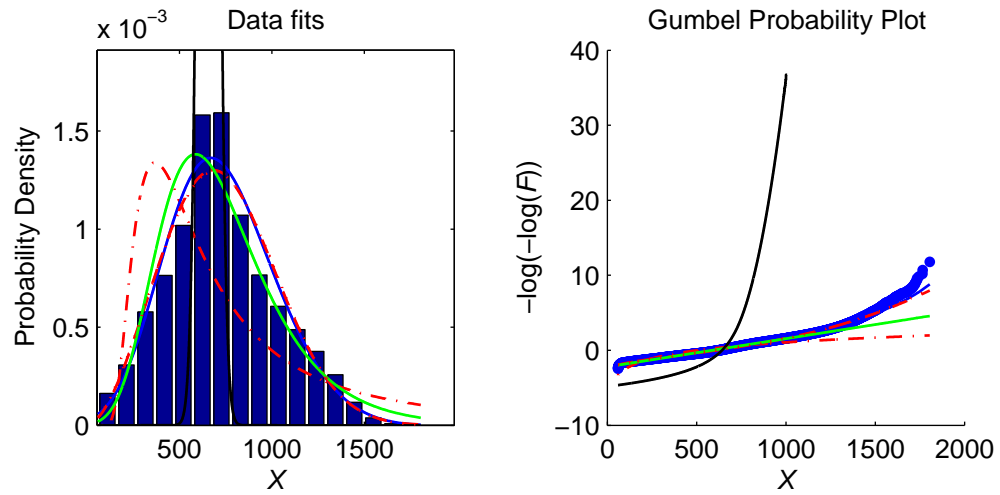
Figure B.28: Parent distribution for Load Effect 2; Length 40 m; 2-truck event.
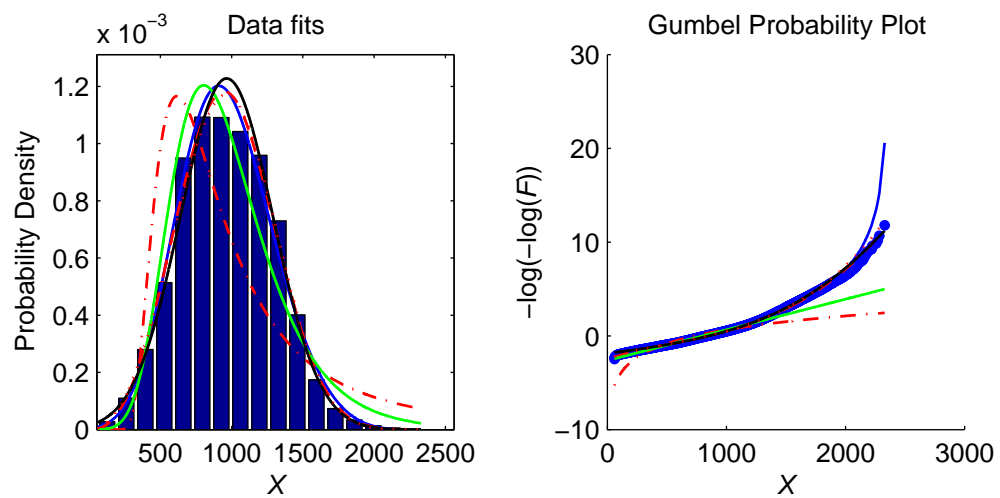
Figure B.29: Parent distribution for Load Effect 2; Length 40 m; 3-truck event.
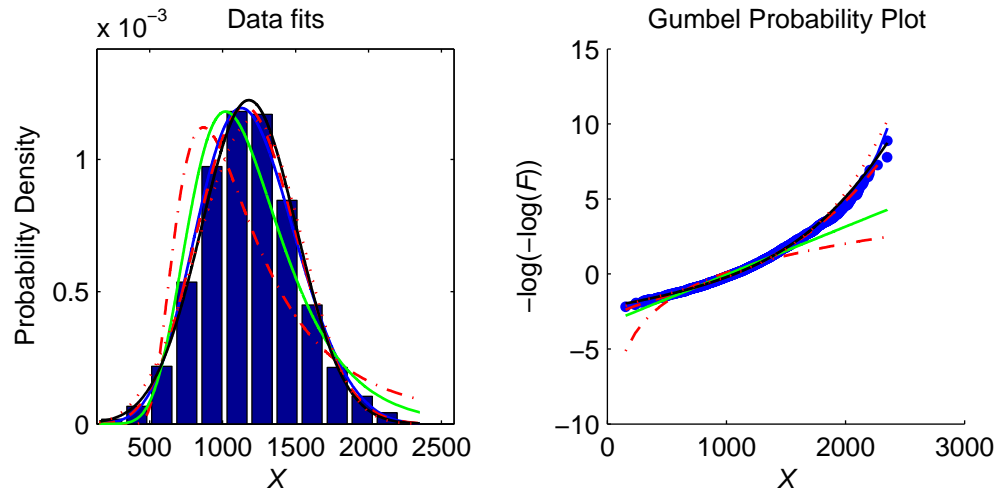
Figure B.30: Parent distribution for Load Effect 2; Length 40 m; 4-truck event.
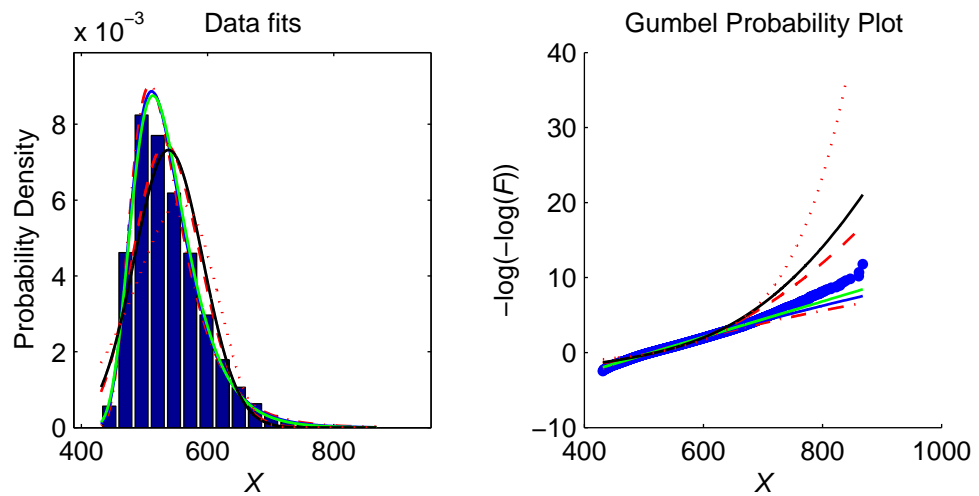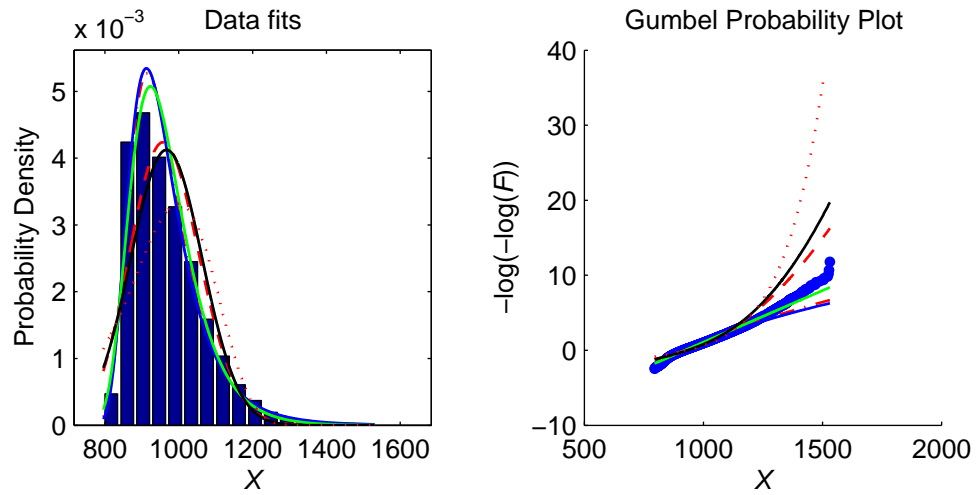

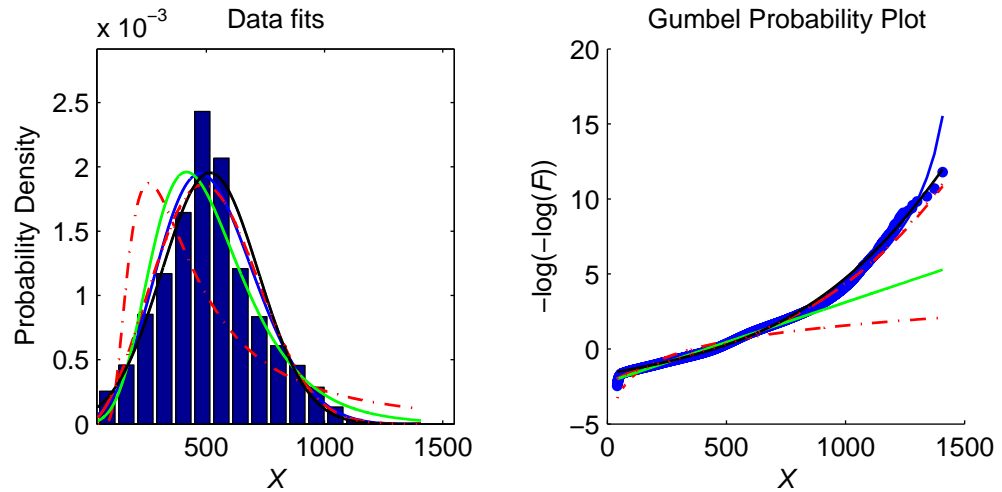Figure B.31: Parent distribution for Load Effect 2; Length 50 m; 1-truck event.
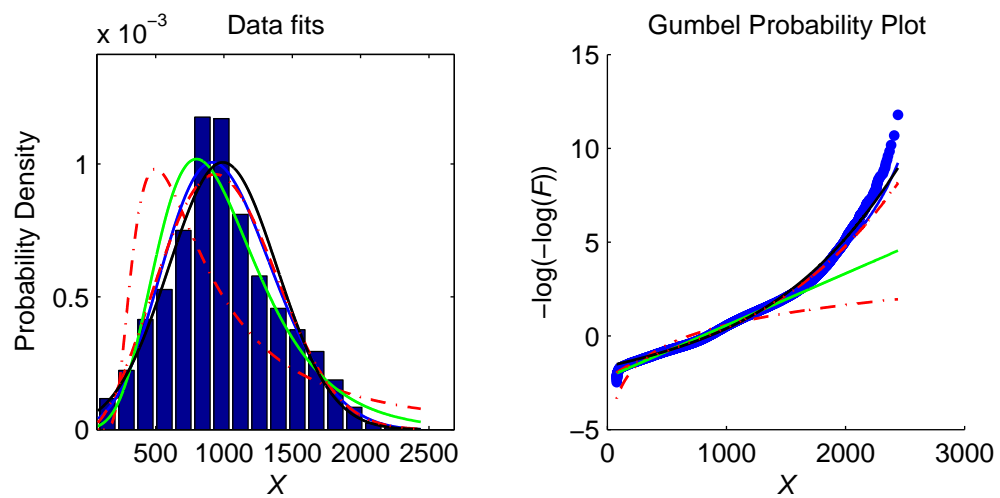
Figure B.32: Parent distribution for Load Effect 2; Length 50 m; 2-truck event.
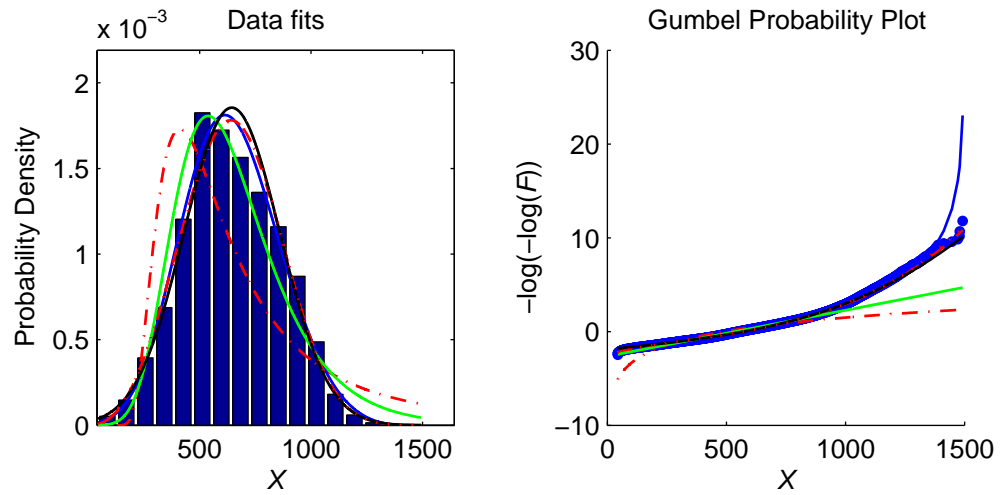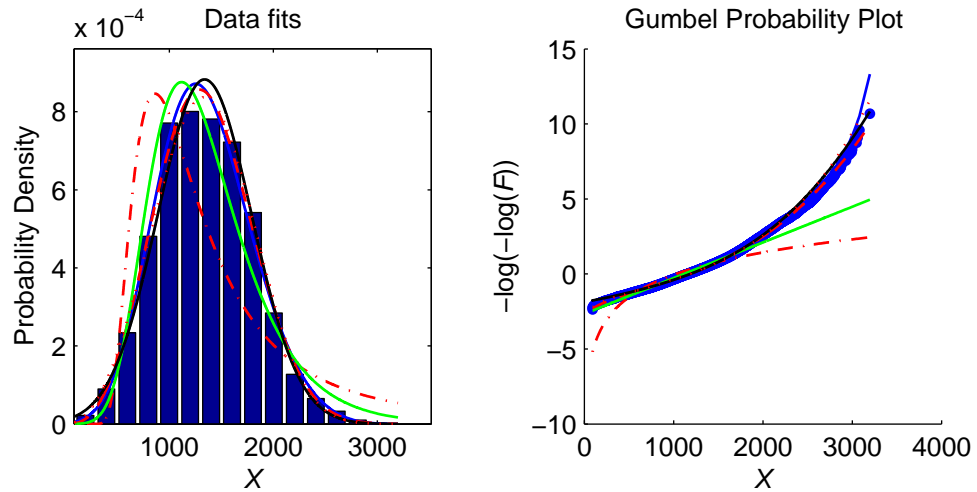
Figure B.33: Parent distribution for Load Effect 2; Length 50 m; 3-truck event.
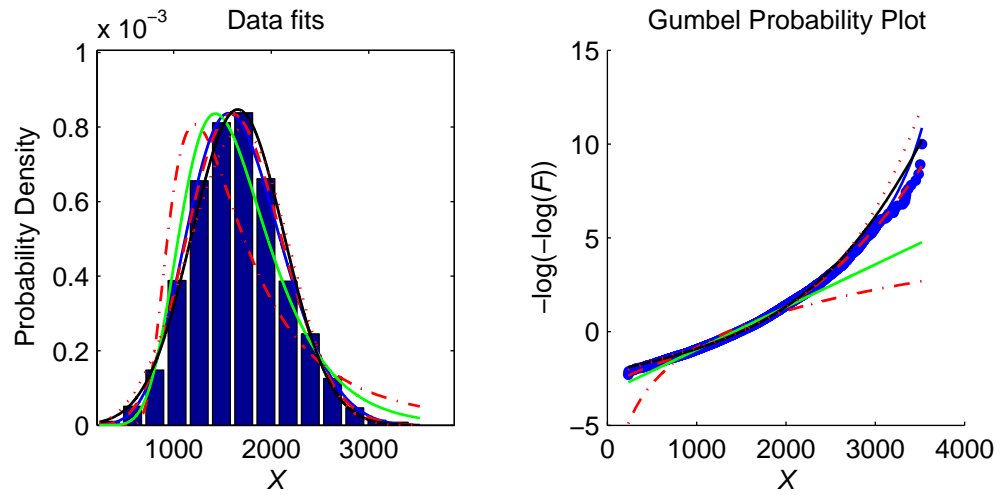
Figure B.34: Parent distribution for Load Effect 2; Length 50 m; 4-truck event.
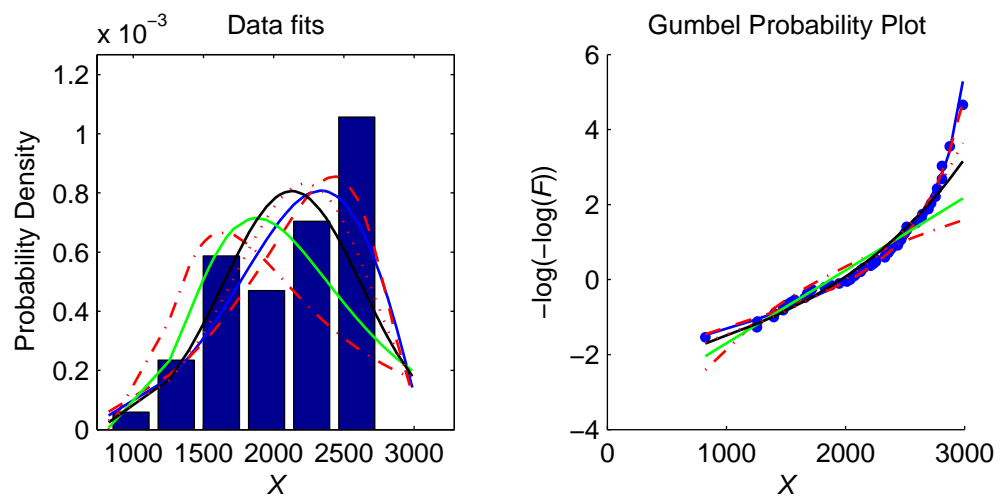
Figure B.35: Parent distribution for Load Effect 2; Length 50 m; 5-truck event.

Load Effect 2			Bridge Length: 20 m		
1-truck event					
Rank	Distribution	Log-likelihood	Parameter vector		
1	GEV	-250986.273	-0.00677	31.09401	381.4966
2	Gumbel	-250991.584	31.073	381.542	0
3	Frechet	-251206.982	380.258	12.465	0
4	G.Gamma	-254140.967	71.637	11.393	1.201
5	Normal	-255434.561	399.673	1602.788	0
6	Weibull	-262179.115	418.595	9.11	0
2-truck event					
Rank	Distribution	Log-likelihood	Parameter vector		
1	GEV	-335674.3988	-0.10795	162.662	397.4217
2	Gumbel	-337603.958	169.1	408.312	0
3	G.Gamma	-338299.935	26.435	0.224	0.427
4	Frechet	-344960.407	369.648	2.03	0
5	Weibull	-348274.208	580.324	1.794	0
6	Normal	-358576.542	510.36	92536.91	0
3-truck event					
Rank	Distribution	Log-likelihood	Parameter vector		
1	Normal	-6643.232	513.57	9975.366	0
2	G.Gamma	-6643.926	3.821	321.856	2.691
3	GEV	-6649.711	0.218	98.419	475.257
4	Weibull	-6668.41	554.485	5.529	0
5	Gumbel	-6726.662	99.611	464.039	0
6	Frechet	-6903.388	455.634	4.53	0

Table B.5: Maximum likelihood estimates for Load Effect 2; Length 20 m.

Load Effect 2			Bridge Length: 30 m		
1-truck event					
Rank	Distribution	Log-likelihood	Parameter vector		
1	GEV	-266808.11	-0.033	41.947	512.749
2	Gumbel	-266848.517	42.467	513.495	0
3	Frechet	-266887.278	511.683	12.383	0
4	G.Gamma	-270124.645	64.12	18.885	1.242
5	Normal	-271418.195	538.476	3037.676	0
6	Weibull	-278093.637	564.453	8.926	0
2-truck event					
Rank	Distribution	Log-likelihood	Parameter vector		
1	G.Gamma	-334782.12	0.843	766.359	4.162
2	Weibull	-334811.812	726.867	3.746	0
3	Normal	-334884.547	656.642	38465.03	0
4	GEV	-334884.797	0.282	197.972	586.837
5	Gumbel	-339308.234	197.217	557.667	0
6	Frechet	-355559.571	515.373	2.168	0
3-truck event					
Rank	Distribution	Log-likelihood	Parameter vector		
1	G.Gamma	-63113.388	1.892	702.728	3.219
2	Normal	-63116.303	808.576	37261.92	0
3	GEV	-63122.761	0.253	191.744	737.507
4	Weibull	-63168.53	883.706	4.634	0
5	Gumbel	-63804.829	190.237	712.236	0
6	Frechet	-65627.234	686.14	3.324	0

Table B.6: Maximum likelihood estimates for Load Effect 2; Length 30 m.

Load Effect 2			Bridge Length: 40 m		
1-truck event					
Rank	Distribution	Log-likelihood	Parameter vector		
1	GEV	-281753.134	-0.069	55.377	687.269
2	Frechet	-281757	686.93	12.456	0
3	Gumbel	-281906.044	56.988	689.361	0
4	G.Gamma	-285495.808	68.83	20.539	1.188
5	Normal	-286878.088	723.285	5637.782	0
6	Weibull	-293548.232	758.644	8.806	0
2-truck event					
Rank	Distribution	Log-likelihood	Parameter vector		
1	GEV	-351780.611	0.264	273.371	796.142
2	G.Gamma	-351855.778	1.046	979.02	3.504
3	Weibull	-351857.448	994.678	3.601	0
4	Normal	-351964.234	896.301	76167.67	0
5	Gumbel	-355178.094	267.764	758.816	0
6	Frechet	-369839.284	704.672	2.255	0
3-truck event					
Rank	Distribution	Log-likelihood	Parameter vector		
1	G.Gamma	-333449.564	2.208	947.285	2.763
2	Normal	-333492.006	1196.907	92133.35	0
3	GEV	-333566.086	0.214	296.075	1079.831
4	Weibull	-333870.979	1313.145	4.308	0
5	Gumbel	-336269.53	293.418	1046.603	0
6	Frechet	-345461.829	1003.4	3.123	0
4-truck event					
Rank	Distribution	Log-likelihood	Parameter vector		
1	G.Gamma	-2237.676	4.335	795.085	2.342
2	Normal	-2237.809	1445.809	90733.62	0
3	GEV	-2240.416	0.189	293.903	1326.59
4	Weibull	-2246.825	1567.09	5.062	0
5	Gumbel	-2258.376	295.736	1297.109	0
6	Frechet	-2311.04	1259.007	3.781	0

Table B.7: Maximum likelihood estimates for Load Effect 2; Length 40 m.

Load Effect 2			Bridge Length: 50 m		
1-truck event					
Rank	Distribution	Log-likelihood	Parameter vector		
1	GEV	-294339.931	-0.104	69.818	919.702
2	Frechet	-294359.954	920.74	13.045	0
3	Gumbel	-294654.784	73.127	923.735	0
4	G.Gamma	-298680.041	68.109	31.119	1.228
5	Normal	-300053.901	967.677	9549.83	0
6	Weibull	-306960.142	1013.931	8.994	0
2-truck event					
Rank	Distribution	Log-likelihood	Parameter vector		
1	GEV	-366657.994	0.27	369.114	1064.172
2	G.Gamma	-366737.552	1.027	1316.776	3.512
3	Weibull	-366738.194	1329.508	3.57	0
4	Normal	-366823.135	1197.642	138005.5	0
5	Gumbel	-370114.356	361.385	1012.489	0
6	Frechet	-385258.176	938.16	2.217	0
3-truck event					
Rank	Distribution	Log-likelihood	Parameter vector		
1	G.Gamma	-373686.354	2.118	1319.331	2.753
2	GEV	-373706.028	0.228	416.578	1477.941
3	Normal	-373772.676	1639.522	182231	0
4	Weibull	-374072.946	1801.892	4.209	0
5	Gumbel	-376533.007	409.552	1428.359	0
6	Frechet	-386302.208	1366.591	3.054	0
4-truck event					
Rank	Distribution	Log-likelihood	Parameter vector		
1	G.Gamma	-10021.813	3.054	1317.937	2.514
2	Normal	-10023.647	1975.198	213064.9	0
3	GEV	-10025.445	0.213	449.256	1797.453
4	Weibull	-10043.114	2156.349	4.629	0
5	Gumbel	-10098.711	444.883	1747.254	0
6	Frechet	-10321.597	1688.231	3.509	0

Table B.8: Maximum likelihood estimates for Load Effect 2; Length 50 m.

Load Effect 3

Figure B.36: Parent distribution for Load Effect 3; Length 20 m; 1-truck event.

Figure B.37: Parent distribution for Load Effect 3; Length 20 m; 2-truck event.

Figure B.38: Parent distribution for Load Effect 3; Length 20 m; 3-truck event.

Figure B.39: Parent distribution for Load Effect 3; Length 20 m; 4-truck event.

Figure B.40: Parent distribution for Load Effect 3; Length 30 m; 1-truck event.

Figure B.41: Parent distribution for Load Effect 3; Length 30 m; 2-truck event.

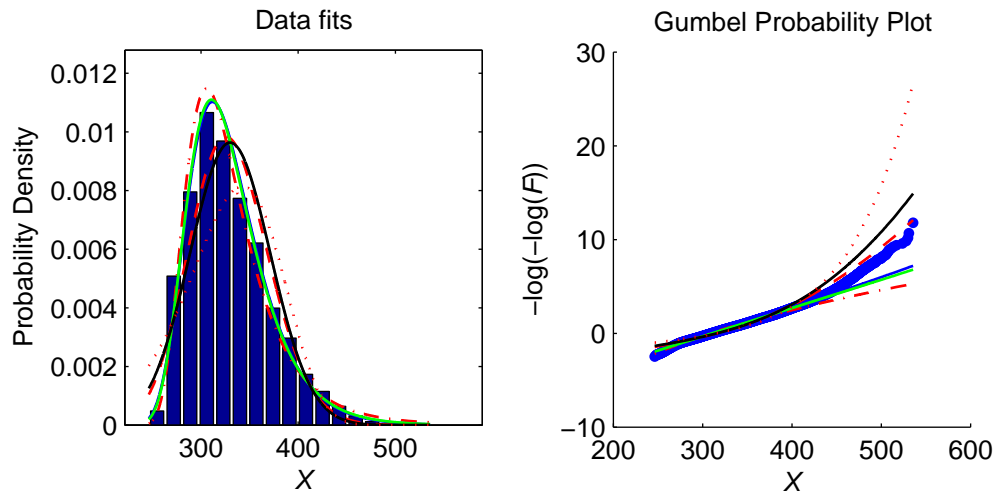Figure B.42: Parent distribution for Load Effect 3; Length 30 m; 3-truck event.
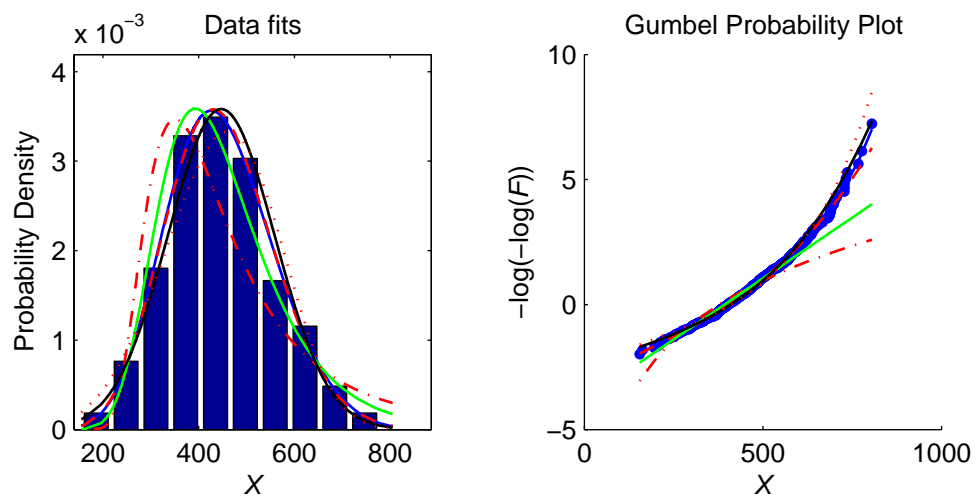
Figure B.43: Parent distribution for Load Effect 3; Length 30 m; 4-truck event.
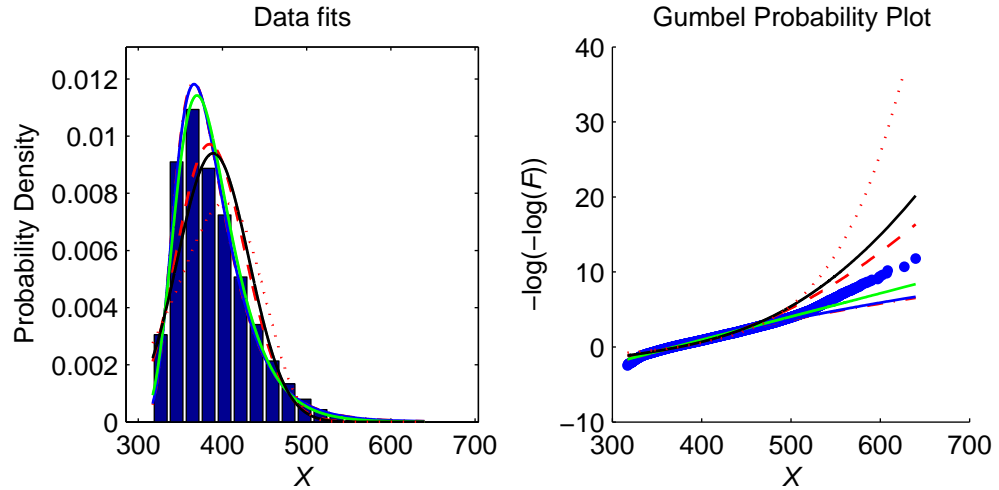
Figure B.44: Parent distribution for Load Effect 3; Length 40 m; 1-truck event.
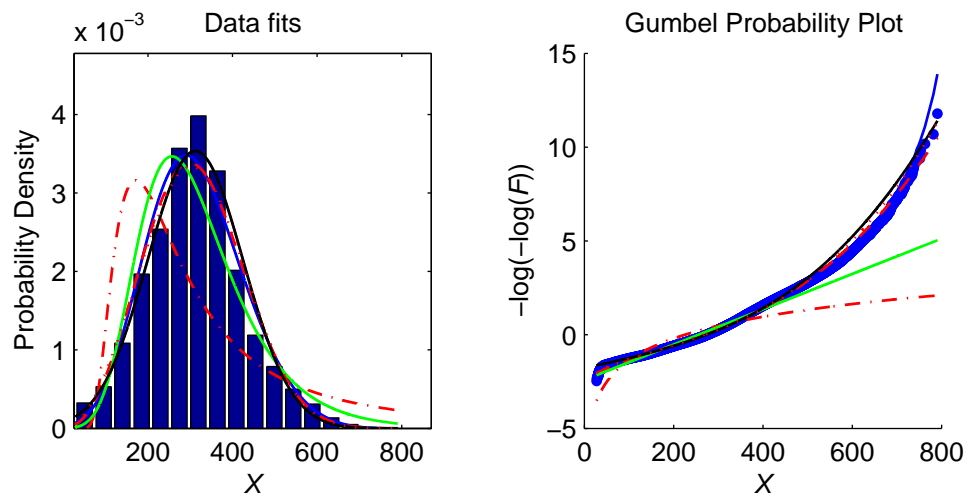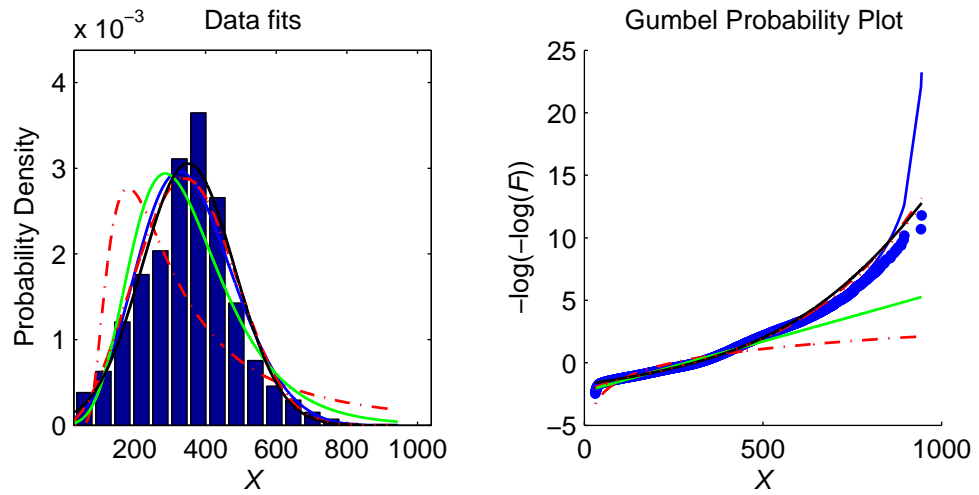

Figure B.45: Parent distribution for Load Effect 3; Length 40 m; 2-truck event.
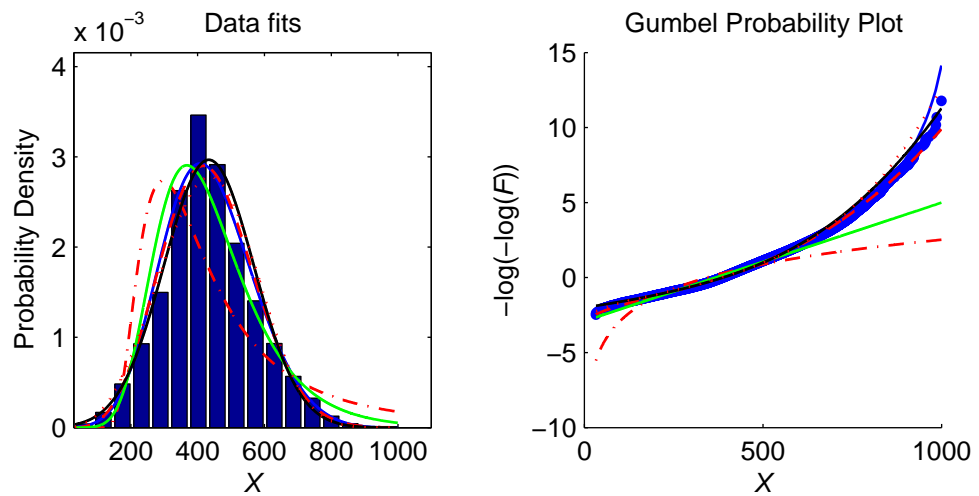
Figure B.46: Parent distribution for Load Effect 3; Length 40 m; 3-truck event.
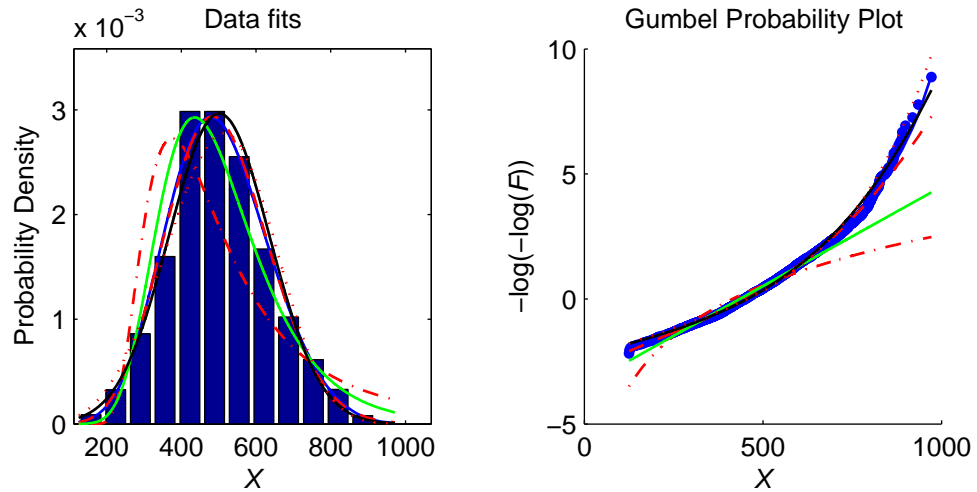
Figure B.47: Parent distribution for Load Effect 3; Length 40 m; 4-truck event.
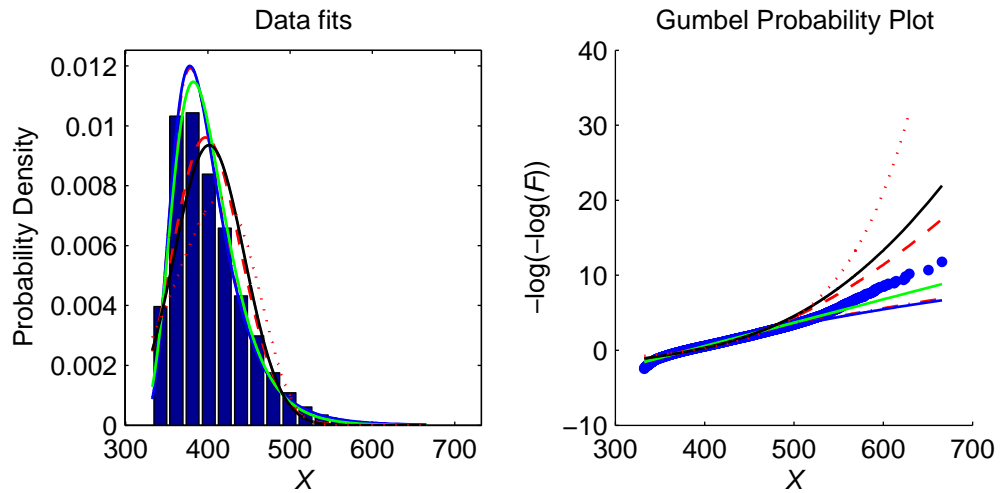
Figure B.48: Parent distribution for Load Effect 3; Length 50 m; 1-truck event.
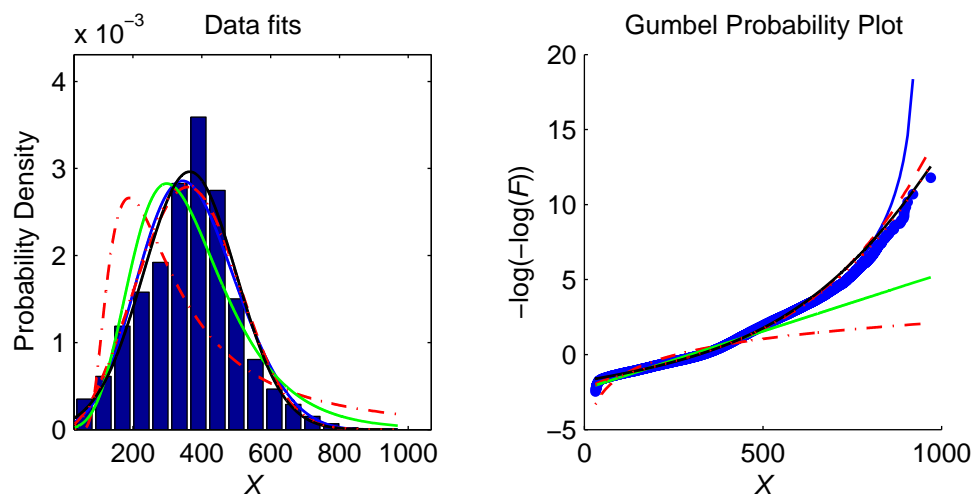
Figure B.49: Parent distribution for Load Effect 3; Length 50 m; 2-truck event.
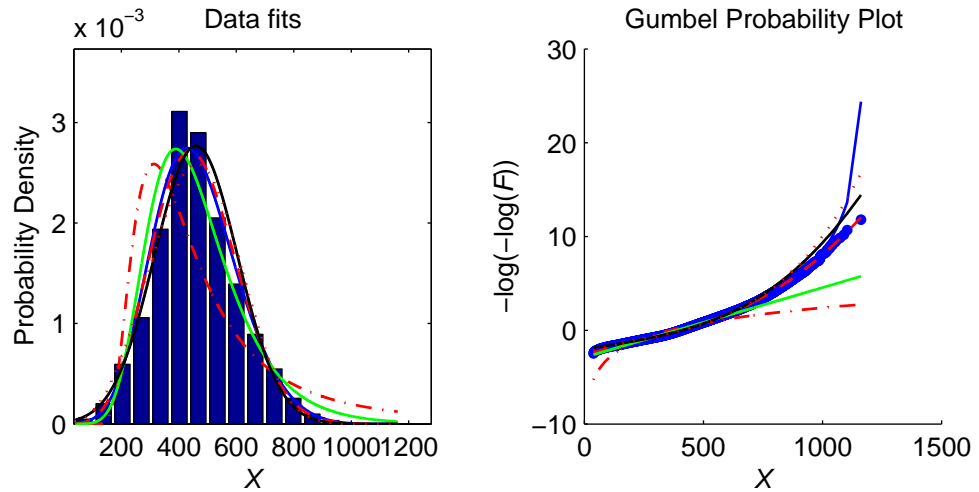
Figure B.50: Parent distribution for Load Effect 3; Length 50 m; 3-truck event.
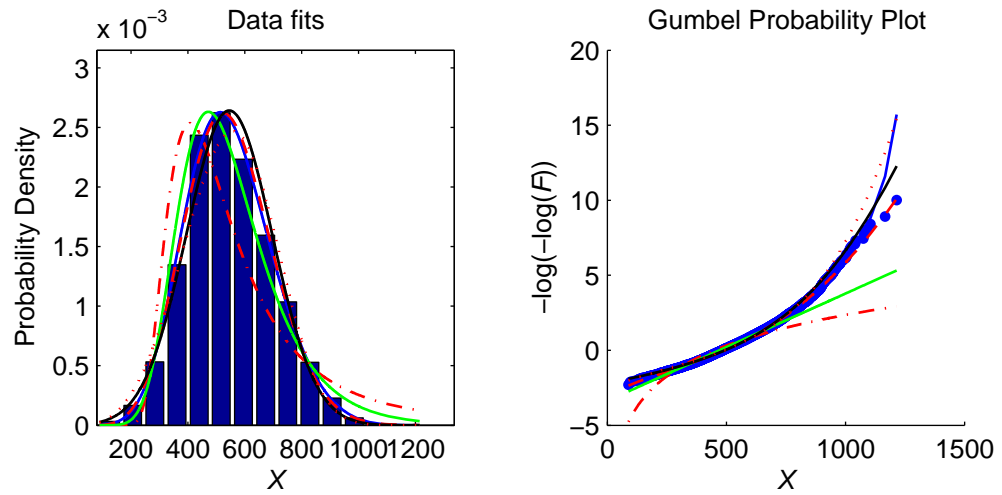
Figure B.51: Parent distribution for Load Effect 3; Length 50 m; 4-truck event.
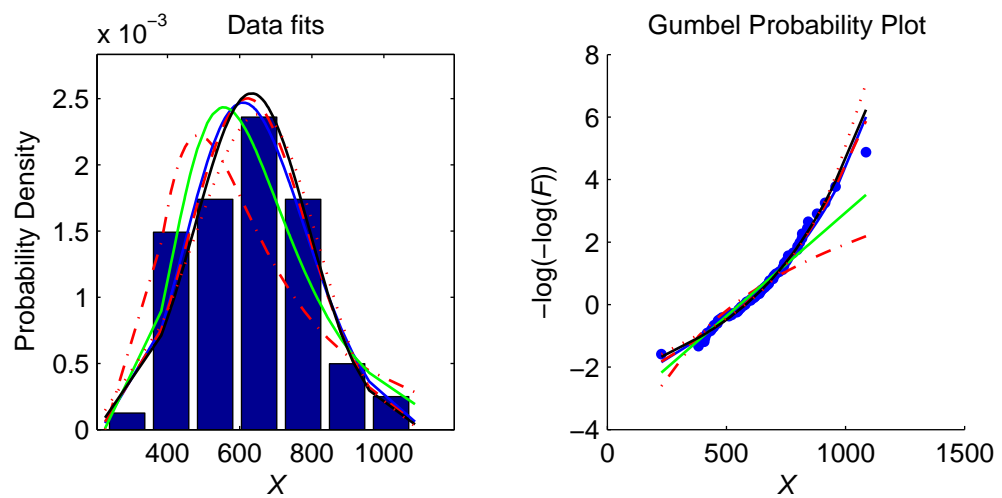
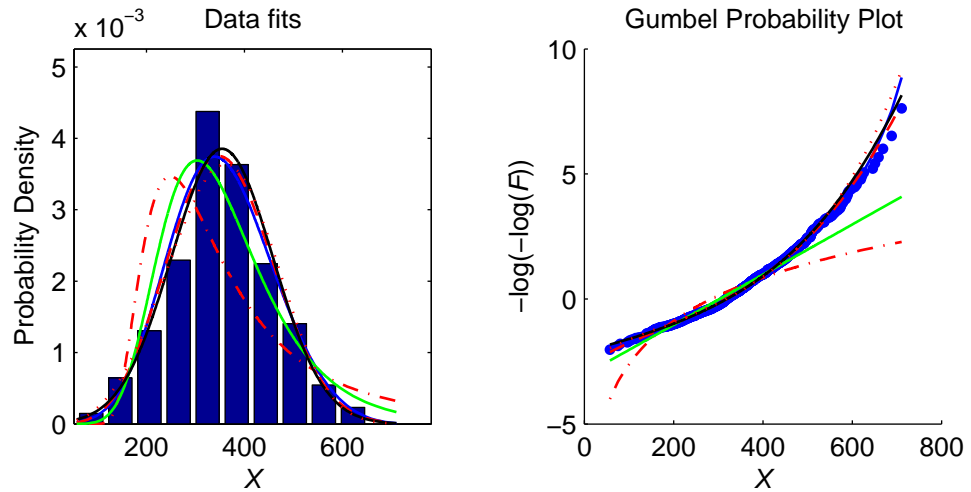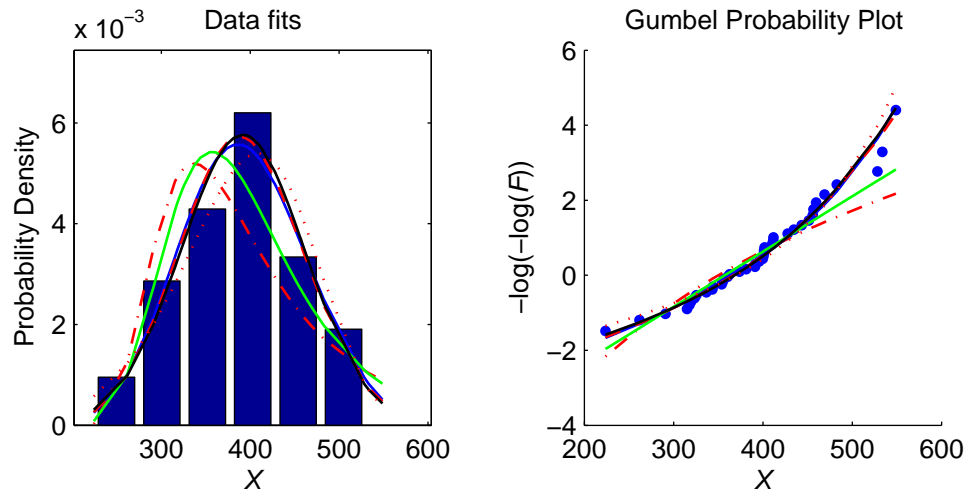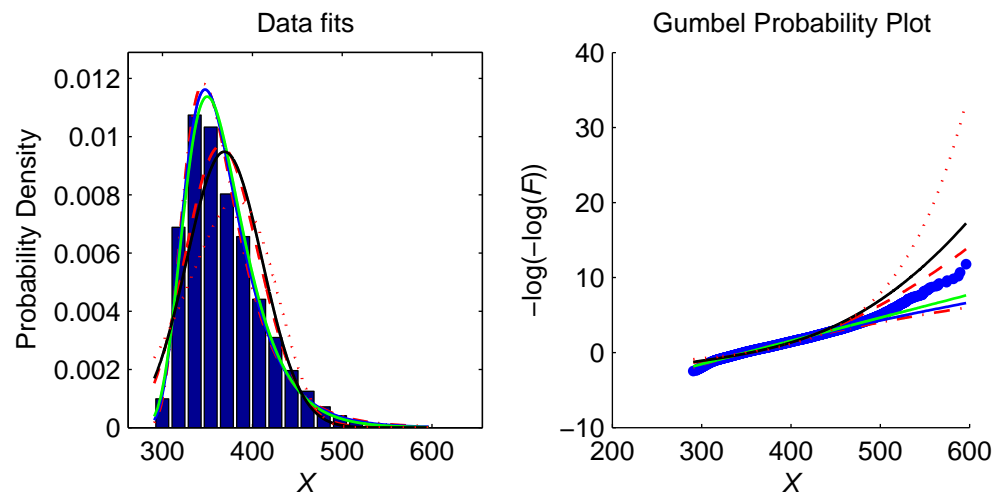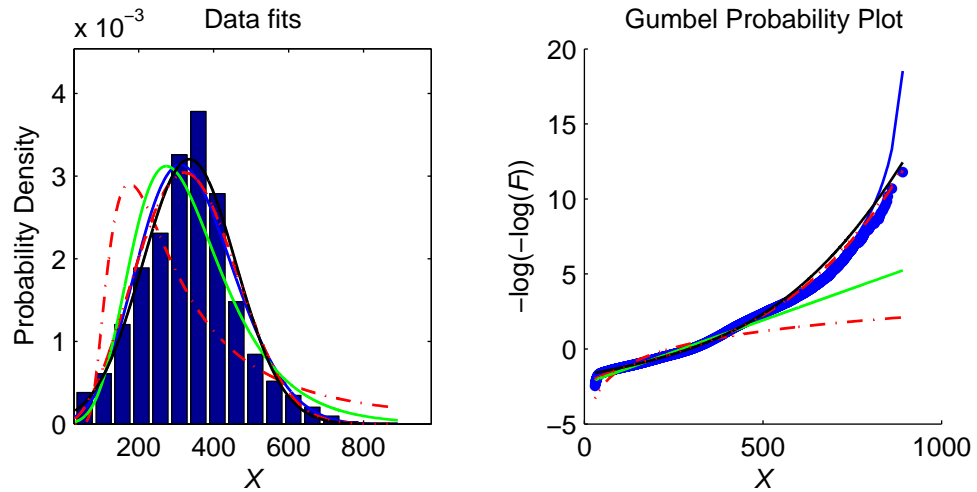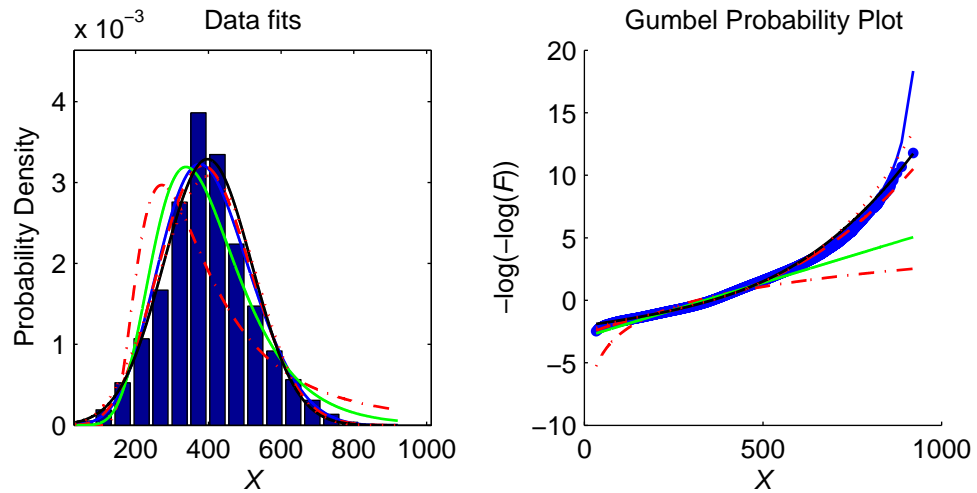Figure B.52: Parent distribution for Load Effect 3; Length 50 m; 5-truck event.

Load Effect 3			Bridge Length: 20 m		
1-truck event					
Rank	Distribution	Log-likelihood	Parameter vector		
1	GEV	-255189.441	0.012	34.055	310.293
2	Gumbel	-255193.717	33.91	310.082	0
3	Frechet	-255588.868	308.186	9.379	0
4	G.Gamma	-257127.077	43.326	14.467	1.205
5	Normal	-258394.246	329.755	1804.237	0
6	Weibull	-263066.922	349.064	7.519	0
2-truck event					
Rank	Distribution	Log-likelihood	Parameter vector		
1	GEV	-306466.627	0.231	108.857	330.973
2	Normal	-306505.14	372.844	12361.33	0
3	G.Gamma	-306524.727	1.431	357.833	2.982
4	Weibull	-306640.239	412.956	3.671	0
5	Gumbel	-309523.22	107.718	317.806	0
6	Frechet	-324054.708	298.032	2.413	0
3-truck event					
Rank	Distribution	Log-likelihood	Parameter vector		
1	G.Gamma	-10062.004	3.369	259.777	2.449
2	Normal	-10064.815	411.47	8779.707	0
3	GEV	-10066.78	0.204	90.826	374.959
4	Weibull	-10091.874	448.541	4.746	0
5	Gumbel	-10157.864	90.172	365.265	0
6	Frechet	-10421.949	353.672	3.653	0

Table B.9: Maximum likelihood estimates for Load Effect 3; Length 20 m.

Load Effect 3			Bridge Length: 30 m		
1-truck event					
Rank	Distribution	Log-likelihood	Parameter vector		
1	GEV	-254079.916	-0.042	32.315	349.349
2	Gumbel	-254136.335	32.864	350.09	0
3	Frechet	-254149.532	348.507	10.966	0
4	G.Gamma	-257099.652	55.424	12.564	1.187
5	Normal	-258471.352	369.491	1809.809	0
6	Weibull	-264168.951	389.242	8.165	0
2-truck event					
Rank	Distribution	Log-likelihood	Parameter vector		
1	G.Gamma	-314716.091	2.322	292.563	2.104
2	GEV	-314753.91	0.142	123.335	359.799
3	Normal	-315009.552	414.138	17370.08	0
4	Weibull	-315405.164	460.296	3.322	0
5	Gumbel	-316451.521	122.828	350.482	0
6	Frechet	-331023.891	326.588	2.303	0
3-truck event					
Rank	Distribution	Log-likelihood	Parameter vector		
1	GEV	-98544.904	0.22	111.374	434.148
2	G.Gamma	-98554.499	2.924	324.418	2.505
3	Normal	-98571.982	477.791	13132.57	0
4	Weibull	-98788.137	522.51	4.521	0
5	Gumbel	-99473.741	110.776	421.383	0
6	Frechet	-102492.932	406.922	3.391	0
4-truck event					
Rank	Distribution	Log-likelihood	Parameter vector		
1	GEV	-321.667	0.156	109.618	474.479
2	G.Gamma	-321.734	17.893	32.012	1.032
3	Normal	-322.605	523.043	14328.5	0
4	Gumbel	-322.865	106.681	465.53	0
5	Weibull	-323.956	570.837	4.612	0
6	Frechet	-328.138	452.554	4.075	0

Table B.10: Maximum likelihood estimates for Load Effect 3; Length 30 m.

Load Effect 3			Bridge Length: 40 m		
1-truck event					
Rank	Distribution	Log-likelihood	Parameter vector		
1	GEV	-253423.262	-0.076	31.292	369.517
2	Frechet	-253425.339	369.371	11.842	0
3	Gumbel	-253597.887	32.314	370.82	0
4	G.Gamma	-257102.393	64.17	10.979	1.166
5	Normal	-258519.913	390.094	1813.329	0
6	Weibull	-264721.157	410.052	8.486	0
2-truck event					
Rank	Distribution	Log-likelihood	Parameter vector		
1	GEV	-328409.794	-0.022	146.421	377.377
2	Gumbel	-328454.1	147.1	379.158	0
3	G.Gamma	-329308.194	16.411	4.391	0.605
4	Weibull	-333877.653	523.396	2.364	0
5	Normal	-336368.712	464.178	40817.6	0
6	Frechet	-339105.664	348.959	2.161	0
3-truck event					
Rank	Distribution	Log-likelihood	Parameter vector		
1	G.Gamma	-313987.349	2.774	355.427	2.458
2	GEV	-313999.666	0.2	124.719	464.731
3	Normal	-314067.836	515.285	16727.95	0
4	Weibull	-314669.967	565.085	4.316	0
5	Gumbel	-316684.807	124.244	451.741	0
6	Frechet	-326834.604	434.793	3.213	0
4-truck event					
Rank	Distribution	Log-likelihood	Parameter vector		
1	GEV	-3285.013	0.262	129.65	550.695
2	G.Gamma	-3286.639	2.852	427.934	2.787
3	Normal	-3287.398	598.342	17283.68	0
4	Weibull	-3292.647	650.934	5.01	0
5	Gumbel	-3318.209	126.903	533.202	0
6	Frechet	-3403.014	516.52	3.634	0

Table B.11: Maximum likelihood estimates for Load Effect 3; Length 40 m.

Load Effect 3			Bridge Length: 50 m		
1-truck event					
Rank	Distribution	Log-likelihood	Parameter vector		
1	GEV	-253146.443	-0.098	30.738	381.618
2	Frechet	-253153.874	381.895	12.344	0
3	Gumbel	-253424.019	32.087	383.28	0
4	G.Gamma	-257291.224	58.704	15.438	1.249
5	Normal	-258663.543	402.533	1823.776	0
6	Weibull	-265137.187	422.644	8.663	0
2-truck event					
Rank	Distribution	Log-likelihood	Parameter vector		
1	GEV	-338246.743	-0.136	166.006	390.128
2	Gumbel	-340112.167	174.852	402.958	0
3	G.Gamma	-340349.79	22.886	0.383	0.439
4	Frechet	-345966.934	365.109	2.023	0
5	Weibull	-347386.841	583.287	1.896	0
6	Normal	-355070.09	514.565	86241.37	0
3-truck event					
Rank	Distribution	Log-likelihood	Parameter vector		
1	GEV	-317306.361	0.199	132.896	489.74
2	G.Gamma	-317339.329	2.98	354.551	2.329
3	Normal	-317471.614	543.762	19167.81	0
4	Weibull	-318099.081	596.882	4.242	0
5	Gumbel	-319815.62	131.959	475.958	0
6	Frechet	-329606.617	457.5	3.185	0
4-truck event					
Rank	Distribution	Log-likelihood	Parameter vector		
1	GEV	-12523.469	0.23	135.48	579.209
2	G.Gamma	-12527.016	3.988	357.751	2.307
3	Normal	-12533.154	631.787	19529.51	0
4	Weibull	-12562.871	687.716	4.914	0
5	Gumbel	-12625.386	132.529	563.035	0
6	Frechet	-12915.213	546.03	3.748	0

Table B.12: Maximum likelihood estimates for Load Effect 3; Length 50 m.

B.3 Full Simulation Results

The results of the 1000-day Auxerre simulation, described in Chapter 6 to assess the implications of the application of the method of Composite Distribution Statistics (CDS), are presented in this section. The parameters of the GEV distributions obtained from the Conventional approach are given in Table B.13. From the application of CDS, Table B.14 gives the parameters of the individual mechanisms determined from the simulation. Following this, Figure B.54 to Figure B.65 are presented showing both the overall behaviour of the mechanisms and the behaviour in the simulation period. The legend used in these figures is given in Figure B.53. For a description of these figures, refer to Chapter 6.

θ	Load Effect 1				Load Effect 2				Load Effect 3			
	20	30	40	50	20	30	40	50	20	30	40	50
ξ	0.123	0.054	0.081	0.081	0.150	0.000	-0.043	0.060	0.092	0.147	0.101	0.076
σ	152.9	258.8	351.5	464.8	46.0	51.3	99.8	178.4	35.6	37.4	40.3	43.5
μ	3086	5512	7975	10508	805	1131	1657	2382	656	747	800	846

Table B.13: GEV parameters derived according to the Conventional approach.
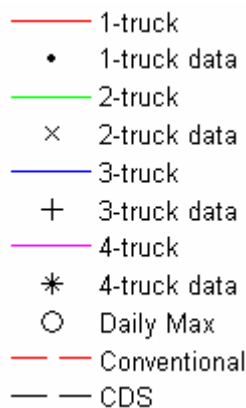
Figure B.53: Legend of parent distribution figures.

Effect	Length	θ	No. of trucks comprising the event			
			1	2	3	4
Load Effect 1	20	ξ	0.085	0.123	0.290	
		σ	91.3	152.8	482.1	
		μ	2209	3086	1891	
	30	ξ	0.098	0.055	0.269	
		σ	155.7	259.7	851.7	
		μ	3858	5509	3429	
	40	ξ	0.104	0.080	0.263	
		σ	222.0	347.5	1111.4	
		μ	5516	7958	5914	
	50	ξ	0.107	0.087	0.211	0.247
		σ	287.5	450.3	1043.0	1411.5
		μ	7174	10441	8988	7518
Load Effect 2	20	ξ	0.094	0.149	0.273	
		σ	23.3	46.0	119.4	
		μ	589	805	482	
	30	ξ	0.079	0.029	0.278	
		σ	31.9	49.3	185.5	
		μ	798	1127	845	
	40	ξ	0.083	0.087	0.191	0.168
		σ	43.0	64.9	194.2	304.1
		μ	1073	1596	1555	1337
	50	ξ	0.092	0.062	0.210	0.200
		σ	56.8	85.0	229.1	426.2
		μ	1428	2177	2348	1829
Load Effect 3	20	ξ	-0.032	0.092	0.182	
		σ	14.5	35.6	85.2	
		μ	493	656	388	
	30	ξ	-0.018	0.146	0.284	
		σ	15.8	37.3	102.2	
		μ	543	746	534	
	40	ξ	0.000	0.107	0.236	0.235
		σ	17.4	39.2	79.0	126.9
		μ	570	793	695	564
	50	ξ	6.488E-03	0.053	0.207	0.214
		σ	18.4	37.6	66.7	138.1
		μ	587	822	798	581

Table B.14: GEV 1000-day simulation daily maximum load effect parameters.

Figure B.54: 1000-day Auxerre simulation results: Load Effect 1; Length 20 m.

Figure B.55: 1000-day Auxerre simulation results: Load Effect 1; Length 30 m.

Figure B.56: 1000-day Auxerre simulation results: Load Effect 1; Length 40 m.
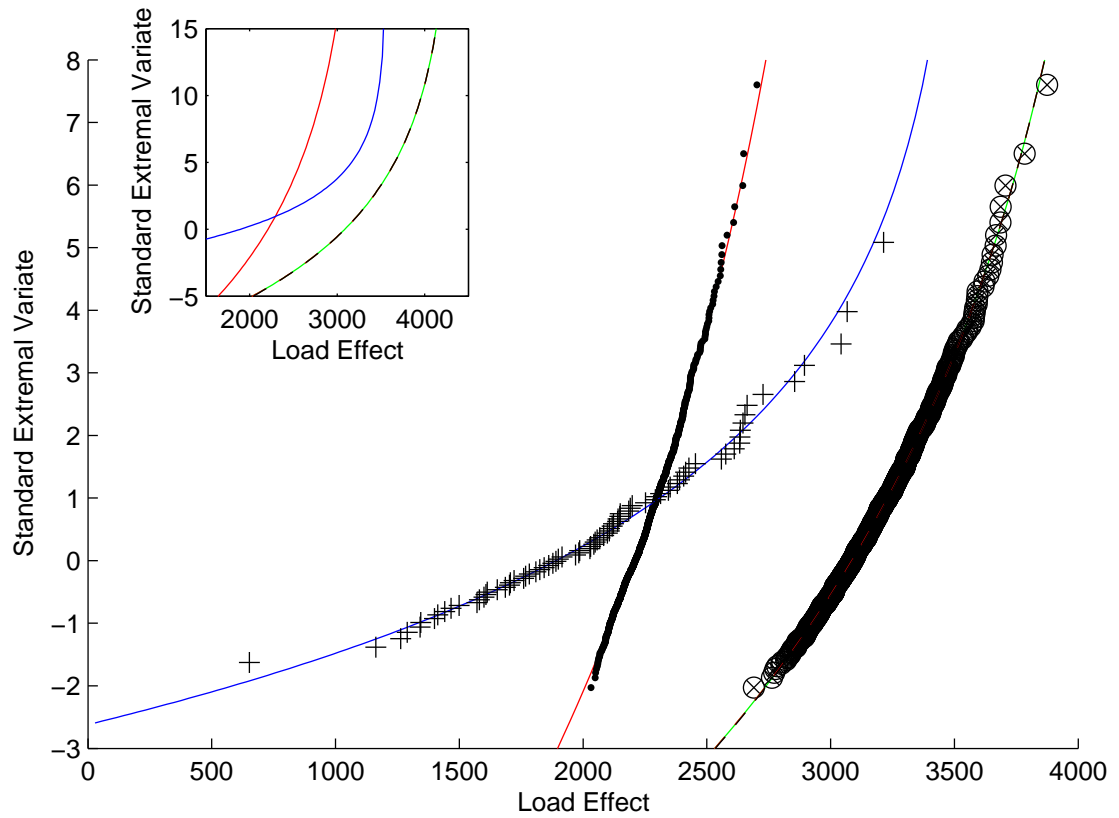

Figure B.57: 1000-day Auxerre simulation results: Load Effect 1; Length 50 m.
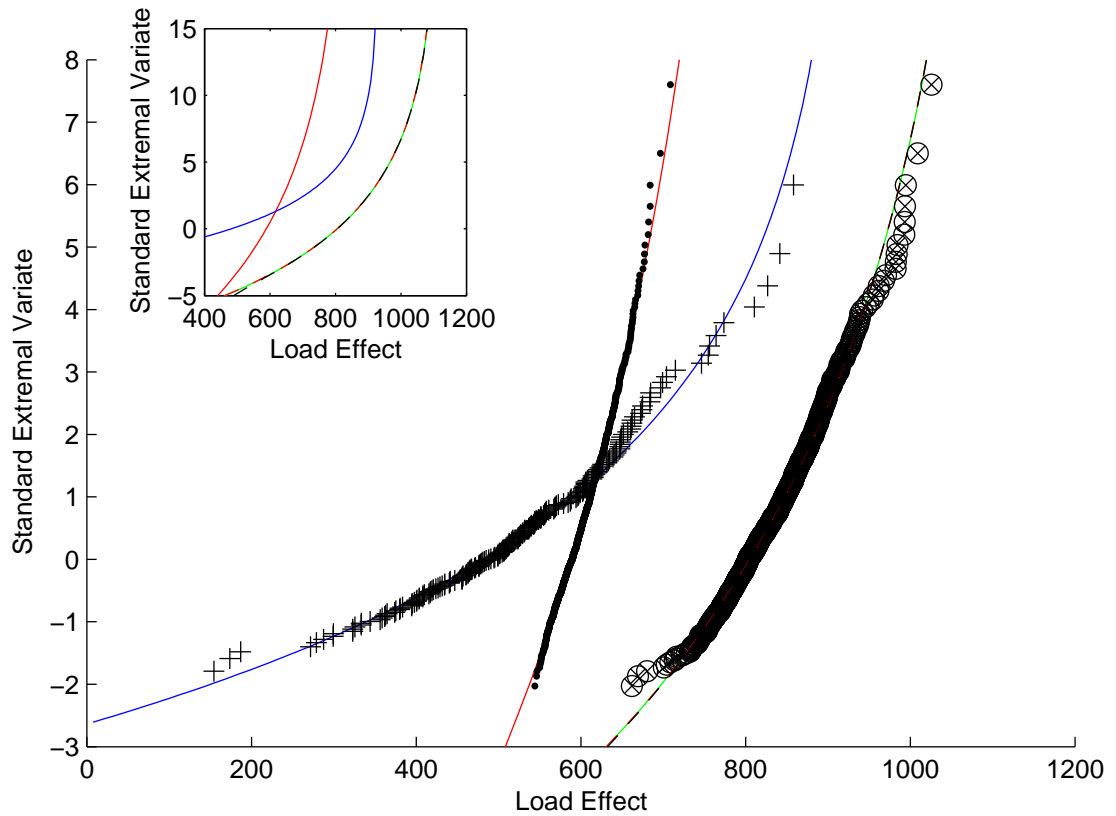
Figure B.58: 1000-day Auxerre simulation results: Load Effect 2; Length 20 m.

Figure B.59: 1000-day Auxerre simulation results: Load Effect 2; Length 30 m.

Figure B.60: 1000-day Auxerre simulation results: Load Effect 2; Length 40 m.

Figure B.61: 1000-day Auxerre simulation results: Load Effect 2; Length 50 m.

Figure B.62: 1000-day Auxerre simulation results: Load Effect 3; Length 20 m.
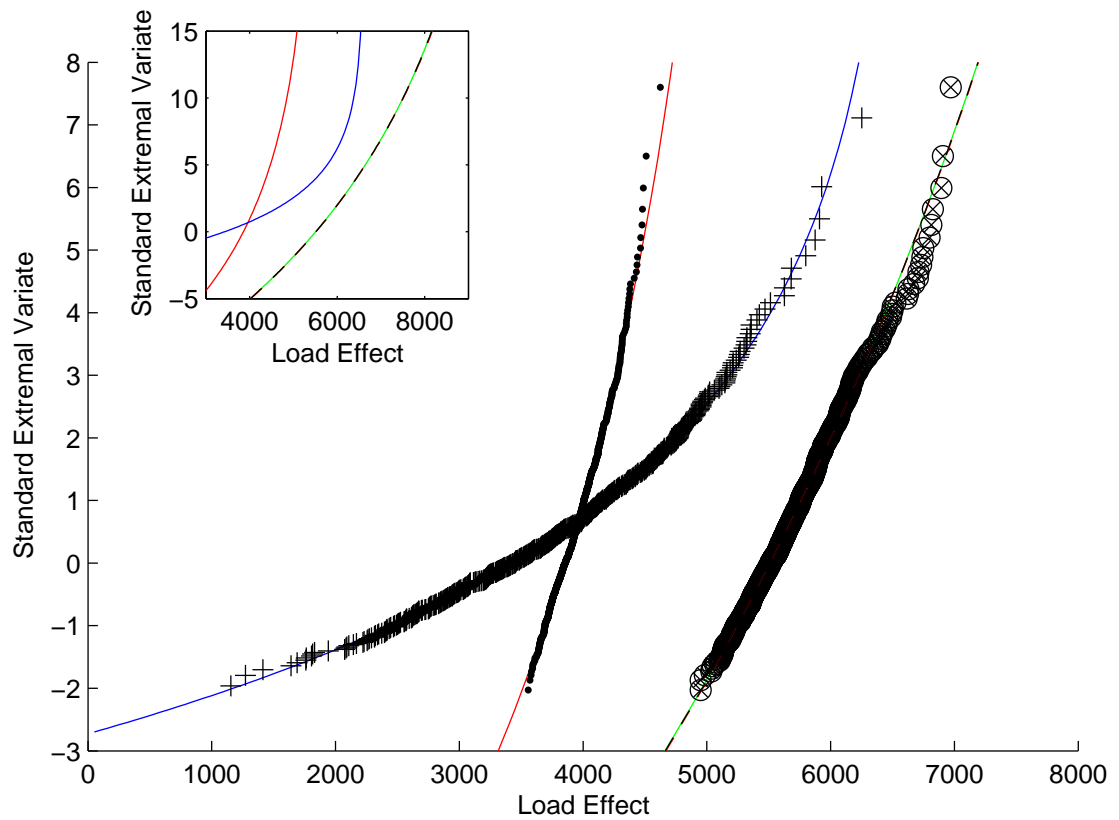

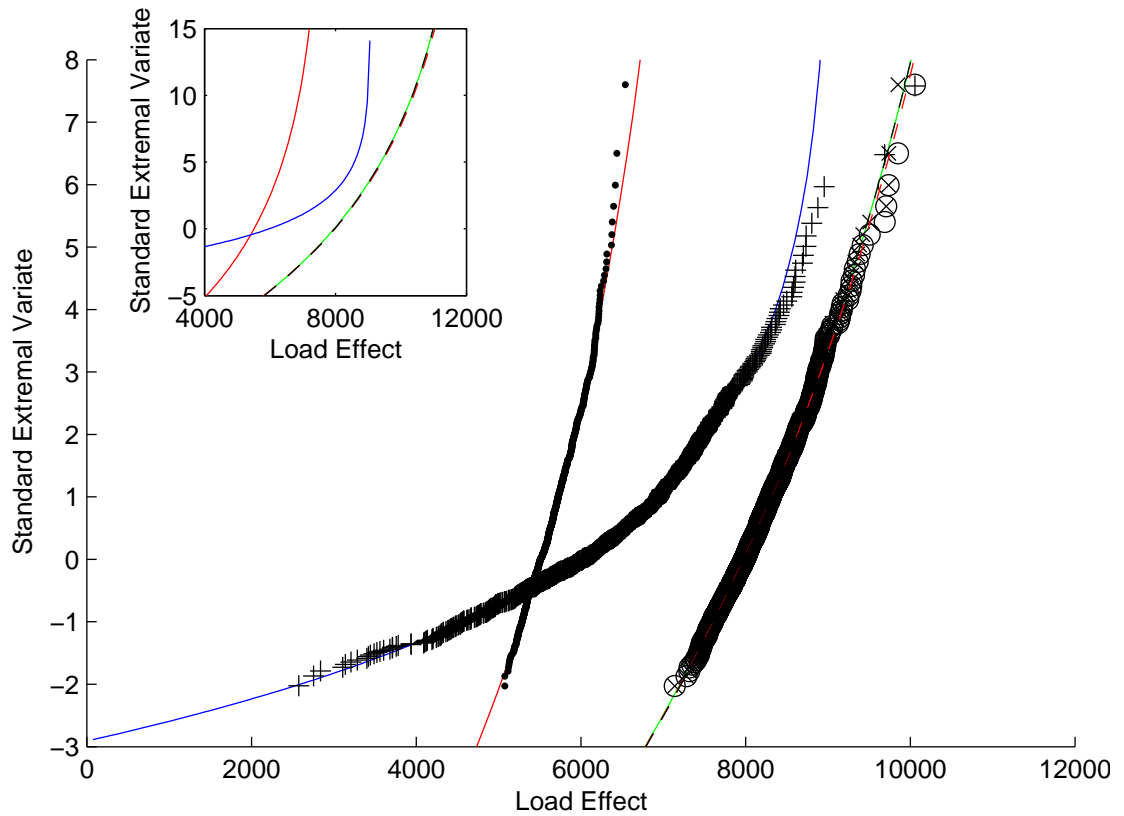Figure B.63: 1000-day Auxerre simulation results: Load Effect 3; Length 30 m.
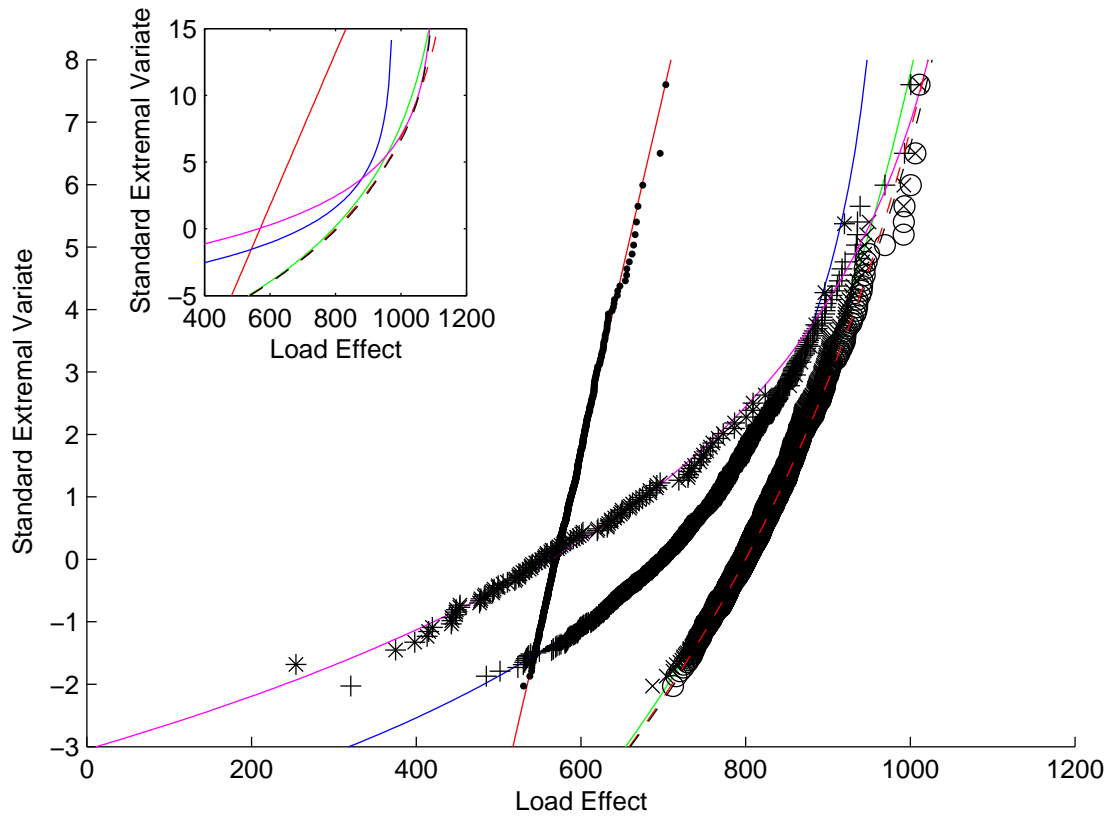
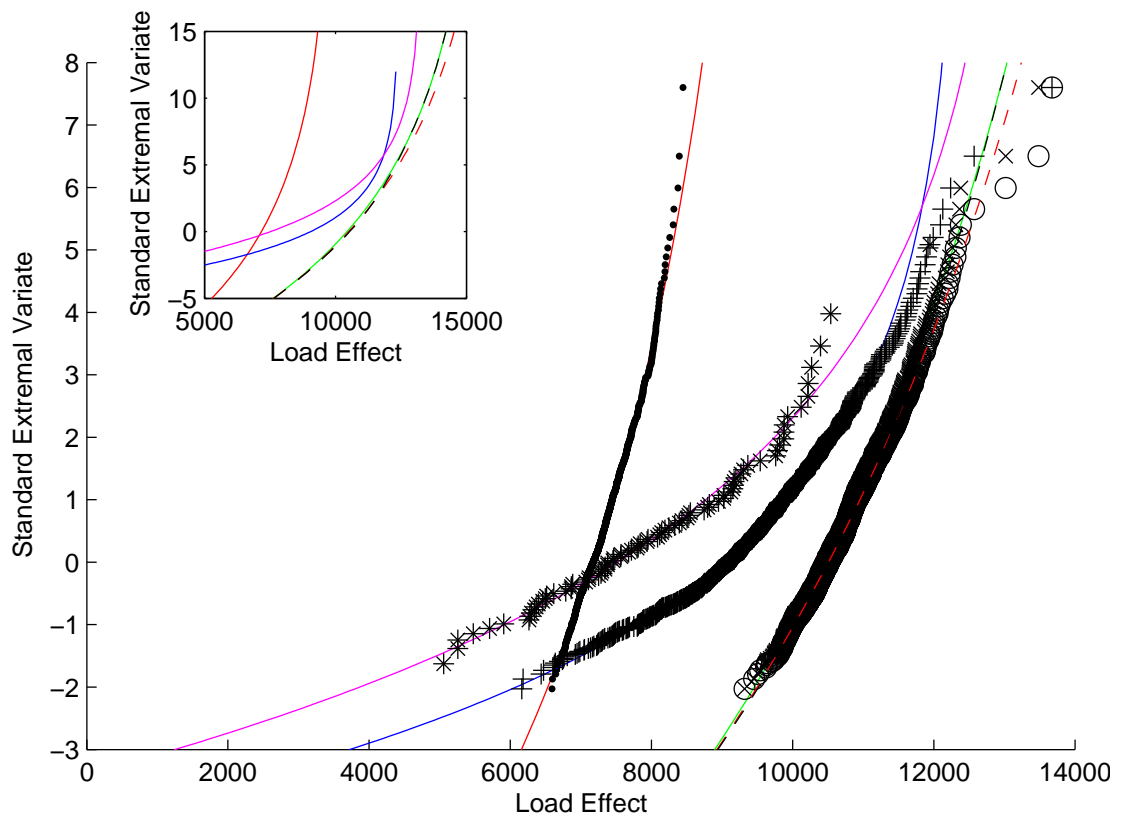Figure B.64: 1000-day Auxerre simulation results: Load Effect 3; Length 40 m.
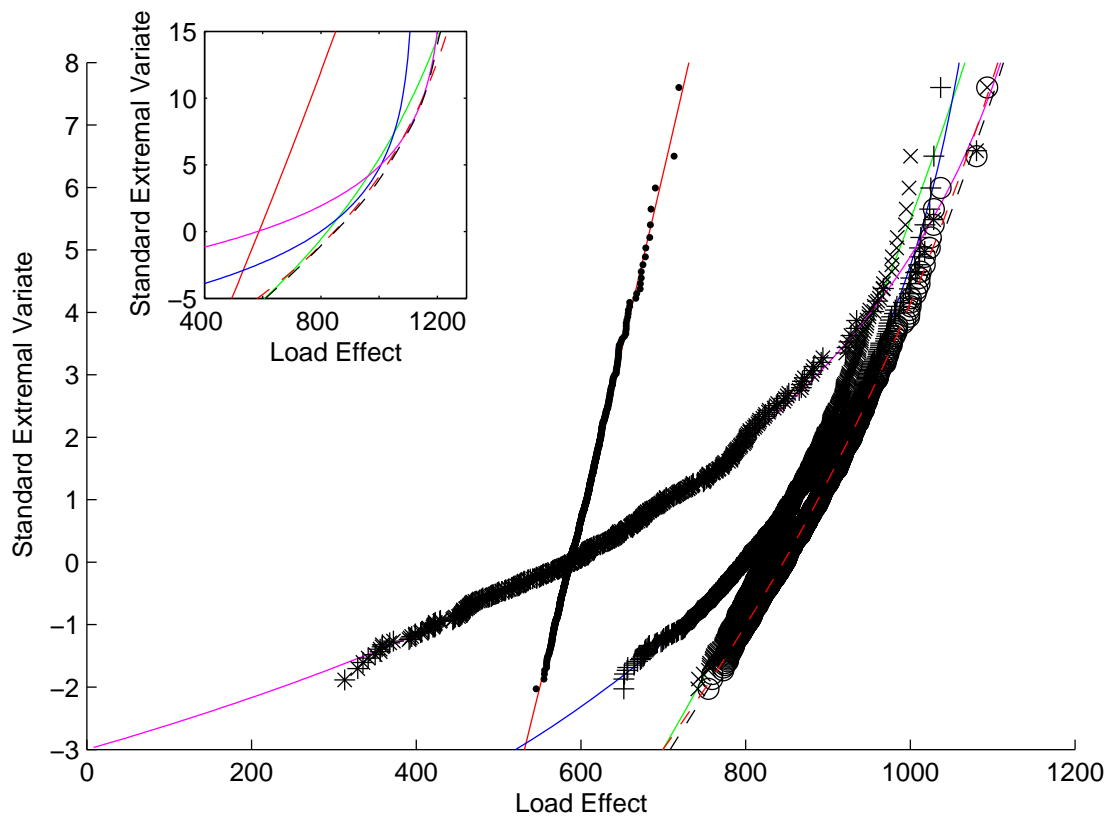
Figure B.65: 1000-day Auxerre simulation results: Load Effect 3; Length 50 m.
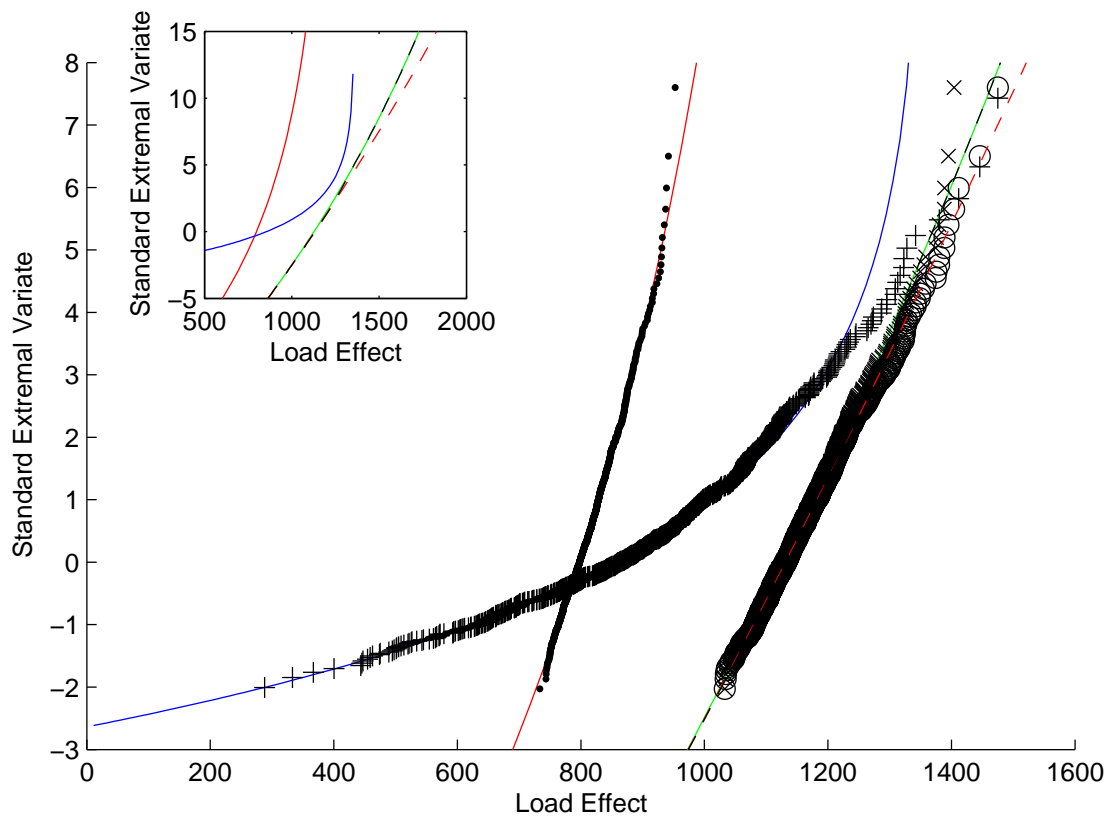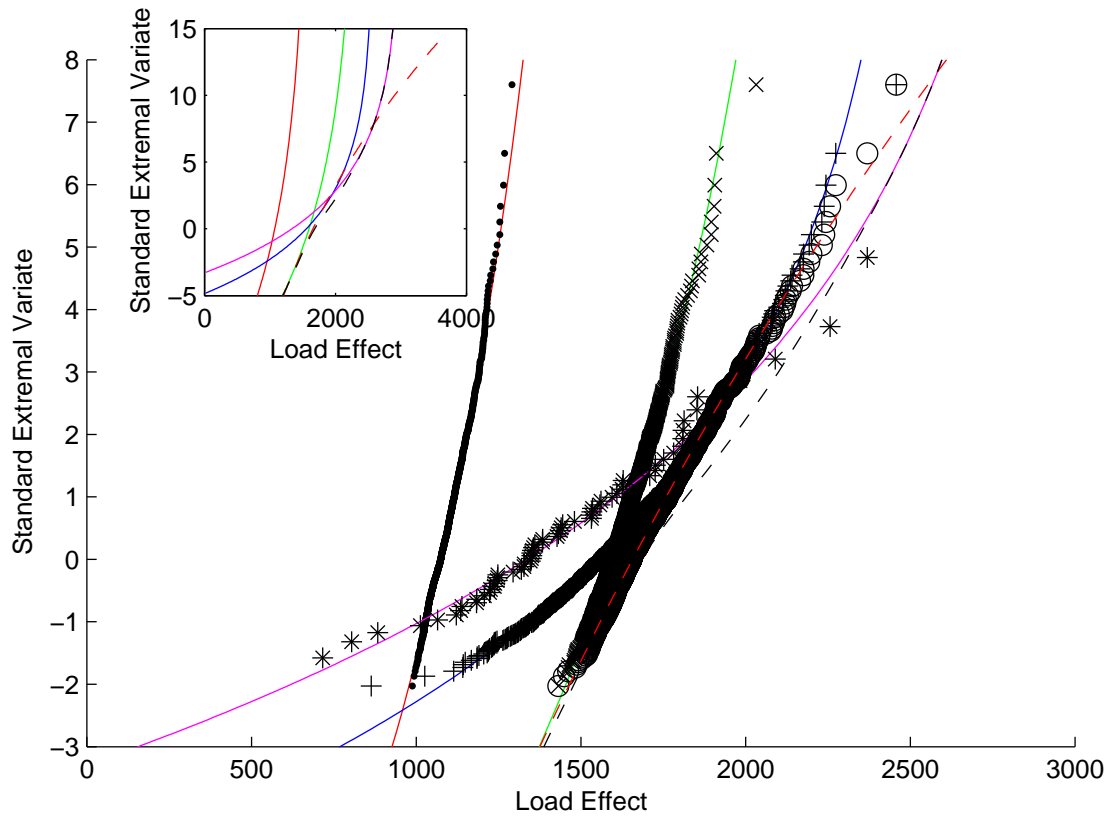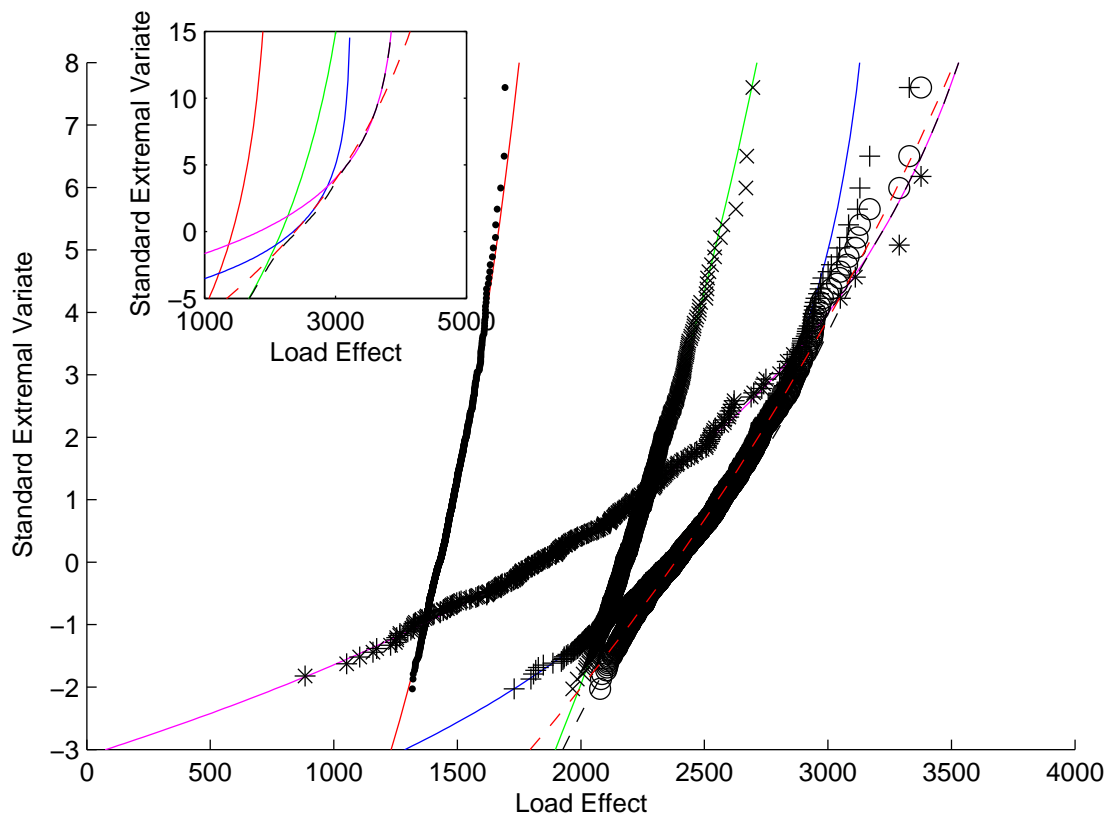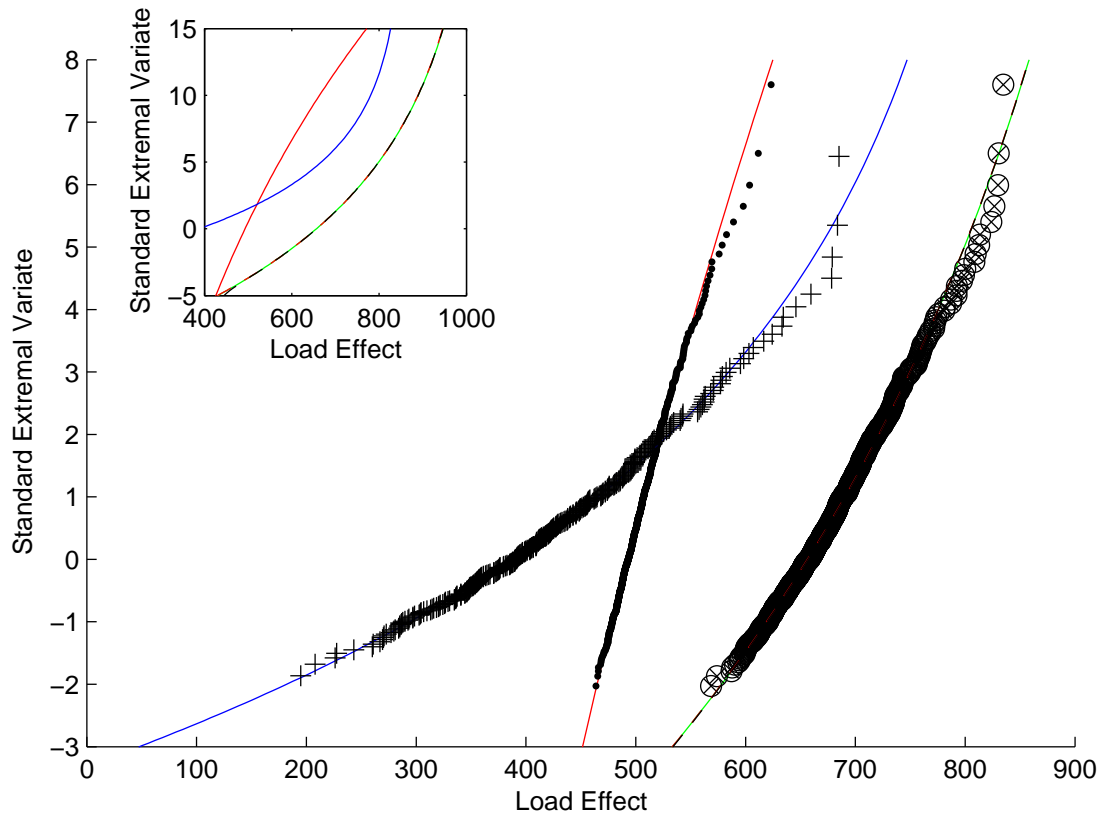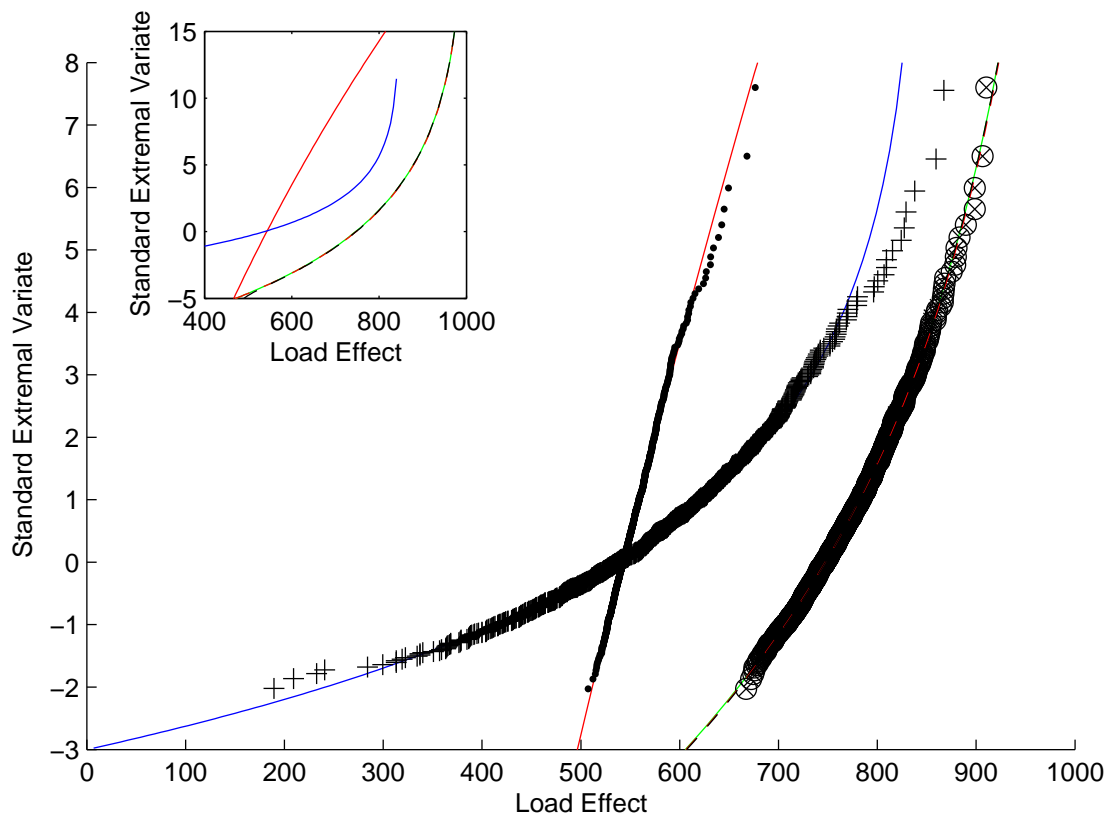
B.4 GEV Parent Distribution Parameters

Chapter 6 describes several variations of GEV distributions of load effect. Firstly, there are the GEV distributions determined from the load effect study of Section 6.2 – these are given in Table B.15. The corresponding 'normalized' parameters are given in Table B.16 – the normalizing process is explained in the next subsection. Table B.17 gives the 'reverted' parent distributions (explained below) from Table B.14 - the GEV parameters of daily maximum load effect determined from the 1000-day simulation of Auxerre traffic. The corresponding normalized parameter values for this reverted parent distribution are given in Table B.18.

Normalized parameters and length ratio

The normalization referred to in Chapter 6 is as follows. Denoting the parameters of the GEV distribution of the **j**-truck event as ξ_j, σ_j, and μ_j, normalization to a 2-truck event location value of 100 is done by:

$$\xi_j^* = \xi_j; \quad \sigma_j^* = \mathrm{cov}_j \cdot \mu_j^*; \quad \mu_j^* = \frac{\mu_j}{\mu_2} \cdot 100;$$

$$\text{where } \mathrm{cov}_j = \frac{\sigma_j}{\mu_j}$$

(B.16)

It is by this method that the impact of the load effect type and bridge length can be eliminated, and insight into the relationship between the types of loading event can be gained.

The length ratio given in the tables of normalized values allows separate quantification of the effect of bridge length. For a bridge length of **L** and a **j**-truck event, whose normalized GEV parameters are given as ξ_j^L, σ_j^L, and μ_j^L

(note that the asterisk notation has been removed for clarity), the length ratio, c_j^L, is given as:

$$c_j^L = \frac{\mu_j^L}{\mu_j^{20}}; \quad \text{for } L = 20, 30, 40 \text{ and } 50 \tag{B.17}$$

Also note, that in the tables presented, only the length ratio corresponding to 2-truck events, c_2^L, has been given.

Reverted parameters

The process described in B.1 applies for all $\mathbf{R}^+$ values of $\mathbf{n}$. Therefore it is possible to calculate a parent GEV distribution from which an observed distribution of maxima is realised.

Given the observed GEV distribution, $G^*\left(x;\theta^*\right)$, for a block size of $\mathbf{m}$, the parent distribution can be expressed as a GEV distribution, $G\left(x;\theta\right)$, such that:

$$\begin{aligned}
G^*(x) &= G^{m^{-1}}(x) \\
&= G^*(a_n + b_n x)
\end{aligned} \tag{B.18}$$

Therefore, equation (B.15) applies. Thus, the parameters of the parent GEV distribution are given by:

$$\xi = \xi^*; \quad \sigma = \frac{\sigma^*}{n^{\xi^*}}; \quad \mu = \frac{\sigma^*}{\xi^*}\left(1 - \frac{1}{n^{\xi^*}}\right) + \mu^* \tag{B.19}$$

where $n = m^{-1}$. It is in this manner that the 'reverted' parent distributions from which the 'measured' GEV parameters for daily maximum load effect are determined. For these transforms, the average number of loading events per day, for each event-type, is taken from the results of the 1000-day Auxerre simulation.

Effect	Length	θ	No. of trucks comprising the event			
			1	2	3	4
Load Effect 1	20	ξ	-0.019	0.216	0.232	
		σ	132.3	520.4	444.5	
		μ	1368	1560	1767	
	30	ξ	-0.083	0.215	0.232	
		σ	202.1	919.7	841.9	
		μ	2442	2708	3211	
	40	ξ	-0.112	0.21	0.243	0.153
		σ	274.4	1297.0	1259.7	1192.8
		μ	3516	3817	4734	5510
	50	ξ	-0.126	0.201	0.235	0.257
		σ	348.3	1655.6	1689.6	1676.8
		μ	4589	4890	6258	7369
Load Effect 2	20	ξ	-0.00677	-0.10795	0.218	
		σ	31.1	162.7	98.4	
		μ	381	397	475	
	30	ξ	-0.033	0.282	0.253	
		σ	41.9	198.0	191.7	
		μ	513	587	738	
	40	ξ	-0.069	0.264	0.214	0.189
		σ	55.4	273.4	296.1	293.9
		μ	687	796	1080	1327
	50	ξ	-0.104	0.27	0.228	0.213
		σ	69.8	369.1	416.6	449.3
		μ	920	1064	1478	1797
Load Effect 3	20	ξ	0.012	0.231	0.204	
		σ	34.1	108.9	90.8	
		μ	310	331	375	
	30	ξ	-0.042	0.142	0.22	0.156
		σ	32.3	123.3	111.4	109.6
		μ	349	360	434	474
	40	ξ	-0.076	-0.022	0.2	0.262
		σ	31.3	146.4	124.7	129.7
		μ	370	377	465	551
	50	ξ	-0.098	-0.136	0.199	0.23
		σ	30.7	166.0	132.9	135.5
		μ	382	390	490	579

Table B.15: GEV parameters of parent load effect distributions.

Effect	Length	θ	No. of trucks comprising event				Length Ratio
			1	2	3	4	
Load Effect 1	20	ξ	-0.019	0.216	0.232		
		σ	8.5	33.4	28.5		
		μ	88	100	113		100
	30	ξ	-0.083	0.215	0.232		
		σ	7.5	34.0	31.1		
		μ	90	100	119		174
	40	ξ	-0.112	0.210	0.243	0.153	
		σ	7.2	34.0	33.0	31.3	
		μ	92	100	124	144	245
	50	ξ	-0.126	0.201	0.235	0.257	
		σ	7.1	33.9	34.5	34.3	
		μ	94	100	128	151	314
Load Effect 2	20	ξ	-0.007	-0.108	0.218		
		σ	7.8	40.9	24.8		
		μ	96	100	120		100
	30	ξ	-0.033	0.282	0.253		
		σ	7.1	33.7	32.7		
		μ	87	100	126		148
	40	ξ	-0.069	0.264	0.214	0.189	
		σ	7.0	34.3	37.2	36.9	
		μ	86	100	136	167	200
	50	ξ	-0.104	0.270	0.228	0.213	
		σ	6.6	34.7	39.1	42.2	
		μ	86	100	139	169	268
Load Effect 3	20	ξ	0.019	0.192	0.218		
		σ	10.7	40.3	32.0		
		μ	116	100	118		100
	30	ξ	-0.049	0.192	0.199	0.196	
		σ	9.1	41.8	33.2	26.1	
		μ	122	100	123	141	109
	40	ξ	-0.074	0.194	0.194	0.207	
		σ	8.5	42.3	33.7	28.6	
		μ	123	100	127	150	114
	50	ξ	-0.094	0.213	0.177	0.185	
		σ	8.1	42.1	33.9	29.3	
		μ	122	100	128	155	118

Table B.16: Normalized GEV parameters of parent load effect distributions.

Effect	Length	θ	No. of trucks comprising the event			
			1	2	3	4
Load Effect 1	20	ξ	0.085	0.123	0.290	
		σ	47.0	81.6	978.3	
		μ	2728	3666	179	
	30	ξ	0.098	0.055	0.269	
		σ	72.5	192.8	873.1	
		μ	4709	6727	3349	
	40	ξ	0.104	0.080	0.370	
		σ	97.9	219.5	701.1	
		μ	6708	9553	7172	
	50	ξ	0.107	0.087	0.318	0.247
		σ	124.0	267.0	512.1	2578.1
		μ	8709	12546	10773	2788
Load Effect 2	20	ξ	0.094	0.149	0.278	
		σ	11.2	21.6	187.1	
		μ	717	968	254	
	30	ξ	0.079	0.029	0.378	
		σ	17.3	42.0	150.1	
		μ	984	1382	958	
	40	ξ	0.083	0.087	0.191	0.180
		σ	22.5	38.1	126.8	493.8
		μ	1320	1905	1908	240
	50	ξ	0.092	0.062	0.264	0.200
		σ	27.8	57.0	103.5	567.8
		μ	1745	2628	2844	1120
Load Effect 3	20	ξ	-0.032	0.092	0.182	
		σ	18.6	22.3	101.6	
		μ	621	802	297	
	30	ξ	-0.018	0.146	0.335	
		σ	18.2	16.7	70.1	
		μ	676	887	637	
	40	ξ	0.000	0.107	0.286	0.235
		σ	17.5	20.8	39.3	240.1
		μ	707	965	838	81
	50	ξ	0.007	0.053	0.207	0.214
		σ	17.5	26.9	34.1	185.9
		μ	728	1021	956	358

Table B.17: Reverted Auxerre 1000-day simulation parent distributions.

Effect	Length	θ	No. of trucks comprising event				Length Ratio
			1	2	3	4	
Load Effect 1	20	ξ	0.085	0.123	0.290		
		σ	1.3	2.2	26.7		
		μ	74	100	5		100
	30	ξ	0.098	0.055	0.269		
		σ	1.1	2.9	13.0		
		μ	70	100	50		183
	40	ξ	0.104	0.080	0.370		
		σ	1.0	2.3	7.3		
		μ	70	100	75		261
	50	ξ	0.107	0.087	0.318	0.247	
		σ	1.0	2.1	4.1	20.5	
		μ	69	100	86	22	342
Load Effect 2	20	ξ	0.094	0.149	0.278		
		σ	1.2	2.2	19.3		
		μ	74	100	26		100
	30	ξ	0.079	0.029	0.378		
		σ	1.2	3.0	10.9		
		μ	71	100	69		143
	40	ξ	0.083	0.087	0.191	0.180	
		σ	1.2	2.0	6.7	25.9	
		μ	69	100	100	13	197
	50	ξ	0.092	0.062	0.264	0.200	
		σ	1.1	2.2	3.9	21.6	
		μ	66	100	108	43	271
Load Effect 3	20	ξ	-0.032	0.092	0.182		
		σ	2.3	2.8	12.7		
		μ	77	100	37		100
	30	ξ	-0.018	0.146	0.335		
		σ	2.1	1.9	7.9		
		μ	76	100	72		111
	40	ξ	0.000	0.107	0.286	0.235	
		σ	1.8	2.2	4.1	24.9	
		μ	73	100	87	8	120
	50	ξ	0.007	0.053	0.207	0.214	
		σ	1.7	2.6	3.3	18.2	
		μ	71	100	94	35	127

Table B.18: Normalized GEV parameters of reverted load effect distributions.

Appendix C

PREDICTIVE LIKELIHOOD

"Everything should be made as simple as possible,
but not simpler"   - Albert Einstein

Appendix C - PREDICTIVE LIKELIHOOD

C.1 Application

The following plots are the output from the predictive likelihood algorithm. In the main plot, on Gumbel probability paper, the large red dot describes the locations of the predictands evaluated. The CDS and component distributions combine to maximize the predictive likelihood function for each predictand and can be seen to do so. In the PDF plots, the red line represents the predictands; for each predictand the component PDFs are also plot. It is clear to see that there is little variation in PDFs, in spite of the significant variation in likelihood of each predictand. The final plot shows the relative predictive likelihood for each predictand. These points are the final predictive likelihood distribution and it is to these that the GEV predictive likelihood distribution is fitted.

The legend used in the Gumbel plots is given by Figure C.1.
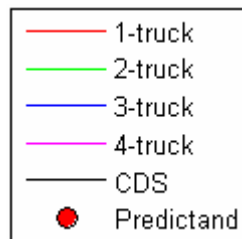
Figure C.1: Legend for the Gumbel plots of the following figures.
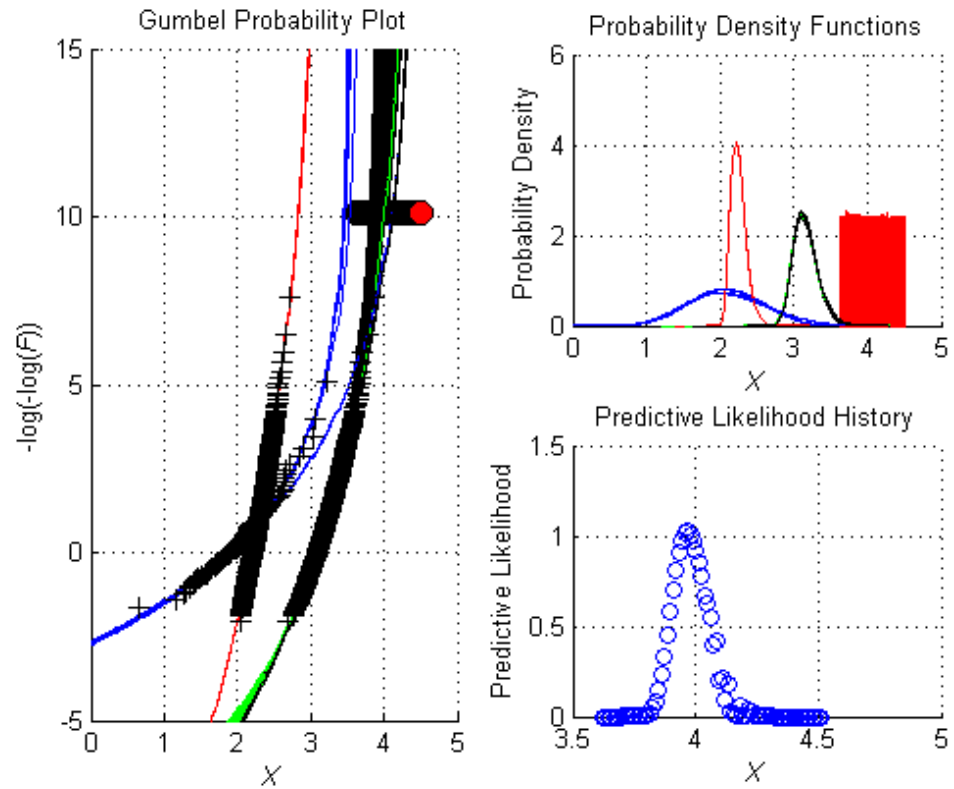
Figure C.2: Load Effect 1; Length 20 m.
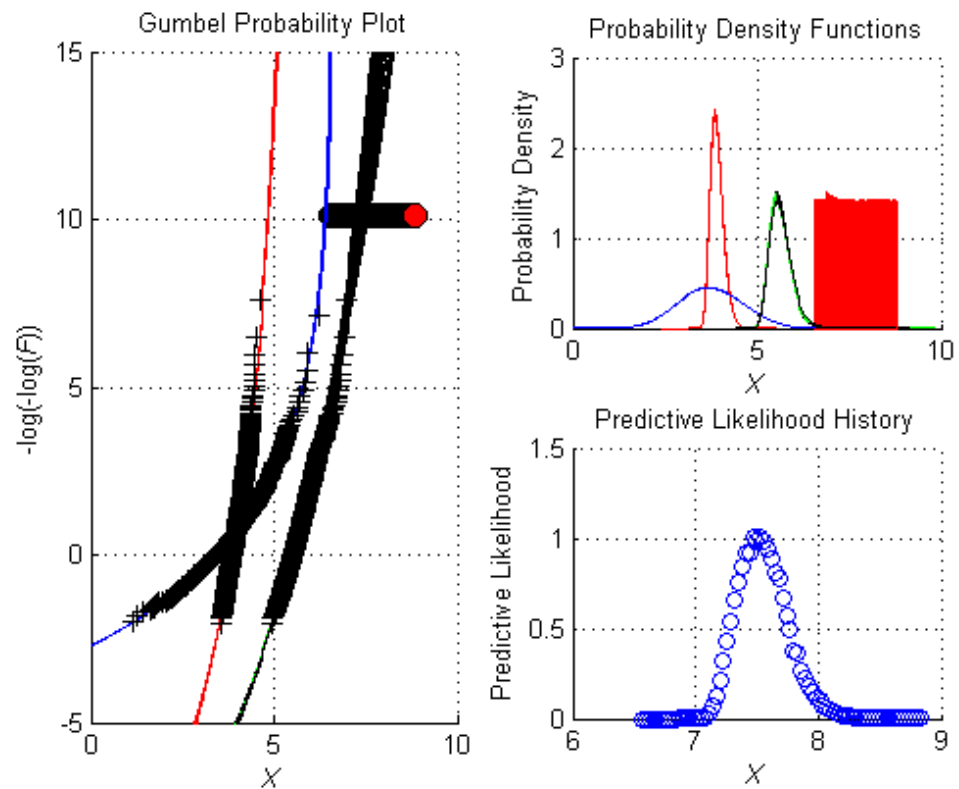
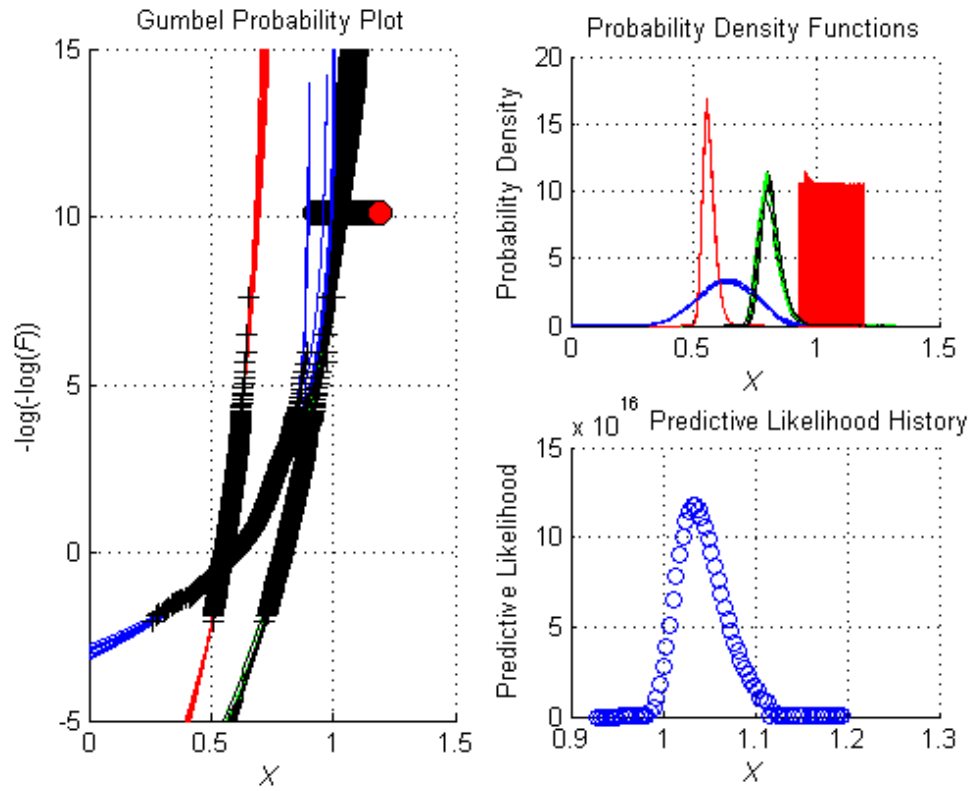Figure C.3: Load Effect 1; Length 30 m.

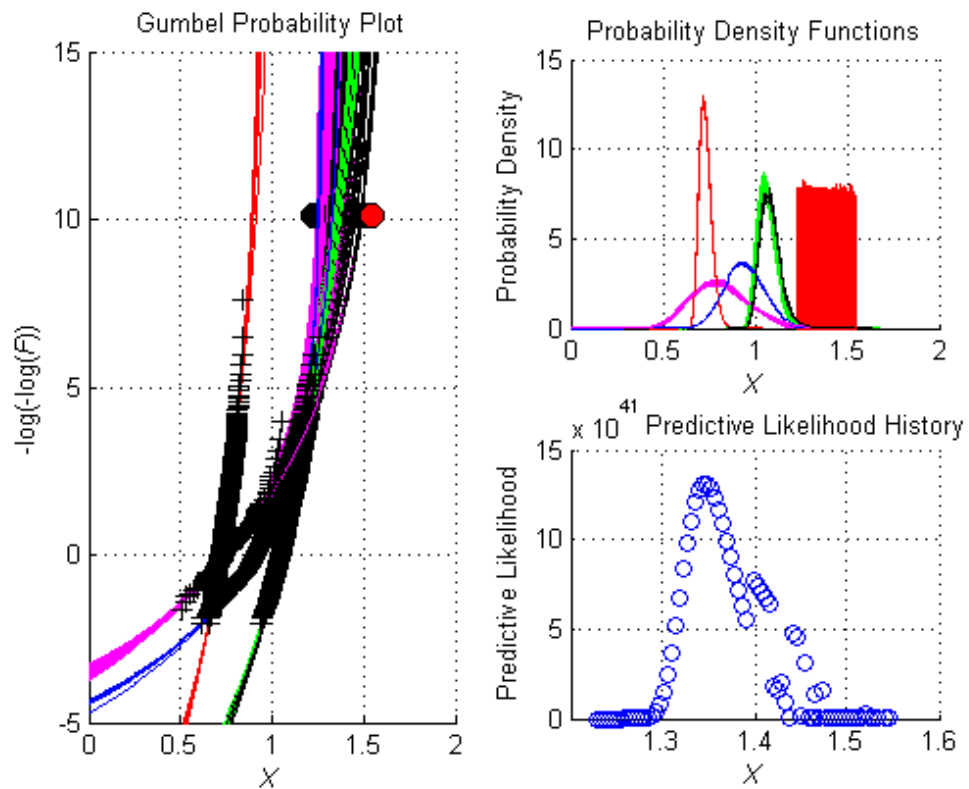Figure C.4: Load Effect 1; Length 40 m.
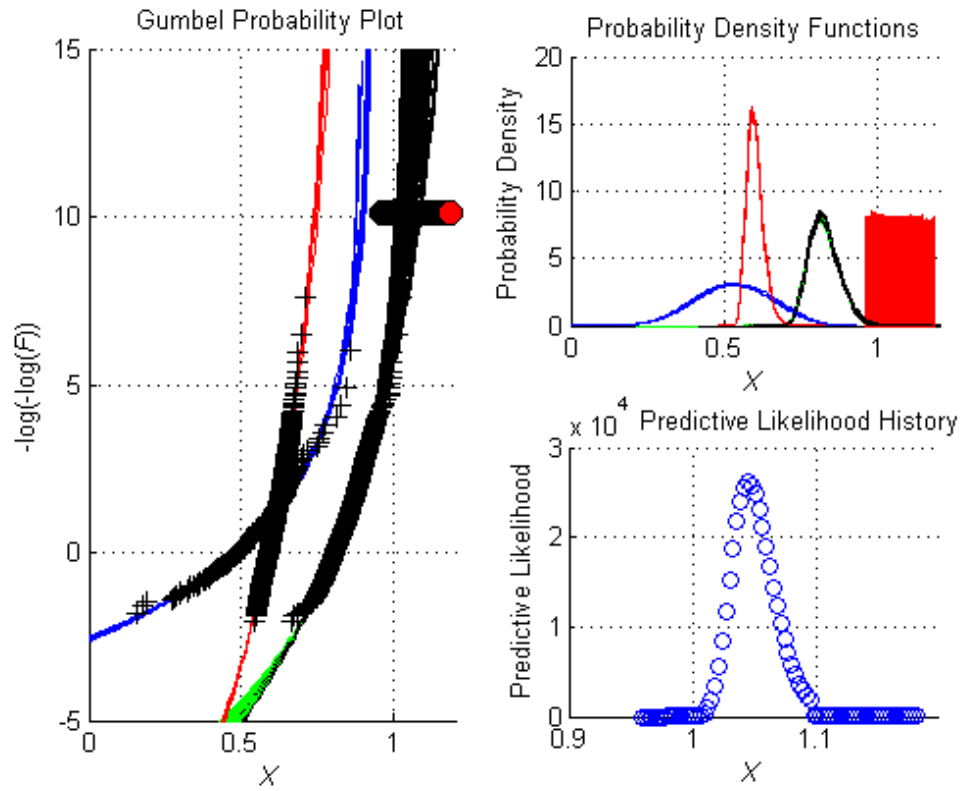

Figure C.5: Load Effect 1; Length 50 m.

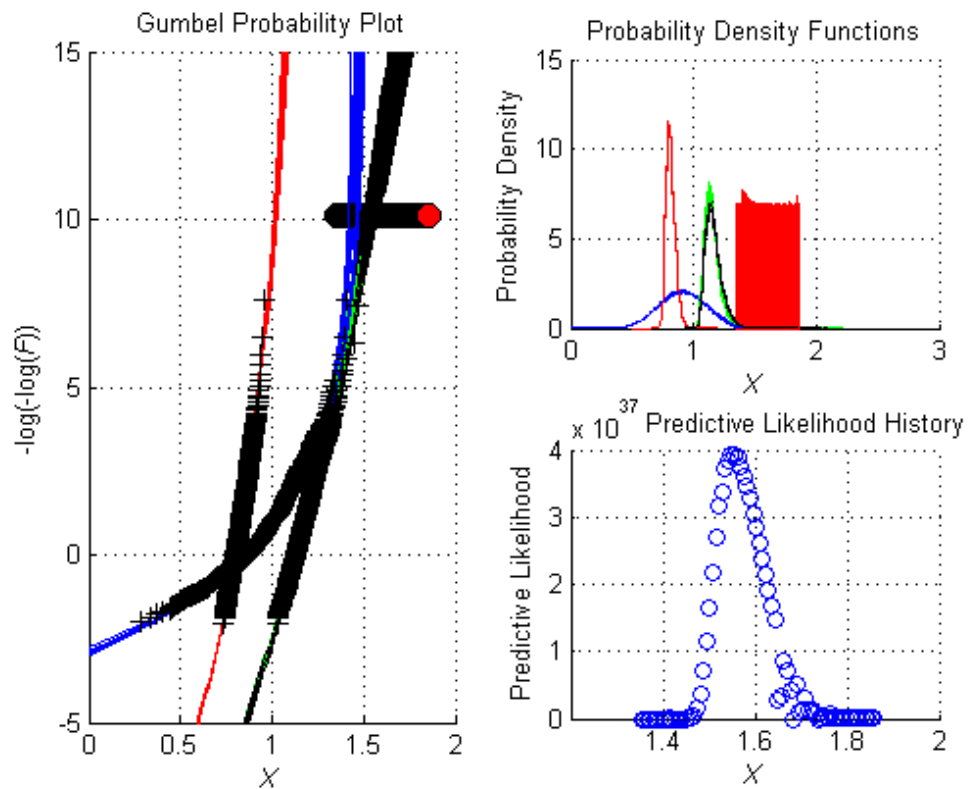Figure C.6: Load Effect 2; Length 20 m.
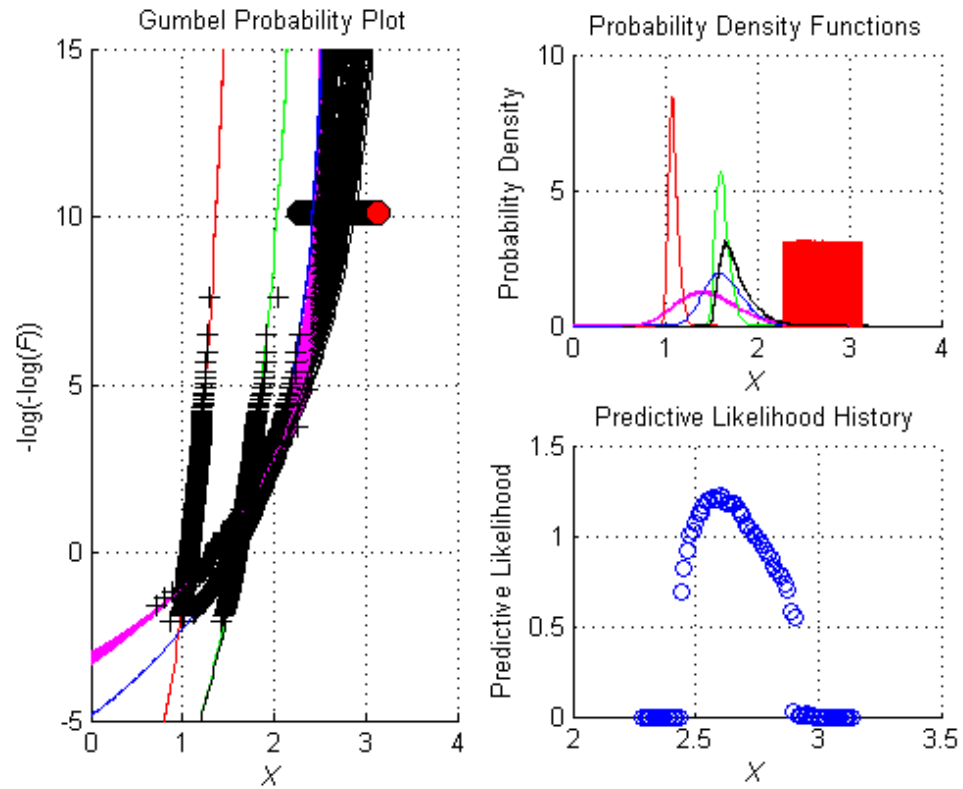

Figure C.7: Load Effect 2; Length 30 m.

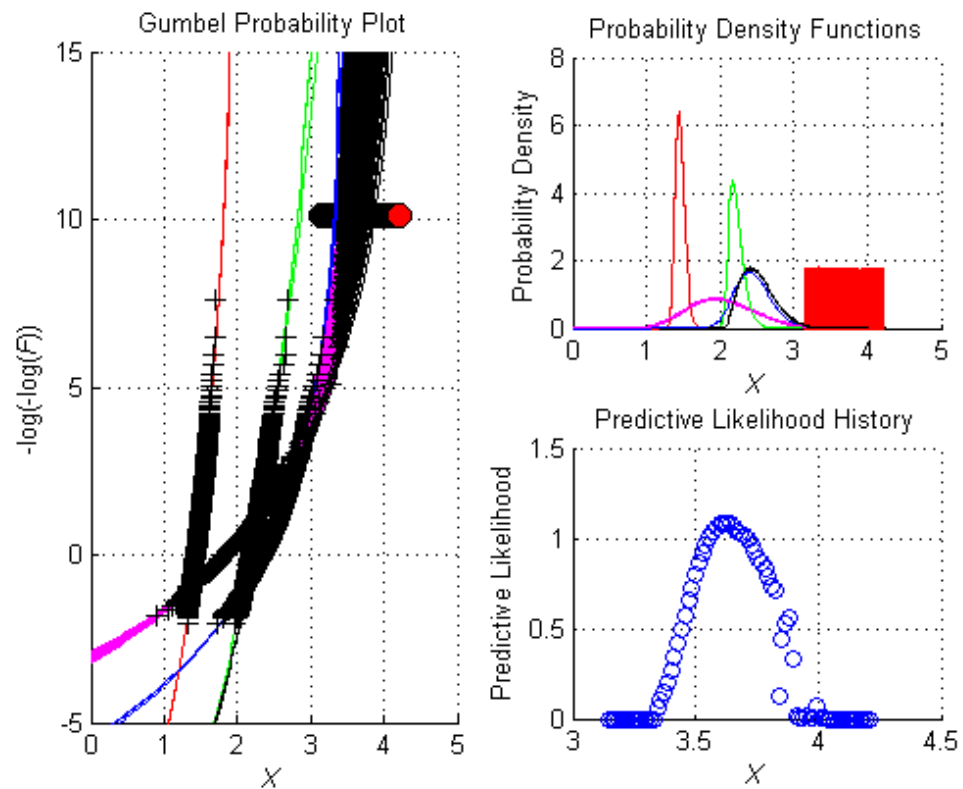Figure C.8: Load Effect 2; Length 40 m.

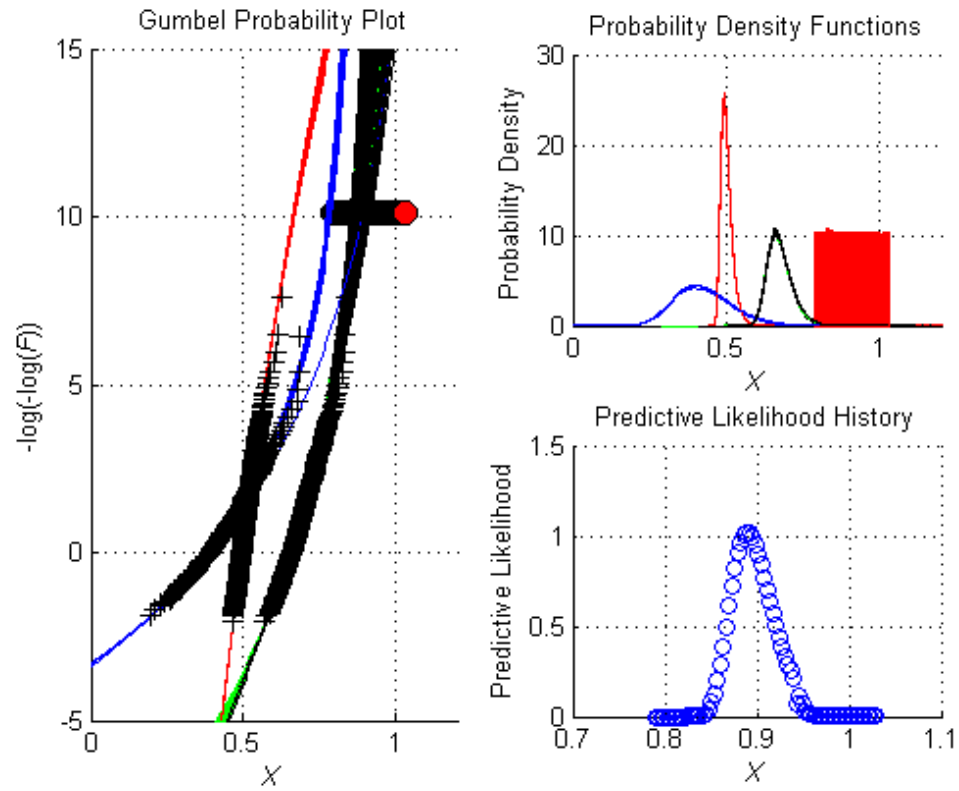Figure C.9: Load Effect 2; Length 50 m.

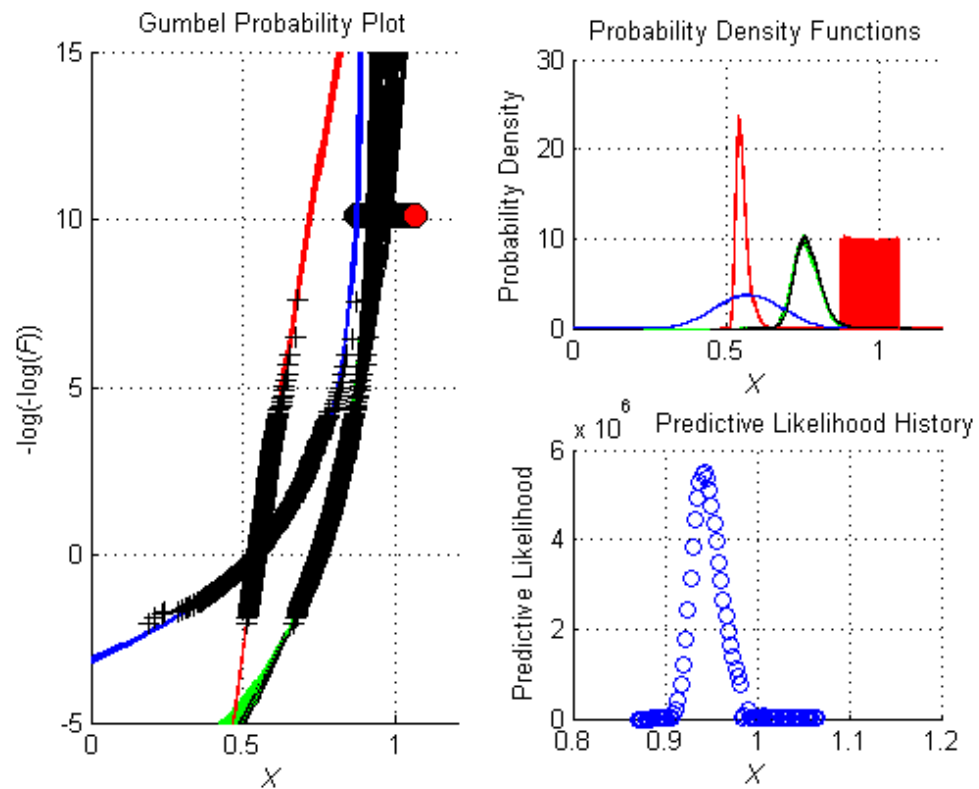Figure C.10: Load Effect 3; Length 20 m.

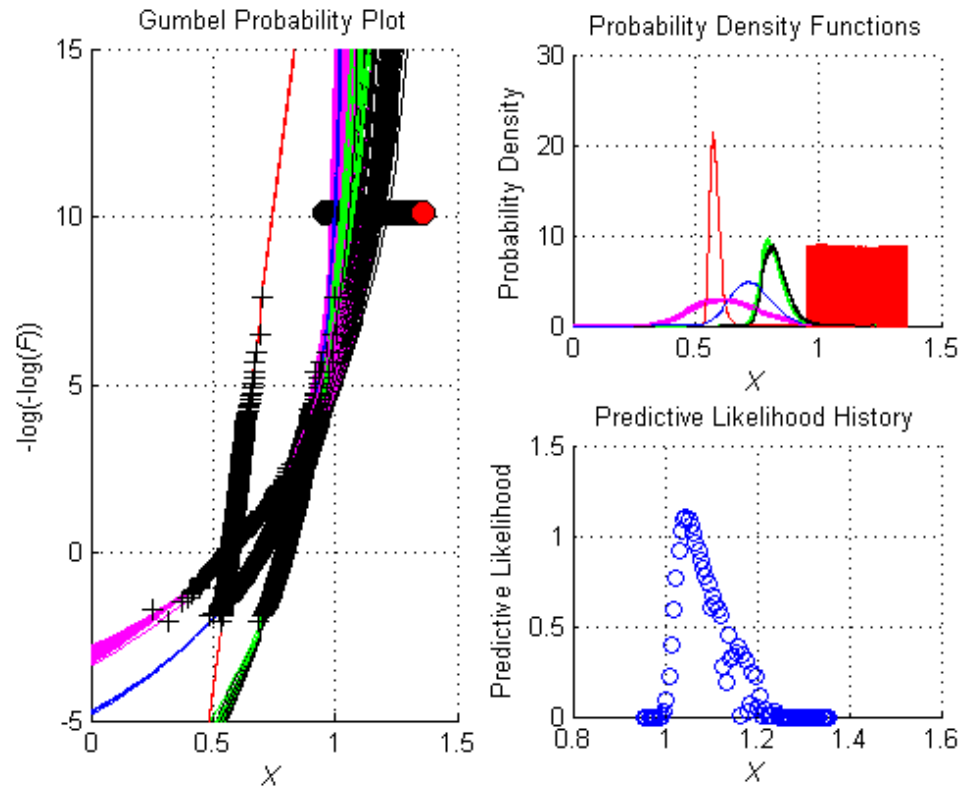
Figure C.11: Load Effect 3; Length 30 m.
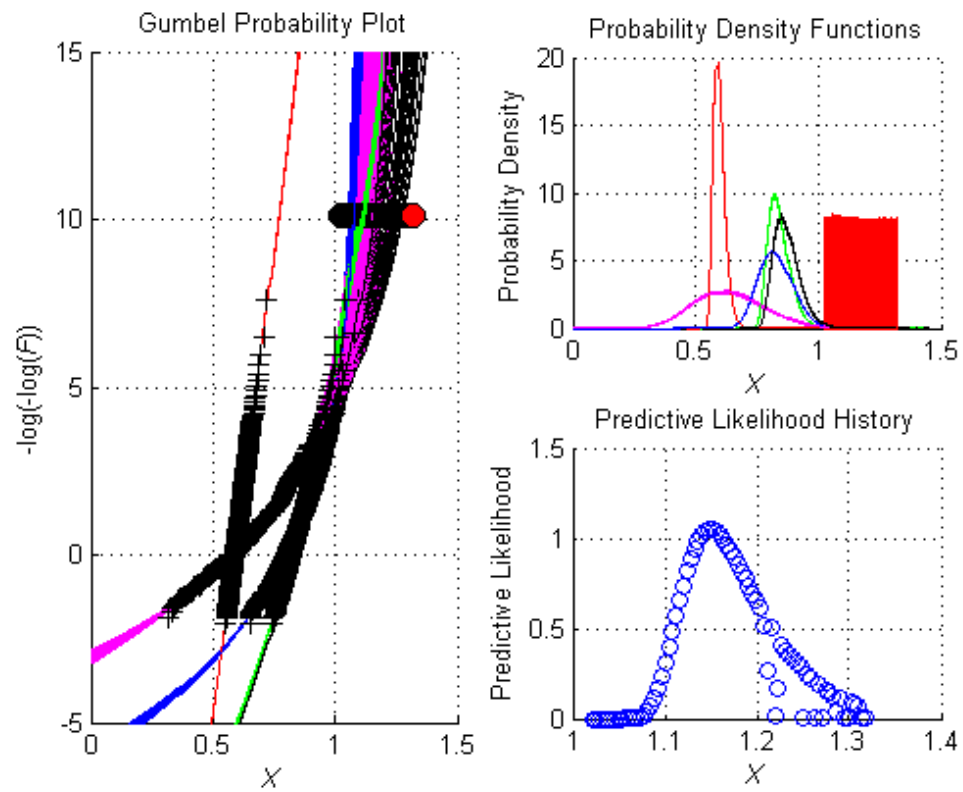
Figure C.12: Load Effect 3; Length 40 m.

Figure C.13: Load Effect 3; Length 50 m.

C.2 GEV Fits

Load Effect	Bridge Length (m)	GEV Fits		
		ξ	σ	μ
1	20	0.2028	66.18	3953
	30	0.1769	189.7	7475
	40	0.08195	233.9	10320
	50	-0.05175	298.9	13460
2	20	0.1208	15.64	1043
	30	0.09644	44.24	1552
	40	0.2478	150.1	2595
	50	0.2671	143.1	3597
3	20	0.1503	20.65	886.8
	30	0.1278	14.48	940.4
	40	-0.1132	46.14	1069
	50	-0.01964	41.21	1158

Table C.1: Table of GEV parameters of fits to predictive likelihood distribution.

C.3 Results

Load Effect	Bridge Length (m)	Characteristic Load Effect			Percentage difference[1]	
		PL[2]	GEV[3]	CDS[4]	PL	CDS
1	20	4074	4073	4067	0.0	-0.3
	30	7830	7827	7852	0.0	0.3
	40	10814	10801	10701	0.1	-1.0
	50	14150	14173	13893	-0.2	-2.2
2	20	1074	1074	1067	0.0	-0.8
	30	1636	1641	1643	-0.3	0.1
	40	2841	2854	2921	-0.5	-1.5
	50	3825	3839	3785	-0.4	-1.5
3	20	927	926	922	0.1	-0.6
	30	969	969	963	0.0	-0.9
	40	1153	1187	1079	-2.9	-9.3
	50	1235	1253	1185	-1.4	-5.5

[1] Relative to GEV PL fit;

[2] 90-percentile of 100-year distribution based on predictive likelihood points;

[3] 90-percentile of 100-year distribution GEV fit to predictive likelihood points;

[4] 1000-year return level based on CDS extrapolation.

Table C.2: Table of predictive likelihood results.